THE USE OF THE SEDIMENT FINGERPRINTING TECHNIQUE TO QUANTIFY THE DIFFERENT SEDIMENT SOURCES ENTERING THE WHANGAPOUA ESTUARY, NORTH ISLAND, IN NEW ZEALAND

A thesis
submitted in fulfilment
of the requirements for the degree of
Doctor of Philosophy in Earth and Ocean Sciences
at the
University of Waikato
by

Brendan Patrick Roddy

University of Waikato
2010

ABSTRACT

New Zealand estuaries are sites of ecological, economic, and recreational significance. Estuaries are vulnerable to the impacts of increased erosion as they act as natural sediment traps. The objectives of this study were to; 1) quantify the relative amounts of sediment entering the estuary from the native forest, exotic forest, and agricultural landscape units in the Whangapoua catchment, Coromandel Peninsula, New Zealand; 2) identify the dominant processes generating the sediment within the native forest, exotic forest, and pastoral landscape units; and 3) assess the utility of the sediment fingerprinting technique in New Zealand by comparing the results with other sediment measurement techniques.

Sediment fingerprinting, which uses geochemical elements to link potential source areas to the estuary sediment, was used to identify sediment sources in the Whangapoua catchment. Three landscape units (referred to as native forest, exotic forest, and agriculture), and three erosion positions (surface, subsurface, and streambanks) were investigated. A radionuclide tracing study, a stream suspended sediment monitoring programme, and catchment modelling were undertaken to compare with the sediment fingerprinting results.

An initial pilot study was undertaken which confirmed that sediment fingerprinting could distinguish sediment derived from the three landscape units and three erosion positions. In a full sampling programme, the landscape units and erosion positions in the Whangapoua catchment were each characterised by analysing 50 samples using ICP-MS to determine the concentrations of 29 elements. The elements Si, P, Se, V, U, In, and Bi were identified as forming a composite fingerprint to distinguish landscape units. The native forest landscape unit (21% of the catchment area) contributed 62% of estuary sediment, with 23% from the exotic forest (61% of the catchment area), and 15% from the agricultural landscape unit (18% of the catchment area). The elements Se, Fe, Ba, Mn, P, and Ca formed a composite fingerprint to distinguish erosion positions and showed that most of the estuary sediment was derived from subsurface (79%), followed by streambanks (13%), and then surface sources (8%).

A radionuclide tracing study was undertaken and 15 samples were used to characterise each of the surface, subsurface, and streambank erosion positions. ^{137}Cs was effective at distinguishing the surface (0-2cm) from other erosion positions, but could not distinguish the subsurface (>20cm) from the streambank sediment. The ^{137}Cs results indicated that up to 98% of the estuary sediment was derived from subsurface and streambank sources.

Stream suspended sediment monitoring was undertaken at four small subcatchment sites over a two year period. Monitoring commenced at the four sites as follows; immediately harvested exotic pines, six month post harvested pines, ten year re-growth pines, and agricultural pastures. The erosion rates were high in pines after harvesting (48 t km^{-2} yr^{-1}), but dropped to 28 t km^{-2} yr^{-1} six months post harvesting and then to 2 t km^{-2} yr^{-1} ten years post harvesting. The agricultural erosion rate was calculated at 7 t km^{-2} yr^{-1}. The lack of a native forest monitoring site, lack of replication, data capture problems, and inherent errors limit confidence in the stream suspended sediment monitoring results which should only be considered indicative.

A stream bed sampling programme used 18 sampling points to estimate how much fine sediment was stored within the rivers and streams. Less than 4% of the annual estuary fine sediment budget was stored within the stream and river beds, indicating that sediment was efficiently conducted from the native forest landscape unit into the estuary.

Two catchment models (Sediment Yield Estimator and the New Zealand Empirical Erosion Model) gave results that were contradictory to the sediment fingerprinting results as they suggested that deforested areas (such as agriculture and harvested pines) were sediment generating areas.

This thesis demonstrated that the use of sediment fingerprinting in New Zealand was an effective means of quantifying various sediment sources based on landscape unit and erosion position. The current pattern of landuse within the Whangapoua catchment is appropriate in providing an economic return while minimising the levels of sediment delivery to the Whangapoua estuary.

ACKNOWLEDGEMENTS

It is my pleasure to acknowledge those who have assisted me in the production of this thesis, some whose contributions has been more than ordinary.

Firstly to my supervisors, Vicki Moon, Megan Balks, and Fiona Dyer. Vicki as Chief Supervisor has been the steady hand on the tiller guiding me in this process. Calm by nature, I would flick through Vicki's edits with nothing written page after page until five or six words in the margin would elicit a pang of panic and then a weeks work to fix the identified problem. Thank you Vicki.

If Vicki was the Captain of the ship up in the bridge, Megan was the ships mechanic down in the engine room with her sleeves rolled up, covered in grease, and no detail escaping her notice. My manuscripts would come back from Megan covered in red pen and resembling a abattoir's drop sheet. Megan's tenacious attitude to 'getting it right' has been a major contribution in the production of this thesis. Cheers a million Megan.

If Megan was the ships mechanic, than Fiona was….sorry, out of nautical analogies! Fiona made the trip over to New Zealand midway to inspect the field work and then reviewed the thesis toward the end of the write up. To Fiona's daughters I offer my apologies, because Mummy really wasn't watching at the swimming carnival because she was editing Chapter 8 (who else takes a lap top to the pool?). Fiona offered an overview of the science and a challenge to the quality of my writing at a critical stage. I thank Fiona for her efforts and friendship.

If George Martin was the fifth Beatle, then Judi McWhirter was the fourth supervisor. Sediment fingerprinting is a statistics heavy technique and Judi provided oversight and unique contributions to this side of the study, as well as unlimited patience when answering my silly questions no matter what time of the day or night (a phone call to Judi at home at 9:50pm on a Saturday night was my record!). I am grateful for Judi's contribution.

This thesis would not have been possible without the generous support of Environment Waikato, initially from Peter Singleton and then from Reece Hill. I also need to thank Dan Borman for GIS and NZeem help, Nick Kim for his knowledge on trace elements, and Bevin Jenkins for the provision of Whangapoua rainfall records. The hydro technicians Ross Jones and Doug Stewart were also important sources of information on the deployment of turbidity probes.

I acknowledge the Department of Earth and Ocean Sciences for material support and the departments academics. Willem De Lange assisted with the writing of a macro and in patching data. All the other academics provided time for discussion and provided pearls of wisdom along the way. I also acknowledge the departments technicians, Craig Burgess, Chris McKinnon, Steve Cooke, Annette Rodgers, and Craig Hosking for their assistance both large and small. I also wish to thank the long suffering Computer Support team headed by Ai Phing Wood, and the team

members Liz Brodie, Brett Loper, and David Nicholls who handled every ‘end of the earth’ computer catastrophe with patience and aplomb.

I would like to thank the many students within the School of Science who have also assisted me. They include Dave Palmer, Adam Vonk, Kyle Bland, and Matt Allen for GIS assistance, and Suus Rutledge provided Matlab processing of suspended sediment data. In particular I wish to thank Fiona Sanders for proof reading and tarting up the thesis just before printing; it was such a better document due to Fionas hard work. Brilliant! Many other students just provided friendship and an ear to bend such as Deb Stokes and the DunGeon Crew.

I have been the recipient of the University of Waikato’s Doctoral Scholarship, which I was grateful to receive. This has been administered by the wonderful staff at the Scholarships Office, in particular Gwenda Pennington who has been an absolute joy to deal with.

It has been my pleasure to meet a great bunch of Kiwi scientists during this PhD who have been generous with their time and advice above and beyond the call of duty. In no particular order they are Les Basher, Chris Phillips, Sandy Elliot, Mike Marden, Rob Davies-Collier, Mal Green, Max Gibbs, Brenda Rosser, and Murray Hicks.

It was vital for this study to gain access to the Whangapoua catchment itself and I would like to thanks the landowners and forest managers. I would especially like to thank Robin and Wendy Denize for access to their property, likewise Dean Woods, and all the lads from Ernslaw One (Lindsay Arthur, Matene Blandford, Graeme Lister, Ropata Shep, and Peter Weir) for their assistance and putting up with me during my field work. Nina Whitley was also most helpful during the establishment of this study. Jo and Russ Scott also provided me accommodation at the ‘Whangapoua Hilton’ and also acted as unofficial safety officers while I was in the field. Cheers guys.

Under the miscellaneous column, I wish to thank Damon Walsh from Chemiplas who assisted with various potions for the size fractionation. I was treated like a million dollar customer rather than a nagging PhD student.

On a personal note, I have had a constant cheer squad of great mates who have barracked for me during the years of working on this PhD and it has been greatly appreciated. In particular, Anthony ‘TT’ Clark proof read my thesis and provided much needed encouragement during the last weeks while all the time juggling a young family, a busy career, and visiting in-laws!

This PhD is dedicated to my dear old Mum, Vera, who has been unwavering in her support not only during this study, but for my entire life. This thesis is only a drop in the ocean of gratitude that I owe to the best Mum in the world.

This PhD is also in memory of Frank Gleeson, a mate of the highest order who didn't make it to the line.

"Soil erosion is a relentless process that is nearly impossible to stop, usually difficult to control, and easily accelerated by man".

H.E. Dregne (1982) as cited in (Cannell & Hawes 1994)

"Today the effects of suspended sediment on estuarine ecosystems remain arguably the biggest threat to the estuarine ecosystems"

(Hume 2003)

"Thus…all New Zealanders should care about muddy rivers, and sooner or later,…are likely to face a problem requiring information on sediment"

(Hicks & Griffiths 1992)

TABLE OF CONTENTS

LIST OF FIGURES

Figure

LIST OF TABLES

CHAPTER ONE

INTRODUCTION

1.1 Introduction

Estuary and harbour environments in New Zealand have high ecological, recreational, and visual values (Environment Southland 2007). Specifically estuaries are: important habitat areas for rare and threatened wildlife; locations of significant salt-marsh, eel-grass and mangrove communities; areas of extensive shellfish beds; and sites of archaeological and cultural significance (Mead & Moores 2004; Environment Waikato 2005b).

Estuaries also act as natural sediment retention systems which makes their intrinsic values vulnerable to accelerated sedimentation caused by human activities (Ellis *et al.* 2004; Thrush *et al.* 2004). The main landuses in the North Island of New Zealand, with the potential to accelerate erosion, are agriculture and exotic (mainly pine) forests. The Whangapoua Harbour in the Waikato region of New Zealand (Figure 1.1) is experiencing increased sedimentation, and this harbour will be the focus of this study. There has been a 1.5 fold increase in sediment accumulation after Polynesian settlement and around a 10 fold increase after European settlement in the Whangapoua estuary (Hume & Dahm 1992). One consequence of increased sedimentation has been an increase in mangrove areas and a decline in sea-grass areas (Halliday *et al.* 2006).

From a management perspective, local authorities (such as Environment Waikato) are empowered under the Resource Management Act (1991) to control the effects of landuse and to promote sustainable management which includes minimising the harmful effects of soil erosion. While the Resource Management Act does not focus on restricting landuse activities, it does state that the effects of landuse should not harm the resource or the environment (Hicks 1995). Consequently, the problems of increased sedimentation are a concern for natural resource managers as well as soil conservators, planners, engineers, and geologists (Hicks & Griffiths 1992).

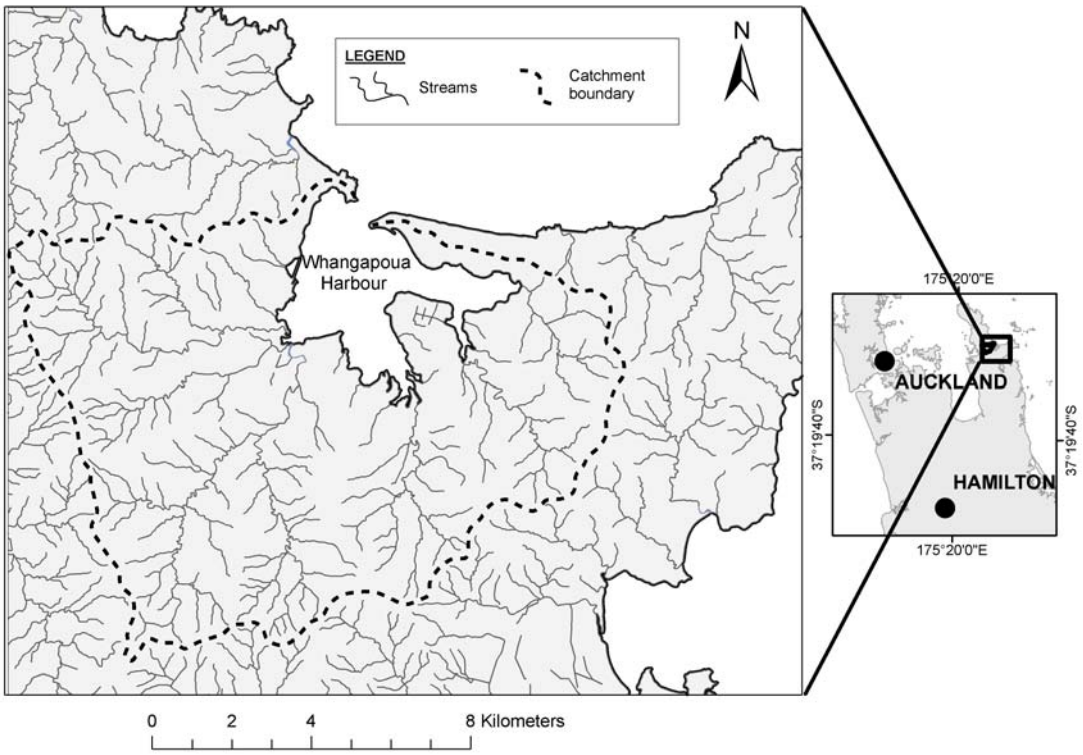

Figure 1.1. Location of Whangapoua Harbour catchment, North Island, New Zealand.

From the research perspective, non-point source suspended sediment has been identified as a threat to the values of New Zealand estuaries. Environment Waikato has identified that the cumulative adverse effects of non-point source suspended sediment can outweigh the adverse environmental effects of point source discharges. Non-point source suspended sediment is considered by Environment Waikato to be a dominant cause in the reduction in water quality in the area under its management (Environment Waikato 2005b). For example, 88% of the sediment transported by North Island New Zealand rivers is the suspended fraction (Adams 1979). To tackle the problems of non-point source suspended sediment, it is critical to identify the sediment sources to implement appropriate erosion control strategies (Mosley & Jowett 1999; Walling *et al.* 1999; Wallbrink 2004; Walling 2005; Douglas *et al.* 2007; Gao 2008). But sediment source identification is hampered by a lack of understanding of the complexities of erosion rates, sediment yields, sediment transfers, and deposition dynamics in a drainage basin system (Walling 2006). The research aim of this thesis is to tackle the problem of sediment source identification.

1.2 Sediment source area identification and sediment fingerprinting

The identification of catchment sediment sources (i.e., measuring erosion contributions from potential source areas) is a problematic and difficult task. Most popular indirect erosion estimation methods (such as erosion plots and erosion pins) measure erosion in 'like' areas (e.g., landuse, geology, or slope) and then extrapolate the result to the rest of the catchment. The problem with the indirect erosion estimation approach is that the techniques only measure sediment past a particular point in the landscape and don't account for the spatial and temporal complexity of sediment detachment, transport, and deposition (Prosser *et al.* 2001b; Phillips *et al.* 2007). Other approaches such as suspended sediment monitoring of catchment streams provide information on sediment fluxes and can be used to construct sediment budgets for the receiving estuary. But suspended sediment monitoring does not provide information on the exact sediment source area within a catchment, nor the process responsible for sediment generation.

The technique of statistically verified composite sediment fingerprinting holds the promise of overcoming the problems of understanding sediment routing through a catchment (Collins *et al.* 1997; Collins & Walling 2002). Sediment fingerprinting seeks to link the different sediment source areas within a catchment to its eventual sink (in this case the Whangapoua estuary). Sediment fingerprinting identifies the important sediment source areas by quantifying their input into the estuary relative to other sediment source areas. The sediment fingerprinting technique will be the main technique used in this thesis for the problem of sediment source area identification, although it has not been previously applied in the New Zealand setting before. Independent comparison of the sediment fingerprinting results was provided by radionuclide analysis, stream gauging, and modelling techniques.

1.3 Aims and objectives

The overall goal of this research was to improve our understanding of catchment scale sediment generation and delivery in a mixed landuse watershed in New Zealand. The specific objectives of this study were to:

1. quantify the relative amounts of sediment generated from the native forest, exotic forest, and agricultural landscape units in the Whangapoua catchment;

2. identify the dominant processes generating the sediment within the native forest, exotic forest, and pastoral landscape units; and
3. assess the utility of the sediment fingerprinting technique in New Zealand by comparing the results with other sediment measurement techniques.

1.4 Thesis structure

In order to address the aims and objectives, this thesis is organised into four main sections:

- Section 1 sets the context of the study and provides a brief introduction outlining the relevance of this research and providing a brief background to the study area (Chapter 1). A more detailed examination of the study area is conducted in Chapter 2 where the physical characteristics of the catchment are presented as well as a summary of previous studies conducted in the area. Three alternative hypotheses of erosion from the landuses are also presented in Chapter 2. A comprehensive review of the literature occurs in Chapter 3 which discusses the problems of sedimentation, the processes of sedimentation, sediment sources, and the various methods of measuring sediment. A case is made for the employment of a sediment fingerprinting approach to answer the aims of this research.
- Section 2 details the methods used for this study including all the sample collection methods and laboratory analysis (Chapter 4)
- Section 3 presents the results of the various techniques employed in this research, including the pilot study (Chapter 5), sediment fingerprinting (Chapter 6), radionuclide soil tracing (Chapter 7), suspended sediment monitoring (Chapter 8), modelling of the catchment (Chapter 9), and the estimation of stream sediment storage (Chapter 10).
- Section 4 discusses the results of Section 3 and quantifies sediment generation from native forest, exotic forest, and agricultural landscape units (Chapter 11). It also identifies the sources of sediment generation within each landuse type from radionuclide analysis and then considers the advantages and problems of the approaches taken in this study. Areas of further work and a summation of the research complete the chapter.

CHAPTER TWO

WHANGAPOUA HARBOUR

2.1 Introduction

The objective of Chapter 2 was to describe the Whangapoua catchment physical setting so as to propose three conceptual models of likely sediment source areas. The three conceptual models will then guide the review of the literature (Chapter 3) and establish the requirements of the experimental design. This chapter describes:

- the physical setting (i.e., geology, climate, etc) of the Whangapoua Harbour;
- the past and present landuses;
- previous studies conducted within the Whangapoua catchment; and
- the observed erosion processes within the native forest, exotic forest, and agricultural landuses.

A synthesis of the information from the four points above was then used to develop three conceptual models of sediment source areas.

2.2 Whangapoua physical setting

2.2.1 Whangapoua catchment

The Whangapoua catchment is approximately 110 km^2 in area. The Whangapoua catchment is typical of the many smaller drainage basins found along the coastline of the North Island (Figure 2.1). It has steep slopes with short first order streams and the area is subject to intense rainfall events. In global terms, this type of catchment is important as small steep drainage basins make disproportionally large sediment contributions to the worlds oceans (Milliman & Syvitski 1992).

Figure 2.1. Drainage basins of the North Island of New Zealand (from White *et al.* 2006).

2.2.2 Whangapoua estuary

Whangapoua Harbour (Figure 2.2) is classified as a barrier-enclosed estuary which is the most common type of estuary found in New Zealand (Healy & Kirk 1991; Hume & Herdendorf 1998). The Whangapoua estuary is relatively small in area at 13.7 km^2 and is enclosed by a single spit of Holocene age that lies across the mouth of a drowned river valley (Healy *et al.* 1996; Hamilton 2003). This type of estuary has extensive sand flats cut by narrow channels so typically around 70% of the surface area is intertidal. Consequently flows are dominated by tides,

and tidal pumping facilitates the exchange and flushing of sediments between the estuary and the sea (Hume 2003). The Whangapoua estuary has been identified in the Waikato Regional Plan as an estuary prone to infilling by sediment, because of high rainfall, which endangers its ecological values (Environment Waikato 2006).

Figure 2.2. The Whangapoua estuary and surrounding catchment. The vertical exaggeration of the image is three. Approximate north direction is indicated by the arrow.

2.2.3 Whangapoua geology, geomorphology, and soils

The main influence on the geology of the Whangapoua Harbour catchment is the andesitic and dacite volcanism that occurred along the Coromandel Peninsula from 19 to 2 million years ago. The volcanics were built on a greywacke basement that is mainly exposed in the north and north-west of the Coromandel Peninsula (Skinner 1986; Adams *et al.* 1994; Malengreau *et al.* 2000). The Whangapoua Harbour catchment is dominated by andesite with small areas of Quaternary deposits (dune sands and alluvial terraces) occurring at the spit enclosure and drowned valleys (Figure 2.3) (Skinner 1993).

The landforms in the Whangapoua catchment are characterised by steep upper slopes with ridge lines extending toward Whangapoua Harbour in a radial pattern (Figure 2.4). Slopes of more than 25° are found in the upper catchment while over

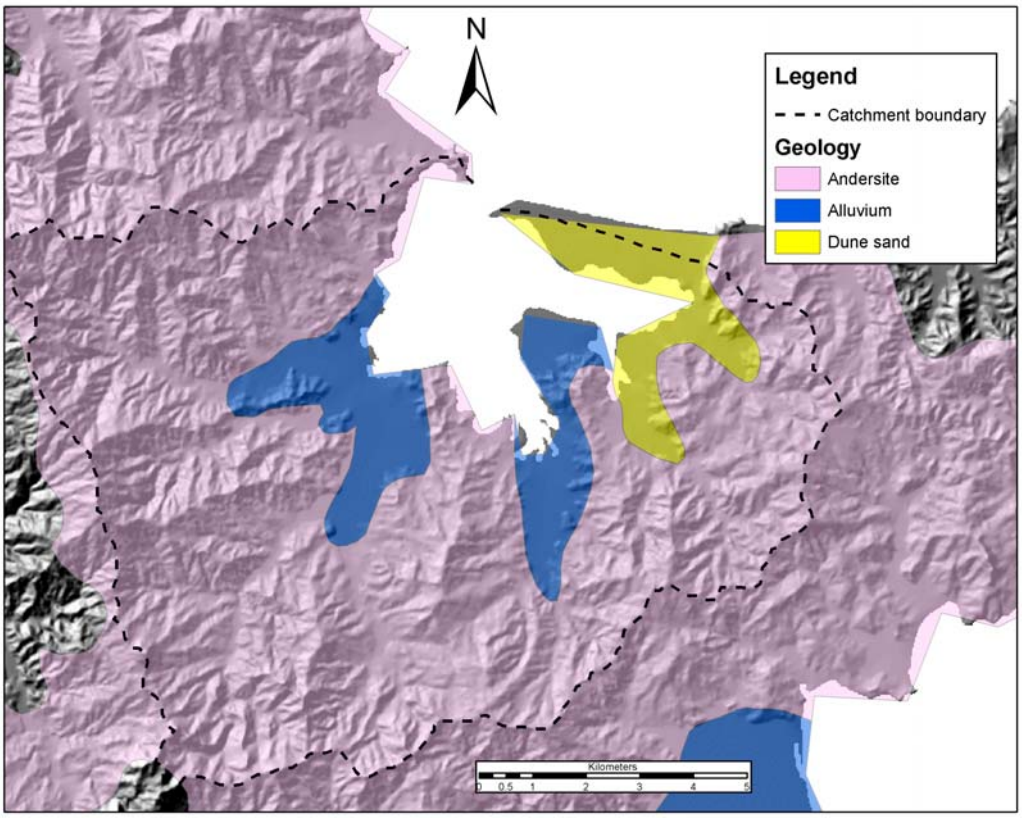

Figure 2.3. Whangapoua Harbour geology at the group level. The catchment is dominated by andesitic geology with low lying areas of Quaternary alluvium, and dune sand along the estuary enclosing spit (Newsome *et al.* 2000).

85% of the entire study area has slopes of more than 20°. Rolling hills are found in the mid-catchment area while flat areas and swamps are found on lower alluvial deposits adjacent to the estuary. Due to the steep slopes, erosion potential is considered severe for 35% of the catchment, moderate for 52%, and slight for the remaining 13% (Hill 2002).

The soils that have developed on the Whangapoua geology have been previously mapped as brown granular clays on the Coromandel uplands and gley soils on lowland areas under the New Zealand Genetic Soil Classification (Orbell 1974). In the study area the soils are classified as Typic Orthic Brown Soils and Mottled Brown Soils on the hill country and a range of Gley, Organic, and Allophanic Soils on the lowlands around the harbour under the New Zealand Soil Classification of (Hewitt 1998) (Figure 2.5) (McLaren & Cameron 1990; Molloy 1993; Hewitt 1998; Newsome *et al.* 2000).

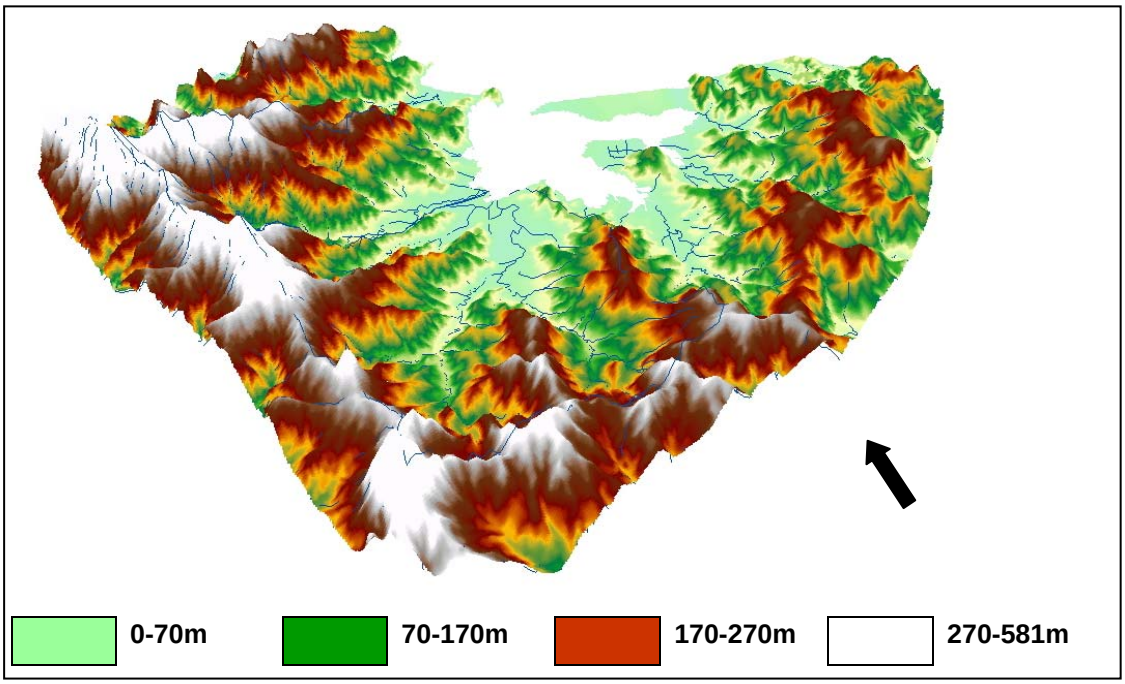

Figure 2.4. Digital elevation model (DEM) of the Whangapoua Harbour catchment showing the steep hinterland and radial ridge line pattern running down to the low lying areas around the estuary. Approximate north is indicated by the arrow.

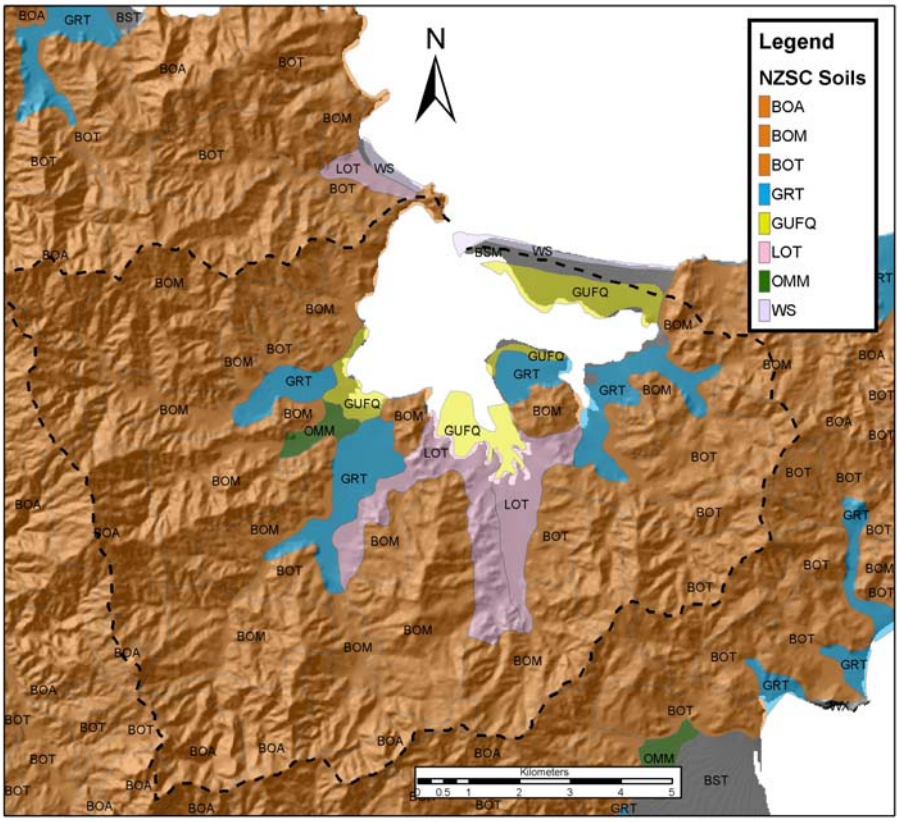

BROWN SOILS
BOM- orthic mottled
BOA- orthic acidic
BOT- orthic typic

GLEY SOILS
GRT- recent typic
GUFQ- sulphuric fluid saline

OTHER
LOT- typic orthic allophanic
OMM-organic mellow mesic
WS- sandy raw soils

Figure 2.5. Soils of the Whangapoua Harbour (Newsome *et al.* 2000).

2.2.4 Whangapoua climate

The Whangapoua Harbour has a temperate climate with a mean daily temperature of 15°C and an annual rainfall of over 1800 mm with wetter months occurring during winter (Figure 2.6). The Whangapoua Forest (4m ASL) rainfall record showed that the return period for storm events of > 50 mm day^{-1} was 55 days or approximately seven times per year, and > 200 mm day^{-1} was 6.5 years.

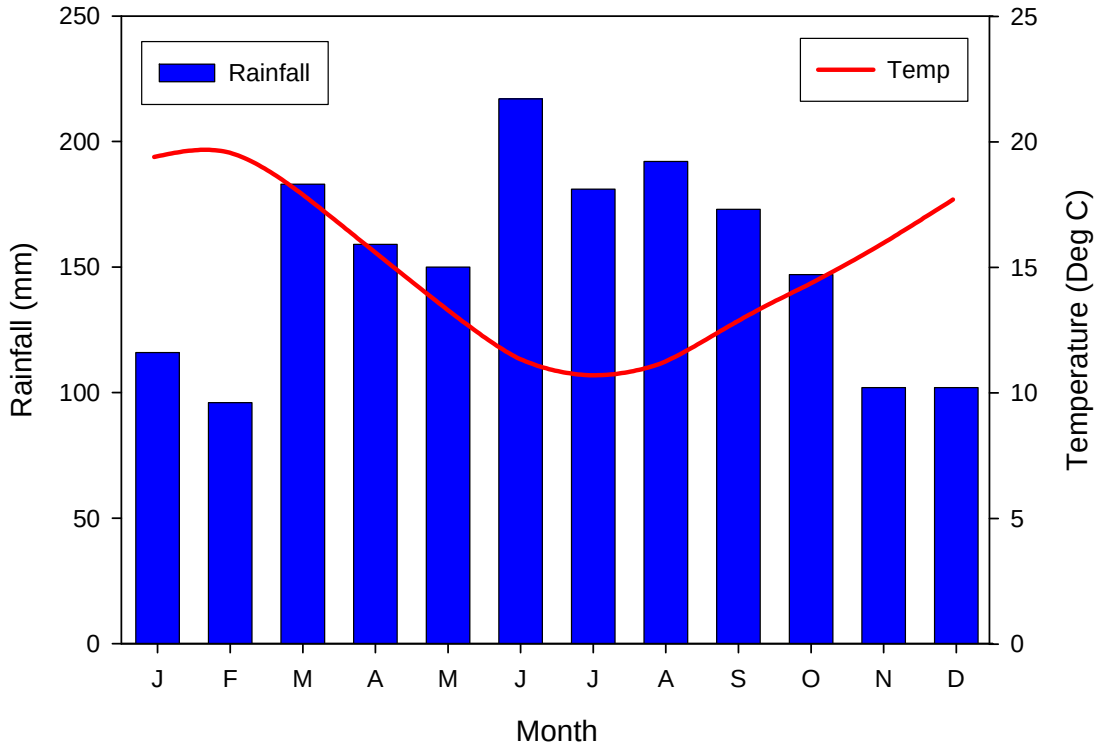

Figure 2.6. Mean monthly rainfall and mean monthly temperature for the Whangapoua Forest station (#1515 Lat -36.76 Long 175.601) 1961 to 1989 record (NIWA 2007).

The Whangapoua catchment is prone to frequent, high intensity, localised storms that are often tropical in their origin (Marden *et al.* 2006). Two examples are the 1995 weather bomb that delivered large quantities of sediment to the harbour (Gibbs 2006) and the 2002 weather bomb that caused severe flash flooding across the Coromandel due to localised intense rainfall (Leslie *et al.* 2005).

Environment Waikato (EW) did an assessment of the spatial pattern of rainfall in the Whangapoua catchment between 2001 and 2006 based on two permanent recording sites at Castle Rock and Opitonui and four temporary Hobomatic rainfall gauges (Jenkins 2006). A linear regression was carried out between

rainfall and elevation and the result was an r^2 of 0.68; this relationship was then used with a 20 m digital elevation model (DEM) to produce an annual rainfall map of the Whangapoua catchment (Figure 2.7). While most of the Whangapoua catchment receives the mean annual rainfall of around 1800 mm, the steep upper parts of the catchment under native forests (lower insert Figure 2.7) may be receiving an annual total rainfall of over 3000 mm.

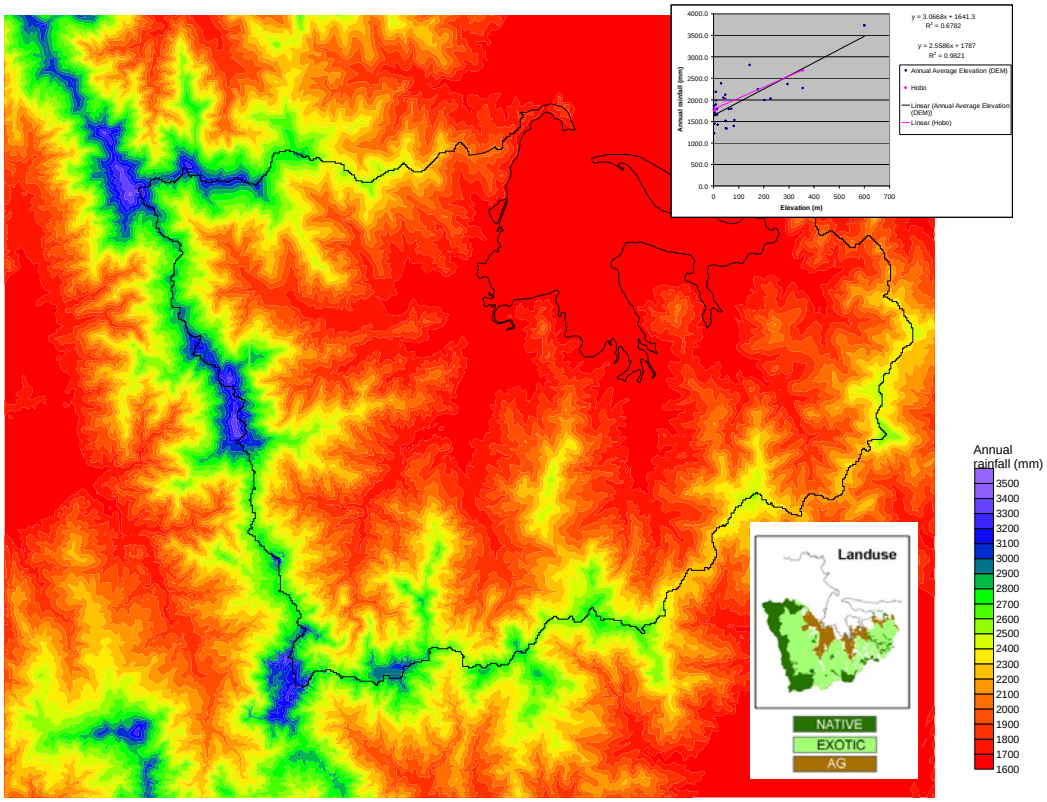

Figure 2.7. Estimated mean annual rainfall for the Whangapoua catchment based on linear regression results for a five year rainfall record and elevation. Regression results shown on the upper inset and landuse is shown on the lower inset (Jenkins 2006).

2.2.5 Whangapoua vegetation and landuse

The Coromandel Peninsula was extensively forested before the arrival of Europeans. The three main vegetation types that were found in the Whangapoua area were a) coastal forest (pohutukawa, kohekohe and puriri) confined to the narrow coastal perimeter, b) dense conifer (kahikatea, matai and totara) forest on flat and poorly drained river terraces, and c) mixed kauri-conifer-broadleaved forest and rimu-tawa forest covering the hills of the catchment (Environment Waikato ND). The arrival of Europeans saw the removal of kauri and other

marketable timbers from the forest. European settlers also removed mature coastal forests creating grasslands and extending mudflats in low lying areas (Donald 1990).

The current vegetation pattern in the catchment sees native forests on the steep hinterland (Figure 2.8). It is important to note that while this type of vegetation is referred to as 'native forest' in this thesis, virtually no mature kauri trees remain due to logging. The native forest currently located on the steep upper slopes is dominated by rata-podocarp/tawa species. The canopy is typically 11-20 m tall, the understory is many tiered with a large diversity of species, and lianas and epiphytes are common. Manuka dominated scrub occurs in small patches south of the Whangapoua settlement and east of Matarangi on steep slopes unsuitable for agriculture. The scrub ranges in height depending on disturbance history, and understory species are diverse (Donald 1990). Exotic forests comprise over half the catchments vegetation on the mid-slope areas and are almost exclusively pines (*P.radiata*) with small patches of the cypress *C.lusitanica* and eucalypt *E.salgina*. The flat areas adjacent to the harbour are predominately agricultural pasture of high producing exotic grasses which are typically clover and perennial ryegrass. Of the 110 km^2 catchment, 56% is exotic forest, 19% native forest, and 16% agriculture (mainly pasture) (Hill 2002). The other 9% of the catchment comprises scrub, coastal vegetation/swamps, and urban areas.

2.3 Landuse history and impacts

2.3.1 Introduction

The first anthropogenic landuse change occurred with Polynesian settlement approximately 650 to 800 years ago (Lowe *et al.* 2000). The main impact of Polynesian settlement on sediment generation was due to deforestation by fire which caused accelerated erosion (Sheffield *et al.* 1995; Wilmshurst 1997; Horrocks *et al.* 2001; Byrami *et al.* 2002; Wilmshurst & McGlone 2005; Ogden *et al.* 2006). 'Polynesian settlement led directly to the destruction of half of the lowland and montane forests' (Horrocks *et al.* 2007). With the arrival of Europeans in the 1770s, landuse changed to logging, gum digging, mining, pastoral activities, and exotic forests establishment.

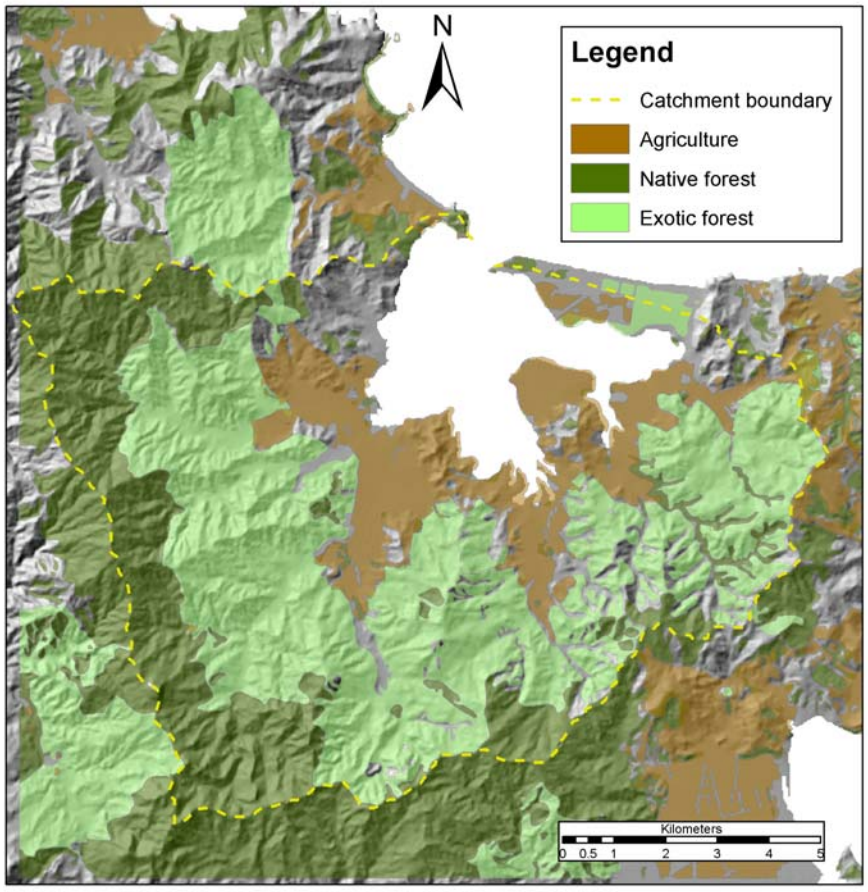

Figure 2.8. Native forest, exotic forest, and agricultural grassland vegetation distribution within the Whangapoua catchment.

2.3.2 Logging

Logging first began when visiting ships would cut spars for repairs from the Coromandel area in the 1770s. The commercial exploitation of kauri trees began in the 1820s but was limited because extraction methods were confined to manual labour and bullock teams. Kauri exploitation increased from the 1850s onwards with the development of tramways and driving dams. Driving dams involved placing temporary timber barriers across stream lines where cut logs would be deposited in the impounded water. The dams would then be tripped sending a cascade of water and logs down the creek toward harbour locations where saw mills were located. Whangapoua was one such receiving harbour and over 50,000 m^3 was exported from Whangapoua harbour. By 1900 over three quarters of Kauri timber had been removed from the Coromandel region. Tightening restrictions and a dwindling resource saw kauri logging in the area all but cease by the 1930s (Harrison 1988).

2.3.3 Gum digging

The kauri tree excretes a resin which was used for paints, varnishes, and other ornamental purposes (Ministry of Culture and Heritage 2007). The first export of kauri gum began in 1830s and by 1845 it comprised over half the exports from Auckland Harbour from source areas such as Whangapoua. Once surface deposits were exhausted, gum digging commenced with subsurface deposits located by a spear and then dug or hooked to the surface. The burning of scrub (such as manuka and kanuka) to facilitate the location of gum was common and this left the land denuded, facilitating erosion down to the clay base and aided the infestation with introduced weeds. Gum production peaked in 1899 but dwindled after this to all but cease after the mid 1930s (Harrison 1988).

2.3.4 Mining

Gold was discovered in the Coromandel in 1852 with the first boom centred on Thames beginning in the 1860s and by 1890 mining had spread along the whole peninsula. Gold was mined in the Whangapoua area at Opitonui and Kuaotunu during the 1890s. The most immediate impact of mining was the disposal of mine waste. Tailings and sediments produced from mining in the Ohinemuri River system caused shoaling and silting in the Firth of the Thames. Sedimentation of this extent in Whangapoua Harbour is not reported, probably due to the less extensive nature of mining in the Whangapoua catchment. Another impact of mining was the clearance of timber in the immediate area of the diggings. Kauri, manuka, and rewarewa were used for mine supports while other timbers were used for fuel (Harrison 1988).

2.3.5 Agriculture

The earliest agriculture was practiced by the Maori population. The local Maori grew large areas of potatoes, mainly for visiting ships. At the beginning of the 20th century European agriculture was confined to the low hill country along the coastal fringe. Dairy farming developed in the 1910s and was assisted by granting of pastoral leases and the opening of dairy factories at Whitianga and Coromandel. Further land development occurred after World War II with the granting of 1,000 ha blocks to returned serviceman in the hill country of the Whangapoua area (Harrison 1988).

The cleared hill country initially produced good pastures but fertility rapidly declined and the country quickly reverted to manuka scrub, which was managed by the local farmers by slash and burn. The advent of aerial top dressing of fertiliser in the 1950s addressed fertility problems but steep pastures were abandoned so today most of the agriculture is practiced on areas close to the Whangapoua Harbour. Through the 1960s and 1970s the main pastoral activity was store sheep and cattle (Harrison 1988). The main agricultural activity today is predominantly cattle and fat sheep with increasing numbers of dairy cattle

2.3.6 Exotic forestry

Large scale planting programmes began in the Coromandel area in the 1930's in the Tairua area with *P.radiata* because of restrictions placed on logging native species (especially kauri) in the early 20th century and the need to rehabilitate eroded mining areas. Plantations in the Whangapoua catchment were developed in the 1960s and 1970's mainly with *P.radiata* and some small pockets of eucalypt and cypress species. Exotic forest expansion continued into the Coromandel region between 1969 and 1975 (Harrison 1988).

The Whangapoua plantation managers (Ernslaw One Ltd) harvest pines on a 30 year rotation and first rotation harvesting began in the early 1990s which means the oldest second rotation trees are around 12 years old (Environment Waikato 2005a). Today approximately 55% of the Whangapoua Harbour's catchment is under exotic pine (*P. radiata*) plantations. The pine plantation in the Whangapoua Harbour catchment (and to the west in the Coromandel area and south in the Whitianga area) are divided into around 120 compartments which range in size from 10 to 100 ha. The compartments form the basis for harvest planning and logging crews will generally harvest several compartments in the one area.

Preparations for harvesting begin by earth moving crews either constructing roads, log landing, and drains, or re-establishing existing ones (Figure 2.9).

Timber extraction by Ernslaw One is achieved by the 'cable logging' method Figure 2.10). This method is used due to the steep slopes and the lower soil disturbance when compared with machine extraction.

A **B**

Figure 2.9. A) Newly constructed access road and batters into a logging compartment; B) newly formed log landing in the background and a metal sealed access road.

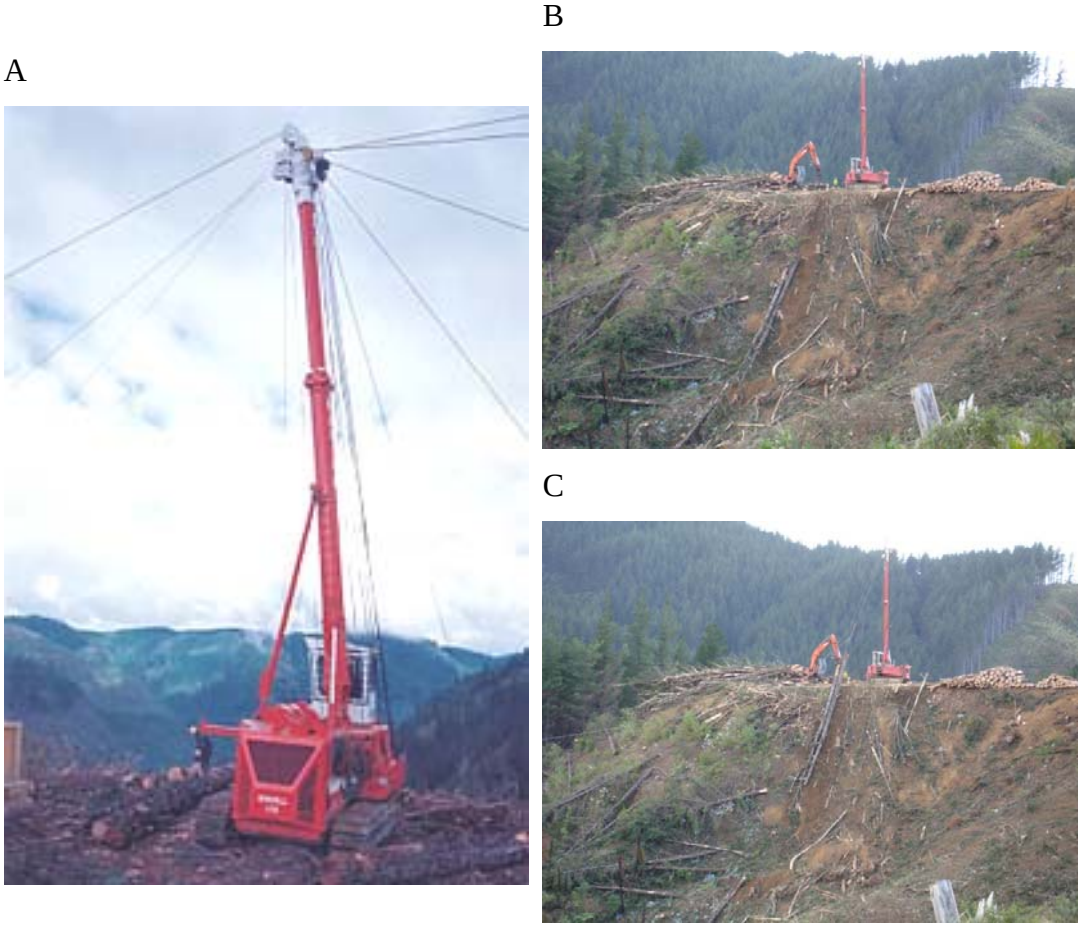

A B C

Figure 2.10. A) The cable logging machine or 'yarder' from which the skylines are run out so that harvested logs can be towed back to the log landing; B-C) A sequence of images where a pair of logs is being towed up to the log landing along a cable. Visible at the top of the log landing is the yarder with skylines running out from the mast, and a modified excavator used to load the logs onto the logging trucks.

A cable logging machine (or 'yarder') is located at the log landing which is located at the highest point in the area (Figure 2.10-A). From the yarder's mast, steel cables (or skylines) are run out and attached to the stumps of trees. Tree fellers cut the pines using chainsaws and remove the branches which are left as trash on the forest floor. The logs are attached by chains to a runner that moves along the skyline and the logs are then 'towed' back to the log landing (Figure 2.10-B and C) where they are graded, cut to size, and loaded onto logging trucks for transport to local timber mills.

The cable logging method has the advantage that relatively steep areas can be harvested for trees and does not require the construction of more roads into the compartment. It also has the advantage that it avoids the dragging of logs to the landing by forwarding tractors which can cause compaction of the soil. The cable logging method causes a characteristic shallow disturbance (or scalping) as the log makes contact with the soil surface while being dragged up to the log landing. The scalping pattern of shallow disturbance emanates outwards in a radial pattern from the log landings (Figure 2.11).

2.3.7 Impacts of landuse on Whangapoua estuary

The main impact that landuse change has had is to accelerate sediment accumulation because of land clearance and soil disturbance for commercial and urban activities (Nichol *et al.* 2000; Hume 2003; Hutchings *et al.* 2005). Pre-settlement rates of sediment accumulation in Whangapoua estuary have been estimated at 0.03-0.08 mm yr^{-1}, increasing to 0.12-0.13 mm yr^{-1} for Polynesian settlement, and 0.9-1.5 mm yr^{-1} for European settlement (Hume & Dahm 1992) as cited in (Jones 2008).

There is an order of magnitude increase in the rates of sedimentation for Whangapoua estuary from pre-settlement to Polynesian settlement to European settlement, but the absolute values are low. A possible explanation for the low values is that Hume & Dahm (1992) had problems with the dating of pollen within the sediment cores and recommended that further work was required.

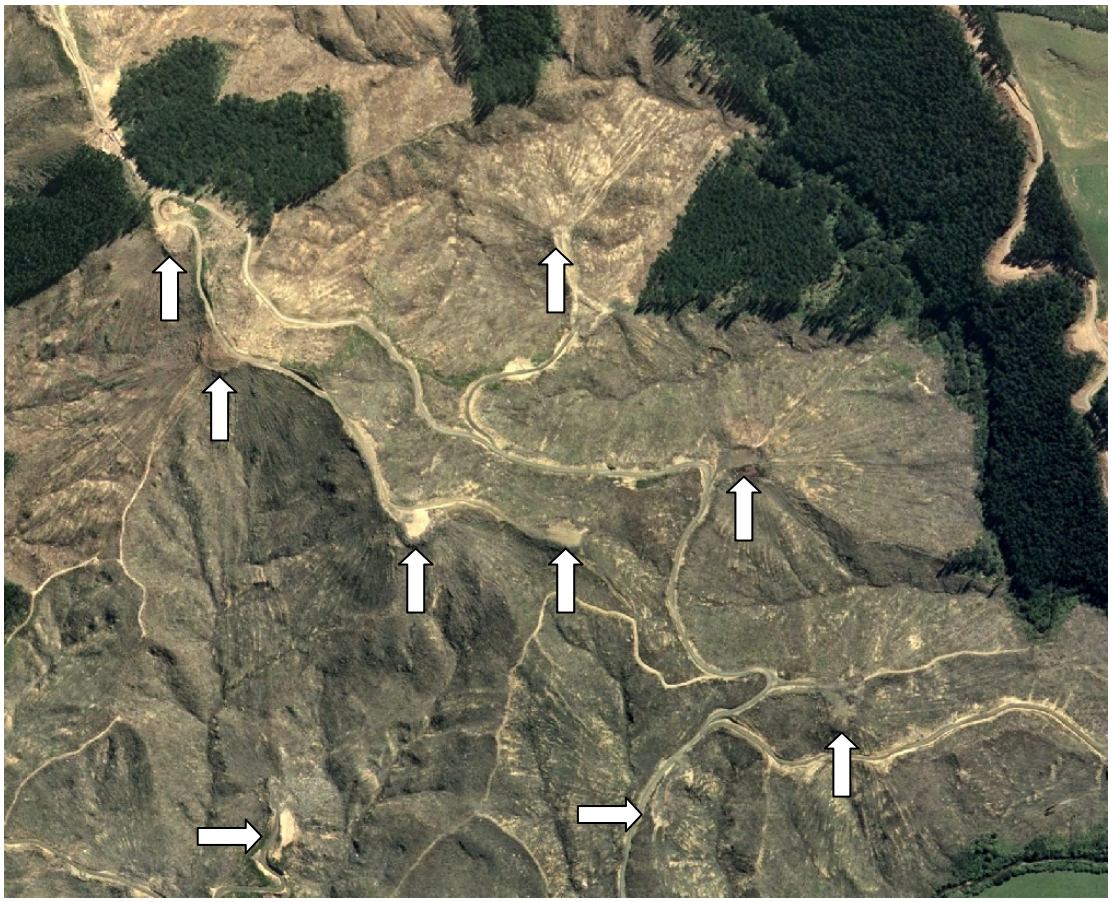

Figure 2.11. Aerial image of a recently harvested compartment north of State Highway 26 and the locations (indicated by arrows) of the log landings used in harvesting operations.

Another possible explanation is that the Whangapoua Harbour reworks and flushes deposited sediment out to sea as around 70% of the estuary bottom is exposed at low tide. The fate of increased sediment quantities onto estuary floors is complex as terrigenous sediment de-waters at low tide and is redistributed and re-suspended by wave action at high tide (Lohrer *et al.* 2006). For example, an estuary in Ohio, USA traps 47% of suspended sediment on one hand, but can be a net exporter of sediment during large events on the other (Wilson *et al.* 2005).

There are ecological impacts to the Whangapoua estuary due to increased sediment. Increasing sedimentation has impacted sea grass (*Zoestera capricorni*) and mangroves (*Avicenna marina*). In the period 1945 to 2006, the sea grass area has decreased while the mangrove area has increased (Schwarz 2004; Halliday *et al.* 2006; Lovelock *et al.* 2007). The mangrove increase appears to be facilitated by fine sediment, while sea grass retreat is due to coarse sand material moving as

'slugs' over the intertidal flats (Halliday *et al.* 2006; Jones 2008). Mangrove expansion in New Zealand estuaries as a result of increased sedimentation from human landuse disturbance has also been observed by Delange & Delange (1994), Ellis *et al.* (2004), Thrush *et al.* (2004), and Swales *et al.* (2007).

2.4 Previous studies

A report by Marden & Rowan (1995) examined the March 1995 storm event (approximately 150-200 mm in < 24 hrs) in the Whangapoua catchment using stereo-photo interpretation and ground truthing of erosion sources. The reports main findings were:

- 51% of derived sediment was from native forest areas (31% of study area), 38% from exotic forests (49% of the study area) and 12% from pastoral areas (20% of the study area). This is due to the native forests being located on the steeper erosion prone hills of the upper catchment.
- Steep slopes (26-35°) accounted for 77% of the sediment volume, moderate slopes (21-25°) 22%, and low slopes only 1%.
- The main sediment generating form was debris avalanches (71%), soil slips (28%), stream banks (0.6%), and log landing failures (0.5%).
- Debris avalanches accounted for 91% of sediment delivered to streams and were the main sediment transport mechanism.
- Sediment production was four times greater from harvested areas compared with mature pines, and the mature pine areas contributed only 4% of the total sediment.

Marden *et al.* (2006) examined sediment generation from a 2-year post-harvest exotic forest subcatchment in the Whangapoua basin. They identified slopewash, soil scraping by cable hauled logs, and storm initiated landsliding as the main sediment generating processes. From the 36 ha site, 1864 tons of sediment was produced of which 64% was generated by soil scraping, 32% was generated by landsliding, and less than 3.5% was generated by slopewash processes. Significantly, the authors found that only 12% (228 t) of the generated material entered the stream network. Of the sediment that was delivered to the streams,

landslides accounted for 72% of the material, soil scraping 26% and slopewash only 2% (Marden *et al.* 2006).

A report by Wild & Hicks (2005) reviewed Environment Waikato's Opitonui Stream monitoring programme in the Whangapoua catchment. The report concluded that there is a significant relationship between event suspended sediment yield and peak discharge, but no clear relationship between sediment yield and exotic forestry activities (Wild & Hicks 2005).

Gibbs (2006) undertook a pilot study into a novel plant compound specific isotope (CSI) technique to fingerprint sediments in the Whangapoua estuary using a plant isotope of ^{13}C that binds onto soil particles. The CSI's provide a different signature for soils under native forest, exotic forest and pasture. Analysis of the CSI's from source areas in the catchment was used to determine the relative proportion that each landuse contributed to estuarine sediments. The report concluded that recently logged exotic pines contributed 54-75% of estuarine sediment, native forest and scrub contributed around 22-26%, pasture was less than 10% at most harbour sites (Gibbs 2006).

2.5 Catchment landuse and erosion

2.5.1 Introduction

A reconnaissance survey of the native forest, exotic forest, and agricultural landuses was conducted to identify potential erosion sources. The landuse patterns in the Whangapoua catchment (as seen in Figure 2.8) generally occur in three topographical zones. The native forest is confined to the steep slopes in the headwater areas of the catchment. The exotic forest occurs mainly on the hilly mid-slope areas, although it also does occur on some steep slopes. The agricultural areas are on mainly flat areas around the Whangapoua estuary, although some pastures do occur on hill country (Figure 2.12). Henceforth the native/steep, exotic/hill, and agricultural/flat zones will be referred to as 'landscape units' in this thesis.

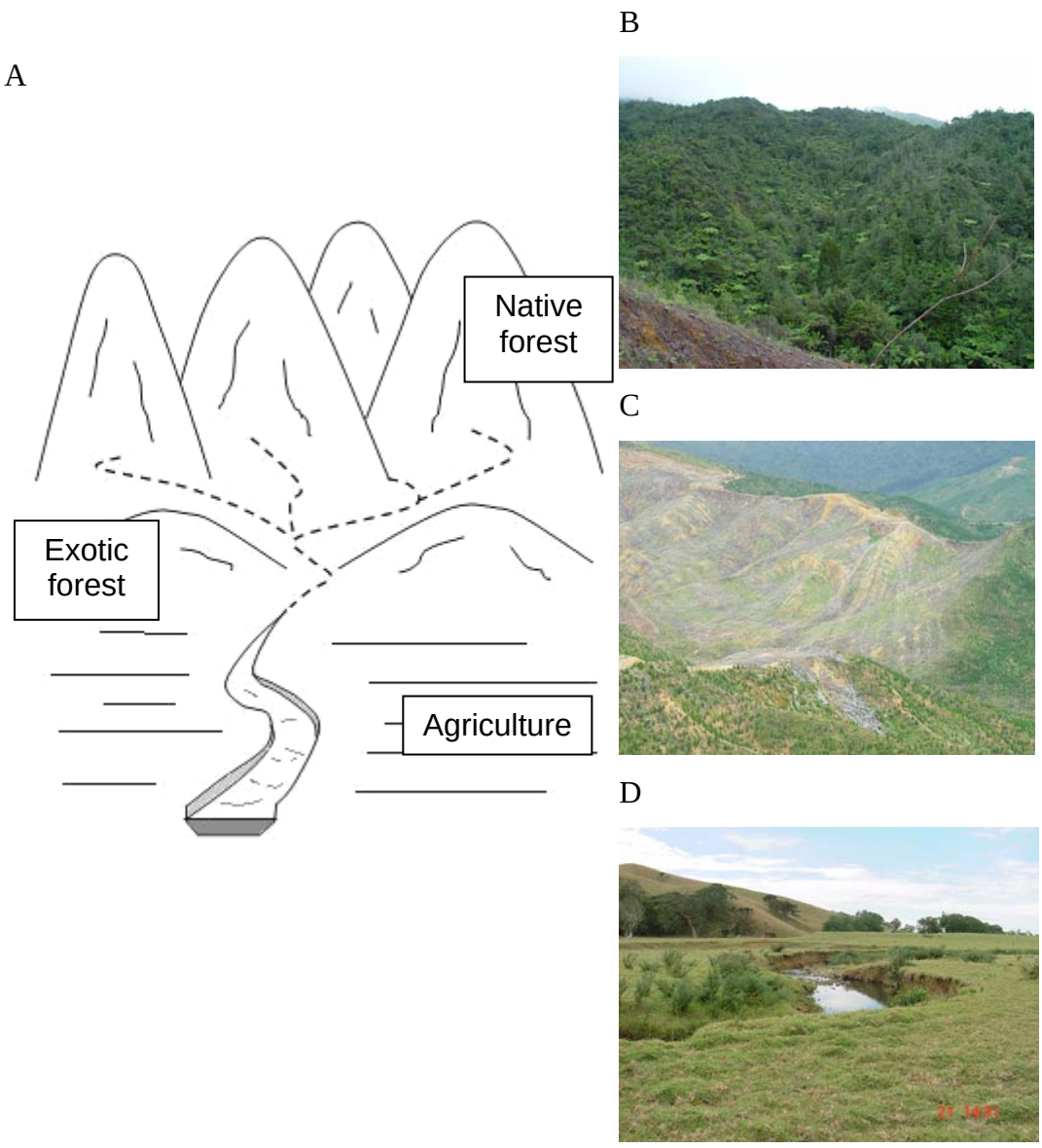

Figure 2.12. A) Simplified diagram of the Whangapoua catchment with the topography/landuse zones; B) example of native forest areas in the steep headwater areas, C) example of harvested exotic forest in the mid-catchment hill area, and D) example of agricultural landuse on flat harbour side area. An area of pasture on sloping land can be seen in the background.

2.5.2 Headwater native forest landscape unit

The native forests in the steep headwater areas have a dendritic drainage pattern which is characterised by short steep streams in the hinterland (Marks & Nelson 1979; Bridge 2003). Permanent and ephemeral streams are found in the headwater area. The ephemeral streams typically have cut down into the clay base to an approximate depth of 0.4m (Figure 2.13-A). The material within the ephemeral stream beds was a poorly sorted mix of fine material, sand, and pebbles that is

potentially available for transport (Figure 2.13-B). The permanent streams in contrast are protected by thick vegetation and within the stream beds cobbles and sand material dominate (Figure 2.13-C).

A

B

C

Figure 2.13. Native forest landscape unit stream beds. A) Ephemeral stream in the headwater area under native forest. Drainage line depth is approximately 0.4m. B) Poorly sorted material in the ephemeral drainage line. Machete in centre image for scale. C) Permanent stream in the headwater area under native forest.

While erosion in ephemeral streams is evident, the main erosion type in the native forest landscape unit is landsliding. Landslide scars can be seen on the steep slopes in the upper catchment (Figure 2.14). The slope failures appear to be

Figure 2.14. Example of a landslide in the steep headwater area under native forest.

depositing significant amounts of soil into the drainage lines due to the steep topography.

Inspection of two examples of native forest landslide shows the potential of landslides to deliver sediment to stream lines. The example in Figure 2.15-A and 2.15-B is a large wide slope failure that has deposited a lens of soil material into a creek. The edges of the re-vegetating scar indicate the depth of the failure to average around 0.5 m. The second example (Figure 2.15-C and 2.15-D) is a narrow landslide that has failed from a ridge top and crossed an access road. The landslide is around 40 m in length and has channelised recent rainfall to continue delivering sediment to the drainage line.

2.5.3 Mid-catchment exotic forest landscape unit

The exotic forests on the mid-catchment areas occur typically on hills, but range from gently rolling hills (adjacent to agricultural areas) to steep slopes where the pines extend into the upper catchment in the south and west. Erosion sources are hard to find in older closed canopy pine forests, but recently harvested pines

exhibit erosion sources from surface scraping, shallow landsliding, and streambank erosion.

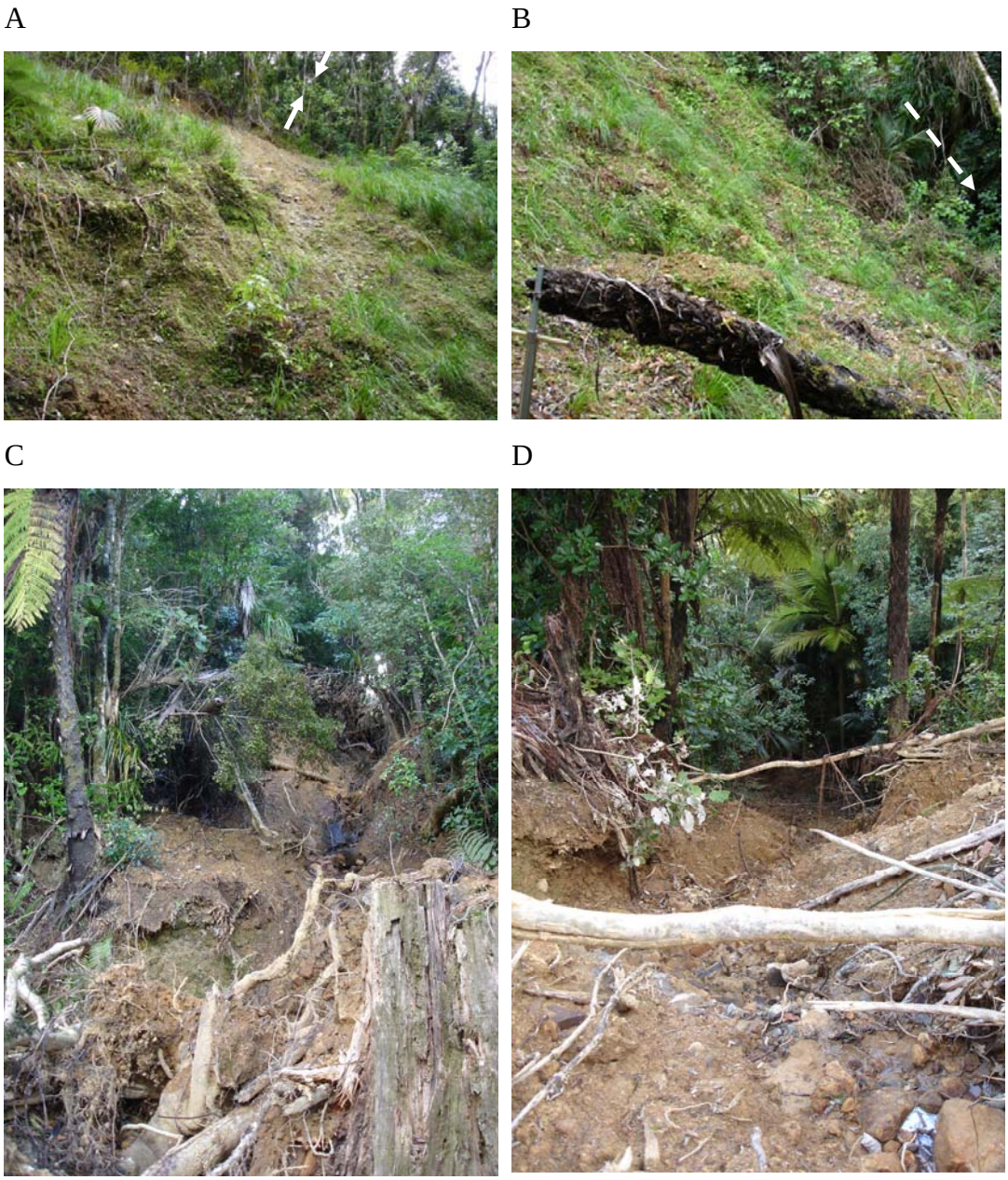

Figure 2.15. A) Landslide scar in the native forest headwater area and landslide depth is indicated by arrows; B) looking down slope to the drainage line (dashed arrow) from the same perspective where the landslide material was deposited; C) a narrow landslide that has been initiated from a ridge top and crossed the road. The perspective is from the road looking up; D) the same landslide viewed from the road looking down into the drainage line.

The potential erosion source of surface scraping (caused by dragging logs up to the log landing) has been identified in Section 2.3.6 (see Figure 2.11). Shallow landsliding occurs after pine harvesting (Figure 2.16) and is caused by soil disturbance and the removal of the protective vegetation. Landsliding is more common on steeper slopes.

Figure 2.16. Landslides (circled) on recently harvested exotic forest on the steeper slopes in the west mid-catchment area. Shallow landslide failures (arrows) caused by the disturbance of a ridge top logging road are also evident. The native forest on the steep upper slopes can be seen in the background.

Landslides are also generated from logging infrastructure. Log landings are flattened areas on ridge tops for the receiving and processing of pine logs. Log landings are constructed by bulldozing soil off the top and pushing it off the edges to create a large flat surface. Logging trash is usually pushed over the top to protect the unconsolidated soil. The unconsolidated material can fail in rain events. The example from Whangapoua shown in Figure 2.17 shows a large failure which has blocked the access road beneath it. The eroded material has been

reworked and channelised by subsequent storms and has the potential to enter the stream network.

A B

Figure 2.17. A) Landslide failure from a log landing that has blocked a logging road. The large lens of failed material has been reworked as evidenced by an erosion scar (arrow); B) the same erosion scar (arrow) looking down to the permanent stream line (dashed arrow).

Streambank erosion was also observed in the exotic forest areas. There appears to be no buffering of riparian zones in harvested areas where higher order streams occur. The logging disturbance appears to increase streambank erosion by stripping away the protective vegetation (Figure 2.18-A). It was also observed that vegetation (mainly exotic weeds) quickly colonised the banks (Figure 2.18-B) and that streambank erosion was hard to find in closed canopy exotic forests (Figure 2.18-C) due to the large variety of shade tolerant understory species (Ogden *et al.* 1997).

The material in exotic forest stream lines varies. In recently harvested areas the material was poorly sorted and contains gravel, sand, and fine material (Figure 2.19-A). In older and mature pines, the material in streams is a more uniform size of predominately sand with finer material in the matrix (Figure 2.19-B).

Figure 2.18. A) Exotic forest mid-catchment stream one year post harvest; B) approximately 10 years post harvest, and; C) mature exotic pine forest stream.

Figure 2.19. A) Poorly sorted material trapped behind a weir after a large storm event from recently harvested exotic pines; B) more uniform sand and fine material in a 10-15 year exotic pine re-growth stream.

2.5.4 Lower plains agricultural landscape units

Streambank erosion was the most obvious erosion process operating in the lowland agricultural areas. The stream network was highly channelised and typically unfenced and open to access from stock. The stream walls were steep sided and there was little if any riparian vegetation (Figure 2.20).

Figure 2.20. A) Example of streambank erosion along the Waitekuri River in the lowland agricultural area. Streambank walls are steep sided, there is little riparian vegetation, and the stream is unfenced and open to stock. B) Streambank erosion along the main channel of the Owera Stream. The bank wall has collapsed directly into the stream and is available for transport during storm event.

Some actively eroding gullies were found in the agricultural areas where grazing was practiced on sloping ground. These were few in number and the biggest gully found in the Whangapoua catchment is shown in Figure 2.21.

Figure 2.21. A gully head-cut found on an area of sloping agricultural pasture. The landowner has tried to ameliorate the gully erosion by depositing rocks into the head-cut area.

The most common form of surface erosion in the agricultural landscape unit was observed to be the result of stock pugging the soil during the wetter winter months (Figure 2.22). There are no areas of cultivation in the Whangapoua catchment. The worst areas of pugging were heavily trampled 'stock camps' which were small in size where cattle tend to congregate.

Figure 2.22. An example of soil pugging by cattle. This stock camp was in a paddock corner and situated on top of a ridge.

The stream bed material found in the lowland catchment streams seems to have a larger percentage of finer material in the sand matrix (Figure 2.23). There are regular in-stream sediment storage deposit banks and with evidence of vegetation colonisation. Large volumes of material have been observed to be transported during high flow events (Fuller & Hutchinson 2007).

Figure 2.23. Lower plains example of in-stream sediment storage. A hole has been dug to show the nature of the material which is a sand and fine clay material mix.

2.6 Alternative hypotheses for main Whangapoua estuary sediment source areas

Three alternative hypothesis of the main sediment source area for the Whangapoua estuary have been developed. The models describe the possible dominant sediment source areas and the processes responsible for sediment mobilisation and delivery.

Hypothesis A. Native forest landscape unit is the main sediment generating area

If the native forest landscape unit was the dominant contributor of sediment to Whangapoua estuary, it would be due to landsliding processes. Landslides have the potential to deliver significant amounts of material. The native forest areas would be susceptible to landslides due to the combination of very steep slopes found in this area and high rainfall experienced in the higher altitude areas (see

Figure 2.7). The removal of kauri trees from the native forest would also increase its susceptibility to disturbance.

The sediment generated by landslides has the potential for efficient delivery to the estuary due the well coupled nature of the head water areas. The hillslope and channel are well coupled because of steep slopes and lack of toe slope features, and the upper channel and lower channel are well coupled because of steep stream gradients which create a higher energy stream environment. Native forests have been identified as the dominant sediment source area by Marden & Rowan (1995) where they concluded that native forests contributed over half the sediment in the March 1995 storm. They also concluded that landslides were the main erosion process (71%) and that 77% of material was derived from steeply sloped areas.

Hypothesis B. Exotic forest landscape unit is the main sediment generating area

If exotic forests were the main sediment source area, this would be due to a combination of landslide, streambank, and surface erosion processes. The exotic forests would be vulnerable to erosion during harvesting operations and for a period after until the replanted pines stabilised the soil surface. As was shown in a Whangapoua study, surface erosion (due to soil scraping by logs) generates more sediment than landsliding. But because landslides are better coupled with the stream network than surface erosion, landslides deliver more sediment than surface erosion (Marden *et al.* 2006). Streambanks would also be active erosion areas after harvesting until they had been stabilised by vegetation.

Exotic forests are the largest landuse in the catchment (56%) and there would usually be an area within the exotic forest estate that would be undergoing harvesting or had been recently harvested. The exotic forest areas in Whangapoua have been identified as being the dominant sediment generating area by a previous report by Gibbs (2006).

Hypothesis C. Agriculture landscape unit is the main sediment generating area

If agricultural areas were the main sediment generating area, this would be mainly due to streambank erosion processes. Very little potential surface erosion sources were found (pugging) and no landslide sources were evident due to low slopes. Soil slumps were observed in the agricultural areas but there were signs that they were generating and delivering sediment to the streams.

Streambank erosion would be assisted by the action of stock as they disturb the streambanks directly and ensure riparian vegetation does not establish to protect the riparian zone. Streambank erosion delivers material directly into the stream and this is an efficient process to convey sediment into the estuary. The location of the agricultural landuse around the harbour also means that the generated sediment has only a short distance to travel to the estuary.

2.7 Conclusion

Whangapoua Harbour provides a good setting to examine sediment source area identification. The Whangapoua estuary and catchment are typical of other North Island estuaries which are relatively small, have steep surrounding catchments, and are subject to heavy rainfall. The exotic forest and agricultural landuse pattern in Whangapoua has the potential to accelerate erosion compared to the native forest landuse, but the native forests have been modified and are located on the steep headwater slopes.

From reviews of the physical setting, past and present landuses, previous studies, and erosion within each landuse, three alternative hypotheses of erosion within the Whangapoua catchment have been proposed. The first is that sediment is mainly generated from native forest areas by landsliding; the second is that most sediment is generated from exotic forest areas by surface, streambank, and landsliding; the third is that agricultural areas generate the most sediment primarily from streambank erosion processes. Any technique that seeks to measure catchment scale erosion to identify the main sediment source areas also needs to account for erosion process within each landuse.

CHAPTER THREE

LITERATURE REVIEW

3.1 Introduction

This chapter will review the literature relevant to catchment scale erosion and to achieve this aim this chapter will be divided into two parts. They are:

A. Impacts of soil erosion. The on-site and off-site impacts of soil erosion will be reviewed. Soil erosion processes and the influencing factors of soil erosion (with emphasis on fluvial erosion) will be presented; and
B. Measuring soil erosion. The techniques available to measure soil erosion within a catchment for sediment source identification will be reviewed and their inherent problems discussed. An erosion measurement technique that will be capable of identifying Whangapoua Harbour's three potential landscape unit/process sediment source areas (Section 2.6) will also be proposed.

PART A:

3.2 Soil erosion

3.2.1 Soil erosion and sedimentation

Soil degradation is the reduction in the current and/or future capacity of the soil to support life through the destruction of soil structure, the removal of parts of the soil, and changes in the soil's biological properties (Ritsema *et al.* 2005). The processes of soil degradation (set in motion by the natural and/or human processes) can be classified into seven main groups. They are water erosion (sheet, rill and gully), wind erosion, mass movement, excess of salts, chemical degradation (e.g., acidification, contamination, nutrient depletion), physical degradation (e.g., crusting, compaction, structural breakdown), and biological (e.g., loss of biodiversity, humus reduction) (Murphy 1993; Lal 2001; Gilley 2005). Thus soil erosion is a process that falls within the broader term of soil degradation. This literature review will focus on soil erosion by water.

Soil erosion is the removal of soil by water and wind at rates in excess of soil formation, and it is generally the result of one or a combination of the soil degradational processes (Jayasuriya 2003). Soil erosion due to natural processes is termed *geological* erosion, and erosion levels above geological erosion caused by anthropogenic perturbations is termed *accelerated* erosion (Chartres 1987).

A product of soil erosion by water is sediment. Sediment is defined as loose, fragmental, solid material that is transported or suspended in water. Sediment includes rock fragments, chemical and biochemical precipitates, and decomposed organic material (Garde & Ranga Raju 1977; Stewart *et al.* 2003). Sediment is principally carried by streams and rivers which dominate the removal of weathering products and link landscapes to their boundaries (Garde & Ranga Raju 1977; Howard *et al.* 1994).

The removal of sediment by water means that landscapes have areas of net erosion and deposition. In particular, storm events remove two components of the soil, the coarse bedload and the fine suspended sediment. Usually the coarse fraction is deposited at the base of hills while the fine fraction is transported in suspension beyond the deposited mantles to adjacent flats or removed completely and delivered to streams (Downes *et al.* 2002; McKenzie *et al.* 2004). This thesis will focus on the suspended or 'fine' fraction of the eroded soil.

The impacts of sediment can be divided into 'on-site' effects (e.g., reduced animal and vegetative production and damage to fixed structures) and 'off-site' effects (e.g., off-site community and environmental effects) (Clough & Hicks 1993).

3.3 On-site effects of erosion

The principal on-site effect of soil erosion by water is the reduction of vegetative production from affected lands and animal performance (i.e., growth rates and general health) (Clough & Hicks 1993). Reduced animal and vegetative production is principally brought about by the loss of soil fertility. Soil fertility is reduced because water erosion selectively removes the finer particles and leaves behind the coarser sands and gravels (Tanberg *et al.* 1998). Major plant nutrients such as nitrogen and phosphorous are associated with the fine clay (< 2 μm)

fraction that is preferentially eroded (DeRose *et al.* 1995; Haygarth & Jarvis 1999; Hatch *et al.* 2002).

Soil erosion contributes to the loss of agrichemicals and fertilisers, lower soil water holding capacity, replanting costs, additional machinery costs, and the repair of infrastructure such as fences, roads, and culverts (Clough & Hicks 1993; Lal 1998). There is also a loss of visual amenity for farming properties and public lands (Krausse *et al.* 2001). One example from New Zealand is that landslides in North Island hill country can have negative impacts to pastoral production up to 80% at paddock scale and 20% at farm scale (DeRose *et al.* 1995; Blaschke *et al.* 2000).

3.4 Off-site effects of erosion

3.4.1 Introduction

"The principal off-site effect of soil erosion is the impact on water quality due to water entrainment of sediments and chemicals in suspended and dissolved forms" (Lal 1998). The impacts of increased delivery of sediment to rivers and streams by accelerated erosion can be divided under two main categories; sediment quantity and sediment quality (Owens *et al.* 2005).

3.4.2 Sediment quantity

Increased sediment quantity increases turbidity in the water column which impacts the ecology of rivers and estuaries. Increased sediment quantity also causes siltation of waterways, which changes channel behaviour and morphology, decreases reservoir storage, increases flooding risk, and impedes navigation of waterways (Vanoni 1975; Ryan 1991; Marden & Rowan 1995; Pimentel *et al.* 1995; Buzzelli *et al.* 1998; Lal 1998; Miller *et al.* 2002; Armstrong *et al.* 2003; Schwarz 2004; Owens *et al.* 2005; Collins & Owens 2006; Lohrer *et al.* 2006; Stanley 1996; Yu 2002). It has been estimated that the annual world cost of off-site sedimentation is around $225 billion per year (Pimentel *et al.* 1995).

3.4.3 Sediment quality

The off-site effects of sediment quality relate to pollutants in the form of nutrients (principally phosphorus and nitrogen) and contaminants (such as pathogens,

heavy metals, and pesticides). Pollutants exist in two phases; particulate (i.e., bound to soil particles) and dissolved in water. Apart from nitrogen, most pollutants are in particulate form and are transported with sediment, particularly the fine fraction (Haygarth & Jarvis 1999; Novotny 1999; Owens *et al.* 2005; Walling 2005; Walling *et al.* 2008). This is because the specific surface area of sediment exerts a major control on surface chemistry and decreases markedly with increasing particle size (Walling & Moorehead 1989). The eroded soil represents the primary source of sediment (and therefore pollutants) to waterways (House *et al.* 1998).

3.4.4 Estuarine impacts

Suspended sediment (fine silts and clays) are highly charged particles that flocculate on contact with salt water and are rapidly deposited. If thick enough, sediment can directly smother the resident fauna. More frequent and extensive lower concentrations of suspended sediment can have chronic effects on physiological conditions and the behaviour of macro fauna, as well as creating biogeochemical gradients in the sediment which encourages the growth of microalgae (Thrush *et al.* 2004).

3.5 Soil erosion processes

3.5.1 Introduction

The energy for the work of soil erosion is principally derived from gravity, chemical reactions, human perturbations, and physical (wind and water) (Lal 2001). Soil erosion by water is the result of rainfall and runoff driven processes that occur simultaneously during rainfall events. Soil erosion by water involves a three stage process; detachment, transport, and deposition (Lal 2001; Asadi *et al.* 2007).

The erosion, transport, and deposition processes are influenced by the physical and chemical properties of the sediment, both at an individual level and as the bulk character of the sediment (Vanoni 1975). The detachment phase is influenced by the grain size distribution, sorting, grain orientation, packing arrangement, porosity, and degree of cohesion. During transport, sediment particles are sorted by size, shape and density and extended transport may fracture or destroy grains

of relatively low hardness (Pye 1994). Grain size and its settling velocity (which in itself is dependant on the sediment grains size, shape, and density) has the greatest influence on the detachment, transport, and deposition erosion process (Vanoni 1975; Pye 1994; Walling *et al.* 2000).

3.6 Soil erosion forms

3.6.1 Coupling definition

Before the review of soil erosion forms, it is necessary to define coupling. Coupling refers to the connectivity that exists between the hillslope and the stream (lateral) and the connectivity of upstream and downstream (longitudinal) (Harvey 2002). The extent of coupling depends on a range of diverse processes, such as climate, slope, and bioturbation (Roering 2008). Coupling should not be confused with the sediment delivery ratio (SDR). The SDR is a ratio of sediment generation within a catchment to the sediment delivery at the catchment mouth (Walling 1983). The better an erosion form is coupled with streams delivering sediment to the catchment mouth, the higher the SDR ratio.

Lateral coupling decreases in a catchment from the headwater zone (highly coupled) to the mid-catchment and then the lowland plains (poorly coupled) (Brierley & Fryirs 2005). Coupling decrease is due to channel and valley slope decline and alluvial accommodation space (i.e., in-stream sediment storage) increasing (Phillips & Slattery 2007).

3.6.2 Surface erosion

Surface erosion by rainfall is not just the action of flowing water, but also the impact of the raindrop itself (Ellison 1944). Erosion by rainfall is the result of the expenditure of the energy of falling raindrops and flowing water, whether these two agents act either singly or together (Kinnell 2005).

Once the soils infiltration capacity is exceeded overland flow is initiated. The movement of water across the soil surface is known variously as Hortonian overland flow, sheet flow, sheetwash, slopewash or wash (Selby 1994). Overland flow rarely occurs as a uniform sheet, but is more commonly a network of braided water courses broken up by the soil surface and vegetation (Morgan 2005).

3.6.3 Gully erosion

Gullies are defined as surface erosion features that are larger than rills and cannot be obliterated by tillage (Poesen *et al.* 2003; Fangmeier *et al.* 2005). A 'classic' gully is characterised by a headcut, steep walls, and flat floors. Gullies have steeper banks, greater depth, and narrower width than stable channels (Selby 1994; Morgan 2005).

Gully development is a threshold dependant process which is controlled by a range of factors including: topographic (slope, critical drainage area); soil and lithology; and landuse (Poesen *et al.* 2003; Belyaev *et al.* 2004; Valentin *et al.* 2005). Gully development is commonly initiated by vegetation removal. Water concentrates in the developed depression which concentrates erosion at the head of the depression where a near vertical scarp develops. Erosion continues at the base of the scarp which causes the headwall to retreat upslope.

The threshold values (i.e., resistance to initiation) for gully development are much higher under native forest than pasture. An example of threshold value change due to landuse from the East Coast region of New Zealand shows a decline after native forest clearance for pasture, a threshold increase from pasture reversion to scrub, and then a restoration of threshold values under exotic pine forest (Figure 3.1) (Parkner *et al.* 2006).

Gullies can be the dominant catchment sediment source because they are well coupled to the drainage network (Selby 1972; Harvey 2002). For example, as much as 90% of catchment sediment yield in Australia can be from gully sources (Olley *et al.* 1993; Wallbrink *et al.* 1996; Wallbrink *et al.* 1998) and 80% in the Mediterranean (Poesen *et al.* 1996).

Gullies can also be the dominant erosion form in New Zealand. For example, studies in the soft rock East Coast country around Gisborne have shown that gully complexes in the Te Weraroa catchment account for 6% of the catchment area, but contributed 62% of the generated sediment (Kasai *et al.* 2001). High resolution Digital Elevation Model measurements from the Waiapu catchment estimated that gullies generated 90% of the sediment (Betts *et al.* 2003).

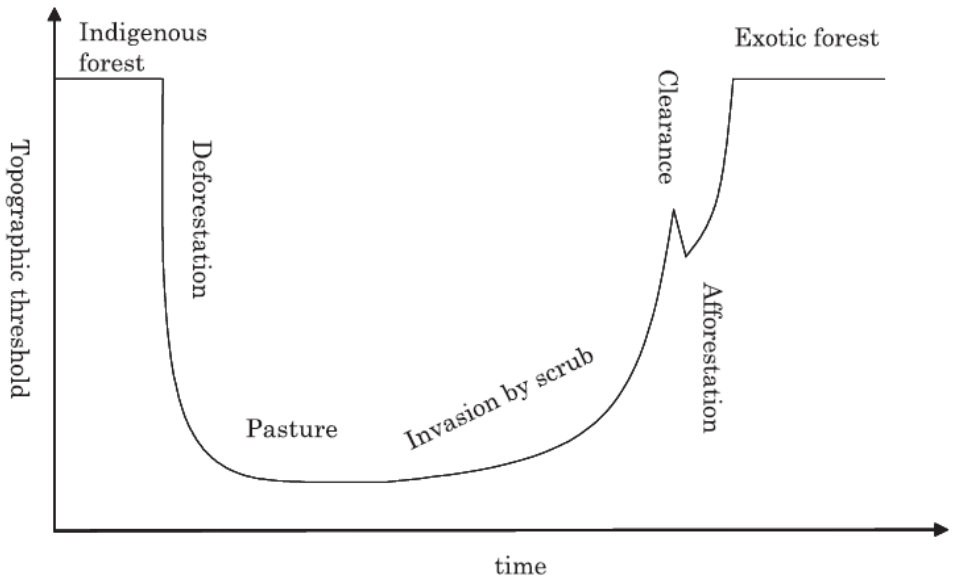

Figure 3.1. Model of different threshold values for gully development under native forest, pasture, scrub, and exotic forest from the east coast region of the North Island, New Zealand (Parkner *et al.* 2006).

3.6.4 Landslide erosion

The term 'landslide' has been used to cover a range of mass movement phenomenon in the literature. Typically, landslide erosion is defined as the sliding, flow, or complex movement of soil, debris and rock without the agent of running water (Crozier 1986; Glade 2003; Schuster & Highland 2007). In this thesis the term landslide will be used in the widest possible sense to describe hillslope mass movement following the classification of (Varnes 1975). Varnes (1975) uses the term landslide to describe falls, topples, shear failures, lateral spreads, flows, and complex failures.

Slopes are stable because they have an excess of resistance over shear stress. Hillslopes become unstable and susceptible to landslides when the excess of resistance is reduced to zero (Crozier 1986). The causes of slope instability can be divided into two categories; quasi-static variables and dynamic variables.

The quasi-static variables refer to factors of landscape stability such as slope, land cover, aspect, gradient, elevation, geology, and soil properties. The dynamic

variables are typically rainfall or earthquakes (Dai & Lee 2003). In other words, the vulnerability of a slope to landslides depends on the combination of quasi-static variables up to a given threshold of triggers (dynamic variables) (Crozier & Glade 2005). For example, a forested slope (quasi-static variable) will require a greater threshold of rainfall (dynamic variable) to initiate landslides than a grassed slope of similar gradient.

Most studies focus on rainfall (dynamic variable) triggered landslides and De Vita & Reichenbach (1998) list a review of over 450 such references. In much of New Zealand's hill country, regolith depths are around 1-2 m especially on steeper slopes. During rainfall events, vertically percolating water meets the bedrock substrate, which has a lower hydraulic conductivity than the rainfall intensity in relative terms. This leads to positive pore water pressure and a reduction in the effective stress of the soil and consequent slope failure (Dai & Lee 2003; Brooks *et al.* 2004).

The rainfall (dynamic variable) frequency/magnitude relationship that triggers landslides is complex. Examples from the East Cape region of the North Island of New Zealand show variable storm frequency/magnitude and landslide occurrence relationships (Figure 3.2). The study concluded that the minimum landslide generating storm threshold was 150 mm for the Te Arai, Waingaromia, and Wharerata, while the value was only 125 mm for the Wharekopae (Reid & Page 2002).

The rainfall frequency/magnitude relationship was also studied by Hicks *et al.* (2000). The authors found that low magnitude/high frequency storm events (< 1 year) delivered the most sediment for the Mangatu basin because the main erosion processes were gully erosion and surface scour. In the same study, the opposite was true for the Te Arai basin where high magnitude/low frequency storm events (> 2 years) generated the most sediment as numerous shallow landslides are generated above this threshold. Similar to the Te Arai basin, in the Tutira catchment it was concluded that high magnitude/low frequency events produce a disproportionally large amount of sediment because landslides are the main erosion process (Page *et al.* 1994a). Low magnitude/high frequency events are

more important if gully and streambank erosion processes are present (Glade 2003).

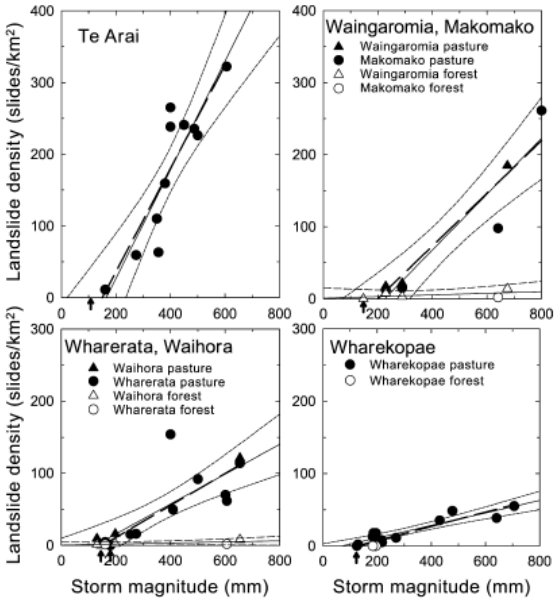

Figure 3.2. A) Storm magnitude and areal landslide density on different catchments in New Zealand; B) storm recurrence interval and averaged areal landslide frequency for eight different areas of New Zealand (Reid & Page 2002).

For quasi-static variable studies, modelling has found that landslide occur disproportionally on steep slopes (Montgomery *et al.* 2000). Landslide risk is mainly on steep slopes > 25°, but slopes over 15° are vulnerable (Eyles 1983). This is an important point for the Whangapoua catchment where around 85% of the study area has slopes over 20° as identified in Section 2.2.3.

The other important quasi-static variable is landuse change. Landuse change is one of the most important variables influencing the occurrence of rainfall-triggered landslides, particularly the conversion of forests to pasture (Glade 2003; Brooks *et al.* 2004). The removal of forests for pasture lowers the cohesion of the soil by the elimination of root strength and changes the equilibrium between slope angle, soil depth and strength, moisture levels, and water tables that leads to slope destabilisation (Glade 1998; Watson *et al.* 1999; Montgomery *et al.* 2000; Istanbulluogulu *et al.* 2004; Sidle *et al.* 2006; Imaizumu *et al.* 2007). One example from New Zealand shows the increasing influence of rainfall triggering

events due to forest clearance (Figure 3.3). Forest clearance in the early 20th century resulted in a sharp spike in storms that led to landslides[1] in the 1920s and 1930s. Post World War II clearance saw the second spike in rainfall triggered landslide occur in the 1960s (Glade 1998).

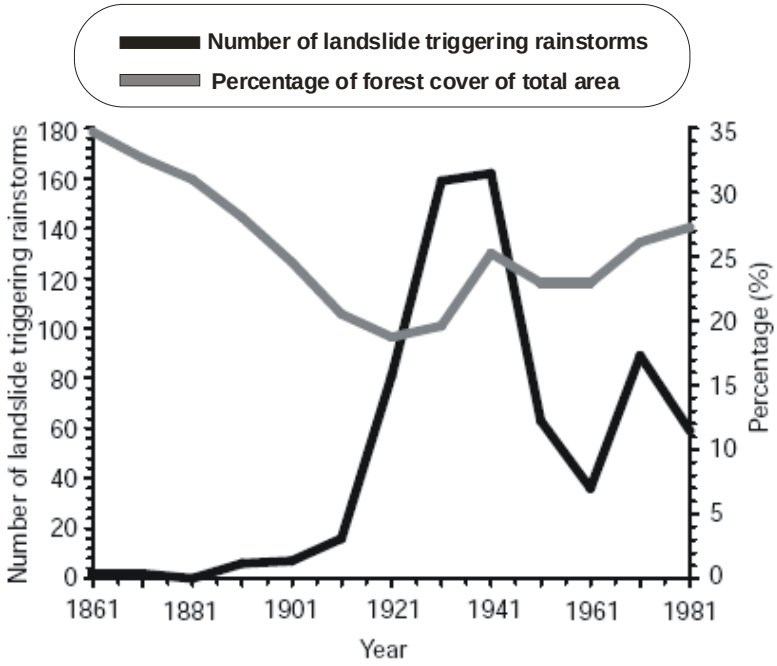

Figure 3.3. Relationship between landuse (forest clearance for pasture – shaded line) and landslide triggering storms (black line) in New Zealand from 1861 to 1981 (Glade 1998).

Landslides are an important erosional form in the North Island hill country (Page *et al.* 1994b). Over 80% of New Zealand is hills and mountains and in the North Island much of the hillslopes are undergoing episodic regolith stripping by the upslope progression of regolith removal by landslides and the consequent exposure of the underlying parent material (Drenge 1995; Brooks *et al.* 2004; Dymond *et al.* 2006). In parts of the North Island landsliding can be the dominant erosion source, triggered by large magnitude rainstorms (Crozier *et al.* 1992; Page *et al.* 1994b; Moon *et al.* 2003; Claessens *et al.* 2005). For example, Page *et al.* (1994b) found that 89% of sediment generated from Cyclone Bola in March 1988

[1] Note: the landslide triggering storms (black line in Figure 3.3) should not be confused with an increase in storm events *per se*, but that the rainfall events that do occur now cause landslides due to land clearance where once they did not when the land was under native forest.

was from landslide sources (Figure 3.4). A study by Page *et al.* (1994b) identified landslides as the major sediment generating process (89%), of which 21% remained stored on hillslopes, 22% was deposited on valley floors, and 51% entered the lake system. Overseas, Peart *et al.* (2005) found that landslides are an important sediment generation process in Hong Kong, and around 50% of material is delivered to drainage systems.

Landslides can be the dominant sediment source as they can be well coupled with the stream network in steep headwater areas. Landslides can deliver large amounts of sediment directly to stream lines and the debris and landslip scar material can be reworked in subsequent storm events and entrain further material (Figure 3.5) (Peart *et al.* 2005). The importance of erosion form coupling was shown in the Whangapoua exotic forest where surface and scraping were the dominant sediment generating processes (64%) and landslides only 32%. But in terms of sediment yield (i.e., delivery of sediment to streams), landslides accounted for 72% whereas surface and scraping processes delivered only 28% (Marden *et al.* 2006).

Photo: Hawkes Bay Catchment Board from (Glade 1998).

Figure 3.4. Example of rainfall triggered landsliding in the hill country in the Hawkes Bay region after Cyclone Bola in March 1988 (Glade 1998).

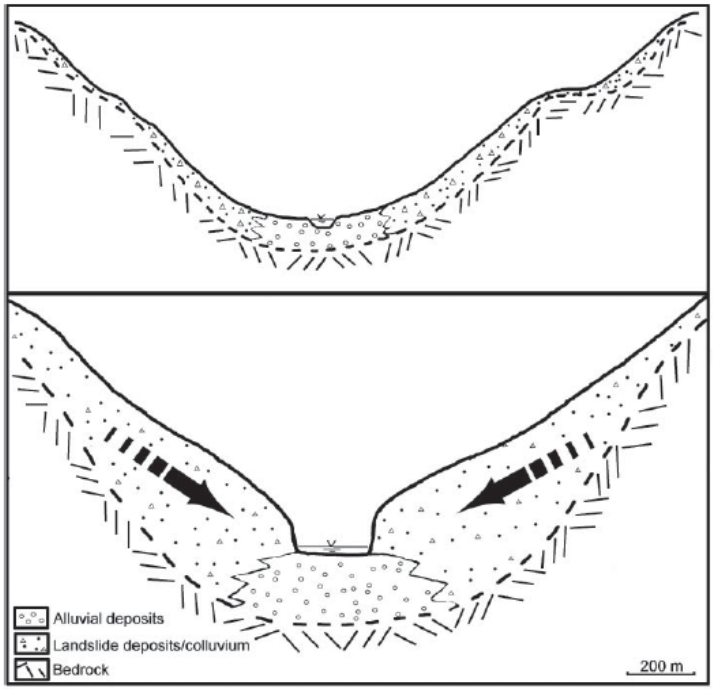

Figure 3.5. Diagram of sediment delivery to stream lines by landslides. Material is injected directly and colluvium is available for reworking during bank full stream discharge (De Vente *et al.* 2006).

3.6.5 Streambank erosion

Streambank erosion is the removal of soil material from streambanks that typically occurs in conditions of high flow (Rosewell *et al.* 1993). Streambank erosion entails two phases, the detachment of sediment particles and their entrainment in the stream. The detachment phase is achieved by two groups of processes, hydraulic action processes and mass failure processes (Figure 3.6) (Green *et al.* 1999; Brierley & Fryirs 2005). For the hydraulic action processes, fluvial entrainment occurs at near bankfull discharge, while mass failure by undercutting occurs at low flows. The most typical streambank erosion occurs mainly as large discrete events rather than a slow continuous process (Lawler *et al.* 1997).

The zonation of streambank erosion processes within a catchment can be generalised (Prosser *et al.* 2000) as researchers have reported that processes occur in spatial domains within a catchment. Sub-aerial processes (such as needle ice formation and clay desiccation) dominate the upper headwater reaches, fluvial erosion the mid basin, and mass failure the lower reaches of a river.

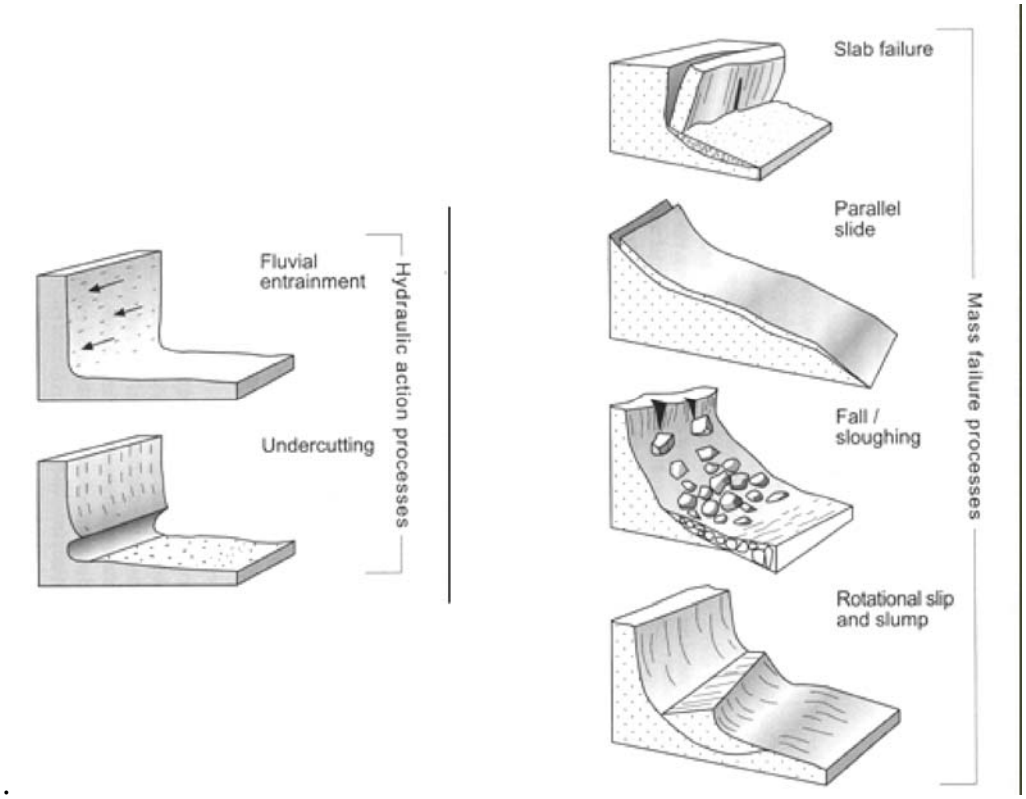

.

Figure 3.6. Streambank erosion hydraulic processes (left) and mass failure processes (Brierley & Fryirs 2005).

The occurrence of these spatial domains is attributed to the upper catchment having weak stream power (or boundary shear stress). Stream power increases mid basin so that fluvial processes dominate. As the channel depth increases and stream gradients decrease in the lower catchment, then bank height will be the dominant factor and thus bank stability/mass failure will be the main erosion process (Lawler *et al.* 1997; Lawler *et al.* 1999; Prosser *et al.* 2000; Couper & Maddock 2001).

Landuse can also influence streambank erosion with the highest rates of streambank erosion found in cropped fields, followed by pasture, and the lowest rates in forests (Zaimes *et al.* 2004). Studies cited in Bull (1997) report that streambanks protected by plant roots (riparian vegetation) may be 20,000 times more resistant to erosion and have ten times the tensile strength than streambanks without riparian vegetation.

Streambank erosion is an important process as the delivery of sediment from stream banks, and ephemeral drainage lines can be the main source of sediment in a drainage basin (Olley *et al.* 1993; Bull 1997; Kronvang *et al.* 1997; Wallbrink *et al.* 1998; Laubel *et al.* 1999; Nagle & Ritchie 1999; Wasson *et al.* 2002; Wallbrink *et al.* 2003a; Thoma *et al.* 2005). Sediment delivery to rivers via streambanks is efficient due to the well coupled nature of streambank erosion to streams as eroded material is deposited directly into the waterways.

While streambank erosion is important, it is a complex process as the interaction between the detachment and entrainment processes occurs at varying spatial and temporal scales. In New Zealand, streambank erosion is a poorly studied process and there is little data on its contribution to river sediment (Watson & Basher 2005).

3.7 Factors influencing soil erosion

3.7.1 Introduction

Soil erosion processes are influenced by the climate, soil/lithology, vegetation, terrain, and landuse, as well as the interaction between them (Selby 1994; Pimentel *et al.* 1995; Lal 2001). The review will focus on the influence of landuse on soil erosion.

3.7.2 Landuse

Human activities often lead to changes in vegetation cover that lead to accelerated erosion by the removal of forests (logging), the change of vegetation cover (forest to grasslands for grazing), or the mechanical interference with the soil (tillage for crops, mining, and road/urban development). Results obtained from erosion plot experiments from different parts of the world show clear evidence of erosion rate sensitivity to landuse and other human activities (Walling 1999). In New Zealand sediment delivery to the continental shelf is sensitive and highly responsive to historic hillslope destabilisation driven by anthropogenic landuse change (Phillips & Gomez 2007).

Generally, sediment yield will increase as vegetation cover is reduced (e.g., forest to pasture) and soil interference is increased (e.g., permanent pasture to tilled crops). Forests have the effect that they buffer soils from erosive forces and consequently erosion rates are lower in forests than in pastoral or arable landuses (Maclaren 1996; Lal 1998). A study examined 61 catchments in Kenya and showed that in terms of sediment yield, landuse was the dominate factor. The study showed that sediment yield followed the pattern of; forestry < forest cover (50% forest, 50% cultivation) < forest/agricultural mix < grazing in terms of sediment yield. The increase in sediment yield was primarily due to decreasing land cover with climate and topographic effects playing lesser roles (Dunne 1979). Table 3-1 shows the results of several studies that examined sediment yield from changing landuse. Sediment yield increases range from an eight fold increase with clearfelling in New Zealand, a 310 fold increase with forest clearance and cultivation in the USA, up to a 1682 fold increase due to deforestation on loess soils in China.

Table 3-1. Results from drainage basin studies of the impact of landuse change on sediment yield.

Region	Landuse change	Increase in sediment yield	Reference
Westland, New Zealand	Clearfelling	× 8	(O'Loughlin *et al.* 1980)
Mahaweli, Sri Lanka	Agricultural plots	× 10 - 100	(Hewawasam *et al.* 2003)
Northern England	Deforestation (ditching and ploughing)	×100	(Painter *et al.* 1974)
Murrumbidgee River, Australia	Tree clearance for grazing	×150	(Olley & Wasson 2003)
Texas, USA	Forest clearance and cultivation	×310	(Chang *et al.* 1982)
Maryland, USA	Building construction	× 126-375	(Wolman & Schick 1967)
Loess Plateau, China	Deforestation for agriculture	× 797-1682	(Zheng 2006)

Landuse change in New Zealand has impacted estuaries mainly by accelerating sediment accumulation because of land clearance and soil disturbance for commercial and urban activities (Nichol *et al.* 2000; Hume 2003; Hutchings *et al.* 2005). In pre-settlement times accumulation rates are generally below 1 mm yr^{-1}, while European settlement can increase siltation rates by an order of magnitude above natural levels (Table 3-2) (Nichol *et al.* 2000; Hume 2003). Modelling of sediment discharge from the Waipaoa River (North Island) has shown sediment

discharge rates were 2.3-14.9 Mt yr^{-1} before human arrival, increasing by 140% after Polynesian settlement; by 350% after European settlement; and by 660% after deforestation of the headwaters (Kettner *et al.* 2007).

As native forests, exotic forests, and agriculture landuse in the Whangapoua catchment is a focus of this study, a further discussion of these three types of landuse and the expected relationship with fluvial erosion follows.

Table 3-2. Summary of sedimentation rates for pre-settlement, Polynesian settlement, and European settlement periods.

Location	Pre-settlement	Polynesian settlement	European settlement	Reference
Whangapoua	0.03-0.08 mm yr^{-1}	0.12-0.13 mm yr^{-1}	0.9-1.5 mm yr^{-1}	(Hume & Dahm 1992)*
Gt. Barrier Island estuary	0.39mm yr^{-1}	0.93 mm yr^{-1}	1.23 mm yr^{-1}	(Ogden *et al.* 2006)
Whangamata	0.1 mm yr^{-1}	0.3 mm yr^{-1}	11 mm yr^{-1}	(Sheffield *et al.* 1995)
Whangape	0.1-0.5 mm yr^{-1}	0.1-0.5 mm yr^{-1}	1.7-4.6 mm yr^{-1}	(Nichol *et al.* 2000)
Hawkes Bay	1.7 mm yr^{-1}	2.7 mm yr^{-1}	13.8 mm yr^{-1}	(Wilmshurst 1997)

* As cited in (Jones 2008)

3.7.2.1 Native forests

Native kauri (*Agathis Australis*) forests used to cover one tenth of the North Island, but now only 10,000 individuals survive (Vrana 2007). Kauri are endemic to New Zealand and it is an emergent tree (35 m) above a mixed angiosperm canopy of 10-20 m (Claessens *et al.* 2006).

Mature kauri trees tend to grow preferentially on ridge tops and moderate to steep slopes with moderate to high landsliding risk. This is attributed to the high occurrence of landslides and soil slips that favour the establishment of light demanding kauri seedlings (Ogden 1985; Claessens *et al.* 2006). After a landslide disturbance, the site is colonised by a dense cohort of kauri seedlings, which is followed by a period of self thinning in which the biomass remains constant.

Lower light demanding species are out competed by the kauri as self thinning continues where only a few tall trees remain in the climax community. This process may take 600-1000 years (Ogden 1985; Burns & Smale 1990; Claessens *et al.* 2006). Kauri also have a competitive advantage in that growing on landslide prone areas, their dense and strong rooting systems combine with tree weight to improve soil cohesion and this postpones landslide disturbance events, where the kauri then uses its long life time to outlive other species (Claessens *et al.* 2006). The removal of kauri from the native forest areas of Whangapoua may potentially increase the landsliding risk.

3.7.2.2 Exotic forest

Exotic forestry influences sediment generation in two main ways; hydrological and physical. A water balance equation may be expressed as:

$$R = P - E - \Delta S \qquad \text{(Eqn 3.1)}$$

where *R* is runoff, *P* is rainfall, *E* is evaporation (including transpiration), and *ΔS* is the change in water stored in the soil profile and in groundwater systems (Fahey *et al.* 2004). Forest harvesting causes a decrease in *E* and a small increase in *ΔS* which will result in increased runoff. Thus forest harvesting generally increases the fraction of precipitation that eventually becomes increased stream flow (Swank *et al.* 2001; Moore & Wondzell 2005). In the paired Pakuratahi exotic forest/pasture study in New Zealand, the forest had a lower water yield than the agricultural catchment until harvesting which caused exotic forest water yields to increase 22% above the pasture catchment (Wood & Fahey 2006). Figure 3.7 shows the increase in water yield and subsequent logarithmic decline in a 23 year harvest cycle of a harvested hardwood forest (Hibbert 1967 as cited in Pereira 1973). Johnson *et al.* (2007) found that the amount of rainfall to cause a 50% saturation of the soil fell from 54mm to 21mm after timber harvesting. Bruijnzeel (2004) cites studies that show water yield can return to original levels within 8 years of harvesting and that water yield may decline if afforestation occurs on degraded or agricultural land, or water hungry trees such as eucalypts are planted.

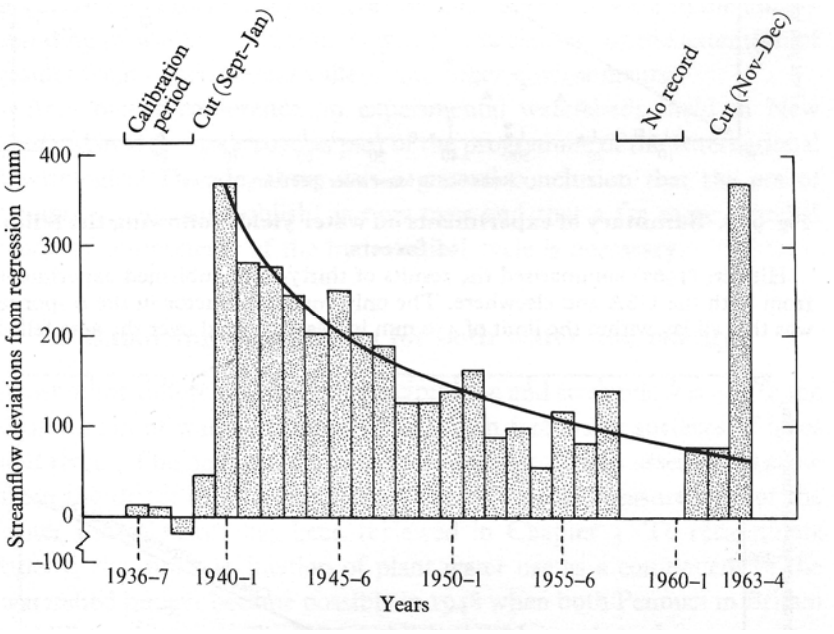

Figure 3.7. Water yield response to harvesting of a hardwood forest (Hibbert 1967 as cited in Pereira 1973).

The direct physical disturbance of the soil surface begins by the removal of native vegetation for site preparation. Further physical disturbance is caused by exposing the soil by removing the tree crop, construction of logging infrastructure (i.e., unsealed roads, road cuttings, drainage features, snig tracks, log landings, etc), and dragging logs across the soil surface (Croke *et al.* 1999; Croke & Mockler 2001; Fransen *et al.* 2001; Lane & Sheridan 2002; Wallbrink *et al.* 2002a; Bruijnzeel 2004; Stott & Mount 2004; Sidle *et al.* 2006). Cable logging disturbs less of the harvested area than machine extraction methods. The main soil disturbance by cable logging is the upper few centimetres of the soil from the centre to the outward edge of the drag lines (Laffan *et al.* 2001). Prepared exotic forest sites that have been ripped, ploughed, furrowed, and residue removed results in no protective vegetative cover and sediment is easily detached and transported (Costantini & Loch 2002).

Physical disturbance in exotic forests can be caused by compaction from features such as snig tracks and roads. Compacted roads increase overland flow which cause increase sediment generation (Wallbrink & Croke 2002).

The hydrological and physical disturbance caused by harvesting trees causes an immediate increase in surface erosion and an increase in landsliding for periods from 3 to 15 years due to a deterioration in root strength (Gomi *et al.* 2005; Marden *et al.* 2006; Sidle *et al.* 2006). Consequently the sediment yield characteristics of exotic forests are an initial increase with site preparation, recovery, and then a more significant increase with infrastructure construction and harvesting (Swank *et al.* 2001; Stott & Mount 2004).

The increase of suspended sediment yields caused by harvesting forests has been reported from various studies in the UK (Table 3-3). The increased sediment yields from logged forests in comparison to undisturbed forests is also supported in a review of the Pacific Northwest region, USA (Gomi *et al.* 2005).

Table 3-3 Mean values and ranges of suspended sediment yield (SSY) in t km^{-2} yr^{-1} for plantation forests in the UK (Stott & Mount 2004).

	Undisturbed	**Mature forest**	**Harvesting**	**Post harvesting**
SSY	14.9	30.3	163.3	98.4
Range	*1.0-41.0*	*15.3-118.0*	*43.8 – 462.8*	*0*

3.7.2.3 Agriculture

Conventional agriculture involves the clearing of native vegetation primarily for the purposes of pasture establishment for the grazing of animals or crop production. This review will examine soil erosion under pastoral systems.

Live stock can cause soil pulverisation and compaction (particularly in moist conditions) which causes lower infiltration rates, an increase in fines production, and the consequent increase in sediment detachment and transport rates (Eldridge 1993). In New Zealand there has been a trend away from sheep and a movement toward dairy cattle and an intensification of agriculture (Parkyn & Wilcock 2004). The effect that high stocking rates of cattle have on soils in high rainfall areas is a condition known as ‘pugging.’ Pugging is when cattle trample wet soils into a slurry like condition and cause considerable pasture damage, particularly to soil drainage due to macropore destruction. Pugging increases the area of bare ground and consequently erosion by overland flow, and pugging damage may take some time to recover (Singleton & Addison 1999; Elliott *et al.* 2002; Adams & Elliott 2006; Drewry 2006).

Grazing stock also impact riparian vegetation and stream bank stability, particularly cattle due to their size and affinity with water (Parkyn & Wilcock 2004; Agouridis *et al.* 2005). Stock also have the indirect effect of reducing vegetative cover and increasing bare areas exposing the soil surface to greater raindrop erosion and lowering the impedance to overland flow (Eldridge 1993).

3.7.2.4 Multi-landuse studies in New Zealand

Studies of sediment generation by different landuse in New Zealand have tended to take the perspective of a landscape history (e.g., Kasai *et al.* 2005) or compared the impacts of a single landuse against some form of forestry to determine the level of accelerated erosion (e.g., Rodda *et al.* 2001). Dissolved organic carbon flowpaths were examined for native forest, exotic forest, and agricultural landuses by Findlay *et al.* (2001).

This review has only been able to identify three multi-landuse studies in New Zealand that compare native forests, exotic forests, and agriculture; one published journal article and two reports. The two reports are detailed in the Whangapoua Harbour background section in Chapter 2.

Briefly Marden & Rowan (1995) used stereo-photo interpretation and field truthing to determine sediment generation from agricultural, exotic forest, and native forest landuse in the Whangapoua catchment. They determined that native forest was the largest sediment source, followed by exotic forest followed by agriculture. Gibbs (2006) used a single novel parameter (a plant compound specific isotope of ^{13}C) to fingerprint sediments from the same landuse types and he found that exotic forests were the largest sediment source, followed by native forest followed by agriculture.

Quinn & Stroud (2002) examined the impacts on water quality from nutrients and sediment from native forest, pine forest, and pasture landuses in sandstone/siltstone hill country of the Mangaotama catchment west of Hamilton. They used stream monitoring (at 15 minute intervals) to determine flow, and used monthly grab samples to determine turbidity and suspended solids and an automated sampler (4.5 hr intervals) to determine sediment and nutrient exports.

Streams draining the native forest had the lower suspended solids and nutrient exports than pines or pasture, and the highest turbidity and suspended solids was derived from a mixed exotic pine/scrub landuse (Table 3-4).

Table 3-4. Landuse effects on average water quality from two native forest streams, a predominantly pine stream, and two pasture streams (Quinn & Stroud 2002).

Parameter	Native	Pine	Pasture
Suspended solids (gm^{-3})	4.5	20.9	11.6
Turbidity (NTU)	8.7	24.7	11.3

Two studies that compared exotic forests with agricultural pasture are also of relevance. A paired catchment study was undertaken in the Hawkes Bay region of New Zealand for a two and a half year period. The results were that the exotic forest was yielding 32.7 t km^2 and the pasture 104.4 t km^2 of sediment, or roughly three times that of the exotic forest. Between a quarter and a third of the total suspended sediment yield for the study was delivered in one storm (Marden & Rowan 1995). In another exotic forest and pasture paired catchment study, it was found that grazed pastures yielded 3.7 times more sediment than mature exotic pines. Although harvesting pines increased the sediment yield, the erosion rates returned to pre-harvest levels within two to three years (Fahey & Marden 2006).

3.8 Synthesis of Part A

Part A has reviewed the literature for erosion processes, erosion forms, and the factors influencing soil erosion. Landslides, gullies, and streambanks have been identified as having the potential to be the main sediment sources within a catchment. Surface erosion due to log scraping (exotic forests) and pugging (agriculture) can also generate significant amounts of sediment.

Landslide erosion on steep slopes is often well coupled to the stream network. On New Zealand hill country, slopes of > 25° are at risk of landslides but slopes > 15° remain vulnerable. Most landslides are triggered by large storm events and thresholds of between 125-150 mm have been identified in New Zealand hill country studies. The type of rainfall most important in triggering landslides is high magnitude and low frequency rainstorms. Landslides on steep slopes in

harvested exotic pine areas can remain a risk for periods of between three and 15 years.

Gully erosion forms can remain active for decades. The most important rainfall threshold for gully sediment generation is low magnitude and high frequency storms because they are well coupled with the stream network. While being major sediment sources in areas such as the soft rock country of the East Coast, their limited extent in the Whangapoua catchment means that they are not a major potential source of sediment generation.

Surface erosion in the forests is caused by dragging logs across the soil surface during cable logging. Shallow furrows are created and they can be the main sediment generating erosion form in exotic forest areas, but in terms of sediment delivery they are not efficiently coupled with the stream network and landslides can deliver more sediment on sloping post harvested areas.

Streambank erosion is most likely to occur in the mid-catchment areas due to fluvial processes and in the lowland catchment area due to mass failure events. The delivery of sediment to the stream network is well coupled and would most likely occur as discrete events during storms rather than at a constant rate during low flow conditions. The action of stock in agricultural areas can exacerbate streambank erosion due to direct disturbance of the streambanks and the destruction of riparian vegetation.

Pugging by stock can disturb the soil surface and be another sediment generating erosion form in agricultural areas. While not extensively found in the Whangapoua catchment, it remains a potential sediment source.

There have only been a few multi-landuse studies conducted in New Zealand comparing native forests, exotic forests, and agriculture. One study identified native forest > exotic forest > agriculture in terms of sediment generation. Another study ordered the landuses as exotic forest > native forests > agriculture, while another ranked them exotic forest > agriculture > native forest. In paired catchment studies between exotic forest and agriculture, agriculture had higher

erosion rates than mature exotic forests. Although recently harvested exotic forest erosion rates far exceeded that of agriculture, exotic forest sediment yields declined to pre-harvest levels within two to three years.

In general, sediment yields decline with drainage basin size so catchments the size of Whangapoua have the potential to deliver greater amounts of sediment to the coastal margins per unit of area than for larger catchment (> 1000 km^2). Studies from the soft rock country of the East Coast identified headwater areas as important sediment sources because they are well coupled to the stream network due to steep slopes and narrow valley floors limiting sediment storage on-slope. Native forests, exotic forests, and agricultural pastures are all potential sediment source areas. There is no landuse and erosion form combination that can be confidently said is delivering the most sediment to Whangapoua estuary. Consequently, any measure of erosion within the Whangapoua catchment to identify sediment source areas will need to account for the various landuses and erosion forms of the three conceptual models.

PART B:

3.9 Measuring catchment scale erosion

3.9.1 Introduction

Reliable information on the nature of catchment suspended sediment sources is important for designing strategies for reducing sedimentation (Collins & Walling 2004). There are a range of techniques available to investigate sediment generation and they can be divided into direct and indirect methods (Loughran & Campbell 1995). Indirect methods seek to infer catchment scale erosion by *in situ* measurement (e.g., erosion plots or erosion pins) and then extrapolating up to the whole catchment (Loughran & Campbell 1995). Direct methods seek to determine catchment erosion by accounting for both sediment mobilisation and delivery to streams via a tracing method (Loughran & Campbell 1995; Collins & Walling 2004).

The technique employed to measure catchment erosion will largely be determined by the dominant type of erosion in the catchment (e.g., erosion pins for stream

bank erosion or erosion plots for surface erosion from agricultural fields) (Lal 2001). Thus indirect methods have proven popular tools in erosion studies, but erosion is a complex process with a range of influencing factors and source types at a catchment scale (Collins & Walling 2004). Table 3-5 summaries a range of potential indirect and direct methods of measuring erosion and provides the advantages and disadvantages of each technique.

3.9.2 The sediment measurement problem with indirect methods

Sediment sources, sinks, and fluxes in a drainage basin are highly variable in space and time and the use of short term sediment yields as determined by indirect methods is of limited utility (Trimble 1999). The difficulties of measuring catchment scale erosion can be divided into the spatial and temporal variability of sediment transport (Walling 1983; Gao 2008).

3.9.2.1 Spatial issues

Catchments are complex environments in which to determine sediment generation and delivery. "Rather than functioning as a conveyor belt moving sediment from the hinterland to terrestrial and marine sinks, the links between erosion and sediment yield are discontinuous, and the relationships among sediment production, transport, storage and export in drainage basins accordingly are complex and nonlinear" (Phillips et al. 2007).

Scale plays an important role in explanations of specific sediment yield (De Boer & Crosby 1996). Measurement of erosion or sediment transport at a plot scale, for example, gives results on sediment passing a particular point in the landscape, but reveals little information on the travel distance of that sediment before it is re-deposited, or if it is remobilised again (Prosser *et al.* 2001b; Ventura *et al.* 2001). Even in areas of high erosion as measured by plots, hillslopes can be poorly coupled with the fluvial system as there are often abundant storage sites with a catchment (Harvey 2002). Thus erosion rates determined at one scale *cannot* be extrapolated to other scales without further testing (De Boer & Crosby 1996).

Table 3-5. A list of indirect and direct erosion measurement techniques and their advantages and disadvantages and an example reference. After (Collins & Walling 2004).

Technique	Description	Advantages	Disadvantages
Indirect	Estimates of erosion from *in situ* measurements		
Mapping (van Dijk *et al.* 2005)	Sediment sources are mapped using semi-quantitative sources. These can identify rilling, gullying, stream bank, percentage of bare ground, and tree root exposure.	Relatively cheap, traditional method, can be combined with other procedures (e.g., soil profiles),	Subjectivity, need for cartographic skills, problems of interpretation of erosion surfaces as to whether they are contributing or non contributing, time consuming.
Surveying	Estimates of erosion and deposition are made in reference to a datum level.		
▪ Profilemeters (Sirvent *et al.* 1997)	A series of rods are lowered onto the surface from set benchmarks and changes are recorded.	Commonly used, low site disturbance, relatively cheap.	Potential loss of data after benchmark disturbance, limited spatial coverage, problems operating on stony and litter layers.
▪ Erosion pins (Couper *et al.* 2002)	Insertion of a pin or nails into surface of stream bank to establish datum point from which changes can be measured.	Relatively cheap, simple method	Potential loss of data after pin disturbance, non erosion changes to datum levels (e.g., ground swelling), spatial representativeness, site interference, unable to measure mass wasting events, time series requirements
▪ Cross-profiling (Hooke 2007)	Accurate surveying establishes datum points on slopes and stream channels	Relatively cheap, can measure stream morphological changes over time,	Spatial representativeness, underestimation of sheet wash from slopes, time series requirements, operator skills
▪ GPS (Malet *et al.* 2002)	Accurate surveying establishes datum points on slopes and stream channels	Data processing through readily available software, precision, data collection out of 'line of sight',	Technical requirements of equipment and operator, need for signal reception (e.g., problems under canopy), identification of fixed survey points,
Photogrammetry (Chandler 1999)	Photographs (terrestrial and aerial) used to examine change of erosional features	Minimal site disturbance, reduces field work costs, documentation of change, applicable to different scales	Frequency requirements, light requirements, availability of records, quantification of sediment generation, resolution of camera, establishment of stable camera points, optical barriers

Technique	Description	Advantages	Disadvantages
Indirect (continued)	Estimates of erosion from *in situ* measurements		
Erosion plots (Coppus & Imeson 2002)	Bounded plots are used to monitor sediment generation from hillslopes and extrapolated to a wider area	Simple, widely used, relatively cheap,	Spatial representativeness, edge effects, calibration and sub sampling of collected sediment, need for many replicates over long periods of time, subsurface process limited
Suspended sediment flux monitoring (Donohue *et al.* 2003)	Manual or automated collection of suspended sediment samples from catchment tributaries	Relative contributions of subcatchments possible, routing of sediment accounted for,	Interval and length of sampling to ensure representativeness, calibration of sediment concentrations and stream flow, equipment requirement, equipment maintenance, laboratory processing of samples, sampling of high intensity events, not process specific
Remote sensing (Pickup & Marks 2001)	Geomorphic processes are monitored using airborne platforms (e.g., satellite, laser-altimetry)	Spatial and temporal resolution	Assumption that erosion process is detectable, cost of data acquisition, small scale studies, technical requirements of operator, error from aerial platform stability
Laser scanning (Flanagan *et al.* 1995)	Soil surface changes are measured by laser	Minimal site disturbance, surface fitting possible, and accurate	Technical requirements of airborne platforms, expensive, and not sensitive for fine sediment movement
Soil tracers	Examination of soil redistribution by measuring detectable properties of transported sediment		
▪ Radionuclide (Wallbrink *et al.* 2002a)	Fallout radionuclides (^{137}Cs, ^{210}Pb, and ^{7}Be) bind with soil particles and emit detectable amount of gamma radiation	Spatial representativeness, retrospective, single site visit, remains conservative during transport, minimal site disturbance	Selection of reference site, expensive laboratory processing, choice of calibrating model, variability of radionuclide deposition
▪ Rare earths (Polyakov *et al.* 2004)	Soil redistribution is measured by natural or tagged rare earths	Ability of tag discrete elements within a landscape (e.g., hillcrest, toe slope)	Relatively new technique, expensive laboratory analysis by neutron activation, heavier elements may not be conservative during transport process
▪ Magnetics (Wasson *et al.* 2002)	The magnetic minerals (e.g., magnetite and haematite) occur in different combinations in soils, can be measured to delineate sediment from different parts of the catchment	Modest cost of mineral magnetic susceptibility analysis	Uniform geology does not provide resolution within a catchment, magnetic signature may not be conservative during transport process

Technique	Description	Advantages	Disadvantages
Direct	Methods that take account of sediment mobilisation and delivery		
Erosion vulnerability indices (Wilson & Gallant 1996)	Values are assigned to various erosion features in a catchment to yield a sediment probability ranking	Provides information for targeting erosion monitoring and/or control measures within a catchment	Subjective, time consuming field component,
Sedigraphs and hysteretic loops (Jansson 2002)	Eroding sections of a catchment are monitored by examining storm hydrographs and sediment concentrations/discharge relationships	Spatial detection of sediment sources possible,	Inability to identify sediment processes
Sediment fingerprinting (Walling *et al.* 1999)	A range of properties (e.g., geochemical, magnetic, organic etc) are used to characterise source soils and then compared to fluvial suspended sediment	Sediment routing accounted for, spatial and temporal patterns possible, can avoid in situ measurements	No generic guide for selecting fingerprint properties or number of samples required, associated uncertainty with current generation of multivariate mixing model outputs.
Catchment modelling (Kinsey-Henderson *et al.* 2005)	Computer models simulate sediment generation and delivery rates	Field costs reduces, highly user friendly outputs (e.g., maps), scenario modelling possible	Availability of reliable catchment information, operator skill requirements, validating data is required

The general rule of the inverse relationship between drainage basin size and sediment yield can be complicated by erosion form, lithology, land cover, climate and topography (de Vente *et al.* 2007). The interplay of erosion forms and sediment storages at different catchment scales changes sediment yield (Figure 3.8). So for small areas (i.e., plot scale 10^{-6}) surface processes dominate and sediment storage is limited to the slope with consequent low sediment yields. Maximum sediment yield is found for basins around 10-100 km^2 where the subsurface erosion forms (gully, streambank, and landslide erosion) come into play. As catchments increase in size from 10 km^2 then so do the sediment storage areas (floodplains, in-stream banks, dams) and sediment yield begins to decrease.

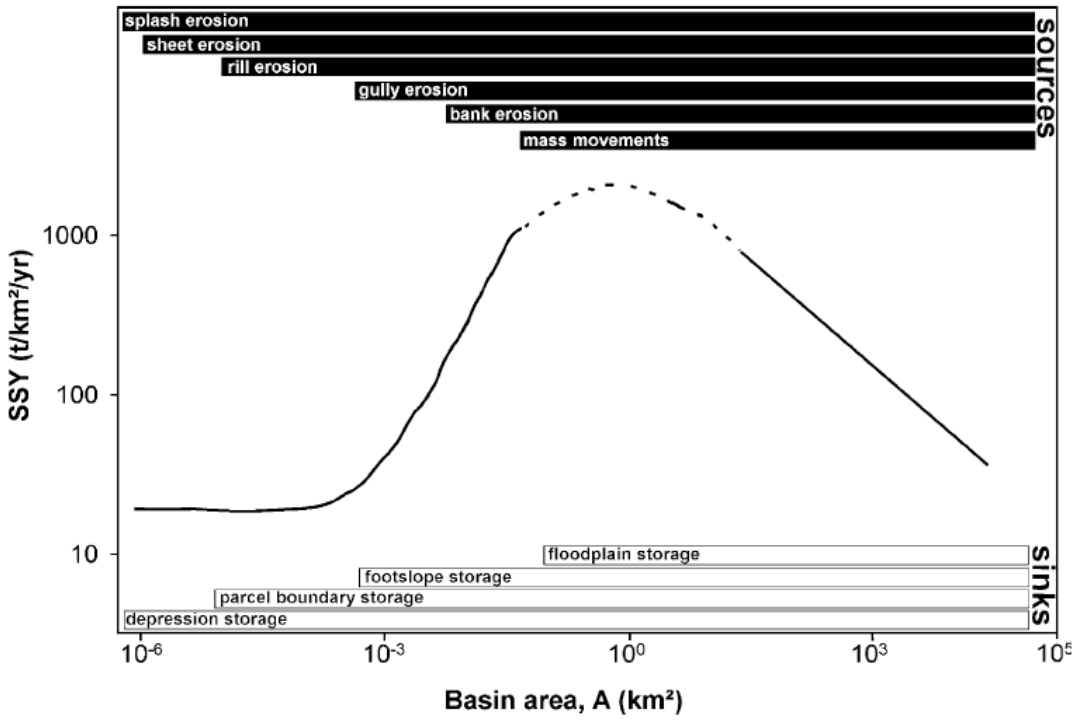

Figure 3.8. Representation of the relationship between the type of sediment sources (dark bars – top), sediment sinks (open bars – bottom), sediment yield and drainage basin area from erosion studies in Spain (de Vente & Poesen 2005).

3.9.2.2 Temporal issues

Measurement of catchment erosion by indirect methods is also complicated by temporal issues. (Parsons *et al.* 2006) argue that the idea of sediment delivery is a fallacy. The widely used sediment delivery ratio (SDR) is calculated by measuring

sediment yield at the catchment outlet in t km^{-2} yr^{-1} to the gross erosion rate measured within the basin (by plots for example) in t km^{-2} yr^{-1} (Walling 1983).

Parsons *et al.* (2006) state that sediment yield measured at the basin outlet (e.g., by stream gauging) will be in the short term derived from in-stream and near stream sources. This is because a considerable portion of the sediment load accumulates on slopes and valley bottoms (Dedkov & Mozzherin 1996). Consequently the measurement of gross erosion at a point in the landscape (by plots) in the catchment may take years to reach the basin outlet, so plot measurement of erosion should be considered to be a measurement of sediment flux only.

Attempting to measure erosion at points in a catchment, many events may have occurred in a single measurement interval, so that measurement is of some aggregated, temporally lumped response which creates further problems in up-scaling results (Lawler 2005). Other temporal issues regarding sediment delivery at a catchment scale are given in Table 3-6.

3.9.2.3 General complexity issues

Widely used indirect methods of measuring soil erosion are plots, erosion pins, sediment budgets, stream monitoring, and modelling, and they provide examples of the complexity of determining catchment sediment yields.

Catchment erosion rates may be over estimated when determined from the erosion plot method. For example, Parsons *et al.* (2004) states that the lowest global rates of soil erosion (extrapolated from plots) are from Europe and the USA, but even at this rate both areas would be eroded to sea level in 500,000 and 1 million years respectively. Schaub & Prasuhn (1993) report that field plots were estimating erosion rates higher than other measures. The Universal Soil Loss Equation (USLE) was developed from data from erosion plots on planar agricultural surfaces and does not account for re-deposition of mobilised sediment (Collins & Walling 2004; Kinnell 2004).

Table 3-6. Examples of temporal complexity of sediment transport within drainage basins.

Authors	Temporal issue
(Collins & Walling 2007a; Collins & Walling 2007b);	Averages of between 18% and 57% of the annual suspended sediment load is stored on the channel bed of five catchments in the UK, but this can range widely (7-92%) throughout the year and local complexity caused no common trend between three river systems
(Owens *et al.* 1999a)	40% of the annual sediment load is stored on the channel bed and 4% is stored on the floodplain of the River Tweed in Scotland. The residence time of bed stored sediment is probably less than a year, while stream bank erosion reintroduces floodplain sediment with a considerably longer residence time
(Phillips & Marion 2001);	'new' sediment (delivered from the catchment) dominates the upper reaches and 'old' sediment (remobilised from the channel) dominates the lower reaches of a Texan catchment
(Bonniwell *et al.* 1999)	In a 389 km^2 Idaho catchment, 'new' sediment dominated the upper reaches and fine sediment had a short residence time (1.6 days) and rapid migration. 'Older' finer grained sediment dominated the lower reaches and residence times increase to 103 days. Transit distances in this environment are between 15 to 60km and that at high discharges, the delivery of fine sediment is high but that it is also flushed through the system. The implications for small basins with stream lengths of < 10km is that the lack of stream storage will mean the effective delivery of sediment to the stream mouth. Extrapolating the results, basins with stream lengths of > 100km could take a substantial period to deliver sediment to the river mouth
(Matisoff *et al.* 2005)	Data from three drainage basins in Ohio, Alabama, and Oregon show the mean age of sediments is 50-80 days in rivers, 80-100 days in estuaries, to 300 days on river bottom sediments. 'New' sediment proportions are 35-50% in rivers, 25-35% in estuaries, and 1-4% on the river bottom

Authors	Temporal issue
(Dosseto *et al.* 2006)	In the Murray-Darling Basin in Australia, sediment transit times have been measured between 2 and 11 km yr^{-1} meaning it would take an average of 1000 years for sediment to travel the approximate 400km of the study river length
(Wallbrink *et al.* 1998)	The mean residence time of fine sediment in a 50km mid-reach section of the Murrumbidgee River in Australia is 10 years
(Phillips *et al.* 2007)	The Waipaoa River Holocene alluvium has a mean age of 4400 years and of the potentially re-mobilisable sediments, they are likely to remain in storage for > 100 years and have a half life (time for 50% removal) of > 2000 years
(Le Cloarec *et al.* 2007)	The average residence times for suspended matter on drainage basin lands in France range from 4,800 to 30,000 years, while once in the fluvial system (or close proximity) this drops to less than a year
(Rommens *et al.* 2005)	A Holocene sediment budget for a 103 ha loess agricultural catchment in Belgium report sediment delivery ratios of between 20% and 42%. These figures show that the majority of historical sediments remain near the source area and have not been delivered downstream
(Rommens *et al.* 2006)	A long term (1000 year) sediment budget for a Belgium catchment (52 km^2) shows that 50% of the eroded Holocene sediment is stored as colluvial deposits on footslopes and dry valley bottoms. Only 29% of sediment was delivered to valleys with permanent streams where it is stored as alluvial deposits. The remaining 21% is transferred out of the system to higher order rivers

Large variability in erosion rate estimation can occur due to natural and measurement variability. Nearing *et al.* (1999), citing the few erosion plot studies that conducted replicates, reported that the coefficient of variability ranged from 18 to 91% in one study and 3.4 to 173% in another. Another study found differences between replica plots up to an order of nine (Boix-Fayos *et al.* 2007). A review of plot data by Boix-Fayos *et al.* (2006) reported that variation in erosion estimation was attributable to exhaustion of material in closed plots, different erosion processes operating at different scales to that measured by erosion plots, and difficulty with extrapolation from plot to catchment scale. A key difficulty is to encapsulate the complexity of system interactions and to represent them by means of erosion plots. The smaller the plot, the larger the hydrological disconnection within the system, the lower the energy flows due to short distances and the quicker the response to runoff due to an artificial decrease of concentration times for continuous flow (Boix-Fayos *et al.* 2007).

Another popular indirect method is the erosion pin method for estimation of soil erosion. But again problems are encountered. As the erosion pin method is quite point specific, a high degree of systematic and random spatial variability is to be expected. Coefficients of variation often exceed 100% (Laubel *et al.* 1999).

The guiding concept behind sediment budgetary approach is that high erosion from sediment sources will lead to high sediment yields (i.e., sediment yield is supply limited). This is contrasted by hydrological modelling based on stream gauging which extrapolates catchment erosion based on sediment-discharge relationships (i.e., sediment yield is transport limited) (McKergow *et al.* 2005).

3.9.2.4 Discussion on erosion measurement

All of the examples above show the problems associated with indirect methods of erosion measurement, mainly because they measure the flux of sediment past a particular point in the landscape. In other words, they are measures of sediment *mobilisation*. Erosion at a catchment scale is a complex process and involves detachment, transport, deposition, and resuspension. The main problem of indirect methods is that they do not account for sediment *delivery*. There are techniques that measure the amount of sediment delivered to the estuary such as estuary

coring or turbidity monitoring, but these techniques do not identify the from where in the catchment sediment is mobilised from nor what erosion form or land management technique is responsible for generating the sediment (Collins & Walling 2004).

The key research aim of this thesis was finding out from where in the catchment the sediment in the Whangapoua estuary was coming from. Also of interest was what erosion form was generating the sediment within the catchment. It would be possible, using indirect techniques, to assemble a suite of measurement methods to estimate comparative erosion rates within different parts of Whangapoua catchment (e.g., erosion plots), and to measure the surface, landslide, and streambank erosion forms within the catchment (e.g., streambank erosion pins). Missing from this approach would be linking catchment erosion (mobilisation) to the deposited estuary sediment (delivery). Say for example indirect methods found that landslides from native forests where the biggest generator of sediment within the catchment based on surveying methods. Would erosion remediation and control strategies be warranted to address this problem if the reality was that most of the eroded material was stored on-slope? Erosion estimation is possible by indirect methods, but they don't account for the numerous uncertainties that have been identified above in regard to sediment delivery. Any targeted sediment control strategy must take into account both sediment mobilisation and delivery.

Sediment flux from a catchment cannot be determined by simply multiplying a yield from a unit area by the catchment area because of the lack of a simple relationship between yield and area (Parsons *et al.* 2004). Since much of the fine sediment transported by river systems will have been mobilised from the catchment from soil erosion, amelioration strategies must be whole catchment focused (Walling 2003). Catchment management strategies for reducing sediment by necessity require information on source types (Collins & Walling 2004), but there are problems using indirect techniques.

3.10 Sediment fingerprinting

3.10.1 Introduction

One method that has been used to address the issues raised in the previous section is the direct method of sediment fingerprinting. Sediment fingerprinting seeks to characterise sediment delivery by linking the catchment mobilisation (or source areas) to where the sediment is delivered (or sink), there by addressing the problem of sediment routing through a catchment. Sediment fingerprinting provides an alternative basis for identifying catchment suspended sediment sources and overcoming the problems of indirect measurement methods (Collins & Walling 2004) and for these reasons has found wider application in erosion studies (Walling & Woodward 1995; Collins *et al.* 1997; Walden *et al.* 1997; Collins *et al.* 1998; Martin & McCulloch 1999; Owens *et al.* 1999b; Walling *et al.* 1999; Franks & Rowan 2000; Kelley & Nater 2000b; Collins *et al.* 2001; Russell *et al.* 2001; Walling *et al.* 2001; Collins & Walling 2002; Motha *et al.* 2002; Douglas *et al.* 2003; Krause *et al.* 2003; Walling *et al.* 2003; Motha *et al.* 2004; Miller *et al.* 2005; Yeager *et al.* 2005; Evans *et al.* 2006; Kelley *et al.* 2006; Walling *et al.* 2006; Collins & Walling 2007b; Minella *et al.* 2008; Walling *et al.* 2008).

3.10.2 Development of the sediment fingerprinting technique

Sediment fingerprinting was developed to determine the sources of suspended sediment in catchments. In the 1970s workers used a range of properties (geochemical, mineralogical, mineral magnetic) to trace sediment from different origins (Walling 2005). The properties of a tracer that make them suitable for such studies are that they (through inherent or delivered properties) are measurable, representative, and conservative (Motha *et al.* 2002). In other words, a tracer should be stable through the physical and chemical processes of fluvial transport and spatially and temporally constant for a given source (Caitcheon 1998; Dyer 1998). An example of a tracer is Caesium-137, which binds to soil particles (delivered property), is conservative during transport, and can identify surface versus subsurface erosion sources (Wallbrink & Murray 1993).

Developments in the late 1980s saw the shift to using several soil tracers (composite fingerprints) to discriminate between multiple source areas and the

development of quantitative methods to increase the precision of source area determination. The quantitative methods included statistical tests such as the Kruskal-Wallis to select properties for the composite fingerprint, Discriminant Function Analysis (DFA) to determine the optimum mix of fingerprint properties, and multivariate mixing models to quantify the relative proportions from different source areas (Walling 2005).

Use of the sediment fingerprinting technique has yielded information for effective sediment and pollution control strategies, the development of more comprehensive sediment budgets and models, understanding of sediment delivery from contrasting landuses in a catchment, and understanding of the temporal and spatial patterns of sediment delivery (Collins *et al.* 1997; Collins *et al.* 1998; Collins & Walling 2002). Sediment fingerprinting has been applied to catchments as small as < 2 km^2 to thousands of square kilometres (Collins *et al.* 1998; Russell *et al.* 2001; Krause *et al.* 2003; Minella *et al.* 2008). Careful assemblage of the data can also mean a range of temporal scales can be investigated (Collins & Walling 2004). For example, Collins *et al.* (2001) determined the dynamic nature of suspended sediment sources for intra-storm, inter-storm, and between seasons (Figure 3.9).

Sediment fingerprinting has shown results that are consistent with existing information on sediment yields from different subcatchments and temporal variations (Collins *et al.* 1998). Two papers in particular by Walling (1999) and Collins *et al.* (1998) validated the results of sediment fingerprinting with other techniques.

Walling *et al.* (1999) identified the relative contribution of sediment derived from three different subcatchments to the River Ouse in the UK. The relative sediment contribution as determined by sediment fingerprinting was 82% from the River Swale, 15% from the River Ure, and 3% from the River Nidd subcatchment. These results were compared with annual suspended sediment loads from gauging stations that gave the contributions at Swale (54%), Ure, (37%), and Nidd (10%).

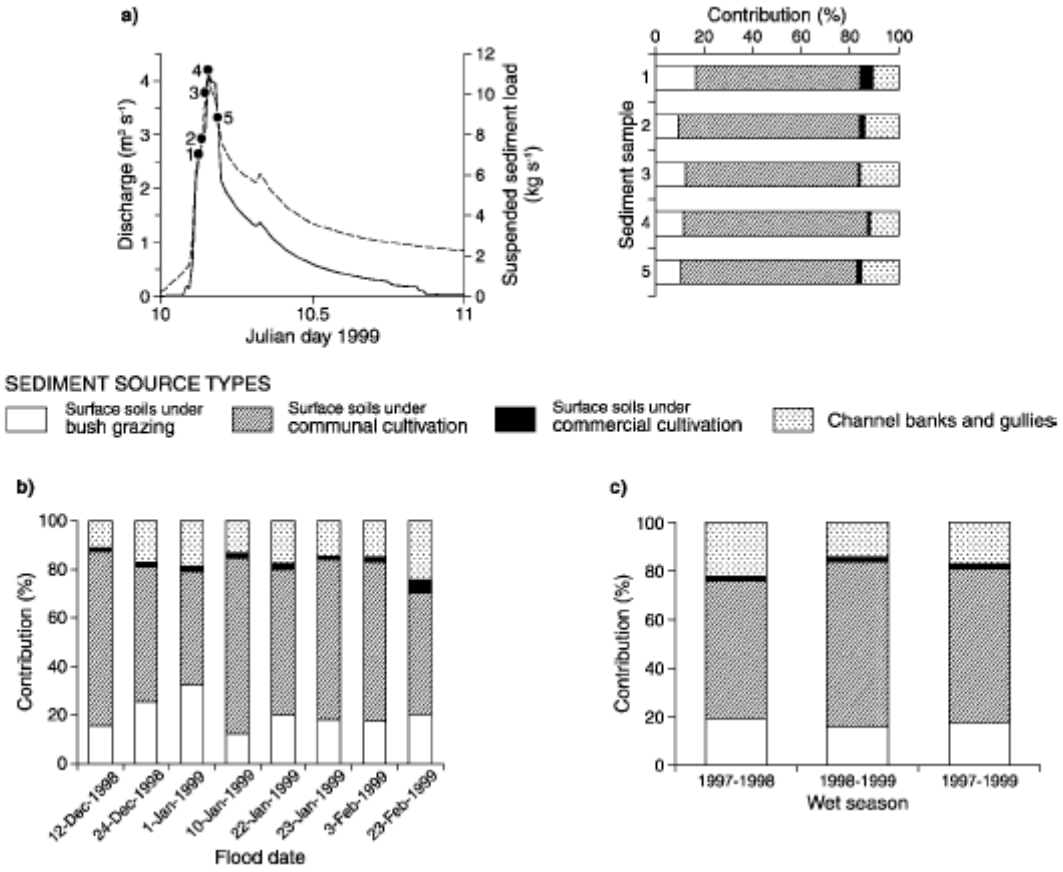

Figure 3.9. Results of sediment fingerprinting showing changes from the contributing sediment source types (surface/bush grazing, surface/communal cultivation, surface/commercial cultivation, and subsurface channel banks and gullies) for: A) intra-storm; B) inter-storm; C) and between seasons (Collins & Walling 2004).

The discrepancies were accounted for by the authors as being caused by spot sampling of water from the rivers during storm events and not being representative of a subcatchments contribution over a longer period as reflected in the gauging results.

Collins *et al.* (1998) identified the relative sediment contributions of geological subareas to the River Exe and Severn River catchments in the UK. The sediment fingerprinting relative contributions were compared with previous findings based on suspended sediment loads and were found to be 'clearly consistent with existing information regarding the suspended sediment yields from different subcatchments', although direct comparison was complicated to the extent that

subcatchments did not correspond directly with geological subareas that were the focus of the study (Collins *et al.* 1998).

3.10.3 The sediment fingerprinting process

The sediment fingerprinting technique (Figure 3.10) is founded on two assumptions. Firstly, that the various source areas can be distinguished on the basis of a range of physical, geochemical and biogenic properties. The use of a number of properties to form the 'composite fingerprint' aims to reduce the spurious source-sediment linkage that may occur when using a single property. Due to the complexity of sediment routing and delivery, a single property will rarely prove adequate to discriminate multiple catchment sources (Walling *et al.* 1999). The second assumption is that the range of selected fingerprint properties can determine the relative importance of various source areas when compared to suspended sediment sink material from a floodplain or estuary (Collins & Walling 2002; Collins & Walling 2004).

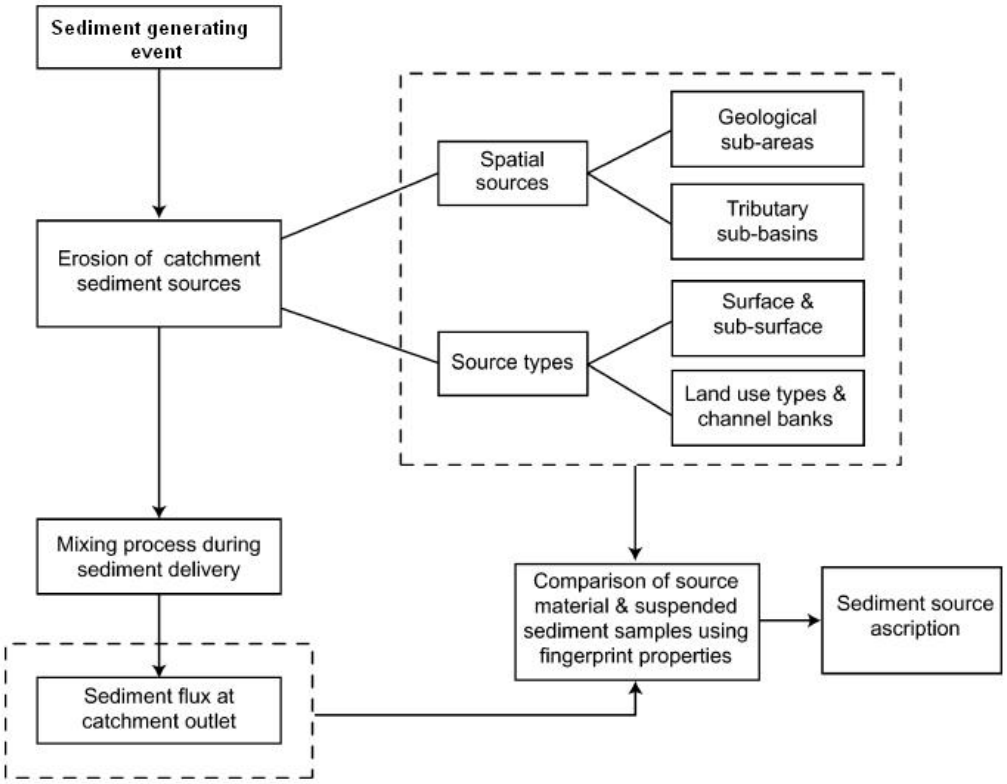

Figure 3.10. Conceptual model of the sediment fingerprinting technique with the erosion, transport and deposition of sediment and the ascription of properties based on either source or spatial types (Collins & Walling 2002).

Some sediment fingerprinting studies have traced sediment source by underlying catchment geology (e.g., Collins *et al.* 1998; Miller *et al.* 2005), subcatchment (e.g., Collins *et al.* 1996), surface vs. subsurface sources (e.g., Collins *et al.* 1997; Owens *et al.* 1999b), or landuse types (e.g., Collins *et al.* 2001). Russell *et al.* (2001) used sediment fingerprinting to examine the contribution of surface, channel bank, and tile drain sources of eroded material.

There have been different statistical approaches taken using the sediment fingerprinting technique such as the Mann-Whitney U-test (Collins *et al.* 1997) or cluster analysis (De Boer & Crosby 1995; Walling & Woodward 1995; Nath *et al.* 2007) to select fingerprint properties, or a chemical mass balance model (Kelley & Nater 2000a), Bayesian statistical approach (Douglas *et al.* 2003), or a Bayesian-Monte Carlo approach (Franks & Rowan 2000) have been used for source ascription. Other authors have adapted mixing models from other fields for sediment source area ascription, such as the US EPA chemical mass balance model that was designed for air quality studies (Kelley & Nater 2000b), or the stable isotope analysis in R (SIAR) mixing model that was designed for determining the diet compositions of consumers based on stable isotopes (Gibbs 2008). For this study, the approach taken will be that of workers from the University of Exeter (Collins *et al.* 1997; Collins & Walling 2002) as this is where the composite sediment fingerprinting approach was developed and this approach has been successfully applied to catchment sediment source ascription in other parts of the world.

Sediment fingerprinting is a three stage process. The first stage is to select the properties that will form the composite fingerprint from analysis of soil samples taken from the source areas. The range of properties may be geochemical, radionuclide, mineral magnetic, or biogenic. Depending on the investigation, suspended sediment source areas may be sampled on geological areas, subcatchments, landuse types, or erosion sources (Collins & Walling 2002; Collins & Walling 2004; Walling 2005).

3.10.3.1 Stage 1: selection of candidate elements for the fingerprint

The method to select the candidate fingerprint properties is the Kruskall-Wallis *H*-test (Appendix A). This is the non-parametric equivalent of a one-way analysis of variance (ANOVA), but uses the sums of the rankings rather than the raw data to determine significant differences between populations.

For example, suppose we wish to find the best properties to distinguish between two subcatchments (source areas) draining into a lake (sink area). Five sites are sampled in the two subcatchments for a total of 10 samples. The 10 sediment samples will be analysed for a range of geochemical properties. The results of a particular property (e.g., magnesium) are ranked from lowest to highest (i.e., 1 ➔ 10) and the ranks are summed for each subcatchment. Hypothesis testing is used to determine if the sums of the ranks are significantly different between the two subcatchments (i.e., their *p-value* being below the 5% level of significance). If in this example all the lowest magnesium concentrations are in one subcatchment (ranks 1 ➔ 5 = 15) and all the highest magnesium concentrations are in the other subcatchment (ranks 6 ➔ 10 = 40). It will be determined that magnesium does vary significantly between the two subcatchments and that it is a useful property to include in the fingerprint to distinguish the two potential subcatchment source areas. All the other geochemical properties will be interrogated independently in this same way.

3.10.3.2 Stage 2: optimisation of the fingerprint elements

The second stage optimises the number of fingerprint properties and this is achieved by Discriminant Function Analysis (DFA) (Appendix B). DFA is similar to multivariate analysis of variance (MANOVA) in that it examines the ability to predict membership to a group (e.g., different landuse types) based on the means of the variables. In other words, can different groups be distinguished as significantly different based on the means of the variables selected?

A common method used in DFA (that will be employed in this research) is forward stepwise analysis. In the first step all the elements (as selected by the Kruskall-Wallis *H*-test) are considered together to find the one element that affords the greatest discriminatory power between groups, testing the null

hypothesis that there is no difference between groups. Matrices are determined for the within-group and between-group sums of squares and are used to find an *F*-ratio to see if the result is statistically significant. The procedure is guided by the *F*-to-enter and *F*-to-remove results. The element with the largest *F*-ratio is chosen and entered into the model, provided that its value is larger than the designated *F*-to-enter value (Tabachnick & Fidell 1996). The second step of the DFA process begins with the new model as the basis for considering the remaining elements (StatSoft Inc 2007). The DFA process does have the potential for any elements already included in the model at an earlier iteration to be removed. Removal occurs if the *F*-ratio for the element is less than the designated *F*-to-remove value. The smallest combination of elements that gives the best discriminating power is found by minimising the Wilks' lambda score (Collins & Walling 2002). The Wilks' lambda is a test statistic used in multivariate analysis of variance to test whether there is a difference between the means of different groups based on a combination of variables (Crichton 2000).

The statistical software package STATISTICA 8.0 goes through the forward stepwise DFA process using a default of the *F*-to-enter of one. In other words, an element will be accepted into the model when its *F*-ratio is larger than one. The value of one has also been used by other researchers (e.g., Collins & Walling 2002). Figure 3.11 shows the *F* distribution with degrees of freedom of 5 and 66, where the *x*-axis shows the *F*-to-enter values from one to four and the corresponding significance levels (α) are in the inserted table. In the example in Figure 3.11, a null hypothesis that there is no difference between groups would be rejected at the 42% level of significance if the observed *F*-ratio was greater than one. This example (like the process in STATISTICA) has the potential of 'accepting' all the elements that were selected by the Kruskal-Wallis *H*-test procedure. Further more, STATISTICA has a default *F*-to-remove value of zero, which means once an element is in the model it will not be removed.

3.10.3.3 Stage 3: determining the source area contributions by a mixing model

The third stage uses a multivariate mixing model to estimate the relative contributions of the suspended sediment source areas to a particular sediment

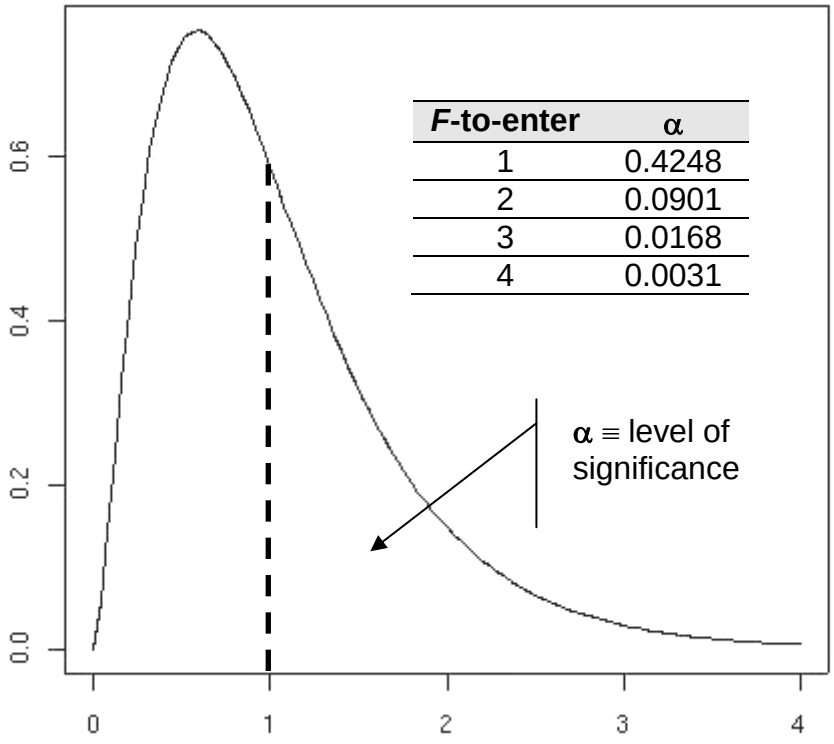

Figure 3.11. Example of the *F* distribution for a degrees of freedom of 5 and 66 with the *F*-to-enter values listed on the *x*-axis (Thompson 2008).

sink. For each of the composite fingerprint member elements, a linear equation is constructed that relates the mean concentration of the element in each source sample to that in the sink sample. Thus, the composite fingerprint is represented by a set of linear equations, one for each element. These are not solved directly, but the least squares method is used and the proportion from the different source areas/groups (*i*) is estimated by minimizing the sum of the squares of the residuals (R_{es}) for the elements (Collins *et al.* 1997). The residual for element (*j*) is:

$$x_{sj} - \sum_{i=1}^{m} P_i \overline{x}_{ij} \qquad \text{(Eqn 3.2)}$$

The residual is scaled by x_{sj} to take into account the differences in the units associated with each element. The least squares equation to be minimised is:

$$R_{es} = \sum_{j=1}^{p} \left(\frac{x_{sj} - \sum_{i=1}^{m} P_i \bar{x}_{ij}}{x_{sj}} \right)^2 \qquad \text{(Eqn 3.3)}$$

In this formulation

p is the number of element in the composite fingerprint

m is the number of source groups (e.g., landuse)

R_{es} is the sum of squares of the residuals

x_{sj} is the concentration of element (j) in the sediment sink sample

$\bar{x}_{ij}$ is the mean concentration of element (j) from the sample in source group (i)

P_i is the relative contribution/relative proportion from source group (i) in the sediment sink sample.

Two linear constraints must be satisfied, and they are the contribution/relative proportion from each source must lie between 0 and 1 ($0 \le P_i \le 1$) and the sum of the contribution/relative proportions from all sources is 1 (or unity). That is:

$$\sum_{i=1}^{m} P_i = 1 \qquad \text{(Eqn 3.3)}$$

(Owens *et al.* 1999b)

Another way of explaining the mixing models is to use a geometric example (Figure 3.12). There are three variables in the example (Landuse 1, 2, and 3) forming a three dimensional open pyramid vector. There are two end members (E_1 and E_2) that can be thought of as the means of two element concentrations (or tracers) from sampling of the three landuse types. The two end members define a plane (shaded) which the mixture X (i.e., the sink sample) must lie within. All mixing models have two natural constraints; 1) that all end members have only positive variables; and 2) that all contributions to a given mixture are positive. In the example below, natural constraint 1 means that the end members must lie

within the positive vector of the three landuses (or the orthant of Landuse 1, 2, and 3), and natural constraint 2 means that the mixture must lie within the shaded plane spanned by the two end members (Akerjord & Christophersen 1996).

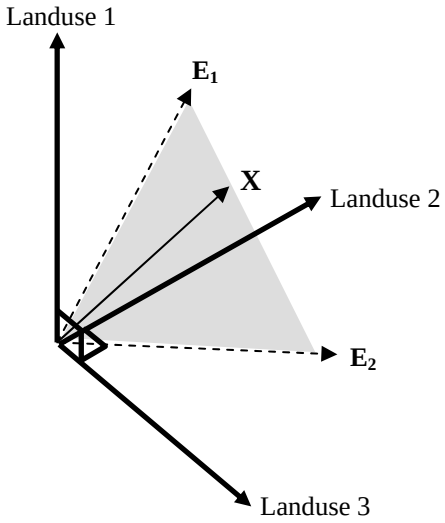

Figure 3.12. Visualisation of a mixing model example where a positive vector is defined by three landuse types (1, 2, 3) and the mean value of two elements (E_1 and E_2) define a plane in which the mixture X (sink sample) must lie. (After Akerjord & Christophersen 1996).

3.10.3.4 Sediment fingerprinting sampling strategy

There are a range of potential source area sample collection strategies reported in the literature. Collection strategies ranged from randomised to targeted. For example, a source area grid sampling pattern was used by (Miller *et al.* 2005), sampling of areas 'likely to be eroded' (but not necessarily actively eroding) was used by (Collins *et al.* 1998), and a targeted sampling strategy of actively eroding sites as identified by preliminary catchment modelling was used by (Wallbrink 2004). This thesis will use the middle course and sample the Whangapoua catchment for areas likely to be eroded.

3.10.4 Limitations of the sediment fingerprinting technique

The limitations of sediment fingerprinting can be categorised into four main areas. The limitations are particle size composition; organic matter composition; mixing model uncertainties; and assumptions on conservativeness of properties during transport (Franks & Rowan 2000; Motha *et al.* 2002; Walling 2005).

It is known that the detachment and transport of sediment is size selective (Slattery & Burt 1997). It is also known that tracer properties such as ^{137}Cs are particle size dependant (He & Walling 1996; Dyer & Olley 1999). Differences in characteristic particle sizes between the source area and sink will alter the tracer signature and lead to erroneous results (Davis & Fox 2009). This problem is largely overcome by either using the simple approach of limiting the analysis to size fractions of < 63 μm (e.g., Wallbrink *et al.* 1998), or using correction factors (e.g., Russell *et al.* 2001). Corrections for organic matter content have been used in sediment fingerprinting studies (e.g., Collins *et al.* 1997), but the relationship between organic matter content of source area and sink samples is complex and difficult to generalise (Walling 2005). A study of the difference between organic matter in source and sink samples found that the highest coefficient of variation was 6.6% (Motha *et al.* 2002).

Optimisation procedures in the mixing model may introduce problems of equifinality, where different property combinations could produce the same goodness of fit (Small *et al.* 2002; Walling 2005). The goodness of fit is how uncertainty is characterised in the application of this mixing model (Collins *et al.* 1997; Walling *et al.* 2006). The problem of equifinality, along with natural variability of source properties, has prompted some workers to apply a Bayesian and Monte Carlo approach to the mixing model (Small *et al.* 2002; Douglas *et al.* 2003; Krause *et al.* 2003).

Sediment fingerprinting is based on the assumption that source area characterisation can determine the relative importance to sediment sources based on selecting fingerprints that link source to sink. Some fingerprints (such as some geochemical properties) do not remain conservative during transport and this area has received little attention (Motha *et al.* 2002). It should also be noted that while

sediment fingerprinting can distinguish the source area of sediment, it cannot determine its residence time in fluvial systems (Phillips & Marion 2001).

3.10.5 Sediment fingerprinting applications in New Zealand

Sediment fingerprinting has not been used in New Zealand, and this review of the literature has found only one study of a novel sediment tracer (a plant compound specific isotope of ^{13}C) that is similar to this technique. Therefore a study trialling sediment fingerprinting in New Zealand to examine catchment suspended sediment sources will require both input data, as well as validation data (Collins & Walling 2004). The validation data will be derived from radionuclides, stream gauging, and modelling techniques. Caution must be exercised when comparing these different results. This is because when different erosion monitoring techniques are employed side by side, they will have different spatial and temporal scales (Brazier 2004). It can also be alternatively argued that by using a range of techniques that focus on different scales, the possibility of misunderstanding the cause and effect (by missing the relevance of processes that operate at different scales) will be reduced (Wilbanks & Kates 1999; Peeters *et al.* 2008). The review continues on the validation techniques.

3.11 Fallout radionuclides

3.11.1 Introduction

Fallout radionuclides (or environmental radionuclides) are found in relatively low levels in the environment but at measurable levels. They are delivered to the earths surface as fallout from the atmosphere, are spatially uniform, and bind strongly to soil particles, and have energies that can be measured which makes them useful in soil erosion studies (Zapata *et al.* 2002; Walling 2006). The principal radionuclides used in geomorphic studies are Ceasium-137 (^{137}Cs), Lead-210 (^{210}Pb), and Berillium-7 (^{7}Be), and have the advantage over methods such as the Universal Soil Loss Equation in that soil deposition is accounted for (Montgomery *et al.* 1997). Radionuclides have been extensively employed in soil erosion studies. (Ritchie & Ritchie 2001) cite over 2,000 publications in a bibliography of soil erosion studies using ^{137}Cs alone. Radionuclides have been found to be conservative during sediment transport (Motha *et al.* 2002; Yeager & Santschi 2003)

3.11.2 Cesium-137

Caesium is an alkali metal with a similar chemistry to sodium, potassium and other elements of Group I in the Periodic Table (Wallbrink *et al.* 2002a). The isotope ^{137}Cs (half life 30 years) is found in the environment as a consequence of above ground nuclear testing that occurred between 1945 and 1974. ^{137}Cs was injected into the stratosphere by the dust cloud that results from nuclear bomb blasts. ^{137}Cs circulated globally in the stratosphere before entering the troposphere where it is scavenged by clouds to return to the earths surface principally as wet precipitation. ^{137}Cs fallout is strongly related to local patterns and rates of precipitation. Once deposited onto the earths surface, it binds onto soil particles in an almost non-exchangeable form (Davis 1963; Lomenick & Tamura 1965; Wise 1980; Ritchie & McHenry 1990; Simkiss *et al.* 1993).

3.11.3 Lead-210

^{210}Pb is a naturally occurring radionuclide (half life 22 years) that forms as part of the ^{238}U decay series (Figure 3.13). ^{238}U decays in the earths lithosphere until it forms ^{226}Ra, which then decays to an inert gas ^{222}Rn which escapes into the atmosphere. Through a number of short lived daughters, ^{210}Pb is formed where it attaches itself to aerosol particles before it is scavenged by rain to return to the earths surface (Koide *et al.* 1972; Turekian *et al.* 1977; Smith 1982) where it also labels soil particles. Lead is located in Group IVA of the Periodic Table, and of the four radioactive isotopes of Lead, ^{210}Pb is the only one to have a half life over 12 hours at 22 years (Doe 1969; Nriagu 1978).

Because not all ^{222}Rn escapes into the atmosphere, ^{210}Pb also forms in situ in the soil. This can confuse studies of soil erosion when using ^{210}Pb as a soil tracer. The in situ ^{210}Pb will be in equilibrium with its parent ^{226}Ra, and is termed 'supported' ^{210}Pb. The atmospherically derived ^{210}Pb is determined by subtracting the supported amount from the total inventory, and is termed the 'unsupported' or 'excess' ($^{210}Pb_{ex}$) (Koide *et al.* 1972; Wise 1980).

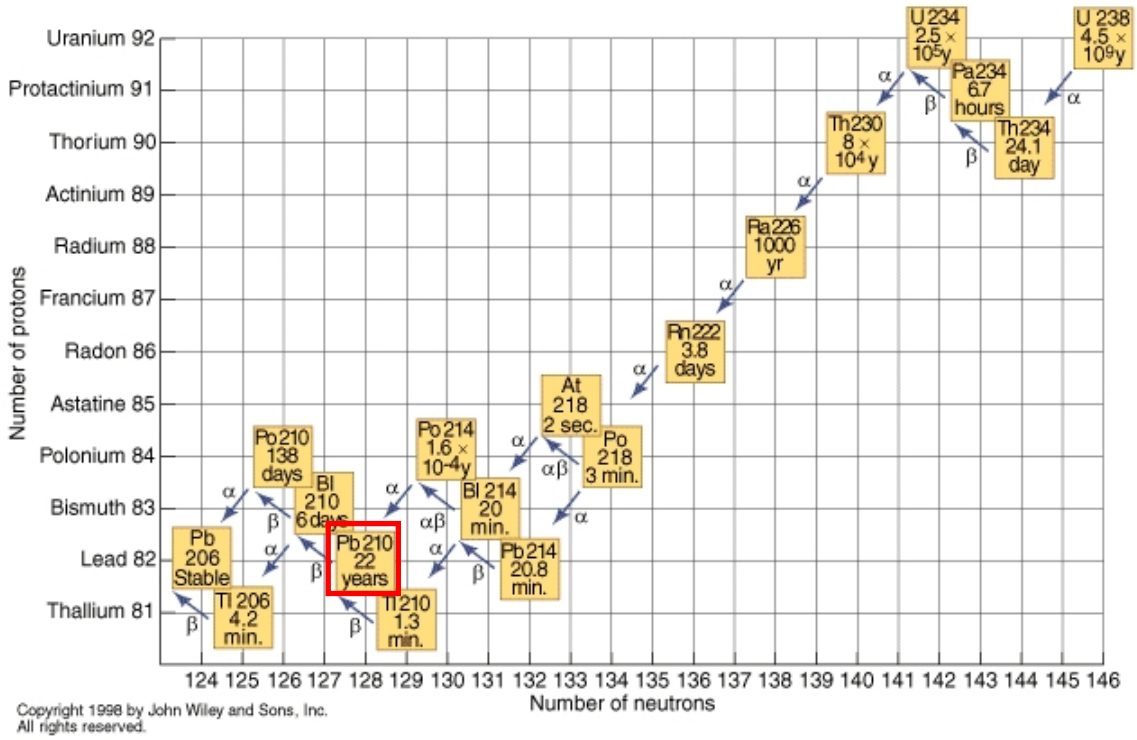

Figure 3.13. Lead-210 (half life 22 years) in the Uranium-238 decay scheme (Trefil & Hazen 2004).

3.11.4 Radionuclides in soil erosion studies

Radionuclides have been used to test erosion models (Di Stefano *et al.* 1999; Porto *et al.* 2003) and to date sediments (Longmore 1982; Wasson *et al.* 1987). The main use of radionuclides has been focused on soil erosion. Studies involving ^{137}Cs and other radionuclides examining soil loss from plots began in the 1960s (Ritchie & McHenry 1990).

The main assumption of radionuclide studies is that the fallout distribution is relatively uniform, at least over a small area (Walling 2003), however spatial variability may be as large as 40% (Fredericks *et al.* 1988; Sutherland 1994; Wallbrink *et al.* 1994b; Sutherland 1996). In New Zealand it has been observed that there is a strong correlation between ^{137}Cs in undisturbed soils and rainfall (Basher & Matthews 1993) and therefore the spatial variation in rainfall is likely to result in a spatial variation in radionuclide distribution.

Typical applications of radionuclides in soil erosion studies involve the establishment of a reference value for the radionuclide at an adjacent undisturbed site. Comparison with this reference level of the radionuclide to the disturbed area will show the patterns of soil loss (below reference value) or deposition (above reference value) (e.g., Wise 1980; Elliott *et al.* 1990; Ritchie & McHenry 1990; Basher *et al.* 1995; Govers *et al.* 1996; Wallbrink & Murray 1996; Walling & He 1997; Di Stefano *et al.* 1999; Walling *et al.* 2002b). The conversion of the proportional differences between reference and disturbed areas is achieved by a number of methods. Some of these relationships are derived from; erosion plot data (e.g., Elliott *et al.* 1990; Sutherland 1991; Loughran *et al.* 1992); theoretical models including proportional models (e.g., Kochanoski & De Jong 1984), gravimetric method (e.g., Brown *et al.* 1981), profile distribution models (e.g., Zhang *et al.* 1990), and depth distribution curves (e.g., Gillison *et al.* 1996; Wallbrink *et al.* 2002a). These models are reviewed in Walling *et al.* (2002a).

Radionuclides have also been used to construct sediment budgets for drainage basins. Using a similar approach to comparing soil deposition/loss within the catchment, an inventory for the radionuclides within the catchment is established and this inventory is then related to the total sediment flux from the basin as measured by other traditional methods such as stream gauging (e.g., Owens *et al.* 1997; Walling *et al.* 2001; Blake *et al.* 2002; Wallbrink *et al.* 2002a; Walling *et al.* 2002b).

Another significant use of radionuclides is the identification of suspended sediment sources. This is based on the different depth distribution profiles of ^{137}Cs, ^{210}Pb, and ^{7}Be (Figure 3.14).

Because of the different half life of the radionuclides and cessation of ^{137}Cs input from the mid 1980s, this means that concentrations down a soil profile differ. ^{210}Pb is concentrated at the surface and declines exponentially down the profile. This is similar to ^{137}Cs, but peak concentrations for ^{137}Cs are usually found several centimetres below the surface because of declining input and downward migration attached to soil particles (Doering *et al.* 2006). The short half life of ^{7}Be means

that it is concentrated at the surface, but is not found in any significant levels below the surface layers (Wilson *et al.* 2003).

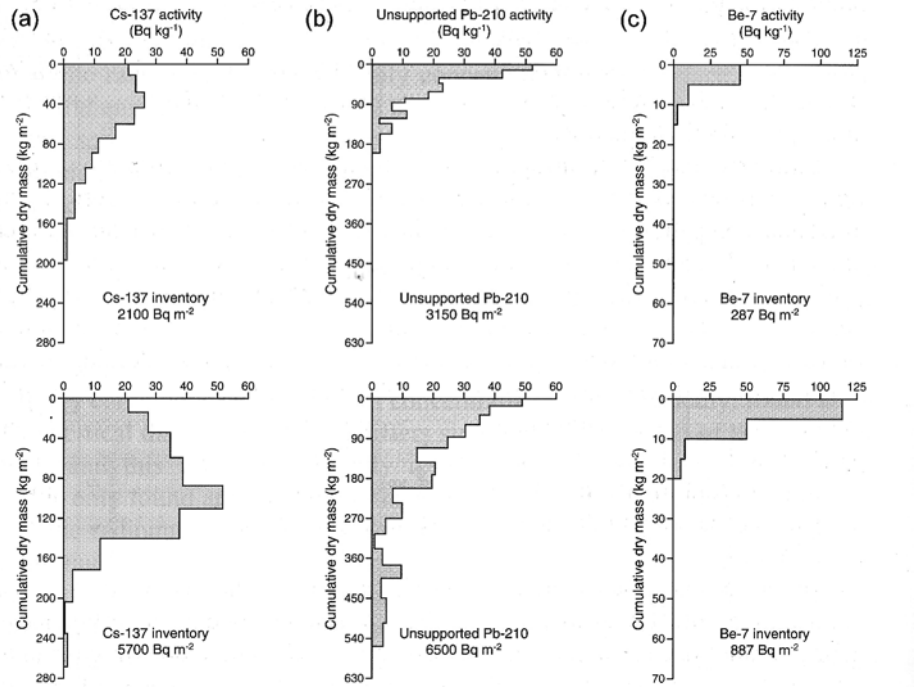

Figure 3.14. Example of depth penetration characteristics down a soil profile (as measured by cumulative dry mass) of ^{137}Cs, ^{210}Pb, and ^{7}Be in undisturbed (top row) and cultivated (bottom row) soils (Walling 2002).

The depth penetration characteristics and differing half lives have been exploited to elucidate the sources of catchment suspended sediment (Walling & Woodward 1992; Olley *et al.* 1993; Wallbrink & Murray 1993; Wallbrink *et al.* 1998; Wallbrink *et al.* 1999; Matisoff *et al.* 2002; Wallbrink 2004; Zhang *et al.* 2004; Matisoff *et al.* 2005; Wilson *et al.* 2005; Yeager *et al.* 2005; Nagle *et al.* 2007; Smith & Dragovich 2008). The different depth penetration characteristics are exploited by using the ratios of the radionuclides and linking them back to the way the sediment sources are tagged. Using ^{137}Cs to ^{7}Be ratios for example, as sheet erosion removes the surface soil the derived sediment will be tagged with high concentrations of ^{137}Cs and ^{7}Be. Rill erosion sediment will be similarly tagged with ^{137}Cs but the sediment will be derived from below the zone of significant ^{7}Be concentration and will have a low concentration of ^{7}Be. Sediment from gully incision will be derived from a zone below ^{137}Cs depth penetration and

will be low in both tracers. Gully floor material will be tagged with ^{7}Be because of the constant input of that radionuclide but low in ^{137}Cs (Figure 3.15).

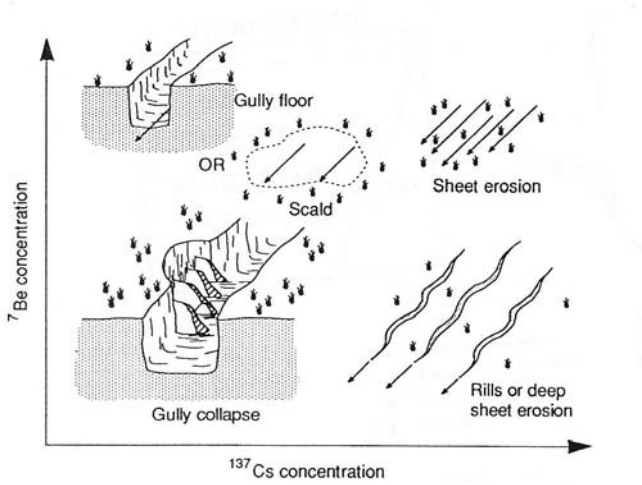

Figure 3.15. The depth penetration characteristics (increasing concentration toward the surface) of ^{137}Cs and ^{7}Be and how the ratios of the two tracers can be used to determine the source of sediment (Olley *et al.* 1993).

The reason for using ratios of radionuclides as opposed to a single tracer is two fold. Firstly, using different ratios can yield information on different sediment sources in a catchment. As shown in Figure 3.15, the ratio of ^{137}Cs and ^{7}Be can discriminate between sheet, rill, gully, and gully floor sediment sources. The second reason is to reduce the spatial variability and extrinsic[2] variability of the radionuclides. Using ratios of radionuclides has been found to increase the precision of radionuclide estimation (Wallbrink & Murray 1996; He *et al.* 2002; Yeager & Santschi 2003).

The use of radionuclide tracers, and in particular various combinations of radionuclide tracers, have been used in geomorphic studies to determine the source of eroded sediment. Examples of combinations of radionuclides include ^{137}Cs and $^{210}Pb_{ex}$ (Wallbrink & Murray 1996; Fukuyama *et al.* 2008; Mizagaki *et al.* 2008; Smith & Dragovich 2008; Zehetner *et al.* 2008), ^{137}Cs and ^{7}Be (Olley *et al.* 1993), $^{210}Pb_{ex}$ and ^{7}Be (Matisoff *et al.* 2005), ^{137}Cs and ^{226}Ra (Wallbrink 2004), ^{137}Cs, $^{210}Pb_{ex}$, and ^{7}Be (Whiting *et al.* 2005; Doering *et al.* 2006), ^{137}Cs,

[2] Examples of extrinsic variables are particle size and radionuclide associations with particulate organic carbon (POC).

$^{210}Pb_{ex}$, ^{232}Th, ^{226}Ra, ^{40}K (Belyaev *et al.* 2004), and radionuclides from the ^{238}U and ^{232}Th series (Yeager & Santschi 2003).

The approach taken by Wallbrink (2004) and Wallbrink *et al.* (2003b) where a limited number of radionuclide samples were analysed to identify different sediment sources areas appeared suitable for use in this research. In one study, uncultivated, cultivated, and subsurfaces were the potential sediment source areas being quantified (Wallbrink 2004), and in the other it was cultivated, uncultivated (forests, pastures, and stock tracks), and gullied areas (Wallbrink *et al.* 2003b). An example of the Wallbrink (2004) approach is shown in Figure 3.16.

Ratios of ^{137}Cs and ^{226}Ra are used to distinguish surface (cultivated and uncultivated) and subsurface sources. The mean concentrations were used to determine the relative proportion of the surface and subsurface sources contributing to the Brisbane and Logan River sediments. The results were that the Brisbane and Logan River sediments were predominantly from subsurface origins.

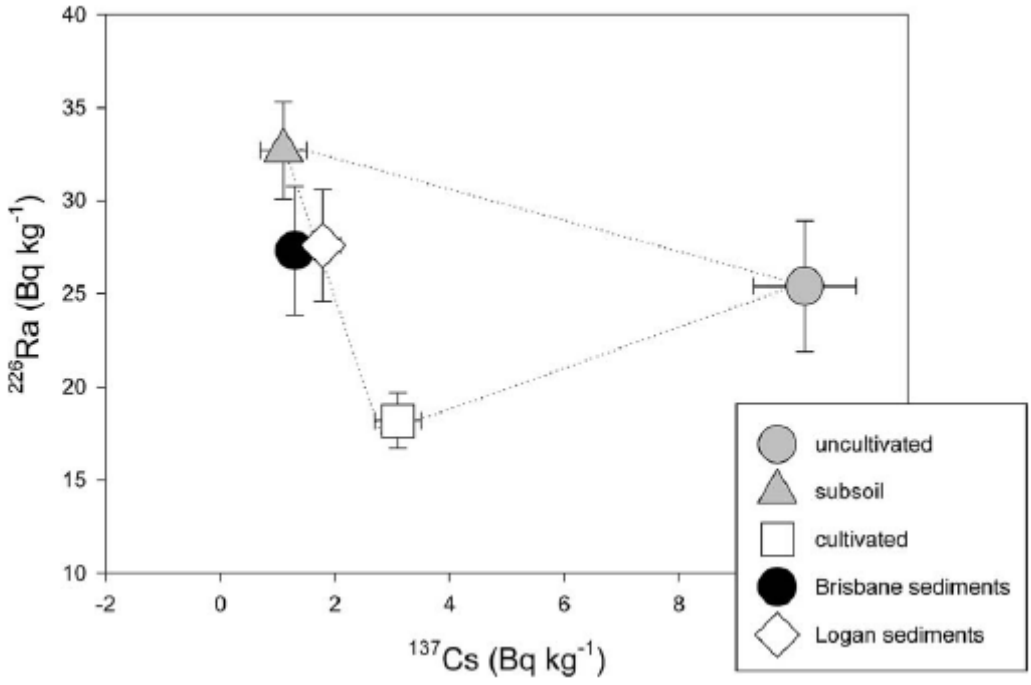

Figure 3.16. Mean values for ^{137}Cs and ^{226}Ra sources samples for uncultivated, cultivated, and subsoil source samples (Wallbrink 2004).

The combination of ^{137}Cs and ^{226}Ra was successful in identifying sediment sources for two reasons; the first is because the ratio of radionuclides

distinguished cultivated, uncultivated, and subsurface derived sediment due to the different depth penetrating characteristics of ^{137}Cs and ^{226}Ra; and secondly the radionuclides appear to have been conservative during transport as mean values of the sediment source areas provided an end member envelope (dashed line in Figure 3.16) in which the river (or sink) sediment fitted.

Following the analysis for radionuclide concentrations, the mean values for the ratio of each sediment source landuse/erosion form is then used in a mixing model based on Collins *et al.* (1997) and similar to that used in the sediment fingerprinting technique. The mixing model was used to quantify the relative contributions of each sediment source areas contributing to the harbour. The graphical representation of the mean values for the sediment source landuse/erosion form and the sinks (Figure 3.16) shows that the uncultivated sediment source area did not contribute to the catchment sinks. The sink was dominated by subsoil and cultivated sources. The results of the mixing model in this example was that approximately 66% (±10) of suspended sediment was derived from subsoil sources, 33% (±10) was from cultivated areas, and 1% (±10) was from uncultivated sources.

3.12 Suspended sediment monitoring

The optical properties of streams (i.e., turbidity) have been widely used to monitor sediment flux in streams (Gippel 1989; Gippel 1994; Gippel 1995; Grayson *et al.* 1996; Sun *et al.* 2001; Armstrong & MacKenzie 2002; Lewis 2002b; Schoellhamer & Wright 2002; Mitchell *et al.* 2003; Lawler *et al.* 2006; McKee *et al.* 2006; Stubblefield *et al.* 2006; Harris *et al.* 2007). More recently the use of Optical Backscatter Sensors (OBS) coupled to data recording instruments has provided a convenient and time/labour/cost effective method of monitoring catchment sediment yields (Sun *et al.* 2001). The OBS work by transmitting light into the water column and the greater the number of particles in suspension, the greater the scatter or absorption of the light which is detected by the probe (Gregory 2006).

The first part of the method is to firstly convert the millivolt (mV) output of the OBS into nephelometric turbidity units (NTU). NTU is not an absolute

measurement, but expressed relative to an artificial standard, usually formazine (Gippel 1994; Anderson 1998). Formazine is a white polymer suspension of particles with a mean weight percent diameter of 2.5 μm. If suspended particle properties do not alter, a linear relationship should be expected between the mV output and NTU. Any deviation of slope or non-linearity at high concentrations is caused by differences in field versus Formazine properties (Gippel 1989).

The next step is to develop a relationship between NTU and suspended sediment concentration (SSC) which is established after field deployment by manual or automated sampling of the stream under various conditions. The relationship may be either a linear regression, a non-linear equation, or a polynomial function (Sun *et al.* 2001). Workers have reported a strong correlation between turbidity and material in suspension, such as total suspended solids and total phosphorus (e.g., Grayson *et al.* 1996; Stubblefield *et al.* 2006)). Once the NTU and SSC relationship is established, then NTUs can act as a proxy for SSC. NTU values are recorded in the field by the data logger along with flow data to arrive at a sediment yield.

The conventional approach to establishing a sediment yield estimate from suspended sediment data is to establish a sediment rating curve which defines the relationship between stream discharge (or flow) and suspended sediment concentration (Phillips *et al.* 2005; Gao 2008; Khanchoul & Jansson 2008). The sediment rating curve method is a well established practice and authors have reported well formed linear relationships (e.g., Gippel 1993; Lewis 2002a). The sediment rating curve relationship and flow records are then used to derive an averaged sediment yield (Figure 3.17-A). The sediment rating curve is unsuitable for data that displays a wide scatter (e.g., Figure 3.17-B).

The storm sediment yield (SSY) method overcomes problems of scattered data by using the data in a different way. The SSY method forms a relationship between individual storm events and the total amount of sediment that was derived during the whole storm event. The SSY method also overcomes the problem of loss of information by inter-annual variation in rainfall. The sediment yield/peak flow

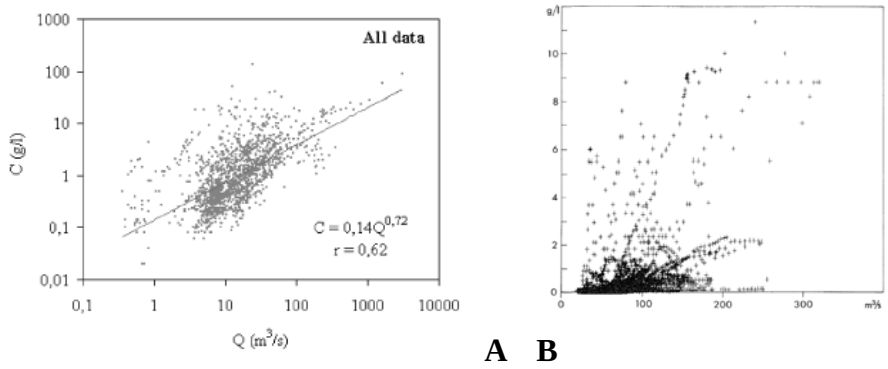

A B

Figure 3.17. A) Example of a sediment rating curve relationship between discharge (Q) and SSC (g/l) (Khanchoul & Jansson 2008); B) example of the data scatter that can occur between discharge (X axis) and SSC (Y axis) (Jansson 2002).

relationships used in the SSY method have been shown to provide the best correlation over other parameters such as runoff factors and rainfall erosivity factors (Hicks 1990 as cited in Hicks 1994a). The SSY method is based on the assumption that most catchment sediment is eroded in larger storm events, and New Zealand studies show the importance of larger events in moving the majority of catchment sediment (e.g., Basher *et al.* 1997; Hicks & Basher 2008).

The SSY method (Hicks 1994b) establishes a relationship between individual storm events (identified by peak flow) and the total sediment amount derived for the event. The SSY method separates the peak (or quick) flow from the base flow in a storm hydrograph and determines the total sediment derived for that storm event (Figure 3.18). This is repeated for a range of storm events so that a number of peak flow/sediment yield observations are recorded so a storm sediment yield/peak flow relationship is formed. The continuous flow record for a catchment is used to firstly identify peak flows, and then from the storm sediment yield/peak flow relationship the total sediment yield for the catchment is calculated to arrive at a catchment erosion rate in t km^{-2} yr^{-1}.

In a review of suspended sediment monitoring techniques using field turbidity, Wren *et al.* (2000) note that while OBS have a wider linear response than other probes and allow good temporal and spatial resolution, they are disadvantaged by particle size dependence. OBS are more sensitive to changes in the smaller size fractions (20-50 μm) than to changes in larger sizes (200-500 μm). The size

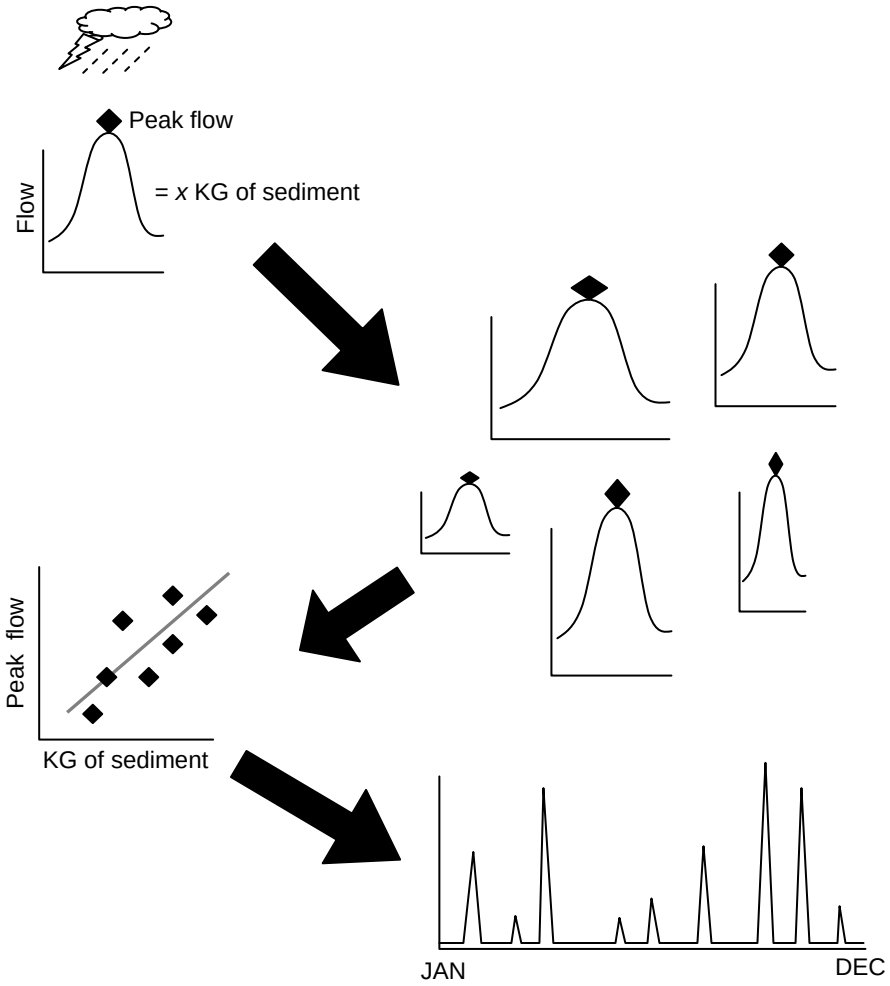

Figure 3.18. Flow diagram of the storm sediment yield method.

sensitivity characteristics of OBS probes has also been noted by other authors (Davies-Colley & Smith 2001; Schoellhamer & Wright 2002). Gippel (1995) observed that particle size variations can cause variations in readings by a factor of four for the same sediment concentration. Gippel (1989) found that relationships between turbidity and suspended solids for stream water samples was site specific and drainage basin subcatchments had slope variations ranging from 0.52 to 1.46.

Armstrong & MacKenzie (2002) examined the impact of gullying on six small grazing catchments in NSW, Australia by turbidity monitoring. The catchments ranged in size from 7.3 ha to 510 ha. Each catchment was instrumented to record rainfall and flow over artificial weirs. Turbidity characterisation was accomplished by automated water sampling and laboratory measurement of NTU. HYDSYS software was used to calculate annual sediment loads. Sediment loads

from gullied catchments were an order of magnitude higher than from un-gullied catchments.

3.13 Modelling

3.13.1 Introduction

There has been a rapid increase in the use of catchment erosion models to identify and quantify suspended sediment sources (Merritt *et al.* 2003). Models can be used to target soil conservation strategies, assist in understanding broad-scale erosion dynamics, allow land managers to design land regulation strategies, and predict long-term sediment and nutrient loadings of streams (Nearing 2006; Bhattarai & Dutta 2007). Models can also suffer from a range of problems including over-parameterisation, unrealistic input requirements, unsuitability of model assumptions/parameters to local conditions, and inadequate testing and documentation of performance (Merritt *et al.* 2003). Most models fall into one of three categories; empirical; conceptual; or physically based (Merritt *et al.* 2003; Aksoy & Kavvas 2005; de Vente & Poesen 2005).

3.13.2 Model selection

Each model will have advantages and disadvantages, but the problem with all models is that they seek to replicate sediment detachment, transport, and delivery processes that are still poorly understood at larger scales (Prosser *et al.* 2001b). The complexity of natural systems in differences in transport media, dimensions, temporal and spatial scales, the thresholds of movement of sediment/water/solutes through the media, and their interactions at catchment scales, makes modelling difficult (Merritt *et al.* 2003; De Vente *et al.* 2006). The equations on which models are based are typically derived from plot scale studies and there is little information to support their validity at larger scales (Pickup & Marks 2001). Scale issues with models have been reported by other authors (de Vente & Poesen 2005; Boix-Fayos *et al.* 2006; Boix-Fayos *et al.* 2007; Govers *et al.* 2007; Peeters *et al.* 2008). There is a paradox between data collection (to improve and validate models) and erosion modelling (to replace data collection) (Brazier 2004).

Consequently there is no ‘right’ model to use. Rather, model selection should be determined by questions that the model user is attempting to address and the

erosion processes that require explicit representation. The spatial and temporal resolution of the model should also match the users requirements (Merritt *et al.* 2003). The argument has been made by Prosser *et al.* (2001b) that the lack of verifying data on large scale natural system complexity has led to models being based on small scale empirical relationships. Empirical model relationships should be replaced by simple physically based predictions of the spatial patterns of sediment transport through fluvial systems. Point sources of sediment such as landslides remain difficult to describe in most models (De Vente *et al.* 2006).

There has been a range of models used in New Zealand for examining soil erosion. They include digital elevation models (DEMs) (De Rose *et al.* 1998; Betts *et al.* 2003; Kasai *et al.* 2005; Marden *et al.* 2005; Kasai 2006; Fuller & Hutchinson 2007), simple conceptual models (Parkyn *et al.* 2005), HydroTrend (Kettner *et al.* 2007), mass balance models (Basher & Ross 2002; Page *et al.* 2004; Phillips & Gomez 2007), MIKE 11 (Gomez *et al.* 2007), BQART (Syvitski & Millman 2007), SHETRAN (Adams *et al.* 2005; Adams & Elliott 2006), TOPMODEL (Claessens *et al.* 2005), HEM (Cogle *et al.* 2003), BNZ (Cooper & Bottcher 1993), CREAMS (Cooper & Bottcher 1993), and sub-components of CREAMS and EUROSEM (Elliott *et al.* 2002). NIWA developed a Catchment Decision Support System (CDSS) which uses a GIS interface and incorporates other models including BNZ, OUTLOOK, TOPMODEL, and GLEANS (Rodda *et al.* 2001). Models have also been used on orogenic studies, such as CHILD (Miller *et al.* 2007). The SEDiment River NETwork Model (SedNet) was developed for addressing land and water management issues at catchment scale (or greater) as part of the Australian National Land and Water Resources Audit (Prosser *et al.* 2001a). Simplified versions and components of SedNet have been used in New Zealand (Schierlitz *et al.* 2006; Landcare Research 2007).

Modelling the Whangapoua catchment provides a third method of comparing the sediment fingerprinting results. From the discussion above there is no right model but selection should be based on accounting for sediment generation from the three landuses and/or the erosion forms identified in the conceptual models. The ease of use of the models was an important factor in model choice. Consequently

two models were selected to estimate sediment generation within the Whangapoua catchment; the Sediment Yield Estimator and the New Zealand empirical erosion model.

3.13.3 Sediment Yield Estimator (SYE)

The SYE was developed as an easy to use tool for planners and researchers and the model was originally run for the North and South Islands of New Zealand (Figure 3.19). A total of 209 M ty^{-1} of eroded material is delivered to the coast from the New Zealand landmass, of which 118 M ty^{-1} is from the North Island and 91 M ty^{-1} is from the South Island (Hicks *et al.* 2003). The results of SYE for New Zealand show that most of the sediment yield from the South Island is derived from the southern alps as a result of a combination of steep slopes, high rainfall, uplifting, and easily erodible schist geology. In the North Island, more than half the sediment is derived from 6% of the land area (East Cape region) where mudstone geology dominates and almost all the native forest cover has been removed.

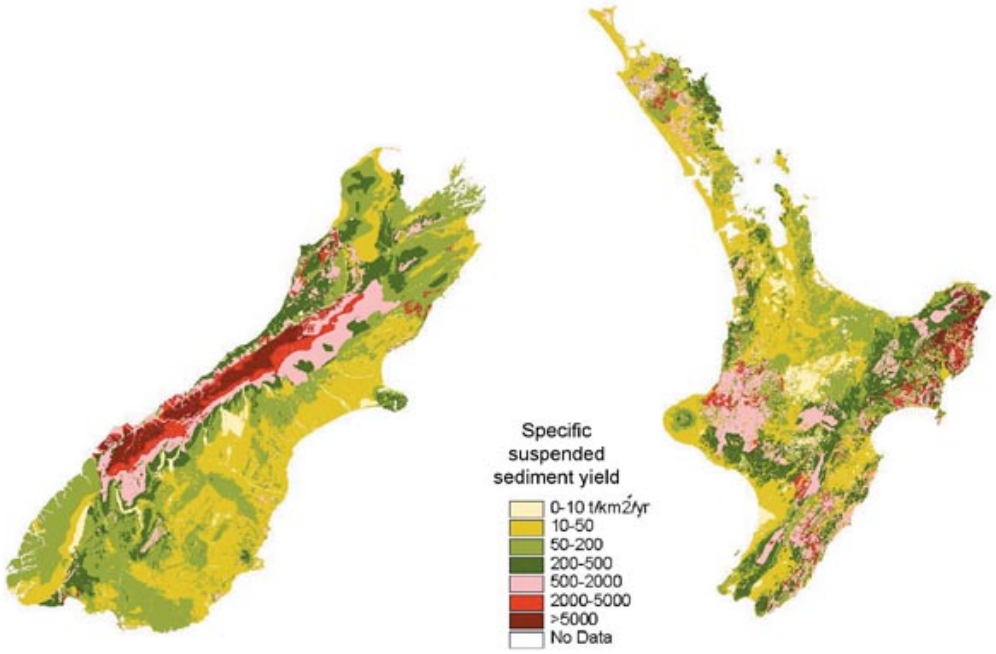

Figure 3.19. Sediment Yield Estimator results for the north and south islands of New Zealand. Areas of high specific sediment yield are shown in red (Hicks *et al.* 2003).

3.13.4 New Zealand empirical erosion model (NZeem)

The NZeem was designed to advance understanding of sediment delivery on a local, regional, and national scale by making better use of higher quality slope and vegetation information. It also uses land cover and land management information as these play an important part in influencing mass movement processes (e.g., landsliding, shallow debris flows etc) which dominate erosion in New Zealand (Eyles 1983). On a national basis, the NZeem model identified 120 M ty^{-1} of mainly human induced sediment eroded off the North Island, and 90 M ty^{-1} of naturally eroded sediment from the South Island (Landcare Research 2007).

3.14 Conclusions

In Chapter 2, three alternative hypotheses of the catchment were proposed as to the potential sources of most of the sediment entering Whangapoua estuary and the models were based on landuse (native forest, exotic forest, and agriculture) and erosion form (surface, landslides, and streambank). A review of the literature in Part A indicated that landslides, streambanks, and gullies can be the dominant source of sediment in catchments. Surface erosion from harvested exotic forests and pugging from stock can also generate significant amounts of sediment. To achieve the research aim of identifying catchment sediment sources contributing to estuary siltation, the erosion measurement technique must account for the potential dominant landuses and erosion forms.

In Part B, indirect measurement techniques of soil erosion such as plots or erosion pins are problematic as they record sediment flux past one point in the landscape and do not account for deposition and remobilisation. In other words, they measure sediment mobilisation but not delivery. The routing of sediment through a catchment is also a problem as the delivery of sediment to the basin outlet may range from hours to millennia which introduces temporal issues. Indirect measurement techniques also have problems of measurement variations. As a consequence, any up-scaling of results from indirect techniques to catchments as a whole can potentially overestimate erosion. Sediment fingerprinting holds promise of overcoming some of the problems inherent in indirect techniques as it routes various suspended sediment source areas to the sinks, and thus accounts for some of the catchment complexity in sediment deposition and remobilisation.

CHAPTER FOUR

METHODS

4.1 Introduction

Sediment fingerprinting was the primary technique used to determine the sources of sediment entering the Whangapoua Harbour. The results of sediment fingerprinting were compared with radionuclide analysis, stream monitoring, and computer modelling. The analytical methods for sediment fingerprinting (both in the pilot study and full programme) and radionuclide analysis are detailed in this chapter. Field methods and experimental designs are described in later chapters.

The sediment fingerprinting approach (Collins *et al.* 1997) was used to determine the relative proportions of sediment contributions by landscape unit (native forest, exotic forest, and agriculture) and by erosion position (surface soils, subsurface soils, and streambanks). The < 10 μm fraction of soil samples characterising catchment source areas and sediment sinks was used for both the sediment fingerprinting and radionuclide analyses.

4.2 Recovery of the < 10μm size fraction from soil samples

A settling method (Atterberg 1916) was used to recover the < 10 μm fraction from the bulk soil material. The method is based on Stokes Law and involved suspending the soil material in water and recovering the < 10 μm fraction after the larger fraction of the soil had settled out.

- Soil samples collected in the field were placed in plastic bags for transport back to the laboratory. Wet soil samples were dried at 50°C upon return to the laboratory to prevent alteration of the samples (Brown 2001). The samples were weighed again when drying was complete.
- The dried material (~3 kg per sample) was broken up into a powder consistency with a wooden mallet and then placed into a 20 L bucket (bucket 1, Figure 4.1). The buckets were filled with laboratory grade deionised (DI) water to 25 cm above the bucket tap. The soil sample was

soaked for 1-2 hours. Any large floating organic material was removed using a strainer.

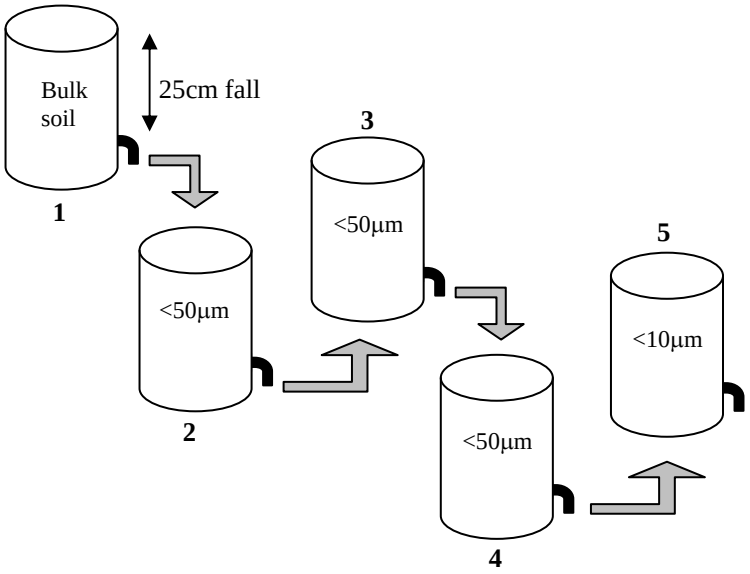

Figure 4.1. Schematic diagram of the settling method used to recover the less than 10 µm particle size fraction.

- The temperature was measured and the time for the < 50 µm particle size to fall 25 cm was determined via a table (Appendix C), which was approximately 2 minutes. The soil/water slurry was stirred again by a high speed electric drill to achieve a homogonous soil/water mix and care was taken to reverse the direction of mixing at the end to minimise turbulence. At the end of mixing a timer was set and after the set time elapsed, the supernatant was drawn off into another 20 L bucket (bucket 2 in Figure 4.1) which was placed on the floor (Figure 4.2).
- After the first < 50 µm recovery step, the residue in bucket 1 was discarded and bucket 2 was filled with DI water to the 25 cm fall line.
- The < 50 µm recovery step was repeated twice more so that material was washed into bucket 3 (bucket 2 material discarded) and then into bucket 4 (bucket 3 material discarded) as in Figure 4.1.
- The last step involved washing material from bucket 4 into bucket 5 to recover the < 10 µm particle size fraction. The bucket was refilled, the water temperature was measured, and the supernatant drawn off as per the

previous steps, but the settling time for the 10 μm particle size fraction was longer (~ 50 minutes).

Figure 4.2. Picture of the settling method where the sediment is stirred in 20 L buckets and the desired fraction is recovered by drawing off the fraction still in suspension in the 25 cm fall zone.

- The recovered < 10 μm fraction was in suspension in around 17 L of DI water. The < 10 μm fraction size was recovered using a coagulant (Ciba Magnafloc LT-510) to flocculate the material in suspension[1]. The coagulant chosen was an organic compound to avoid addition of elements that might influence the fingerprinting profile.
- The coagulant was applied drop-wise to the < 10 μm sediment mixture and stirred with a high speed electric drill and left for 30 minutes until the supernatant became clear and a sediment layer formed on the bottom of the buckets (Figure 4.3).

[1] Coagulation and flocculation have different meanings in different contexts. For this study the term *coagulant* will be the agent to cause a change among sediment particles so that they are attracted to one another, and *flocculation* will be used to describe the action of particles attracting one another to form flocs. Gregory, J. 2006, *Particles in water: properties and processes*, IWA Publishing and CRC Press, .

- The supernatant was decanted by gently tilting the buckets to allow the surplus liquid to drain off via the bucket tap. The remaining sediment slurry was washed into 750 ml plastic containers using DI water.
- The samples were dried at 50°C. The solid dry sediment was then ground in a tungsten mill prior to analysis by ICP-MS, magnetic susceptibility, XRF, and gamma spectroscopy.

Figure 4.3. The recovered < 10 μm sediment after the addition of the coagulant. A) The suspended sediment approximately two minutes after the addition of the coagulant and mixing, where the sediment begins to floc and takes on a 'miso soup' like appearance. B) The same bucket where the sediment is beginning to fall to the bottom of the bucket so the excess water can be drained off and only a small amount of slurry needs to be dried down.

4.3 Analytical processing

4.3.1 ICP-MS

Inductively Coupled Plasma Mass Spectrometry (ICP-MS) was used for trace (ppb-ppm) and ultra-trace (ppq-ppb) elemental analysis. A plasma (or gas) consisting of ions, electrons, and neutral particles is formed from Argon gas. The plasma is used to atomise and ionise the elements in a sample. The resulting ions are then passed through a series of apertures into the high vacuum mass analyzer. The isotopes of the elements are identified by their mass-to-charge ratio (m/e) and the intensity of a specific peak in the mass spectrum is proportional to the amount of that isotope (element) in the original sample (University of Missouri Research Reactor Center 2007).

The < 10 μm sediment samples were prepared using the following methods:

- Approximately 0.2 g of the sediment sample was placed in a 50 ml falcon tube into which reverse aqua regia (1 ml of HNO_3 and 0.33 ml of HCl) was placed and left to predigest overnight.
- The next day the falcon tubes were placed into an aluminium digestion block set at 50°C and left for 60 minutes. 50 ml of DI water was added to the tubes, mixed, and then centrifuged at 4000 rpm for 10 minutes.
- A 10 ml aliquot was taken and placed into a 15 ml falcon tube and the tubes were placed into racks for counting by technicians on a Perkin Elmer Elan DRC II ICP-MS. Two Merck IV standards were prepared to 50 PPB and one is run as a check and the other standard is run with the sediment samples. A flush function was carried out every 8 samples and recalibration was undertaken every 24 samples to monitor any instrument drift.

4.3.2 XRF

When an x-ray excitation source (e.g., an x-ray tube or a radioactive source) strikes a sample, the x-ray can either be absorbed by the atom or scattered through the material. The process in which an x-ray is absorbed by the atom (by transferring all of its energy to an innermost electron) is called the photoelectric effect. If the primary x-ray has sufficient energy during the photoelectric processes, electrons are ejected from the inner shells and this creates vacancies. The resulting vacancies are an unstable condition for the atom. As the atom returns to its stable condition, electrons from the outer shells are transferred to the inner shells. Electron transference gives off a characteristic x-ray whose energy is the difference between the two binding energies of the corresponding shells (Figure 4.5). Because each element has a unique set of energy levels, each element produces x-rays at a unique set of energies, allowing for the non-destructive measurement of the elemental composition of a sample (Osan *et al.* 2002; Amp-Tek 2007).

Samples were analysed for major and trace elements by a Spectro X-Lab 2000 fully automated X-ray fluorescence (XRF) spectrometer. Samples were prepared following (Norrish & Hutton 1977) and (Chappell 1992). Glass fusion disks were

prepared with 0.33-0.35g of sample powder and 2.5-2.55 g of 1.2:2.2 flux, and trace element briquettes were prepared with 5g of dried powder with 10-20 drops of liquid PVA binder.

4.4 Sediment fingerprinting statistical process

4.4.1 Kruskall_Wallis *H*-test

The sediment fingerprinting technique involved two stages to select the geochemical elements that will comprise the composite fingerprint to be used in the mixing model. The first was the Kruskall-Wallis *H*-test (Appendix A), which is the non-parametric equivalent of the one-way ANOVA, but uses the sums of the rankings rather than the raw data. Elements were eliminated on the basis that there was no significant difference in the mean concentrations between the discrete groups of interest (i.e., landscape unit).

4.4.2 Discriminant Function Analysis (DFA)

The second step was to optimise the number of first stage elements to be used in the composite fingerprint and this was achieved using Discriminant Function Analysis (DFA) (Appendix B).

Forward stepwise DFA was run in the STATISTICA 8.0 software package. The process of DFA in STATISTICA is an iterative procedure whereby at each step, the elements not already in the model are considered separately and are guided by the *F-to-enter* and *F-to-remove* values. STATISTICA reports the results of the DFA in a table form.

The DFA process in STATISTICA can be illustrated by way of an example (using the same data contained in Table B-2, Appendix B) where four elements (A, B, C, and D) have been selected as potential fingerprint candidates by the Kruskall-Wallis *H*-test. The aim of the example was to form a composite fingerprint to distinguish three landuses (native forest, exotic forest, and agriculture). The first process was at step zero where there are no elements in the DFA model. An *F*-ratio is computed for each element, as if it were in the model (Table 4-1). The most important result is the *F-to-enter* column which is the primary guide to enter elements into the model; the *F-to-enter* value is the computed *F*-ratio. The largest

F-to-enter value from Table 4-1 is for element C and this was the first element selected for the model.

Table 4-1. Step zero table of results for the DFA calculation in STATISTICA.

	Variables currently not in the model (Spreadsheet in DFA_example.stw) Df for all F-tests: 2,6					
N=9	Wilks' Lambda	Partial Lambda	F to enter	p-level	Toler.	1-Toler. (R-Sqr.)
A	0.803304	0.803304	0.734577	0.518369	1.000000	0.00
B	0.579545	0.579545	2.176471	0.194654	1.000000	0.00
C	0.471698	0.471698	3.360000	0.104952	1.000000	0.00
D	0.881912	0.881912	0.401699	0.685924	1.000000	0.00

The next process is for the step one calculation where element C has been entered into the model and the *F*-ratio for the remaining three elements were obtained (Table 4-2). Note that these *F*-ratios are calculated for each two element model. That is, for a model with element C and for the particular element under consideration. These two element calculations are not the same as reported in Table 4-1. The step one results show that element B now has the largest *F*-ratio value and it will be the second element entered into the model.

Table 4-2. Step 1 table of results for the DFA calculation in STATISTICA. The first element entered into the model is element C (top table) and the remaining three elements not yet in the model results (bottom table). Values reported in red are for elements that have a *p* value of < 0.05.

	Discriminant Function Analysis Summary (Spreadsheet in DFA_example.stw) Step 1, N of vars in model: 1; Grouping: Landuse (3 grps) Wilks' Lambda: .47170 approx. F (2,6)=3.3600 p< .1050					
N=9	Wilks' Lambda	Partial Lambda	F-remove (2,6)	p-level	Toler.	1-Toler. (R-Sqr.)
C	1.000000	0.471698	3.360000	0.104952	1.000000	0.000000

	Variables currently not in the model (Spreadsheet in DFA_example.stw) Df for all F-tests: 2,5					
N=9	Wilks' Lambda	Partial Lambda	F to enter	p-level	Toler.	1-Toler. (R-Sqr.)
A	0.148860	0.315583	5.42185	0.055948	0.370990	0.629010
B	0.075430	0.159912	13.13361	0.010226	0.201944	0.798056
D	0.368251	0.780691	0.70229	0.538516	0.885027	0.114973

The DFA process keeps entering elements into the model until all the *F*-ratios of the remaining elements are smaller than the *F-to-enter* values, which has a default

setting of one. The final result for elements C, B, and A shows the discrimination is highly significant (Wilks' lambda = 0.1233; F = 10.672; p = 0.0019) (Table 4-3).

Table 4-3. Last step table of results for the DFA calculation in STATISTICA. Element C was the first element entered into the model down to the last, element A (top table). Element D was not selected for the model (bottom table).

	Discriminant Function Analysis Summary (Spreadsheet in DFA_example.stw) Step 3, N of vars in model: 3; Grouping: Landuse (3 grps) Wilks' Lambda: .01233 approx. F (6,8)=10.672 p< .0019					
N=9	Wilks' Lambda	Partial Lambda	F-remove (2,4)	p-level	Toler.	1-Toler. (R-Sqr.)
C	0.095927	0.128575	13.55511	0.016532	0.199379	0.800621
B	0.148860	0.082855	22.13842	0.006865	0.091251	0.908749
A	0.075430	0.163514	10.23139	0.026737	0.167635	0.832365

	Variables currently not in the model (Spreadsheet in DFA_example.stw) Df for all F-tests: 2,3					
N=9	Wilks' Lambda	Partial Lambda	F to enter	p-level	Toler.	1-Toler. (R-Sqr.)
D	0.010477	0.849418	0.265916	0.782856	0.532780	0.467220

The results of the DFA can be visualised by way of graphing the canonical scores (Figure 4.4). The canonical scores are obtained from the discriminant functions, also known as canonical functions or roots. The discriminant functions are optimal linear combinations of the original elements, which provide decreasing power to discriminate between the groups (Hardle & Simar 2007). That is, the first function provides the best overall discrimination, the second provides the second best, and so on. These functions are also independent so that their contribution to the discrimination will not overlap. The easiest way of thinking of the canonical graph in Figure 4.4 is as a dimension reduction of four groups in Table 4-1 down to two groups which show the two best discriminators.

The maximum number of canonical functions computed is equal to the number of groups minus one or the number elements in the analysis, whichever is smaller. The standardised coefficients of these functions are known as canonical weights and the relative magnitude of these is an indication of how much each element is able to discriminate between the groups (StatSoft Inc 2007). A full explanation is contained in Appendix D.

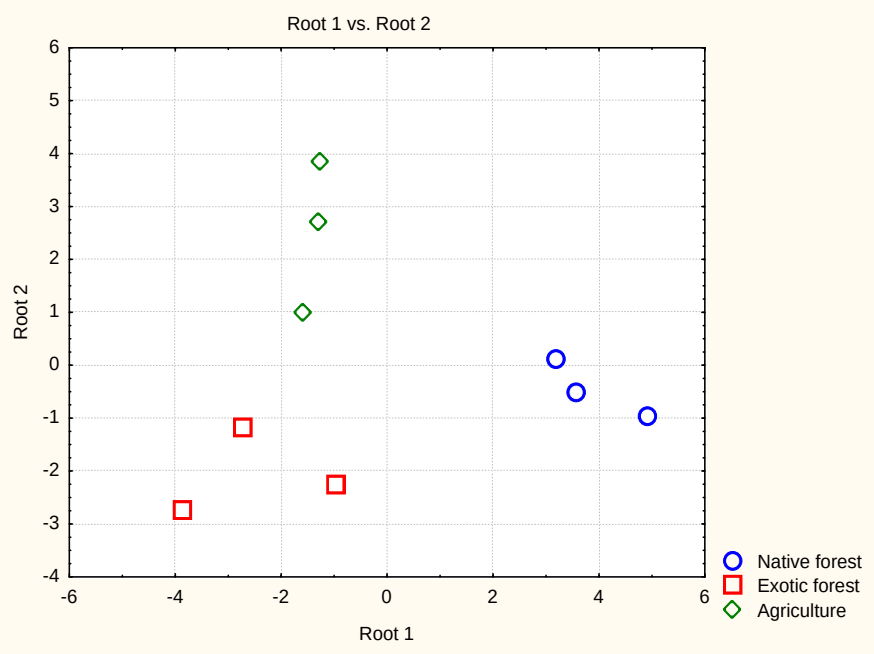

Figure 4.4. Canonical scores for elements C, B, and A as selected by DFA to distinguish three landuse types.

The individual canonical scores are found by evaluating these canonical functions (using the raw coefficients) for each observation and the discrimination of each canonical function can be assessed by looking at the means of the scores across the groups. The canonical scores can also be examined visually by plotting the individual scores for the first two canonical roots. The farther apart points of one group are away from the points of another, the better the elements have been able to differentiate the groups being examined. The greater the overlap of points from different groups, the greater the chance of erroneous classification (Garson 2007).

In the above example, there are m=3 groups, and p=3 elements, so that there will only be two canonical roots. The first root explains 68.55% of the discrimination and the remaining 31.4% is explained by the second (Table 4-4). From the standardised coefficients, it can be seen that the first canonical function is weighted heavily by element B, while the second function is characterised mainly by the remaining two elements. Thus the result of the canonical analysis of this simple example shows that the use of elements A, B, and C affords good discrimination between the three landuse types.

Table 4-4. Raw coefficients for the canonical variables for root 1 and root 2 that have been used in the graph of canonical scores (Figure 4.4).

	Raw Coefficients for Canonical Variables	
Variable	Root 1	Root 2
C	0.3012	-0.329000
B	-1.2013	0.025620
A	0.1287	0.097474
Constant	-11.3385	1.706986
Eigenval	11.7179	5.375082
Cum.Prop	0.6855	1.000000

4.4.3 Mixing model

After selecting and optimising the geochemical elements of the composite fingerprint, a mixing model was used to quantify the relative contributions of the potential sediment source areas (e.g., landuse). A linear equation is constructed that relates each element's mean concentration in the three landuses, to that element's concentration in the sink sample. So the composite fingerprint is represented by a set of linear equations, one for each of the selected geochemical elements. The linear equations are not solved directly, but rather by minimising the sums of squares of the residuals (Walling *et al.* 1999), and the details of the mixing model are presented in Section 3.10.3.3.

The mixing model produces a single estimate of the mixing proportions (or relative contribution) of each landuse to the sink sample. The estimate in this study was obtained using the Solver function in Microsoft Excel. To give a measure of the uncertainty associated with each of the estimates in the main sediment fingerprinting project, a Monte Carlo procedure was used to produce empirical sampling distributions for the estimates. Details of the procedure are given in Appendix E.

CHAPTER FIVE

PILOT STUDY

5.1 Introduction

A pilot study was undertaken in the Waitekuri subcatchment within the Whangapoua Harbour to test the potential use of sediment fingerprinting in the New Zealand environment. The pilot study was designed to determine if sediment fingerprinting could be used to differentiate between sediment derived from the three principal landscape units, as well as sediment derived from three different 'erosion positions' (surface soils, subsurface soils, and streambanks). The null hypothesises posed were:

$H_{o\ (1)}$: geochemical properties will not be able to distinguish between sediment derived from the three major landscape units (native forest, exotic forest, and agriculture) in a subcatchment of Whangapoua Harbour.

$H_{o\ (2)}$: geochemical properties will not be able to distinguish between sediment derived from the three erosion 'positions' (i.e., surface < 2 cm, subsurface > 20 cm, and streambank) in a subcatchment of Whangapoua Harbour.

The methods principally follow Collins *et al.* (1997) (Chapter 3). This chapter describes the sampling design and sediment fraction recovery used in the pilot study and the subsequent results.

5.2 Site selection

Site selection for the pilot study began by partitioning the Whangapoua catchment into smaller subcatchment areas using CatchmentSIM (Cooperative Centre for Catchment Hydrology 2004). Whangapoua catchment was partitioned based on the five major streams draining into the harbour; Waitekuri River, Waingaro and Opitonui, Owera, Otanguru, and Mapauriki streams (Figure 5.1). Small areas of swamp around the harbour, scrub areas to the east of the harbour and the urban

areas of Whangapoua and Matarangi (around 10% of the catchment) were excluded from consideration.

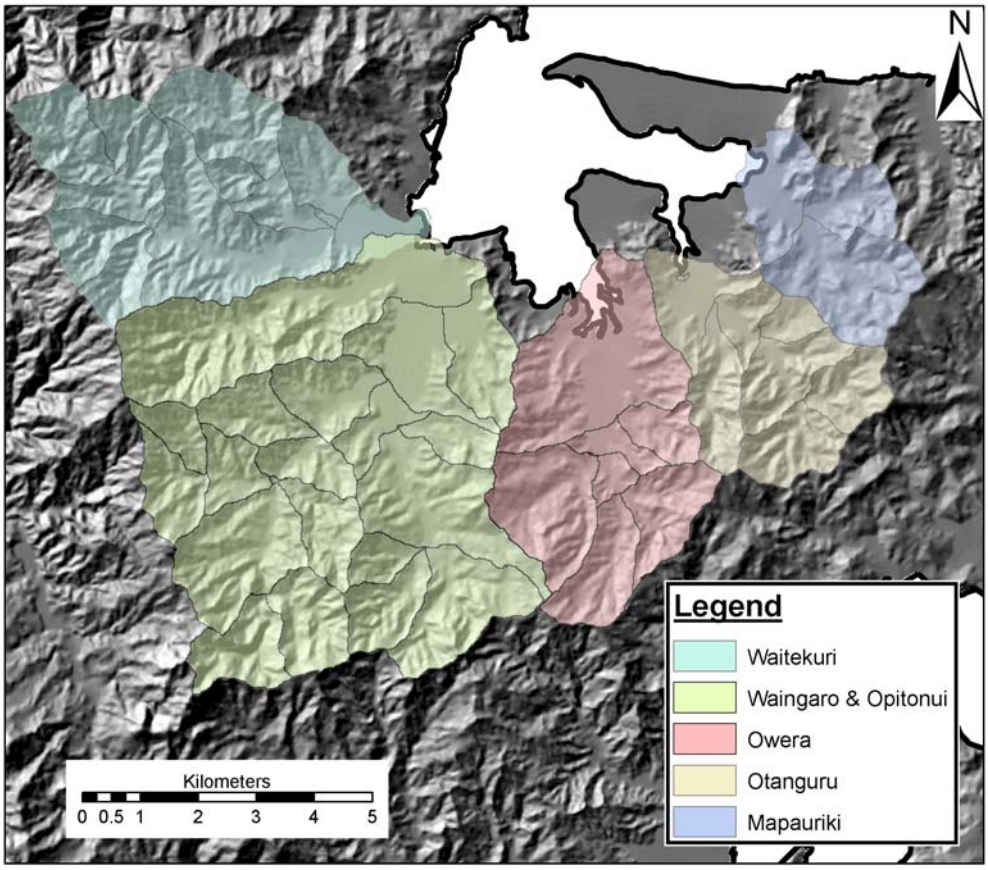

Figure 5.1. The five subcatchment areas of the Whangapoua Harbour catchment.

The Waitekuri subcatchment (Figure 5.2) was chosen for the pilot study as it was representative of the landuse and slope patterns in the greater catchment with steep upper slopes under native forest, mainly intermediate slopes under exotic forest, and lower slopes and flat areas on alluvial soils under agriculture. While the slope/landuse patterns were typical of the Whangapoua catchment, the Waitekuri had the highest average channel slope and channel slope range of any of the subcatchments (Table 5-1).

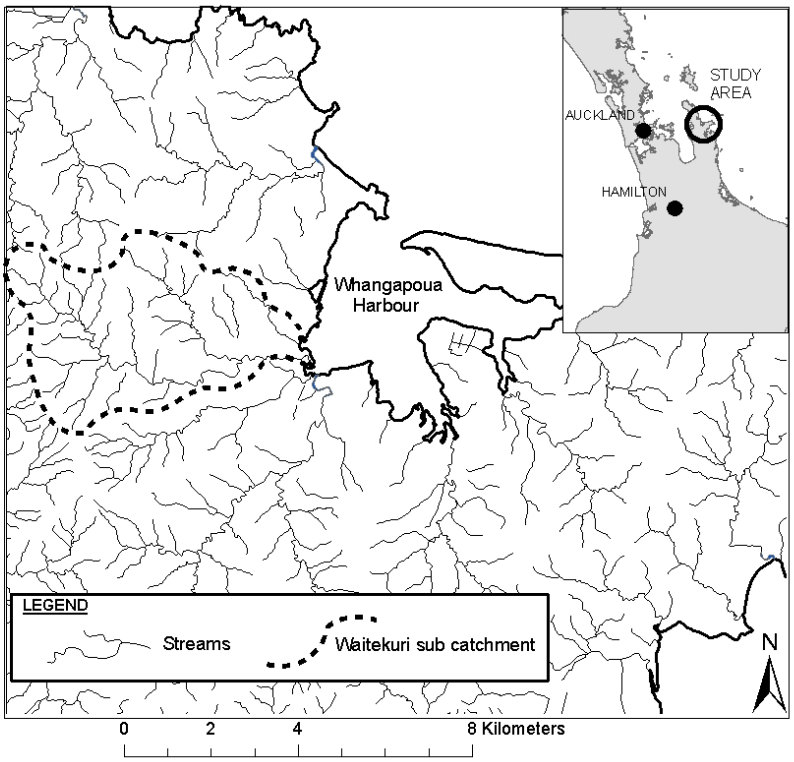

Figure 5.2. The Whangapoua Harbour catchment and the boundary of the Waitekuri subcatchment.

Table 5-1. The five sub-catchments of the Whangapoua Harbour area, average channel slope, and channel slope range.

Subcatchment	Area (ha)	Average slope	Slope range
Waitekuri	1922	6.1	0.9 – 18.6
Waingaro and Opitonui	4214	3.7	0.1 – 12.2
Owera	1605	4	1.8 – 5.3
Otanguru	1046	4.1	0.6 – 5.7
Mapauriki	745	3.1	2.5 – 3.2

5.3 Sampling design rationale and assumptions

The rationale guiding the sampling comes from the three alternative hypotheses of catchment erosion identified in Chapter 2. Thus surface, subsurface, and streambank samples were taken from each one of the native forest, exotic forest, and agricultural landscape unit.

To characterise sediment originating from surface erosion forms, the top 2 cm of the surface soils were sampled. To characterise sediment originating from landslides, soil samples from greater than 20 cm depth were collected. Material was collected from along drainage channels to characterise streambank erosion forms.

Soil samples were collected from source areas that are 'likely to be eroded' (Section 3.10.3.4) or as I interpreted it, likely to deliver sediment to streamlines. The soils were sampled *in-situ* as opposed to actively transported material so as to characterise source areas and not material in transit. Sampling areas were selected close to drainage lines which are likely to deliver sediment to streams (i.e., proximal sources); surface and subsurface samples were taken from within 10 m of drainage lines on flat land and up to 20 m on steep land. For streambank samples, material was taken from bare or exposed banks that were not fortified by vegetation.

5.4 Sample collection

5.4.1 Catchment soil samples

Within each of the three landscape units, nine areas of equal size adjacent to the stream network were identified of which three were randomly selected. A push tube soil sampler was used to take 10 cores in an area of approximately 100 m^2 and these were bulked in the field to make up the sample. The top 2 cm of the core was retrieved for the surface sample, the 2-20 cm section discarded, and the greater than 20 cm section retrieved for the subsurface sample. Streambank material was retrieved using a stainless steel trowel and 10 samples were taken from approximately 20 lineal meters of the channel and were bulked in the field. Consequently, each landscape unit had three sites containing three different positions, totalling 27 source area samples for the pilot study (Figure 5.3).

5.4.2 Catchment sink samples

A time integrated sediment sampling device (TISSD) (Figure 5.4) was used to represent sediment entering the Whangapoua estuary (Phillips *et al.* 2000). The TISSD was deployed in the lower reach of the Waitekuri River above the tidal influence (Figure 5.3). Stream sampling using the TISSD was to ensure that the

collected sediment was of a contemporary nature and to assess the performance of the TISSD for later use in the full sampling programme.

The TISSD was deployed from 8-11-2007 until 28-4-2008. The TISSD was placed in around 60% of the low flow water depth after it was filled with native water. Once it was secured with metal stakes, the TISSD received a constant water inflow and by virtue of its inlet to chamber ratio, decreased the receiving water velocity by a factor of 600. This induced sedimentation within the chamber before the water circulated out the exhaust tube (Phillips *et al.* 2000).

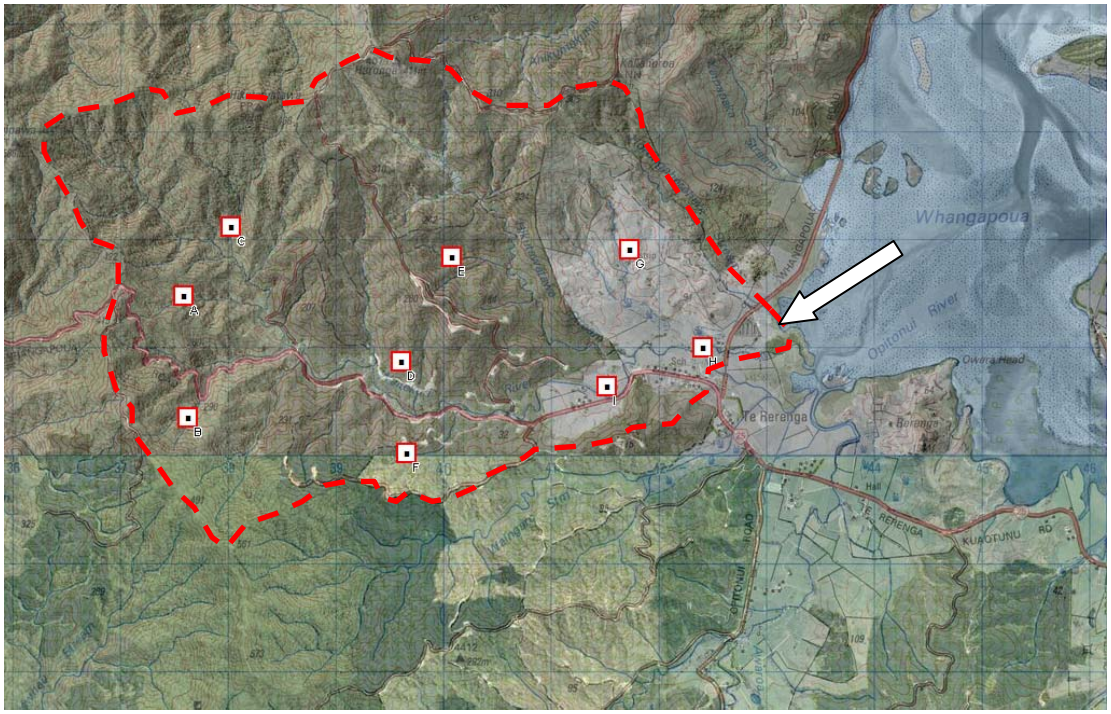

Figure 5.3. Sampling sites locations for native forest (A B C), exotic forest (D E F) and agriculture (G H I). At each site indicated, soil was sampled from three positions (surface, subsurface, and streambank). The approximate boundary of the Waitekuri subcatchment is shown by the dashed line and the approximate location of the time integrated sediment sampler is indicated by the arrow.

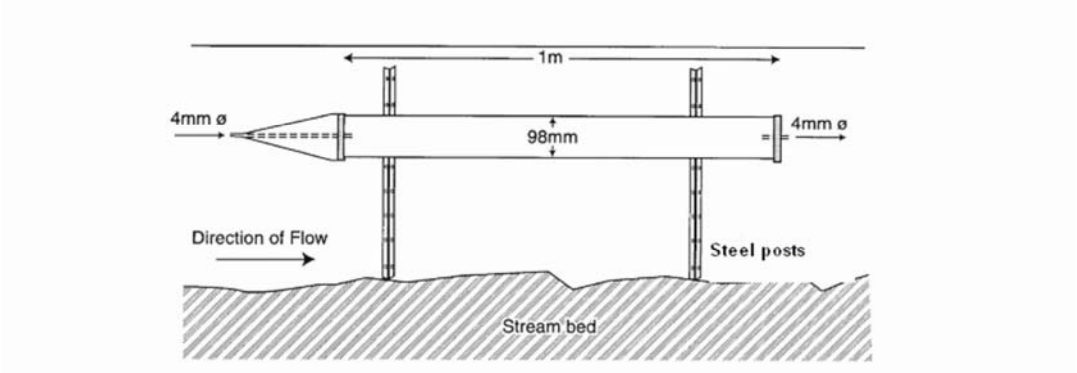

A

B

Figure 5.4. A) Schematic drawing of the time integrated sediment sampler; B) field deployment of the time integrated sediment sampler in the Waitekuri River.

5.5 Sample preparation and analysis

The 27 source area and one sink sediment samples were returned to the laboratory and air dried at 45°C for 48 hours. Each sample was then manually disaggregated using a mortar and pestle, mixed to ensure sample homogenisation, and dry sieved to recover the < 63 μm fraction for analysis by X-ray Florescence (XRF).

5.6 Results

5.6.1 XRF analysis

The XRF reported the results for 39 trace and 12 major geochemical elements. Due to the analytical unreliability of the XRF instrument with respect to certain trace elements (Co, Ni, Ga, Ge, Se, Br, Nb, Mo, Ag, Cd, In, Sn, Sb, Te, I, Cs, Pr, Nd, Hf, Ta, W, Hg, Ti, and Bi) (Roger Briggs *pers. comm*.), these 24 elements were eliminated before the first stage of statistical treatment. Consequently 27 elements were potential fingerprint candidates. The full geochemical element results are presented in Appendix F.

5.6.2 Sediment fingerprinting statistical process

The sediment fingerprinting technique is a three stage process. Firstly, the geochemical elements that vary significantly between groups (i.e., landscape unit or erosion position) were identified as candidate elements by the Kruskall-Wallis *H*-test (Section 3.10.3.1). The number of candidate elements were then optimised by Discriminant Function Analysis (DFA) (Section 3.10.3.2). The optimised elements are then used in a composite fingerprint to determine the relative contribution of the landscape units or erosion positions by using a mixing model (Section 3.10.3.3). The sediment fingerprinting statistical process was run firstly for the landscape units and then erosion position.

5.6.3 Statistical analysis to determine fingerprint candidates for landscape units

Candidate elements to distinguish between the landscape units (native forest, exotic forest, and agriculture) were selected using the Kruskall-Wallis *H*-test. Elements were eliminated on the basis that their *p*-values were above the 5% level of significance (i.e., $p \geq 0.05$). Seven elements were below the 5% level of significance and were identified as candidate fingerprint elements. They were chromium, magnesium, calcium, iron, zinc, phosphorus, and manganese (Figures 5.5 and 5.6). The full Kruskall-Wallis *H*-test results are contained in Appendix G.

The concentrations of Mg, Zn, P, and Mn were higher in the agricultural areas. Fe showed an increase from native to exotic to agricultural landscape units. Cr was

found in similar concentrations in the exotic forest and agricultural landscape units, but in much lower concentrations in the native forest. The lowest concentration for Ca was found in the exotic forest landscape unit.

The second step was to optimise the selected seven candidate elements by forward stepwise discriminant function analysis (DFA). As detailed in Chapters 3 and 4, DFA is an iterative process that is guided by the *F-to-enter* / *F-to-remove* value, which was set at three. The rationale for the *F-to-enter* value will be discussed later in this chapter. The DFA result (Table 5-2) was that Mn, Zn, and Cr were selected for the model with a highly significant result (Wilks' lambda = 0.22726; $F = 8.0375$; $p < 0.0000$) (Table 5-2).

Table 5-2. Results for the forward step-wise DFA process for landscape units using an *F-to-enter* value of three. Zn was the first element entered into the model and Mn the last (top) while Mg, P, Ca, and Fe were not selected for the model (bottom).

Discriminant Function Analysis Summary (DFA_LANDUSE.sta in Pilot_Study_ALL.stw)
Step 3, N of vars in model: 3; Grouping: **Landuse** (3 grps)
Wilks' Lambda: .22762 approx. F (6,44)=8.0375 p< .0000

N=27	Wilks' Lambda	Partial Lambda	F-remove (2,22)	p-level	Toler.	1-Toler. (R-Sqr.)
Zn	0.255024	0.892540	1.324381	0.286354	0.590425	0.409575
Cr	0.395143	0.576042	8.095819	0.002317	0.645102	0.354898
Mn	0.311833	0.729940	4.069727	0.031344	0.452829	0.547171

Variables currently not in the model (DFA_LANDUSE.sta in Pilot_Study_ALL.stw)
Df for all F-tests: 2,21

N=27	Wilks' Lambda	Partial Lambda	F to enter	p-level	Toler.	1-Toler. (R-Sqr.)
Mg	0.202271	0.888636	1.315859	0.289469	0.707322	0.292678
P	0.217163	0.954061	0.505587	0.610308	0.691159	0.308841
Ca	0.197626	0.868231	1.593563	0.226813	0.714291	0.285709
Fe	0.199455	0.876266	1.482655	0.249851	0.551347	0.448653

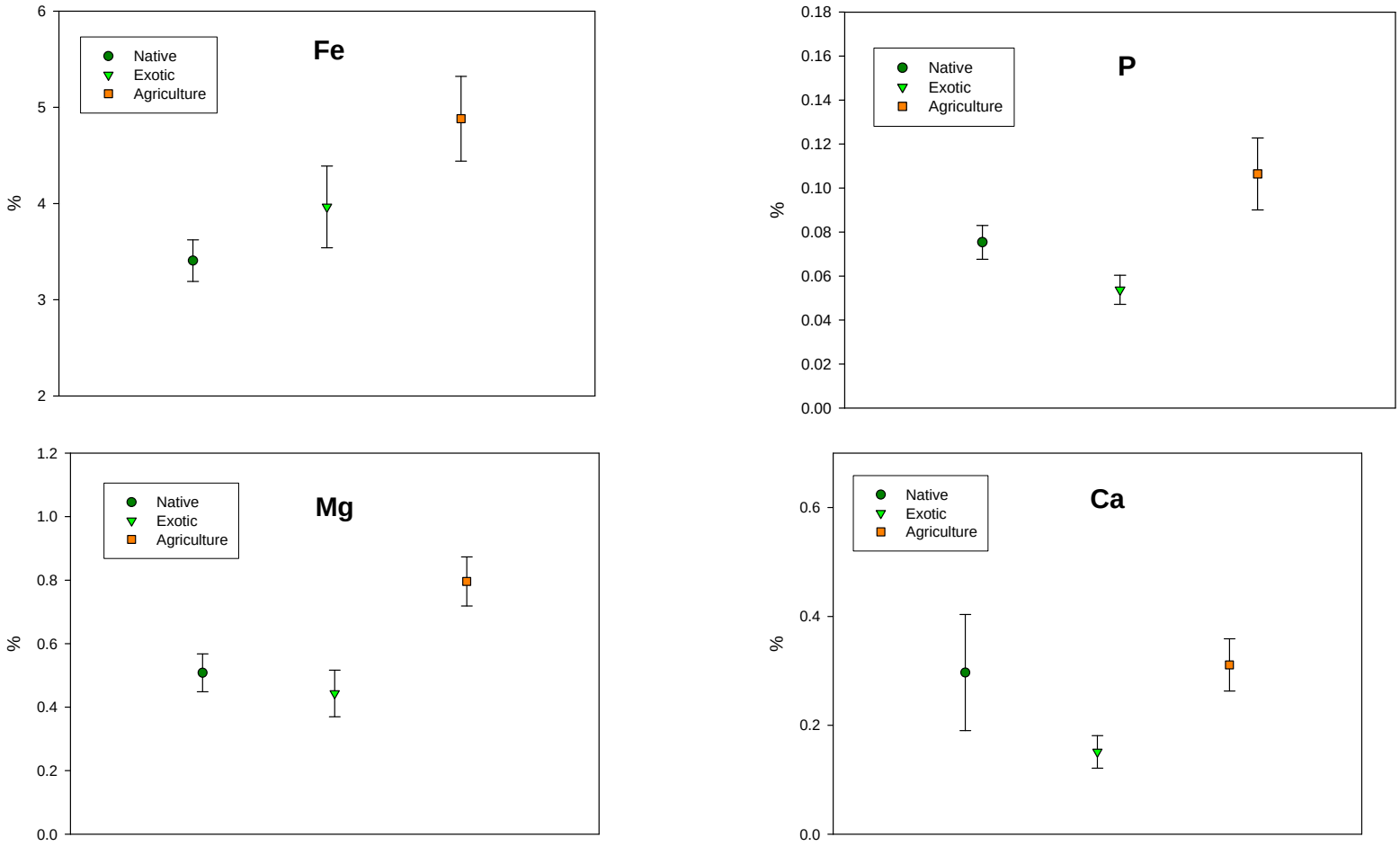

Figure 5.5. Mean concentrations of Fe, P, Mg, and Ca for the three landscape units. Error bars represent one standard error of the mean values.

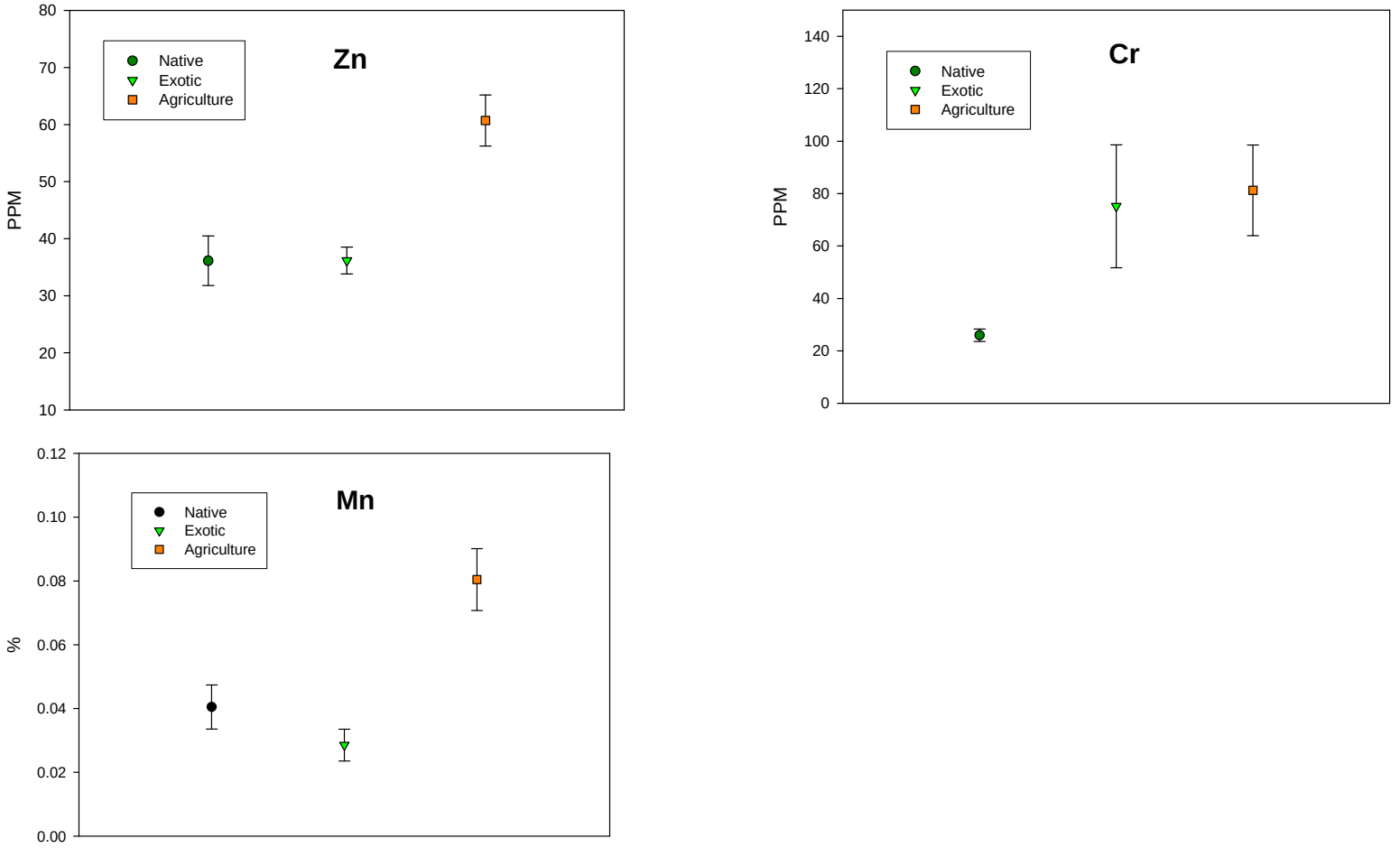

Figure 5.6. Mean concentrations of Zn, Cr, and Mn for the three landscape units. Error bars represent one standard error of the mean values.

Canonical analysis was used to visualise the DFA results (Figure 5.7). There was good separation of the agricultural landscape unit and the native and exotic landscape units using Zn, Cr, and Mn. There was also separation between exotic and native forests landscape units although there was some overlap evident between them. This reflects that of the three elements, only Cr clearly distinguishes the native forest from the exotic and agricultural landscape units (Figure 5.6). Consequently, the null hypothesis $H_{o\ (1)}$ posed is rejected as the pilot study had shown that there are geochemical elements that can distinguish between the three landscape units.

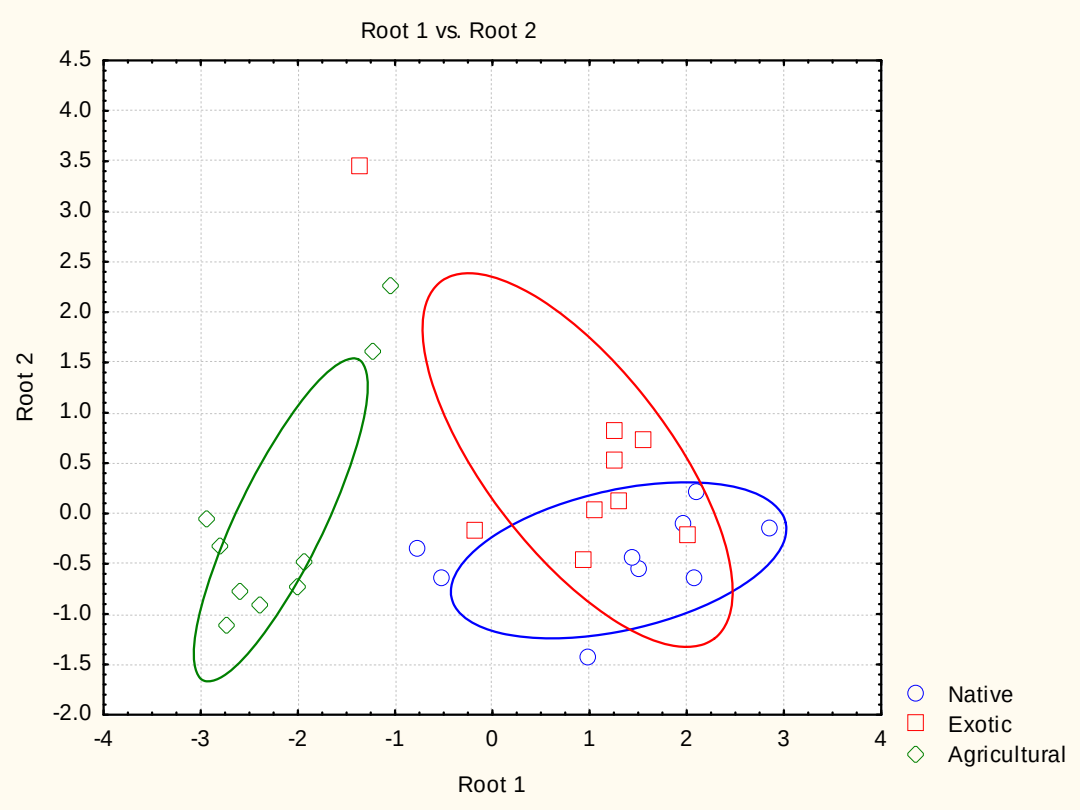

Figure 5.7. Canonical analysis of the DFA results for landscape units using Zn, Cr, and Mn. Ellipses are 0.95 of data range for each landscape unit.

I have drawn 95% range ellipses on all of the canonical graphs in this thesis. A 95% range ellipse is one where the length of its horizontal and vertical proportions onto the *x*-axis and *y*-axis respectively, is equal to mean ± range ∗ 0.95. These ellipses have no statistical meaning but are drawn to highlight the clustering of the groups. (StatSoft Inc 2007).

5.6.4 Statistical analysis to determine fingerprint candidates for erosion position

The statistical process was repeated using the Kruskall-Wallis *H*-test, except this time the grouping variable was erosion positions (surface soils 0-2 cm, subsurface soils > 20 cm, and streambank material). Seven elements (aluminium, phosphorus, sulphur, chlorine, calcium, vanadium, and uranium) were identified as potential candidate elements (Figure 5.8 and 5.9) and the full results are contained in Appendix G.

The pattern of the geochemical results in Figures 5.8 and 5.9 is a contrast between the surface sample concentrations and both the subsurface and streambank sample concentrations. S, Ca, Cl, and P all show increased concentrations in the surface samples compared to low concentrations in the subsurface/streambank samples. Al, U, and V show low surface concentrations compared to higher subsurface/streambank concentrations.

The seven elements selected to distinguish erosion position were run through the DFA process with the *F-to-enter* value of three. Only Cl and P were entered into the model for a still highly significant result (Wilks' lambda = 0.31335; $F = 9.0438$; $p < 0.001$) (Table 5-3).

Table 5-3. Results for the forward step-wise DFA process for position using an *F-to-enter* value of three. Cl was the first element entered into the model and P the last (top) while Al, S, Ca, V, and U were not selected for the model (bottom).

	Discriminant Function Analysis Summary (DFA_POS_elements.sta in Pilot_Study_ALL.stw) Step 2, N of vars in model: 2; Grouping: Position (3 grps) Wilks' Lambda: .31335 approx. F (4,46)=9.0438 p< .0000					
N=27	Wilks' Lambda	Partial Lambda	F-remove (2,23)	p-level	Toler.	1-Toler. (R-Sqr.)
Cl	0.567620	0.552048	9.331522	0.001078	0.996570	0.003430
P	0.434508	0.721169	4.446335	0.023304	0.996570	0.003430

	Variables currently not in the model (DFA_POS_elements.sta in Pilot_Study_ALL.stw) Df for all F-tests: 2,22					
N=27	Wilks' Lambda	Partial Lambda	F to enter	p-level	Toler.	1-Toler. (R-Sqr.)
Al	0.284360	0.907473	1.121570	0.343694	0.829939	0.170062
S	0.304166	0.970680	0.332265	0.720834	0.552032	0.447968
Ca	0.309601	0.988025	0.133317	0.875889	0.807494	0.192506
V	0.295388	0.942666	0.669032	0.522320	0.978219	0.021781
U	0.289424	0.923633	0.909489	0.417345	0.934505	0.065495

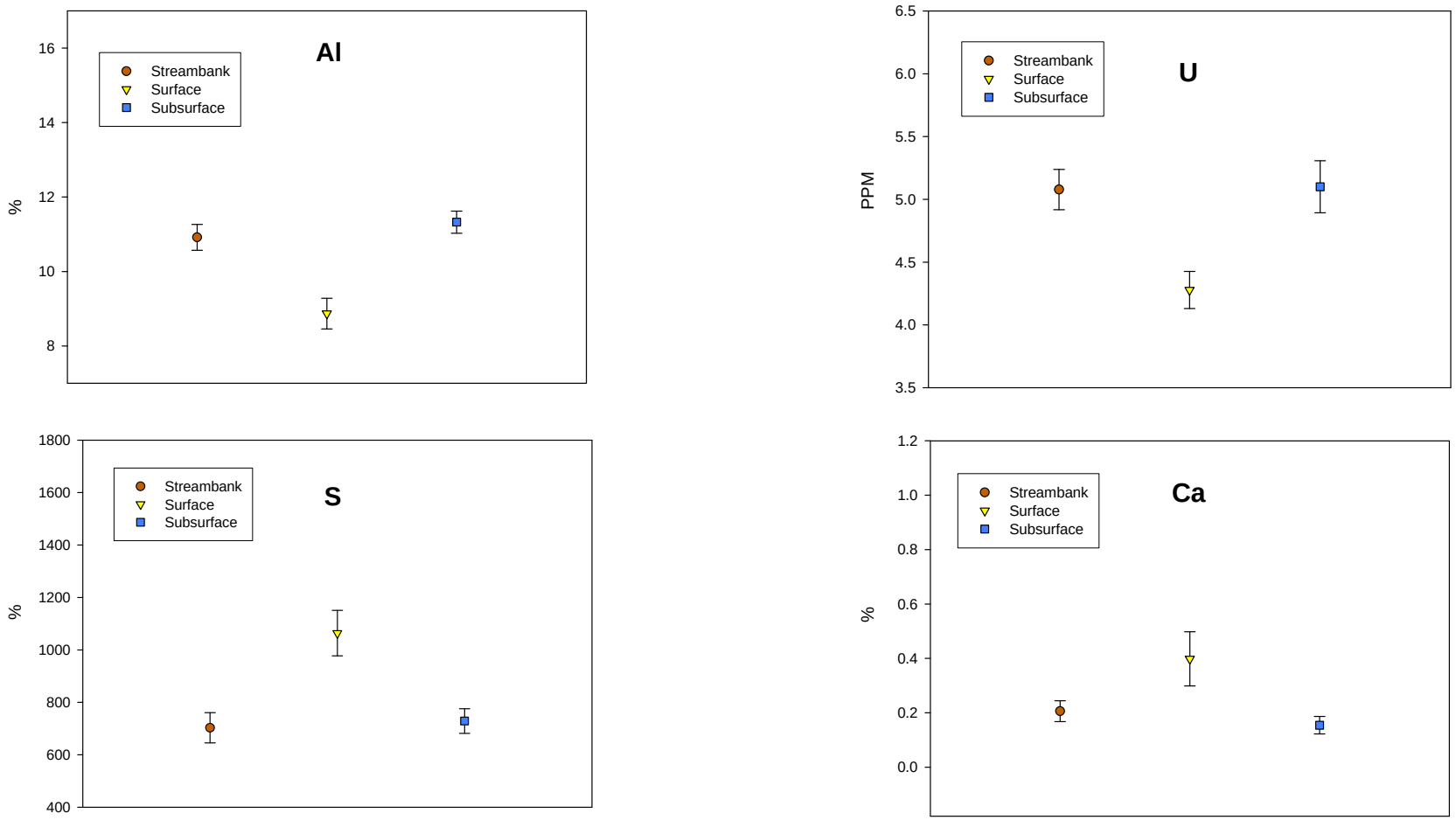

Figure 5.8. Mean concentrations of Al, U, S, and Ca for the three erosion positions. Error bars represent one standard error of the mean values.

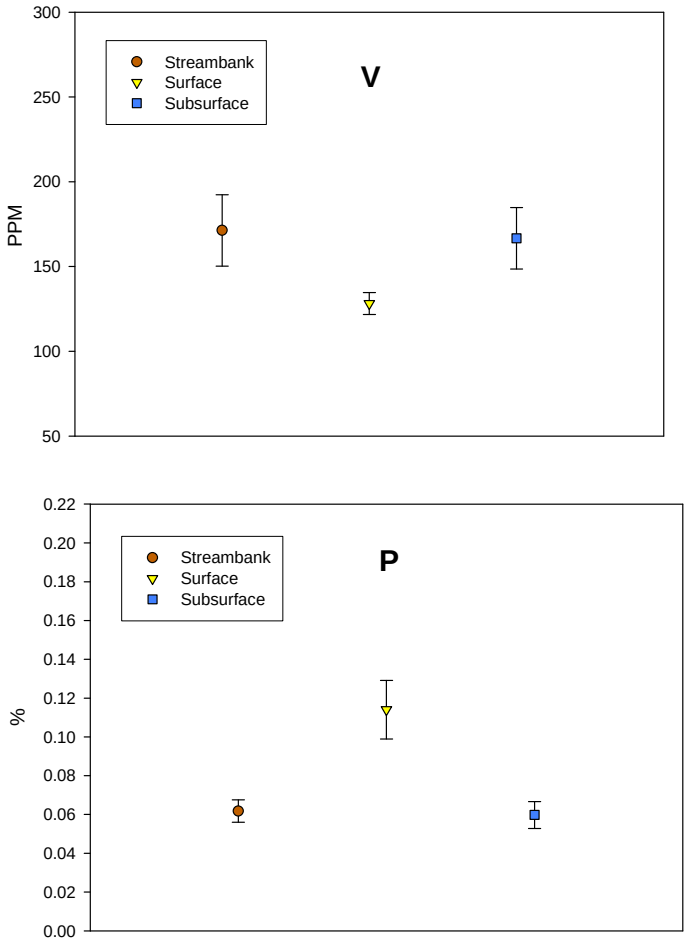

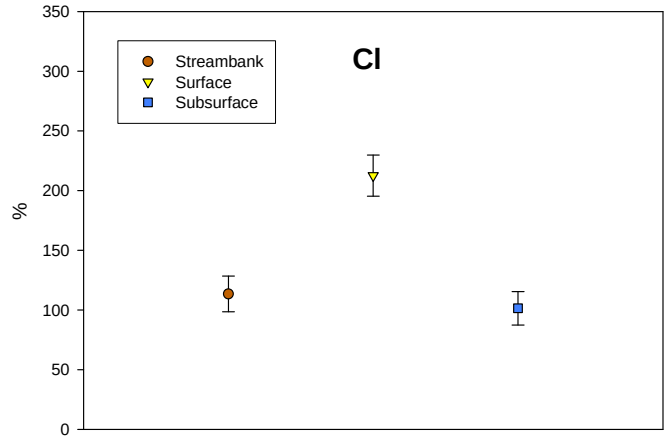

Figure 5.9. Mean concentrations of Ca, V, and U for the three erosion positions. Error bars represent one standard error of the mean values.

The canonical analysis of elemental concentrations (Figure 5.10) is characterised by good separation between surface sources and the two subsurface positions (streambank and > 20 cm). There was not good separation between streambank and subsurface positions. This reflects the higher concentrations of Cl and P in surface soils and the lower concentrations in both subsurface soils and streambanks. The overall result is still significant and there is enough evidence to reject the null hypothesis $H_{o\ (2)}$ as the pilot study had shown that there are geochemical properties that can be used to distinguish erosion source positions.

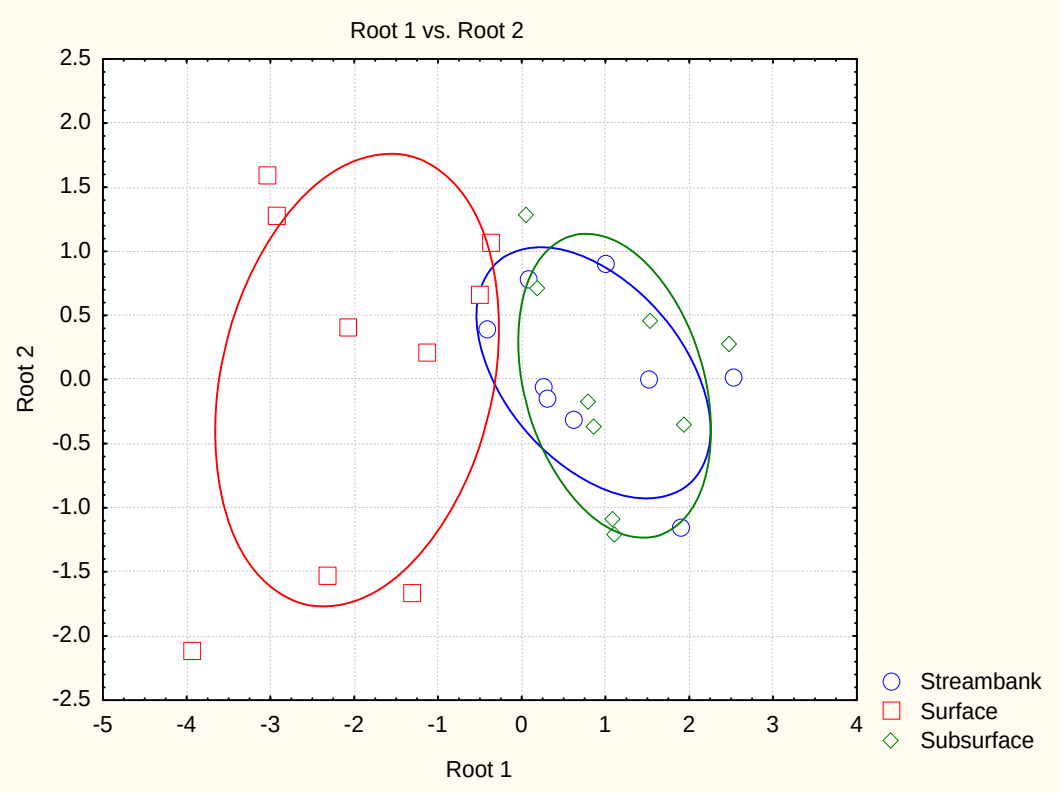

Figure 5.10. Canonical analysis of the DFA results for position using Cl and P. Ellipses are 0.95 of data range for each landuse type.

5.6.5 Mixing model results

The mixing model produces a single estimate of the mixing proportions (or relative contribution) from each landscape unit/erosion position to the sink sample. The sink sample result is contained in Appendix H. The mixing model (Section 3.10.3.3) was run in an Excel spreadsheet using the Solver function (Appendix E). The elements Mn, Zn, and Cr were used to estimate the relative contributions from the native, exotic, and agricultural landscape units in the

Waitekuri subcatchment. Cl and P were used to estimate the relative contributions from surface, subsurface, and streambank positions in the Waitekuri subcatchment. The Solver function was run once to provide a single estimate of the relative contributions and the results are contained in Table 5-4. The main contributor of sediment by landscape unit was the native forest and the main process of sediment delivery appears to be landslides due to the dominance of subsurface sources.

Table 5-4. Results of the mixing model for the relative contribution from landuse and position from the Waitekuri subcatchment.

Landuse	Relative proportion (%)	Position	Relative proportion (%)
Native	40	Surface	10
Exotic	33	Subsurface	62
Agricultural	27	Streambank	28

5.6.6 Review of objectives

The objective of the pilot study was to test the hypotheses (Section 5.1) that no geochemical elements could be found to distinguish either landscape units or erosion position in the Waitekuri subcatchment. Both hypotheses $H_{o\ (1)}$ and $H_{o\ (2)}$ were rejected as the DFA identified Zn, Cr, and Mn to distinguish landscape units and Cl and P to distinguish erosion position. Both results were highly significant. Using the elements for the composite fingerprint determined the relative contribution results in Table 5-4.

5.7 Discussion

5.7.1 Sediment fingerprinting results

Following the sediment fingerprinting process, geochemical elements were found that could distinguish landscape units and erosion position, and that using the elements in a composite fingerprint it was possible to calculate the relative sediment contribution. It is evident from Section 5.6 is that both sets of DFA results were highly significant with acceptable Wilks' lambda scores. But the canonical analysis (Figures 5.7 and 5.10) indicates that there may be greater difficulty distinguishing exotic forests from native forests landscape units and

subsurface from streambank erosion positions due to the overlap observed of these groups in the graphs.

The overlap of groups in the canonical graphs (Figures 5.7 and 5.10) reflects the reality of the geochemical elements selected to distinguish the groups. For landscape units, Zn and Mn clearly has different concentrations in the agricultural landscape units but not native or exotic forests, while Cr has a different concentration in the native forest but not agricultural or exotic landscape unit (Figure 5.6). None of the elements clearly distinguishes exotic forests. For erosion position, both Cl and P (Figure 5.9) have higher concentrations in the surface positions and are similar in the subsurface and streambank positions.

Classification matrices were generated for the DFA analysis for landscape units (Table 5-5) and position (Table 5-6) to attempt to examine the level of discrimination of groups within the landscape units and erosion position.

Table 5-5. Classification matrix for the DFA analysis of native forest, exotic forest, and agricultural landscape units.

	Classification Matrix (DFA_LANDUSE.sta in Pilot_Study_ALL.stw) Rows: Observed classifications Columns: Predicted classifications			
Group	Percent Correct	Native p=.33333	Exotic p=.33333	Ag p=.33333
Native	77.77778	7	0	2
Exotic	55.55556	3	5	1
Ag	88.88889	0	1	8
Total	74.07407	10	6	11

Table 5-6. Classification matrix for the DFA analysis of surface, subsurface, and streambank erosion positions.

	Classification Matrix (DFA_POS_elements.sta in Pilot_Study_ALL.stv Rows: Observed classifications Columns: Predicted classifications			
Group	Percent Correct	Surface p=.33333	Subsurf p=.33333	St.bk p=.33333
Surf	66.66666	6	0	3
Subsurf	77.77778	2	7	0
St.bk	66.66666	3	0	6
Total	70.37037	11	7	9

The classification matrices results are based on the distance of a single observation from the centroid of the data group which is analogous to a mean. Thus the position results which show the lowest classification rate for surface when it should be expected to be the highest based on Figure 5.10, reflects the surface data having large variability about the centroid. The classification results also suffer from the low sample number which means that one misclassification changes the results by 11%. The classification matrices therefore do not quantify the discrimination between landscape unit or erosion position groups.

The DFA result is highly significant for landscape units and erosion position, but quantifying how well native/exotic/agricultural landscape units and surface/subsurface/streambank positions are distinguished from one another remains difficult. The best indication seems to be the canonical graphs which would suggest it is sensible to interpret the final sediment fingerprinting results with greater caution for native and exotic forests and subsurface and streambank erosion positions.

5.7.2 Optimisation of geochemical elements

An advantage of sediment fingerprinting is that it is based on the premise that using multiple properties to form the fingerprint reduces the potential error of spurious source-sink links by being more representative (Collins & Walling 2002). There is also the competing aim to ensure the number of fingerprint properties is kept to a minimum. This is to ensure parsimony (or simplicity) in the mixing model, as models should have as few parameters as possible to ensure their simplest functional form (Crawley 2005; Miller 2005). Fewer parameters avoid errors such as multiple comparisons.

When using confidence intervals, the null hypothesis is rejected when it is proved false by a very significant level ($p < 0.05$). The problem arises when testing not a single hypothesis, but many and this is the problem of multiple comparisons. For example, if four independent tests are carried out using the acceptance criteria of 5%, the probability that one of the hypothesis is accepted by chance alone is 19% (Dallal 2007)

When the sediment fingerprinting statistical process was first run on the data for landscape units, the DFA process did not optimise the number of candidate elements identified by the Kruskall-Wallis *H*-test (Figures 5.5 and 5.6). In other words, the DFA did not reduce the seven candidate elements (Table 5-7). The result showed the discrimination is highly significant (Wilks' lambda = 0.1205; $F = 4.8361$; $p < 0.001$).

Table 5-7. Step seven table of results for the forward step-wise DFA process. Zn was the first element entered into the model down to the last Fe.

	Discriminant Function Analysis Summary (StepwiseDFA_analysis) Step 7, N of vars in model: 7; Grouping: **Landuse** (3 grps) Wilks' Lambda: .12050 approx. F (14,36)=4.8361 p< .0001					
N=27	Wilks' Lambda	Partial Lambda	F-remove (2,18)	p-level	Toler.	1-Toler. (R-Sqr.)
Zn	0.142836	0.843660	1.667810	0.216524	0.420234	0.579766
Cr	0.171251	0.703672	3.790060	0.042299	0.410286	0.589714
Mn	0.139602	0.863200	1.426327	0.266073	0.265141	0.734859
Ca	0.140015	0.860657	1.457125	0.259103	0.504995	0.495005
Mg	0.143333	0.840734	1.704934	0.209858	0.437563	0.562437
P	0.148994	0.808789	2.127752	0.148087	0.390937	0.609063
Fe	0.137387	0.877118	1.260882	0.307270	0.352999	0.647001

Canonical analysis of the DFA results with all seven elements showed that there was clear separation of the agricultural landscape unit and overlap of the native forest and exotic forest landscape unit (Figure 5.11).

Likewise for erosion position, the initial processing of the candidate elements by DFA selected three elements (Cl, P, and Al) and rejected S, Ca, V, and U as they all had an *F*-ratio below the default *F-to-enter* value of one (Table 5-8). Therefore the DFA forward-stepwise process only ran to three steps. The final result shows the discrimination is highly significant (Wilks' lambda = 0.28436; $F = 6.4187$; $p < 0.001$).

Canonical analysis of the position DFA results with Cl, P, and Al showed that there was clear separation of the surface position and overlap of the subsurface and streambank positions (Figure 5.12).

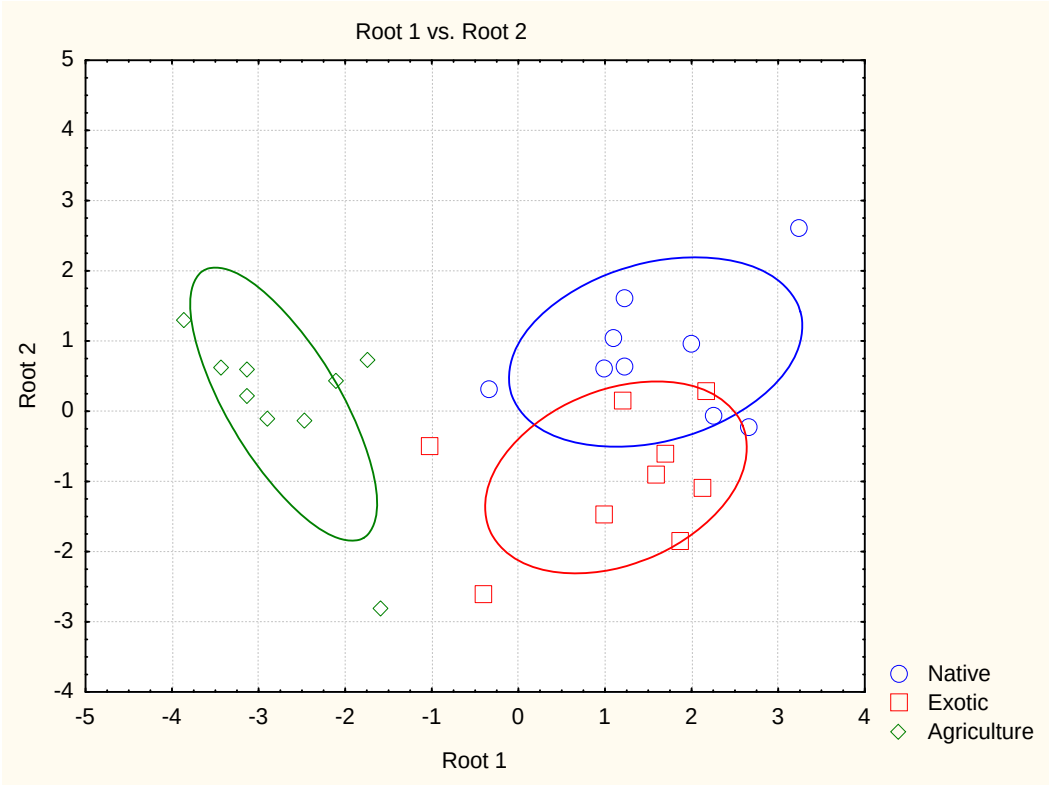

Figure 5.11. Canonical analysis of the DFA results for landscape units using Cr, Mg, Mn, Ca, Fe, Zn, and P. Ellipses are 0.95 of data range for each landuse type.

Table 5-8. Step three table of results for the forward step-wise DFA process for position. Cl was the first element entered into the model down to the last Al (top). Rejected elements are displayed in the bottom table.

	Discriminant Function Analysis Summary (DFA_POS_elements.sta in Pilot_Study_ALL.s Step 3, N of vars in model: 3; Grouping: Position (3 grps) Wilks' Lambda: .28436 approx. F (6,44)=6.4187 p< .0001					
N=27	Wilks' Lambda	Partial Lambda	F-remove (2,22)	p-level	Toler.	1-Toler. (R-Sqr.)
Cl	0.406290	0.699894	4.716667	0.019740	0.934453	0.065547
P	0.330733	0.859785	1.793889	0.189798	0.867032	0.132967
Al	0.313353	0.907473	1.121570	0.343694	0.829939	0.170062

	Variables currently not in the model (DFA_POS_elements.sta in Pilot_Study_ALL.stw) Df for all F-tests: 2,21					
N=27	Wilks' Lambda	Partial Lambda	F to enter	p-level	Toler.	1-Toler. (R-Sqr.)
S	0.277191	0.974790	0.271547	0.764836	0.550912	0.449089
Ca	0.282624	0.993896	0.064486	0.937734	0.780215	0.219785
V	0.275736	0.969672	0.328399	0.723707	0.811643	0.188358
U	0.273304	0.961122	0.424733	0.659438	0.825809	0.174191

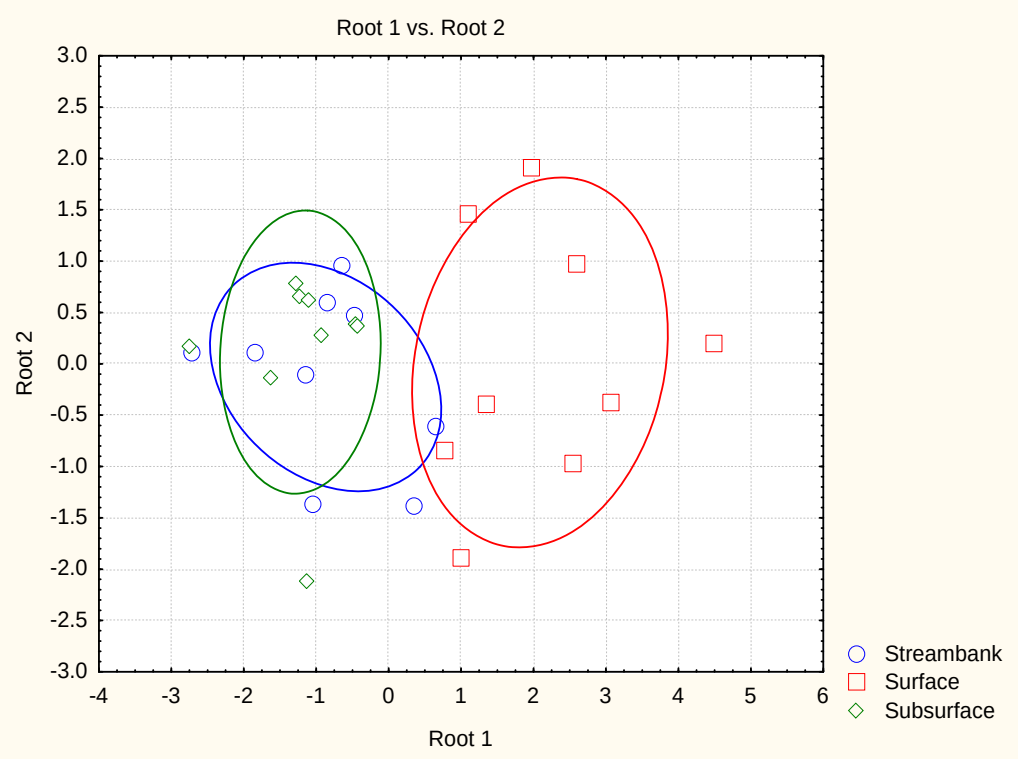

Figure 5.12. Canonical analysis of the DFA results for position using Cl, P, and Al. Ellipses are 0.95 of data range for each landuse type.

As detailed in Section 3.10.3.2, DFA is an iterative process that is guided by the *F-to-enter* / *F-to-remove* value and the default value used by STATISTICA and previous studies is an *F-to-enter* value of one. When the *F-to-enter* value of one was used for the first statistical processing of the pilot study data, there was no optimisation of candidate landscape unit elements, and an extra element was accepted into the erosion position DFA model (Al). It was decided to investigate the potential of further optimisation of candidate elements at the DFA stage.

5.7.3 Optimisation by DFA

To examine the issue of optimisation of elements further, it is important to know that the degrees of freedom for the pilot study data for landscape units was determined by degrees of freedom of the numerator (df_1) which is k-1 (the number of groups or landuse types minus one), and the degrees of freedom of the denominator (df_2) which is n-k (the number of predictor values or elements minus three). Thus the pilot study has degrees of freedom of 2 and 24.

Consider the first results of pilot study data for landscape units (Table 5-7) where no DFA optimisation occurred. Using the corresponding table for the *F*-distribution (Table 5-9), and elements were accepted (because the null hypothesis was rejected) into the DFA model when their *F*-ratio was greater than one at the 38% level of significance (i.e., *F-to-enter* value of one). The level of significance (38%) is at odds with the hypothesis testing which is typically conducted at the $p \leq 0.05$ level of significance, which would correspond to the *F-to-enter* value in Table 5-9 of approximately three. So was there a case to change the default value used in STATISTICA for the DFA process from one to three?

Table 5-9. Level of significance (α) for the *F-to-enter* values for the degrees of freedom of 2 and 24 (Hale 2000).

F-to-enter	Level of significance (α)
1.0	0.382697
2.0	0.157267
3.0	0.068719
4.0	0.031676
5.0	0.015303

The forward stepwise DFA was run again on the seven selected elements for the landscape unit grouping, but this time with the default *F-to-enter* value changed from one to three. The results were that only three elements (Zn, Cr, and Mn) were accepted into the model while four elements (Mg, P, Ca and Fe) were rejected (Table 5-2). The change in the default *F-to-enter* value from one to three reduced the number of elements in the model from seven to three and reduced the problems of multiple comparisons with the overall result remaining highly significant ($p < 0.001$). The use of fewer element in the models led to a larger Wilks' lambda score (0.22762), whereas for the model including all seven elements the Wilks' lambda score was 0.1205 (Table 5-7). The *F*-ratio determines how much variation exists within and between the landscape unit group of elements and the significance level of the variance. The Wilks' lambda calculates how useful a given element is in the forward-stepwise discriminant function (Purkait 2005).

The problem with the larger Wilks' lambda in Table 5-2 is that it is at odds with published literature which uses the minimisation of the Wilks' lambda as the key

factor in determining the number of elements in the model. However, the reduction in Wilks' lambda with more elements included is not significant. This is because the *F*-ratios, each computed to assess the improvement in discriminatory power of a model with each additional element (and given in the "F to enter" column in Table 5-2 and 5-7), are not statistically significant. As shown in Appendix B, these *F*-ratios are a function of Wilks' lambda and essentially give a measure of the reduction in the Wilks' lambda score, which would occur with the inclusion of an additional element in the model. If the *F*-ratio is not significant, then neither is the reduction in the Wilks' lambda score.

To summarise at this point, the DFA process did not reduce (or optimise) the number of elements selected by the Kruskall-Wallis *H*-test when the published method was followed of using an *F-to-enter* value of one (Wilks' lambda score = 0.1205). This is at odds with the aim of ensuring the least number of elements are used in the model to ensure simplicity and reduce the problem of multiple comparisons.

The pilot study had a degrees of freedom of 2 and 24, and when the *F*-distribution for this situation is examined, an *F-to-enter* value of one corresponds to a level of significance of 38% when it is normal to test at the 95% level. The 95% level of significance for the pilot study data corresponds to an *F-to-enter* value of three. The DFA process was rerun using an *F-to-enter* value of three which optimised the number of elements in the fingerprint to three instead of all seven, but the Wilks' lambda score was larger (0.28436). The larger Wilks' lambda score is at odds with the published method of minimising the Wilks' lambda score as a way of determining the optimum number of elements in the composite fingerprint.

5.7.4 Testing optimisation by 'Jackbooting'

To investigate the opposing results of element optimisation (to ensure simplicity and avoid multiple comparisons) while increasing the Wilks' lambda, a resampling of the pilot study data was undertaken based on the landscape unit groupings. Typically any resampling of the data would involve techniques such as Bootstrapping or Jackknifing. The Bootstrapping and Jackknifing techniques are used to estimate the precision of statistics (e.g., medians) and the dispersion

(e.g., standard deviation). Bootstrapping is the technique whereby the data set is resampled by sequential removal and replacement of each point and running over many iterations, typically in the thousands. Jackknifing is the resampling of a dataset by the creation of many other subsets, usually by a one off removal. For example, in a data set with 20 elements, 20 pseudo-replicate datasets (each of $n = 19$) will be created. For this reason Jackknifing is considered to be a means of approximating Bootstrapping (Efron 1982; Lanyon 1987; Kohavi 1995; Shao & Tu 1995).

For the pilot study data, neither Bootstrapping nor Jackknifing would be applicable. For Bootstrapping the removal of one point and its replacement by one chosen randomly from the entire data set would bias the results as the data is organised into the three landscape unit groups and would unbalance the groups. Similarly, the creation of subsets by Jackknifing would also unbalance the data that had been grouped into landscape units.

A variation of the Bootstrapping and Jackknifing methods was developed in this thesis and termed Jackbooting. This involved the removal and replacement of not one but three observations, one each from the three landscape units. Jackbooting involved sequentially removing an observation at each 'step' from the native forest, exotic forest, and agriculture landscape unit data sets and then running forward-stepwise DFA analysis (Roddy *et al.* 2008). After each step, the observations were returned and three more removed (Figure 5.13). At each step, the first element entered into the model (or 'ranked') by DFA through to the fifth was recorded to ascertain if there is a hierarchy of importance of the candidate elements. To execute the Jackbooting resampling, a macro was written for STATISTICA which automated the procedure as well as recording the ranking of elements, the classification matrix percent, the Wilks' lambda statistic and the significance level (Appendix I). The resampling of the pilot study data by Jackbooting resulted in 729 iterations of the data.

The results from Jackbooting showed that there was a hierarchy of elements to distinguish landuse types (Table 5-10). Out of a possible 729 iterations, Mn was the first ranked element 369 times, closely followed by Zn at 351. Mg was the

only other element to appear in the first ranked position nine times. Neither Mn nor Zn were ranked second, but this position was dominated by Cr 707 times out of a possible 729. In the third ranked position, Mn again appears the most (321 times) with Fe the next best with 198. It should be noted that the columns in Table 5-7 don't all sum to 729 as for some iterations less than five elements were entered into the model by the DFA process.

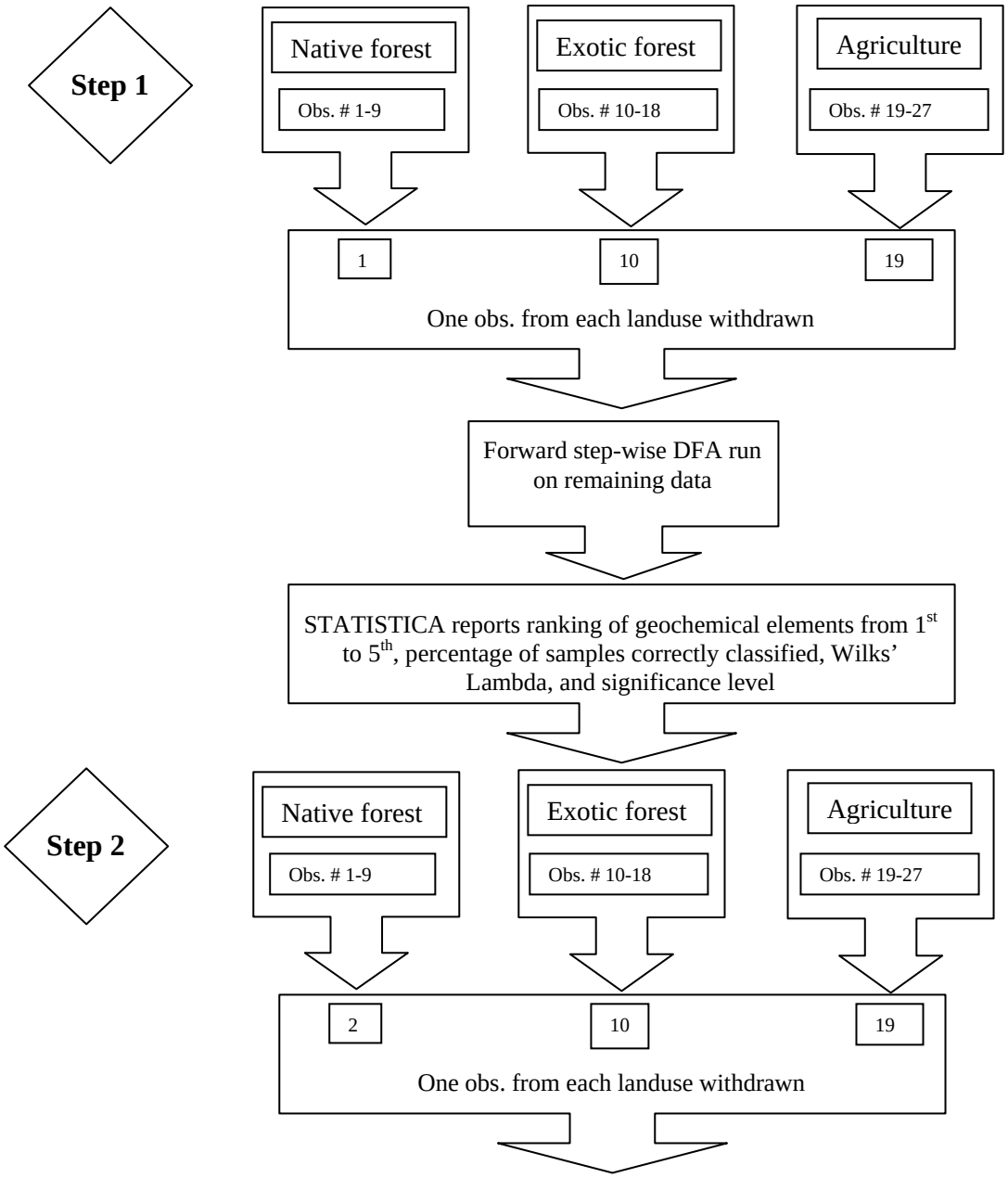

Figure 5.13. Flow chart showing the Jackbooting process for the first and second step in the macro written for STATISTICA.

Table 5-10. Results of forward stepwise DFA analysis Jackboot resampling showing the ranking of elements from first to fifth.

	Rank				
Element	**1st**	**2nd**	**3rd**	**4th**	**5th**
Mn	369	0	321	0	1
Zn	351	0	52	27	27
Cr	0	707	2	4	16
Ca	0	0	72	244	41
P	0	1	58	210	180
Fe	0	21	198	66	32
Mg	9	0	23	175	412

A clear break can be seen in the results (Figure 5.14). Mn, Zn, and Cr account for over 96% in the first and second rankings, and over 50% in the third ranked position. Of the other elements, Fe accounts for 27% in the third ranked position and Ca 34% in the fourth ranked position. There is a definite hierarchy (or 'importance') of Mn, Zn, and Cr which dominate the first to third ranked positions on the right hand side of the graph. The elements Mg, Fe, P, and Ca dominate the rankings third through to fifth on the left hand side of the graph (Figure 5.14).

The result of the Jackbooting resampling leads to the conclusion that the default *F-to-enter* value of one used in STATISTICA and reported in the literature is in fact too low. A more appropriate *F-to-enter* value is three, as it better matches a $p \leq 0.05$ level of significance for the pilot study number of observations and number of groups data (Table 5-10) and is a more rigorous qualifier of candidate elements while reducing the potential of multiple comparisons. Even though the use of an *F-to-enter* value of three results in a larger Wilks' lambda score, the Jackboot resampling shows that only Mn, Zn, and Cr are required to distinguish the three landscape units because of their hierarchy of importance and using only Mn, Zn, and Cr still produces a highly significant result (Wilks' lambda = 0.22726; $F = 8.0375$; $p < 0.0001$) (Table 5-2).

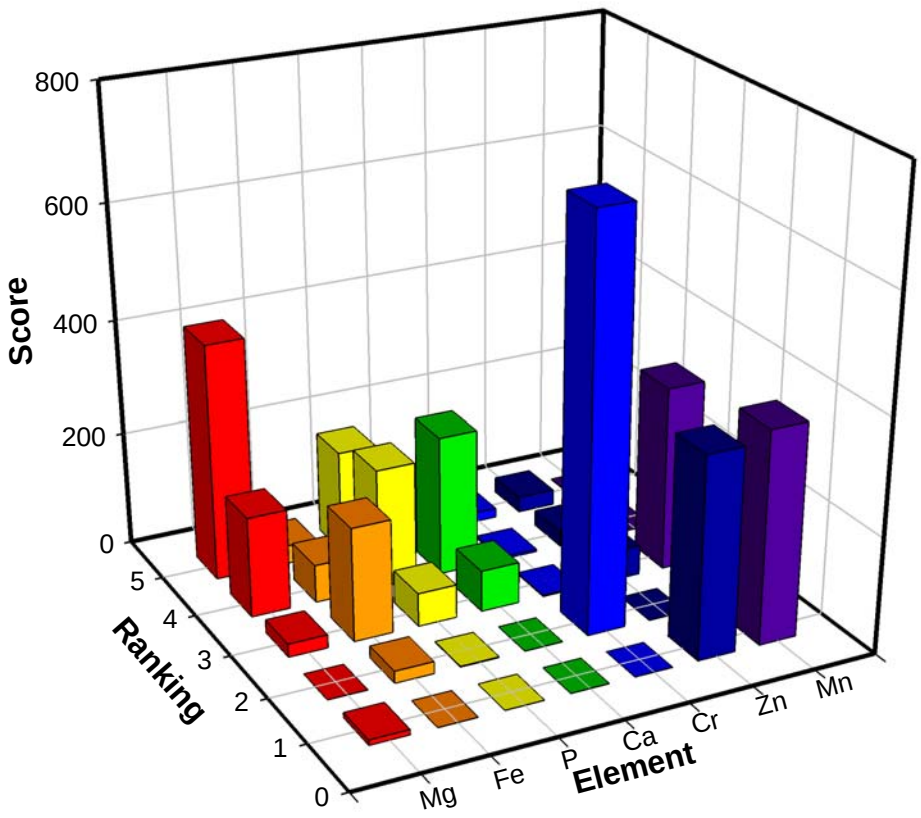

Figure 5.14. Results of the Jackbooting resampling method showing the rankings of elements from first to fifth.

5.7.5 Discussion of mixing model results

The landscape unit mixing model used three elements to determine the relative contribution of three different landscape units (native, exotic, and agricultural), and the position mixing model used two elements to determine the contribution from three positions (surface, subsurface, and streambanks). When the number of elements in the mixing model is less than the number of sources, then the problem of dimensionality is encountered. That is to say, the problems of dimensionality occur where the discriminating powers of the tracers is compromised when the number of tracers used is less than the number of sources trying to be identified (Small *et al.* 2002).

The erosion position mixing model was posed using only two elements (Cl and P) to distinguish three groups (surface, subsurface and streambanks), thus encountering the problems of dimensionality. It has already been observed from canonical analysis of position that the two elements do not distinguish well between the subsurface and streambank positions. For this reason the mixing

model was run again using the two elements to distinguish only two groups, surface positions and *all* subsurface position (subsurface and streambanks combined) so as the rule of dimensionality was not broken. The result was that the mixing model would not leave the 0.5/0.5 starting assumption for the surface and all subsurface positions, so no result was obtained.

The Waitekuri subcatchment landscape unit/erosion position sediment fingerprinting results indicate that the majority of entering the lower reaches is sourced from the native forest landuse and is most likely generated by landslide erosion. The pilot study results indicate that native forest/landslide alternative hypothesis (Section 2.5.2) of catchment erosion is primarily how sediment is delivered to the Whangapoua estuary.

Interpretation of the pilot study results requires some caution. Firstly, there are only nine observations representing each landscape unit/erosion position in a 1900 ha subcatchment. Secondly, the rule of dimensionality was broken to obtain the mixing model result using two elements to distinguish three groups for the erosion position scenario, and a result was not obtained when using two elements to distinguish two groups for erosion position. Thirdly, the low number of observations also limits the confidence in which we can say that landscape units and erosion position interact. That is, that sediment is being predominantly generated from subsurface sources in native forest areas. These three problems are largely due to the low sample numbers in the pilot study and will be addressed by a larger sample number in the full sediment fingerprinting programme (Chapter 6).

5.8 Summary

The Waitekuri subcatchment was selected to conduct a pilot study into the feasibility of applying the sediment fingerprinting technique to sediment source ascription in New Zealand. Two null hypothesis were posed that there are no geochemical properties that would distinguish the native, exotic, and agricultural landscape units nor the surface, subsurface, and streambank erosion positions. After sampling the subcatchment and analysis of the < 63 μm fraction by XRF, geochemical candidate elements were identified by the Kruskall-Wallis *H*-test and

then optimised by discriminant function analysis. This process identified the elements Mn, Zn, and Cr for landuse discrimination and Cl and P for position discrimination and the two null hypotheses were rejected. It was also shown by Jackboot resampling that the default *F-to-enter* value used in STATISTICA is too low and that a more rigorous value of three should be used in this case.

The sediment fingerprint elements were then used in the mixing model to determine the relative sediment contribution from the landscape units and erosion position sources. The results indicate that native forest is the main contributor and it is delivering sediment via subsurface (i.e., landslide) sources. The mixing model results must be used with caution because of low sample numbers and problems of dimensionality.

CHAPTER SIX

SEDIMENT FINGERPRINTING

6.1 Introduction

In Chapter 5 it was shown that the sediment fingerprinting technique could distinguished sediment from the different landscape units (native forest, exotic forest, and agriculture) and erosion 'positions' (surface, subsurface, and streambank). This chapter outlines the application of sediment fingerprinting to the whole Whangapoua catchment. The full sampling programme was modified from the method used in the pilot study. The aim of the full sediment fingerprinting sampling programme was to quantify the relative contributions from the landscape unit/erosion position sediment source areas.

6.2 Source area sample collection

6.2.1 Introduction

Typically the native forest landscape unit occurs on steep slopes, exotic forests on rolling hills, and agriculture on flat land, although there are exceptions (e.g., where agricultural pastures occur on hill country). To include all the landscape unit variations in the sampling programme, it was necessary to map the landscape unit variability within the Whangapoua catchment.

6.2.2 Mapping catchment area categories

The Whangapoua Harbour catchment was mapped to ascertain the variations that occur within each landscape unit. The variables mapped were landuse, slope, and soil type. Fifty sampling sites were allocated to ensure the sediment source areas were representative. For example, in the Waitekuri subcatchment (Figure 6.1), the native forest and exotic forest occur on uniform slope and soil classes so the sampling points can be allocated to ensure spatial representativeness. However, the agricultural landuse occurs on three different soil and slope classes, so sampling points were allocated to ensure spatial representativeness of landscape unit variability.

Coverages and their categories from the New Zealand Land Resource Information System (NZLRI) (Newsome *et al.* 2000) were used to construct the maps used to define the sampling programme. The NZLRI themes include soil, geology, vegetation, and erosion risk. The method for producing the field sampling maps was as follows:

- The landuse and soil shapefiles were imported into ArcGIS where the Whangapoua Harbour catchment area was extracted to give a landuse and soil coverage for the catchment.
- The landuse coverage was reclassified so that the NZLRI high producing grassland and low producing grassland (Table 6-1) were merged to represent agricultural landuse. The NZLRI native forest and exotic forest was found to accurately represent these landuses in the catchment.
- The NZLRI soil coverage units were merged into two groups. The first was the Brown Soil Order, and the other was the Gley, Allophanic, and Organic Soil Orders that were merged to give 'Lowland Soil Associations' located mainly around the harbour margins.
- A digital elevation model (DEM) was built for the Whangapoua catchment and the raster surface was reclassified to group the eight NZLRI slope classes into two slope groups: flat to rolling (0°-15°) and strongly rolling to precipitous (16°- > 42°) (Table 6-1). The two slope categories were created for the purpose of identifying atypical areas of agriculture on steep slopes, and atypical areas of exotic forest on gentle slopes.
- Once the shapefiles for landuse, soil, slope, and subcatchment area inputs were prepared, the Query Builder tool in ArcGIS was used to merge these coverages for each of the five major subcatchments (Table 6-1). The final output was a map for each subcatchment delineated by landuse and showing the categories of soil and slope within each landuse. In other words, the maps show the variability of slope and soil within each landscape unit.
- Sampling sites were allocated on the spatial extent of each category and are indicated on the maps by the numbered boxes (Figures 6.1 to 6.5).

Table 6-1. Classification groupings for landuse, slope and soil type.

Category	NZLRI Code	New code
Landuse		
- Native	N – native forest	**n**
- Exotic	N6 – exotic forest	**e**
- Agriculture	P1 – High producing grassland P2 – Low producing grassland	**a**
Slope		
- Flat to rolling (0° - 15°)	A to C	**f**
- Strongly rolling to precipitous (16° - > 42°)	D to H	**h**
Soils		
Steep land soils	BOM – Brown Orthic Acid BOT – Brown Orthic Typic	**B**
Lowland soils	GRT – Gley Recent Typic GUFQ – Fluvial Saline Sulphuric Gley LOT – Typic Orthic Allophanic OMM – Mellow Mesic Organic	**L**

The catchment maps were colour coded to show the landuse/slope/soil variability within each landuse within each subcatchment. The legend for each colour code is labelled to show the subcatchment, the landuse, slope class, and soil class using the codes from the 'new codes' column (Table 6-1). For example, Wait_n_h_B is an area with the Waitekuri subcatchment (Wait), native forest (n), on strongly rolling to precipitous topography (h), on Brown soils (B).

The maps showed the areas that needed to be represented in the sampling programme and the number of samples were apportioned based on the spatial extent of each category within each landuse. For example, the majority of exotic forests in the subcatchments were located on the steeper slopes with Brown soils, so 20 sampling sites were allocated. Only two sampling sites were allocated to the small areas of exotic forest on low slopes with lowland soils, and two sampling sites allocated to the small area of exotic forest on low slopes with Brown soils. The maps show the originally planned 51 sampling sites, but due to lack of access permission only 50 sites were sampled.

The Waitekuri catchment (Figure 6.1)[1] was dominated by native vegetation on high slope classes under Brown soils (Waite_n_h_B) and exotic forests on high slope classes under Brown soils (Waite_e_h_B). Agriculture was practiced on a mix of low slopes under Brown and Lowland soils (Waite_a_f_B and Waite_a_f_L). There was also a small area where agriculture was practiced on a high slope class under Brown soils (Waite_a_h_B).

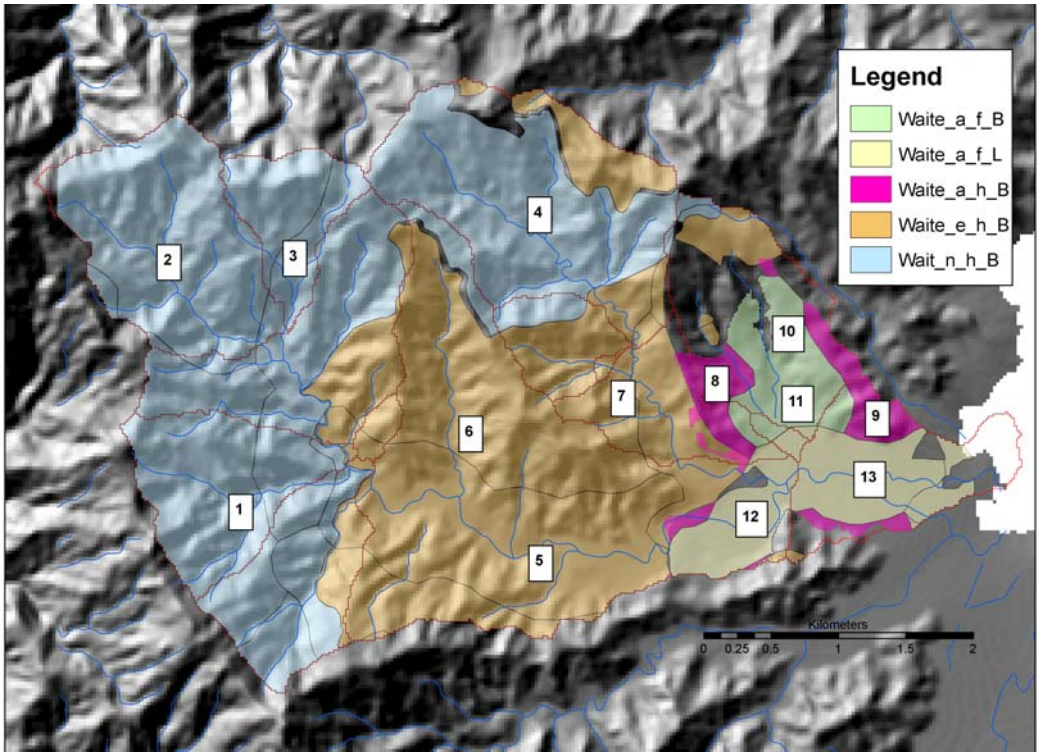

Figure 6.1. Waitekuri subcatchment sampling sites, where the first letter is landuse (a=agriculture, e=exotic, n=native), second letter is slope group (f=flat 0°-15° and h=high 16°- > 42°), and the third letter is soil group (B=Brown, L=Lowland associations).

The Waingaro and Opitonui subcatchment (Figure 6.2) was the largest of the subcatchments and was dominated by exotic forest on high slopes under Brown soils (Wain_e_h_B). A smaller area of exotics exists on low slopes under Brown soils (Wain_e_f_B) and this was the only area in the catchment where this occurs. A large section of agricultural land was on low slopes under Lowland soils (Wain_a_f_L).

[1] Some of the maps show areas of no data, and this is due to areas of vegetation not considered in the sampling categories, such as scrub or estuarine vegetation.

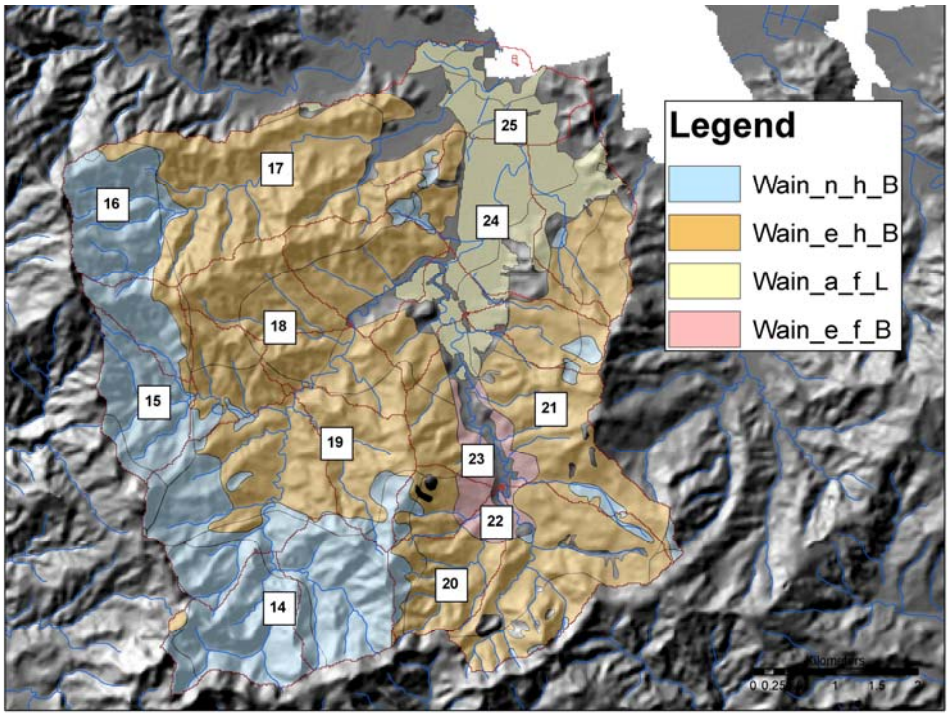

Figure 6.2. Waingaro and Opitonui subcatchment sampling sites, where the first letter is landuse (a=agriculture, e=exotic, n=native), second letter is slope group (f=flat 0°-15° and h=high 16°- > 42°), and the third letter is soil group (B=Brown, L=Lowland associations).

Only a small section of native forest was present in the Owera subcatchment (Figure 6.3) and was typical of the Whangapoua catchment in that it was on high slopes under Brown soils (Owera_n_h_B). The Owera subcatchment was dominated by exotic forest on high slope classes under Brown soils (Owera_e_h_B). A rare area of exotic forest on low slope classes under Lowland soils was also present in this subcatchment (Owera_e_f_L). The low slope areas were more typically found under agricultural landuse. Characteristic of the Whangapoua catchment was a large area of agricultural land on low slopes under Lowland soils (Wain_a_f_L).

A small section of native forest occurred in the top part of the Otanguru subcatchment (Figure 6.4) along with areas that are restricted to drainage lines within the exotic forest (Otang_n_h_B). The subcatchment was also dominated by exotic forests on high slope under Brown soils (Otang_e_h_B). Similar to the Waitekuri subcatchment, there was also a small area with agriculture on a high slope class under Brown soils (Otang_a_h_B), but more typically agriculture was on low slope classes under Lowland soils (Otang_a_f_L).

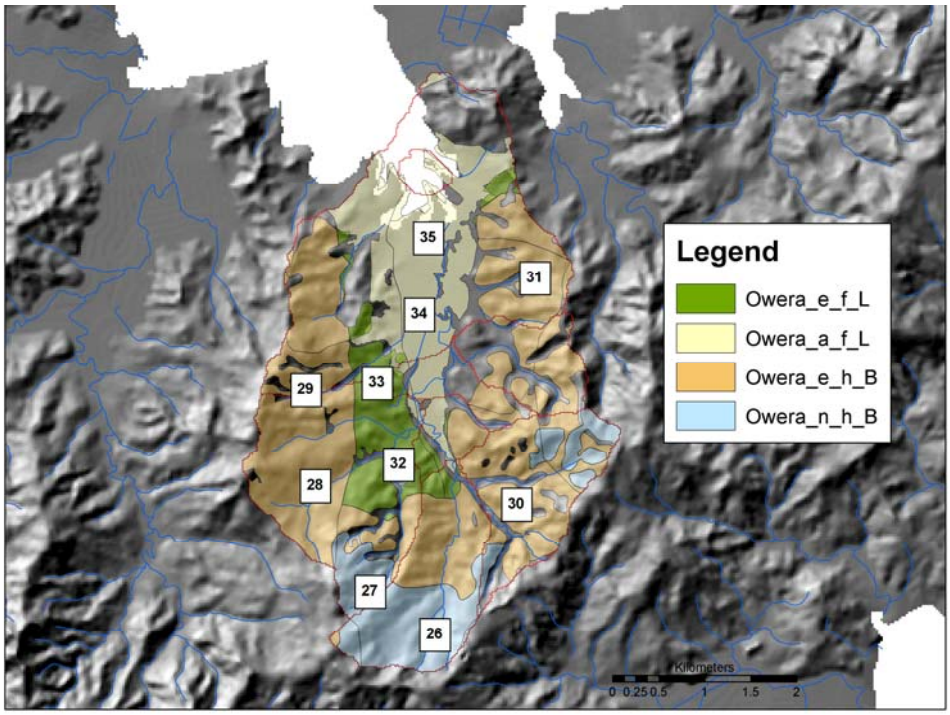

Figure 6.3. Owera subcatchment sampling sites, where the first letter is landuse (a=agriculture, e=exotic, n=native), second letter is slope group (f=flat 0°-15° and h=high 16°- > 42°), and the third letter is soil group (B=Brown, L=Lowland associations).

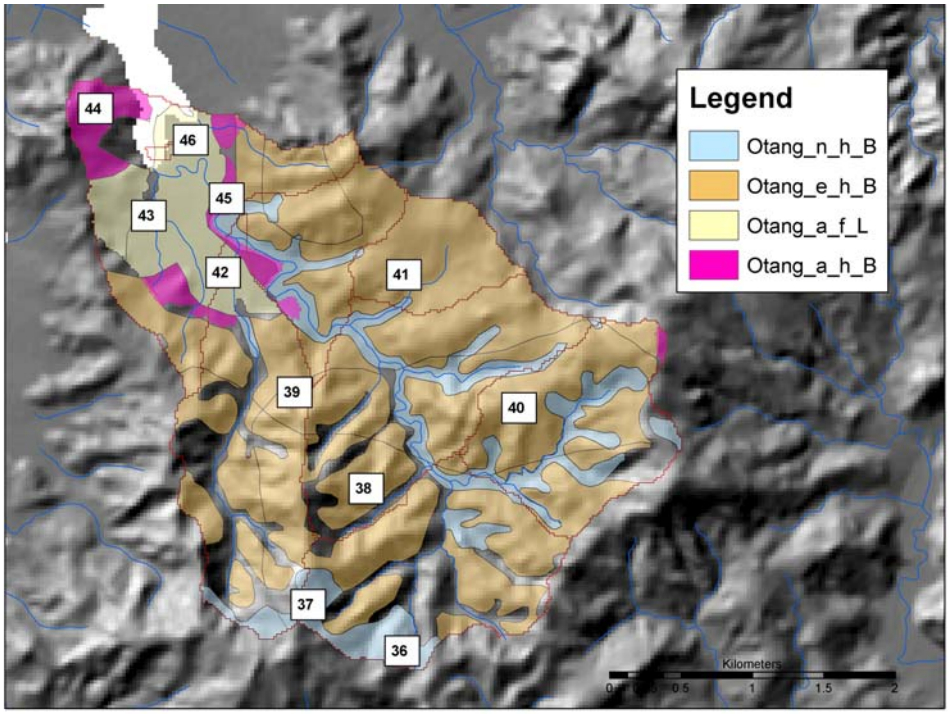

Figure 6.4. Otanguru subcatchment sampling sites, where the first letter is landuse (a=agriculture, e=exotic, n=native), second letter is slope group (f=flat 0°-15° and h=high 16°- > 42°), and the third letter is soil group (B=Brown, L=Lowland associations).

The Mapauriki subcatchment (Figure 6.5) is dominated by exotic forest on high slopes under Brown soils (Mapa_e_h_B). Native forest was limited to drainage lines and some small pockets at the top of the subcatchment (Mapa_n_h_B). Agriculture occurs on flat land with Lowland soils (Mapa_a_f_L) and a large area left void in the north of the subcatchment was an area of coastal scrub.

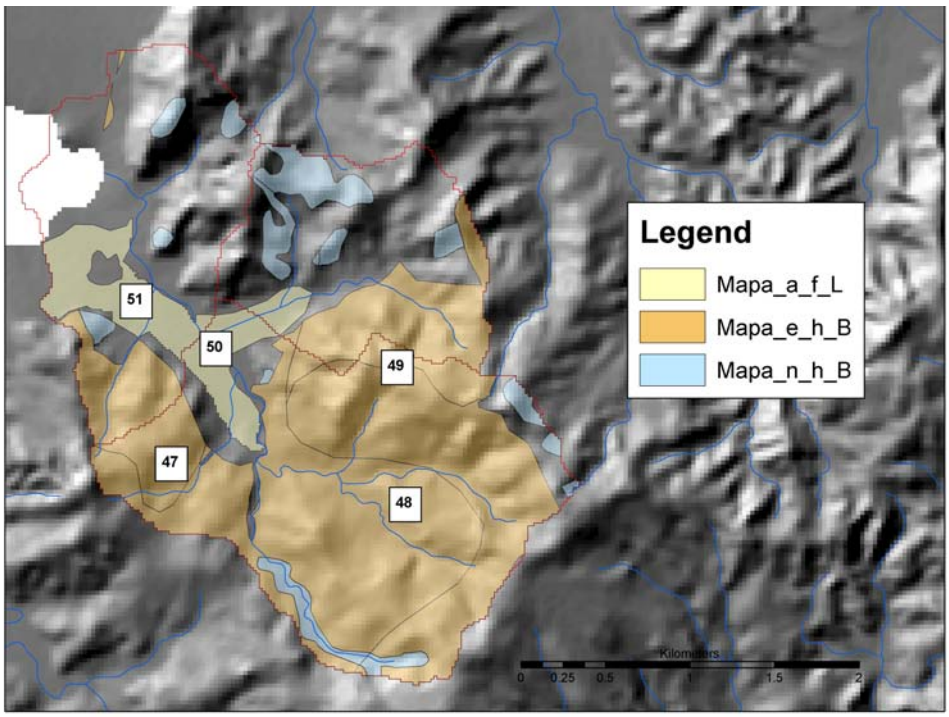

Figure 6.5. Mapauriki subcatchment sampling sites, where the first letter is landuse (a=agriculture, e=exotic, n=native), second letter is slope group (f=flat 0°-15° and h=high 16°- > 42°), and the third letter is soil group (B=Brown, L=Lowland associations).

6.2.3 Soil sampling

The allocation of sampling sites was 11 for native forest, 23 for exotic forest, and 16 for agriculture (Table 6-2). The percentage of the sample site allocation was native 22%, exotic 46%, and agriculture 32% which reflects the actual landuse of the total catchment area (native 19%, exotic 55%, agriculture 16%). The higher representation of agriculture in the sample allocation reflects the need to capture the greater variation of slope and soils within the agriculture landscape unit. The sample allocation number for landuse and erosion position is shown in Table 6-2, along with total sample allocation for the subcatchment, slope and soil categories.

Table 6-2. Number of sampling sites allocated (bold type) for landscape unit, subcatchment, slope and soil classes.

Category	Number of classes	Class description
Landuse	3	Native forest **(11)**, exotic forest **(23)**, agriculture **(16)**
Subcatchment	5	Waitekuri **(13)**, Waingaro & Opitonui **(13)**, Owera **(10)**, Otanguru **(9)**, Mapauriki **(5)**
Slope class	2	Flat to rolling **(16)**, strongly rolling to precipitous **(34)**
Soil type	2	Hill slope associations (Brown) **(38)**, flat associations (Allophanic, Gley, Organic) **(23)**

The coordinates of each sampling site were recorded from the subcatchment maps and loaded into a hand held GPS. The GPS was used in the field to navigate to the sampling site location, or as near as practically possible. Once the sampling site has been determined, the actual coordinates were recorded using a hand held GPS and the actual sampling sites are shown in Figure 6.6. Some planned sampling point's locations had to be modified because of restrictions to access. Originally there were 51 sampling sites planned (Figures 6.1 to 6.5), but because of the inability to gain permission for access from the landowner sample site #46 was not sampled.

At each of the 50 sampling sites, three soil samples were taken to characterise the surface (0-2 cm), subsurface (> 20 cm), and streambank erosion positions. The subsurface sample acts as a proxy for landslide erosion processes. Ten individual soil samples were taken in an approximate 10 m square and bulked in the field to represent surface and subsurface erosion positions. The same assumptions about sampling areas 'likely to erode' (defined here as likely to deliver sediment to streamlines) by identifying proximal sources of soil erosion (Section 5.3) meant that sampling points were within 10 m of drainage lines on flat land and up to 20 m on steeper land for surface and subsurface samples. Ten individual samples were taken along around 20 m of streamline to represent streambank erosion processes. Thus surface, subsurface and streambank samples from 50 sites meant that 150 soil samples were analyzed.

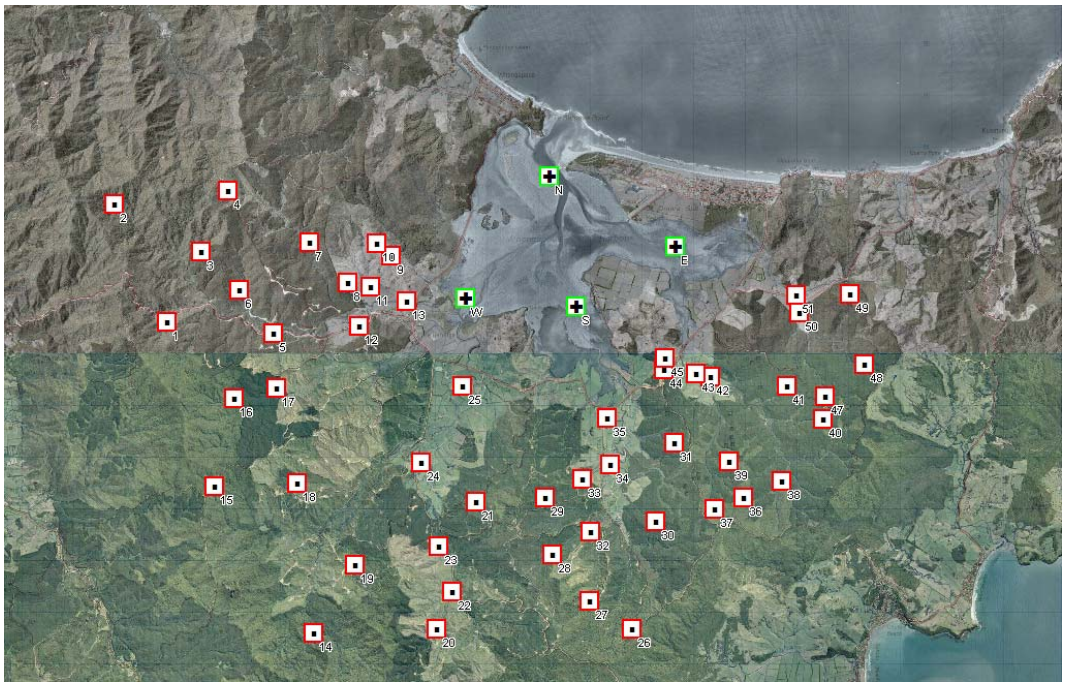

Figure 6.6. Sampling sites for the sediment fingerprinting study of the Whangapoua catchment. Sampling sites N, S, E, and W (green boxes with crosses) are the sink sampling locations).

The 150 soil samples were collected, handled, and transported as per the methods outlined in Section 5.4.1. The method of extracting the < 10 μm size fraction from the soil samples for analysis by ICP-MS is detailed in Sections 4.2 and 4.3. The rationale for using the < 10 μm size fraction is contained in Appendix J.

6.3 Sink area sample collection

A minimum of 10 g of sediment of the < 10 μm size fraction was needed for radionuclide analysis. Only small quantities of sediment were collected using the time integrated sediment sampler in the pilot study (Section 5.4.2), so this method was not practical for the full sampling programme. Thus sink sediment samples were obtained from the Whangapoua Harbour.

The Whangapoua Harbour was sampled in four locations (Figure 6.7). Three of the sampling points were in the upper intertidal flats draining the Waitekuri/Waingaro/Opitonui ('W' for harbour west), the Owera ('S' for harbour south), and Waingaro/Mapauriki ('E' for harbour east) subcatchments respectively. The fourth sampling point was taken from the northern sector near

the harbour mouth ('N').The samples were collected by grab sampling either at low tide or by diving from a boat. Ten individual sediment samples of the top 2 cm were collected from within a 30 m grid using a stainless steel spade. The amount of sediment collected averaged around 4 kg and was bulked in the field then stored in plastic bags and refrigerated during transport and storage. To ensure a contemporary and representative sample, material was taken from the shoulder area of the channels. This was to avoid the coarse sediments in the channel bottom and reworked sediments from the flat tidal areas (Malcolm Green NIWA, *pers comm*).

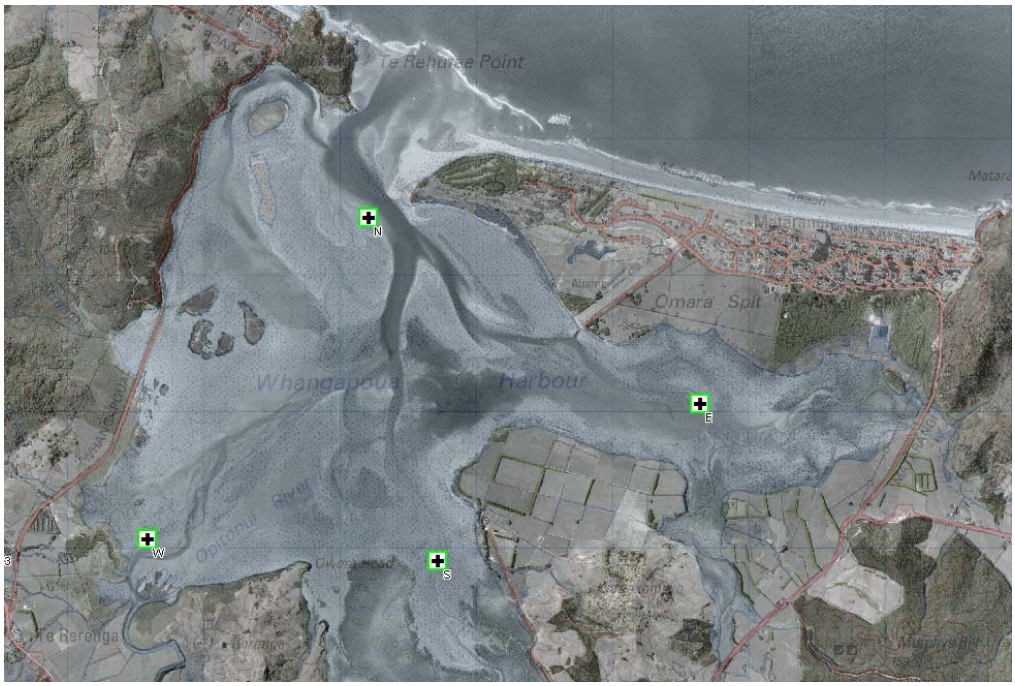

Figure 6.7. Whangapoua Harbour sink area sampling points.

The harbour sediment samples were returned to the laboratory where they were sieved to 1mm to remove debris, shells, and unbound organic matter. The samples were oven dried and the < 10 μm fraction recovered by the same method used for the catchment soil samples (Section 4.2). The < 10 μm fraction was analysed using ICP-MS, mineral magnetic, and radionuclide techniques (Section 4.3). ICP-MS was used for the geochemical analysis instead of XRF (Chapter 5) due to ICP-MS analysing for a larger range of elements and with a lower detection level.

6.4 Results

6.4.1 Geochemical results

The ICP-MS analysis on the < 10 μm sediment fraction reported the results for Lithium (Li), Sodium (Na), Magnesium (Mg), Aluminium (Al), Silicon (Si), Phosphorus (P), Sulphur (S), Potassium (K), Calcium (Ca), Vanadium (V), Chromium (Cr), Iron (Fe), Manganese (Mn), Cobalt (Co), Nickel (Ni), Copper (Cu), Zinc (Zn), Arsenic (As), Selenium (Se), Strontium (Sr), Silver (Ag), Cadmium (Cd), Indium (In), Barium (Ba), Thallium (Tl), Bismuth (Bi), Lead (Pb), Boron (B), and Uranium (U). The full ICP-MS results for the source area geochemical elements are presented in Appendix K, and the geochemical estuary sink results are presented in Appendix L. Where readings were below detection limits, the results adjusted to the lowest detection level of the ICP instrument. Boron was not considered as almost all of readings were below the detection limits of the ICP-MS instrument. Sodium was not considered as a potential fingerprint candidate (although presented), as terrestrial sources could not be distinguished from salt water additions in the catchment sink sample.

6.4.1.1 Geochemical results for landscape units

The mean concentration for the elements are presented in Figures 6.8 to 6.12. The first stage Kruskall-Wallis *H*-test to select elements uses the *sums of ranks* of the elements to find the best potential discriminator between groups, rather than the general mean concentrations which are presented in the graphs below. The graphs are used here to summarise the geochemical results and to display the differences that occur between landscape units.

The elements Cd, Na, Zn, U, Al, P, S, K, Ca that have a high concentration in the agricultural landscape unit, most likely due to human inputs (Figures 6.8 and 6.9). V, Cr, Cu, and particularly Si have an increasing pattern from native forest to exotic forest to agricultural landscape units (Figures 6.9 and 6.10). Co, Ni, Mn, Tl, Ba, Li, Sr, and Pb have the lowest concentrations in the exotic forest (Figures 6.10 and 6.11), while Ag, In, Bi, and Se show a declining pattern from native to exotic to agricultural landscape units (Figures 6.11 and 6.12). Ag, Mg, and Fe do not show any discernable pattern between the landscape units (Figure 6.12).

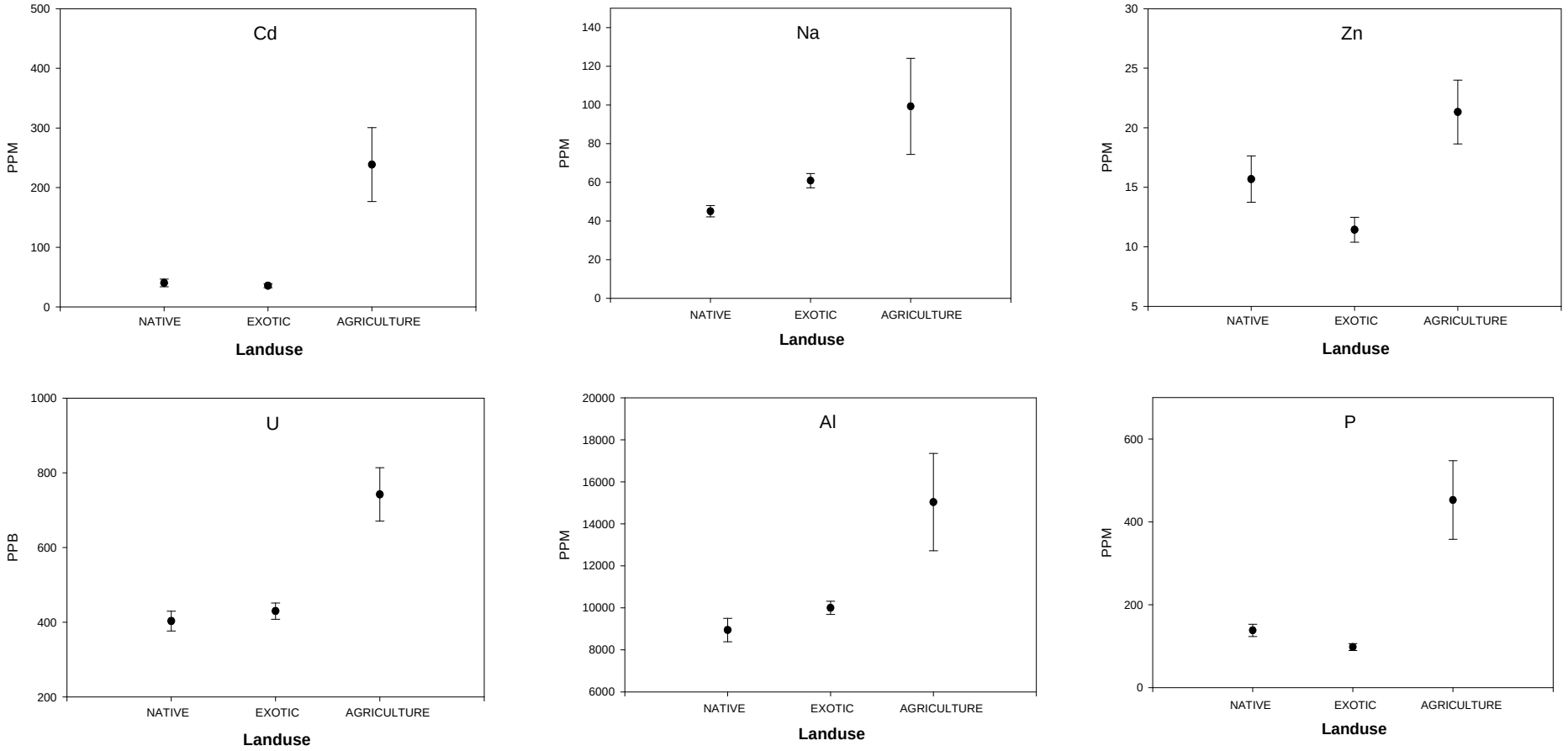

Figure 6.8. Mean concentration of Cd, Na, Zn, U, Al, and P for the native forest, exotic forest, and agricultural landscape units. Error bars represent one standard error.

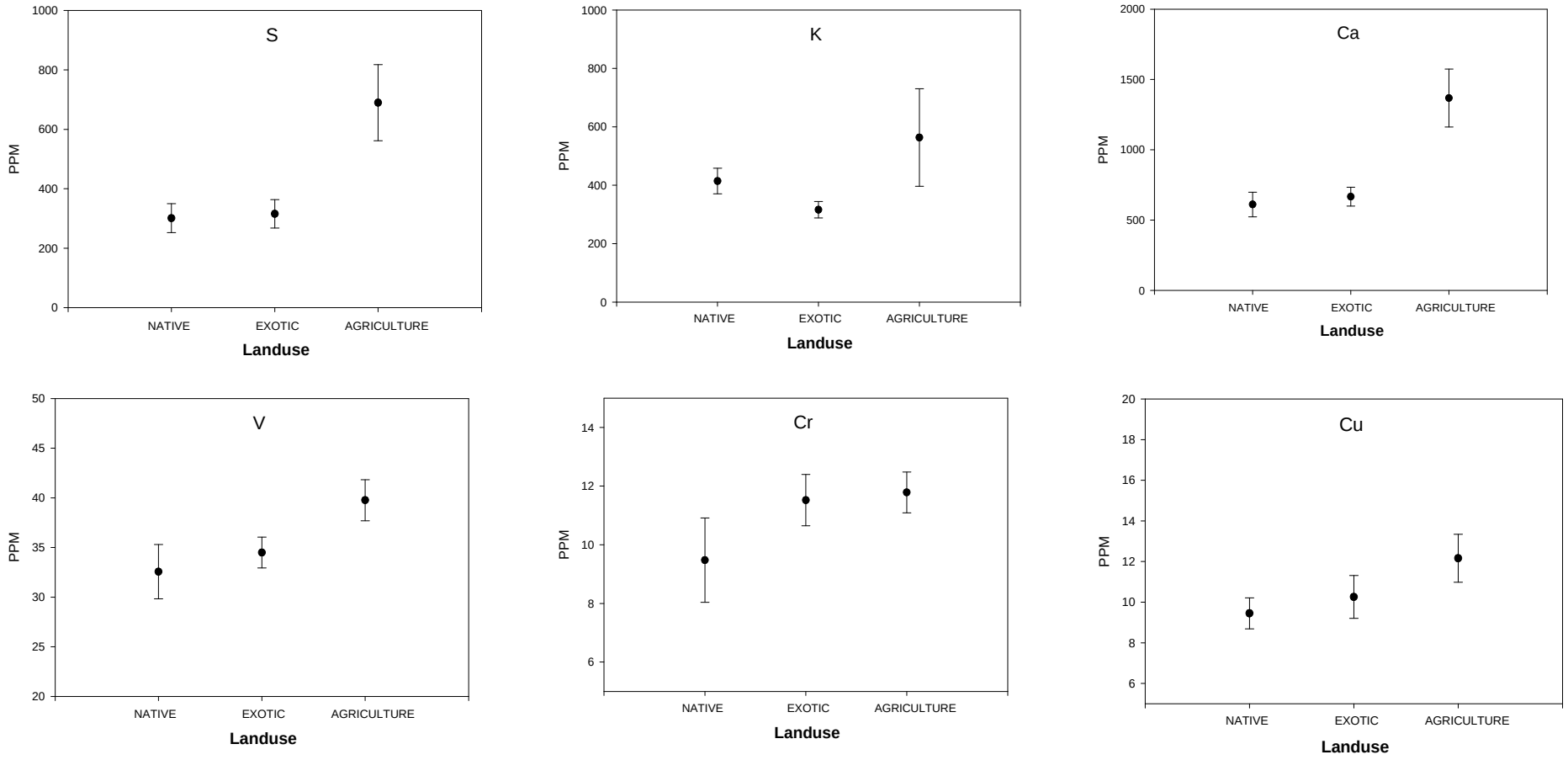

Figure 6.9. Mean concentration of S, K, Ca, V, Cr, and Cu for the native forest, exotic forest, and agricultural landscape units. Error bars represent one standard error.

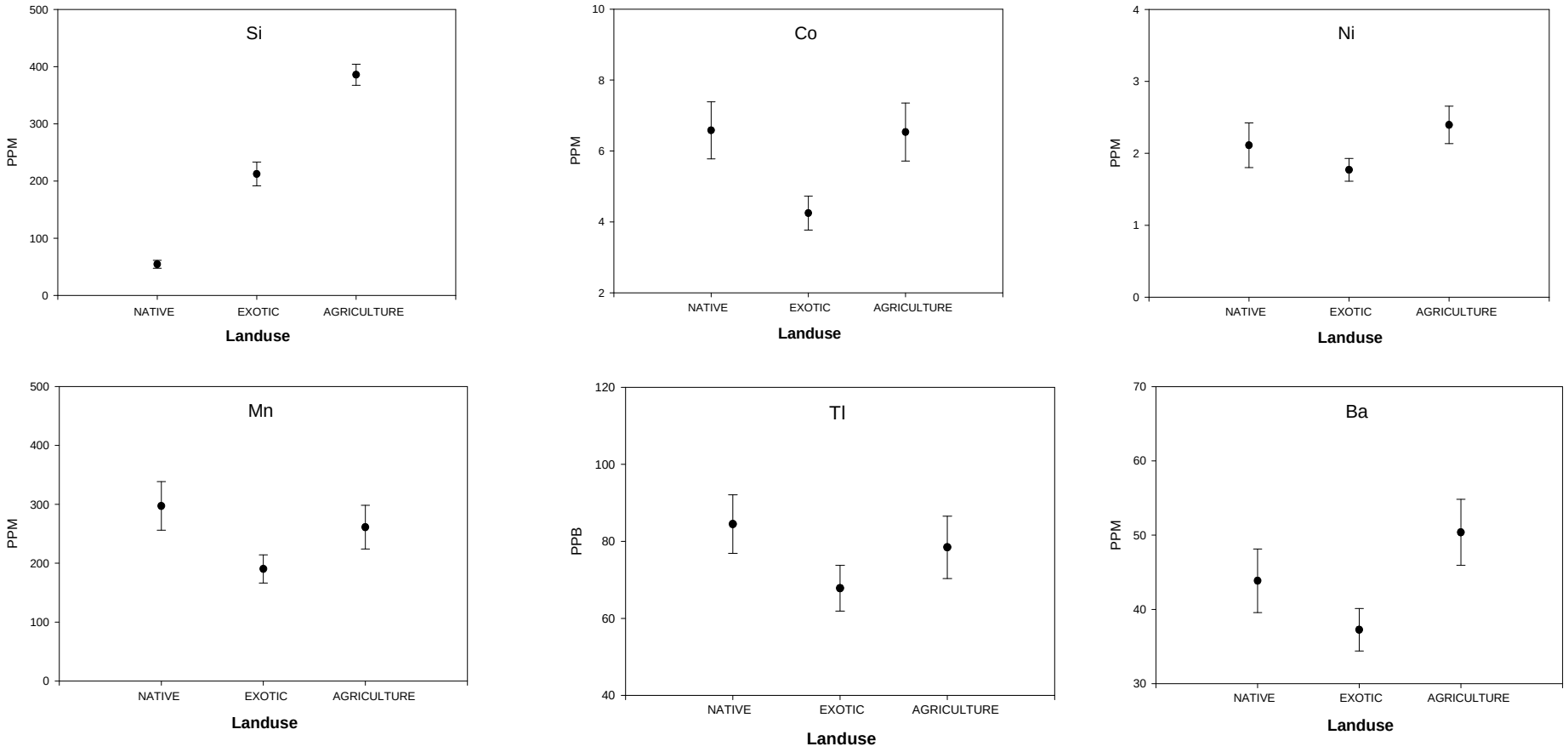

Figure 6.10. Mean concentration of Si, Co, Ni, Mn, Tl, and Ba for the native forest, exotic forest, and agricultural landscape units. Error bars represent one standard error.

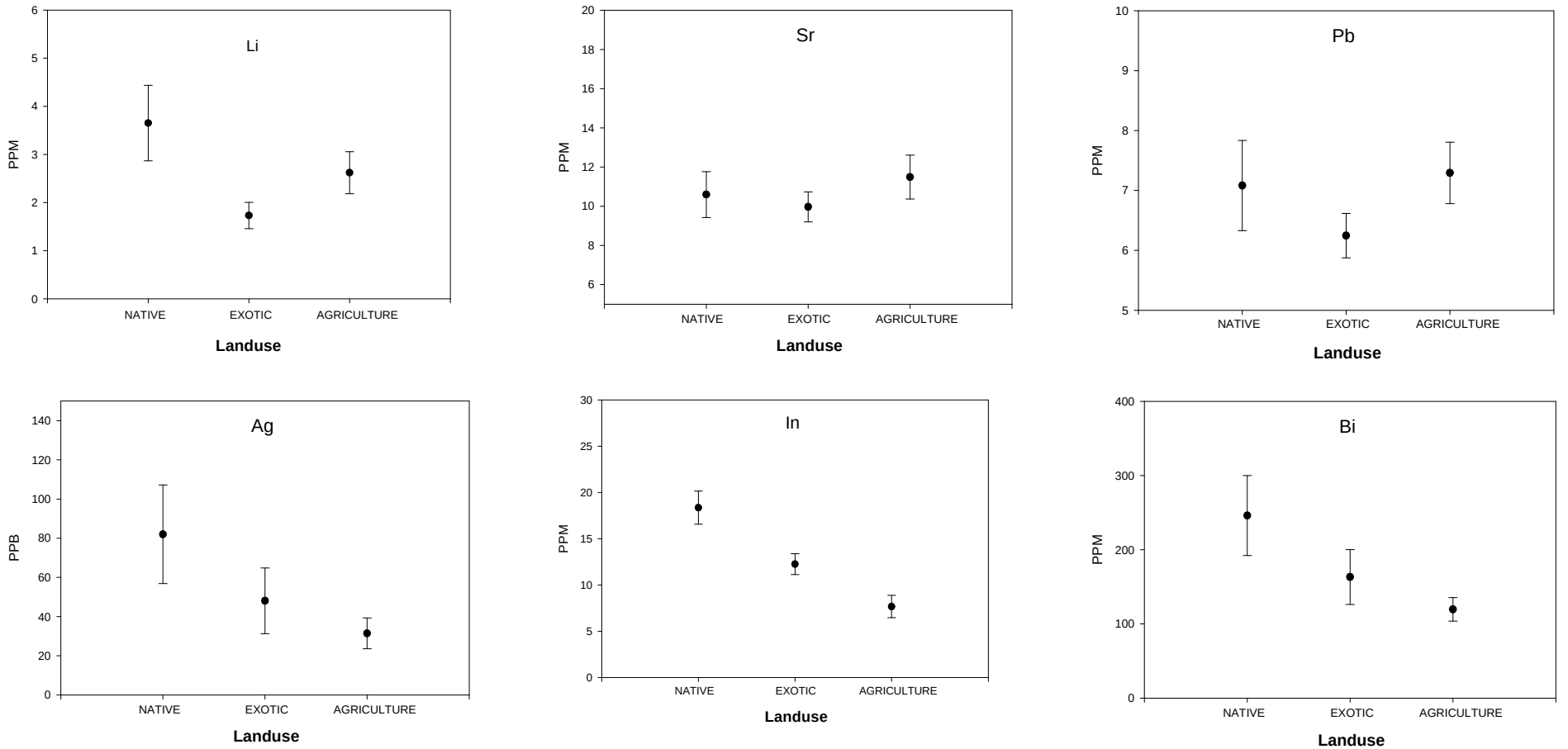

Figure 6.11. Mean concentration of Li, Sr, Pb, Ag, In, and Bi for the native forest, exotic forest, and agricultural landscape units. Error bars represent one standard error.

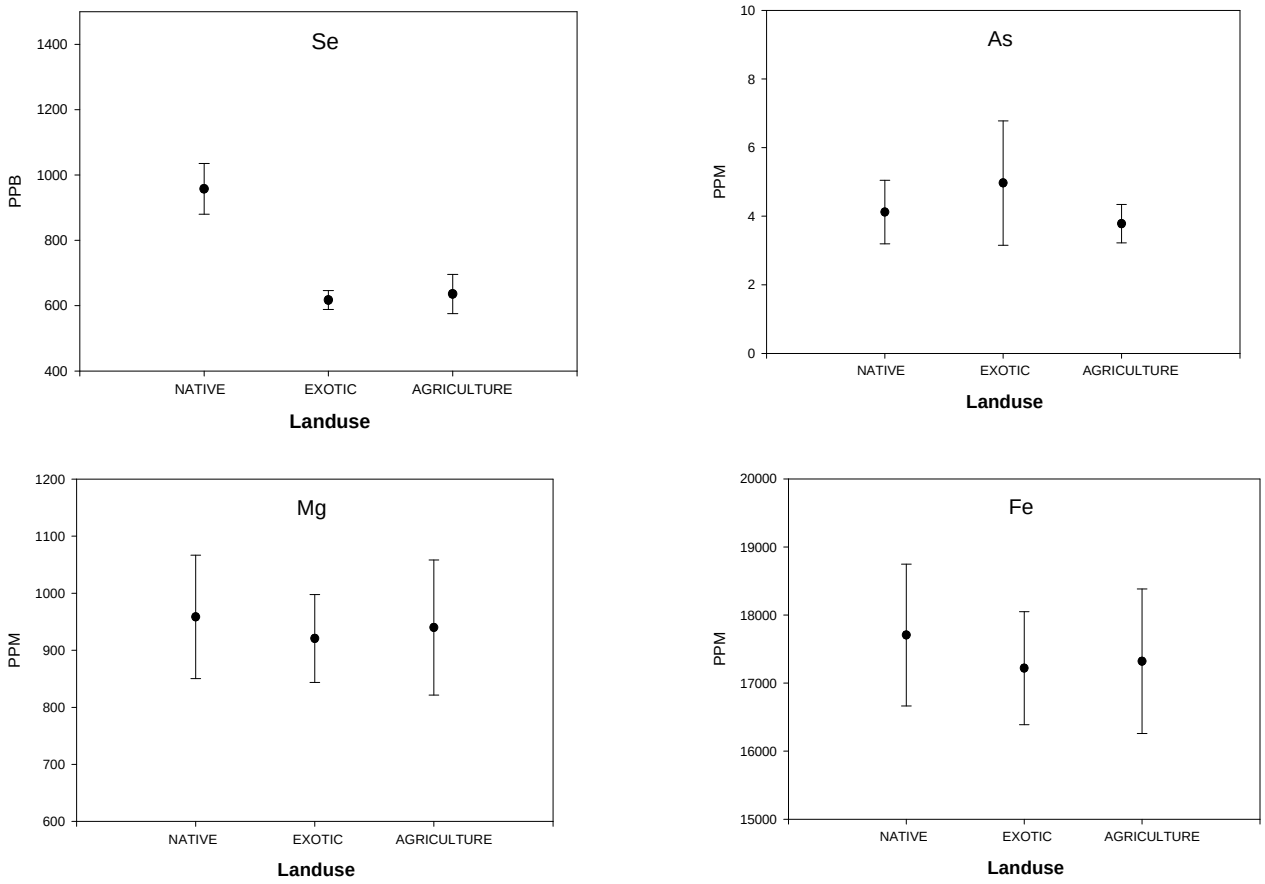

Figure 6.12. Mean concentration of Se, As, Mg, and Fe for the native forest, exotic forest, and agricultural landscape units. Error bars represent one standard error.

6.4.1.2 Geochemical results for surface, subsurface, and streambanks

The mean concentration for the elements for erosion position (surface soils, subsurface soils, and streambanks) are presented in Figures 6.13 to 6.17.

The elements K, Na, Ca, S, Cd, P, and to a lesser extent Se and Tl show a pattern of surface soil concentration (Figures 13 and 6.14). Pb, V, Cr, Fe, Ag, Si, and In show the opposite pattern of low surface concentrations and increase from subsurface to streambanks (Figures 6.14 and 6.15). Ni, Cu, Sr, Mg, Ba, Mn, Co, Zn, and to a lesser extent Li have their lowest concentrations in the subsurface position (Figures 6.15 and 6.16). U has similar concentrations in the surface and subsurface, Al in the subsurface, and Bi and Ag are similar throughout all positions (Figure 6.17).

6.4.1.3 Potential explanations of geochemical variation between landscape units and between erosion positions

One of the most obvious causes of geochemical variability between the landscape units (native forest, exotic forest, and agriculture) is human influence of silvicultural and agricultural systems. The main soil fertility constraints in New Zealand are N, P, and S (Loganathan *et al.* 2003). In the Whangapoua catchment, geochemical variability has been influenced in the agricultural landscape unit by the addition of fertilisers and chemicals (Figure 6.18), and in the exotic forests primarily by the aerial application of rock phosphate (Matene Blandford, *pers comm.*).

In a review of Waikato agricultural soils, Kim *et al.* (2008) identified five main sources that increase the concentrations of geochemical elements. They are;

- fertilisers and lime,
- animal remedies,
- pesticides,
- accelerated weathering of aluminosilicates, and
- associations with hydrated oxides of Fe and Mn.

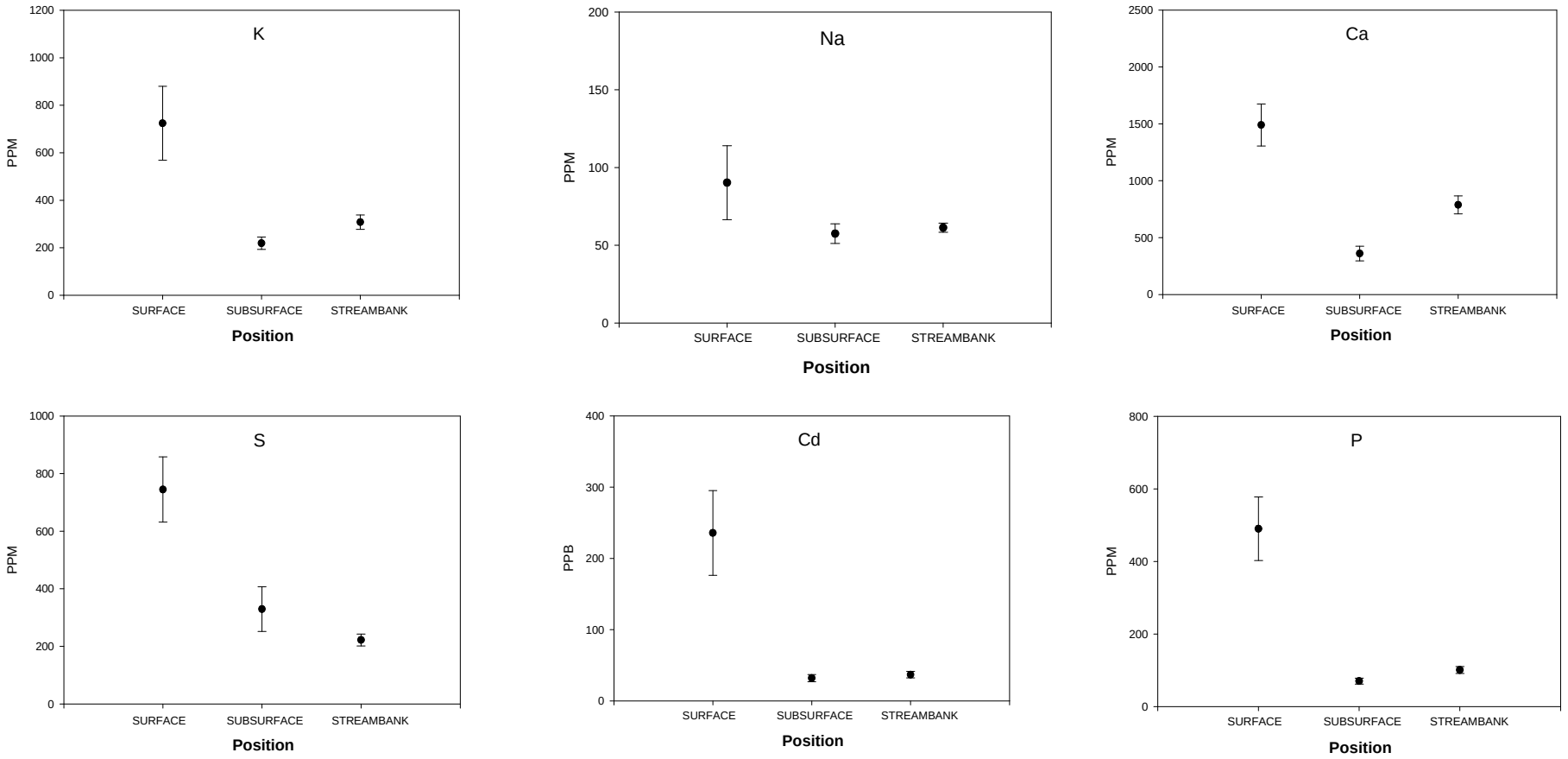

Figure 6.13. Mean concentration of K, Na, Ca, S, Cd, and P for position (surface, subsurface, and streambank). Error bars represent one standard error.

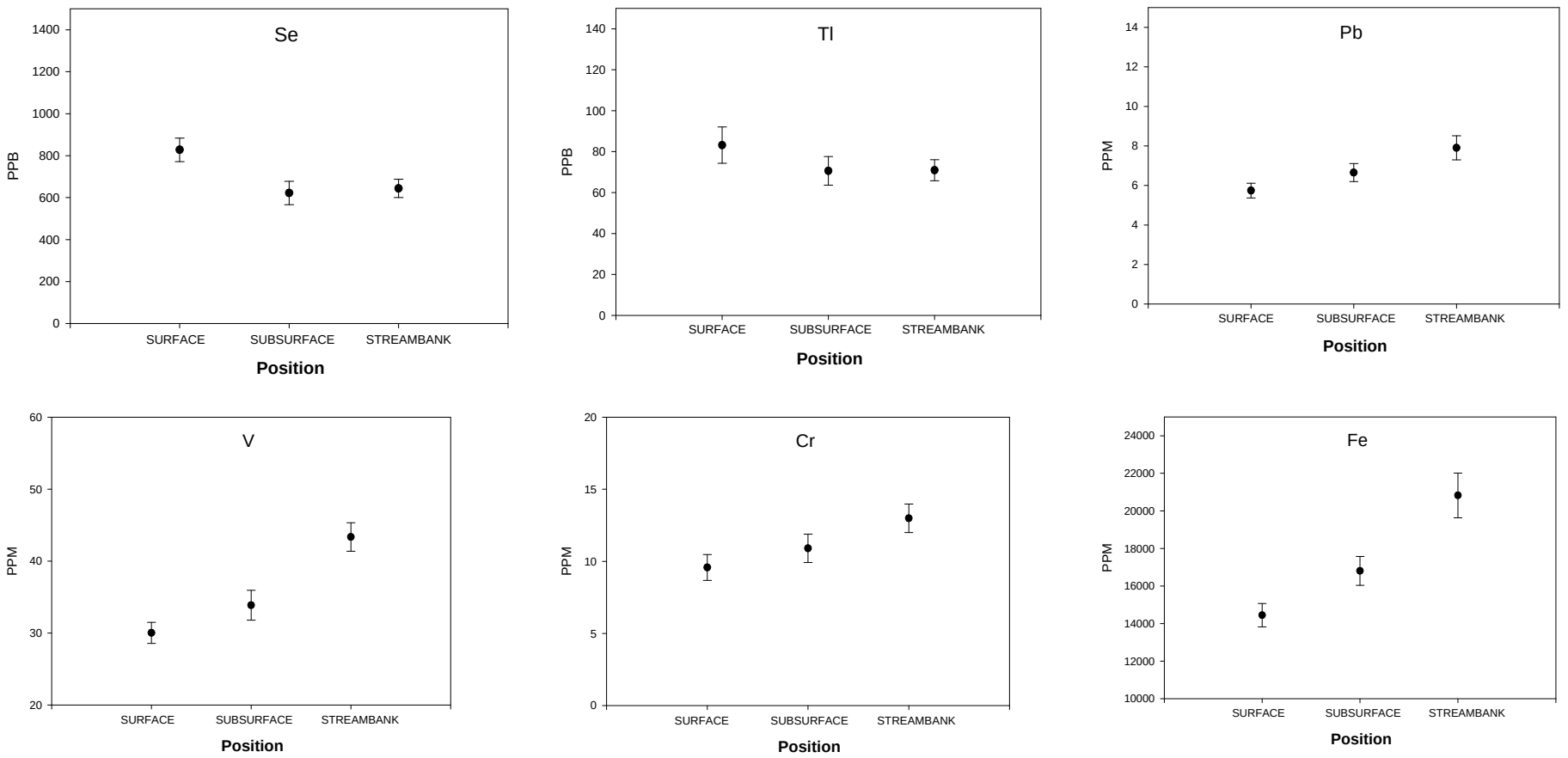

Figure 6.14. Mean concentration of Se, Tl, Pb, V, Cr, and Fe for position (surface, subsurface, and streambank). Error bars represent one standard error.

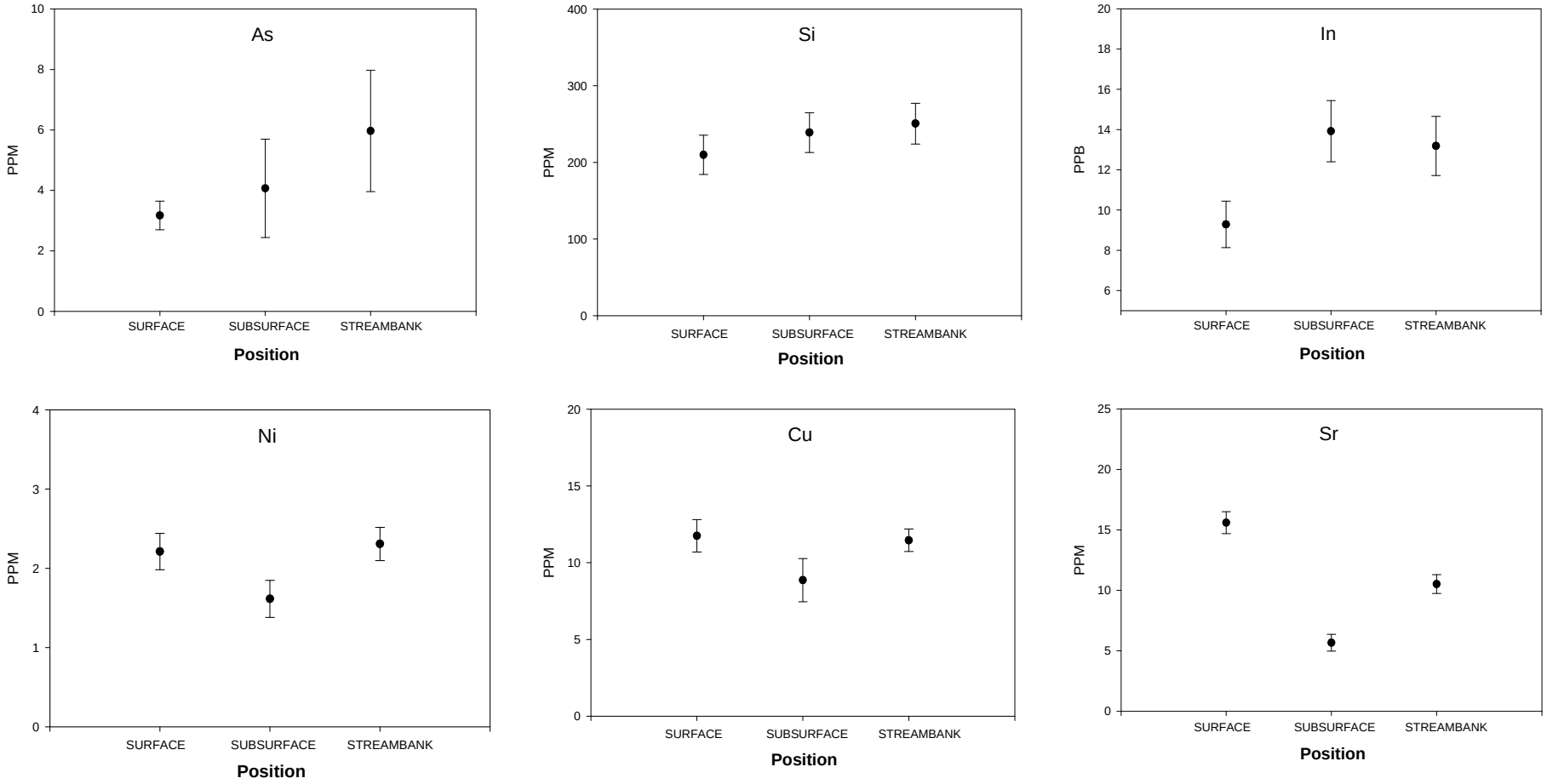

Figure 6.15. Mean concentration of As, Si, In, Ni, Cu, and Sr for position (surface, subsurface, and streambank). Error bars represent one standard error.

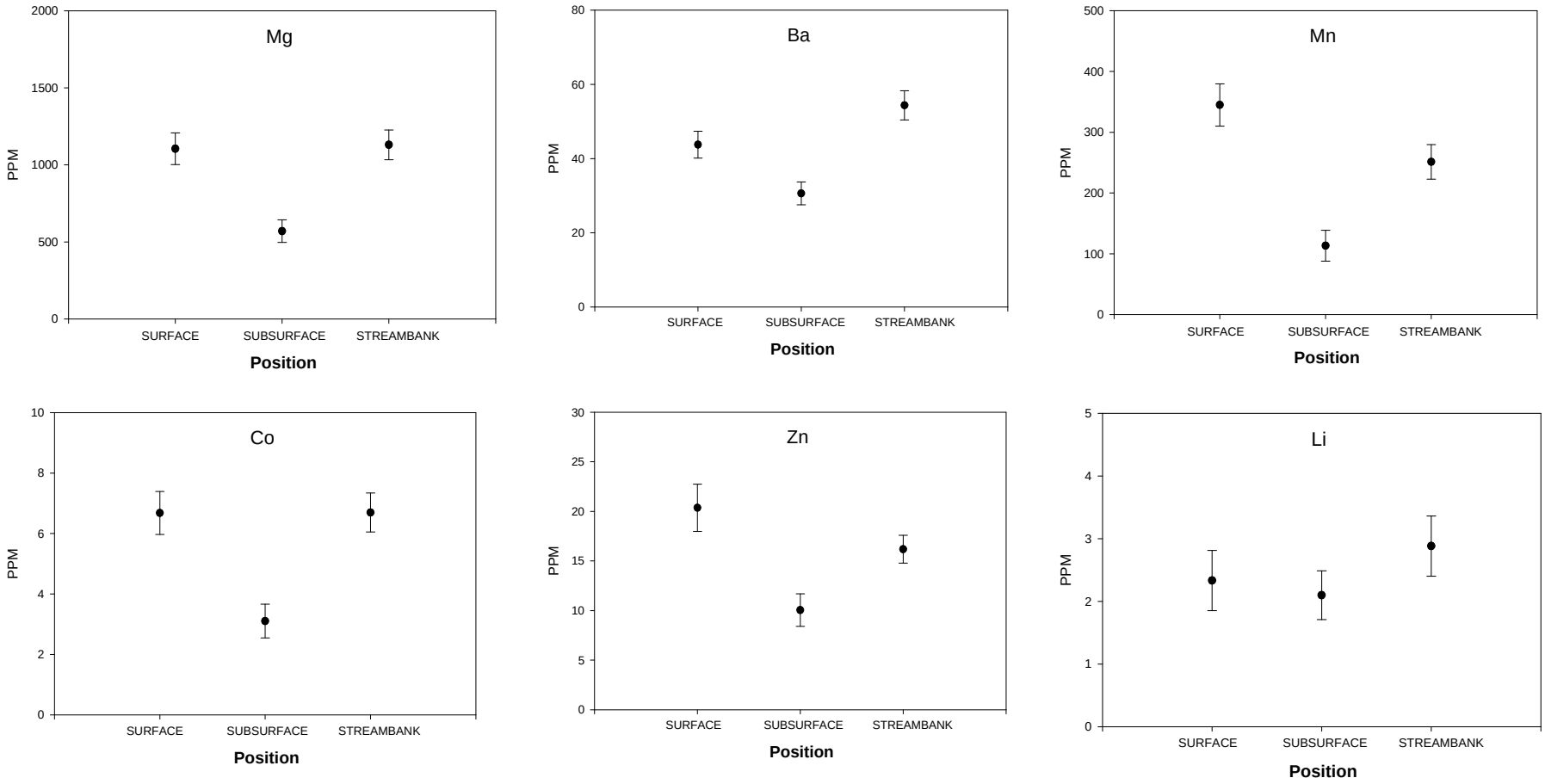

Figure 6.16. Mean concentration of Mg, Ba, Mn, Co, Zn, and Li for position (surface, subsurface, and streambank). Error bars represent one standard error.

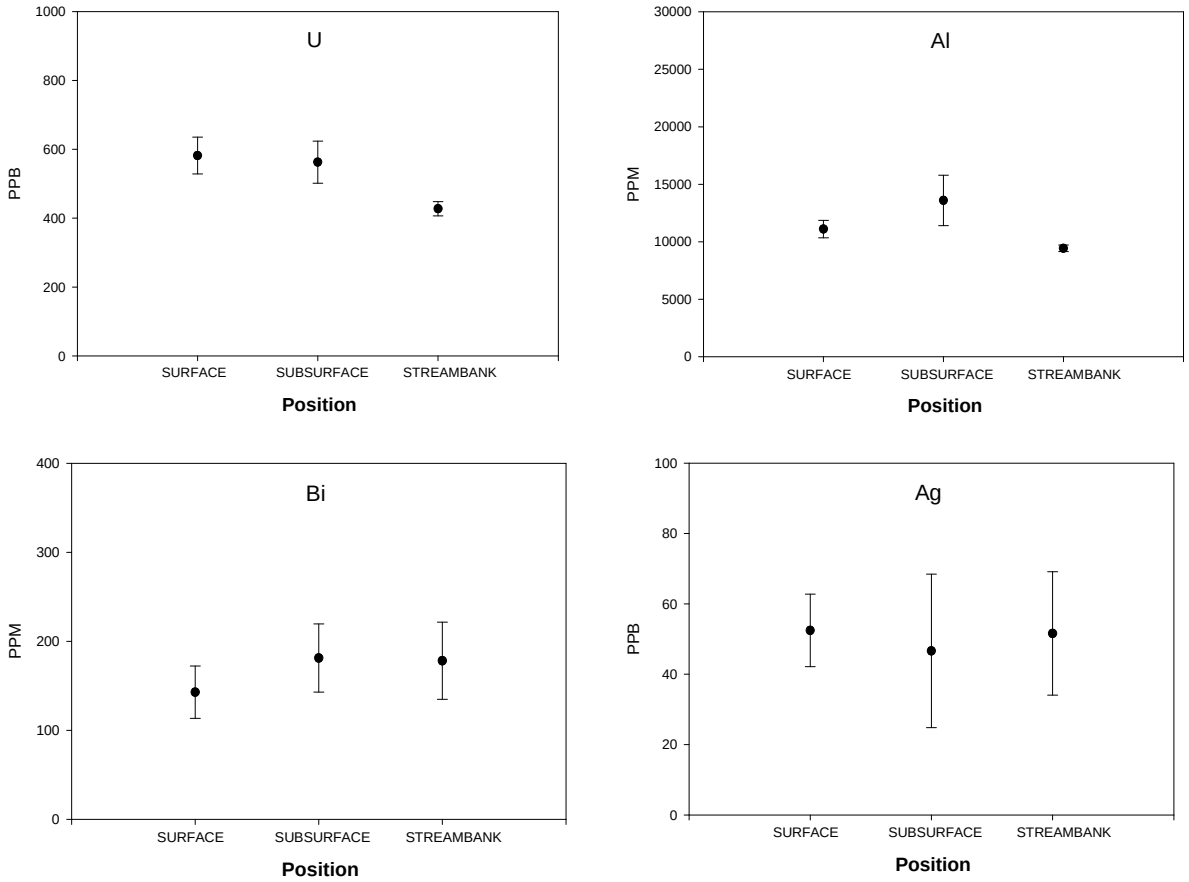

Figure 6.17. Mean concentration of U, Al, Bi, and Ag for position (surface, subsurface, and streambank). Error bars represent one standard error.

Figure 6.18. Fertiliser application in the agricultural lowland area of the Whangapoua catchment.

Fertilisers add the macro-nutrients N, P, K, S, and Ca (also from liming) to the soil. Contaminants in fertilisers may also increase trace element concentrations in the soil. Potential fertiliser additives consist of U, Cd, Cr, Ni, As, Pb, Hg, V, and Flourine (F) (McLaughlin *et al.* 1996; Cronin *et al.* 2000; Glendinning 2000; Loganathan *et al.* 2003). The main soil additives from the animal remedies source are Zn and Cu from facial eczema and supplements. The third source group of potential soil contaminants is from pesticide use, and they are most likely to be Cu, Zn, As, and Pb. The accelerated weathering of aluminosilicates means that elements normally held within the aluminosilicate lattice are released into the soil. The weathered elements are mainly Al, but also include La, Li, Ba, and Ag. The fifth category, Fe and Mn hydrated oxides, are Fe and Mn, as well as Co, Tl, Ni, Sn, and Mo (Kim *et al.* 2008). In a study of Waikato agricultural soils, Taylor & Kim (2009) found enrichment of many major and trace elements when compared to native or background soils (Figure 6.19).

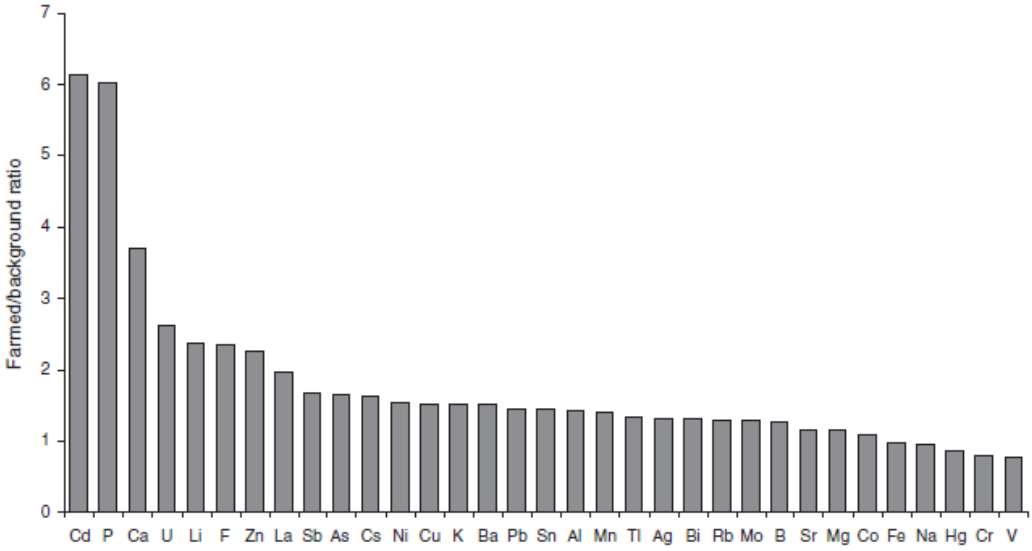

Figure 6.19. Enrichment ratios of major and trace elements in Waikato agricultural soils in comparison with native soils (Taylor & Kim 2009).

In my study, the mean concentrations of P, Ca, K, and S were higher within the agricultural areas compared with the other landscape units, which is consistent with the application of fertilisers and lime (Figures 6.8 to 6.12). The concentration of P was lower in the exotic forest than in native forests. While the nutrient demands on the soil of exotic forests are lower than for agriculture, it has been identified that the P and N demand of exotic pines peaks in years 6-8 and that successive tree crops will lead to nutrient depletion that could retard exotic pine growth (Will 1968; Turner & Lambert 1986). Exotic forests have been fertilised by aerial applications of rock phosphate, but these have been reduced in recent years due to lower timber prices (Matene Blandford, *pers comm.*). U and Cd in agricultural areas also show higher concentrations than the other landscape units and is probably due to the contamination of fertilisers. It has been reported that fertilisers sourced from Morocco and used in New Zealand had U concentrations around 140 mg kg^{-1} (Kim *et al.* 2008).

Another element showing higher concentrations in agricultural areas is Al, possibly due to accelerated weathering of aluminosilicates. This is thought to be caused by the fertiliser contaminant F which accelerates the removal of interlayer Al and increases its concentration in the soil solution (Egli *et al.* 2001; Manoharan *et al.* 2007; Kim *et al.* 2008).

Of the other elements, Zn shows an increased concentration in agricultural areas possibly due to animal remedies (e.g., to prevent facial eczema) or from contaminants in lime (Montagne *et al.* 2007). Cu and V have increasing concentrations from native forest to exotic forest to agriculture, and these two elements have also been shown to be contaminants associated with fertilisers (Molina *et al.* 2009).

The increasing pattern of the elements Na and Si from native forest to agriculture could be explained by Na inputs to near harbour areas by seawater aerosol and groundwater sources, while Si might reflect higher clay content down the catchment gradient. The other patterns of elements identified in Section 6.4.1.1 are not readily explainable. Elements that might be expected to behave similarly such as Cu/Pb/Zn or Cr/Ni or three plus valency elements Cr/V/Fe or two plus valency elements Mn/Mg, display different patterns (Nick Kim and Roger Briggs *pers. comm.*).

The reasons for the other observed trends in the landscape unit geochemical results is speculation. It might be due to the precipitation/dissolution, adsorption/desorption, and complexation factors differing between landuse types (Zhenli *et al.* 2005), or age factors of the productive exotic and agricultural landuses (Herpin *et al.* 2002). A study of elements down a forested Spanish toposequence found associations with carbonates (Ca and Sr), silicates and clay minerals (Al, K, Na) and Fe and Mn oxides (Cr, Cu, Ni, Co, and Zn) (Navas *et al.* 2005), but the pattern of elemental concentrations in this thesis didn't correspond to these findings.

Geochemical concentration variability could be caused by the different forest types and tree species, as they can also impact element levels in the soil. An example from Denmark showed that different tree species affect heavy metal solubility in the soil. Grand fir enhances the solubility of Cd and Zn, while Norway spruce enhances the solubility of Cu, Ni, and Pb (Andersen *et al.* 2003). A Norwegian study showed that Mg, Th, Ni, Sc, Cr, Co, Ti, Al, Fe, and La were not preferentially taken up by trees and plants while Ag, Au, Bi, Cd, Hg, Pb, S, Sb, Se, and Sr show a strong enrichment in the upper layers of the soil. This

enrichment was due to trees ridding toxic elements via litter fall (Reimann *et al.* 2007).

The use of *P. radiata* also changes the soil chemistry (Rivaie *et al.* 2008). A long term study in New Zealand showed a drop in soil pH under pine. Also, there was a drop in total cations reflecting a fall in the CEC while organic P increased (Yeates *et al.* 2000). Another study of the long term changes under *P. taeda* also showed an increase in acidity and decline in exchangeable Ca and Mg, but only a modest decline in K (Richter *et al.* 1994). Ethiopian data shows that forest soils subject to disturbances tend to have a lower CEC and nutrient retention capacity (Eshetu *et al.* 2004). Counter to these elemental differences is that one study found heavy metal concentrations did not differentiate urban landuse or cover types (Pouyat *et al.* 2007), and landuse was the least important factor in influencing geochemical variables in Irish soils (Zhang *et al.* 2008).

The variation of elements by position (Figures 6.12 to 6.15) shows the highest concentration of elements associated with fertiliser input (P, S, K, and Ca) to be in the surface soils. The fertiliser contaminant Cd was also found in high levels in surface soils. Explanations for the other patterns of concentrations are not readily apparent.

The expected pattern of elemental concentrations should be highest in surface positions and lowest in the sub-soils (Burt *et al.* 2003). For example, Figure 6.20 shows the concentration of phosphorus down two reference profiles in a native eucalypt forest in south east NSW. What is more difficult to account for is variation in geochemical concentrations between subsurface and streambank positions, so why might this variation occur?

The sediment fingerprinting statistical verification process selected P, Ca, Fe, Mn, Sr, and Ba (Section 6.4.4) to distinguish sediment derived from the surface, subsurface, and streambank erosion positions. All six of the fingerprint elements had higher concentrations in the streambank position than in the subsurface position (Figures 6.13 to 6.17). While it can be speculated that perhaps the streambank material is more recent deposited alluvial material that may contain

higher concentrations or 'legacy sediments' (Weitzman 2008), the pattern is not consistent with other major and trace elements and no definitive explanation can be proposed.

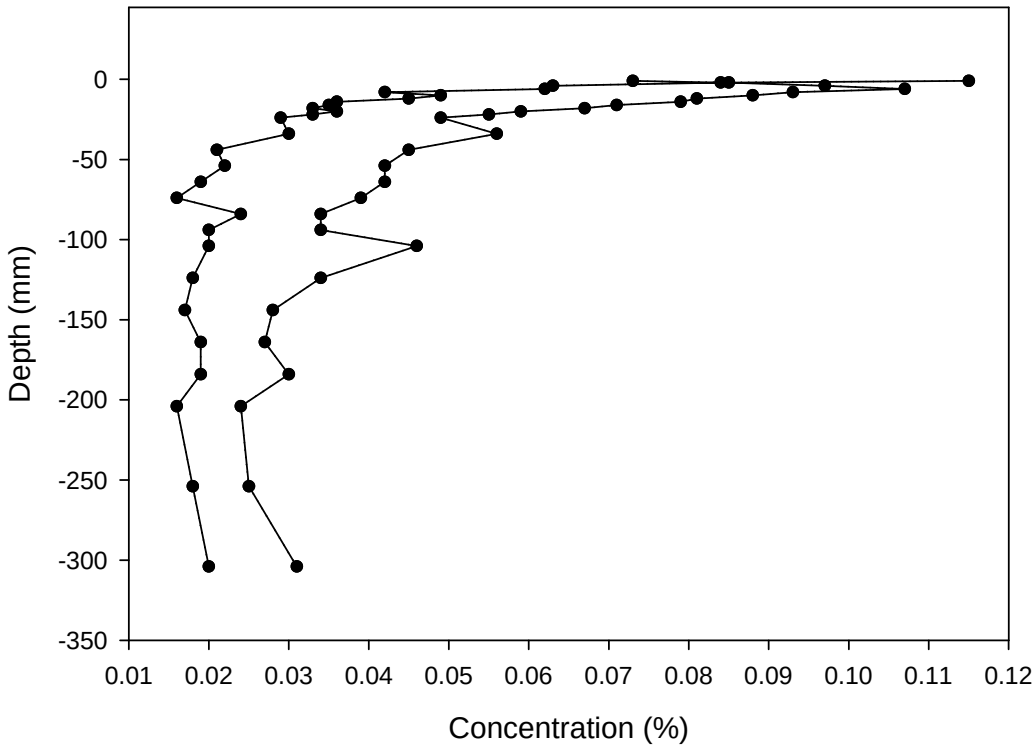

Figure 6.20. Phosphorus XRF concentrations down two reference profiles in a native eucalypt forest in south eastern NSW (Roddy 1997).

6.4.2 Statistical analysis to determine fingerprint candidates for landscape units

The sediment fingerprinting statistical process firstly involves selecting candidate elements to distinguish between the landscape units (native forest, exotic forest, and agriculture) and was achieved using the Kruskall-Wallis *H*-test. Elements were eliminated on the basis that their *p*-values were above the 5% level of significance (i.e., $p \geq 0.05$). The Kruskall-Wallis *H*-test identified 17 elements (Li, Al, Si, P, Ca, V, Cr, Mn, Co, Zn, As, Se, Ag, Cd, In, Bi, and U) that were significantly different ($p \leq 0.05$) between the three landscape units (Table 6-3). Full Kruskall-Wallis *H*-test results are contained in Appendix M.

Table 6-3. Kruskall-Wallis *H*-test results for elements that vary significantly between landscape units based on $p \leq 0.05$ between the sums of ranks. The sum of ranks result column adds up to 11,325 which is the sum of the 1, 2, 3, …150 ranks.

Element	*p* value	Sum of ranks: Native	Sum of ranks: Exotic	Sum of ranks: Agriculture
Li	0.0057	2899	4361	4065
Al	0.0042	1844	5239	4242
Si	0.0000	978	5041	5306
P	0.0056	2763	4361	4201
Ca	0.0094	2147	4806	4372
V	0.0269	2125	4937	4263
Cr	0.0059	1852	5271	4202
Mn	0.0394	2969	4620	3736
Co	0.0358	2888	4548	3889
Zn	0.0155	2697	4457	4171
As	0.0105	2666	4433	4226
Se	0.0000	3543	4757	3025
Ag	0.0061	3188	4833	3304
Cd	0.0035	2319	4555	4450
In	0.0000	3364	5408	2552
Bi	0.0064	3064	4448	3813
U	0.0000	1984	4586	4755

The selected elements (Table 6-3) were further optimised by forward stepwise Discriminant Function Analysis (DFA). The elements were examined to see what combination afforded the greatest discrimination between the native, exotic, and agricultural landscape units based on the minimisation of the Wilks' lambda statistic. The *F-to-enter* value for the forward stepwise DFA process was set at three (see Chapter 5 for details). Eight elements were selected for the model and nine rejected on the basis of the DFA model. The eight elements selected to discriminate between landscape units were Si, P, Se, V, U, In, Bi, and Ca (Table 6-4). The combination of the eight elements to distinguish landscape elements was highly significant (Wilks' lambda = 0.28982; $F = 15.007$; $p < 0.001$) and the eight elements selected by the DFA process were themselves significant as indicated by the red colour in Table 6-4. Note that with the adjusted *F-to-enter* value of three, all of the selected elements are significant as indicated by the red colour of the output in Table 6-4.

Table 6-4. Results of the forward stepwise DFA for landscape units. Eight elements were selected for the model (top) and nine were rejected (bottom).

N=150	Discriminant Function Analysis Summary (ICP_data in Project_KWall&DFA.stw) Step 8, N of vars in model: 8; Grouping: Landuse (3 grps) Wilks' Lambda: .28982 approx. F (16,280)=15.007 p<0.0000					
	Wilks' Lambda	Partial Lambda	F-remove (2,140)	p-level	Toler.	1-Toler. (R-Sqr.)
Si-corr	0.382901	0.756918	22.48030	0.000000	0.787335	0.212665
P-corr	0.308752	0.938696	4.57153	0.011933	0.224823	0.775177
Se-corr	0.304593	0.951513	3.56705	0.030834	0.572533	0.427468
V-corr	0.359749	0.805630	16.88850	0.000000	0.652016	0.347984
U-corr	0.357902	0.809788	16.44241	0.000000	0.468617	0.531383
In-corr	0.351087	0.825506	14.79644	0.000001	0.326342	0.673658
Bi-corr	0.317024	0.914205	6.56927	0.001875	0.616549	0.383451
Ca-corr	0.303929	0.953593	3.40658	0.035926	0.239823	0.760177

N=150	Variables currently not in the model (ICP_data in Project_KWall&DFA.stw) Df for all F-tests: 2,139					
	Wilks' Lambda	Partial Lambda	F to enter	p-level	Toler.	1-Toler. (R-Sqr.)
Li-corr	0.282037	0.973131	1.918952	0.150629	0.755477	0.244523
Al-corr	0.287322	0.991366	0.605317	0.547334	0.318976	0.681025
Cr-corr	0.285983	0.986747	0.933478	0.395634	0.759692	0.240308
Mn-corr	0.285588	0.985383	1.030974	0.359370	0.672130	0.327870
Co-corr	0.280859	0.969067	2.218465	0.112614	0.745482	0.254518
Zn-corr	0.288905	0.996827	0.221238	0.801808	0.421346	0.578654
As-corr	0.288229	0.994496	0.384675	0.681394	0.948854	0.051146
Ag-corr	0.288313	0.994785	0.364350	0.695309	0.776490	0.223510
Cd-corr	0.287363	0.991505	0.595438	0.552721	0.316134	0.683866

Canonical analysis showed good separation between the native forest and agricultural landscape units, with the exotic forest landscape unit partially overlapping both the native forest and agricultural landscape units (Figure 6.21). As shown in the pilot study (Chapter 5), it is difficult to quantify the discrimination between the landscape unit groups. The canonical graphs are the best way to interpret the discrimination between groups. So while the result is significant and there is separation between landscape units, some overlap does occur.

6.4.3 Mixing model results for landscape units

The eight fingerprint elements optimised by DFA were then used in the mixing model to determine the relative proportions of sediment contribution from the three landscape units. In the pilot study (Chapter 5) the mixing model problem was posed once to generate a single relative contribution solution with no estimate of uncertainty. Greater confidence was expected for the full sampling programme

Figure 6.21. Canonical analysis of DFA results using Si, P, Se, V, U, In, Bi, and Ca for landscape units. Ellipses are 0.95 of the data range.

data (n = 150 for each element) in comparison with the pilot study (n = 27 for each element). The larger sample number allowed for the generation of synthetic data (by way of resampling) to test how well the mixing model problem is posed (Akerjord & Christophersen 1996). The uncertainty estimation was achieved by using a Monte Carlo simulation to generate an empirical distribution (Appendix E). A one-third contribution (or mixing proportion) from each of the native forest, exotic forest, and agricultural landscape units was used as the starting assumption. The mixing model was run for 100 iterations with the Monte Carlo simulation and the relative proportion result for each landscape unit was then used as the starting model proportions for a 5000 iteration run. The mean of the 5000 iteration run served as the final estimate of the relative sediment contribution from each landscape unit. The uncertainty was estimated by calculating the standard deviation of the 5000 iteration run for each landscape unit.

The results show that the dominant contributor of sediment to Whangapoua Harbour was native forest (62% ± 17%), followed by exotic forest (23% ± 12%), and then agriculture (15% ± 10%).

The Monte Carlo 5000 iteration run to estimate native forest contributions showed a right skew of the empirical distribution (Figure 6.22). The highest count (1360) was for the contribution of 0.52, but the right skew of the distribution led to a higher final mean contribution. The contribution estimates for the exotic forest result are relatively uniformly distributed from 0.0 to 0.6, with the exception of the highest count (1427) for the contribution of 0.26 corresponding reasonably well with the overall mean contribution of 0.23 (Figure 6.23). The second largest count (452) for the contribution of 0.004 lowers the overall mean. The contribution estimates for agriculture is grouped around 0.23, where the highest count was recorded (1356) (Figure 6.24). Two other large counts of 885 for the contribution of 0.002 and 189 counts for 0.03 lower the overall mean to 0.15 from the mode value of 0.23.

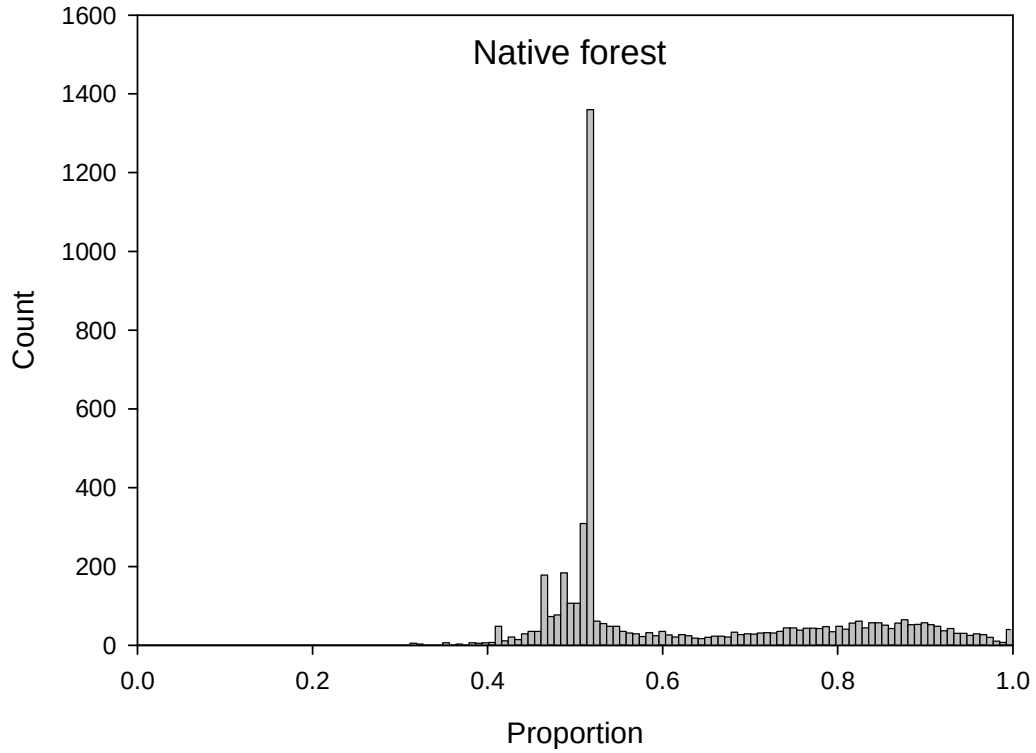

Figure 6.22. Mixing model 5000 iteration distribution for the native forest landscape unit.

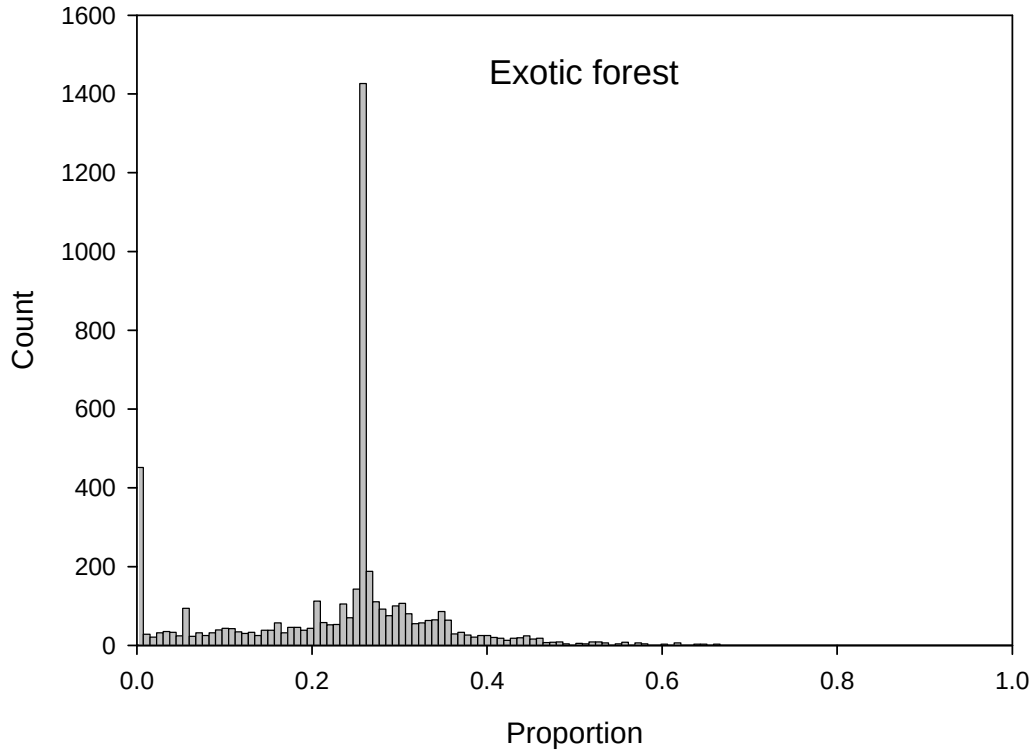

Figure 6.23. Mixing model 5000 iteration distribution for the exotic forest landscape unit.

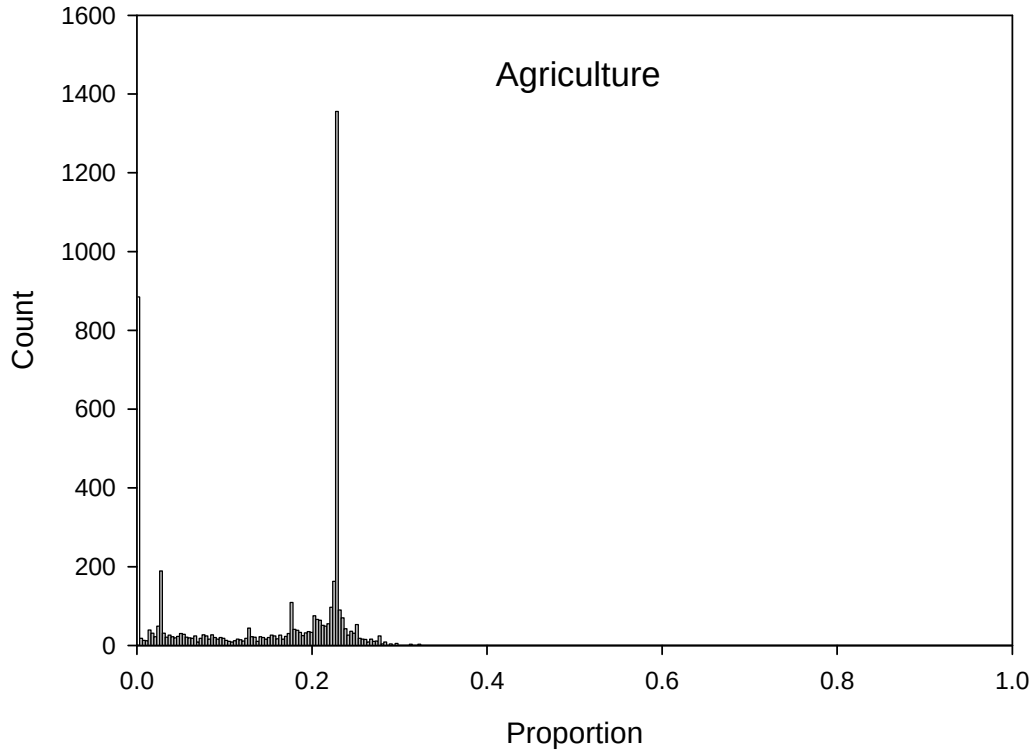

Figure 6.24. Mixing model 5000 iteration distribution for the agricultural landscape unit.

6.4.4 Statistical analysis to determine fingerprint candidates for 'position'

All the geochemical data was reassembled and the sediment fingerprinting analysis was conducted for erosion position. The first step in selecting candidate elements to distinguish between erosion positions (surface, subsurface, and streambank) was the Kruskall-Wallis *H*-test. Elements were eliminated on the basis that their *p*-values were above the 5% level of significance (i.e., $p \geq 0.05$). The Kruskall-Wallis *H*-test identified 20 elements (Mg, P, S, K, Ca, V, Cr, Fe, Mn, Co, Ni, Cu, Zn, Se, Sr, Ag, Cd, In, Ba, and Pb) that were significantly different ($p \leq 0.05$) between the three erosion positions (Table 6-5). The full Kruskall-Wallis *H*-test results are in Appendix M.

Table 6-5 Kruskall-Wallis *H*-test results for elements that vary significantly between position based on $p \leq 0.05$ between the sums of ranks. The sum of ranks result column adds up to 11,325 which is the sum of the 1, 2, 3, …150 ranks.

Element	*p* value	Sum of ranks: Surface	Sum of ranks: Subsurface	Sum of ranks: Streambanks
Mg	0.0000	4439	2359	4527
P	0.0000	5711	2336	3278
S	0.0000	5385	3009	2931
K	0.0000	5367	2480	3478
Ca	0.0000	5281	2040	4004
V	0.0000	2893	3558	4874
Cr	0.0055	3139	3660	4526
Fe	0.0001	2862	3697	4766
Mn	0.0000	4942	2250	4133
Co	0.0000	4422	2439	4464
Ni	0.0037	4031	2954	4340
Cu	0.0002	4143	2750	4432
Zn	0.0000	4502	2520	4303
Se	0.0026	4620	3185	3520
Sr	0.0000	5329	2105	3891
Ag	0.0297	4398	3279	3648
Cd	0.0000	5142	2781	3401
In	0.0425	3152	4171	4001
Ba	0.0000	3876	2751	4698
Pb	0.0071	3072	3816	4437

The twenty candidate elements were then optimised by the forward stepwise DFA with the *F-to-enter* value adjusted to three. Of the twenty candidate elements, six were selected to form the composite fingerprint (Table 6-6). The result was highly

significant (Wilks' lambda = 0.36142; F = 15.700; p < 0.001) and the DFA process selected six significant elements for the model (indicated by the red colour in Table 6-6) and rejected the other 13 elements. The six elements selected to discriminate between erosion position were Sr, Fe, Ba, Mn, P, and Ca.

Table 6-6. Results of the forward stepwise DFA for position. Six elements were selected for the model (top) and 13 were rejected (bottom).

	Discriminant Function Analysis Summary (ICP_data in Project_KWall&DFA_v2.stw) Step 6, N of vars in model: 6; Grouping: Position (3 grps) Wilks' Lambda: .36142 approx. F (12,284)=15.700 p<0.0000					
N=150	Wilks' Lambda	Partial Lambda	F-remove (2,142)	p-level	Toler.	1-Toler. (R-Sqr.)
Sr-corr	0.496518	0.727916	26.53872	0.000000	0.214998	0.785002
Fe-corr	0.380510	0.949839	3.74955	0.025890	0.734617	0.265383
Ba-corr	0.425330	0.849748	12.55418	0.000010	0.415797	0.584203
Mn-corr	0.382779	0.944210	4.19517	0.016977	0.599848	0.400152
P-corr	0.441850	0.817977	15.79946	0.000001	0.184674	0.815326
Ca-corr	0.412046	0.877144	9.94456	0.000091	0.099354	0.900646
	Variables currently not in the model (ICP_data in Project_KWall&DFA_v2.stw) Df for all F-tests: 2,141					
N=150	Wilks' Lambda	Partial Lambda	F to enter	p-level	Toler.	1-Toler. (R-Sqr.)
Mg-corr	0.361034	0.998923	0.076010	0.926845	0.426965	0.573035
S-corr	0.357245	0.988440	0.824513	0.440551	0.430570	0.569430
K-corr	0.358225	0.991151	0.629452	0.534374	0.456316	0.543684
V-corr	0.356931	0.987571	0.887264	0.414067	0.532838	0.467162
Cr-corr	0.360127	0.996414	0.253693	0.776284	0.839386	0.160614
Co-corr	0.351621	0.972879	1.965333	0.143929	0.408974	0.591026
Ni-corr	0.358569	0.992104	0.561125	0.571836	0.505109	0.494891
Cu-corr	0.361122	0.999165	0.058925	0.942801	0.664537	0.335463
Zn-corr	0.360432	0.997258	0.193863	0.823990	0.308484	0.691516
Se-corr	0.355440	0.983444	1.186854	0.308210	0.747672	0.252328
Ag-corr	0.360888	0.998519	0.104536	0.900812	0.938461	0.061539
Cd-corr	0.361305	0.999673	0.023039	0.977228	0.347758	0.652242
In-corr	0.360727	0.998072	0.136210	0.872774	0.789847	0.210153

Canonical analysis showed reasonable separation between the surface and subsurface/streambank positions, but there was greater overlap between the subsurface and streambank positions similar to the pilot study results. This probably reflects the combination of fingerprint elements in Table 6-6. Ca and P are good identifiers of surface sediment. Sr, Ba, and Mn are good identifiers of subsurface sediment, and only Fe distinguishes between all three erosion positions. The canonical results indicate that these three groups have not been distinguished as clearly as were the landscape unit groups (Figure 6.25).

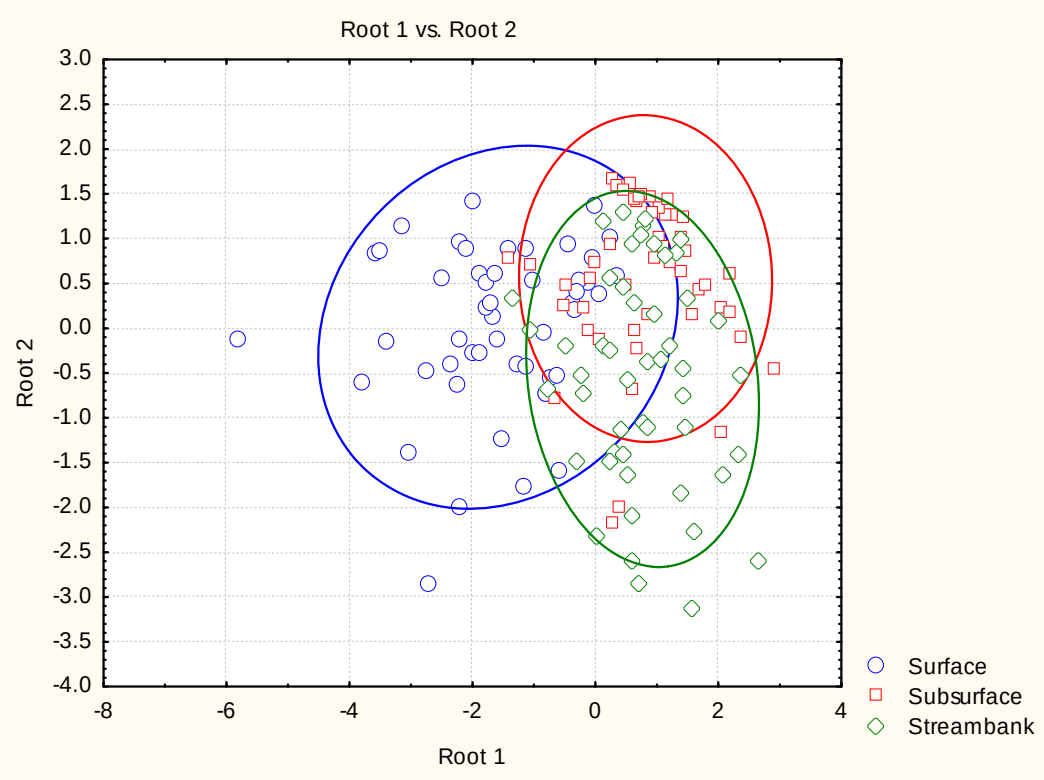

Figure 6.25. Canonical analysis of DFA results using Sr, Fe, Ba, Mn, P, and Ca for erosion positions. Ellipses are 0.95 of the data range.

6.4.5 Mixing model results for position

The six fingerprint elements optimised by DFA were then used in the mixing model to determine the relative proportions of sediment contribution from the three positions. The procedure was to run the mixing model initially for 100 iterations (with the Monte Carlo simulation) assuming a one-third starting contribution from each position for the model assumptions. The mean relative proportion results of the 100 iteration run were then to be used as the model assumptions for a run of 5000 iterations.

A problem occurred at this point with the position data in the mixing model. After 100 iterations using a one-third proportion assumption, the results were close to 0.3333 for each of the surface, subsurface, and streambank positions. To overcome this problem, the Solver function was used to calculate the mixing proportions from the data with a one-third starting contribution assumption, but for only one iteration and without the Monte Carlo uncertainty step.

The result from the one iteration step was that 6% of the sediment was derived from the surface, 78% from the subsurface, and 16% from streambank positions. The proportions were then used for a 100 iteration run of the mixing model with the Monte Carlo uncertainty step included and the results were 7% for surface, 79% for subsurface, and 14% for streambanks. The 100 iteration results were then used as the proportion assumptions for the 5000 iteration run and the results were 8% ± 6% for surface, 79% ± 6% for subsurface, and 13% ± 5% for streambank positions.

Estimates for the surface position contribution (Figure 6.26) show a result dominated by a count of 3224 that corresponds to the 0.065 proportion with little spread of the data. The highest count for subsurface (1129) is for the 0.78 proportion, although other large counts of 503 for the 0.73 proportion and 369 for the 0.76 proportion are also recorded. There is a right skew to this distribution which is distributed up to 1.0 (Figure 6.27). The streambank contribution result has the highest count of 1039 for the 0.16 proportion, but is also distributed from a proportion of 0.0 to 0.3 (Figure 6.28). Overall there was less uncertainty around the position results than for landscape units.

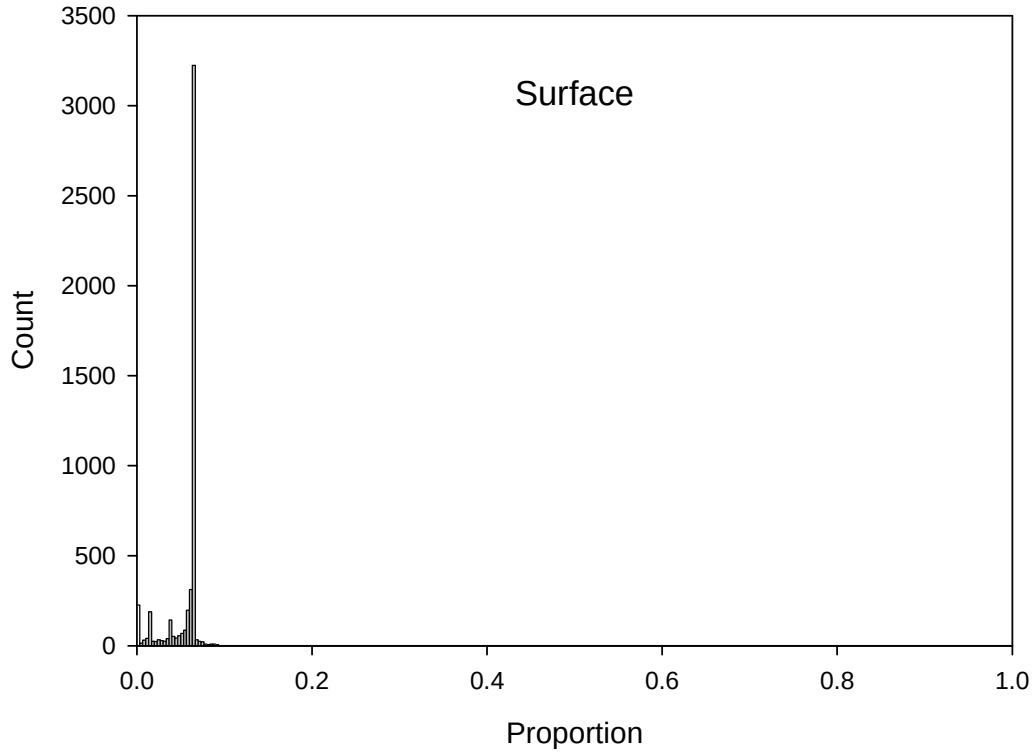

Figure 6.26. Mixing model 5000 iteration distribution for the surface position.

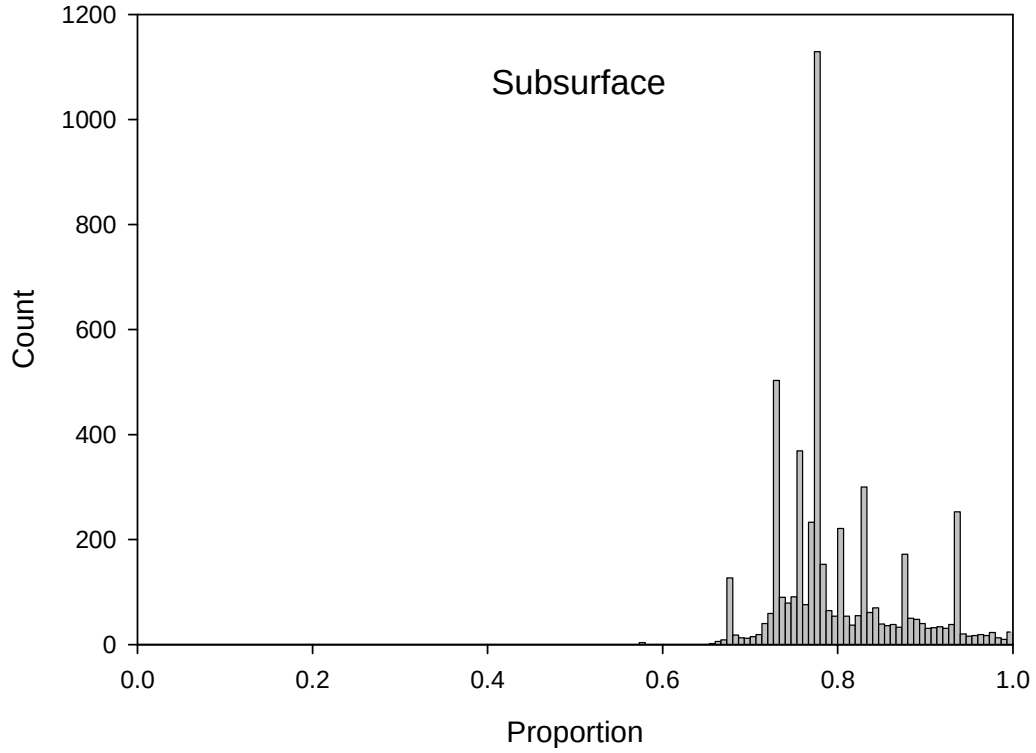

Figure 6.27. Mixing model 5000 iteration distribution for the subsurface position.

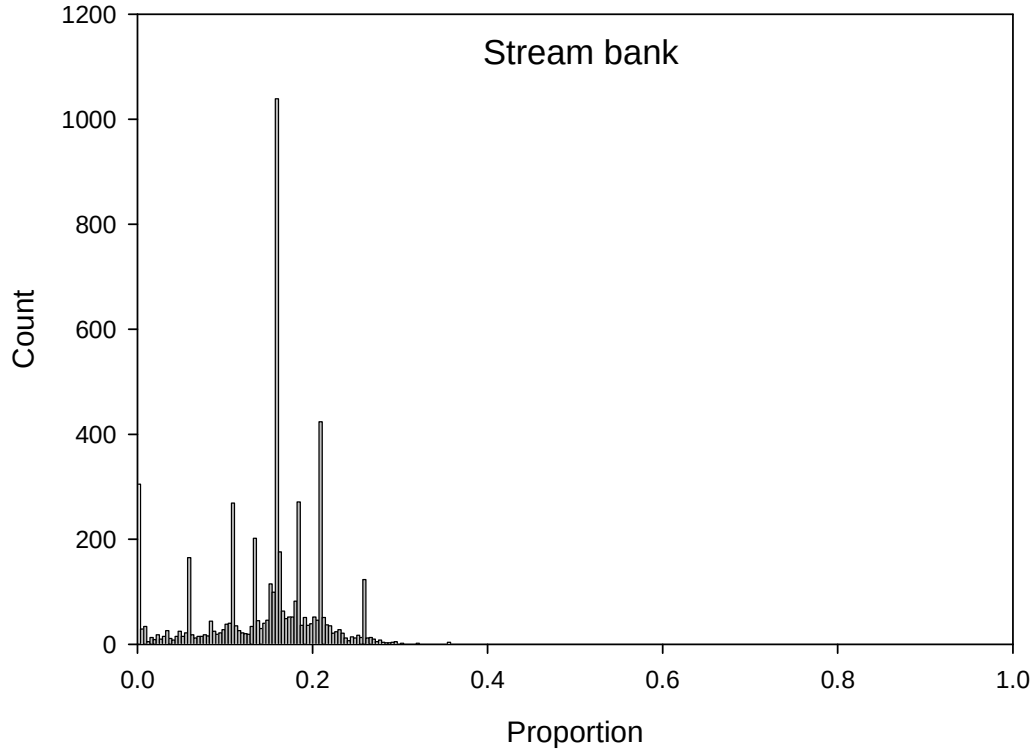

Figure 6.28. Mixing model 5000 iteration distribution for the streambank position.

6.5 Discussion

6.5.1 The results of sediment fingerprinting

The sediment fingerprinting results determined that the largest contributor of sediment to the Whangapoua Harbour was from the native forest landscape unit (62% ± 17%) followed by exotic forest (23% ± 12%) and then agriculture (15% ± 10%). The dominant erosion position was subsurface (79% ± 5%), then streambanks (13% ± 5%), and then surface soils (8% ± 6%). The results are consistent with the first alternative hypothesis proposed of Whangapoua Harbour sedimentation (Section 2.5.2) where most of the sediment was derived from the native forest landscape unit due to landslides (i.e., from subsurface positions). While the native forest landscape unit is furthest away from the estuary, the results indicate that the steep headwater channels are well coupled (laterally) to the slopes and that sediment is efficiently delivered by well coupled (longitudinally) high energy streams. If the results are normalised for the area each landscape unit occupies, then the erosion ratio is 1:2:8 for exotic forests, agriculture, and native forests.

The sediment fingerprinting results are also consistent with those obtained in the pilot study (Table 6-7). The identification of the native forest/subsurface as the main contributions of sediment in the pilot study was not of the same magnitude as that for the full programme, but in both cases the ordering was consistent and the subsurface position was clearly the most important source. The variation in the two sets of results could be attributed to different size fraction analyses, slightly different analytical methods, different sink sample collection methods, and greater confidence in the full programme results due to a larger sample size.

Table 6-7. Sediment fingerprinting results for the relative proportions (%) of sediment derived from landscape unit and position for the pilot study and the full programme.

Landuse	**Native**	**Exotic**	**Agriculture**
Pilot study	40	33	27
Full programme	62	23	15
Position	**Surface**	**Subsurface**	**Streambank**
Pilot study	10	62	28
Full programme	7	79	14

It is worth comparing the geochemical elements identified as varying significantly by the Kruskall-Wallis *H*-test for the full programme with the pilot study. Of the seven elements identified as candidates for landscape unit in the pilot study (Zn, Cr, Mn, Mg, P, Ca, and Fe), five were also identified in the full programme. The exceptions were Mg and Fe. For position, the seven elements identified as candidates in the pilot study (Al, P, S, Cl, Ca, V, and U), four were also identified in the full programme with the exceptions being Al, Cl, and U.

One reason for the difference is that Cl was not reported by the ICP-MS instrument. Other reasons that account for the discrepancy is that ICP-MS has a greater detection limit and therefore sensitivity (Winter *et al.* 2002). There were also differences between the two studies where the full programme collected more samples and thus more accurately captured the variation between elements than the pilot study. Another difference was that the analysis in the pilot study was on the < 63 μm sediment size fraction, while the full programme used the < 10 μm size fraction.

The estimation of the uncertainty (one standard deviation) around the results from the Monte Carlo simulation indicated that there was a greater degree of uncertainty associated with the landscape unit results than for the position results. When uncertainly was taken into consideration, native forests had the largest relative contribution but exotic forests and agriculture were within uncertainty of each other (Figure 6.29). The uncertainty around the position results was not so large (Figure 6.30).

6.5.2 Comparison with previous work

The sediment fingerprinting results can be compared with two previous multi-landuse studies conducted in the Whangapoua catchment by Marden & Rowan (1995) and Gibbs (2006) (Table 6-8).

The Marden & Rowan (1995) report results for landuse correspond with the sediment fingerprinting results as they identify the native forest area as the dominant sediment source area, followed by exotic forest and then agriculture. The Marden & Rowan (1995) process results follow the pattern of the sediment

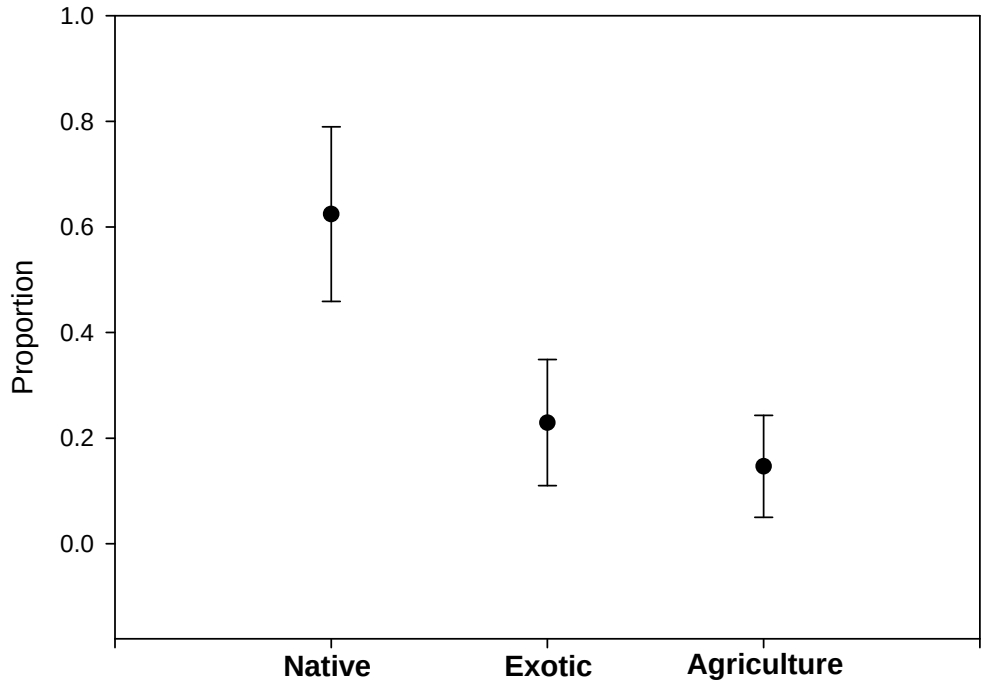

Figure 6.29. Mixing model mean relative proportions for landscape unit. Error bars are one standard deviation.

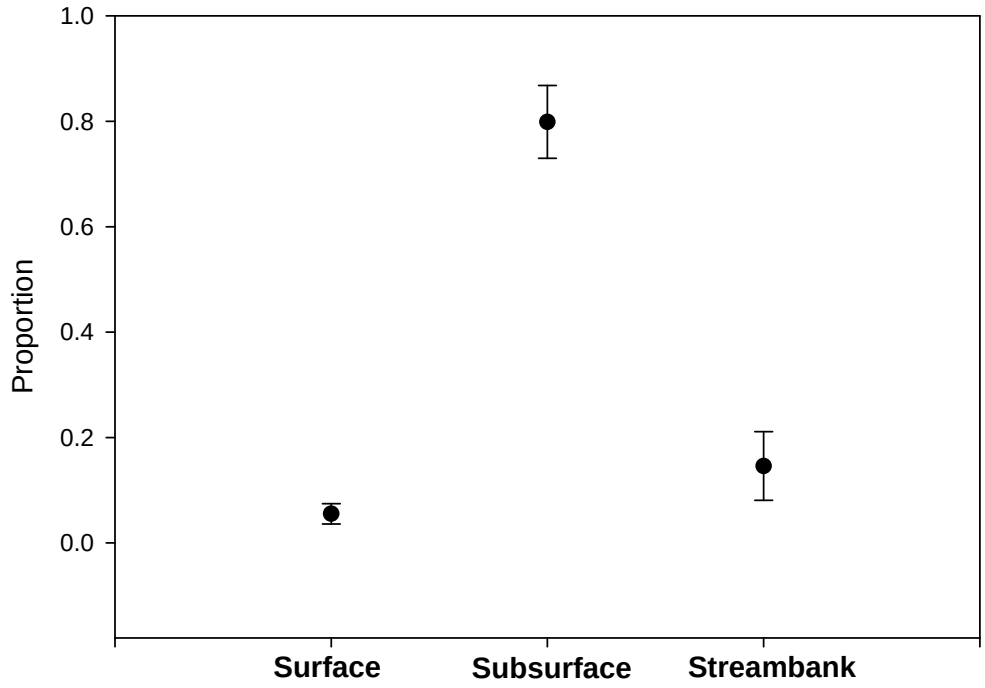

Figure 6.30. Mixing model mean relative proportions for position. Error bars are one standard deviation.

Table 6-8. Relative contributions (%) for landscape unit from the pilot study and full programme sediment fingerprinting, as well as from Marden and Rowan (1995) and Gibbs (2006) reports.

Landuse	Pilot study	Full programme	Marden and Rowan (1995)	Gibbs (2006)
Native	40	62	51	22-26
Exotic	33	23	38	54-75
Agriculture	27	15	12	<10

fingerprinting position results which showed the dominance of landslide sources at 98% (debris avalanches and soil slips).

The Marden & Rowan (1995) results differ from sediment fingerprinting as the sediment fingerprinting results indicated that streambanks contributed 13% and surface sources at 8% of estuary sediment, while Marden & Rowan (1995) report streambank contributions at 0.6% and virtually no surface erosion . The surface and streambank discrepancies could possibly be accounted for by the aerial photo technique not being sensitive to surface and streambank forms of erosion, while sediment fingerprinting is better at tracing surface and streambank sources. Using aerial photographic techniques to quantify streambank erosion is better suited to detecting large scale channel events (Lawler 1993).

Gibbs (2006) undertook a pilot study to assess the ability of a compound specific isotope (CSI) of ^{13}C to trace landuse derived sediment into the Whangapoua estuary from native forest, exotic forest and pasture. The top 2 cm of soil were collected at 14 sites in the Whangapoua catchment. The Gibbs (2006) results were that native forest contributed around 22-26% of harbour sediment, pasture was less than 10% at most harbour sites, and that recently logged exotic pines contributed 54-75%. While Gibbs (2006) study agrees with the sediment fingerprinting results in terms of the lowest contribution from agricultural areas, it is in contrast in identifying the exotic forests as the main contributor followed by native forests. No validating evidence was presented with the CSI results, nor was a potential subsurface signature sampled during the study. Limiting sampling to the < 2 cm soil depth could potentially bias the CSI signal to the surface

disturbance that takes place during forest harvesting. The analysis of only eight samples to characterise the catchment is also a potential limit of the findings.

6.5.3 Testing the sediment fingerprinting results

One of the underlying assumptions of sediment fingerprinting is that sediment source areas can be distinguished by a range of properties; in this case using geochemical properties to distinguish sediment from different landuse and erosion position sources. The soils parent material has a large influence on its chemical composition (Corbett 1969). Sediment fingerprinting studies have used the different underlying geologies of different subcatchments to distinguish them as sediment source areas (e.g., Collins *et al.* 1998; Miller *et al.* 2005). So tracing sediment from different geological areas seems logical.

The results of this chapter and Chapter 5 show that there are geochemical elements that could distinguish sediment derived from different landscape units and erosion positions in Whangapoua Harbour. The sediment fingerprinting technique has been applied to distinguish different sediment sources in geologically uniform areas, including paddocks of < 2 km^2 in size (Krause *et al.* 2003). So how does the sediment fingerprinting technique distinguish landscape units and erosion position geochemically in a catchment with relatively uniform underlying geology (Figure 2.2.3)? The geochemical fingerprinting of landscape units and erosion position were tested by comparing the sediment fingerprinting results with other erosion measures (Chapters 7-10).

6.6 Summary

After establishing that geochemical elements could be used to distinguish landscape units and position in the Waitekuri subcatchment (Chapter 5), a full sampling programme of the Whangapoua Harbour was undertaken to establish the relative sediment contribution of landscape units and position to the estuary. The sampling was guided by catchment mapping to account for soil and slope variability and ICP-MS analysis was undertaken on the < 10 μm fraction of 150 catchment samples and four sink samples.

Eight elements were selected to determine the relative contribution of sediment derived from different landscape units to the estuary. The highest sediment contribution came from the native forest (62% ± 17), followed by exotic forest (23% ± 12), and then agricultural landscape units (15% ± 10). Most sediment was derived from subsurface (79% ± 6), then streambanks (13% ± 5) and then surface (8% ± 6) sediment sources.

The results for landscape units and position in terms of relative contribution was consistent with the first alternative hypothesis of catchment erosion (Section 2.5.2) of the native forest landscape unit delivering most of the sediment by landsliding processes (i.e., subsurface positions). The native forest/subsurface highest contribution result was consistent with the results for the pilot study, although there was some variation. The variation can be accounted for by differences in sample number, sample fraction, and analytical methods.

CHAPTER SEVEN

RADIONUCLIDES

7.1 Introduction

Radionuclides were used in this study is to determine the relative sediment contribution from surface, subsurface, and streambank erosion positions to provide a comparison with the sediment fingerprinting results. Previous studies have shown that radionuclides can be used as soil tracers as they possess the property of being conservative during transport (Section 3.11). This chapter investigates the use of radionuclides to identify sediment sources and compares the effectiveness of the use of radionuclides with sediment fingerprinting.

7.2 Methods

7.2.1 Field sample collection and laboratory processing

Soil samples for radionuclide analysis were subsets of the material collected for the sediment fingerprinting study (Chapter 6). The analytical budget constraints limited the number of samples that could be processed to a maximum of 50 compared with 150 for sediment fingerprinting.

From the 150 sediment fingerprinting samples, the subset of 50 samples were selected to ensure a spread across each native forest, exotic forest, and agricultural landscape unit (Figure 7.1). At each sampling site, surface (0-2 cm), subsurface (> 20 cm), and streambank material was collected according to the procedure outlined in Section 6.2. Subsets were taken from the four Whangapoua estuary sediment fingerprinting samples (Figure 7.1) to characterise the catchment sink. The method of sink sample collection is outlined in Section 6.3.

The catchment and sink samples were handled and processed to recover the < 10 μm sediment fraction (Section 4.2). Subsets of the homogenised sediment fingerprinting material were then sent to the National Radiation Laboratory (NRL) in Christchurch, New Zealand for radionuclide analysis.

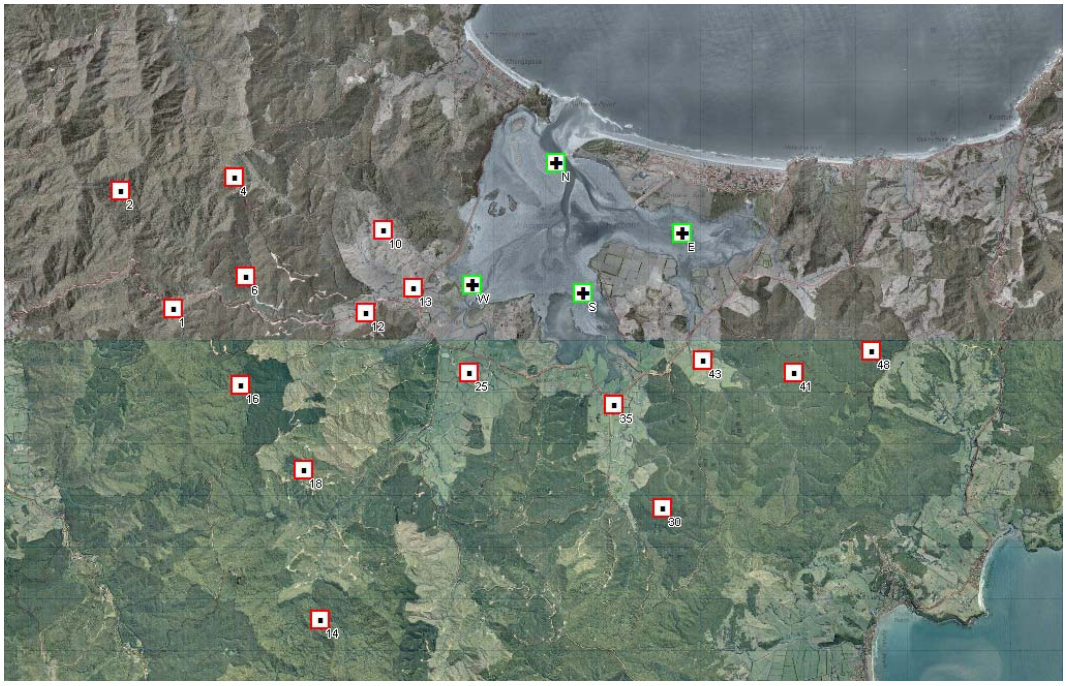

Figure 7.1. Location of radionuclide sampling sites for the Whangapoua catchment. Sink samples are denoted by crosses inside green boxes.

7.2.2 Analysis for radionuclide activity

The < 10 μm sediment fraction was analysed for ^{137}Cs, ^{210}Pb, ^{228}Ra, and ^{226}Ra by high-resolution gamma spectroscopy using HpGe detectors of 20% or 43% relative efficiency. The geometry used was a 500ml Marinelli beaker and counting times of 24 hours was used because of the low level of radionuclide activity in the samples. Calibration factors for the 662 keV ^{137m}Ba gamma emissions were determined by analysis of aqueous and sand (density 1.54 g cm^{-3}) calibration samples of the same geometry, containing known amounts of a ^{137}Cs standard. Small corrections to counting efficiency were made for variations in the soil packing density in the Marinelli beakers (1.0 – 1.5 g cm^{-3}) by interpolation between calibration factors derived from the aqueous and sand samples. Gamma spectra were analysed by a computer programme used in the NRL routine environmental radioactivity monitoring operations (Basher & Ross 2002). The full radionuclide results are contained in Appendix N.

7.3 Results

7.3.1. ^{137}Cs results

The concentrations of ^{137}Cs in the soil samples showed a distinct labelling of all native, exotic and agricultural surface soils in comparison to the subsurface and streambank soils (Figure 7.2). Surface soils from the agricultural areas had lower mean concentrations of ^{137}Cs compared with the surface soils of the native and exotic forests, but there was no significant difference. There is also no significant difference between the concentrations of ^{137}Cs in the subsurface and streambank soils. The mean concentration of ^{137}Cs in the estuary sediment was very low.

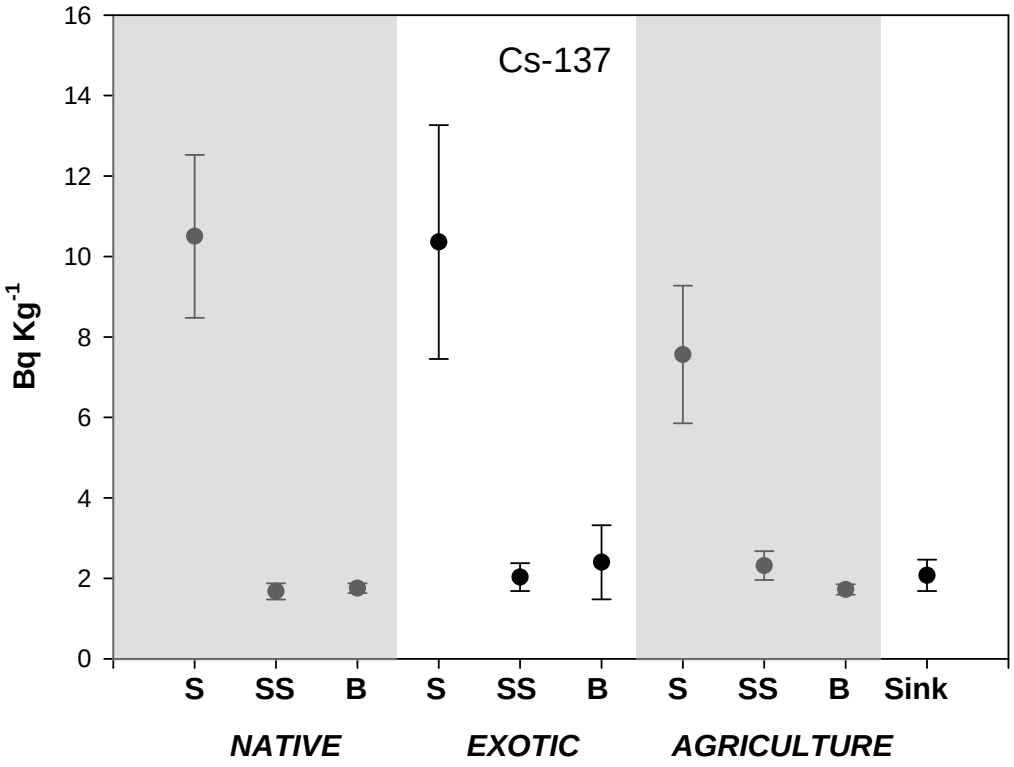

Figure 7.2. Mean concentrations of ^{137}Cs for soils sampled from the surface (S), subsurface (SS), and streambank (B) positions within landscape units and the estuary sediment (sink). Error bars are one standard error of the mean.

7.3.2. ^{210}Pb$_{ex}$ results

^{210}Pb forms both *in situ* in the soil as well as in the atmosphere. It is the atmospherically derived ^{210}Pb that is of interest in this study as it labels surface soil particles at higher concentrations than subsurface particles, and so has the

potential to distinguish between sediment derived from surface and subsurface positions. To determine the atmospherically derived ^{210}Pb, the ^{226}Ra concentration was subtracted from the total inventory of ^{210}Pb. This is because the *in situ* ^{210}Pb will be in equilibrium with its parent ^{226}Ra, and so ^{226}Ra acts as a proxy for the *in situ* ^{210}Pb which is also termed 'supported.' The atmospherically derived ^{210}Pb was termed the 'unsupported' or 'excess' and is denoted as $^{210}Pb_{ex}$ (Koide *et al.* 1972; Wise 1980; Zapata *et al.* 2002).

Similar to ^{137}Cs, the highest concentrations of $^{210}Pb_{ex}$ are in the surface soils of the three landscape units and there was no significant difference between the concentrations of the subsurface and streambank positions (Figure 7.3). The concentration of $^{210}Pb_{ex}$ in the estuary sediment was higher than the potential catchment source area concentrations.

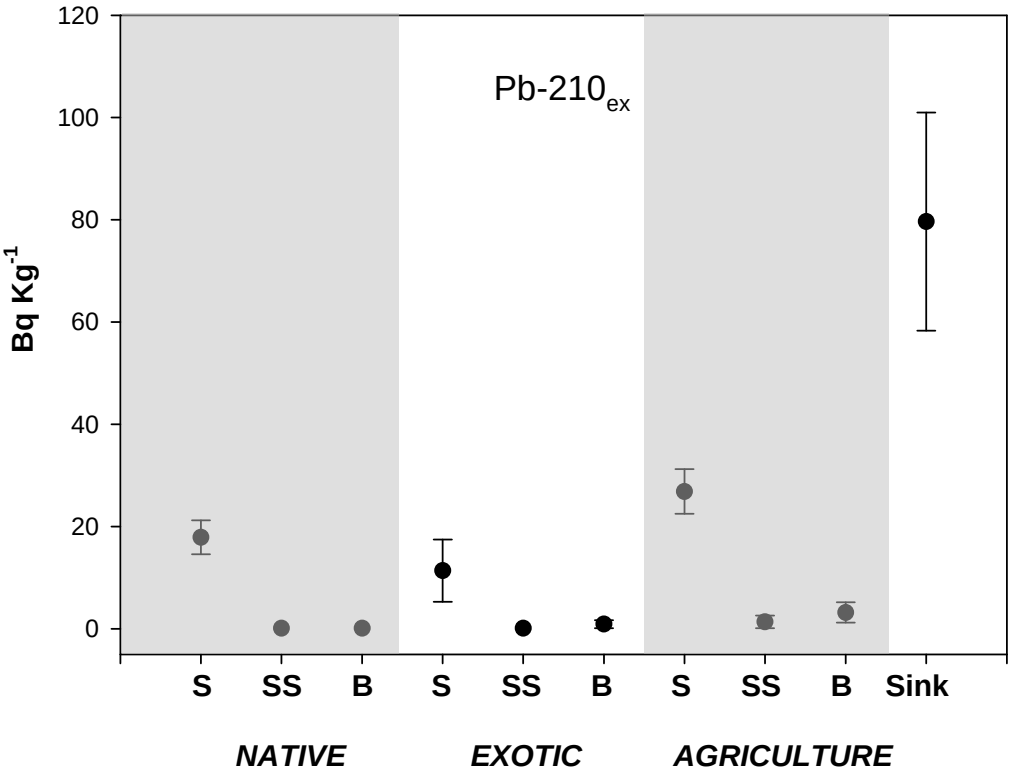

Figure 7.3. Mean concentrations of $^{210}Pb_{ex}$ radionuclide for soils sampled from the surface (S), subsurface (SS), and streambank (B) positions within landscape units and the estuary sediment (sink). Error bars are one standard error of the mean.

7.3.3. ^{226}Ra results

There was no significant difference between the ^{226}Ra concentrations between landscape units and erosion position, although there was an elevated concentration in surface agricultural soils (Figure 7.4). The sink ^{226}Ra concentration was lower than all the potential catchment source concentrations.

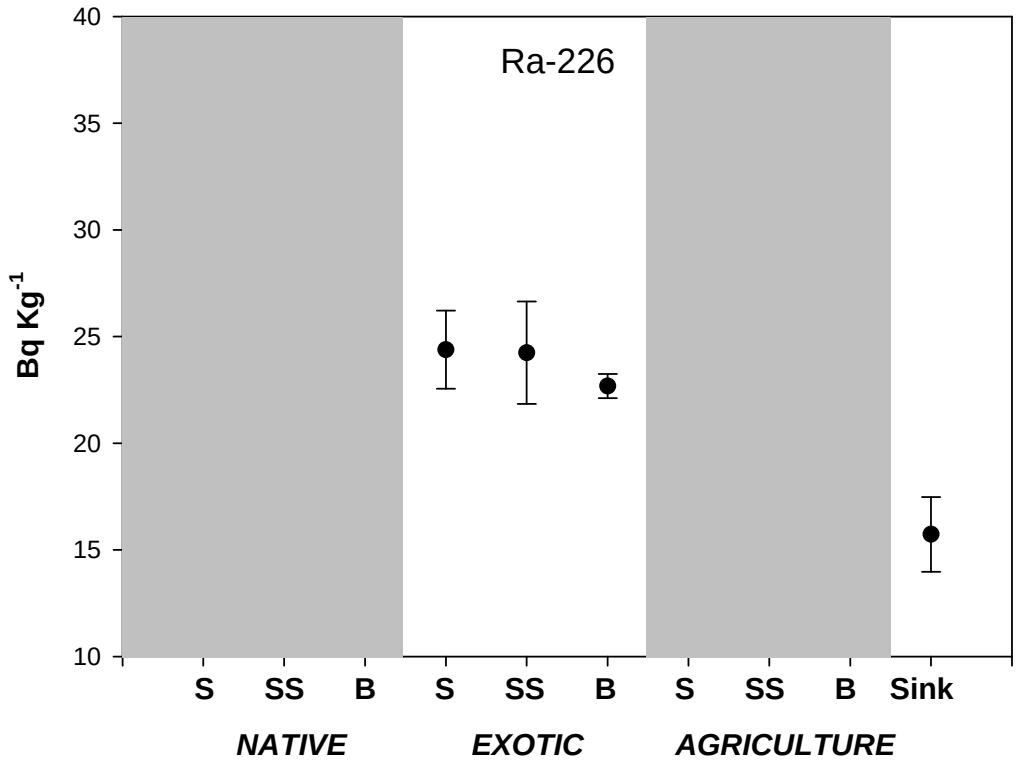

Figure 7.4. Mean concentrations of ^{226}Ra radionuclide for soils sampled from the surface (S), subsurface (SS), and streambank (B) positions within landscape units and the estuary sediment (sink). Error bars are one standard error of the mean.

7.3.4. ^{228}Ra results

The ^{228}Ra concentrations vary between the surface and subsurface/streambank positions across the three landuses (Figure 7.5). The subsurface and streambank ^{228}Ra concentrations were higher than the surface position in the native forest landuse. The subsurface and streambank ^{228}Ra concentrations were only slightly higher than the surface position in the exotic forest and agricultural landuses. The ^{228}Ra concentration in the estuary sediment was lower than any of the potential catchment source area concentrations.

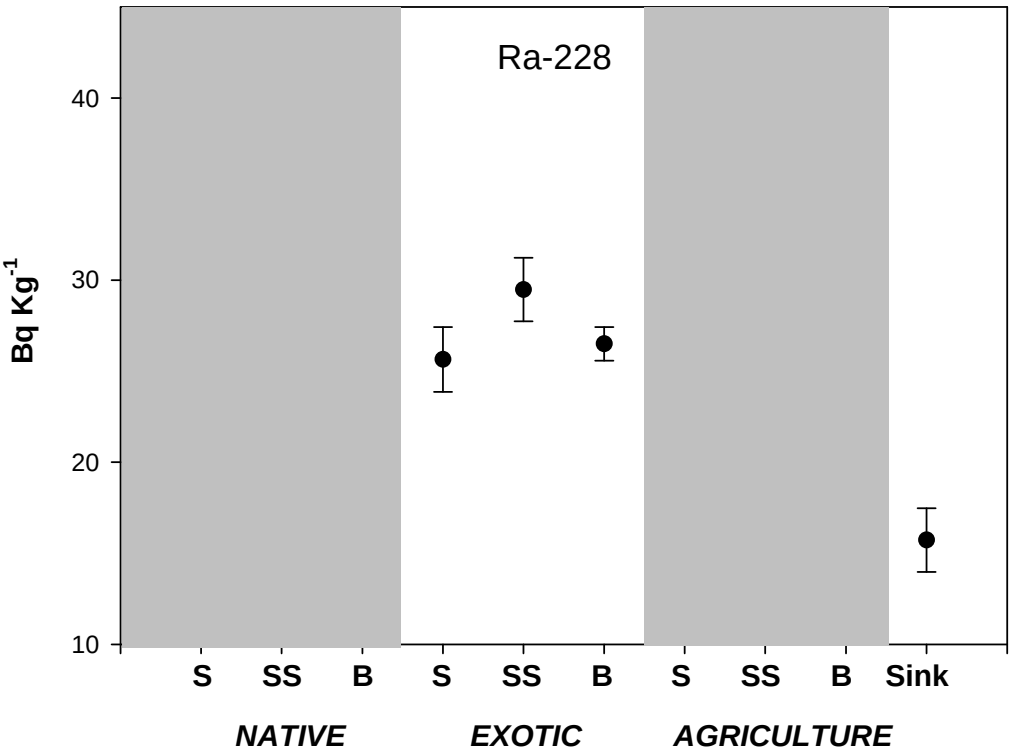

Figure 7.5. Mean concentrations of ^{228}Ra radionuclide for surface (S), subsurface (SS), and streambank (B) positions within landscape units and the estuary sediment (sink). Error bars are one standard error of the mean.

7.3.5. Discussion of radionuclide results

Overall, there is little influence of landuse on the radionuclide results. There was a slightly lower concentration of ^{137}Cs in the agricultural surface soil, but not significantly so.

For $^{210}Pb_{ex}$, there was a small non-significant elevation of concentration in the agricultural surface soil. Tree cover is known to cause perturbations in radionuclide concentrations as tracers are delivered to the ground surface principally by wet precipitation. The lack of tree cover interception in agricultural areas may account for the higher agricultural surface value (Wise 1980; Wallbrink *et al.* 1994a).

Unlike the enriched surface concentrations of ^{137}Cs and $^{210}Pb_{ex}$, it was expected that the concentrations of ^{226}Ra should be relatively uniform throughout the soil profile or show some increase with depth (Baeza *et al.* 1994; Akyil *et al.* 2002;

Dowdall *et al.* 2003; Navas *et al.* 2005; El-Reefy *et al.* 2006; Akyil *et al.* 2008). Such concentrations of ^{226}Ra at depth could be due to sorption onto Fe-oxides and clay surfaces (VandenBygaart & Protz 1995).

In the agricultural landuse, there is a higher concentration of ^{226}Ra in the surface samples compared to the subsurface and streambank samples. The elevated concentrations in agricultural surface soils could be attributed to the addition of fertilisers. Fertiliser additions such as U, Cd, and Hg are found in elevated concentrations in agricultural soils (McLaughlin *et al.* 1996). Uranium has been found in elevated concentrations in agricultural areas as shown by the geochemical ICP-MS results in Chapter 6. As ^{226}Ra is a product of the ^{238}U decay series, then it is reasonable to expect higher concentrations of the radionuclide in agricultural surface soils (Akyil *et al.* 2002).

^{228}Ra is part of the ^{232}Th decay scheme and only has a half life of 5.75 years (Leroy 1995). The short half life of ^{228}Ra means that sink samples can quickly become depleted of this radionuclide limiting its potential as a source tracer in this study. More typically, ^{228}Ra is used in combination with ^{226}Ra for geochronology or a tracer of recent soil erosion (e.g., (Bai *et al.* 2000; Tims *et al.* 2004). Due to its short half life, ^{228}Ra will not be used as a sediment tracer in this thesis.

The ^{137}Cs and ^{210}Pb$_{ex}$ results show a difference between surface soil concentrations and subsurface/streambank concentrations. There is no delineation between the ^{137}Cs and ^{210}Pb$_{ex}$ results of subsurface and streambanks. The low depth penetration characteristics of the two tracers has meant that subsurface and streambank material is virtually unlabelled and therefore cannot be discriminated by radionuclide techniques.

An immediate problem with the radionuclide results is that with the exception of ^{137}Cs, the sink concentrations of ^{210}Pb$_{ex}$ and ^{226}Ra do not relate to the potential catchment surface, subsurface, and streambank sediment sources. That is, the ^{210}Pb$_{ex}$ sink concentration is too high and the ^{226}Ra is too low.

7.4 Soil tracing using radionuclides

7.4.1 Radionuclide selection for soil tracing

For radionuclides to be useful in this study, they must satisfy the criteria of being able to distinguish sediment derived from different source areas, and remain conservative during transport. An indication of conservativeness during transport is that the tracer is not altered, depleted, or enriched during transport or deposition. The results (Section 7.3) indicate that $^{210}Pb_{ex}$ and ^{226}Ra have been altered, depleted, or enriched during transport because of the sink concentrations being outside the range of the possible catchment sediment sources.

Hypothesis testing (Students t-test) was used to examine if $^{210}Pb_{ex}$ and ^{226}Ra sink concentrations were significantly different from surface mean concentrations and from the subsurface/streambank mean concentrations. The mean subsurface and streambank concentrations have been combined ('all subsurface') as the subsurface and streambank material could not be distinguished by the radionuclides.

The mean sink concentration for $^{210}Pb_{ex}$ was significantly different from the surface ($p < 0.01$) and all subsurface ($p < 0.01$) potential source erosion positions. The mean sink concentration for ^{226}Ra was also significantly different from the surface ($p = 0.01$) and all subsurface ($p < 0.01$) potential source erosion positions. The tables are contained in Appendix O. Thus neither $^{210}Pb_{ex}$ nor ^{226}Ra was considered suitable for sediment tracing in this study. The potential explanations for their unsuitability will be discussed later in this chapter. Thus ^{137}Cs was the only radionuclide suitable to quantify catchment sediment sources.

7.4.2 Sediment source determination using ^{137}Cs

The ^{137}Cs soil tracing method is well understood with over 3,400 publications to date (Ritchie & Ritchie 2001; Hancock *et al.* 2008). It was the aim of this study to find another suitable radionuclide to use in ratio with ^{137}Cs such as ^{210}Pb (Smith & Dragovich 2008). As no other suitable radionuclide was found, it was necessary to determine the Whangapoua estuary sediment sources by position using only ^{137}Cs. There were two possibilities when using only ^{137}Cs to determine catchment

erosion positions; hypothesis testing and using an upper limit calculation. Both the hypothesis testing and the upper limit calculation were used to form multiple lines of evidence (e.g., Lind *et al.* 2007) to determine estuarine sediment sources.

7.4.2.1 Hypothesis testing

To formally test if there is a difference between the sink samples and the surface samples and the 'all subsurface' samples, the hypotheses posed were that:

$H_{o\ (1)}$: there is no difference between the mean activity levels of ^{137}Cs between the surface (0-2 cm) position and the sink

$H_{o\ (2)}$ there is no difference between the mean activity levels of ^{137}Cs between all subsurface (subsurface >20 cm and streambank) position and the sink

The ^{137}Cs concentrations in the < 10 μm fraction of the surface soils ranged from 2.4 to 18.6 Bq kg^{-1} (Figure 7.6). The ^{137}Cs concentrations in the 'all subsurface' soils (subsurface and streambank positions) were lower than the surface soils with most samples having concentrations around 2.6 Bq kg^{-1}. The ^{137}Cs concentrations in the estuary sediment sink samples were 2.99, 2.34, 1.8, and 1.17 Bq kg^{-1}. The mean ^{137}Cs concentration in the estuary sink samples was close to the mean concentration of the 'all subsurface' but differed from the surface concentration.

There was a significant difference in the mean ^{137}Cs concentrations between the estuary sediment sink and the surface samples (p = 0.01), but there was no significant difference between the sink and the 'all subsurface' samples (p = 0.86). Table contained in Appendix O. So the null hypothesis $H_{o\ (1)}$ is rejected for the sink/surface comparison as there is a significant difference, but the hypothesis $H_{o\ (2)}$ was not rejected for the sink/subsurface as there was no significant difference between the two groups.

7.4.2.2 Upper limit calculation

The second method used to determine catchment erosion positions using only ^{137}Cs was the upper limit calculation. The upper limit calculation was previously used to determine the relative contribution from surface sources (sheet and rill)

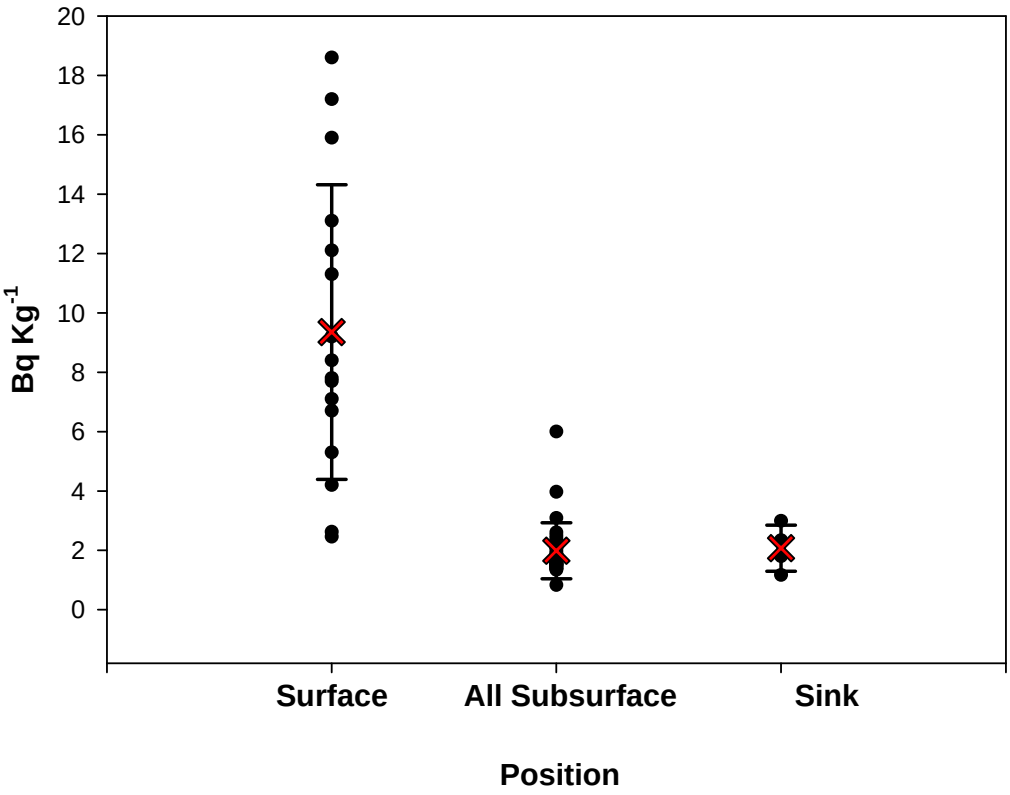

Figure 7.6. ^{137}Cs concentrations for the surface, 'all subsurface' (combined streambank and subsurface), and sink samples. The mean values are indicated by red crosses and the error bars represent one standard deviation.

and subsurface sources (gully erosion) to Murrumbidgee River (sink) sediments (Wallbrink *et al.* 1996). The calculation was used to determine the upper limit of the ratio of the surface erosion source alone to the total river sink sediments. The modified calculation relevant to this thesis is:

$$C_s = \left[\frac{S_k - SS}{S - SS} \right] \times 100 \qquad \text{(Eqn 7.1)}$$

Where C_s is the upper limit ratio of catchment surface positions,
S is the mean concentration of ^{137}Cs in the surface position (0-2 cm),
S_k is the mean concentration of ^{137}Cs in the sink (estuary), and
SS is the mean concentration of ^{137}Cs in all subsurface positions (subsurface > 20 cm and streambanks).

The upper limit of surface positions (C_s) is 1.2% meaning the majority of harbour sink sediment (98.8%) was derived from all subsurface (combined subsurface and streambank) erosion positions.

7.5 Discussion

7.5.1 ^{137}Cs results

The multiple lines of inquiry approach indicates that the subsurface erosion positions (subsurface and streambanks) was the dominant contributor of sediment to the estuary. The hypothesis test found that there was no significant difference (p = 0.01) between the sink sample and 'all subsurface' positions for ^{137}Cs concentrations, and that there was a significant difference between the sink sample and the surface sample. The upper limit calculation resulted in a 98% estimation for the contribution of all subsurface positions.

7.5.2 Radionuclide variability

For radionuclides to be used in this study, they had to satisfy the criteria of being able to distinguish sediment derived from different source areas, and remain conservative during transport. It is also advantageous to use radionuclides in ratios to reduce their spatial variability (Section 3.11.4). For example, Figure 3.16 shows that ^{137}Cs and ^{226}Ra distinguish cultivated, uncultivated, and subsurface sediment sources. The sink sediments (Brisbane and Logan River sediments) were within the end member source envelope (dashed line). Because the sink concentration was within the end member envelope, this indicates that the sink relates to the potential source areas and that the radionuclides were conservative during transport and deposition.

Confidence testing (Section 7.4) showed that only ^{137}Cs sink concentrations related to the potential source area concentrations, while $^{210}Pb_{ex}$ and ^{226}Ra did not. Ratios of ^{137}Cs and $^{210}Pb_{ex}$ have been widely used (e.g., Wallbrink *et al.* 2002a) to discriminate between sediment derived from surface and sub-surface sources. Using the concentrations of ^{137}Cs and $^{210}Pb_{ex}$ from this thesis as a ratio shows that surface and all subsurface catchment sources are distinguished, but that the estuary sink ratio lies outside the source end member envelope (dashed line) (Figure 7.7) due to higher sink concentrations for $^{210}Pb_{ex}$.

When the ^{137}Cs concentrations were used in ratios with ^{226}Ra in this thesis, surface and all subsurface catchment sources could be distinguished, but again the combined sink ratio was outside the end member envelope (dashed line) (Figure 7.8). The non-relation of the sink sample to the source area end member envelope was due to depleted ^{226}Ra sink concentrations.

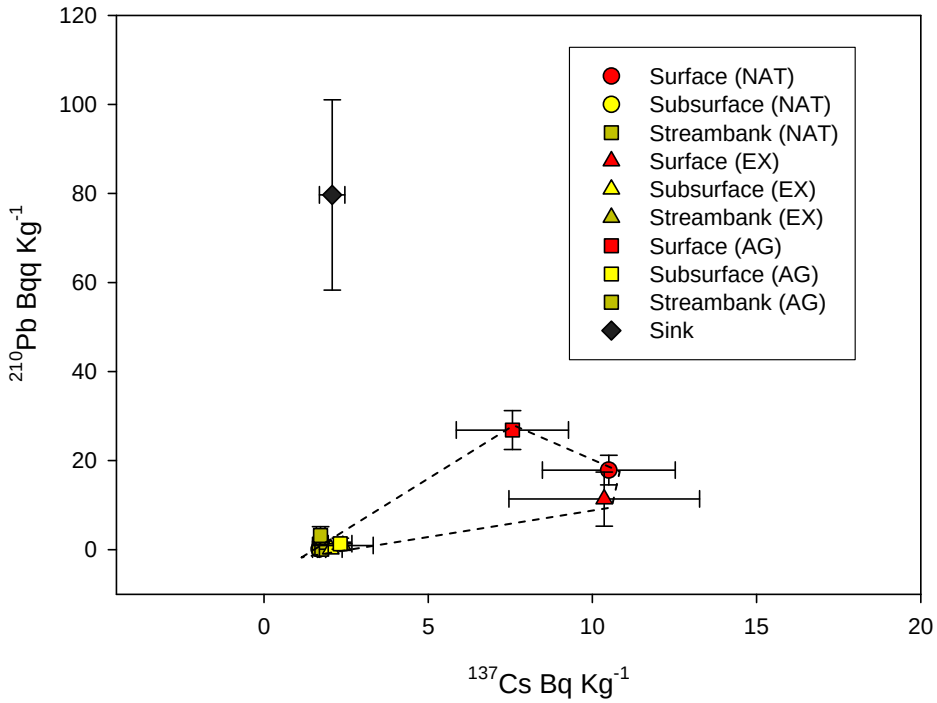

Figure 7.7. Results of ^{137}Cs and ^{210}Pb$_{ex}$ concentrations in soils derived from surface, subsurface, and streambank positions and the estuary (sink) sample. Error bars are one standard error.

7.5.3 ^{210}Pb$_{ex}$ enrichment

The enrichment of ^{210}Pb$_{ex}$ in sediment has been observed before (e.g., Wallbrink *et al.* 2003b) and Figure 7.9 shows the ratio of ^{137}Cs to ^{210}Pb$_{ex}$ for source (cultivated, uncultivated, and subsurface soils) and sink (Cardinia, Bunyip, and Yallock subcatchments) activity values in a study to determine the sediment sources entering Western Port in Victoria, Australia. While the sediment source areas were distinguished by the ratio of the two tracers, the Cardinia, Bunyip, and Yallock sink concentrations show elevated results for the ^{210}Pb$_{ex}$.

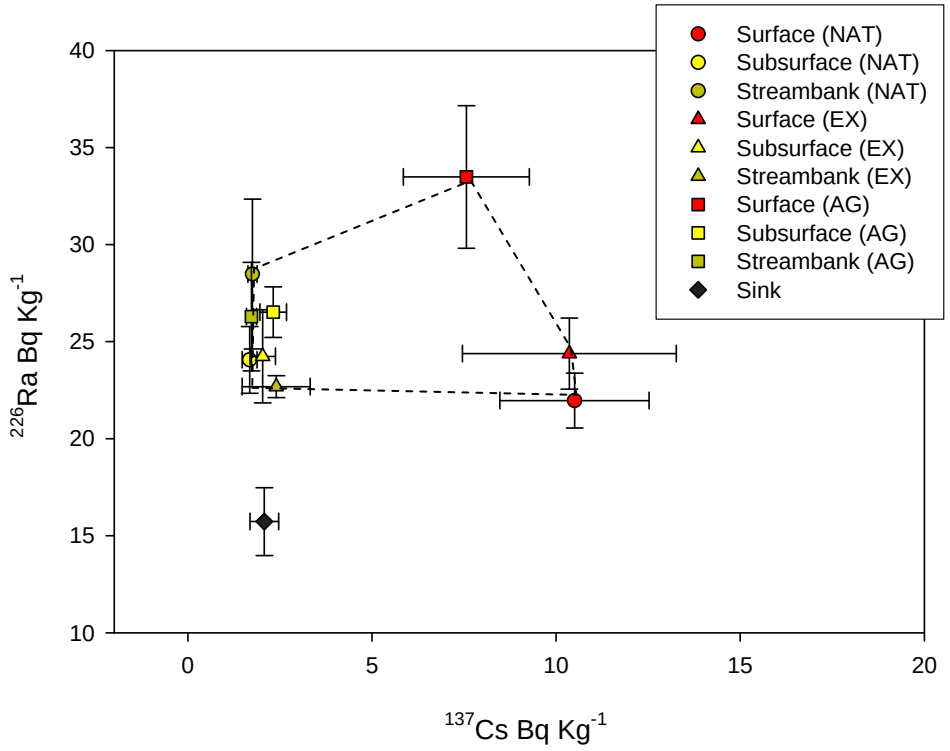

Figure 7.8. Results of for the ratio of ^{137}Cs and ^{226}Ra concentrations in soils derived from surface, subsurface, and streambank positions and the estuary (sink) sample. Error bars are one standard error.

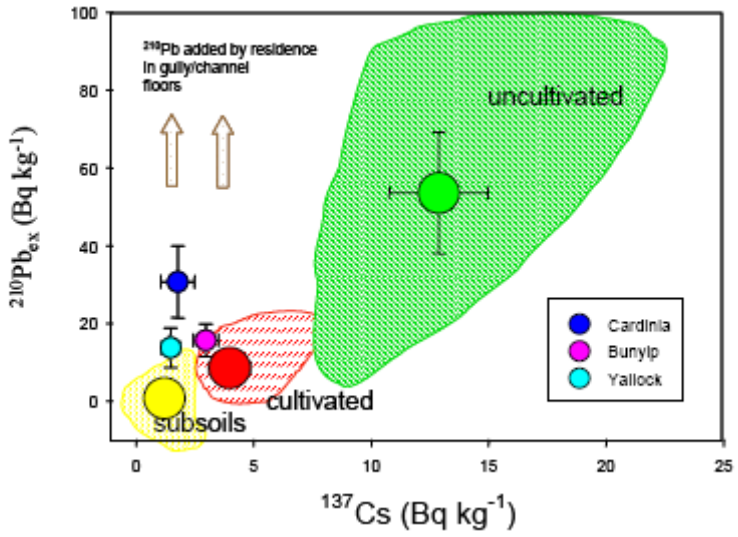

Figure 7.9. ^{137}Cs and ^{210}Pb$_{ex}$ radionuclide concentrations for cultivated, uncultivated, and subsoil sources and three subcatchment sink results. Elevated ^{210}Pb$_{ex}$ concentrations for the Cardinia, Bunyip, and Yallock sediment sink samples are due to gully floor enrichment while the sediment is in transport (Wallbrink *et al.* 2003b).

There are three possibilities that could account for the high $^{210}Pb_{ex}$ estuary concentration; surface soil erosion dominance of sediment delivery, $^{210}Pb_{ex}$ enrichment during transport, or $^{210}Pb_{ex}$ enrichment during deposition.

The first possible explanation of $^{210}Pb_{ex}$ enrichment is the delivery of $^{210}Pb_{ex}$ labelled surface soils to the estuary from the catchment. This possibility is unlikely as the sink concentration is far above those found in the catchment surface soils. Also, if surface erosion was dominant in the catchment then a concomitantly high level of ^{137}Cs labelled material would be expected in the sink sediment samples as well which is not the case.

The second possible explanation of $^{210}Pb_{ex}$ enrichment is some form of post erosion addition of $^{210}Pb_{ex}$ to the sediment before it reaches the sink. The authors of the Western Port study (Figure 7.9) concluded the addition occurred as a result of the fallout of $^{210}Pb_{ex}$ onto gully floor material which would have resulted in a higher concentration of $^{210}Pb_{ex}$ (Wallbrink *et al.* 2003b). Another study concluded that $^{210}Pb_{ex}$ addition occurred to sediment temporarily stored in stream banks, and the enrichment concentrations were used to calculate residence times of fine grained sediment in river channels (Wallbrink *et al.* 2002b). The catchment area in the Wallbrink *et al.* (2003b) study is 3250 km^2 and 14785 km^2 in the Wallbrink *et al.* (2002b) study and located in Australia. This means the river channels would be much longer than found in Whangapoua and subject to long seasonal periods of low or no flow. The Whangapoua catchment has short (< 15 km) length streams in a steep catchment subject to high rainfall which appears to ensure that very little (< 4%) of the annual fine sediment budget is stored within the stream network (Chapter 10). This makes the enrichment of sediment undergoing transport by $^{210}Pb_{ex}$ unlikely in this environment as sediment residence times within the streamlines would be short.

A third explanation is that there is a post depositional enrichment of estuary sediment with $^{210}Pb_{ex}$. Atmospherically derived $^{210}Pb_{ex}$ is stripped from the water column and deposited onto estuary sediments. This is achieved by agents such as particulate organic matter (POM) or particulate organic carbon (POC) which have high trapping efficiencies for $^{210}Pb_{ex}$ (Kato *et al.* 2003). The process of

'scavenging' or 'stripping' of $^{210}Pb_{ex}$ and consequent enrichment of coastal sediments has been observed by other authors (Moore *et al.* 1996; Carvalho 1997; Peng 2003; Wan *et al.* 2005). As the sink concentrations of $^{210}Pb_{ex}$ did not relate to terrigenous inputs, Yeager & Santschi (2003) concluded that $^{210}Pb_{ex}$ could not be used to trace watershed erosion sources. As the agents of stripping can include algae and diatoms, Wan *et al.* (2005) concludes that elevated levels of ^{210}Pb are more indicative of biological primary productivity and has implications for geo-chronological use. The unlikelihood of surface erosion dominance/ transport enrichment and the observation of biological scavenging of $^{210}Pb_{ex}$ in estuarine environments in the literature make scavenging the most likely process of sink sediment enrichment.

7.5.4 ^{226}Ra depletion

The estuary sink samples show low concentrations of ^{226}Ra, placing it outside of the end member sources. A possible explanation for this low sink concentration is the post depositional mobility of ^{226}Ra. Unlike ^{137}Cs which binds to soil particles in an almost non-exchangeable form, radium is essentially completely reversibly adsorbed (Smith & Amonette 2006). Radium in rivers is strongly adsorbed to particles. Waters high in iron oxide and manganese surfaces are found to readily scavenge radium ((Turekian 1997; EPA 2004). But once radium isotopes encounters salt water it is desorbed from the particle surface and is found mainly in dissolved forms in salt water (Moore & Shaw 2008). Thus the sink inventory naturally occurring radionuclides such as ^{226}Ra can be different from the activity originally deposited (El-Reefy *et al.* 2006). A study of the Tagus River estuary in Portugal found that sediment bound ^{226}Ra was desorbed and that atmospherically derived ^{210}Pb was scavenged by estuary processes. This led to estuarine water flowing out to sea containing enhanced levels of ^{226}Ra and depleted levels of ^{210}Pb (Carvalho 1997).

^{226}Ra can also be quite mobile in sediments under anoxic conditions, and in a coastal environment oxygen depletion can be caused by benthic macrophytes (Martin *et al.* 2003). Anoxic sediments may occur in mangrove areas of the Whangapoua Harbour. But as the sink samples for this thesis were taken in the central sections of the estuary away from mangrove areas, the most likely reason

for radium depletion would be post depositional desorption in the salt water environment.

7.6 Summary

Radionuclide sediment tracing was used to compare the sediment fingerprinting results for erosion positions in the Whangapoua catchment. Forty eight samples were used to characterise the catchment with the aim of distinguishing between surface, subsurface, and streambank erosion positions as per the sediment fingerprinting programme. The results showed that subsurface and streambanks were not distinguishable from one another and were, therefore, treated as one erosion position (all subsurface). $^{210}Pb_{ex}$ was found to be enriched in the sink samples and ^{226}Ra was found to be depleted of the sink samples in comparison with source area concentrations. $^{210}Pb_{ex}$ sink sample enrichment was most likely due to a scavenging process of atmospherically derived $^{210}Pb_{ex}$ principally by organic matter, and ^{226}Ra sink depletion was most likely due to being desorbed in a saline environment.

^{137}Cs hypothesis testing and an upper limit calculation were used to identify the main erosion position. The sink and subsurface samples were not significantly different, and the upper limit calculation indicated that around 98% of estuary sediment was from all subsurface positions. Both estimates using only ^{137}Cs supported the findings of sediment fingerprinting which indicated that 92% of estuary sediment was derived from subsurface and streambank erosion positions.

CHAPTER EIGHT

SUSPENDED SEDIMENT MONITORING

8.1 Introduction

Suspended sediment monitoring was undertaken to generate empirical data on erosion rates from the different landuses within the Whangapoua catchment as a way of comparing the sediment fingerprinting results. Streams draining four small subcatchments under different landuses (Figure 8.1) were monitored to compare their responses to rainfall events and to derive an erosion rate in tonnes per square kilometre per year. Unlike the typical landscape units identified in the Whangapoua catchment where native forest is on steep slopes, exotic forest on moderate slopes, and agriculture on flat lowlands, the monitoring sites were located on similar slopes to better compare the effects of landuse.

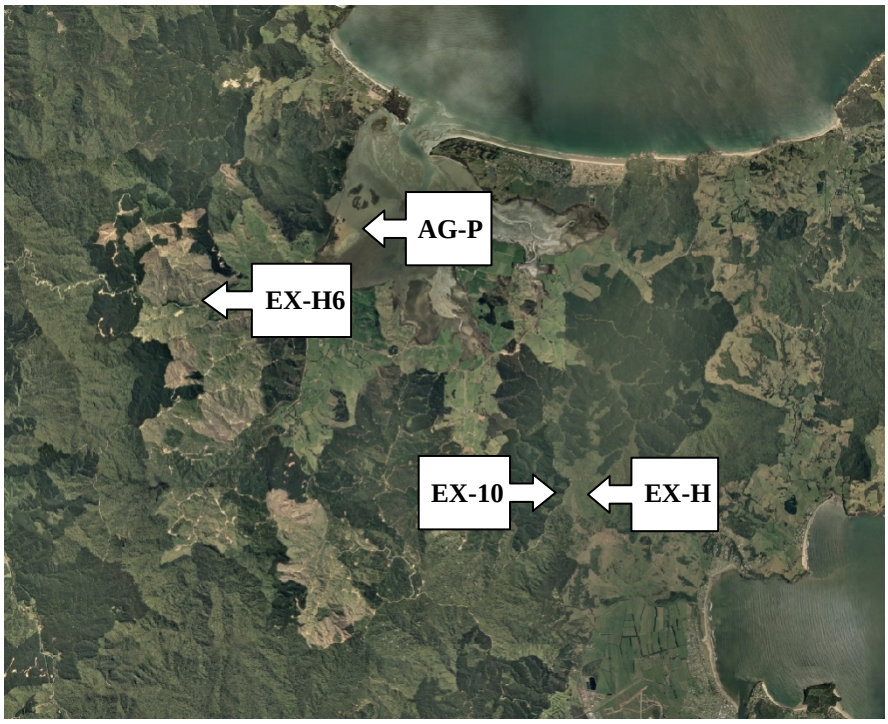

Figure 8.1. Location of the four suspended sediment monitoring sites in relation to one another in the Whangapoua Harbour catchment.

8.2 Experimental design and site description

Four sites were monitored to record turbidity and flow to ascertain an erosion rate in tonnes per square kilometres per year. It was predicated (based on reviews of the literature and site inspections) that the main contributors of sediment to Whangapoua Harbour would be the exotic forest and the agricultural areas because of human induced accelerated erosion. As the erosion rate from mature pines versus recently harvested pines is different, the various stages of exotic pine harvesting were represented within the experimental design to gather information on how quickly erosion rates dropped after pine harvesting.

Thus, the landuses selected for suspended sediment monitoring were agricultural pastures (AG-P), exotic pine forest where harvesting had just taken place (EX-H), exotic pine forest six month post harvest (EX-H6), and exotic pine forest with ten year re-growth (EX-10) (Table 8-1). Continuous stream monitoring was undertaken on each site for about two years.

Table 8-1. Summary statistics of the four stream monitoring subcatchments.

	EX-H#	**EX-H6#**	**EX-10**	**AG-P**
Landuse	Exotic pine harvested	Exotic pine 6 month post harvest	Exotic pine 10 year re-growth	Agriculture pasture
Lat/long	36.47.556E 175.38.937E	36.45.376S 175.33.455E	36.47.471S 175.38.769E	36.44.748S 175.35.422E
Size (ha)	5.02	1.56	9.95	2.48
Elevation	28 m	87 m	26 m	35 m
Aspect	W	NE	E	SW
*Soil**	Brown	Brown	Brown	Brown
Topography	Rolling	Rolling	Rolling	Rolling
Record (begin/end)	11-12-2005 14-3-2008	24-2-2006 20-12-2007	13-4-2006 11-1-2008	23-2-2006 14-3-2008
Missing record	7%	20%	14%	29%

* New Zealand Soil Classification (Hewitt 1998).
# Denotes the harvesting cycle at the commencement of monitoring

The subcatchment size that could be monitored was limited to around 10ha as only temporary plywood weirs could be constructed without Resource Consent permission. The plywood weirs proved inadequate to handle rainfall events draining larger areas. Ideally subcatchments would be similar in size, aspect, soil type, topography, and altitude, but this aim was not wholly achieved (Table 8-1).

8.2.1 Exotic pines harvested – EX-H

The subcatchment draining a 5 ha subcatchment of harvested exotic pines was located in compartment 87 off Owera Rd (Figure 8.2). Clearfelling operations in EX-H began in April 2006 using the cable logging method. No major erosion features were observed before felling took place. No roads or other constructed features drained directly into the EX-H subcatchment. The EX-H subcatchment had a 20m riparian buffer strip along a section of the main Owera Stream which the subcatchment drained into. The riparian strip comprised mostly native vegetation and the monitoring equipment was located in the buffer strip to avoid damage when logging took place. Figure 8.3 shows EX-H pre and post harvest. The riparian strip along the Owera Stream was evident after harvesting.

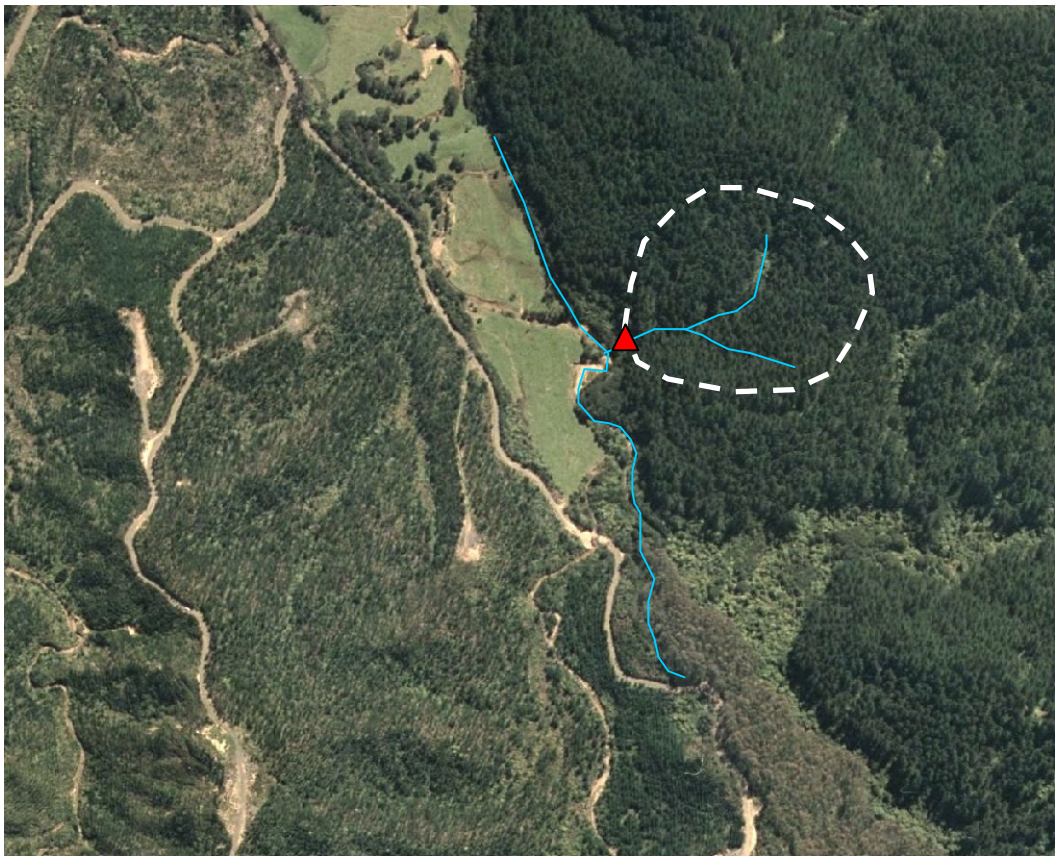

Figure 8.2. The EX-H subcatchment area and the weir/instrument site is marked with a red triangle. The subcatchments main drainage lines are shown (blue line) as is a short section of the Owera Stream into which the subcatchment drains.

Figure 8.3. The EX-H site pre-harvest (top) and post harvest (below). All the pines were removed by cable logging and the forwarder mast is visible in the bottom image sitting atop the log landing. The approximate location of the weir and monitoring equipment in the riparian strip is indicated by an arrow in the bottom image.

8.2.2 Exotic pines six months post harvest – EX-H6

Harvesting at the EX-H6 subcatchment was undertaken six months prior to the installation of the monitoring equipment. The EX-H6 subcatchment was the highest of all the monitored sites and was located off State Highway 26 in compartment 51 and was harvested using cable logging methods (Figure 8.4). The suspended sediment monitoring site was located where it drained the harvested area, the log landing, part of a constructed batter, and an artificial drain (Figure 8.5).

Figure 8.4. Location of the EX-H6 subcatchment off State Highway 26. The approximate catchment area is marked and the monitoring site is indicated by a red triangle. The image is taken before harvesting. Log landings constructed in preparation for logging operations can be seen (arrows).

A  **B** 

Figure 8.5. A) The EX-H6 subcatchment before the installation of monitoring equipment. A drain has been cut and to the left is the edge of the log landing and to the right of the drain is a formed batter. B) The eventual location of the temporary plywood weir and monitoring equipment.

The vegetation colonisation of the EX-H6 subcatchment over 18 months post harvest was marked (Figure 8.6). In February 2006 (Figure 8.6-A) the surface was devoid of any ground cover apart from logging trash (smaller trees and cut limbs) discarded during the harvesting operations. The log landing and batter surface were bare and there was evidence of surface erosion and shallow disturbance in the EX-H6 subcatchment.

Six months later in August 2006 (Figure 8.6-B) the area had been aerially sowed with grasses to increase surface cover which was evident in the photo, although the grass coverage was only about 50%. The compartment has been replanted with pine seedlings during this time (indicated by the arrow) and new sproutings of Gorse were visible in the bottom left hand corner of the photo.

The condition of the subcatchment 12 months after harvesting in February 2007 is shown in Figure 8.6-C. The photo was not taken within the EX-H6 subcatchment, but within the same compartment. On the right of the photo the increasing ground cover is evident (nearly 100%). The dry summer of 2006/07 kept the ground cover low.

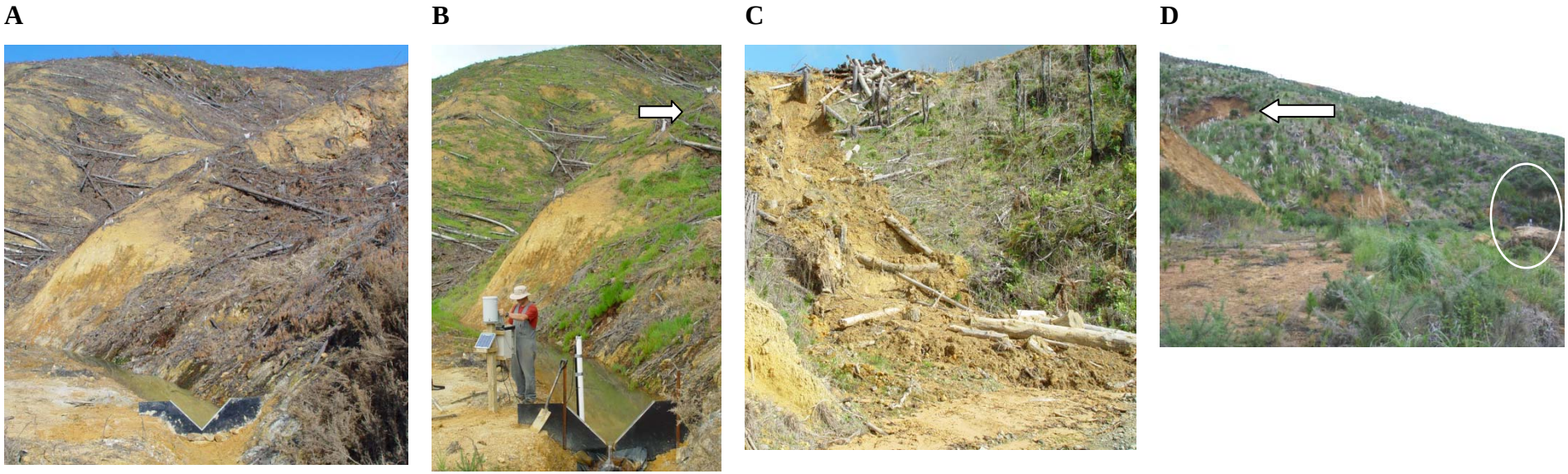

Figure 8.6. The EX-H6 subcatchment A) six months after harvesting just after weir installation; B) 12 months post harvest. Planted pine seedlings example is indicated by the arrow; C) A small debris avalanche from the edge of a log landing within compartment 51 approximately 12 months post harvest; D) 18 months post harvest. The photo is taken from across the log landing. A new erosion feature (shallow landslide) is indicated by the arrow and the monitoring instruments are indicated by a circle.

The subcatchment condition 18 months post harvest in August 2007 is shown in Figure 8.6-D. The perspective of this photograph is from the log landing at the bottom of the EX-H6 subcatchment and the monitoring site can is visible in the image. Ground cover consisted of a mix of grasses and weeds including Pampas Grass and Gorse. Typically after clearing the invasion phase was dominated by adventive weeds (Ogden *et al.* 1997). The ground cover is also higher and would average around 0.5m on average. The log landing has been colonised mainly by exotics and a replanting with pine seedlings can be seen in the foreground of the photo. Sections of the batter have been colonised, but large steep sections remain exposed. The rapidly growing older pines in the compartment can be made out emerging from the ground cover. While increasing ground cover was inhibiting erosion, a shallow landslide on the edge of a small steep ridge is indicated by the arrow (Figure 8.6-D).

8.2.3 Exotic pines 10 year re-growth – EX-10

The 10 year exotic pine re-growth area was the largest of the subcatchments at nearly 10ha (Figure 8.7). It was located in compartment 32 off the Owera Rd, close to the EX-H subcatchment. At the time of instrument installation, the pines had formed a closed canopy with no obvious sign of erosion evident. Some old logging infrastructure was found in the EX-10 subcatchment such as log landings and roads, but had been colonised by ferns and grasses.

8.2.4 Agricultural pastures – AG-P

An approximately 2.5ha pastoral area on the Denize property on the western side of the harbour was monitored (Figure 8.8). Beef cattle grazing was the predominant agricultural landuse in the Whangapoua catchment. Beef cattle were the only pastoral activity on the AG-P site. The rolling hills make this site somewhat atypical as most of the agricultural land in the Whangapoua was on mainly flat land. The topography of the agricultural site was selected to make for better comparisons with the forestry sites.

The agricultural subcatchment was dominated by improved pastures and there were no trees in the subcatchment (Figure 8.9). The stream line was choked by exotic grasses and there were some small areas of bank erosion along its length.

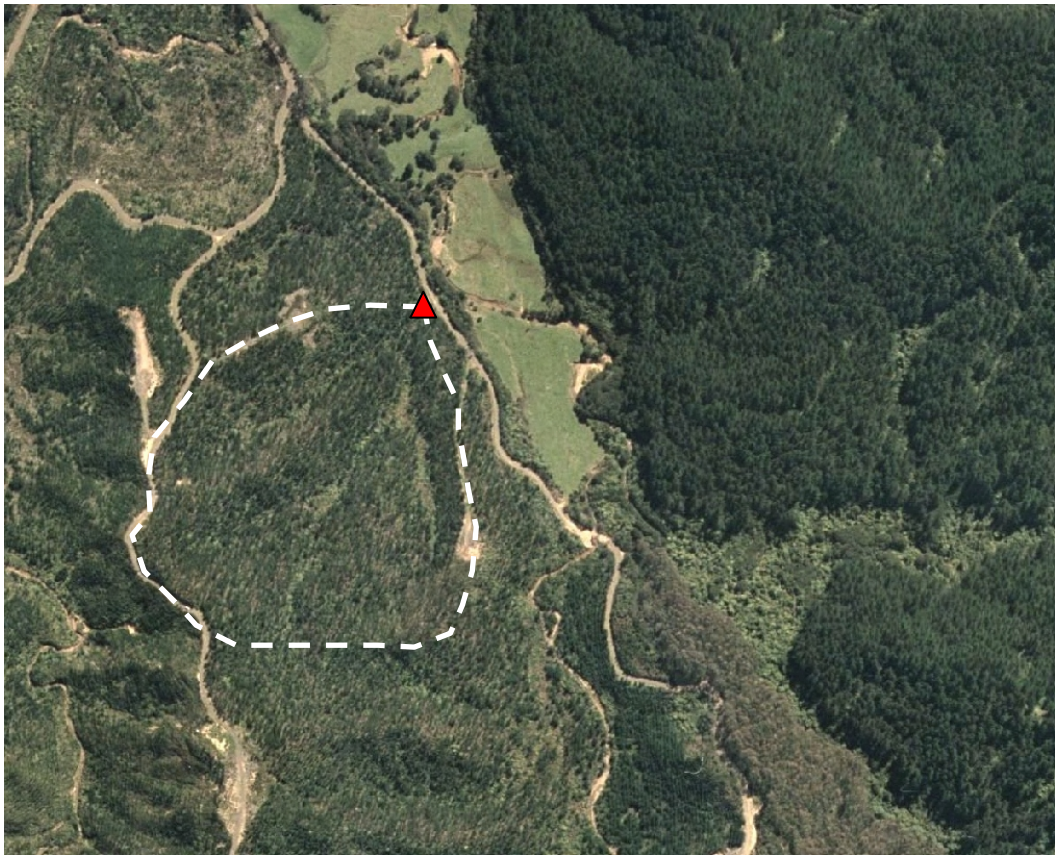

Figure 8.7. The EX-10 subcatchment with the boundary marked and the monitoring station location indicated by a red triangle.

At the top of the subcatchment there were some larger areas of bank erosion, most likely initiated and kept active by cattle trampling. The landowner had attempted to minimise the erosion by dumping rocks into the drainage line (Figure 8.10). The condition of the pasture changed depending on season and stocking phase (Figures 8.9 and 8.10).

8.3 Suspended sediment monitoring methods

8.3.1 Instrumentation setup

The monitoring equipment was installed at the drain-point of each subcatchment. The equipment consisted of an optical backscattering probe (OBS - Greenspan) and a capacitance sensor (Hydrological Services) linked to a Campbell CR10 data logger to measure the height of water passing over a temporary plywood 90° v-notch weir. The OBS probe measured nephelometric turbidity units (NTU) and the capacitance sensor measured the water height in millimetres.

Figure 8.8. The AG-P subcatchment with the boundary marked and the monitoring station location marked by a red triangle.

Figure 8.9. The AG-P subcatchment looking east toward the top of the catchment. The pasture is tall and the drainage line choked with exotic grass and reeds. Gorse bush is also evident.

Figure 8.10. The bank erosion feature at the top of the AG-P subcatchment. Rocks have been dumped into the drainage line to minimise erosion. The pasture cover is good but not long because of stocking with cattle in the winter season.

Three of the sites (EX-H6, EX-10, and AG-P) were also fitted with tipping bucket rain gauges recording at 0.2 mm intervals. All instruments were mounted in a weather proof box and powered by a solar panel to provide continuous monitoring (Figure 8.11). The OBS probes were calibrated as per Appendix P.

The OBS turbidity probe can be mounted in a variety of ways (Eads & Lewis 2002) and was originally mounted perpendicular to the stream flow in a housing of 80 mm PVC pipe which also contained the capacitance sensor. The OBS probe was moved to an overhead suspension to avoid fouling by in-stream debris, burial, and to limit algae growth (Figure 8.12).

8.3.2 Flow measurement

Temporary 90° v-notch weirs were constructed to provide a known cross section for the calculation of water flow (Ackers *et al.* 1978; Fenwick 1994; Campbell 2006) (Figures 8.11 and 8.12). Flow was estimated from the depth readings of the capacitance sensor and by the development of a calibration curve from onsite stream gauging measurements.

Figure 8.11. EX-H6 site showing the housing for the logger, rain gauge (mounted on top) and the power supply via the solar panel. The OBS turbidity probe was mounted using the suspension method and a low flow condition over the V-notch weir.

The theoretical formula for a V-notch weir follows that of (White 1978):

$$Q = \frac{8}{15}\sqrt{2g}C_d \tan\left(\frac{\theta}{2}\right)h^{\frac{5}{2}} \qquad \text{(Eq. 8.1)}$$

Where:

Q = the discharge (m^3s^{-1})

g = acceleration due to gravity = $9.81 m/s^2$

C_d = an empirical 'coefficient of discharge' = 0.578*

h = the measured head of water above the base of the weir notch (m)

θ = the angle of the V-notch

* This constant is for 90° V-notch weirs with negligible velocities of approach

Figure 8.12. Monitoring equipment installed at the AG-P site emptied of water after weir failure (note water height stain on the weir face). A) The original mounting for the turbidity probe at right angles to the stream flow. The original mounting was around 30 cm above the stream bed but course material has deposited behind the weir. B) The suspension deployment of the turbidity probe upstream of the V-notch weir.

The theoretical discharge calculation for a range of stage heights compared reasonably well with field measurements carried out to check the reliability of the calculation at low flow conditions (Figure 8.13). Calibration was undertaken by placing a large bucket under the weir to collect the flow and by timing how long it took to fill. The amount of water collected was then measured using a measuring cylinder and the result recorded in litres per second. The measurements from the capacitance sensor were converted to flow using Equation 8.1.

8.3.3 Sediment measurement

The millivolt (mV) readings from the OBS probes were converted to NTU values by pre-deployment calibration with known standards (Appendix P). Suspended sediment concentration (SSC) values were obtained from the OBS probe NTU values using the relationships developed in a previous study conducted in the

Whangapoua catchment. The SSC and NTU values for 54 samples gave a relationship between NTU and SSC (r^2 = 0.85) where SSC is equal to 1.602 $(NTU)^{0.9787}$; slope equal to 1.03; standard error equal to 0.058; and $p < 0.0001$ (Phillips *et al.* 2005) (Figure 8.14).

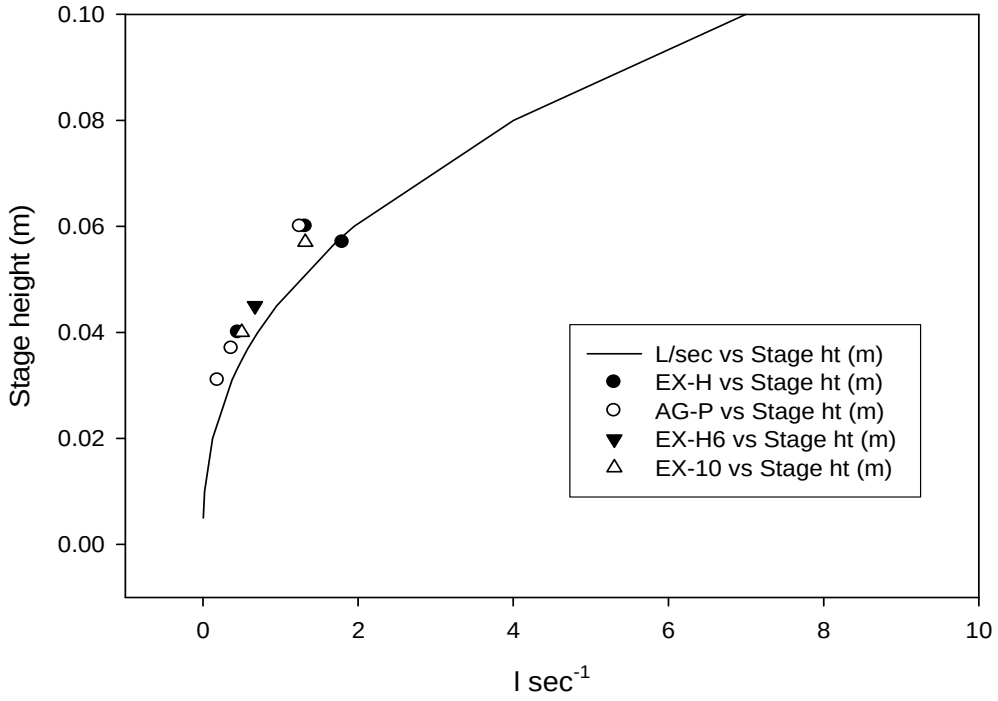

Figure 8.13. Comparison of calculated flow from Equation 8.1 (line) and field calibration points from the four monitoring stations. Only low flow calibration points were obtained.

8.3.4 Establishing a sediment yield

With field turbidity and flow data being measured, the next step was to establish a sediment yield for each subcatchment. The most popular method is the sediment rating curve (Section 3.12), but there was a wide scatter of suspended sediment concentration (SSC) data versus flow data for the four suspended sediment monitoring subcatchments (Figure 8.15). There was an unexpected high flow/low SSC and low flow/high SSC trend, particularly at sites AG-P and EX-10. The r^2 values for the monitoring sites were 0.007 (AG-P), 0.0009 (EX-H), 0.02 (EX-H6), and 0.3 (EX-10) (i.e., no significant relationship). The scatter of the data meant that sediment yield could not be determined using a sediment rating curve.

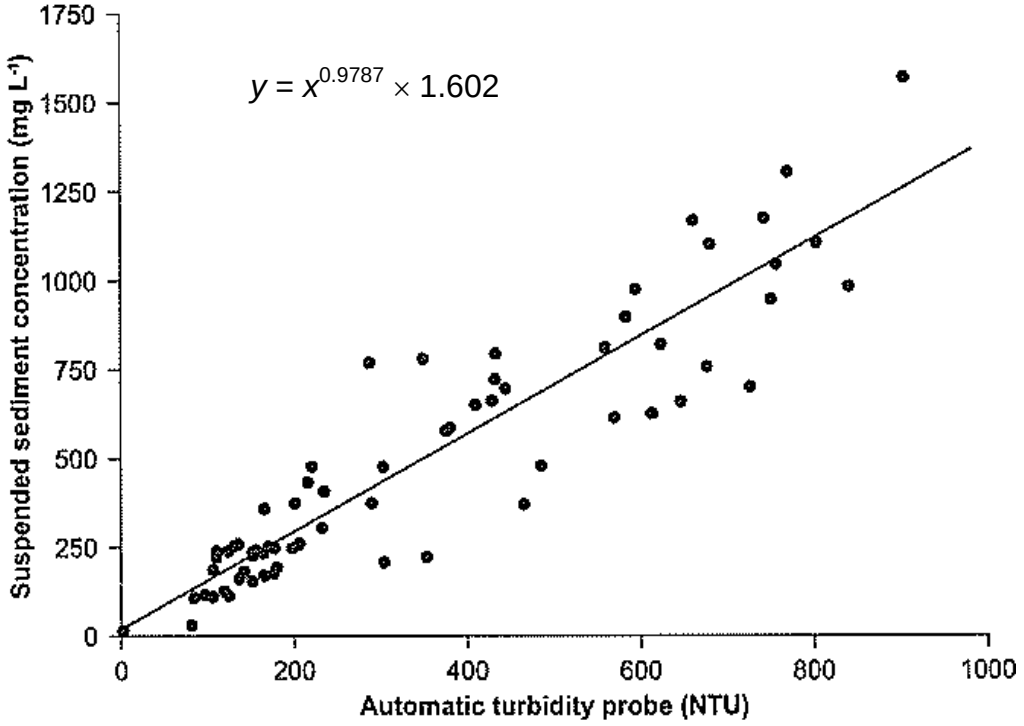

Figure 8.14. Relationship between OBS NTU values and SSC from 54 samples taken in the Whangapoua catchment (Phillips *et al.* 2005).

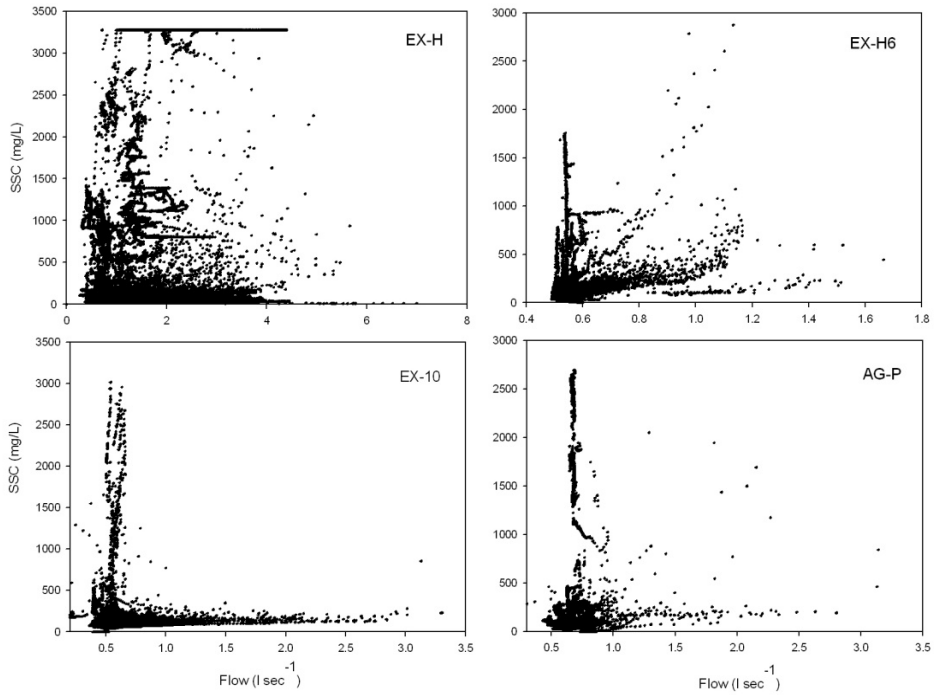

Figure 8.15. Flow vs. suspended sediment concentrations for the four monitoring subcatchments.

The wide scatter of data from the four suspended sediment monitoring subcatchments may be attributed to the small drainage size. In small streams with catchment areas measuring less than a few square kilometres, the sediment concentration for a given discharge can vary greatly as the sediment concentration responds primarily from random injections of sediment from various erosion sites (Hicks & Griffiths 1992). The unsuitability of the sediment rating curve method to the suspended sediment monitoring data in this thesis required another method to establish sediment yield.

8.3.5 The storm sediment yield (SSY) method

The storm sediment yield (SSY) method determines sediment yield by establishing a relationship between the magnitude of storm events and the magnitude of sediment yield. The SSY method is based on the assumption that most sediment is transported by larger storm events and the SSY method has been successfully applied to New Zealand studies (Section 3.12) (Hicks 1994b).

The process of determining total sediment yield by the SSY method is shown in the flow diagram (Figure 8.16). For each monitoring site, a range of storm events was identified and the peak flow and sediment yield were calculated. A peak flow/sediment yield relationship was formed by log-log regression. The complete flow record was used to identify each peak flow for which a sediment yield was calculated, giving a total storm sediment yield for 2007.

It is common practice to separate the base flow component from the peak flow of each storm hydrograph, and there are a range of methods for accomplishing this task (Appendix Q). In this study, a modified constant discharge method was used (Figure Q.2, method 2a, Appendix Q). The start point of the storm was marked by an increase in flow, and the end point when the receding limb of the storm hydrograph flow ‘settles down’ to become reasonably constant, either at the pre-storm level or a new post storm level. The base flow (in terms of litres and sediment quantity) was not separated in this thesis due to the low sediment levels during base flow conditions.

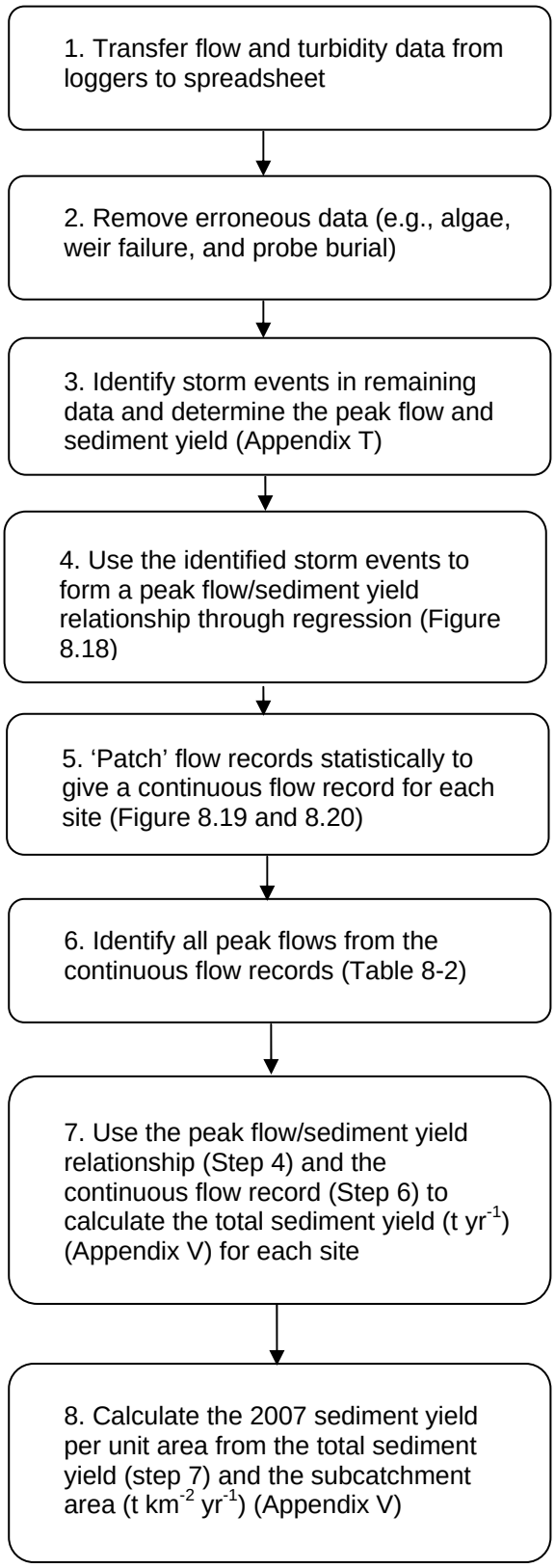

Figure 8.16. Flow diagram of calculating the average sediment yield from a catchment using the Storm Sediment Yield (SSY) method.

8.3.5.1 Identifying storm events (Step 1-3, Figure 8.16)

Firstly, the flow records and turbidity records of all four subcatchments were incomplete (Table 8-1, 'Missing record'). Data was lost due to power or instrumentation failure, or erroneous data (algae on OBS probe, probe burial, probe blown out of water). The corrupted data was removed (or 'cleaned') from the data set prior to analysis (details Appendix R).

For each of the four monitoring sites, the data was examined to find storm events of varying sizes to form the peak flow/sediment yield relationship. The rainfall record was used to identify the dates of rainfall activity. Then the flow and suspended sediment concentration (SSC) records for each site were examined to see if a 'clear' response in both flow and SSC had occurred. A clear response was defined as an increase in flow and SSC, and also a decrease in flow where an end point of the storm event could be identified. Thus, 16 clear storm events were identified for the EX-H site, 16 for EX-H6, 15 for EX-10, and 13 for AG-P.

8.3.5.2 Forming the peak flow and sediment yield relationship (Step 4)

For each storm event:

- the start and end dates/times were recorded, along with the peak flow rate (L sec^{-1}),
- the suspended sediment concentration (SSC in mg L^{-1}) for each 15 minute period of the storm event was calculated from the NTU readings and the (Phillips *et al.* 2005) relationship,
- the SSC mg L^{-1} values for each 15 minute period of the storm event were multiplied by the corresponding flow values (in L sec^{-1}) and summed to obtain a total sediment yield in kilograms for the whole storm event,
- the peak flow/sediment yield pairs for each storm event were plotted, and the regression equation derived for each monitoring site.

8.3.5.3 Identifying all peak flows (Step 5-7)

Because a continuous flow record was required to calculate total sediment yield by the SSY method, it was necessary to patch the flow records of the four monitoring sites because of gaps in the data. The method of patching the flow record is contained in Appendix R.

The continuous flow records (both actual data and patch data) for each site was examined to identify all storm flow events (defined as a 20% increase of peak flow above base flow due to the 'noise' of the data) from which the peak flow was identified and recorded. Each peak flow value was converted into a sediment yield (kg) by the appropriate peak flow/sediment yield relationship.

8.3.5.4 Calculation of the average sediment yield (Step 8)

The sediment yields for each site were summed for 2007 and divided by the area of the monitoring site to arrive at a total erosion value in t km^{-2} yr^{-1}.

8.4 Results

8.4.1 Rainfall

The rainfall records for this study were from rain gauge instruments on EX-H6, EX-10, and AG-P, as well as two records from Environment Waikato (EW) sites. One of the EW sites (Castle Rock) was a permanent station at the top of the catchment at around 300 m ASL, while the other (Opitonui) was located in the lower agricultural area (Figure 8.17). Of the five rainfall records, the Castle Rock site was the only one not to suffer any data loss.

Summary graphs of 2006 and 2007 rainfall are contained in Appendix S. The Castle Rock site receives the most rainfall and generally has larger magnitude storm events than comparison to the other sites. For example, in 2006 Castle Rock received 1665 mm and Opitonui 1358 mm, while in 2007 Castle Rock received 2401 mm and Opitonui 1574 mm, a difference of more than 800 mm between the recording sites.

8.4.2 Peak flow and sediment yield (Steps 1-4)

Storm events identified as suitable for developing the peak flow/sediment yield relationships are tabulated in Appendix T and graphed in Appendix U. Graphs of the sediment yield/peak flow are presented in Figure 8.18.

Two events (2-3-2006 and 7-3-2006) were removed from the data in order to define the relationship for the EX-H6 site. The removal the two storm events changing the r^2 value from 0.02 to 0.62. The two storm events were the first

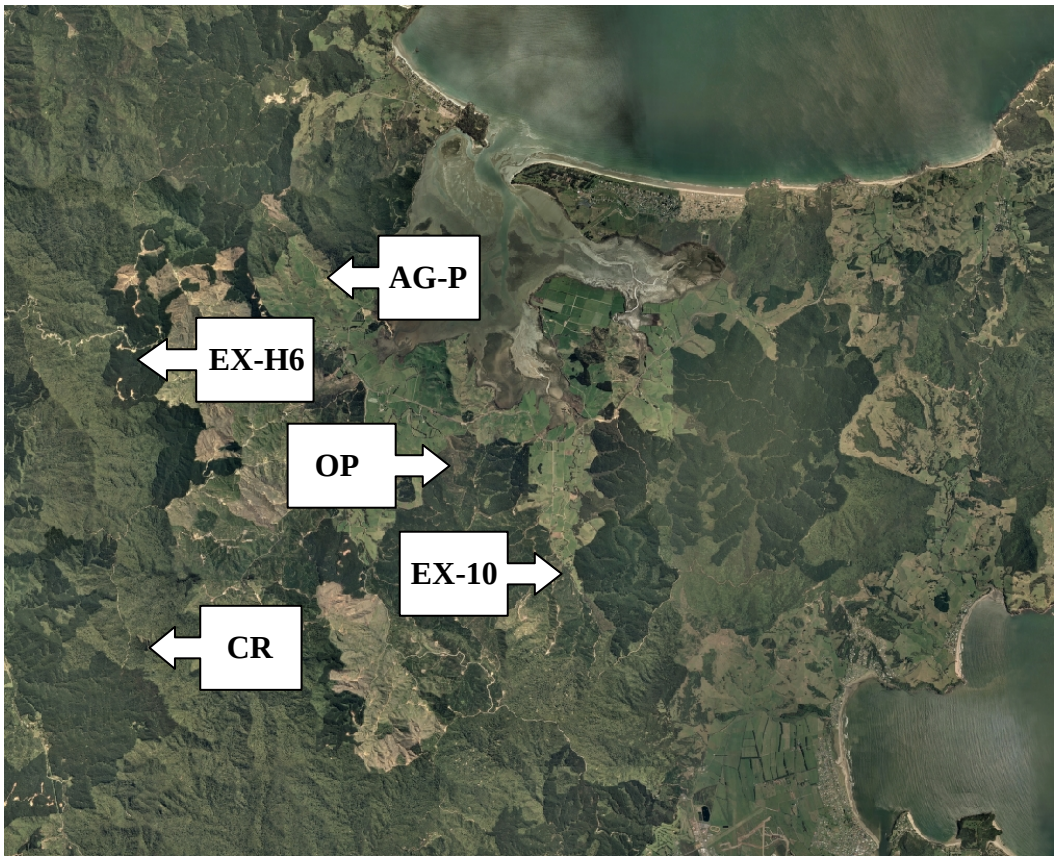

Figure 8.17. Location of the rainfall monitoring stations at the AG-P, EX-H6, and EX-10 sites. Also shown are the locations of the Opitonui (OP) and Castle Rock (CR) sites.

recorded after the establishment of the monitoring site 6 days prior to the first event (in italics Table T-2, Appendix T). The anomalously low and high respectively sediment yields for the corresponding peak flow are believed to be due to disturbance of the site during construction of the weir.

8.4.3 Flow results (Step 5-6)

The details of patching the flow record are in Appendix R and the raw flow record is in Appendix S. The patched flow results which provided a 15 minute record for the four stream monitoring subcatchments are shown in Figures 8.19 and 8.20. As monitoring of all four sites didn't begin until 51 days into the 2006 period and the unreliable nature of the data for 2006, the catchment sediment yield for all four sites was calculated only for 2007.

The continuous (patched) flow record was used to identify all peak flow events in each of the monitoring sites for 2007 (Table 8-2).

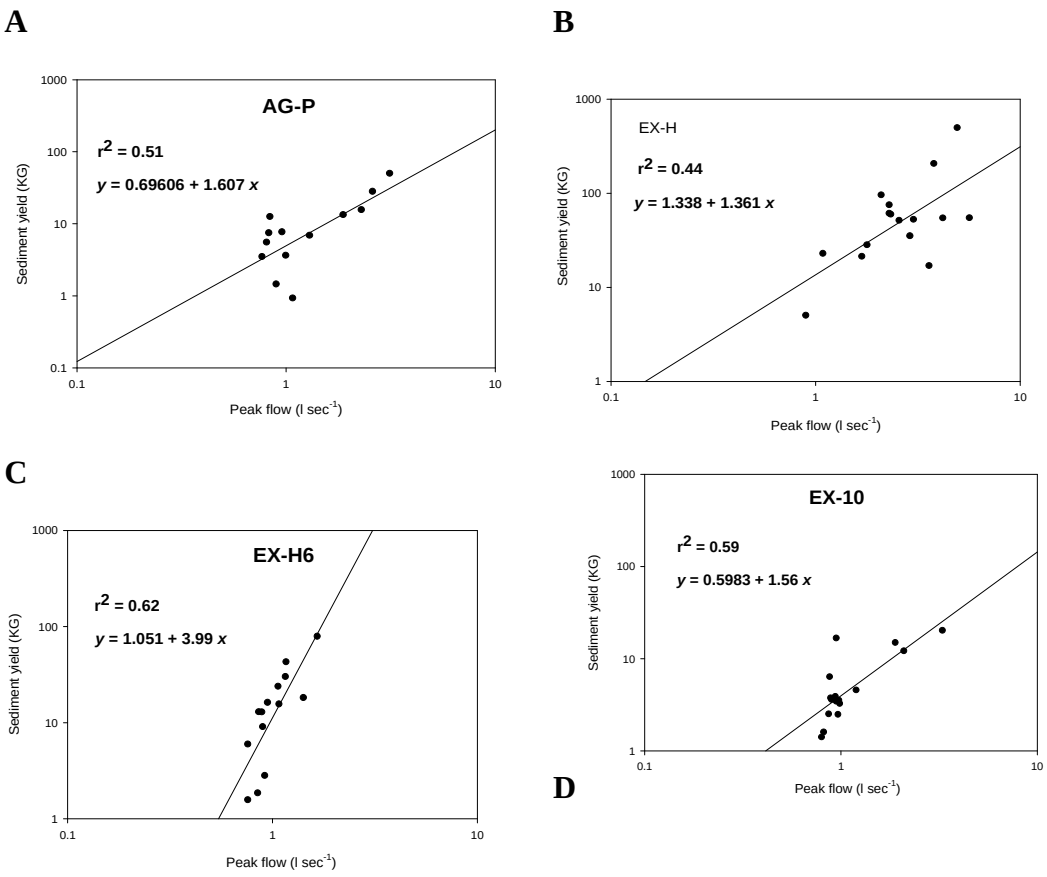

Figure 8.18. Peak flow and sediment yield relationships for A) AG-P; B) EX-H; C) EX-H6; and D) EX-10.

8.4.4 Catchment sediment yield (Step 7-8)

The peak flow values in Table 8-2 were then used to calculate a sediment yield for each storm event for each monitoring site for 2007 (Appendix V) from which an erosion rate for each monitoring site was derived (Table 8-3).

The most recently harvested exotic pine site (EX-H) had the highest erosion rate, followed by the recently harvested exotic pines (EX-H6), followed by the agricultural pastures (AG-P), and the lowest erosion rate was found in the 10 year exotic pine (EX-10).

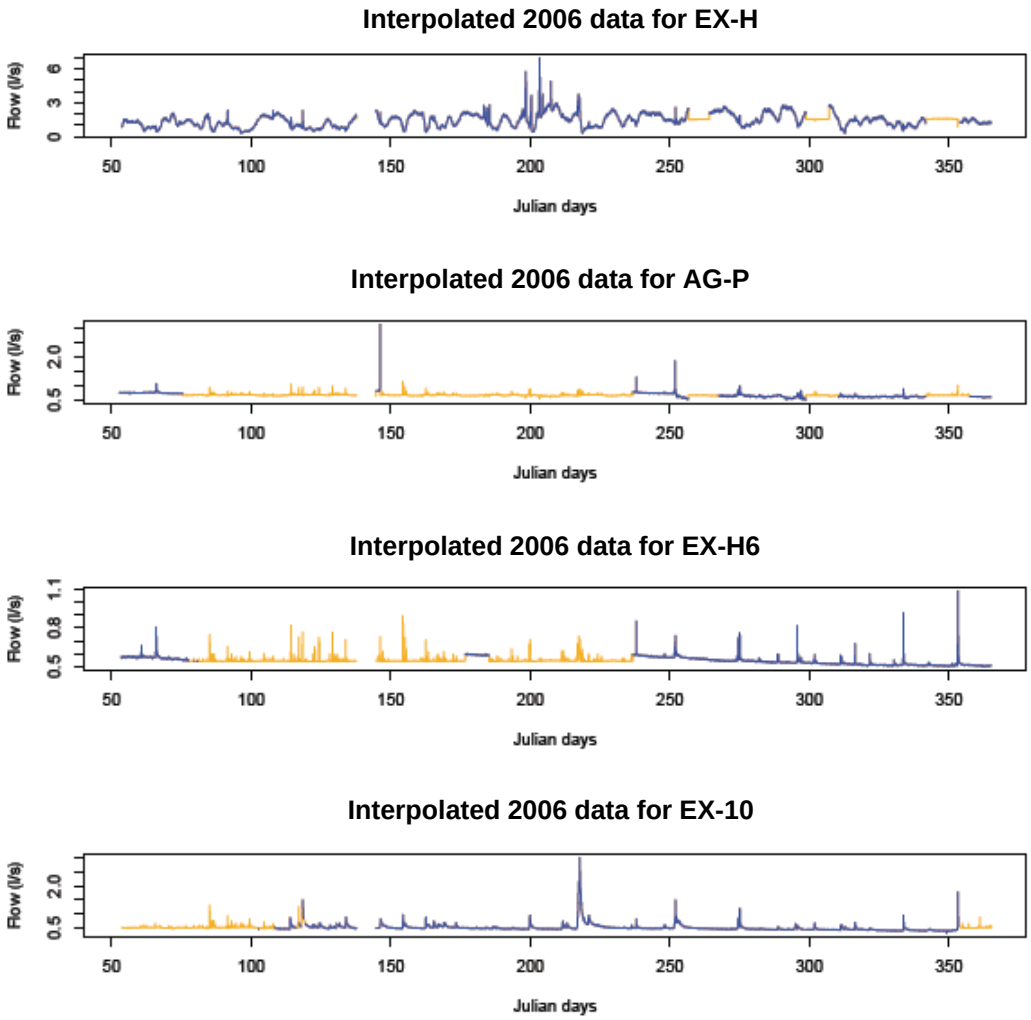

Figure 8.19. Patched stream flow data (orange) for the exotic harvested (EX-H), agricultural pasture (AG-P), exotic 6 month post harvest (EX-H6), and exotic 10 year post harvest (EX-10) monitoring sites, 2006.

8.5 Discussion

8.5.1 Subcatchment erosion rate results

Harvesting of pine trees causes accelerated erosion due to direct ground surface disturbance during harvesting and tree removal leaves the soil exposed to rainfall events and increases the water yield. Erosion rates in pine forests decrease over the harvesting cycle. By year 10 of a rotation the harvested area has 'settled down' due to the rapid growth and canopy closure of the pines to result in a lower erosion rate than agricultural pastures or harvested pines.

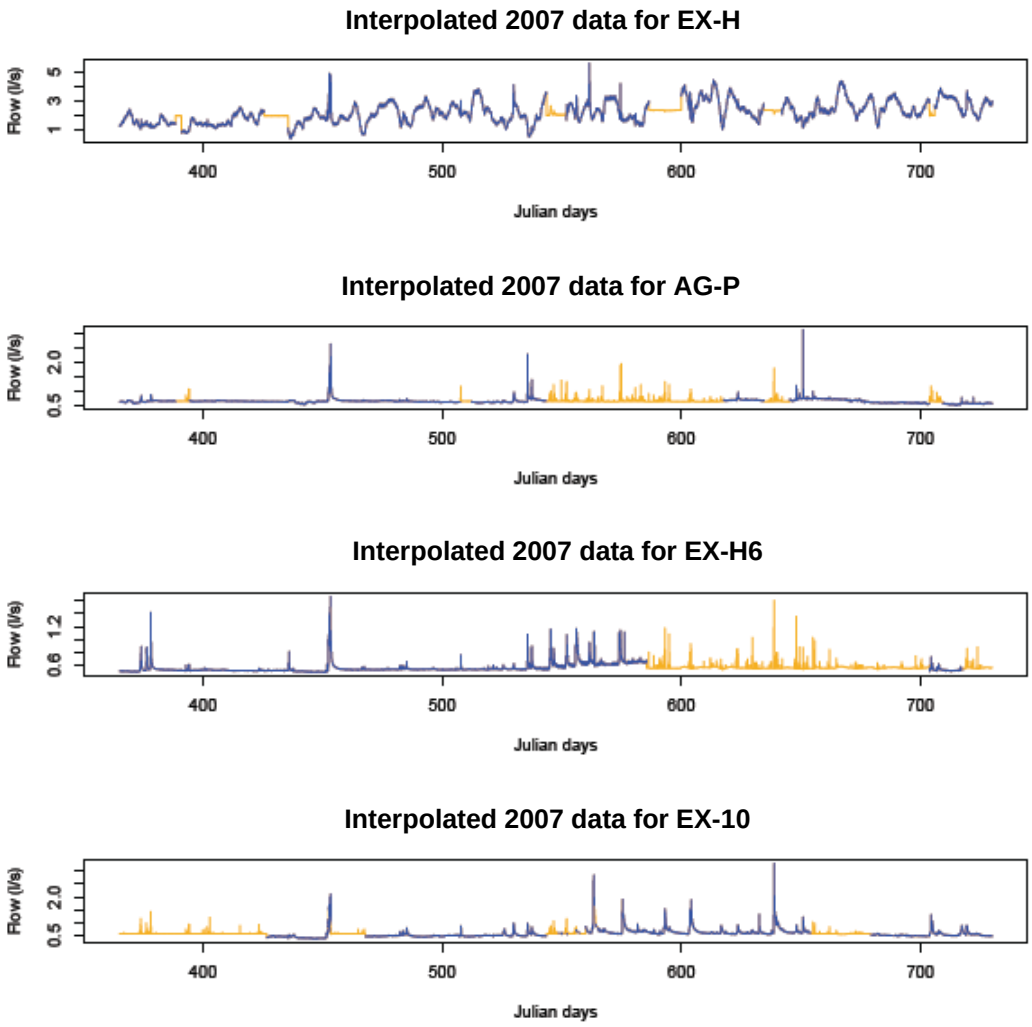

Figure 8.20. Patched stream flow data (orange) for the exotic harvested (EX-H), agricultural pasture (AG-P), exotic 6 month post harvest (EX-H6), and exotic 10 year post harvest (EX-10) monitoring sites, 2007.

The 10 year post harvest pine (EX-10) returned the lowest erosion rate suggesting that when the tree canopy has closed it protects the ground surface from erosive rainfall events. The closed canopy also increases interception of rainfall and there is ground cover vegetation and litter increase. In a study in the Mangatu exotic pine forest, it was found that *P.radiata* increased root mass at a rate of 1-2 t ha year^{-1} from planting up to age 8-10 years, and this rate doubles up to age 25 years. At age 8, the *P.radiata* tree has developed strong lateral roots and an interlocking root structure that reinforces the upper soil horizons (Watson *et al.* 1999). Similar trends of slope instability from harvesting up until 10 years under other types of forest have also been observed with sediment yield ten times higher during the period of instability than under mature forest (Imaizumu *et al.* 2007).

Table 8-2. Peak flow results for all four sites for 2007.

Date	Peak flow (l sec^{-1})			
	EX-H	**EX-H6**	**EX-10**	**AG-P**
09/01/2007	1.68	0.89	0.70	0.83
12/01/2007	1.44	1.42	1.42	0.86
30/01/2007	1.18	*	*	*
28/03/2007	4.94	1.66	2.10	2.60
28/04/2007	1.85	*	*	*
30/04/2007	1.81	*	0.80	*
21/05/2007	3.02	*	0.87	1.16
14/06/2007	4.13	*	0.98	0.96
21/06/2007	1.44	1.08	0.97	2.27
20/06/2007	2.04	0.90	0.83	1.38
23/06/2007	2.04	*	*	*
29/06/2007	2.64	1.16	0.88	1.00
06/07/2007	2.75	1.07	1.15	1.32
09/07/2007	3.35	1.17	0.83	0.95
15/07/2007	5.67	1.12	2.85	0.74
28/07/2007	4.21	1.14	1.91	1.94
04/08/2007	*	*	0.94	*
15/08/2007	2.34	1.18	1.53	1.31
26/08/2007	3.62	0.93	1.88	1.06
07/09/2007	1.98	0.69	0.89	0.79
13/09/2007	3.09	0.85	0.90	0.96
30/09/2007	2.34	1.60	3.31	1.78
10/10/2007	1.98	1.36	0.91	1.19
11/10/2007	1.94	0.88	1.21	3.13
15/10/2007	2.22	1.03	1.02	0.98
24/10/2007	2.08	0.84	0.84	*
05/12/2007	2.77	*	1.31	1.16
18/12/2007	2.47	*	0.89	*
21/12/2007	3.72	0.86	0.88	*

* No rise in flow levels above threshold value.

Table 8-3. Results for storm flow and sediment yield for all four sites.

Site	Description	Erosion rate (t km^{-2} yr^{-1})
EX-H	Exotic pine – recent harvest	48
EX-H6	Exotic pine – 6 month post harvest	28
EX-10	Exotic pine – 10 year regrowth	2
AG-P	Agriculture – pasture	7

The pasture catchment (AG-P) erosion rate was around 7 t km^{-2} yr^{-1}. Neither mass movement nor cattle pugging was observed in the subcatchment monitored by the turbidity probes. A small area of head cut gully was in the monitored site at the top of the agricultural subcatchment. Sediment generated from the gully could be

intercepted by the grassed stream line before reaching the monitoring site (Figure 8.9). The majority of the subcatchment was under healthy pasture cover which protects the soil surface from erosion and there were no landslides evident within the agricultural monitoring area.

8.5.2 Subcatchment erosion rate results in the New Zealand context

The results for the two harvested exotic pine sites (48 t km^{-2} yr^{-1} for EX-H and 28 t km^{-2} yr^{-1} for EX-H6) were within the range of reported values from other New Zealand studies, but at the lower end. One study of post harvesting erosion rates in pine plantations, (Phillips *et al.* 2005) reports erosion rates as low as 21 t km^{-2} yr^{-1} on weathered granites and as high as 450 t km^{-2} yr^{-1} on gravels. A study conducted in the Whangapoua catchment on harvested pines derived values of 59-116 t km^{-2} yr^{-1}. One estimate of the specific sediment yield of the Opitonui River was 160 t km^{-2} yr^{-1} (Blair 2004). At Pakuratahi New Zealand, monitored storm events from mature pines gave low sediment yields (0.09-2.7 t/km^{-2}) (Fahey & Marden 2006) which compared to the low erosion rates of the 10 year pine (2 t km^{-2} yr^{-1} EX-10) found in this thesis.

For agricultural pasture erosion rates, (Quinn & Stroud 2002) reported New Zealand ranges of 60-200 t km^{-2} yr^{-1} and as low as 2.2 t km^{2} yr^{-1} for the mid-North Island. Erosion on a Waikato dairy farm was 14.2 t km^{2} yr^{-1} (Wilcock *et al.* 1999) and 0.25-8.83 t/km^{-2} for sheep and beef pastures (Fahey & Marden 2006). Fahey & Marden (2000) report values of around 100 t km^{-2} yr^{-1} for pastures on hill country tertiary sediments in the Hawke's Bay, some of the most erodible country in New Zealand. The AG-P result of 7 t km^{-2} yr^{-1} was similar to the exotic pine results in that it is within the reported ranges for New Zealand, but at the lower end of the erosion estimates.

8.5.3 Comparison of exotic pine and agricultural erosion rates

The recently harvested pine (EX-H), six month post harvested pine (EX-H6), and the 10 year post harvested pine (EX-10) results show a declining erosion rate of exotic pine areas with increasing time after harvesting. The decrease in exotic pine erosion rates after harvesting was also observed in a study in the Whangapoua forest (Figure 8.21) (Marden *et al.* 2006). The harvesting process directly disturbs

the ground surface and removes the ground cover that protects the soil surface from rainfall events. Slope instability increases if no replanting takes place due to the decomposition of roots that lowers the effective soil strength. In New Zealand, trees are replanted and grasses sowed to protect the soil surface. The lower erosion rate of EX-H6 compared to EX-H probably reflects the more advanced stage of recovery from harvesting (i.e., ground cover increase) EX-H6 was at during the monitoring period compared with the EX-H.

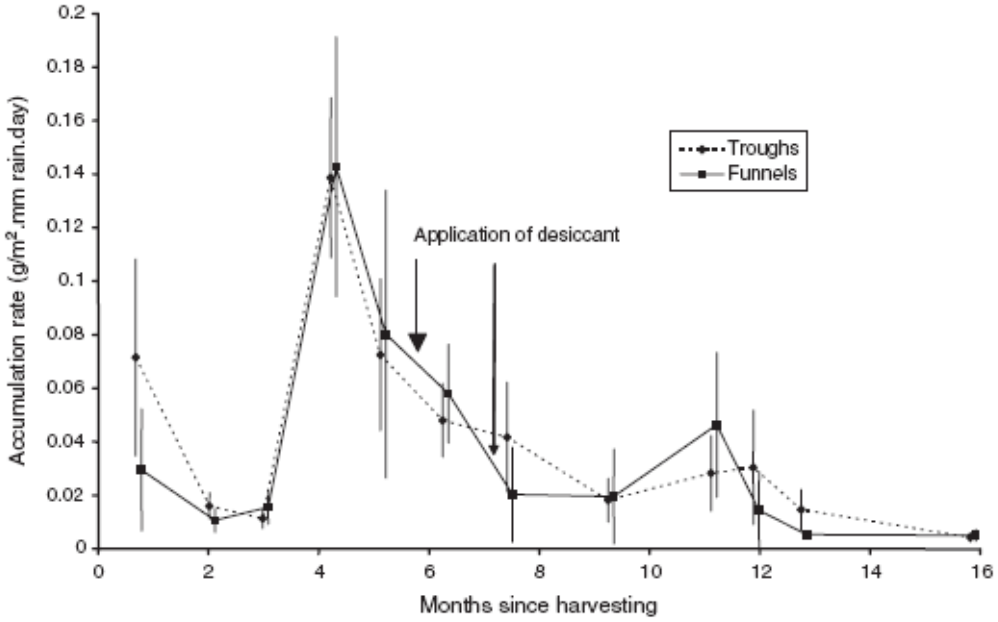

Figure 8.21. Sediment accumulation normalised for rainfall over a 16 month period after pine tree harvesting. Desiccant application refers to the aerial application of a chemical to kill weed competition for the newly planted pine seedlings (Marden *et al.* 2006).

While the agricultural landuse erosion rate would vary because of seasonal change, pasture condition, and stocking rates, overall it would be more constant compared to exotic forests that undergo major soil disturbance at harvest time. If exotic forests erosion rates are compared with agricultural erosion rates over a 30 year harvest cycle, a simple conceptual model would have the agricultural landuse yielding more sediment over that time than the exotic forests (Figure 8.22). The suspended sediment monitoring results (Table 8-3) has the recently harvested exotic forests eroding at over four times the rate of the agricultural landuse and six month post harvested exotic pines eroding at around three times the rate. But 10 years after harvesting the exotic pine erosion rate is only one fifth that of the

agricultural landuse. Both Marden *et al.* (2006) (Figure 8.21) and Eyles & Fahey (2006) report a similar rapid decline in sediment yield following pine harvesting.

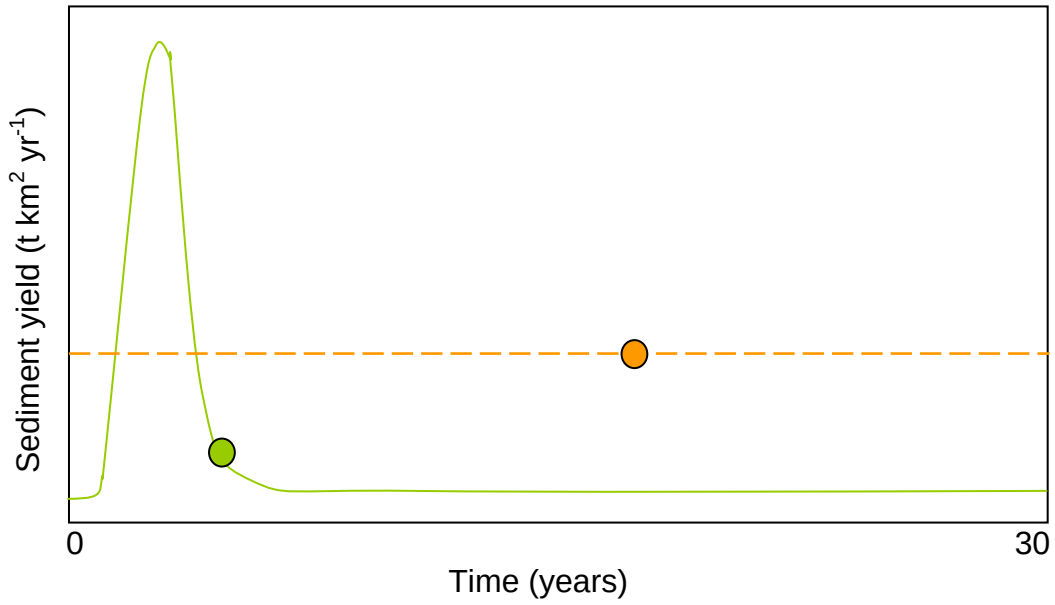

Figure 8.22. Conceptual model of a 30 year erosion cycle of exotic pines (green) compared to agricultural pastures (orange) as indicated by the suspended sediment monitoring results.

8.5.4 Comparison of exotic pine and agricultural erosion rates by peak flow/sediment yield relationships

The slopes of the peak flow/sediment yield relationships regressions (Figure 8.18) for the four monitoring sites were compared using analysis of covariance to test the null hypothesis that there was no difference between the slopes of the equations. The null hypothesis was accepted for EX-10, AG-P, and EX-H. The null hypothesis was rejected for EX-H6. The slopes of EX-10, AG-P, and EX-H were similar while EX-H6 had a steeper slope which means it yields more sediment at higher peak flow rates than the other three monitoring subcatchments (Figure 8.23).

The most likely explanation for the steeper slope for EX-H6 is that it indicates the presence of logging infrastructure (roads, batters, drains, log landing) at EX-H6 that were absent from EX-H. The EX-H6 monitoring site was located adjacent to a log landing and a batter and the subcatchment drained to the weir via a drainage ditch cut by the logging contactors. Studies have shown the importance of logging

infrastructure in relation to sediment yield. For example, unsealed roads have been shown to be important sediment sources and can account from 4.4% to 39% of the sediment budget (Croke *et al.* 1999; Croke & Mockler 2001; Fransen *et al.* 2001; Madej 2001; Swank *et al.* 2001; Lane & Sheridan 2002; Wallbrink & Croke2002; Motha *et al.* 2003; Sheridan *et al.* 2006; Sheridan & Noske 2007). Low infiltration runoff is generated from roads and other compacted and disturbed features during storms and accelerates the delivery of sediment to streams (Sidle *et al.* 2006). New infrastructure such as young forest roads have a greater landslide susceptibility than old forest roads (Fransen *et al.* 2001). EX-H did not have any logging infrastructure features draining to the monitoring site such as at EX-H6, but instead had a strip of riparian vegetation (Figure 8.3) which is widely recognised as reducing the impact of sediment into streams (Wallbrink *et al.* 2002a; Boothroyd *et al.* 2004; Quinn *et al.* 2004; Parkyn *et al.* 2005). The riparian strip may have buffered the EX-H site from the more extreme storm flows and sediment yields. The riparian strip should only have had a small influence at this site as most of the sediment carried in the flow monitored at EX-H should have been entrained and channelised by the time it reached the weir and recording instruments.

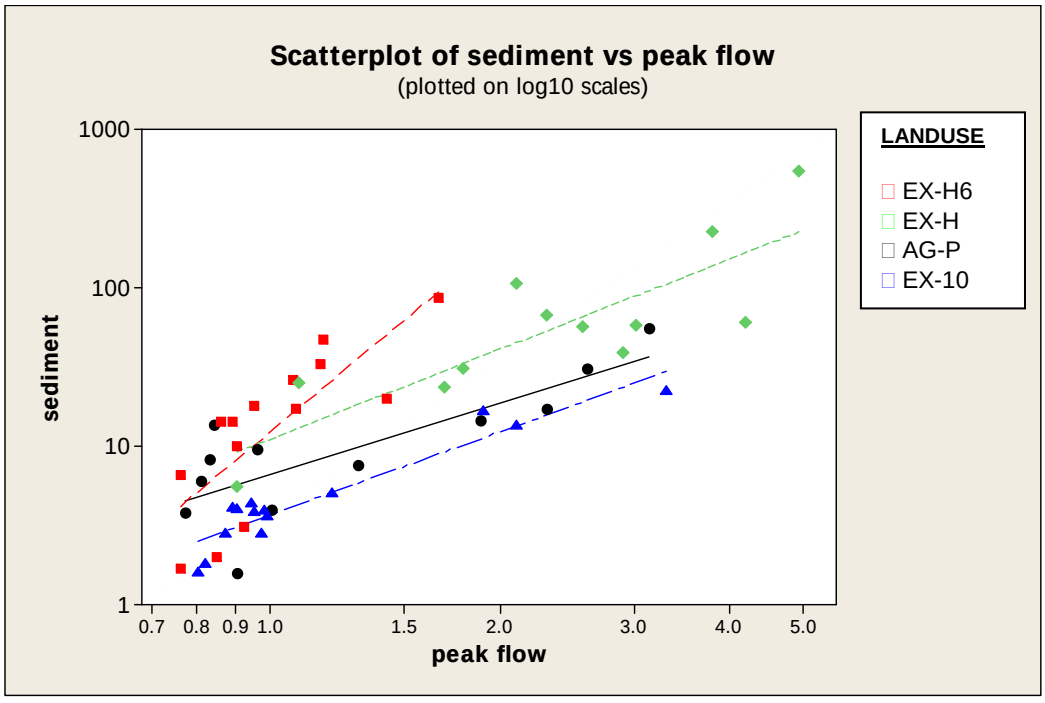

Figure 8.23. Peak flow and sediment yield relationships for the AG-P, EX-H, EX-H6, and EX-10 monitoring sites.

8.5.5 Comparison of exotic pine and agricultural erosion rates by storm hysteresis

An examination of the storm hysteresis of the four subcatchments was undertaken to compare the sediment yield characteristics between the exotic pine and agricultural landuses. The storm hysteresis relationships were generally not well formed. Of the good storm hysteresis relationships found, all landuses had a clockwise relationship indicating sediment supply exhaustion during a storm event. The exception to this was the EX-H site soon after harvesting which had an anti-clockwise relationship indicating high levels of soil erosion as could be expected. The details are contained in Appendix W.

8.5.6 Sources of error

8.5.6.1 SSC and NTU relationships

The best method of converting NTU readings into suspended sediment concentrations (SSC) is by direct field calibration by employing automatic samplers to sample turbid water over a range of flow conditions (Gippel 1989; Gippel 1994; Sun *et al.* 2001; Eads & Lewis 2002; Lewis 2002b). Automatic sampling equipment was not available for this study and instead NTU was converted to SSC by an existing published relationship (Section 8.3.3).

The problem with not having direct field calibration is that the main assumption underlying the use of OBS probes is that the more suspended sediment in the water column, the more light will be attenuated (scattered/refracted) by the sediment particles and the backscattered signal will be registered with the probe. The size/attenuation relationship is also assumed to be approximately linear (Gippel 1989; Lewis 2002a), and the linear relationship was borne out in the laboratory calibration with Formazin solution. The problem in a field setting is that the material present in the water column will vary in size depending on the magnitude of the rainfall event and from changing sediment sources within an event. For example, clay particles will dominate at base flow conditions. During a storm event, larger particles such as quartz spheres become entrained in the flow (Davies-Colley & Smith 2001). The light attenuation characteristics with increasing particle size are non-linear (Figure 8.24). Particle size differences are the main problem with OBS probes (Wren *et al.* 2000). While the NTU/SSC

relationship used was derived in the same catchment over a range of flows in another study, the lack of extensive sampling of all four sites over a wide range of conditions is a potential source of error.

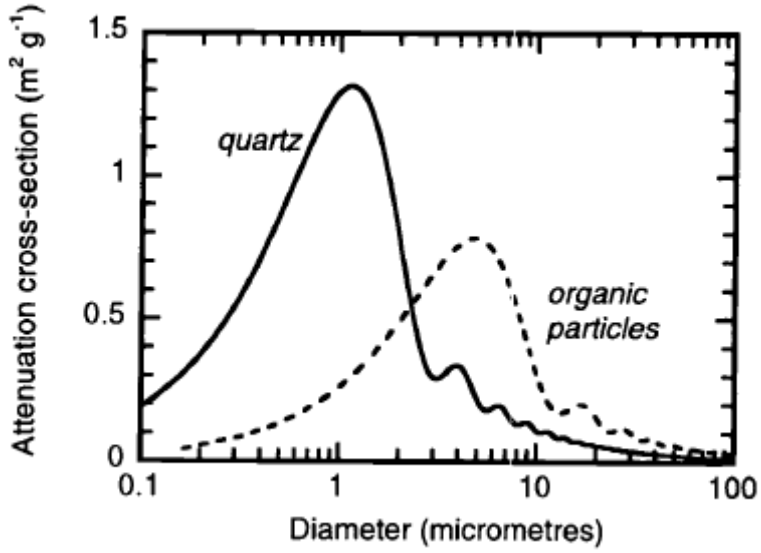

Figure 8.24. Non-linear attenuation characteristics of OBS probes for quartz and organic particles of varying sizes (Davies-Colley & Smith 2001).

8.5.6.2 Biological changes

The placement of a weir across the streams in the Whangapoua catchment created a body of standing water which, apart from the EX-H site, was also open to direct sunlight. The still body of water behind the weir exposed to sunlight created the conditions for algae build up and this was a constant problem during the study (Figure 8.25). While the algae was mitigated to some extent by the addition of pumps to the probe heads, data was rendered useless during summer peaks when algae build up would over-come the cleaning action of the pumps. Algae and other plant life also grew immediately behind the weir. The aquatic plants were periodically removed during site maintenance visits and when disturbed threw up plumes of fine sediment that had collected in the aquatic plants. While not directly observed, it was a concern that the sediment could be flushed out during higher energy events and interfere with the measuring of the true character of sediment generation within the subcatchments.

A

B

C

D

Figure 8.25. The biological changes that are potential sources of error in the stream monitoring study. A) a new turbidity probe before installation in the field with a copper surround to stop algal growth; B) same probe showing algal growth over the lens and body of the probe several months after installation; C) turbidity probe with washer pump installed showing effects of algal growth; D) turbidity probe site showing aquatic plant growth behind the weir which potentially acts as a sediment trap.

8.5.6.3 Flow data patching and flow calculation

The flow record data was patched using the records of other sites. The assumption that a storm event caused significant peak flow events in all four monitoring sites was not found to be true in all cases in the Whangapoua catchment (Table 8-2). Thus estimating flows from other sites may have added or eliminated storm flow events to the sites where the data was patched.

The flow across the v-notch weir was calculated by employing the stage height in an equation, so the flow conditions are assumed to be constant over the period of monitoring. Sediment deposition behind the weir (especially at EX-H) can change

the approach water velocities (Bonta 1998), meaning that the flow calculation assumptions used in this study could have changed during the monitoring period.

8.5.6.4 Lack of replication and period of monitoring

Resources only allowed for four sites to be monitored during the course of two years. Factors such as difference in altitude, aspect, localisation of storm events, and the difference in logging infrastructure between the EX-H and EX-H6 introduce a greater level of uncertainty when interpreting the results.

The stream monitoring was conducted for two years. Cleared forests may remain unstable for up to 10 years. Most studies focus on large landslides from large storms using methods such as aerial photos, but small landslides from common storms also increase sediment yield and are often overlooked (Montgomery *et al.* 2000). Thus a two year period may not have been long enough to capture a range of storm events and the episodic nature of sediment delivery from a regenerating exotic forest.

8.5.6.5 Reliability of the stream monitoring results

Sun *et al.* (2001) found that the establishment of sound relationships between suspended sediment concentration and NTU requires extensive data collection across all sizes of events at short sampling time intervals, and then the data should only be used for interpolation and not extrapolation. Sun *et al.* (2001) conclude that if a sound suspended sediment concentration/NTU relationship is not achieved, then the data may contain errors and therefore should only be used as a *general guide* rather than a serious estimate of catchment erosion. Thus, I consider that the suspended sediment monitoring results show the broad differences between erosion rates in the different landuses within the catchment, but that they are an underestimation of the true rates of erosion.

8.6 Conclusion

Constructing sediment rating curves was not possible with the collected data, most likely due to the behaviour of very small (< 10 ha) catchments. Consequently the suspended sediment yield (SSY) method was applied to determine erosion rates for each monitoring area. The EX-H (exotic pines recently harvested) had the

highest erosion rate at 48 t km^{-2} yr^{-1} followed by the EX-H6 (exotic pines six month post harvest) at 28 t km^{-2} yr^{-1}, most likely due to increased soil surface protection and lower runoff in the older EX-H6 site, although location differences cannot be eliminated. The EX-H6 site peak flow/sediment regression had the steepest slope (Figure 8.23), most likely due the presence of logging infrastructure. The AG-P (agricultural pastures) site erosion rate of around 7 t km^{-2} yr^{-1} was the second lowest, while the EX-10 (exotic pines 10 year re-growth) had the lowest recorded erosion rate of the four sites (2 t km^{-2} yr^{-1}). The erosion rates for all four monitoring sites were within the reported ranges for erosion rates for New Zealand, but at the lower end.

There were many sources of potential error, including a lack of replication, data corruption and patching, biological changes, and relationship assumptions. Therefore the most appropriate use of the results from this chapter is for explanation rather than extrapolation.

CHAPTER NINE

MODELLING CATCHMENT SEDIMENT GENERATION

9.1 Introduction

Modelling was undertaken to compare with the results of the sediment fingerprinting technique. Two modelling packages were used; the Sediment Yield Estimator (SYE) (Hicks *et al.* 2003) from the National Institute of Water and Atmosphere (NIWA), and the New Zealand empirical erosion model (NZEEM) (Dymond *et al.* 2006) from Landcare Research. Both models have been developed in New Zealand and have been calibrated using New Zealand data, but had not been calibrated to the Whangapoua catchment.

9.2 Sediment Yield Estimator (SYE)

9.2.1 Background

The SYE is a landscape scale model developed to estimate how much sediment is carried by rivers and streams to the coast annually. The SYE is a raster-based GIS layer for New Zealand that specifies suspended sediment yield (SSY) in t km^{-2} y^{-1} for drainage basins. It was developed based on gauged sediment yields from over 200 gauging stations that were used to calibrate the model. The model input data is annual rainfall and erosion terrain (slope, lithology, and soils). The model output was adjusted so that predicted yields matched the actual yields for the 200 river gauging sites and was corrected for lake trapping of sediment (Hicks *et al.* ND).

The empirical model bases sediment delivery on:

$$SSY = b\,P^{1.7} \qquad \text{(Eqn 9.1)}$$

Where P is the local mean annual rainfall (mm) and b is the coefficient that is determined by erosion terrain. P can be thought of as the driving factor and b as the availability of sediment. The rainfall coverage P was interpolated from a 30 year record of national rain gauges. The erosion terrain b was defined on a

hierarchical basis with the primary components identified as slope and lithology and the secondary components being soil type, the dominant erosion processes, and expert knowledge.

9.2.2 Method

To estimate the erosion rates for the Whangapoua catchment, the following procedure was followed. The data set for New Zealand was used to create shapefiles of the various Whangapoua Harbour subcatchments and landuses. A new raster was created for each subcatchment and the mean for all of the cell values in the new raster's table of properties was equivalent to the mean erosion value for that subcatchment in t km^{-2} y^{-1}. To enhance the visualisation of the results, the rasters for the Whangapoua catchment were reclassified into categories of 0-10, 10-20, etc to 100 t km^{-2} y^{-1} for final presentation.

9.3 New Zealand empirical erosion model (NZeem)

9.3.1 Background

The NZeem was designed to improve understanding of sediment delivery from local to national scales by using rainfall, slope, vegetation, and landuse information. The NZeem estimates the erosion rate as:

$$\bar{e}(x,y) = a(x,y)C(x,y)R(x,y) \qquad \text{(Eqn 9.2)}$$

Where the erosion rate at each pixel (x,y) $\bar{e}$ is a function of three main factors; land cover factor C, mean annual rainfall R, and an erosion coefficient a that depends upon the erosion terrain (Dymond *et al.* 2008; Dymond & Betts In prep.). If C and R are known, then they can be estimated for each erosion terrain by:

$$a_i = \frac{\overline{s_i}}{\iint\limits_{\substack{erosion\\terrain\\i}} D(x,y)C(x,y)R(x,y)dxdy} \qquad \text{(Eqn 9.3)}$$

To estimate the erosion coefficient for each erosion terrain a_i, the cover factor $C(x,y)$, the rainfall factor $R(x,y)$, the sediment delivery ratio $D(x,y)$, and the sediment yield $\overline{s_i}$ must be known.

The land cover *C* is the long term mean erosion rate at *x,y* relative to forest. The estimation of *C* has been influenced by New Zealand studies (e.g., Page & Trustrum 1997; Luckman *et al.* 1998) that deforestation increases landsliding events, usually by an order of magnitude. Therefore:

C(x,y) = 1 (woody vegetation)
= 10 (grassland)
= 10 (bare ground)

The mean annual precipitation (*P*) used is based on a 100m grid provided by Land Environment New Zealand (LENZ). The rainfall factor *R* multiplier was investigated by the NZeem authors who cite previous New Zealand studies that define *R* as ranging from:

$R(x,y) = P^{1.7} \leftrightarrow P^{2.3}$

Both ranges were tested by the NZeem authors and it was found that there was very little difference in accuracy, so a value of $R(x,y) = P^{2.0}$ was used.

On a national scale, the sediment delivery ratio *D* is defined as 1. On a regional scale, D for each pixel is defined by an algorithm that determines if each erosion terrain pixel is linked to the stream network, and the values are assigned:

D(x,y) = 1 if (*x,y*) is connected to the stream network
= 0 if (*x,y*) is disconnected from the stream network

The sediment yield $\overline{s_i}$ in kg s^{-1} m^{-2} for each erosion terrain was derived from the national estimate produced by the SYE model as described in Section 9.2 above.

Figure 9.1 is a conceptual diagram of the model showing the three input functions into the susceptibility model (slope, landcover, and rock type) which identifies land susceptible to landsliding. This is land that has no woody vegetation protecting the surface; if woody vegetation is present the land is classified ‘not at risk.’ Land susceptible to landsliding is also identified as land that is above a

certain slope threshold. The threshold values vary depending on the land type; for example 'weak to very weak Tertiary-aged mudstone' has a threshold value of 26° (Dymond *et al.* 2008). All 'high risk' pixels were then examined to see if they can deliver sediment to streams ('sediment delivery model' Figure 9.1), using an algorithm to see if two consecutive pixels of low slope (< 5°) were encountered before the drainage line. The algorithm then produced five classes of highly erodible land from which the erosion rate was calculated:

- High landslide risk – deliver to streams
- High landslide risk – non-delivery to streams
- Moderate earthflow risk
- Severe earthflow risk
- Gully risk

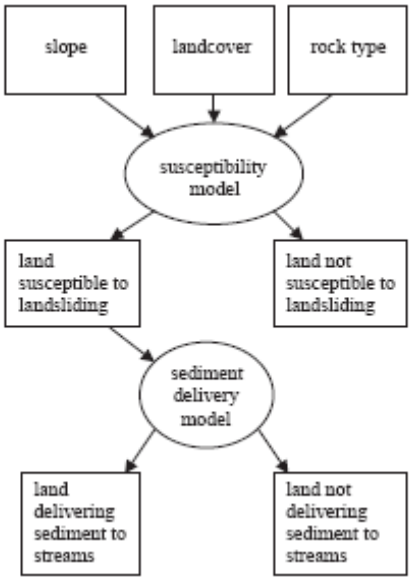

Figure 9.1. A conceptual model of NZeem showing the three determinants of the susceptibility component, the classification of landslide susceptible land, and the sediment delivery component that determines if sediment will be delivered to streams (Dymond *et al.* 2006).

The output file is a digital map with 15 m pixel resolution giving erosion rates as a continuous variable. The version supplied to Environment Waikato does not have the same spatial resolution and calculates erosion values on subcatchment units.

Recent versions of NZeem used a Sednet component (Prosser *et al.* 2001a) for in-stream sediment modelling, but this was not available on the NZeem version used in this study.

9.3.2 Method

The NZeem used for this study was run by Environment Waikato's (EW) Spatial Analyst Officer Dan Borman. Catchment boundaries were supplied as shapefiles by the author and the model was run on the 2002 landuse classification for the Whangapoua catchment. New aerial photographs (2007) were available and areas of landuse change were digitised and included in a second run of the model (Figure 9.2). The landuse change that had occurred between 2002 and 2007 was that areas of exotic forest had been harvested (woody to non-woody) and areas of harvested exotic forest where the trees had been replanted and were around five years old (non-woody to woody). The NZeem uses a landcover factor *C* that is 1 for woody cover and 10 for non-woody. In other words, the model inherently defines erosion from non-forested land as an order of magnitude higher than forested land for the landcover component.

9.4 Results

9.4.1 Sediment yield estimator (SYE)

The results for the SYE are provided for both the whole of the Whangapoua catchment and for the native forest, exotic forest, and agricultural landscape units (Table 9-1).

Table 9-1. Sediment yield results for the SYE model for the Whangapoua Harbour catchment in total and for the native, exotic, and agricultural landscape units as total yields and average yields.

Landscape units	**Average yield (t km^{-2} y^{-1})**	Total yield (t y^{-1})
Native forest	**67.79**	1319.88
Exotic forest	**59.03**	3274.39
Agriculture	**58.34**	773.59
Whangapoua	**60.86**	5367.86

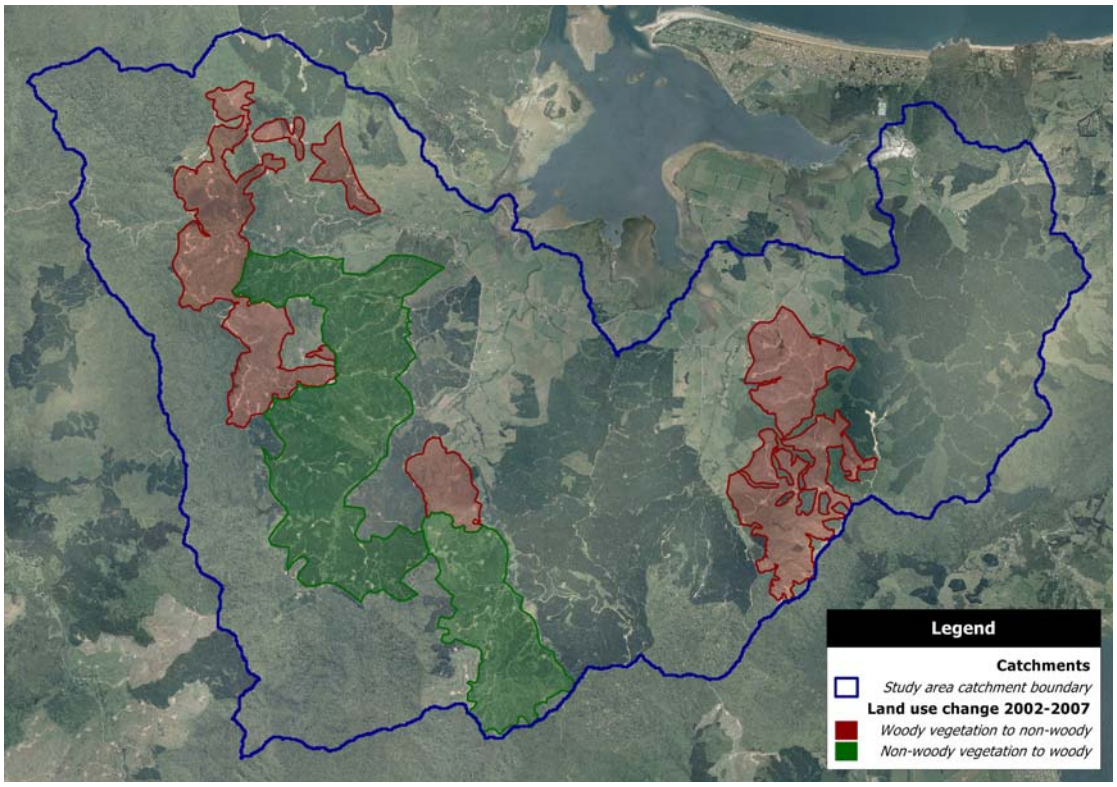

Figure 9.2. The Whangapoua Harbour catchment showing the changes in landuse scenario between 2002 and 2007 with the harvesting of exotic forest (woody to non-woody) and the classification of five year old pines as 'woody' vegetation.

The results for the SYE model show the average yield for the Whangapoua catchment is 61 t km^{-2} y^{-1} and approximately 5,400 tonnes of sediment to the estuary per year. The greatest sediment yield is from the native forest (68 t km^{-2} y^{-1}), followed by exotic forest at 59 t km^{-2} y^{-1} and agriculture at 58 t km^{-2} y^{-1}. The exotic forest and agricultural yields were similar and there is not much difference between all three landscape units.

The patterns of average yield (t km^{-2} y^{-1}) for the catchment (Figure 9.3) show that the native forest areas (shown in the inset as dark green) have areas yielding the lowest rates (most areas between the 10-30 t km^{-2} y^{-1}), and one of the highest rates of 90-100 t km^{-2} y^{-1}. The high yielding area identified by the model was on the western margin of the catchment, which results in a large portion of the sediment yield being derived from the native forest landscape unit. The band of exotic

forest (light green in the inset) has mid-range sediment yield values of 40-50 t km^{-2} y^{-1} (as indicated by the yellow areas in the north and east), but then increases up to the 60-70 t km^{-2} y^{-1} (dark brown areas) in the south of the catchment. The higher sediment yield in the south reflects the increase in slope values that were detected by the model. A large proportion of the agricultural areas (dark brown on the inset) have upper ranges of sediment yield values > 60 t km^{-2} y^{-1}, except for some areas along the western-most finger of land butting into the exotic forest in which the model predicted yields of 20-40 t km^{-2} y^{-1} t. The areas identified as relatively high yielding are on low slopes with no forest cover on alluvial soils.

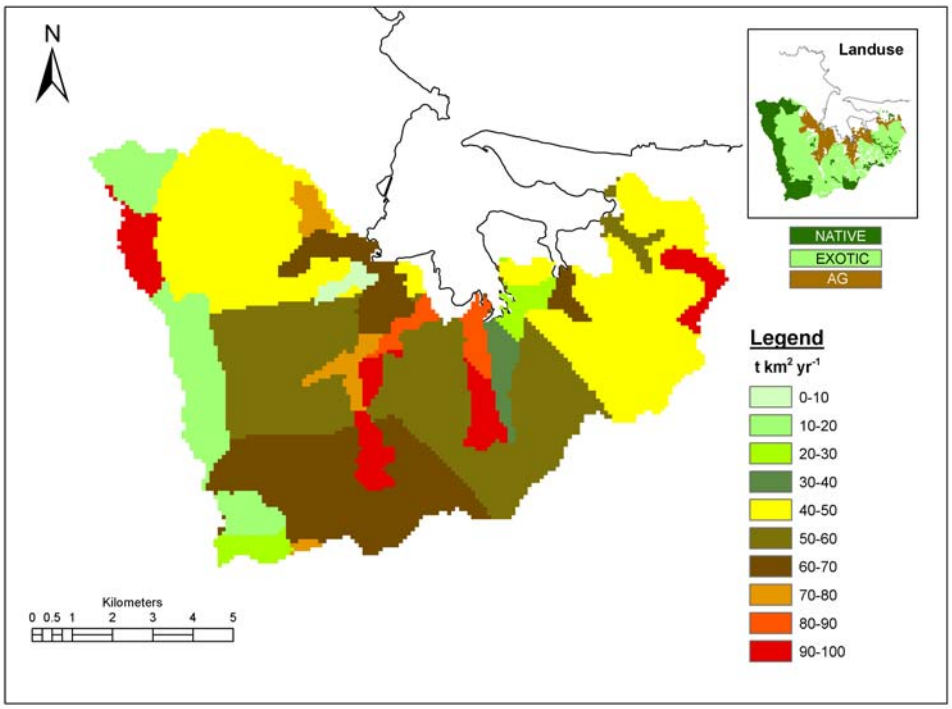

Figure 9.3. Results of the SYE model for Whangapoua Harbour catchment showing average yields in t km^{-2} y^{-1}. Inset shows the landuse pattern in the catchment for native forest (dark green), exotic forest (light green), and agriculture (brown).

9.4.2 NZeem

The NZeem model focuses on land cover as either woody or non-woody. Thus the model did not differentiate between woody native or exotic forest landcover, nor between non-woody agricultural pasture and recently harvested exotic pines. The model was run for the Whangapoua catchment as a whole. Two model scenarios

were run to look at the landcover change between 2002 and 2007 as a result of exotic pine harvesting and the classification of five year old pines as 'woody' (Table 9-2).

Table 9-2. Sediment yield results for the NZeem for the Whangapoua Harbour catchment in total for the 2002 and 2007 landuse scenarios.

Whangapoua Harbour	**Average yield (t km^{-2} y^{-1})**	Total yield (t y^{-1})
2002	**75.23**	7188
2007	**80.34**	7676

The 2002 pattern of sediment yield in the Whangapoua catchment (Figure 9.4 top) shows the lower values based around the native forest on the upper slopes and mature exotic forest. The darker green areas indicating higher yielding areas correspond to harvested exotic pines and agricultural pastoral areas. The landcover changes in the 2007 scenario (Figure 9.4 bottom) show a larger area of lower sediment yield because of the maturing pines in the south west corner of the catchment. The conversion of woody to non-woody vegetation led to higher sediment yielding (dark green/yellow) areas in the east and north of the catchment, and the appearance of a high yielding area (105-1100 t km^{-2} y^{-1}) in the northern area where slopes are steeper. The increase in higher yielding areas from 2002 to 2007, as a result of changes from mature to harvested pine forest, contributes to the increase in the estimated total yield from 7188 t km^{-2} y^{-1} to 7676 t km^{-2} y^{-1}.

9.5 Discussion

The two models provide information on the predicted pattern of sediment yield within the Whangapoua catchment based on the assumptions of each model. Both models identify the native forest landuse as low sediment yielding areas, except for a small area in the western section of the catchment in the SYE output. Both models identify agricultural areas as relatively high areas of erosion located in a band around the estuary. Both models also identify the exotic pine as areas of high sediment yield with the NZeem model more sensitive to picking up the harvesting schedule in the areas of exotic forestry.

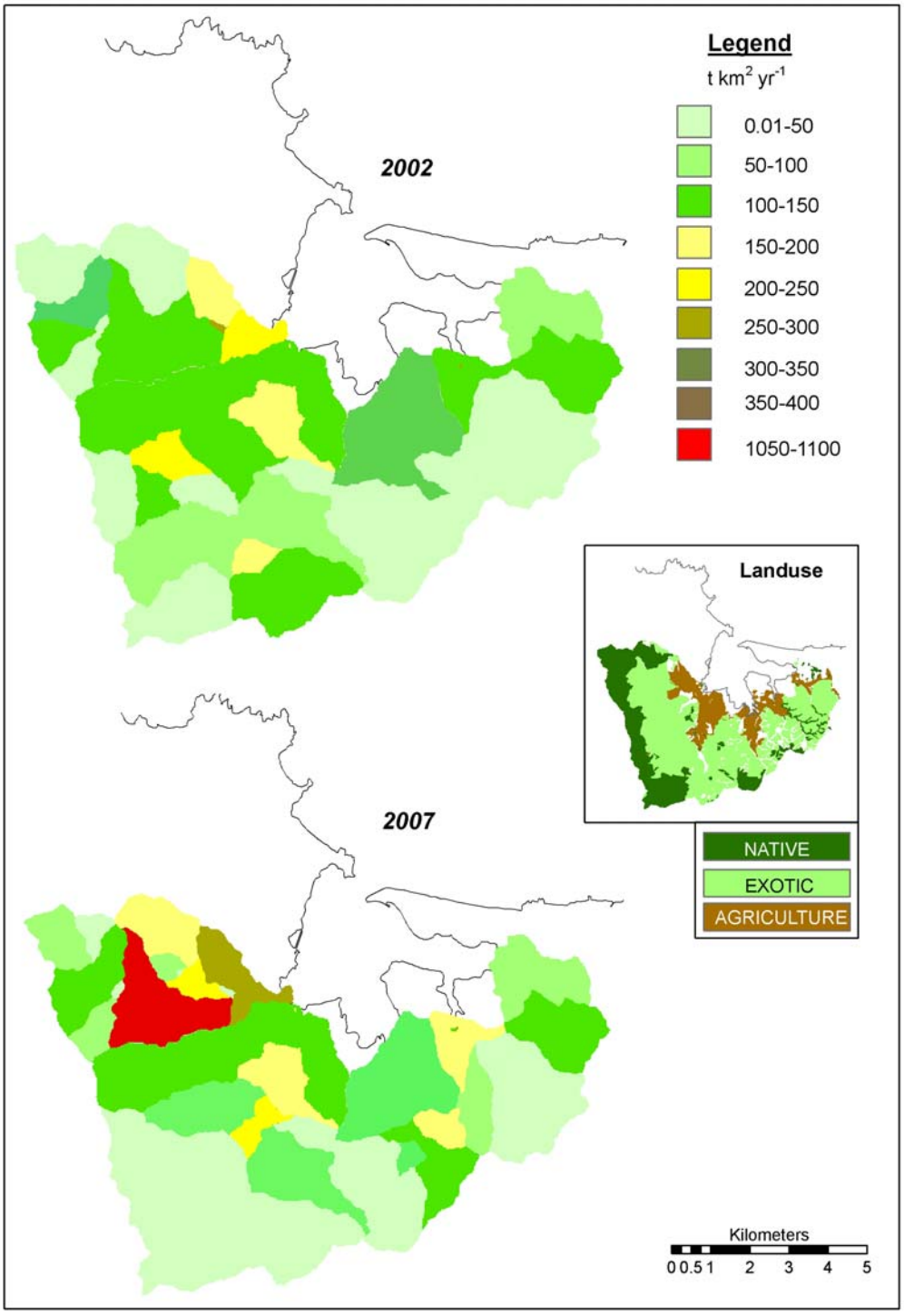

Figure 9.4. NZEEM model results for the Whangapoua catchment based on 2002 landuse scenario (top) and the 2007 landuse scenario (bottom). Inset shows the landuse pattern in the catchment for native forest (dark green), exotic forest (light green), and agriculture (brown).

The NZeem estimates of average and total yield are about 25% higher than that of the SYE model (Table 9-3). The NZeem's 2002 result was used in the comparison with the SYE model in Table 9-3 as the 2002 landuse data was closer to that used by the SYE model. A possible cause of the difference between the two models may be some of the assumptions used in the NZeem, which has been found to overestimate erosion in the Manawatu-Wanganui region (Dymond *et al.* 2006). The overestimation was considered to be caused by the model using a 30° slope threshold to identify highly erodible areas where susceptibility to landslides was rated 'high' if above 30° and 'low' if below 30°. The slope/landsliding relationship was linear and more complex than the NZeem model assumption of a high and low threshold.

Table 9-3. Mean and total sediment yield results for the SYE and NZeem for the Whangapoua catchment.

Whangapoua Harbour	**Average yield (t km^{-2} y^{-1})**	Total yield (t y^{-1})
SYE	**60.86**	5368
NZeem (2002)	**75.23**	7188

The average yield results of the two models were compared with the Environment Waikato SedRate software that incorporates five year monitoring of flow and turbidity of the Opitonui River which is one of the five subcatchments draining into the Whangapoua estuary (Jones 2008). The monitoring station was located on the Opitonui River where it was predominately recording the sediment delivered from exotic pine areas with some areas of pasture on low slopes and native forest on steep slopes. The SedRate gave a mean yield of 140 t km^{-2} y^{-1} with 4000 tonnes of sediment per year delivered to the estuary from the Opitonui subcatchment alone. It may be that both the SYE and NZeem models are underestimating Whangapoua catchment erosion. The underestimation could be because of the assumptions of both models that significant amounts of sediment cannot be generated from areas under wooded forests such as the native forest areas on steep slopes in the Whangapoua catchment.

9.6 Summary

Whangapoua catchment erosion was estimated using two models; the Sediment Yield Estimator (SYE) and the New Zealand empirical erosion model (NZeem). The SYE is a GIS raster based coverage of New Zealand based on rainfall and erosion terrain and was calibrated from over 200 gauging stations around New Zealand. The NZeem is based on landcover, rainfall, and an erosion coefficient for each *x*,*y* pixel, as the three main drivers of erosion.

The SYE model suggested that the most erodible landuse was the native forest at 68 t km^{-2} y^{-1}, followed by exotic forest at 59 t km^{-2} y^{-1}, and agriculture at 58 t km^{-2} y^{-1}. The total sediment delivery to the Whangapoua estuary was 5,368 t y^{-1}. The NZeem outputs were not available for each landuse, but the sediment delivery to the estuary was estimated at 7188 t y^{-1} for 2002 and 7676 t y^{-1} for the 2007 period. The areas of high sediment yield identified by both models were centred on agricultural areas on sloping land, recently harvested exotic forests and a patch of native forest on steep land in the north west of the catchment.

The total catchment yield estimated by the two models (5368 to 7676 t y^{-1}) was under the SedRate estimate of around 4000 t y^{-1} from one subcatchment alone. This would indicate that the two models might be underestimating catchment sediment yield based on assumptions that areas under wooded forests are not major sediment source areas.

CHAPTER TEN

STREAM SEDIMENT STORAGE

10.1 Introduction

Fine sediment may be transported through a river system either as one event or as a series of deposition and resuspension events where the channel bed acts as a temporary storage. Ignoring in-channel process will result in the inaccurate estimation of suspended sediment (Gao 2008). Of more importance to this thesis is estimating how much sediment is stored with the Whangapoua catchments streams as the sediment fingerprinting results indicate that the native forests in the headwater areas are the main sediment source area. The sediment fingerprinting result would indicate that fine sediment is efficiently conveyed from the headwater areas through the stream network to the Whangapoua estuary. If large amounts of fine sediment are stored within the streams, this would indicate inefficient sediment delivery and be inconsistent with the sediment fingerprinting result. Thus the aim of this chapter was to estimate the amount of fine sediment stored in the Whangapoua catchment streams.

10.2 Method

The method used to estimate stream fine sediment storage follows that of Lambert & Walling (1988) and Walling *et al.* (2006). A 200 litre cylindrical drum was cut so a double open ended straight section of a known area (0.221 m^2) was formed. The cylinder was carefully pushed into the stream bed to make a seal and then the upper 5cm of the bed was agitated using a plastic raking device (Figure 10.1). A 1L sampling bottle was dipped into the agitated water to collect the suspended sediment, and then returned to the laboratory where the sediment concentration (g m^{-3}) was determined gravimetrically by vacuum filtration suspended solid analysis.

Figure 10.1. Sampling drum used for stream sediment storage estimation.

Suspended solids analysis was carried out by filtering the water samples using a Buchner Funnel and vacuum filtration unit following the methods of the (American Public Health Association and American Water Works Association and Water Environment Federation 1992).

- Advantec Glass Fibre GC-50 70 mm filter papers were prewashed using 150 ml of deionised water and dried overnight at 105ºC. The filter papers were cooled to room temperature in a desiccator and weighed.

- A filter paper was placed on the Buchner funnel. Sample bottles were pre-shaken to ensure thorough mixing of the contents. The stream sediment samples were placed into volumetric measuring cylinders and poured onto the filter paper. The exact amount of sample used depended on how 'thick' (or concentrated) the sample was, so only enough sample was used to cover approximately 50% of the paper and this was judged by eye when pouring the sample. The amount of sample (L) used was determined from the before/after readings on the volumetric cylinder.

- The filter papers were oven dried at 105ºC overnight and then allowed to cool to room temperature in a desiccator and then weighed. The suspended solid concentration (g L^{-1}) was determined by the formula:

$$SS = \frac{W_{ss} - W_{pw}}{l_s} \qquad \text{(Eqn 10.1)}$$

Where:
SS = suspended solids
W_{ss} = weight of the dried filter paper plus suspended solids (in grams)
W_{pw} = weight of the pre-washed filter paper (in grams)
l_s = litres of sample

The amount of sediment yielded per unit area of stream (g m^{-2}) was estimated by multiplying the sediment concentration (g L^{-1}) and the volume of water contained in the drum (m^3, the product of the mean depth and cross sectional area), divided by the area of stream bed enclosed by the drum (m^2). Samples were collected from two points in the stream; the thalweg (deepest part of the stream) where it was assumed that sediment storage will be the lowest; and close to the river bank where it was assumed to be the highest (Walling *et al.* 2006). The mean of the

thalweg and stream edge samples was considered representative of the surrounding reach.

The sampling sites were located at the lower confluence of each landuse in the Waitekuri, Waingaro, and Opitonui catchments (Figure 10.2). These catchments were selected as they have the largest areas of native, exotic and agricultural landuses. Within the native forest landuse, two sites were used to estimate the sediment storage at a 'high' elevation and one site at a 'low' elevation. The high and low elevation sites were used to differentiate the difference between streams in the steep headwater areas of the native forests and the lower gradient streams toward the bottom of the native forest areas.

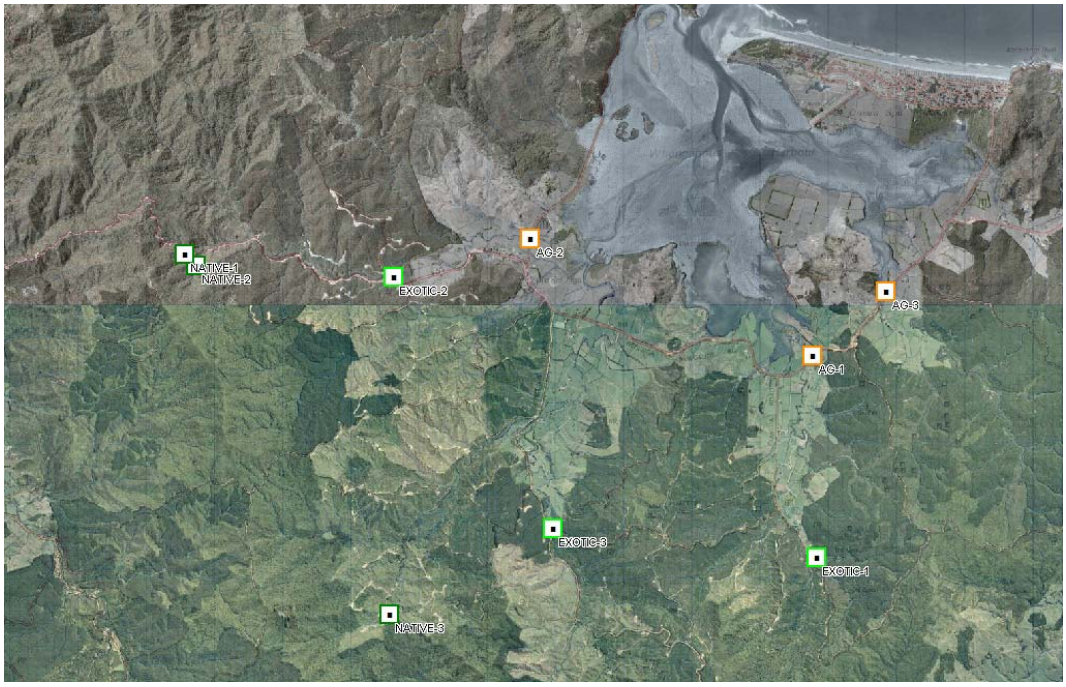

Figure 10.2. Stream sampling sites for the native forest (dark green), exotic forest (light green), and agricultural (orange) landscape units.

10.3 Results

The results (Figure 10.3 and Appendix X) show that sediment storage increases from the upper to lower catchment. Very low levels of sediment are found in the steep headwater (upper) native forest catchment (mean 26.6 g m^{-2}). The lower native forest streams (mean 75.2 g m^{-2}) had individual sediment storage observations within the range of exotic forest values. The highest values are for

the lower energy streams in the agricultural landuse (mean 446.1 g m^{-2}) which includes one particularly large observation of 1144 g m^{-2}.

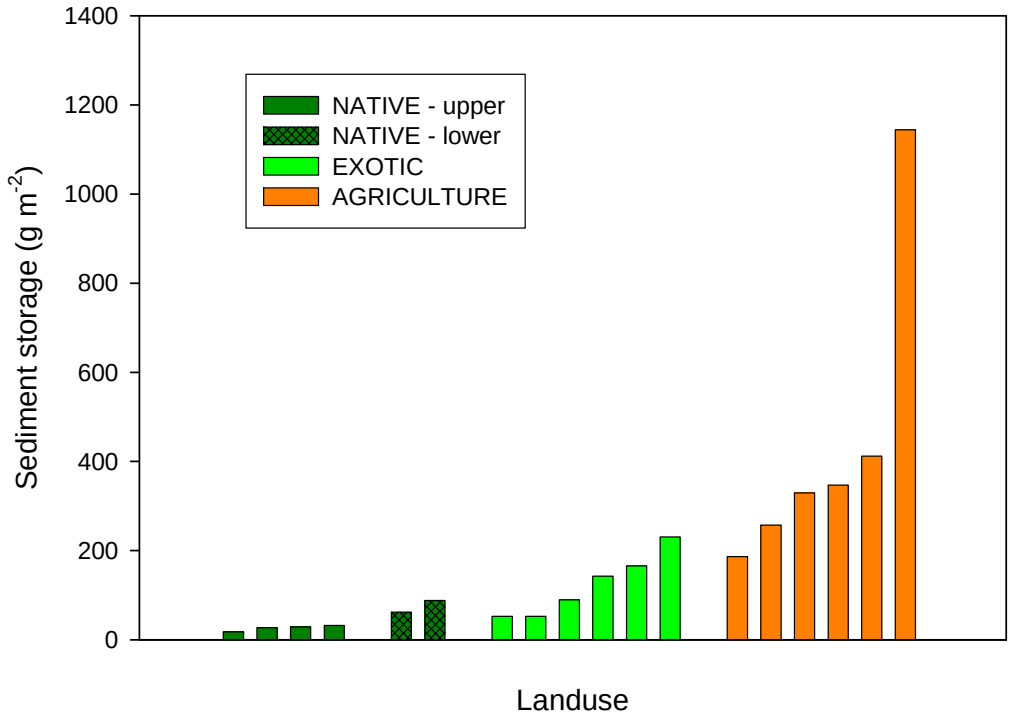

Figure 10.3. Stream sediment storage results (g m^{-2}) for the native forest (upper and lower), exotic forest, and agricultural landscape units.

The mean sediment storage values (g m^{-2}) for streams within each landuse were then used to calculate the in-stream sediment storage within each landuse. The stream length within each landuse was determined from GIS data and stream widths were estimated based on field observations (Table 10-1).

Table 10-1. Stream fine sediment storage for the native forest, exotic forest, and agricultural landscape units.

Landuse	Sediment storage ($\overline{X}$ g m^{-2})	Stream length (m)	Stream width (m)	Total sediment (t)
Native (upper)	$26.6_{6.1*}$	20950	2	$1.12_{0.25}$
Native (lower)	$75.2_{18.9}$	26440	4	7.95_{2}
Exotic	$122.4_{70.4}$	104950	4	$51.4_{29.56}$
Agriculture	$446.1_{350.6}$	32910	5	$73.4_{57.7}$
TOTAL				$133.86_{64.85}$

* Subscripts are one standard deviation

10.4 Discussion

The stream sediment storage results can be viewed in two ways; as a percentage of the total sediment budget and as concentrations per unit area of stream bed. If the Sediment Yield Estimator (SYE) figure of 5368 t yr^{-1} of sediment (Chapter 9) being delivered to the estuary is assumed to be correct, than the stream sediment storage value of 133.86 t ± 64.85 t is a very small percentage (< 4%) of the annual sediment load. Studies of the Tern and Pang/Lambourn lowland catchments in the UK found stream sediment storage values to range from as low as 21% to as high as 149% (Collins & Walling 2007b). Another study of Dorset lowland catchments found the stream storage ranges between 18% and 57% of the total annual budget (Collins & Walling 2007a). The UK river systems studied were lower energy, wider channels draining larger catchments than the Whangapoua. The Whangapoua stream storage results indicate that the catchment is a high energy, efficient deliverer of sediment from the landuse areas to the estuary.

The other method of comparison is to examine the sediment concentrations per unit area of stream bed. The Whangapoua mean values ranged from 26.6 g m^{-2} in the upper native forest to 446.1 g m^{-2} in the agricultural landscape unit. Values from the lowland Pang and Lambourn catchments in the UK ranged from 770 to 2290 g m^{-2} (Walling *et al.* 2006). The Dorset (UK) rivers ranged from 260 to 4340 g m^{-2} (Collins & Walling 2007a), the River Severn (UK) ranged between 630 to 8000 g m^{-2} (Walling & Quine 1993), and river sediment storage from Ontario Canada had ranged from 660 to 2200 g m^{-2} (Droppo & Stone 1994). Again, the UK and Canadian comparisons probably reflect the lower energy of the river systems that allows in-stream sediment storage, but the comparison supports the view that the Whangapoua catchment is an effective transporter of sediment through the river system and out into the estuary. The efficient delivery of sediment has also been observed by other authors who state that the implication for small basins with stream lengths of < 10 km is that the lack of stream storage will mean the effective delivery of sediment to the stream mouth (Bonniwell *et al.* 1999).

The Whangapoua stream sediment storage results should be viewed in the context of the sample size and the lack of replication. The results were based on a study

where n = 18 and more extensive sampling would no doubt increase the reliability of the estimate. While the stream lengths in the catchment were reliably estimated using ArcGIS, the stream widths were estimated from field observations which are another potential source of error.

The sampling was conducted over two days in autumn and was not replicated at other times of the year. Sediment transmission from reach to reach is susceptible to both natural and human induced environmental change and can change quickly (Harvey 2002). For example, Walling & Amos (1999) found that in a Dorset river (UK), sediment accumulated on upper and middle reaches during winter, and was then slowly moved as a slug during the summer months. Consequently seasonal sampling may be necessary to characterise the Whangapoua catchment more accurately.

10.5 Summary

A stream bed sampling method (Lambert & Walling 1988) was used to estimate the amount of sediment that is stored in the channels of the Whangapoua catchment. A total of 18 samples were taken to characterise the stream sediment storage within the native forest, exotic forest, and agricultural landscape units.

The results showed an increase in sediment stored within the channel down-catchment. The streams of the upper native forest stored 26.6 g m^{-2} and those of the lower native forest stored 75.2 g m^{-2}. The streams of the exotic forest and agricultural areas were estimated to be storing 122.4 g m^{-2} and 446.1 g m^{-2} respectively. The mass of sediment stored within the streams of the entire catchment was estimated as 133.86 ± 64.85 t, or less than 4% of the annual sediment yield as estimated by the Sediment Yield Estimator (5368 t yr^{-1}). Such figures are low when compared with other studies. However, the only studies available for comparison were conducted in lower energy environments in larger catchments. The in channel estimate of sediment indicates that the streams of the Whangapoua catchment are high energy environments which efficiently convey sediment through the drainage system to the estuary.

CHAPTER ELEVEN

DISCUSSION AND CONCLUSIONS

11.1 Introduction

This chapter reviews the results of the sediment fingerprinting technique and the three comparative techniques (radionuclides, stream monitoring, and modelling). The sediment fingerprinting results are then used to explain catchment function and implications for land managers are discussed.

11.2 Overview of key findings

The aims of this thesis were to quantify the amounts of sediment generated from the native forest, exotic forest, and agricultural landscape units in the Whangapoua catchment; identify the main processes generating the sediment; and assess the usefulness of sediment fingerprinting for application in the New Zealand environment.

A pilot study was conducted as the sediment fingerprinting technique had not been applied before in New Zealand. The pilot study tested the null hypotheses that the sediment fingerprinting technique could not distinguish between the three landscape units (native forest, exotic forest, and agriculture) in the Whangapoua Harbour catchment, nor that it could distinguish between the three erosion positions (surface, subsurface, and streambank erosion) that had been identified as potential sediment sources in the catchment (Chapter 2). The pilot study showed that sediment fingerprinting could distinguish between the landuses and the sediment positions, thus the null hypotheses were rejected. The relative contribution of sediment to the estuary by landscape unit determined in the pilot study was 40% from native forest, 33% from exotic forests, and 27% from agriculture. The relative contribution by erosion position was 10% from surface sources, 62% from subsurface sources, and 28% from streambank sources (Table 5-4). It was observed that the sediment fingerprinting statistical verification method did not optimise the number of geochemical elements identified by the Kruskall-Wallis H-test by discriminant function analysis (DFA). A resampling

method (Jackbooting) identified that there was a hierarchy of importance of geochemical elements and that the default *F-to-enter* score of one in the DFA process was too low. An *F-to-enter* score of three provided a better optimisation of elements in the DFA process and meant that only geochemical elements that were statistically were used in the mixing model.

A full sediment fingerprinting programme was conducted in the Whangapoua catchment (Chapter 6) and showed that the native forest landscape unit was the main sediment contributor to the estuary (62% ± 17%) followed by exotic forests (23% ± 12%) and then agriculture (15% ± 1%) (Table 6-7). The results for 'process' was that the majority of sediment was derived from subsurface sources (79% ± 6%) followed by streambanks (13% ± 5%) and then surface sources (8% ± 6%) (Table 6-7).

Radionuclide sediment tracing (Chapter 7) using ^{137}Cs tracer indicated that the majority of sediment delivered to the estuary (>90%) was derived from 'all subsurface' (> 20cm depth plus streambanks) sources (Section 7.4.2). ^{137}Cs was the only radionuclide tracer that could be used in this thesis as the results indicated that $^{210}Pb_{ex}$ was enriched after deposition in the estuary and ^{226}Ra was mobile after deposition in the estuary.

Suspended sediment monitoring in streams (Chapter 8) undertaken using the storm sediment yield technique, showed that the highest erosion rate was in the recently harvested exotic pines (48 t km^{-2} yr^{-1}), followed by the six month post harvest pine (28 t km^{-2} yr^{-1}), then agricultural pastures (7 t km^{-2} yr^{-1}) and the lowest erosion rate was the 10 year re-growth exotic pine (2 t km^{-2} yr^{-1}) (Table 8-3). The erosion rates for the exotic pine and agricultural landuses were within the ranges reported in the New Zealand literature, but at the lower end. There were significant sources of error encountered in estimating erosion rates (Section 8.5.6) and the results are best used for explanation rather than extrapolation.

The Sediment Yield Estimator (SYE) and the New Zealand Empirical Erosion Model (NZeem) were used to identify erosion pattern within the Whangapoua

catchment (Chapter 9). For the SYE there was little difference in the mean sediment yield values for the native, exotic, and agricultural landscape units (58-68 t km^{-2} yr^{-1}) and the NZeem estimated the mean sediment yield for the Whangapoua catchment at 75 t km^{-2} yr^{-1}. The SYE total catchment sediment yield was 5368 t yr^{-1} (Table 9-1) and 7188 t yr^{-1} as determined by the NZeem (Table 9-2).

An estimation was made on how much sediment was stored in the Whangapoua catchment's stream beds (Chapter 10). Samples were taken from the native forest, exotic forest, and agricultural streams and the results showed that there was an increasing trend of storage down catchment. Less than 4% of the Whangapoua catchment sediment budget (as estimated by the Sediment Yield Estimator) was stored in the stream beds (Table 10-1). The 4% value and the ranges of stream bed sediment concentration were low when compared to overseas literature.

11.3 Sediment fingerprinting comparisons

11.3.1 Comparison between sediment fingerprinting results and pilot study results

The sediment fingerprinting pilot study (Waitekuri River subcatchment) gave similar results to the full programme (Whangapoua catchment) in that the native forest landscape unit was identified as the dominant sediment source, as was subsurface erosion positions (Figure 11.1).

There are several possible explanations for the differences between the pilot study and full programme results. At the time of the pilot study, almost all of the exotic forest had been recently harvested in the Waitekuri subcatchment. The harvested exotic forest area may have increased its relative sediment contribution. The sink sample was collected in the pilot study using a sediment trap placed in the lower reach of the Waitekuri River above the tidal influence that ensured the material was contemporary, whereas in the full programme samples were obtained from the estuary bottom. The pilot study results may reflect the relative contributions of the subcatchment at that particular time, whereas the full programme may be representing a more time averaged effect from the three landscape units. The differences may also be a result of the different size fractions and analytical

A) **Pilot study – landscape unit** B) **Pilot study - position**

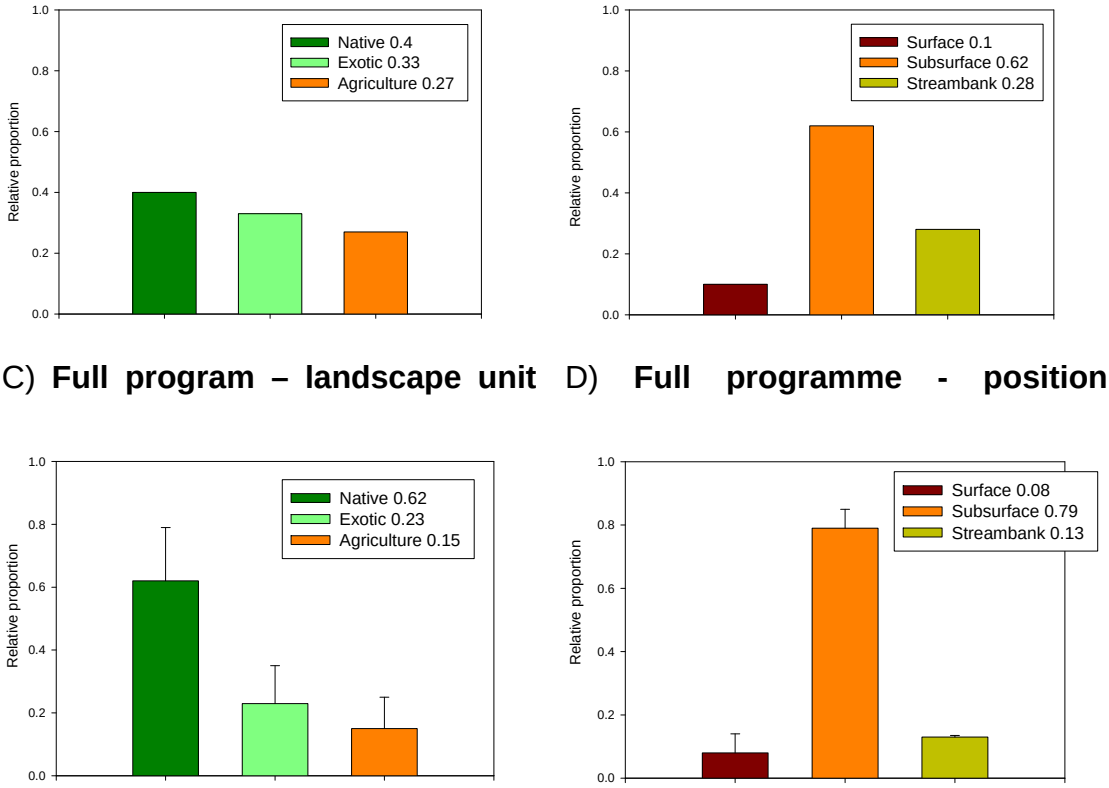

C) **Full program – landscape unit** D) **Full programme - position**

Figure 11.1. Sediment fingerprinting results from the Waitekuri River subcatchment pilot study (top row) and the full Whangapoua catchment (bottom row). A) Pilot study relative contribution of sediment by landscape unit; B) pilot study relative contribution of sediment by position; C) full programme relative contribution of sediment by landuse; D) full programme relative contribution of sediment by position. Error bars are one standard deviation of the mean.

techniques used between the pilot and full programmes, although recent work would suggest that the < 10 μm fraction is comparable with the < 63 μm in terms of relative contribution results (Fu *et al.* 2008). The last possibility for the difference could be the statistical treatment of the data and the data itself. The pilot study only had nine samples per landuse and the mixing model was run for one iteration to arrive at the final result. The full programme had 50 samples per landuse and the mixing model was run for 100 iterations to arrive at proportions that were then used as the inputs for a 5000 iteration run. It may be that the full programme results are more accurate than the pilot study results.

If the sediment fingerprinting technique is measuring a random variation of geochemical properties in different parts of the landscape, then the results of two studies should also show random variability and not be comparable at all. The fact that both studies have identified consistent trends of major relative contributions from native forests and from subsurface sources lends weight that the sediment fingerprinting technique is statistically verifying tracer properties that are then tracing a 'real' effect.

11.3.2 Comparison between sediment fingerprinting results and radionuclide results

The radionuclide results support the findings from sediment fingerprinting. Sediment fingerprinting determined the relative contribution to estuary sediment was 79% for subsurface (> 20 cm) and that 13% from streambanks for a total of 92% from 'all subsurface' positions (Figure 11.2-A). Using only ^{137}Cs, a Students *t*-test found that catchment surface sources were significantly different from the estuary sink values, whereas 'all subsurface' sources were not significantly different from the sink (Figure 11.2-B). The upper limit calculation showed that only 2% of sediment was derived from surface sources, so 98% of estuary material was derived from 'all subsurface' position.

A

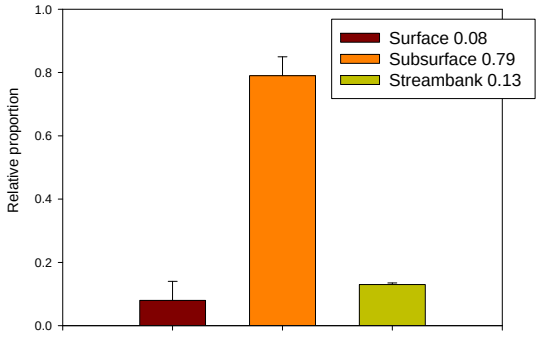

B

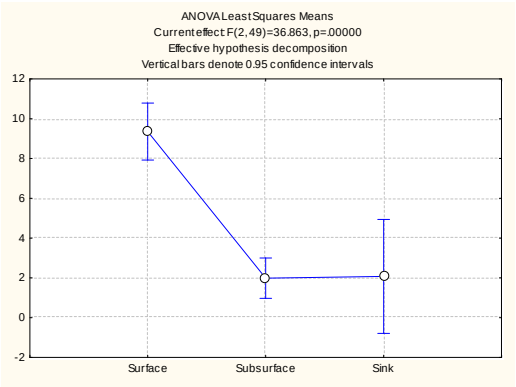

Figure 11.2. A) Sediment fingerprinting results for process compared against B) ^{137}Cs radionuclide ANOVA least squares results for process. Error bars are 95% confidence intervals.

Radionuclides were able to provide validating evidence for the sediment fingerprinting results in terms of erosion position, but could not validate the sediment fingerprinting results in terms of the landscape unit results. Radionuclides are radioactive isotopes that bind to soil particles in an almost non-exchangeable form and move about the landscape with sediment (Chapter 3). It would not be expected that ^{137}Cs would show the same influence of landuse as fertiliser derived elements (e.g., P, Ca) that was used by the sediment fingerprinting technique. It was not possible to distinguish between subsurface and streambank erosion positions with only ^{137}Cs due to its depth penetration characteristics, so the subsurface and streambank erosion positions were combined ('all subsurface'). The sediment fingerprinting surface and 'all subsurface' relative contribution estimates compare favourably with the radionuclide results. The use of ^{137}Cs as a soil tracer has been widely applied (> 4000 published uses) and is well understood. The radionuclide result provides strong evidence that the sediment fingerprinting technique is tracing a 'real' dynamic within the catchment.

Reports of subsurface dominance of erosion sources is not unusual. In a recent example Smith & Dragovich (2008) found that over 80% of catchment sediment contribution was from subsurface sources in a south-eastern Australian catchment as determined by $^{210}Pb_{ex}$ and ^{137}Cs.

11.3.3 Comparison between sediment fingerprinting results and suspended sediment monitoring results

Comparison of sediment fingerprinting results with suspended sediment monitoring results is difficult due to a lack of a native forest monitoring site and the precision of the result due to the errors involved. The main conclusion is that while exotic forest erosion rates were high during harvesting, they rapidly decline and 10 years post harvest are far below the levels for agricultural areas. Other studies in New Zealand also show a rapid decline of erosion rates after pine harvesting that can return to near pre-harvest rates within two to three years (Fahey & Marden 2000; Eyles & Fahey 2006; Marden *et al.* 2006).

The rapid decline of exotic forest erosion rates after tree harvesting is an important finding if the sediment fingerprinting results are to stand up. Exotic forests account for 61% of the land area within the catchment, but sediment fingerprinting estimates that it contributes 23% of the estuarine sediment. This would only be possible if exotic forests are viewed from a 30 year harvesting cycle that while post harvest erosion rates can be high, for most of the time, in most of the catchment, exotic forests contribute little sediment (Figure 8.22).

11.3.4 Comparison between sediment fingerprinting results and catchment modelling

The SYE model generally contradicts the sediment fingerprinting results. While the SYE identified the native forests landscape unit as having the highest mean erosion rate (68 t km^{-2} yr^{-1}), the total yield estimates showed that the exotic forest was the dominant sediment contributor at nearly 2.5 times that of native forest and over four times that of agriculture (Table 9-1) .

The NZeem results are also contradictory to the sediment fingerprinting results. The NZeem total catchment sediment yield was 7188 t yr^{-1} for the whole catchment. It was not possible to split the NZeem results by landuse as the SYE did, because the NZeem results are based on subcatchments. However, some inference of the relative erosion rates can be made by examining the mapped results for 2002 landuse (Figure 11.3). The higher erosion values (dark green and yellows) are clustered around the non-forested agricultural areas around the harbour and the recently logged exotic forests. The lower erosion values (light green) occur on the upper southern slopes under mature exotic forests and native forests. If the NZeem results corroborated the sediment fingerprinting results then the model output should have indicated high erosion rates in the steep upper slopes under native forest. Lower erosion rates should have been found in the exotic forests (reflecting the harvesting cycle) and agricultural areas (reflecting lower slope).

The discrepancy between the model results and the sediment fingerprinting results most likely lies within the assumptions made by each model, as the modellers attempt to simplify complex realities. The models have been developed for use on

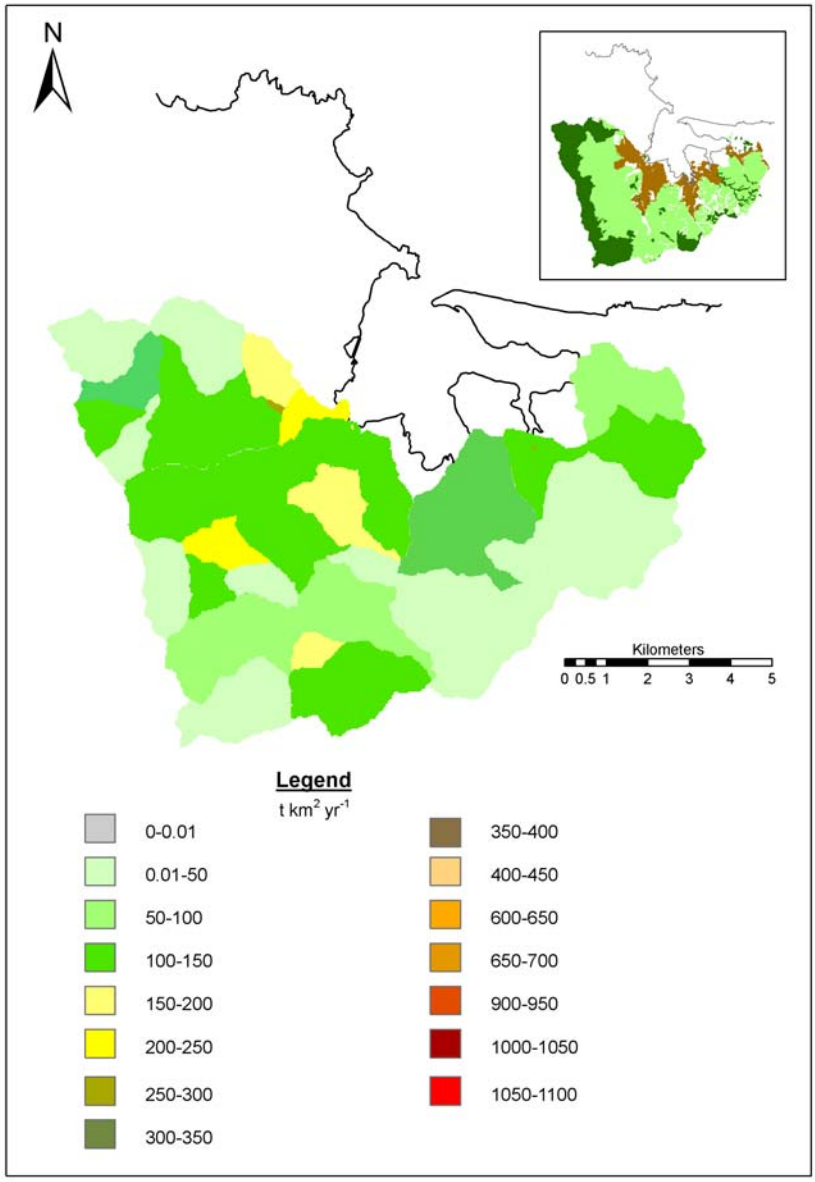

Figure 11.3. NZEEM results for the Whangapoua Harbour catchment for 2002 landuse scenario. Insert is Whangapoua landuse for native forest (dark green), exotic forest (light green), and agriculture (dark brown).

a national scale and have been calibrated with national scale river gauging data. The SYE model uses lithology and rainfall (raised to the power of 1.7) as the main drivers for erosion. The NZeem used lithology, landform (which includes slope angle) and rainfall (raised to the power of 2.0) as the main drivers. It also accounts for landuse which gives it a greater sensitivity at a regional/local scale. The NZeem uses a multiplier of 10 for everything not under woody vegetation and assumes that the land is not vulnerable to landsliding if under woody vegetation.

The assumptions used by the Sediment Yield Estimator and New Zealand Empirical Erosion Model are challenged by the sediment fingerprinting results. The Sediment Yield Estimator did show that the native forests had the highest erosion rate, but only by a small margin, compared to the exotic and agricultural landscape units. The SYE is a nationally based model that has used calibration from North and South Island river gauges, but the assumptions of the main drivers of erosion (rainfall and geology) means that it may not be applicable to estimate erosion at the Whangapoua catchment scale. The NZeem assumes that lands under woody vegetation (i.e., forests) are not as susceptible to landslides as grasslands by an order of magnitude and thus results in identifying harvested exotic forests and agriculture as the most important sediment source areas. The underlying model assumptions are challenged by the sediment fingerprinting findings at a catchment scale. The NZeem has been identified as the most promising method of estimating nationwide reductions in erosion based on landuse change (i.e., reforestation) for climate change mitigation (Blaschke *et al.* 2008). Improving the assumptions of the NZeem to better reflect forested erosion rates will improve the function of the model.

11.3.5 Comparison between sediment fingerprinting results and stream sediment storage results

Sampling of the Whangapoua streams was undertaken to estimate the amount of sediment stored within the catchment's drainage lines following the method of (Lambert & Walling 1988). The results showed the upper native forest had mean storage values of 26.6 g m^{-2} and lower native forest was 75.2 g m^{-2} and 122.4 g m^{-2} for exotic forests and 446.1 g m^{-2} for agriculture. The total stream sediment storage value of 133.86 ± 64.85 g m^{-2} was less than 4% of the total annual sediment budget of 5368 t yr^{-1}) as estimated by the Sediment Yield Estimator.

The results indicate that while sediment storage increases down catchment, very little sediment is stored within the stream lines. The small storage of sediment in the stream channels supports the Chapter 2 alternative hypothesis of the catchment and the sediment fingerprints results that native forests supply the bulk of the catchment's sediment from landsliding (or from subsurface positions) as the

sediment is efficiently delivered from well coupled (lateral) hillslopes to channel, and then through well coupled (longitudinal) stream channels to the estuary.

11.3.6 Comparison between sediment fingerprinting results and previous Whangapoua studies

There are two multiple landuse studies in the Whangapoua catchment, one by Marden & Rowan (1995) and the other by Gibbs (2006). The findings of (Marden & Rowan 1995) support the sediment fingerprinting results both in terms of landscape unit and erosion position sediment sources as described in Section 6.5.2 and Table 6-8. The findings of Gibbs (2006) contradict the sediment fingerprinting results (Table 6-8) as Gibbs (2006) identifies exotic forests as the main sediment contributor.

The compound specific isotope (CSI) technique used by Gibbs (2006) was a new technique that was tested in the Whangapoua catchment. Only the top 2 cm of soil was collected at 14 sites in the Whangapoua catchment source area to characterise native forest, native scrub, pasture, and exotic pine landscape units, while eight estuary sink samples were collected. It is possible that the CSI technique is a good indicator of surface erosion processes only as the CSIs concentrate in the surface soils and only the top 2 cm was sampled. If CSIs are mainly tracing surface erosion processes, then the CSI technique would be consistent with the sediment fingerprinting results. I conclude that most of the surface erosion in the catchment occurs in exotic forests due to harvest disturbance and would lead to the 54-75% exotic forest relative contribution estimation by Gibbs (2006).

11.3.7 Comparison between sediment fingerprinting results and mass balance approach

Another comparison is to use a mass balance approach. Assume the Sediment Yield Estimator (SYE) estimate of annual sediment delivery to Whangapoua Harbour of approximately 5000 t yr^{-1} is correct. Using the sediment fingerprinting relative contribution results for landscape units, a total sediment budget was calculated (t yr^{-1}) for each landscape unit (Table 11-1). Using the land area that each landscape unit occupies, an erosion rate (in t km^{-2} yr^{-1}) was calculated which resulted in an erosion rate for native forests of 147 t km^{-2} yr^{-1}, exotic forests at

19 t km^{-2} yr^{-1}, and agriculture at 42 t km^{-2} yr^{-1}. The stream monitoring results are shown in the last column in Table 11-1 as a comparison.

Table 11-1. Mass balance of fingerprinting results and suspended sediment monitoring results.

Landuse and relative contribution	Sediment (t yr^{-1})	Land area (km^2)	Erosion rate (t km^{-2} yr^{-1})	Monitoring results (t km^{-2} yr^{-1})
Agriculture (15%)	750	18	42	7
Exotic (23%)	1150	61	19	2 - 48
Native (62%)	3100	21	147	N/A

Firstly, the mass balance calculation normalises the sediment fingerprinting results for area occupied by each landscape unit showing the higher relative erosion rate of native forest compared to agriculture and exotic forest. The mass balance comparison does not normalise for the slope on which each landscape unit is found in the Whangapoua catchment.

Secondly, the mass balance comparison shows that if the sediment fingerprinting results and SYE estimate are correct, then the suspended sediment monitoring results (Chapter 8) is underestimating the actual erosion rates. The suspended sediment agricultural erosion estimate of 7 t km^{-2} yr^{-1} (Table 11-1) is lower than the mass balance estimate of 42 t km^{-2} yr^{-1}. If the mass balance estimate of exotic forest average erosion of 19 t km^{-2} yr^{-1} is correct, then this means that a 30 year harvest cycle sediment yield is 570 t km^{-2} yr^{-1}. Assuming a 100 t km^{-2} yr^{-1} erosion rate in the first and second year after harvest, this still results in an average erosion rate of 13 t km^{-2} yr^{-1} for the next 28 years which is higher than the 10 year post harvest erosion rate of 2 t km^{-2} yr^{-1}.

The mass balance calculation was also made for erosion position. Taking the sediment fingerprinting results (Table 11-2) for erosion position and SYE budget 5000 t estimate, annual tonnages can be assigned for the surface (400 t), subsurface (3950 t), and streambank (650 t).

Table 11-2. Mass balance of sediment fingerprinting results for erosion position.

Position and relative contribution	Sediment (t)
Surface (8%)	400
Subsurface (79%)	3950
Streambank (13%)	650

The alternative hypotheses of catchment erosion (Chapter 2) propose that most of the native forest erosion would be caused by landslides, most agricultural erosion because of stream banks, and exotic forest erosion would be a mix of surface erosion and landslides. Apportioning the position tonnages in Table 11-2 to the landscape unit tonnages in Table 11-1 using the alternative hypotheses assumptions means that all 3100 t of native forest erosion comes from landslides and all 650 t of agricultural erosion comes from streambanks. This leaves exotic forest erosion at 850 t from landslides, 400 t from surface, and 100 t from streambank erosion. The mass balance estimation of the mix of exotic forest erosion is similar to the results of Marden *et al.* (2006) in the Whangapoua exotic forest where they found approximately 70% of the delivered sediment was caused from landslides and around 30% was from surface sources.

The mass balance assumptions are open to criticism, but the exercise shows that the sediment fingerprinting results for landscape unit and erosion position are consistent with one another and fit in with field observations and the literature.

11.4 Catchment function

Three alternative hypotheses of catchment erosion were proposed in Chapter 2 based on the literature and field inspections. It was speculated that the majority of estuary sediment could be sourced from either landslides in native forest headwater areas; surface, streambank, and landslide erosion from mid-catchment exotic forest areas; or streambank erosion from lowland agricultural areas. The sediment fingerprinting results indicate that the steep headwater areas under native forest was the dominant sediment source generating sediment by landslide processes (Figure 11.4). It is evident that rainfall and slope were important factors in sediment generation in the Whangapoua catchment. It does not follow that

therefore landuse is not important, but that in the Whangapoua catchment rainfall and slope overcome the armouring effects of the native forest.

Figure 11.4. A cluster of landslides in the native forests in the steep upper slopes of the Whangapoua catchment from a 2002 aerial photo. A ridge top logging road and exotic forest areas are visible in the top left hand corner.

For a landslide to occur, the land surface must be mobilised. “Mobilisation requires failure of the mass, sufficient water to saturate the mass, and sufficient conversion of gravitational potential energy to internal kinetic energy” (Iverson 1997). In the native forest areas, the slopes are the steepest in the catchment and provide the potential gravitational energy. The steep headwater slopes ensure that the slopes are well coupled with the streams (lateral coupling), and Chapter 10 results indicate that sediment is effectively conveyed down to the estuary

(longitudinal coupling). The other important factor is rainfall to saturate the soil to cause an increase in pore pressure that will result in a failure. If rainfall is the important variable in causing landslides, then what type of rainfall?

Reviews of the literature (Chapter 3) cite New Zealand landslide studies that report landslide initiating thresholds of 120-150 mm of rainfall in East Coast soft rock rolling hill country. The damaging 1995 storm was between 150-200 mm (Marden & Rowan 1995). The two year rainfall record from Castle Rock (top of catchment) and Opitonui (lower catchment) show daily rainfall above 150 mm (low frequency/high magnitude) occurred at the top of the catchment twice yearly during 2006 and 2007 (Figure 11.5). To generate landslides in native forest areas (as the sediment fingerprinting indicates), high magnitude/low frequency events are required and the Environment Waikato analysis (Section 2.2.4) shows that the upper catchment may receive 1000 mm more rainfall than the lower catchment.

The low magnitude/high frequency events would be more important for the mid-slope exotic forest and lowland agricultural areas as the absence of steep slopes means that large amounts of sediment are not delivered to streams via landslides. Low magnitude/high frequency storm events would keep streambank erosion active in the exotic forest and agricultural landscape units as streambank erosion is an efficient deliverer of sediment to streams in the moderate and lowly coupled mid and low slope areas. Low magnitude/high frequency events would also remobilise sediment from surface erosion and smaller landslides in the exotic forest landscape unit.

This study has referred to the indigenous vegetation as ‘native forest’, but in fact these areas have been extensively logged in the late 1800s for kauri. A more correct term would be ‘regenerating native forests.’ As reviewed in Section 3.7.2.1, kauri grows on steeper slopes where landslide risk is moderate to high where this type of disturbance favours kauri succession. Kauri have the added competitive advantage in that they can delay disturbance events due to root reinforcement and tree weight to outcompete other species by their long life.

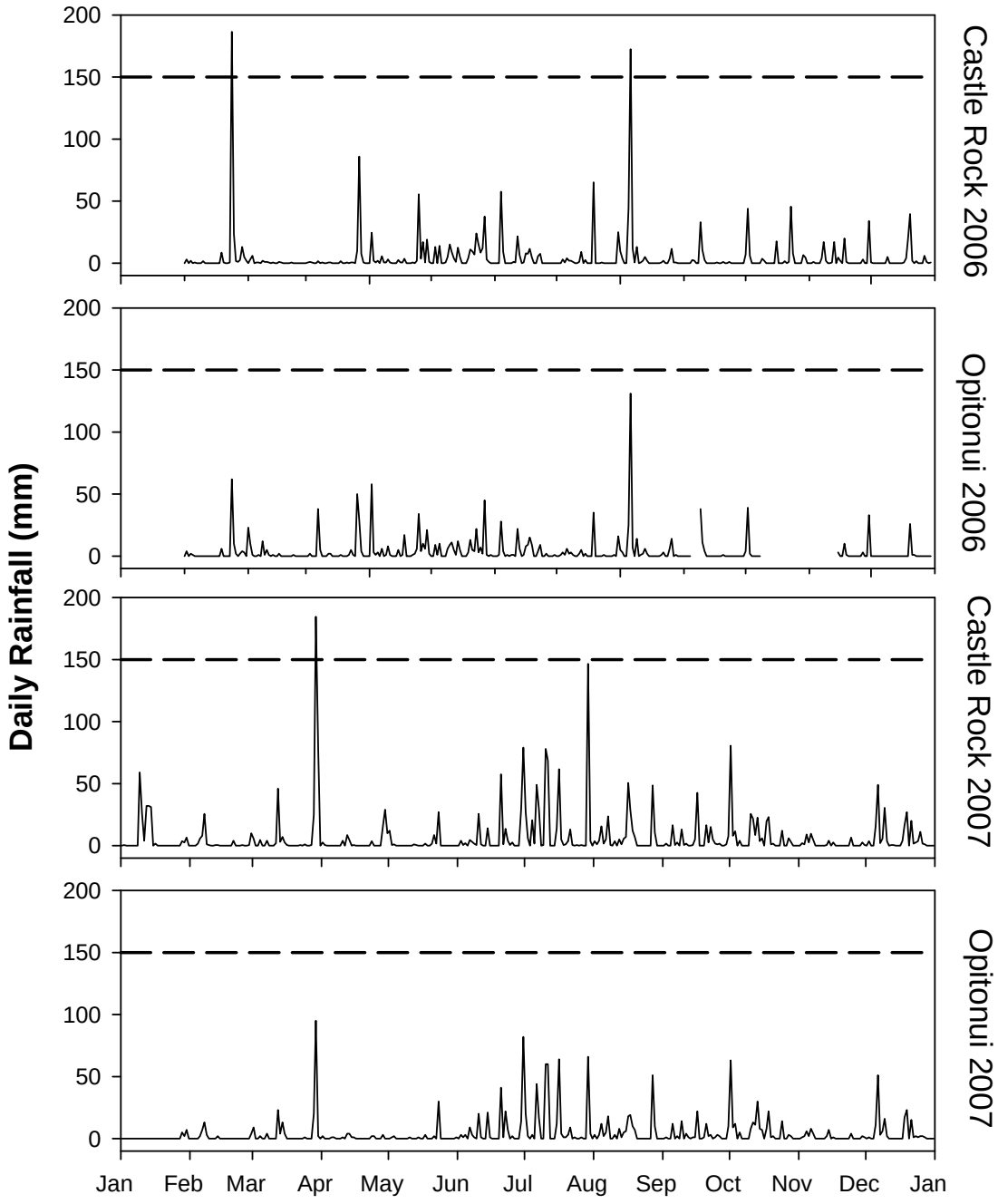

Figure 11.5. Daily maximum rainfall for the Castle Rock and Opitonui stations for the 2006 and 2007 period. The 150mm daily maximum is marked with a dashed line.

The removal of kauri from the steep Whangapoua slopes has no doubt had an influence on slope stability. Vegetation cover is one of the most influential and sensitive elements for landslide vulnerability, and hill country and mountain soils have proved very sensitive to vegetation changes (Crozier 1986). After native kauri forest disturbance, the initial building phase may take at least 200 years with a kauri dominated forest requiring a period of 600-1000 years (Ogden 1985;

Burns & Smale 1990). The sediment fingerprinting results may also indicate that the upper part of the catchment under native forest is undergoing a period of post disturbance disequilibrium and will not return to stability for several centuries. Disequilibrium stream conditions brought about by landuse change have been a recognised phenomena (Happ *et al.* 1940).

Native forest landscape unit disequilibrium has been reported by Gabet & Dunne (2002). Native sage-scrub had been converted to grasslands for pasture and increased the incidence of landslides as a result of weaker and shallower grass roots. Gabet & Dunne (2002) state that there is now a disequilibrium between root reinforcement and soil depth (Figure 11.6). The soil depth will decrease (via landslides) for a given slope angle to adjust to a new equilibrium from sage root reinforcement (high) to grassland root reinforcement (low). The most important point of Figure 11.6 is the diminishing protective effects of native vegetation to landslides at increasing slope angles.

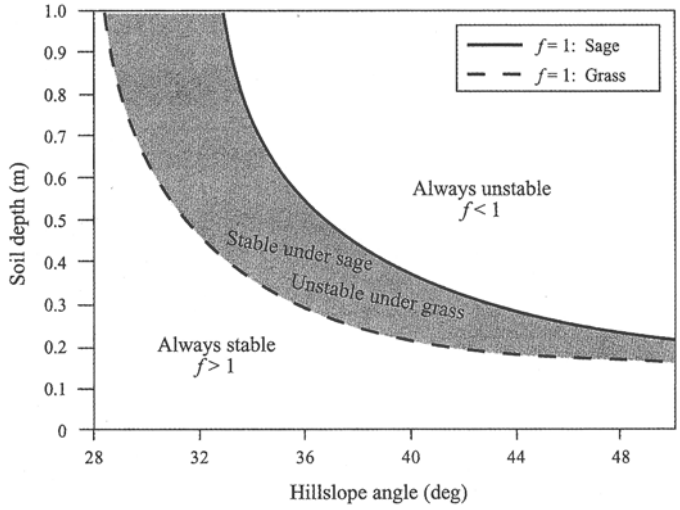

Figure 11.6. Landslide stability analysis for varying soil depth and slope angles under native sage (solid line) and grassland (dashed line) landuse. The shaded area is the depth of soil that is unstable and susceptible to landslides due to conversion from native to grassland landuse (Gabet & Dunne 2002).

11.5 Management implications

The first and most important management implication is that the pattern of landuse within the Whangapoua catchment is about the best in terms of

minimising sediment entering the harbour while maintaining some economic use of the catchment. The sediment fingerprinting results indicate that around 60% of the estuary sediment is derived from the native forest landscape unit, most likely generated by landslides due to the high rainfall and steep slopes. The steep headwater areas are under permanent forest and apart from the reintroduction of kauri trees (Section 11.4), native forest is the best landuse to minimise the impacts of landslides.

The mid-slope areas are under exotic pine forests. The suspended sediment monitoring (Chapter 8) and New Zealand studies indicate that the post harvest erosion rates fall quickly to below agricultural landuse rates after two to three years after vegetation recolonisation and pine replanting. In a 30 year harvest cycle, the Whangapoua exotic forest slopes are protected for 90% of the time. If it is assumed that all of the native forest sediment is landslide generated, the most likely source of the other 20% of landslide sediment is from the exotic forest areas that are on steep slopes (Figure 11.7). The potential exists to reduce estuary sedimentation by allowing areas of exotic forests on steep slopes to revert back to native forest. Surface and streambank erosion could be lowered in exotic forest areas by the buffering of stream and drainage lines by riparian planting.

Agriculture is largely confined to the lowland areas of low relief. While hill country under agriculture can be a major sediment source area (Chapter 3), the low gradient of the agricultural landscape unit in the Whangapoua catchment means that landslides are virtually absent in the pasture areas and thus agriculture is practiced in the best location.

Sediment fingerprinting relative contribution results indicate that streambank erosion (13%) is an important erosion process in the agricultural landscape unit (15%) (Figure 11.8). Almost all of the agricultural activity in the Whangapoua catchment involves livestock which are not excluded from streamlines. The potential exists to reduce the amount of streambank erosion by the introduction of riparian zones on agricultural areas. Riparian zones would also reduce biological contamination of streams and estuary from animal and agricultural derived nutrients and faecal material.

Figure 11.7. Area of exotic forest landuse on steep slopes toward the top of the catchment with the native forest in the background.

Figure 11.8. Area of streambank erosion in the agricultural landscape unit.

11.6 Review of objectives

11.6.1 Objective 1

There were three primary objectives outlined at the beginning of this thesis. The first was to:

> *quantify the amounts of sediment generated from the native forest, exotic forest, and agricultural landscape units in the catchment.*

This objective has been met with the unexpected result that the native forest landscape unit was the greatest contributor of estuary sediment, followed by exotic forest and agricultural landscape units, although exotic forest and agriculture are within uncertainty of each other.

11.6.2 Objective 2

The second objective was to:

> *identify the dominant processes generating the sediment within the native forest, exotic forest, and pastoral landscape units.*

This objective has been met with the identification that the main sediment source was from subsurface (i.e., landslide), followed by streambank erosion, and then surface erosion. The dominance of subsurface sources was confirmed by radionuclide tracing techniques. To be consistent with the first objective results, it appears that low frequency/high magnitude rainfall events in the native forest/headwater areas trigger landslides that efficiently deliver sediment to streams. High frequency/low magnitude events are more important in the harvested exotic forest/mid-catchment area and agricultural/lowland plains area where streambank and surface erosion are more important, but decoupling buffers some of the impacts.

11.6.3 Objective 3

The third objective was to:

> *assess the utility of the sediment fingerprinting technique in the New Zealand landscape for examining catchment sediment delivery.*

The sediment fingerprinting results were compared with radionuclide analysis, stream monitoring, and modelling. Previous studies were also taken into account. Sediment fingerprinting results should be compared with other methods because "…results from sediment mixing models should not be used in isolation…but should be combined with other forms of data that can provide insights into the validity of the models output" (Miller *et al.* 2005). Sediment fingerprinting results were compared and supported by the radionuclide tracing study, and the sediment fingerprinting results were consistent with the pilot study results and the stream sediment storage results indicate that sediment is not stored within the catchments rivers, but efficiently conveyed to the estuary. On the balance of evidence, it is therefore my opinion that the sediment fingerprinting technique was tracing real processes in the Whangapoua catchment. Sediment fingerprinting appears to be overcoming the problems of linking sediment sources to the sink in a drainage basin where sediment sources, sinks, and fluxes are highly variable in space and time and difficult to measure with indirect methods (Trimble 1999).

Contrary comparisons come from another previous study using compound specific isotopes (CSI) (Gibbs 2006) and modelling. The CSI study used only 14 surface soil samples to characterise the catchment, and as a new technique presented no validating evidence for the results. Models will always encounter problems of simplification of real world complexity by the assumptions used. The model used in this study was based on national scale drivers such as rainfall and geology (SYE and NZeem) and from more regional/local assumptions about landuse and landsliding (NZeem). All models suffer from the paradox that they characterise erosion without the need for data collection, but their assumptions are underpinned by the quality of collected data (Brazier 2004).

There have been many studies on the individual components of catchment dynamics such as hillslope erosion, flood plain accumulation, and landslide frequency and magnitude. But studies of dynamics of the coupled systems with all their interlinked components "are rare, but urgently needed" (Wasson 2002). Sediment fingerprinting has provided information on the function of a multilanduse catchment in New Zealand, and provides a comparison for those developing models to better understand sediment dynamics and landuse impacts.

11.7 Conclusions of this thesis

The following conclusions were reached:

- Based on the pilot study results, the sediment fingerprinting technique can distinguish between landscape units and erosion positions using geochemical elements in the Whangapoua catchment.
- Based on the full sediment fingerprinting programme, the main contributing landuse in terms of sediment delivery is the native forest (62% ± 17%) followed by exotic pine forests (23% ± 12%) and then agriculture (15% ± 10%). In terms of the relative proportion for erosion process, the main source was from subsoil (79% ± 6%), then streambanks (13% ± 5%), then surface soils (8% ± 6%).
- Radionuclide analysis (using ^{137}Cs) identified 'all subsurface' (> 20 cm depth and streambanks) as the dominant erosion source of estuary sediment.
- Stream suspended sediment monitoring identified harvested pines had a greater erosion rate than six month post harvest pines, then agricultural pastures, then 10 year post harvest pines. The results supported previous studies that suggest that post harvesting erosion rates fall quickly. Assumptions and potential errors meant that the suspended sediment monitoring results should only be used for explanation rather than extrapolation. The lack of a native forest monitoring site hindered comparison to the sediment fingerprinting results.
- Two catchment models (Sediment Yield Estimator and the New Zealand Empirical Erosion Model) identified the total sediment yield to the harbour to be in the range of 5400-7200 t $year^{-1}$, although neither identified native forest as the dominant contributor of sediment.
- The sediment fingerprinting results were supported by the radionuclide results and the report from Marden & Rowan (1995). The sediment fingerprinting results were also indirectly supported by the stream sediment storage results which indicated an efficient longitudinal coupling within the stream network that conveys sediment from the top of the catchment to the estuary. To a lesser extent, the sediment fingerprinting results were supported by the suspended sediment monitoring which

showed the pattern of rapidly declining erosion rates after pine harvesting to rates below that of the agricultural landuse.

- The sediment fingerprinting results were contradicted by the Sediment Yield Estimator and the New Zealand Empirical Erosion Model and the report by Gibbs (2006). The two models were not calibrated for the Whangapoua catchment and use national scale assumptions (rainfall and geology) for erosion estimation. The Gibbs (2006) novel use of compound specific isotopes (CSI) in Whangapoua only sampled the top 2 cm of the soil which would indicate that the CSI technique traces surface erosion. Only 14 samples were used to characterise the Whangapoua catchment in the Gibbs (2006) report.
- Sediment fingerprinting was concluded to be a useful method for determining sediment sources in the Whangapoua estuary environment.
- The main erosion drivers in the catchment are slope and rainfall which in the steep headwater areas of the catchment overcome the protective landcover of native forests. The well coupled native forest/headwater areas efficiently deliver sediment most likely during low frequency/high magnitude storm events that trigger landslides.
- The pattern of landuse in the Whangapoua catchment is well suited to the physical conditions in terms of minimising sediment delivery to the estuary. The steep headwater areas are under permanent native regenerating forests, the mid-slopes are under exotic pines that are harvested once in 30 years, and the lowland areas are under agricultural pastures. Scope remains to lower the levels of sediment entering the estuary by better management of all three landscape units.

11.8 Recommendations for further work

There are a number of areas that warrant further investigation:

- A more extensive use of radionuclides could provide information on soil loss and deposition on the native, exotic, and agricultural slopes. The confounding behaviour of $^{210}Pb_{ex}$ and ^{226}Ra in the estuary environment also merits further investigation.

- Further stream monitoring of native forest catchments needs to be undertaken to assess if the magnitude of sediment contribution from native forests has been correctly estimated against the contributions of exotic forests and agriculture.
- The sediment contribution from the process of streambank erosion could be directly measured using techniques such as erosion pins. A monitoring programme could shed light on the importance of the streambank erosion process within the three landuse types.
- Continued work is required on the underlying assumptions of the sediment fingerprinting technique. These include testing why the fingerprint properties behave differently between the sediment source areas under investigation, their conservativeness during transport, and comparison of sediment fingerprinting results with other established erosion techniques such as radionuclide analysis.
- Sediment fingerprinting data could be run with other types of mixing models such as those developed for use in the biological sciences (e.g., stable isotope analysis in R – SIAR) to understand the sensitivity of sediment fingerprinting results to the type of mixing model. Different mixing models may also allow greater precision or level of detail about potential sediment source areas.
- This study has made assumptions about the nature of coupling and the efficiency of sediment delivery in North Island estuary environments. Work to test the coupling assumptions by sediment fingerprinting or other tracing methods (e.g., rare earths) or indirect methods would yield information on the efficiency of sediment delivery from different coupling zones.
- While much attention has been focused on the removal of commercial crops of trees from the landscape and their impact, little is known about the historic logging of such species as Kauri and what the long term impacts are on slope stability. It was postulated here that the native forest areas are large sources of sediment because they are still undergoing change to a new equilibrium after logging disturbance last century. Investigation into the interaction of Kauri and slope stability, particularly in very steep areas, would assist in explaining the results of the sediment

fingerprinting technique and contribute to understanding of landscape modification in New Zealand. Small undisturbed Kauri stands in the Coromandel have potential to be monitored for sediment generation on a paired catchment basis.

APPENDIX A

KRUSKALL-WALLIS H-TEST

The Kruskal-Wallis *H*-test is the non-parametric equivalent of the one-way analysis of variance (ANOVA). It uses ranks to determine whether three or more independent groups are the same or different. The test procedure is a direct generalisation of the Mann-Whitney rank sum test. The test begins by ordering and assigning ranks from the smallest to the largest to all the sample values regardless of group membership. The test statistic *H* is then:

$$H = \frac{12}{n(n+1)}\left[n_1\left(\overline{R}_1 - \frac{n+1}{2} \right)^2 + n_2\left(\overline{R}_2 - \frac{n+1}{2} \right)^2 + \ldots + n_m\left(\overline{R}_k \frac{n+1}{2} \right)^2 \right] \quad \text{(Eqn A.1)}$$

Eqn A.1 can be rewritten:

$$= \frac{12}{n(n+1)} \sum_{i=1}^{m} n_i \left(\overline{R}_i - \frac{n+1}{2} \right)^2 \quad \text{(Eqn A.2)}$$

Now *H* can be written in an alternative form, for ease of calculation:

$$H = \frac{12}{n(n+1)}\left[\frac{W_1^2}{n_1} + \ldots + \frac{W_m^2}{n_m} \right] - 3(n+1) \quad \text{(Eqn A.3)}$$

where $\overline{R_i} = \frac{W_i}{n_i}$ and $n = \sum_{i=1}^{m} n_i$. W_i is the sum of the ranks and n_i is the number of observations in group *i*.

In a simple example, the test results for Al_2O_3 for soil samples from three different soil groups A, B, and C are presented in Table A-1. The null hypothesis (H_0) to be

tested is that there is no significant difference between the soil group test results at the 5% significance level.

Table A-1. Test results for Al_2O_3 for three different soil groups and their ranking from lowest to highest as per the Kruskal-Wallis *H*-test.

Soil group	A	Rank	B	Rank	C	Rank
	23.0	15	17.3	6.5	11.5	1
	21.4	13	17.8	8	14.9	3
	16.6	5	18.4	9	11.6	2
	22.1	14	17.3	6.5	15.8	4
	18.8	10	19.1	11	19.5	12
W_i (sum of ranks)		57		41		22
n_i		5		5		5
$\overline{R}_i$		11.4		8.2		4.4

272

Note that in the event of ties (as in Soil Group B), the average of the ranks of the tie are assigned, which in this case is (6+7)/2=6.5. So using equation A.3 yields:

$$H = \frac{12}{15(15+1)}\left[\frac{57^2}{5}+\frac{41^2}{5}+\frac{22^2}{5}\right]-3(15+1)=6.14 \qquad \text{(Eqn A.4)}$$

Under the null hypothesis, *H* has an approximate chi-squared distribution with *m*-1=2 degrees of freedom. The critical chi-square value, at the 5% level of significance, is 5.99 and we reject H_0 if *H* is larger than the critical value. Thus, in this instance there is sufficient evidence to reject the null hypothesis. It can be concluded that there is a significant difference between the soil groups at the 5% level of significance. It is worthy to note that if this example was tested at the 4% level of significance, the null hypothesis is not rejected, as the critical chi-square value is 6.44.

APPENDIX B

DISCRIMINANT FUNCTION ANALYSIS (DFA)

Discriminant function analysis (DFA) is used to determine whether a set of variables is effective in predicting membership to a group. DFA can be considered as the statistical inverse of multivariate analysis of variance (MANOVA). In MANOVA, the group membership is the independent variable and is used to predict or explain the observed values in the response variables. In DFA, the independent variables are the observed values and is used to explain the group membership. In other words it answers the question, can a set of variables (i.e., geochemical elements) be used to predict membership to a group (i.e., a landuse type)?

DFA essentially gives a linear transformation of the p predictor variables, (X_1, …, X_p), to create another set p variables (Z_1, …, Z_p). These new set of variables describe surfaces (in p-dimensional space), which provide the best possible separation of the group means in decreasing order of importance. In most instances the higher orders of elements in these new variables are zero. For example, if we have two predictor variables, the first element in the new vector defines a line which best separates the groups centres. The second vector also gives a line, but it does not separate the groups as well as the first. (Environmental Protection Agency 2007).

Discrimination can be based on Mahalanobis distances, Canonical Discriminant functions, or Eigen values. The computational approach taken by STATISTICA 8.0 parallels that taken by MANOVA. A matrix is developed containing the within-group sums of squares (SS_{WG}) and sums of cross-products of each dependent variable. A second matrix, containing the between-group sums of squares (SS_{BG}) and cross-products is also obtained. The test of significance is then based on the Wilks' Lambda and F-test. The test of significance involves finding a function of the determinants of these two matrices and their sums.

The sum of squares for a variable is a measure of the deviation between the observations and their mean value. In practical terms, the sums of squares is the sum of the squared differences between the scores and their mean. For a single variable, X_j, the sum of squares for a sample of size n, is defined as:

$$\sum_{k=1}^{n}(x_{jk} - \overline{x_{j\bullet}})^2 \qquad \text{(Eqn B.1)}$$

where $\bar{x}_{j\bullet}$ is the usual sample mean for variable j. Dividing this by n-1, gives the usual definition of the sample variance. For two variables, X_j and X_{j*}, the sum of the cross-product is defined as:

$$\sum_{k=1}^{n}(x_{jk} - \bar{x}_{j\bullet})(x_{j*k} - \bar{x}_{j*\bullet}) \qquad \text{(Eqn B.2)}$$

where $\bar{x}_{j\bullet}$ and $\bar{x}_{j*\bullet}$ are the usual sample means for the two variables. Dividing by n-1, gives the usual definition of the sample co-variance.

Generally, there will be random samples of size n_1, …, n_p from each of m different groups. For each member of each sample, we record the values for X_1, …, X_p the p predictor variables. That is, we have $N = \sum_{i=1}^{m} n_i$ observations x_{ijk} and is the score for variable j for the kth member of the sample from group i. Consequently the data takes the form of a data matrix in DFA, as shown in Table B-1.

Table B-1. DFA data matrix table for predictor variables X_1, …, X_p and observations n_1, …, n_p for m groups.

	Observation	X_1	⋯	X_j	⋯	X_p
Group 1	1	x_{111}	⋯	x_{1j1}	⋯	x_{1p1}
	⋮	⋮	⋱	⋮	⋱	⋮
	n_1	x_{11n_1}	⋯	x_{1jn_1}	⋯	x_{1pn_1}
⋮	⋮	⋮	⋱	⋮	⋱	⋮
Group i	1	x_{i11}	⋯	x_{ij1}	⋯	x_{ip1}
	⋮	⋮	⋱	⋮	⋱	⋮
	k	x_{i1k}	⋯	x_{ijk}	⋯	x_{ipk}
	⋮	⋮	⋱	⋮	⋱	⋮
	n_i	x_{i1n_i}	⋯	x_{ijn_i}	⋯	x_{ipn_i}
⋮	⋮	⋮	⋱	⋮	⋱	⋮
Group m	1	x_{m11}	⋯	x_{mj1}	⋯	x_{mp1}
	⋮	⋮	⋱	⋮	⋱	⋮
	n_m	x_{m1n_m}	⋯	x_{mjn_m}	⋯	x_{mpn_m}

For the data in the table, calculations are made for $\bar{x}_{ij\bullet}$ (the sample means for each individual group within variable j), and also $\bar{\bar{x}}_{\bullet j\bullet}$ (the sample mean of all observations for variable j, regardless of group membership).

Consider the following hypothetical example of the results for four geochemical elementals (A, B, C, and D) from the analysis of soil samples taken from three different landuse types (native forest, exotic forest, and agriculture) (Table B-2).

Table B-2. DFA hypothetical example of soil analysis results for four elements (A, …, D) from three different landuse types (native forest, exotic forest, and agriculture).

Group	Element A (j=1)	Element B (j=2)	Element C (j=3)	Element D (j=4)
Group 1	87	5	31	6.4
Native forest	97	7	36	8.3
(i=1)	112	9	42	7.2
Means ($\bar{x}_{1j\bullet}$)	*98.67*	*7*	*36.33*	*7.3*
Group 2	102	16	45	7.0
Exotic forest	85	10	38	7.6
(i=2)	76	9	32	6.2
Means ($\bar{x}_{2j\bullet}$)	*87.67*	*11.67*	*38.33*	*6.93*
Group 3	120	12	30	8.4
Agriculture	85	8	28	6.3
(i=3)	99	9	27	8.2
Means ($\bar{x}_{3j\bullet}$)	*101.33*	*9.67*	*28.33*	*7.63*
Grand mean ($\bar{\bar{x}}_{\bullet j\bullet}$)	***95.89***	***9.44***	***34.33***	***7.29***

Note: in this example $i = 3$, $p = 4$, and $n_i = 3$ for $i = 1,\ldots,m = 3$.

The next step is to calculate the matrix of within-group sums of squares (SS_{WG}) and sums of cross-products of each dependent variable. This is a p by p symmetric matrix and the (j, j*) element is defined as:

$$\sum_{i=1}^{m}\sum_{k=1}^{n_i}(x_{ijk}-\bar{x}_{ij\bullet})(x_{ij*k}-\bar{x}_{ij*\bullet}) \qquad \text{(Eqn B.3)}$$

for j, j^*=1, …, p. Note that for $m = i$ and $j = j^*$,

$$\sum_{k=1}^{n_i}(x_{ijk} - \bar{x}_{ij^*\bullet})(x_{ij^*k} - \bar{x}_{ij^*\bullet}) \qquad \text{(Eqn B.4)}$$

Becomes:

$$\sum_{k=1}^{n_i}(x_{ijk} - \bar{x}_{ij\bullet}) \qquad \text{(Eqn B.5)}$$

which is $(n_i\text{-}1)Var(X_{ij})$ while for $j \neq j^*$,

$$\sum_{k=1}^{n_i}(x_{ijk} - \bar{x}_{ij\bullet})(x_{ij^*k} - \bar{x}_{ij^*\bullet}) \qquad \text{(Eqn B.6)}$$

is $(n_i\text{-}1)CoVar(X_{ij}, X_{ij^*})$.

In a similar fashion the matrix of the between-group sums of squares (SS_{BG}) and cross-products can be defined. This is also a p by p symmetric matrix and the (j, j^*) element is defined as:

$$\sum_{i=1}^{m} n_i(\bar{x}_{ij\bullet} - \bar{\bar{x}}_{\bullet j\bullet})(\bar{x}_{ij^*\bullet} - \bar{\bar{x}}_{\bullet j^*\bullet}) \qquad \text{(Eqn B.7)}$$

So for the hypothetical example in Table B-2, for $j = 1$, and $i = 1$, the sums of squares calculation (SS_{WG}) is:

$$\sum_{k=1}^{n_1=3}(X_{i1k} - \overline{X}_{i1\bullet})^2 = (87 - 98.67)^2 + (97 - 98.67)^2 + (112 - 98.67)^2 = 316.67$$

Thus, $\sum_{i=1}^{m=3}\sum_{k=1}^{n_i}(X_{i1k}-\overline{X}_{i1\bullet})^2 = 316.67+348.67+620.67 = 1286.00$

which gives the (1,1) entry in the within-group matrix (SS_{WG}), and the matrix is populated firstly with these results along the diagonal (or trace).

$$SS_{WG} = \begin{bmatrix} 1286.00 & * & * & * \\ * & 45.33 & * & * \\ * & * & 150.00 & * \\ * & * & * & 5.49 \end{bmatrix}$$

Next the calculation is made for the off diagonal (or cross products). For $j = 1$ and $j^* = 2$, with $i = 1$, gives:

$$\sum_{k=1}^{n_1=3}(X_{11k}-\overline{X}_{11\bullet})(X_{12k}-\overline{X}_{12\bullet}) =$$

$$(87-98.67)(5-7)+(97-98.67)(7-7)+(112-98.67)(0-7) = 50$$

so that:

$$\sum_{i=1}^{m=3}\sum_{k=1}^{n_i=3}(X_{ijk}-\overline{X}_{ij\bullet})(X_{ij*k}-\overline{X}_{ij*\bullet}) =$$

$$50+97.67+72.33 = 220$$

and will give the (1,2) and (2,1) entries in SS_{WG} matrix. The other cross products are calculated and the matrix can be populated to give:

$$SS_{WG} = \begin{bmatrix} 1286.00 & 220.00 & 348.33 & 50.00 \\ 220.00 & 45.33 & 73.67 & 6.37 \\ 348.33 & 73.67 & 150.00 & 9.73 \\ 50.00 & 6.37 & 9.73 & 5.49 \end{bmatrix}$$

For the symmetric between-group sums of squares matrix (SS_{BG}) again for $j = 1$, and $j^* = 2$, the calculation is:

$$\sum_{i=1}^{m=3} n_i (\overline{X}_{i1\bullet} - \overline{\overline{X}}_{\bullet 1\bullet}) =$$

$$3\left[(98.67 - 95.89)^2 + (87.67 - 95.89)^2 + (101.33 - 95.89)^2\right] \times 3 = 314.89$$

These sums of squares are entered into the matrix for SS_{BG} diagonally:

$$SS_{BG} = \begin{bmatrix} 314.89 & * & * & * \\ * & 32.89 & * & * \\ * & * & 168.00 & * \\ * & * & * & 0.74 \end{bmatrix}$$

in the (1,1) position in SS_{BG}, while

$$\sum_{i=1}^{m} n_i (\overline{X}_{i1\bullet} - \overline{\overline{X}}_{\bullet 1\bullet})(\overline{X}_{i2\bullet} - \overline{\overline{X}}_{\bullet 2\bullet}) =$$

$$3\begin{bmatrix} (98.67 - 95.89)(7 - 9.44) + (87.67 - 95.89)(11.67 - 9.44) \\ + (101.33 - 95.89)(9.67 - 9.44) \end{bmatrix} = -71.56$$

gives the (1,2) and (2,1) entries for the off diagonal cross products. The other entries are populated in the same way to give:

$$SS_{BG} = \begin{bmatrix} 314.89 & -71.56 & -180.00 & 14.49 \\ -71.56 & 32.89 & 8.00 & -2.22 \\ -180.00 & 8.00 & 168.00 & -10.40 \\ 14.49 & -2.22 & -10.40 & 0.74 \end{bmatrix}$$

From the above two matrices of sums of squares and cross products, a third matrix is defined; SS_{TOTAL} which is the $SS_{WG} + SS_{BG}$. The usual matrix addition rules apply

where the corresponding cells in SS_{WG} and SS_{BG} are added to give the corresponding entry in $SS_{TOTAL.}$ The next step is to calculate the determinants of SS_{WG} and $SS_{TOTAL.}$

The determinant of a matrix is usually denoted **|A|** and is a scalar value which is calculated from a matrix. This number can determine whether a set of linear equations are solvable, or in other words whether the matrix can be inverted. In the simple example below, the determinant of a 2×2 matrix:

$$|A| = \begin{bmatrix} a & b \\ c & d \end{bmatrix} \text{ would be } |A| = ad - bc$$

As the matrix increases in order, so does the complexity. For a 4×4 matrix:

$$|A| \det = \begin{bmatrix} a & b & c & d \\ e & f & g & h \\ i & j & k & l \\ m & n & o & p \end{bmatrix}$$

the determinant is equal to:

$$\begin{aligned} |A| &= a\left[f\{kp - lo\} - g\{jp - \ln\} + h\{jo - kn\}\right] \\ &- b\left[e\{kp - lo\} - g\{ip - lm\} + h\{io - km\}\right] \\ &+ c\left[e\{jp - \ln\} - f\{ip - lm\} + h\{in - jm\}\right] \\ &- d\left[e\{jo - kn\} - f\{io - km\} + g\{in - jm\}\right] \end{aligned}$$

Since the sums of squares matrices here are symmetric, the expression is somewhat simplified.

The determinant for the matrix SS_{WG} is:

$$|SS_{WG}| = \det \begin{bmatrix} 1286.00 & 220.00 & 348.33 & 50.00 \\ 220.00 & 45.33 & 73.67 & 6.37 \\ 348.33 & 73.67 & 150.00 & 9.73 \\ 50.00 & 6.37 & 9.73 & 5.49 \end{bmatrix} = 864{,}884.76$$

The determinant for the matrix SS_{TOTAL} is:

$$\left|SS_{TOTAL}\right| = \det\begin{bmatrix} 1600.89 & 148.44 & 168.33 & 64.49 \\ 148.44 & 78.22 & 81.67 & 4.15 \\ 168.33 & 81.67 & 318.00 & -0.67 \\ 64.49 & 4.15 & -0.67 & 6.23 \end{bmatrix} = 82{,}717{,}969.24$$

The next step is to calculate the Wilks' lambda (Λ). The Wilk's lambda is a test statistic used in multivariate analysis of variance (MANOVA) to test whether there are differences between the means of identified groups of subjects on a combination of dependent variables. The statistic is defined as the ratio of the determinants of the matrix of the within-group sums of squares of the matrix of the total sums of squares, which for this example is:

$$\Lambda = \frac{\left|SS_{WG}\right|}{\left|SS_{TOTAL}\right|} = \frac{864{,}884.76}{82{,}717{,}969.24} = 0.010456$$

Next the *F*-ratio is determined. A random variable that has an *F* distribution is the value of two estimates of variance. The *F* distribution is defined by two parameters; the degrees of freedom of the numerator (df_1) and the degrees of freedom of the denominator (df_2). The shape of the *F* distribution will depend on the value of the two degrees of freedom and the smaller they are, the larger the *F*-ratio will need to be to be significant. By definition, the *F*-ratio is:

$$F - ratio = \left(\frac{1-y}{y}\right)\left(\frac{df_2}{df_1}\right)$$

where $y = \Lambda^{\frac{1}{s}}$, and $s = \sqrt{\frac{p^2(dfn)^2 - 4}{p^2 + (dfn)^2 - 5}}$ and $dfn = m\text{-}1$

In this case *p* is the number of elements and *m* is the number of groups (as has been defined earlier).

So $p = 4$, $m = 3$, giving $dfn = 2$. So:

$$s = \sqrt{\frac{(4)^2(2)^2 - 4}{(4)^2 + (2)^2 - 5}} = 2 \text{ and } y = (0.010456)^{\frac{1}{2}} = 0.102255$$

Now the F-ratio has an approximate F distribution with degrees of freedom df_1 and df_2 value. So:

$$df_1 = p \times df_n \text{ and } df_2 = s\left[(dfd) - \frac{p - dfn + 1}{2}\right] - \left[\frac{p(dfn) - 2}{2}\right]$$

where $dfd = m(k-1)$, and k is the number of observations (or cases) in each group. Thus:

$$df_1 = 4 \times 2 = 8 \text{ and}$$

$$df_2 = 2\left[(6) - \frac{4 - 2 + 1}{2}\right] - \left[\frac{4(2) - 2}{2}\right] = 6$$

And so the observed F-ratio is:

$$\left(\frac{1 - 0.102255}{0.102255}\right)\left(\frac{6}{8}\right) = 6.58$$

The critical F value with 8 and 6 degrees of freedom at $\alpha = 0.05$, is 4.15. Because the observed F-ratio exceeds the critical F, there is sufficient evidence to reject the null hypothesis. It is concluded in this example that the three landuse types can be distinguished on the combination of the four geochemical elements or predictors.

APPENDIX C

THE 25cm FALL TIMES FOR DIFFERENT PARTICLE SIZES AT DIFFERENT TEMPERATURES

Sedimentation Times for 25 cm fall

Particle size (μm)

Temp	2	5	10	20	30	40	50
(°C)	Hr min	Hr min	Min sec	Min sec	Min sec	Min sec	Min sec
5	30 15	4 50	72 35	18 10	8 04	3 32	2 54
6	29 20	4 41	70 30	17 35	7 49	4 24	2 49
7	28 25	4 33	68 15	17 05	7 35	4 16	2 44
8	27 35	4 25	66 15	16 35	7 22	4 08	2 39
9	26 50	4 17	64 20	16 05	7 09	4 01	2 34
10	26 05	4 10	62 30	15 40	6 59	3 54	2 30
11	25 20	4 03	60 45	15 10	6 45	3 48	2 26
12	24 35	3 56	59 05	14 45	6 34	3 42	2 22
13	23 55	3 50	57 30	14 20	6 23	3 36	2 18
14	23 20	3 44	56 00	14 00	6 13	3 30	2 14
15	22 45	3 38	54 30	13 35	6 03	3 24	2 11
16	22 05	3 32	53 05	13 15	5 54	3 19	2 07
17	21 30	3 27	51 45	12 55	5 45	3 14	2 04
18	21 00	3 22	50 25	12 35	5 36	3 09	2 01
19	20 30	3 17	49 10	12 20	5 28	3 04	1 58
20	***20 00****	***3 12****	***48 00****	***12 00****	***5 20****	***3 00****	***1 55.2****
21	19 30	3 07	46 50	11 45	5 12	2 56	1 52
22	19 05	3 03	45 45	11 25	5 05	2 52	1 50
23	18 35	2 59	44 40	11 10	4 58	2 48	1 47
24	18 10	2 55	43 40	10 55	4 51	2 44	1 45
25	17 45	2 50	42 40	10 40	4 44	2 40	1 42
26	17 20	2 47	41 40	10 25	4 38	2 36	1 40
27	17 00	2 43	40 45	10 10	4 32	2 33	1 38
28	16 35	2 40	39 55	10 00	4 26	2 30	1 36
29	16 15	2 36	39 00	9 45	4 20	2 26	1 34
30	15 55	2 33	38 10	9 35	4 15	2 23	1 32

* Exact values by International definition of particle size in sedimentation range

Settling times in the above table are based on the calculation of Stokes Law:

$$t = \frac{18\eta h}{\left(g\left(\rho s - \rho l\right)X^{2}\right)} \qquad \text{(Eqn C.1)}$$

Where:

t = time (seconds)
η = coefficient of viscosity
h = distance of settling (cm)
g = gravity (corrected for elevation and latitude) cm^2/sec
ρs = density of soil (assumed to be 2.6 g/cm^3)
ρl = density of liquid
X = particle diameter (cm)

APPENDIX D

CANONICAL ANALYSIS

D.1 Introduction

Canonical analysis can best be understood by comparison with multiple regression:

> *In regression, there are several variables on one side of the equation and a single variable on the other side. The several variables are combined into a predicted value to produce, across all subjects, the highest correlation between the predicted value and the single variable. (Tabachnick & Fidell 1996)*

Canonical analysis seeks to understand the relationship between two sets of variables. The difference between the multiple liner regression quote above and canonical analysis is that there are several variables on either side of the canonical equation. On each side these sets of variables are combined to produce a predicted value that has the highest correlation with the predicted value on the other side (Tabachnick & Fidell 1996). The basic canonical technique is based on projections with the aim of maximising the association between the low dimensional projections of the two data sets (Hardle & Simar 2007).

In other words, canonical analysis is interested in investigating relationships between two sets of variables $Y = (Y_1 , Y_2 ,..., Y_p)$ and $X = (X_1 , X_2 ,..., X_p)$. In addition one may also have sets of covariates $Z = [Z_1 , Z_2 ,..., Z_p]$ and $W = [W_1 , W_2 ,..., W_p]$. The aim of canonical analysis is to construct two new sets of canonical variates $U = \alpha Y$ and $V = \beta X$ that are linear combinations of the original variables such that the simple correlation between U and V is maximal (Timm 2002).

D.2 Calculation

The first step in canonical analysis is the creation of a correlation matrix, and it is divided into four parts. The first is the correlation between the dependant variables (DV) R_{yy}, the correlation between the independent variables (IV) R_{xx}, the two matrices of correlations between the DVs and the IVs, R_{xy} and R_{yx}. The canonical correlation matrix is a product of four correlation matrices, between DVs (inverted), IVs (inverted), and between DVs and IVs.

$$R = R_{yy}^{-1} R_{xy} R_{xx}^{-1} R_{xy}$$

The equation can be thought of as a product of regression coefficients for predicting Xs from Ys ($R_{yy}^{-1} R_{yx}$) and the regression coefficients for predicting Ys from Xs ($R_{xx}^{-1} R_{xy}$) (Tabachnick & Fidell 1996).

Canonical analysis then proceeds to solve the matrix R by calculating the eigenvalues. The eigenvalues are the proportion of variance accounted for by the correlation between the respective canonical variates (a canonical variate is a linear combination of variables, one combination on the IV side and the second on the DV side). Solving the eigenvalues of a matrix is a process that redistributes the variance of a matrix and consolidates it into a few composite variates rather than many individual variables (Tabachnick & Fidell 1996; StatSoft Inc 2007).

In practical terms for this research, if we had five elements (x_1, x_2, …x_5) that have been selected for the composite fingerprint, they will be transformed in canonical analysis thus:

x_1, x_2, x_3, x_4, x_5

$y_1, y_2, 0, 0, 0$

The y_1 and y_2 represent the canonical roots which are displayed on the X and Y axis of the canonical graphs. The better visual discrimination (i.e., separation of points) between groups of variables in the graphs, the better the selected variables (i.e., elements) should be able to discriminate between the grouping variable (e.g., landuse) (Figure D.1) (Garson 2007).

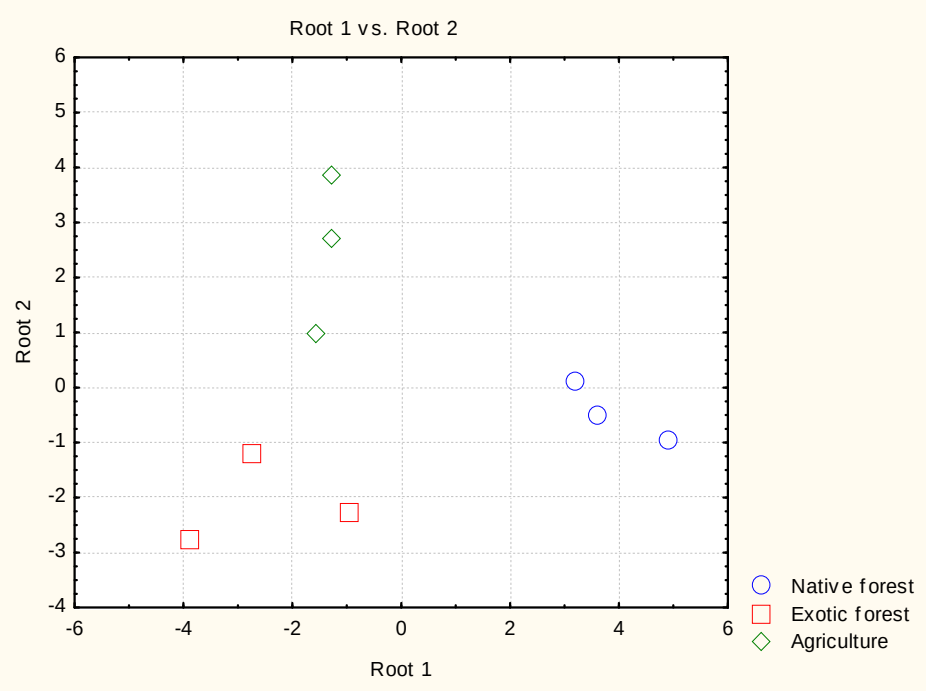

Figure D.1. Graph of canonical analysis between hypothetical native forest, exotic forest, and agricultural landuse.

APPENDIX E

MIXING MODEL PROCUDURE IN AN EXCEL SPREADSHEET

The mixing model that was used to quantify the relative contributions of the potential source areas (e.g., landscape units) was described in Section 3.10.3.3. Essentially, a set of linear equations, $\sum_{i=1}^{m} P_i \bar{x}_{ij}$ is obtained for each element (j) to 'predict' each landuse's contribution to the sink sample. For each element, the residual (or difference) between this predicted value and the observed value x_{sj}, is obtained. This residual is scaled by x_{sj} to take into account the differences in the units associated with each element, and the scaled residual is then squared and summed over the elements, to yield the least squares equation to be minimised. This is

$$R_{es} = \sum_{j=1}^{p} \left(\frac{x_{sj} - \sum_{i=1}^{m} P_i \bar{x}_{ij}}{x_{ij}} \right)^2 \qquad \text{(Eqn E.1)}$$

where:

- p is the number of elements in the composite fingerprint
- m is the number of source groups (e.g., landuse)
- R_{es} is the sum of squares of the residuals
- x_{sj} is the concentration of the element property (j) in the sediment sink sample
- $x_{ij.}$ is the mean concentration of the element (j) in source group (i)
- P_i is the relative contribution/relative proportion from the source group (i) in the sediment sink sample.

This least squares procedure is a common technique in statistics to estimate the parameters of a model. In the above model, it is the P_is (or mixing proportions) that

are being estimated, and they must also satisfy two linear constraints: 1) they must lie between 0 and 1 ($0 \le P_i \le 1$), and 2) their sum is one ($\sum_{i=1}^{m} P_i = 1$) (Collins *et al.* 1997; Owens *et al.* 1999b). Using the observed mean values ($\bar{x}_{ij}$), the least squares procedure gives the actual estimated mixing proportions, for the observed data.

It is a well known statistical result that under certain conditions the sampling distribution for a sample mean can be represented by a Normal distribution with a standard error estimated by the sample standard deviation divided by the square root of the sample size. The Monte Carlo procedure essentially takes a single observation from this sampling distribution and calculates the mixing proportions as if this were the actual observed sample mean for that element. The Monte Carlo result is then used in the mixing model to produce another estimate for the mixing proportions. If this is repeated a large number of times, an empirical distribution of mixing proportions are produced from which an estimate of the uncertainty can be obtained. Since the population mean for the sampling distribution is unknown, this is estimated by the observed sample mean.

The process was run using the Solver function in Microsoft Excel. An example spreadsheet is shown in Figure E.1 and the process was as follows:

- Each of the selected fingerprint element results were arranged in columns and grouped using codes (e.g., landuse).
- The mean and standard error was calculated for each element within each landuse.
- Using the mean and standard error (as obtained above) as estimates of the mean and standard deviation for the sampling distribution of the sample mean, and assuming that the Normal approximation is appropriate, a single observation is taken from the sampling distribution. The appropriate Excel command is:

  =NORMINV(RAND(),Grouped_element_mean,Grouped_element_std_dev

The NORMINV(probability,mean,standard_dev) function returns the inverse of a normal distribution for the specified mean and standard deviation. That is, it returns the value of an observation which has associated the cumulative probability as given. The use of RAND() for probability, ensures a random observation is obtained, since this function returns a uniformly distributed random number between zero and one. At each recalculation of the Excel spreadsheet (F9), new mean values for the element concentrations in each landuse are estimated for use in the least square procedure.

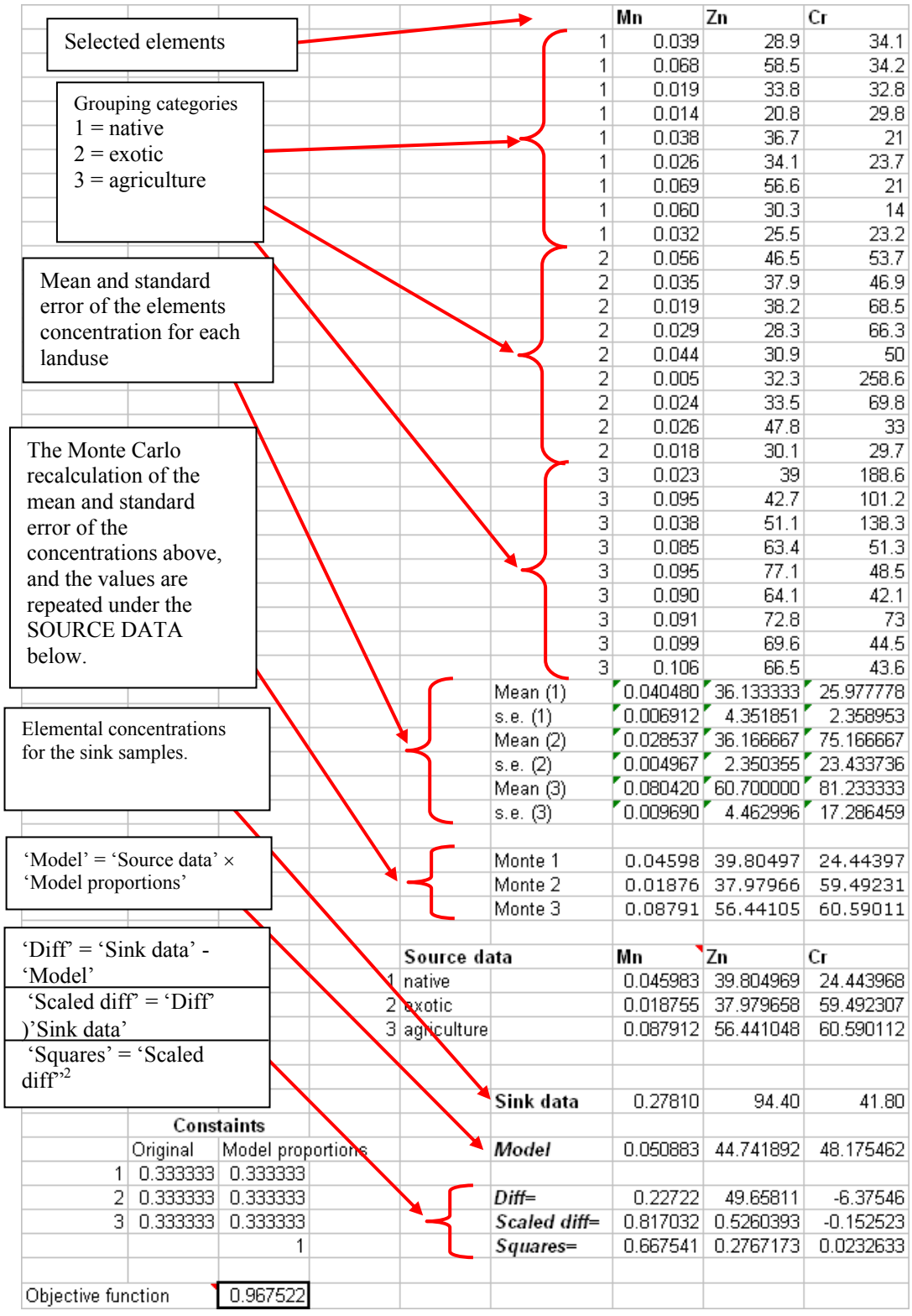

Figure E.1. Screen grab of an example of the mixing model set up in an Excel spreadsheet with annotations of the row calculations used.

- The solver function requires starting values for the parameters to be estimated. It is assumed that the contributions from each landuse are the same, so starting values of 1/3 are used. The "estimated mean element values for each landuse were then multiplied by the starting model proportions and then added together to give the 'model'.
- The difference or residual between the actual elements concentration in the sink (or estuary) sample ('sink data') and the 'model' value, was then calculated The result ('diff') is scaled so that the differing elemental concentrations and units could be compared together in the mixing model ('scaled diff').
- The 'scaled diff' was squared and all the 'squared diff' values for each element were added together to form the 'objective function' that is to be minimised in the Solver equation
- The target cells, constraints, and cells to change were specified in the Solver programme. The 'target cell' was set to the result of the 'objective function' and is the value that was minimised (Figure E.2). The 'constraints' are set so that the 'model proportions' are greater than zero but sum to one. The 'by changing cells' that are changed are set to those labelled 'model proportions' and are set to the initial values of $\frac{1}{3}$ for each landuse, to start. The Solver programme posts the results under the 'model proportions' and these cells are overwritten with each iteration.

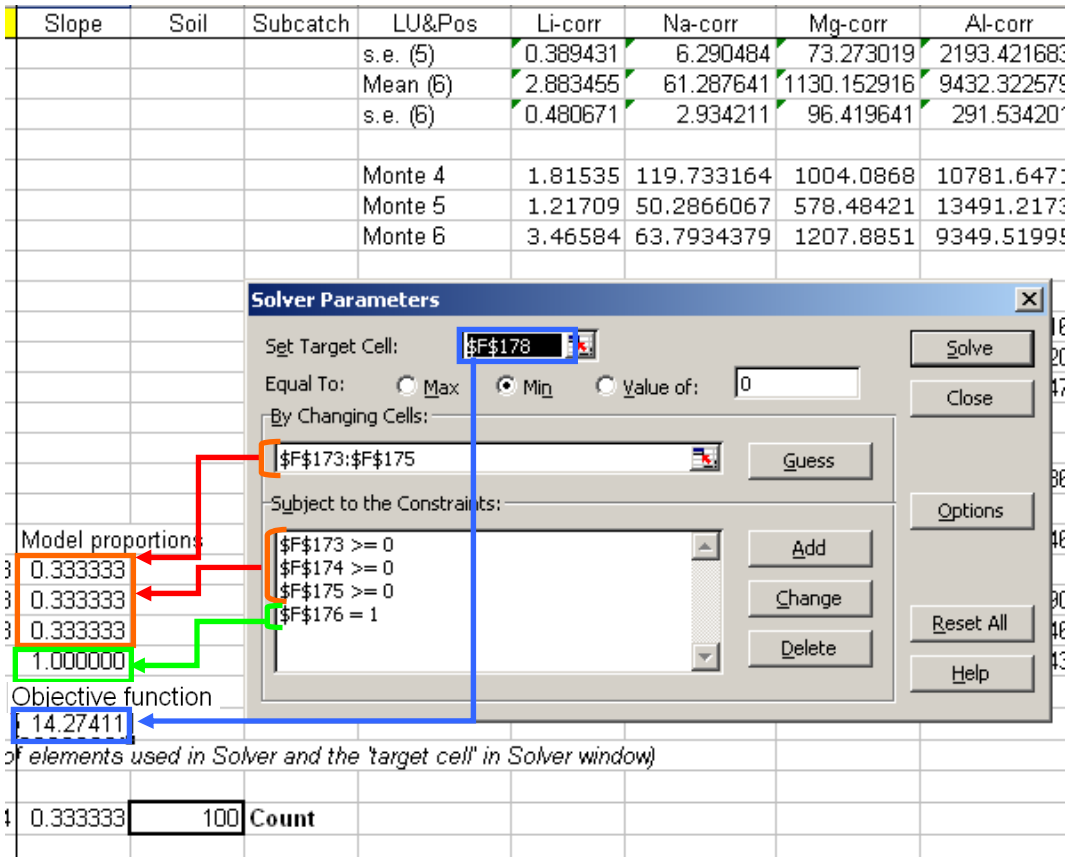

Figure E.2. Screen grab of an example of the mixing model operation using the Solver function in Excel and the relating parameters.

- The Excel worksheet was then recalculated by pushing the F9 key, the Monte Carlo simulation calculates new means for each of the landuse elements, and the process begins again. A Visual Basic macro was written to rerun the Monte Carlo simulation and record the results. The model run was begun with a $\frac{1}{3}$ assumption for each group and then cycled for 100 iterations. The mean of the 100 iteration results (i.e., the model proportions) were then used as the starting values for the proportions for a 5000 iteration cycle.
- At the end of the 5000 iteration run, there are 5000 "estimates" of mixing proportions The mean of the 5000 results was calculated for the mixing proportions of each group, and the standard deviation of the 5000 "estimates" of mixing proportions of each group was calculated to give a measure of the uncertainty of the overall results.

APPENDIX F

XRF RESULTS – SOURCE AREA

	XRF RESULTS: MAJOR ELEMENTS					All results are in part per million (PPM)								
Sample #	Landuse	Position	Na	Mg	Al	Si	P	S	Cl	K	Ca	Ti	Mn	Fe
1	1	1	0.144	0.461	11.050	27.160	0.076	787	128	1.606	0.347	0.490	0.039	3.364
2	1	2	0.633	0.585	7.928	25.140	0.106	1177	229	1.412	1.118	0.413	0.068	2.983
3	1	3	0.239	0.334	11.190	28.220	0.069	634	109	1.795	0.200	0.427	0.019	3.192
4	1	1	0.059	0.865	12.450	28.610	0.033	497	53	2.333	0.120	0.587	0.014	4.425
5	1	2	0.153	0.416	8.477	25.910	0.100	1064	285	1.014	0.289	0.624	0.038	3.500
6	1	3	0.091	0.429	11.510	27.240	0.072	739	101	1.086	0.102	0.665	0.026	4.376
7	1	1	0.311	0.715	9.603	30.710	0.076	581	170	1.767	0.241	0.680	0.069	3.515
8	1	2	0.143	0.414	9.183	27.060	0.093	1004	190	1.375	0.167	0.619	0.060	2.705
9	1	3	0.146	0.356	9.237	32.130	0.052	540	63	1.251	0.088	0.740	0.032	2.600
11	2	1	0.089	0.632	11.580	26.170	0.038	846	134	1.580	0.072	0.492	0.056	6.179
12	2	2	0.194	0.508	9.439	25.510	0.071	912	180	1.019	0.205	0.493	0.035	3.611
13	2	3	0.049	0.351	11.670	26.420	0.040	797	102	1.138	0.060	0.477	0.019	4.715
14	2	1	0.048	0.367	9.348	29.170	0.058	710	163	1.022	0.189	0.562	0.029	3.695
15	2	2	0.152	0.352	8.603	30.180	0.059	758	188	0.871	0.174	0.587	0.044	2.932
16	2	3	< 0.022	0.914	12.650	26.920	0.027	754	62	1.946	0.030	0.492	0.005	5.686
17	2	1	0.129	0.437	9.992	32.010	0.051	588	89	1.317	0.119	0.668	0.024	2.745
18	2	2	0.236	0.230	10.120	24.650	0.094	1003	298	0.541	0.315	0.645	0.026	2.788
19	2	3	0.314	0.199	11.630	25.900	0.046	922	179	0.566	0.195	0.650	0.018	3.332
21	3	1	< 0.022	0.893	11.630	22.940	0.075	1041	132	0.102	0.086	0.751	0.023	7.792
22	3	2	0.143	0.385	6.255	26.030	0.202	1689	221	0.298	0.570	0.857	0.095	3.206
23	3	3	0.055	0.441	11.390	26.010	0.058	936	157	0.191	0.138	1.058	0.038	5.545
24	3	1	0.186	0.968	11.250	27.680	0.073	543	42	1.437	0.370	0.602	0.085	4.853
25	3	2	0.125	0.901	9.815	26.780	0.158	1023	181	1.378	0.414	0.573	0.095	4.240
26	3	3	0.187	0.863	11.280	28.040	0.086	575	72	1.600	0.323	0.584	0.090	4.530
27	3	1	0.185	1.069	11.350	27.190	0.075	734	111	1.478	0.309	0.575	0.091	5.534
28	3	2	0.150	0.778	10.000	27.220	0.143	944	140	1.357	0.333	0.588	0.099	3.899
29	3	3	0.159	0.863	11.360	27.650	0.088	663	68	1.503	0.255	0.596	0.106	4.338
	CODE	CODE												
	1=Native	1=Str.bank												
	2=Exotic	2=0-2cm												
	3=Ag	3=>20cm												

	XRF RESULTS: TRACE ELEMENTS					All results are in part per million (PPM)																
Sample #	Landuse	Position	V	Cr	Co	Ni	Cu	Zn	Ga	Ge	As	Se	Br	Rb	Sr	Y	Zr	Nb	Mo	Ag	Cd	In
1	1	1	134	34.1	6.8	7.8	28	28.9	16.4	1.8	9.6	3.7	41.5	75.3	55.4	14.9	199.9	7.9	2.3	< 0.4	< 0.5	< 0.7
2	1	2	114.5	34.2	8.6	7	44.5	58.5	13.5	1.6	6.9	1.3	22.3	63.6	121	13.3	165.9	6.9	2.1	< 0.4	< 0.5	< 0.7
3	1	3	121.4	32.8	< 5.9	5.5	47.8	33.8	16.5	1.9	10.9	3	31.2	84.7	46.4	11.2	201.9	7.3	3.1	< 0.4	< 0.5	< 0.7
4	1	1	155.9	29.8	< 7.3	3.7	27.6	20.8	19.9	1.2	10.9	5.7	18.7	106.8	25.5	14.5	206.8	8.3	2.5	< 0.4	< 0.5	< 0.7
5	1	2	120.9	21	7.6	5.4	40.2	36.7	13.7	1.7	17.4	2.4	38	53.2	41.9	13.3	192.4	9.5	1.3	< 0.4	< 0.5	< 0.7
6	1	3	145.5	23.7	6.7	7.6	38.9	34.1	18.2	1.5	24.9	3.4	37.4	55	26.2	15.1	211.7	10.3	1.3	< 0.4	< 0.5	< 0.7
7	1	1	127.9	21	9.9	7.2	27.1	56.6	14.1	1.3	18.1	1.1	23.4	81.3	44.2	16.8	272.6	12.1	1.3	< 0.4	< 0.5	< 0.7
8	1	2	116	14	< 5.5	4	16.1	30.3	15.3	1.4	17.5	3	34.3	77.8	31.6	13.5	187.7	10	1.2	< 0.4	< 0.5	< 0.7
9	1	3	116.2	23.2	< 5.5	5.2	13.8	25.5	15.1	1.7	14.2	2.3	27.7	67.2	25.6	15	207.1	11.4	1.5	< 0.4	< 0.5	< 0.7
11	2	1	171.8	53.7	< 8.5	9.9	16	46.5	17.4	1.4	48.7	2.6	22.6	103.5	25.7	12.4	202.8	8.1	2.1	< 0.4	< 0.5	< 0.7
12	2	2	143.3	46.9	6.2	7.2	17.5	37.9	15.7	1.2	23.5	1.8	51.9	85.5	38.9	10.8	195.2	8	1.2	< 0.4	< 0.5	< 0.7
13	2	3	162.6	68.5	< 7.3	14.2	39.5	38.2	17.2	1.6	31.9	2.2	36.9	81.7	18.7	11.3	185.1	7.6	1.5	< 0.4	< 0.5	< 0.7
14	2	1	141	66.3	< 6.5	11.4	19.5	28.3	15.4	1.7	25.4	2.2	32.2	66.8	30	11.7	220.6	9.6	3	< 0.4	< 0.5	< 0.7
15	2	2	114.7	50	< 5.8	5.3	13.5	30.9	15.9	2	9.3	2.2	37.5	50.5	33.1	9.7	254.3	11.3	1.2	< 0.4	< 0.5	< 0.7
16	2	3	224.8	258.6	< 8.3	13	42	32.3	21.7	1.5	41.3	3.9	22.7	112.9	21.7	13.3	166	7.2	2.1	< 0.4	< 0.5	< 0.7
17	2	1	125.2	69.8	5.2	13.7	26.5	33.5	15.4	1.3	9.5	1.4	27.3	72.1	20.2	12.1	265.5	11.3	1.4	< 0.4	< 0.5	< 0.7
18	2	2	109.9	33	7.3	5.4	45	47.8	22.2	2	10	5.9	94.3	37	40.1	17.4	315.5	15.2	3.7	< 0.4	< 0.5	< 0.7
19	2	3	101.2	29.7	< 5.2	4.8	7.4	30.1	19.6	1.8	8.8	4.3	67.5	36.7	46.4	15.5	296.1	13.8	3.5	< 0.4	< 0.5	< 0.7
21	3	1	330.4	188.6	< 9.6	17.4	29	39	22.1	1.6	2.7	2.5	40.6	8.6	21.4	12.8	268.7	10.5	1.7	< 0.4	< 0.5	< 0.7
22	3	2	133.4	101.2	< 5.5	9.6	28.6	42.7	12.1	1.3	1.6	1	39	17.3	42.4	10.7	473	14.1	1.6	< 0.4	< 0.5	< 0.7
23	3	3	276	138.3	7.4	22.7	27.5	51.1	20.8	1.7	2.2	2.7	48.2	14.2	20.6	12.1	369.7	15.8	2	< 0.4	< 0.5	< 0.7
24	3	1	179.2	51.3	11.5	14.3	31.6	63.4	17.6	1.5	18.2	1.3	15.9	70.2	45.3	18.6	191.4	8.4	1.6	< 0.4	< 0.5	< 0.7
25	3	2	154.9	48.5	12.8	12.8	42.5	77.1	15.8	1.1	16.2	0.9	17.9	65.3	44.5	15.9	189.7	8.1	1.5	< 0.4	< 0.5	< 0.7
26	3	3	168	42.1	10.3	12.8	36.9	64.1	17.4	1.6	18.5	1.6	17.6	75.2	40.2	18.2	192	8.2	1.9	< 0.4	< 0.5	< 0.7
27	3	1	176.3	73	11.9	15.2	34.1	72.8	17.3	1.1	23.4	1.1	9.5	72.3	46.4	17.2	197.7	8.3	2	< 0.4	< 0.5	< 0.7
28	3	2	154.8	44.5	8.9	12.8	37.2	69.6	16.3	1.3	16.1	1.2	22.5	71.9	40.1	15.1	192.2	8.7	1.9	< 0.4	< 0.5	< 0.7
29	3	3	175.8	43.6	13.7	13.1	34.5	66.5	17.4	1.5	17.6	1.3	27.8	76.4	39	17.8	189.3	8.5	1.8	< 0.4	< 0.5	< 0.7
	CODE	CODE																				
	1=Native	1=0-2cm																				
	2=Exotic	2=>20cm																				
	3=Ag	3=Str.bank																				

	XRF RESULTS: TRACE ELEMENTS					All results are in part per million (PPM)																
Sample #	Landuse	Position	Sn	Sb	Te	I	Cs	Ba	La	Ce	Pr	Nd	Hf	Ta	W	Hg	Tl	Pb	Bi	Th	U
1	1	1	2.9	< 0.9	< 1.2	17	6.8	266.6	14.8	43.3	12.4	12.5	5.8	2.2	3.1	< 0.4	1.4	20.2	0.9	9.1	4.4
2	1	2	2	< 0.9	< 1.2	4.6	3.9	270.4	14.4	31.5	12.9	11.7	3	3.2	1.4	< 0.4	0.9	20.8	< 0.3	8	3.6
3	1	3	2.9	< 0.9	< 1.2	10.8	6.8	268.6	11.7	22.8	9.1	< 10	6.7	< 3.3	4.2	0.6	1.8	22.1	0.9	9.2	4.2
4	1	1	4.2	0.7	< 1.2	12.2	6.7	271.3	5.4	6	8.9	< 10	4.9	< 2.9	3.7	< 0.4	1.6	13.7	1.1	9.1	5.7
5	1	2	4.4	0.9	< 1.2	14.4	3.8	190.7	7.7	20.5	11.5	< 10	5.1	< 3.1	3.8	< 0.4	1.3	24.4	1.5	7.8	4
6	1	3	3.6	< 0.9	< 1.2	24.5	6.9	194.6	8.5	20.7	8.9	< 10	4.4	< 3.2	3.9	< 0.4	1.2	29.1	2.2	9.3	4.4
7	1	1	1.3	1	< 1.2	7.2	6.5	281.2	7.6	21.2	12.7	11.2	6.3	5.8	3.1	< 0.4	1	12.7	< 0.4	9.6	5.1
8	1	2	2.9	0.8	< 1.2	9.6	6.5	201.7	7.9	17.3	11.3	< 10	3.7	< 2.3	3.4	< 0.4	0.8	19.1	0.9	8.2	4.5
9	1	3	5.1	0.6	< 1.2	12.2	6.1	185.9	9	18.2	12.1	< 10	6.7	2.7	3.7	< 0.4	1.3	17.5	0.7	9.4	4.9
11	2	1	1.2	1.5	< 1.2	33	14.3	242.9	< 4.9	11.3	< 8.0	< 10	5.1	< 2.7	4.8	< 0.4	0.5	16.9	< 0.4	9.6	5.8
12	2	2	0.4	0.6	< 1.2	14.7	11.2	194.3	8.2	16.5	10.4	< 10	4.5	< 2.4	3.9	< 0.4	0.9	10	< 0.3	9.1	4.8
13	2	3	1.9	0.9	< 1.2	22.5	10.1	191.9	4.9	11.1	8.5	< 10	4.6	< 3.2	3.2	0.4	0.9	11.3	< 0.4	9.3	5.2
14	2	1	2.2	1.6	< 1.2	14.6	8.3	181.7	9.5	19.9	11.6	< 10	5.7	2.8	6.4	< 0.4	0.8	10.8	< 0.3	9.7	4.8
15	2	2	1.2	0.9	< 1.2	11.4	6.1	188.6	10.5	18.5	8.3	9.3	6.1	< 2.2	4.9	< 0.4	0.9	9.2	< 0.3	9.2	3.9
16	2	3	7.5	3.4	0.7	13.1	11	253.3	4.7	10	9	< 10	3.7	< 3.5	3.9	< 0.4	0.9	26.2	< 0.4	10.4	5.9
17	2	1	1.1	1.3	< 1.2	7.9	7.3	203.2	6.7	15.1	8	9.9	5.6	< 2.7	6.1	0.4	0.5	54.4	< 0.4	10	5.1
18	2	2	3.7	< 0.9	0.8	68.2	9.5	179.1	19	45.7	22.6	21.2	7.3	3.6	5.2	< 0.4	1.4	19.1	0.4	14.7	5.8
19	2	3	3.7	< 0.9	< 1.2	39.3	7.3	169.3	16.5	37.3	16.1	12.9	6.9	3.6	5	< 0.4	1	20.6	0.4	11.4	4.3
21	3	1	1.2	< 0.9	< 1.2	10.7	< 2.6	52.9	12.9	14.1	< 8.0	< 10	5.5	< 3.2	1.1	< 0.5	< 0.5	13.4	< 0.4	8.9	5.4
22	3	2	1.5	< 0.9	< 1.2	7.3	3.9	130.9	12	18.2	10.5	< 10	9	< 2.7	2.3	< 0.4	0.3	12.1	< 0.3	8.5	4.3
23	3	3	2	< 0.9	< 1.2	10.8	< 2.6	90.9	< 4.9	12	< 8.0	< 10	8.5	< 3.0	2.7	< 0.4	< 0.5	55.3	< 0.4	11.8	5.7
24	3	1	1	0.3	< 1.2	9.1	4.5	282.9	8.4	20.7	12.1	9.1	4.7	4.8	2.6	< 0.4	0.7	13.1	< 0.4	8.1	4.6
25	3	2	3.5	0.9	< 1.2	6	5.8	267.6	10.2	20.1	9.4	< 10	4.6	< 3.3	4.1	< 0.4	0.9	20.6	< 0.4	7.6	4.1
26	3	3	1.5	0.6	< 1.2	8.6	5.6	287.4	9.8	21.6	7.5	10.1	5.1	< 3.1	3.2	< 0.4	1.5	16	< 0.4	8.2	4.6
27	3	1	1.8	< 0.9	< 1.2	7.5	5	300.8	8.4	21.1	8.2	< 10	3.9	< 3.3	3.7	< 0.4	0.9	16.6	< 0.4	8.2	4.8
28	3	2	2.3	0.7	< 1.2	7	5	258.7	8.4	18.3	< 8.0	< 10	4.1	< 3.1	4.3	< 0.4	0.8	22.9	< 0.4	8.3	5
29	3	3	1.3	0.7	< 1.2	12.2	6.5	285.7	10.6	22.5	8.7	9.9	4.5	< 3.1	3.8	< 0.4	0.7	13.6	< 0.4	8.7	5.2
	CODE	CODE																			
	1=Native	1=0-2cm																			
	2=Exotic	2=>20cm																			
	3=Ag	3=Str.bank																			

APPENDIX G

PILOT STUDY KRUSKALL-WALLIS H-TEST RESULTS

G-1 Landscape units

Kruskal-Wallis ANOVA by Ranks; **Cr** (Satistica)
Independent (grouping) variable: **Landuse**
Kruskal-Wallis test: H (2, N= 27) =15.08397 p =.0005

Depend.: **Cr**	Code	Valid N	Sum of Ranks
1	1	9	51.0000
2	2	9	156.0000
3	3	9	171.0000

Kruskal-Wallis ANOVA by Ranks; Mg (Pilot study majors)
Independent (grouping) variable: Landuse
Kruskal-Wallis test: H (2, N= 27) =8.394097 p =.0150

Depend.: Mg	Code	Valid N	Sum of Ranks
1	1	9	109.0000
2	2	9	88.0000
3	3	9	181.0000

Kruskal-Wallis ANOVA by Ranks; Ca (Pilot study majors)
Independent (grouping) variable: Landuse
Kruskal-Wallis test: H (2, N= 27) =6.077601 p =.0479

Depend.: Ca	Code	Valid N	Sum of Ranks
1	1	9	127.0000
2	2	9	84.0000
3	3	9	167.0000

Kruskal-Wallis ANOVA by Ranks; **Zn** (Satistica)
Independent (grouping) variable: **Landuse**
Kruskal-Wallis test: H (2, N= 27) =13.37919 p =.0012

Depend.: **Zn**	Code	Valid N	Sum of Ranks
1	1	9	87.0000
2	2	9	94.0000
3	3	9	197.0000

Kruskal-Wallis ANOVA by Ranks; P (Pilot study majors)
Independent (grouping) variable: Landuse
Kruskal-Wallis test: H (2, N= 27) =8.736353 p =.0127

Depend.: P	Code	Valid N	Sum of Ranks
1	1	9	136.0000
2	2	9	72.0000
3	3	9	170.0000

Kruskal-Wallis ANOVA by Ranks; Mn (Pilot study majors)
Independent (grouping) variable: Landuse
Kruskal-Wallis test: H (2, N= 27) =10.69136 p =.0048

Depend.: Mn	Code	Valid N	Sum of Ranks
1	1	9	111.0000
2	2	9	80.0000
3	3	9	187.0000

Kruskal-Wallis ANOVA by Ranks; Fe (Pilot study majors)
Independent (grouping) variable: Landuse
Kruskal-Wallis test: H (2, N= 27) =6.617284 p =.0366

Depend.: Fe	Code	Valid N	Sum of Ranks
1	1	9	86.0000
2	2	9	120.0000
3	3	9	172.0000

G-2 Erosion position

Kruskal-Wallis ANOVA by Ranks; Al (Pilot study majorsv1.sta
Independent (grouping) variable: Position
Kruskal-Wallis test: H (2, N= 27) =12.87959 p =.0016

Depend.: Al	Code	Valid N	Sum of Ranks
1	1	9	146.5000
2	2	9	58.0000
3	3	9	173.5000

Kruskal-Wallis ANOVA by Ranks; S (Pilot study majors
Independent (grouping) variable: Position
Kruskal-Wallis test: H (2, N= 27) =12.28924 p =.0021

Depend.: S	Code	Valid N	Sum of Ranks
1	1	9	88.0000
2	2	9	194.0000
3	3	9	96.0000

Kruskal-Wallis ANOVA by Ranks; Ca (Pilot study majo
Independent (grouping) variable: Position
Kruskal-Wallis test: H (2, N= 27) =6.786596 p =.0336

Depend.: Ca	Code	Valid N	Sum of Ranks
1	1	9	116.0000
2	2	9	174.0000
3	3	9	88.0000

Kruskal-Wallis ANOVA by Ranks; **V** (Pilot study trace.
Independent (grouping) variable: **Position**
Kruskal-Wallis test: H (2, N= 27) =6.268078 p =.0435

Depend.: **V**	Code	Valid N	Sum of Ranks
1	1	9	157.0000
2	2	9	78.0000
3	3	9	143.0000

Kruskal-Wallis ANOVA by Ranks; P (Pilot study majorsv1.sta ir
Independent (grouping) variable: Position
Kruskal-Wallis test: H (2, N= 27) =10.96631 p =.0042

Depend.: P	Code	Valid N	Sum of Ranks
1	1	9	100.0000
2	2	9	190.0000
3	3	9	88.0000

Kruskal-Wallis ANOVA by Ranks; Cl (Pilot study major
Independent (grouping) variable: Position
Kruskal-Wallis test: H (2, N= 27) =15.88360 p =.0004

Depend.: Cl	Code	Valid N	Sum of Ranks
1	1	9	95.0000
2	2	9	203.0000
3	3	9	80.0000

Kruskal-Wallis ANOVA by Ranks; **U** (Pilot study trace.
Independent (grouping) variable: **Position**
Kruskal-Wallis test: H (2, N= 27) =10.20711 p =.0061

Depend.: **U**	Code	Valid N	Sum of Ranks
1	1	9	156.0000
2	2	9	64.0000
3	3	9	158.0000

APPENDIX H

XRF RESULTS – SINK

	XRF RESULTS: SINK					All results are in part per million (PPM)														
Sample #	Na	Mg	Al	Si	P	S	Cl	K	Ca	Ti	Mn	Fe								
30	0.425	1.352	17.35	56.28	0.2449	1819	2839	1.395	0.9304	0.8614	0.2781	7.681								
	V	Cr	Co	Ni	Cu	Zn	Ga	Ge	As	Se	Br	Rb	Sr	Y	Zr	Nb	Mo	Ag	Cd	In
30	175	42	< 8.4	18.6	60	94	17.7	1.1	23	1.8	84	63	57	21	159	6.9	0.9	< 0.4	< 0.5	< 0.7
	Sn	Sb	Te	I	Cs	Ba	La	Ce	Pr	Nd	Hf	Ta	W	Hg	Tl	Pb	Bi	Th	U	
30	1.8	< 0.9	< 1.2	31	4.3	300	13	26	< 8.0	18.3	6.4	< 3.8	2.3	< 0.4	0.7	24	< 0.4	6.9	2.7	

APPENDIX I

RESAMPLING MACRO

The resampling macro was authored by Dr. W.P. de Lange, Earth and Ocean Science Department, University of Waikato, to automate the resampling of the pilot study geochemical landuse data.

```
_
' This program is intended to undertake repeated discriminant function analyses
' while removing triples of the existing cases
' Created for Brendan Roddy

Option Base 1

' Define variables
Dim newanalysis As Analysis
Dim raw As Spreadsheet
Dim Atemp As Spreadsheet
Dim Btemp As Spreadsheet
Dim outcome As Spreadsheet
Dim Pos1 As Integer
Dim Pos2 As Integer
Dim ii0 As Integer
Dim ii1 As Integer
Dim ii2 As Integer
Dim ii3 As Integer
Dim jj1 As Integer
Dim CaseCount As Integer
Dim label As String
Dim label2 As String
_____
Sub Main
' Open spreadsheet to contain results
Set outcome = Spreadsheets.New ("E:\Stats files\BS_outcome.sta")
outcome.SetSize 730,10
outcome.Visible = False
```

```
' Add header information to outcome
outcome.Header = "Summary of repeated discriminant analyses with omitted
cases"
outcome.InfoBox="Three cases" + vbCrLf + "omitted" + vbCrLf + "1 per
landuse"
outcome.VariableName(1) = "Case L1"
outcome.VariableName(2) = "Case L2"
outcome.VariableName(3) = "Case L3"
outcome.VariableName(4) = "Rank 1"
outcome.VariableName(5) = "Rank 2"
outcome.VariableName(6) = "Rank 3"
outcome.VariableName(7) = "Rank 4"
outcome.VariableName(8) = "Rank 5"
outcome.VariableName(9) = "Total %"
outcome.VariableName(10) = "Wilks' Lambda"
outcome.AutoFitCase
outcome.AutoFitVariables


ii0 = 0
For ii1 = 1 To 9
For ii2 = 11 To 19
For ii3 = 21 To 29

        ii0 = ii0 + 1
        label = Str(ii1) + " " + Str(ii2) + " " + Str(ii3)

' Open Brendan's data file
        Set raw = Spreadsheets.Open ("E:\Stats files\BS_spreadsheet.sta")
        raw.Visible = False

' Define discriminant function analysis
        Set newanalysis = Analysis (scDiscriminantAnalysis, raw)
        With newanalysis.Dialog
        .Variables = "2 | 6-12"
        .Codes = "1-3"
        .CasewiseDeletionOfMD = True
        .AdvancedOptions = True
        End With

        newanalysis.SelectionConditionSource = scSourceLocal
        With newanalysis.SelectionCondition
        .Enabled = True
        .ExcludeList = label
        End With

        newanalysis.Run
```

```
'       If ii0 = 1 Then
        With newanalysis.Dialog
           .Variables = "6-12"
        .Method = scDisForwardStepwise
        .Tolerance = 0.01
        .FToEnter = 1
        .FToRemove = 0
        .NumberOfSteps = 7
        .DisplayResults = scDisSummaryOnly
        End With

        newanalysis.Run
'       End If

        With newanalysis.Dialog
        .APrioriProbabilitiesProportionalToGroupSizes = True
        .SaveClassifications = True
        .MaxNumberOfCasesInSpreadsheetsAndGraphs = 100000
        End With

        Set Atemp = newanalysis.Dialog.Summary(1)
        Atemp.Visible = False
        Set Btemp = newanalysis.Dialog.ClassificationMatrix(1)
        Btemp.Visible = False
        outcome.Cells(ii0,1) = ii1
        outcome.Cells(ii0,2) = ii2
        outcome.Cells(ii0,3) = ii3
        CaseCount = Atemp.Cases.Count
        If CaseCount > 5 Then
                CaseCount = 5
        End If
        For jj1=1 To CaseCount
                label = Atemp.CaseHeaderCell(jj1)
                outcome.Cells(ii0,3+jj1) = label
        Next jj1
        outcome.Cells(ii0,9) = Btemp.Cells(4,1)
        label = Atemp.Header
        Pos1 = InStr(label,"Wilks")
        Pos2 = InStr(label,"Exclude")
        If Pos1 = 0 Then
                outcome.Cells(ii0,10) = label
        Else
                Pos1 = Pos1 + 14
                If Pos2=0 Then
                        Pos2 = Len(label)
                Else
```

```
                    Pos2 = Pos2 - 2
                End If
                Pos2 = Pos2 - Pos1 + 1
                label2 = Mid(label,Pos1,Pos2)
                outcome.Cells(ii0,10) = label2
        End If
        Atemp.Close(False)
        Btemp.Close(False)
        raw.Close(False)

Next ii3
Next ii2
Next ii1
outcome.Variable(10).AutoFit
outcome.Visible = True

End Sub
```

APPENDIX J

RATIONALE FOR THE ANALYSIS AND RECOVERY OF THE <10 MICRON PARTICLE SIZE FRACTION

Sediment fingerprinting studies have used the < 63 μm fraction to analyse for geochemical or other properties (e.g., Owens *et al.* 1999b; Collins *et al.* 2001; Walling *et al.* 2006). The < 63 μm fraction is used because it constitutes over 95% of the suspended sediment load transported in rivers (Walling *et al.* 2000). The problem of using the <63μm for sediment fingerprinting is that there is a wide range of particle sizes present within the sediment, and particle size exerts a large influence on a range of sediment properties, especially mineralogy (Walling & Moorehead 1989). Nutrients such as phosphorus and nitrogen are also preferentially associated with the very fine fraction (< 2 μm). Some studies have tried to account for the particle size difference within the < 63 μm by using particle size correction calculations (e.g., Krause *et al.* 2003), but this assumes a linear relationship and should only be used if such a relationship is established for all tracers used (Fu *et al.* 2008; Davis & Fox 2009).

A simple and cost effective way of eliminating issues associated with tracer variation with particle size is to limit the size fraction for analysis to the < 10 μm. While there are precedents for the < 10 μm fraction in the literature (e.g., Wallbrink 2004; Douglas *et al.* 2007; Smith & Dragovich 2008; Hughes *et al.* 2009), this approach is open to accusation that it is not representative of the suspended sediment transported from source to sink. The Walling *et al.* (2000) study that concluded that most of the suspended sediment load of rivers was < 63 μm, also found that the median (d_{50}) values ranged between 4.1 and 13.5 μm, so on one hand it could be argued that the < 10 μm is still measuring around half of the fluvial suspended sediment load. In another study of four UK rivers, the mean particle size distribution for the 0-10 μm ranged from 76% to 95% (Table L-1) (Walling & Kane 1982).

Table L-1. Mean particle size distribution by percent for four rivers in the Devon catchment, UK (Walling & Kane 1982).

	0-0.5μm	0.5-2μm	2-10μm	10-62μm	*0-10μm %*
Exe	19	22	38	21	***79***
Creedy	29	24	33	14	***86***
Dart	26	19	31	24	***76***
Jackmoor	54	26	15	5	***95***

A recent study has found that the selection of < 10 μm or < 63 μm fractions makes little difference to the mixing model results from a sediment fingerprinting investigation (Fu *et al.* 2008). Another investigation of metals and trace element affinity with either the < 2 μm or the < 20 μm fraction of fluvial suspended sediment found that there is a general positive correlation with both size fractions and the < 20 μm should be used for ease of separation by sieving (Muller *et al.* 2001).

Another argument for using the smallest possible fraction is the selective erosion/delivery process. Only a small fraction of eroded soils are delivered to the river mouth, and the delivered sediment will be enriched with the fine fraction (Walling & Moorehead 1989). The fine fraction (particularly clays) has the lowest enrichment between source and sink as they are readily transportable compared to loams and sands and therefore potentially provide the 'best' signal of erosion at a catchment scale (Walling & Moorehead 1989).

Most soil and sediment studies fully disperse the sediment into its primary particles or its 'ultimate' particle size, but it is the 'effective' particle size that governs the actual behaviour of the transported sediment (Slattery & Burt 1997). There is an order of magnitude difference between the effective and ultimate particle sediment size and there is no clear understanding of whether the aggregates are survivors of the primary erosion process or caused by secondary in-stream processes (Walling & Moorehead 1989; Walling & Amos 1999). As the Whangapoua catchments streams are relatively

short and non-saline, the assumption will be that the aggregation is mainly due to primary erosion processes. The aim of sediment fingerprinting is to link source areas with the sink, and that this link is best established by analysing the effective particle size. Consequently the effective < 10 μm was used as the size fraction for analysis in this research.

The settling process by which the <10μm particle size is recovered is based on the principles described by (Oden 1915 as cited in Lovell & Rose 1988), that after a given time particles settling down a certain height can be separated in this way (McCave & Syvitski 1991; Bungartz & Wanner 2004). The settling method is based on Stokes Law that spherical sediment grains of a uniform density will settle at given rates in non-turbulent fluid at a known temperature (Vanoni 1975). While the settling method based on Stokes Law and is a widely used and cost effective method for particle size determination or particle size separation, some problems have been reported such as a modal distribution around the target size fraction, density and turbulence variations in the settling tube (Clifton *et al.* 1999). Also, the settling velocity is a function of a particles shape, surface texture, and degree of roundness (Lovell & Rose 1988) and these properties are not uniform in a sediment sample and the implicit assumptions within Stokes Law is that the sediment is comprised of spherical grains that settle freely in non-turbulent flow which is rarely found in laboratory conditions (Clifton *et al.* 1999).

APPENDIX K

ICP-MS RESULTS – SOURCE AREA

Landuse	Position	Sample	Weight	Li 7	Li-corr	B 10	B-corr	Na 23	Na-corr	Mg 24	Mg-corr	Al 27	Al-corr	Si 28	Si-corr	P 31	P-corr
1=N,2=Ex, 3=Ag	4=surf, 5=sub	#			PPM		PPB		PPM		PPM		PPM		PPM		PPM
4=sink	6=bank, 100=slip																
1	4	34	0.2139	81.30	19.51	0.17	41.04	184.26	44.22	11135.28	2672.15	65942.27	15824.30	67.13	16.11	863.52	207.22
1	4	38	0.2004	13.00	3.33	0.28	72.49	193.44	49.55	1933.77	495.31	20878.27	5347.71	66.39	17.00	661.50	169.44
1	4	41	0.2016	18.42	4.69	0.02	5.60	221.00	56.27	4181.30	1064.61	47100.50	11992.40	91.81	23.38	576.16	146.70
1	4	47	0.2018	11.52	2.93	-0.12	-29.25	135.45	34.45	2555.73	650.08	24543.13	6242.81	28.34	7.21	875.55	222.70
1	4	53	0.2005	10.73	2.75	0.15	39.17	261.46	66.94	2541.84	650.74	24176.21	6189.35	0.85	0.22	1479.82	378.85
1	4	56	0.2079	1.80	0.44	-0.30	-73.82	168.46	41.59	4244.05	1047.85	34593.34	8541.01	218.57	53.96	645.92	159.48
1	4	63	0.207	4.42	1.10	-0.41	-101.17	132.01	32.74	4588.07	1137.71	47882.16	11873.39	273.27	67.76	1209.34	299.88
1	4	R-63	**0.2012**	6.68	1.70	0.62	158.17	193.26	49.30	4126.10	1052.65	87937.75	22434.62	248.01	63.27	622.43	158.79
1	4	66	0.2026	4.35	1.10	-0.85	-214.34	206.26	52.26	2269.44	574.98	32330.19	8191.06	78.67	19.93	454.71	115.20
1	4	69	0.2053	3.31	0.83	-1.05	-263.53	257.24	64.32	4040.09	1010.12	24213.65	6054.00	117.76	29.44	754.73	188.70
1	4	72	0.2042	1.27	0.32	-1.29	-325.02	293.47	73.77	4272.99	1074.11	25921.39	6515.89	119.01	29.91	834.92	209.87
1	4	75	0.2023	1.03	0.26	-0.96	-243.84	246.28	62.49	7032.63	1784.40	28889.23	7330.12	267.48	67.87	572.71	145.32
1	5	35	0.2031	52.08	13.16	-0.04	-9.86	97.76	24.71	6624.70	1674.28	31789.85	8034.33	316.60	80.01	828.67	209.43
1	5	39	0.2025	10.51	2.66	-0.08	-19.52	81.50	20.66	360.05	91.27	10712.47	2715.41	365.08	92.54	86.40	21.90
1	5	42	0.2068	17.35	4.31	-0.40	-100.03	113.44	28.16	2604.53	646.47	46523.14	11547.55	158.79	39.41	171.85	42.66
1	5	48	0.2031	6.05	1.53	-0.49	-124.34	60.55	15.30	692.71	175.07	21991.98	5558.09	381.87	96.51	403.19	101.90
1	5	54	0.2021	24.76	6.29	0.45	114.80	233.09	59.20	1879.89	477.46	56809.05	14428.54	29.55	7.51	676.69	171.87
1	5	57	0.206	3.79	0.95	-0.55	-137.54	97.74	24.35	3088.22	769.51	44284.69	11034.63	825.71	205.75	369.02	91.95
1	5	64	0.2094	9.60	2.35	-1.19	-290.48	189.84	46.53	3019.55	740.18	73229.66	17950.71	432.73	106.07	215.54	52.83
1	5	67	0.2025	5.22	1.32	-1.24	-313.05	167.65	42.50	958.23	242.89	32195.92	8161.07	78.48	19.89	160.85	40.77
1	5	70	0.2031	4.65	1.18	-1.66	-418.27	117.14	29.61	1008.07	254.77	30958.16	7824.14	396.44	100.19	184.99	46.75
1	5	73	0.2046	2.10	0.53	-1.25	-313.85	158.86	39.85	3301.88	828.37	34917.12	8760.00	291.86	73.22	413.48	103.73
1	5	76	0.2017	1.55	0.39	-1.38	-351.70	176.65	44.95	2978.48	757.98	33960.19	8642.42	182.00	46.32	300.93	76.58
1	6	37	0.2086	38.85	9.56	-0.26	-64.47	98.39	24.21	4920.24	1210.72	40805.38	10040.94	157.92	38.86	1059.37	260.68
1	6	40	0.2047	25.86	6.48	-0.04	-9.78	251.67	63.11	2778.30	696.68	34423.05	8631.83	182.04	45.65	466.86	117.07
1	6	43	0.2033	32.03	8.09	-0.26	-64.64	219.50	55.42	10072.55	2543.16	42341.33	10690.51	173.16	43.72	526.06	132.82
1	6	49	0.2225	28.65	6.61	-0.47	-108.66	117.05	27.00	3560.63	821.43	32344.64	7461.80	152.44	35.17	341.63	78.81
1	6	55	0.2007	49.06	12.55	-0.35	-88.75	95.05	24.31	7181.62	1836.73	36131.98	9240.93	217.77	55.70	577.19	147.62
1	6	58	0.204	3.51	0.88	-0.64	-161.04	165.89	41.74	2968.49	744.41	37373.85	9403.92	367.66	92.51	249.80	62.85
1	6	65	0.2066	7.05	1.75	-1.38	-342.12	195.23	48.51	6213.68	1543.80	40959.12	10176.34	176.70	43.90	233.72	58.07
1	6	68	0.2036	2.26	0.57	-1.59	-401.87	160.07	40.36	1027.11	258.95	16792.49	4233.59	144.84	36.52	197.19	49.71
1	6	71	0.2029	3.15	0.80	-1.35	-340.26	244.29	61.80	2047.17	517.90	26860.02	6795.09	209.78	53.07	215.77	54.59
1	6	R-74	0.2086	3.43	0.84	-0.38	-93.51	324.58	79.87	5394.86	1327.51	47341.47	11649.27	393.36	96.79	1031.26	253.76
1	6	77	0.2033	1.88	0.48	-1.61	-405.74	258.80	65.34	5178.79	1307.56	32061.56	8095.03	225.37	56.90	563.72	142.33
2	4	50	0.205	2.32	0.58	-0.16	-39.56	197.69	49.50	969.35	242.72	16741.89	4192.01	89.07	22.30	539.45	135.07
2	4	59	0.2037	10.60	2.67	0.35	86.94	96.09	24.21	1396.29	351.85	43325.14	10917.43	163.46	41.19	356.31	89.79
2	4	78	0.2026	22.99	5.82	-1.28	-324.55	142.59	36.13	6001.26	1520.46	22976.29	5821.19	246.02	62.33	1343.15	340.30
2	4	81	0.2037	17.22	4.34	-1.38	-348.50	207.31	52.24	2315.71	583.53	37681.19	9495.21	250.90	63.22	341.76	86.12
2	4	84	0.2059	9.33	2.33	-1.26	-314.61	220.62	55.00	2880.10	718.00	54940.84	13696.52	196.48	48.98	841.28	209.73
2	4	87	0.2237	3.33	0.76	-1.26	-289.12	222.83	51.13	2728.59	626.10	35288.37	8097.24	257.97	59.19	923.49	211.90
2	4	90	0.2038	2.37	0.60	-1.08	-271.76	114.34	28.80	2750.01	692.63	54213.05	13654.35	656.25	165.29	454.49	114.47
2	4	93	0.2022	7.59	1.93	-1.29	-327.22	324.18	82.30	9089.78	2307.51	47878.56	12154.34	357.25	90.69	755.20	191.71
2	4	96	0.2026	3.09	0.78	-0.37	-93.24	197.29	49.98	2290.96	580.43	49014.94	12418.25	325.40	82.44	355.88	90.16
2	4	99	0.2099	1.54	0.38	-1.44	-352.14	284.03	69.46	4668.26	1141.60	43403.13	10614.02	855.97	209.32	531.24	129.91
2	4	102	0.2016	0.97	0.25	-1.29	-328.45	229.00	58.31	3162.23	805.15	31238.42	7953.71	222.08	56.54	444.06	113.06
2	4	105	0.2103	2.07	0.51	-1.51	-367.83	283.25	69.13	5320.53	1298.63	43870.68	10707.95	212.64	51.90	835.66	203.97
2	4	108	0.2088	1.81	0.44	-1.45	-356.70	332.52	81.74	3112.64	765.19	43459.52	10683.80	135.58	33.33	407.90	100.28
2	4	111	0.2028	8.12	2.05	-0.82	-208.56	314.96	79.72	14380.16	3639.71	41925.37	10611.58	2058.20	520.94	1101.21	278.72
2	4	114	0.2061	1.50	0.37	-1.38	-344.19	226.03	56.29	3830.79	954.07	33892.02	8440.94	1339.07	333.50	599.68	149.35
2	4	117	0.2016	5.75	1.46	-1.27	-322.09	205.68	52.37	4741.32	1207.20	49644.39	12640.11	2007.30	511.08	490.09	124.78
2	4	120	0.2063	9.42	2.34	-1.61	-400.84	310.15	77.17	2598.14	646.45	53843.55	13396.94	991.63	246.73	547.31	136.18
2	4	123	0.2034	1.81	0.46	-1.19	-300.06	350.61	88.48	6214.40	1568.26	28951.84	7306.28	1755.97	443.14	785.62	198.26
2	4	126	0.2036	1.69	0.43	-1.53	-386.74	277.46	69.95	5719.26	1441.89	46037.32	11606.66	2007.65	506.15	706.91	178.22
2	4	129	0.2026	12.39	3.14	-1.28	-323.54	253.39	64.20	2024.48	512.91	51160.70	12961.89	883.85	223.93	516.43	130.84
2	4	132	0.207	1.93	0.48	-1.43	-354.10	220.97	54.79	2404.67	596.29	31286.98	7758.26	914.07	226.66	392.37	97.30
2	4	135	0.2048	1.15	0.29	0.32	80.45	233.12	58.43	3627.49	909.18	17411.11	4363.83	658.97	165.16	686.36	172.03
2	4	138	0.2084	2.20	0.54	-1.13	-277.59	314.60	77.49	5087.49	1253.08	47645.10	11735.24	2248.88	553.91	336.53	82.89
2	5	51	0.2034	4.18	1.05	-0.32	-80.00	70.72	17.85	221.14	55.81	22096.83	5576.35	216.63	54.67	31.30	7.90
2	5	60	0.2015	5.80	1.48	-0.25	-64.19	61.97	15.79	498.22	126.92	35974.73	9164.18	207.22	52.79	48.47	12.35
2	5	79	0.2021	46.50	11.81	-1.16	-293.86	262.76	66.74	7780.96	1976.23	45823.11	11638.30	379.29	96.33	701.13	178.08
2	5	82	0.2091	15.52	3.81	-1.45	-354.96	159.68	39.20	1811.55	444.70	40768.73	10007.93	241.22	59.21	166.64	40.91
2	5	85	0.2028	7.53	1.91	-1.37	-346.50	135.05	34.18	766.11	193.91	50306.81	12732.98	229.09	57.98	134.44	34.03
2	5	88	0.2087	0.34	0.08	-0.94	-231.69	401.63	98.78	806.65	198.40	12586.62	3095.69	61.64	15.16	311.55	76.63
2	5	91	0.2096	5.93	1.45	-1.53	-375.18	152.66	37.38	2898.41	709.81	61617.93	15089.93	561.51	137.51	227.85	55.80
2	5	94	0.2007	2.51	0.64	-1.53	-391.56	137.02	35.04	1982.86	507.12	48796.43	12479.92	616.28	157.62	104.83	26.81
2	5	97	0.2047	1.89	0.47	-1.57	-392.44	143.62	36.01	810.68	203.28	45023.14	11289.88	786.12	197.13	25.73	6.45
2	5	100	0.2072	1.39	0.35	-1.51	-374.07	196.17	48.60	2615.56	647.96	42179.43	10449.18	918.18	227.46	71.04	17.60
2	5	103	0.2031	1.84	0.46	-1.73	-436.22	289.93	73.27	707.67	178.85	51855.35	13105.54	177.26	44.80	64.16	16.21
2	5	106	0.2052	1.60	0.40	-1.58	-395.73	270.92	67.77	2180.56	545.46	54155.82	13546.87	382.50	95.68	192.18	48.07
2	5	109	0.2204	1.26	0.29	-1.45	-337.23	304.85	71.00	1797.97	418.74	44518.68	10368.17	135.84	31.64	164.08	38.21
2	5	112	0.2015	2.21	0.56	-1.30	-329.89	212.64	54.17	1933.46	492.53	38846.45	9895.72	1725.23	439.48	203.07	51.73
2	5	115	0.2029	0.59	0.15	-1.10	-277.02	187.26	47.37	2443.73	618.22	33949.03	8588.49	1439.24	364.10	245.67	62.15
2	5	118	0.2043	4.25	1.07	-1.87	-468.83	136.75	34.36	2632.43	661.39	47639.57	11969.35	1781.81	447.68	558.00	140.20
2	5	121	0.1714	4.60	1.38	3.99	1194.31	866.23	259.41	1453.18	435.19	47503.51	14226.11	1285.68	385.03	84.83	25.40
2	5	124	0.2159	1.56	0.37	-1.99	-472.17	295.93	70.36	6641.34	1578.97	31257.09	7431.34	516.06	122.69	219.38	52.16
2	5	127	0.2014	0.61	0.16	-1.92	-489.85	262.13	66.81	3854.40	982.36	31230.75	7959.66	2022.67	515.51	353.03	89.96
2	5	130	0.2027	10.35	2.62	-1.88	-476.58	255.98	64.82	1459.16	369.51	42454.03	10750.69	842.05	213.23	278.22	70.45
2	5	133	0.2059	13.26	3.31	-1.84	-457.96	169.79	42.33	1830.84	456.42	38872.72	9690.81	1361.14	339.33	172.06	42.89
2	5	136	0.2044	0.33	0.08	0.22	54.75	118.52	29.76	496.10	124.58	27290.95	6853.45	768.11	192.89	111.14	27.91
2	5	139	0.2098	3.89	0.95	-1.16	-283.32	302.22	73.94	3829.32	936.89	52451.16	12832.78	2322.92	568.33	83.47	20.42
2	6	52	0.2022	25.52	6.48	0.03	8.12	157.77	40.05	2271.15	576.55	40413.40	10259.25	73.39	18.63	660.06	167.56
2	6	61	0.2037	9.34	2.35	-1.01	-254.76	281.45	70.92	6809.09	1715.81	40104.30	10105.81	424.93	107.08	401.15	101.06
2	6	80	0.2067	46.76	11.61	-1.32	-326.80	235.16	58.40	8863.37	2201.05	35109.46	8718.76	320.18	79.51	780.48	193.82
2	6	83	0.2036	16.84	4.25	-1.36	-343.63	251.01	63.28	3049.28	768.76	52505.42	13237.25	181.82	45.84	515.91	130.07
2	6	86	0.2041	4.72	1.19	-1.37	-343.29	68.16	17.14	789.67	198.60	34693.99	8725.34	148.68	37.39	451.21	113.48
2	6	89	0.2063	5.75	1.43	-1.44	-357.05	256.82	63.90	5240.65	1303.94	38715.58	9632.92	476.29	118.51	610.92	152.01

Landuse	Position	Sample	Weight	Li 7	Li-corr	B 10	B-corr	Na 23	Na-corr	Mg 24	Mg-corr	Al 27	Al-corr	Si 28	Si-corr	P 31	P-corr
1=N,2=Ex, 3=Ag	4=surf, 5=sub	#			PPM		PPB		PPM		PPM		PPM		PPM		PPM
4=sink	6=bank, 100=slip																
2	6	**92**	0.2015	5.77	1.47	-1.36	-346.45	217.56	55.42	5362.87	1366.14	43877.22	11177.26	507.67	129.32	438.85	111.79
2	6	**95**	0.2033	6.31	1.59	-1.73	-436.80	263.25	66.47	6246.65	1577.18	50777.46	12820.50	823.52	207.93	211.81	53.48
2	6	**98**	0.2006	2.85	0.73	-1.44	-368.47	234.95	60.12	2990.78	765.29	40869.33	10457.74	443.89	113.58	182.36	46.66
2	6	**101**	0.206	2.35	0.59	-1.54	-384.23	226.01	56.32	5954.60	1483.74	53055.60	13220.12	313.63	78.15	460.07	114.64
2	6	**104**	0.2009	1.05	0.27	-1.62	-412.63	197.38	50.43	2241.57	572.72	32509.10	8306.08	491.77	125.65	69.64	17.79
2	6	**107**	0.207	2.12	0.53	-1.56	-385.59	285.03	70.68	4653.62	1153.96	39291.31	9743.11	275.09	68.21	333.04	82.58
2	6	**110**	0.2027	1.98	0.50	-0.63	-158.27	424.55	107.51	2500.88	633.30	44429.76	11251.01	1573.05	398.35	103.85	26.30
2	6	**113**	0.2041	6.92	1.74	-1.47	-369.95	332.60	83.65	8105.10	2038.39	42129.57	10595.35	1835.24	461.55	453.40	114.03
2	6	**116**	0.2038	2.22	0.56	-1.75	-440.01	208.70	52.56	2772.49	698.29	36125.79	9098.81	1563.64	393.82	504.21	126.99
2	6	**119**	0.2009	3.11	0.79	-2.08	-531.70	238.10	60.83	4575.66	1169.08	28592.45	7305.38	1098.76	280.73	362.87	92.71
2	6	**122**	0.2076	11.88	2.94	-1.66	-411.43	224.19	55.43	4862.80	1202.35	37674.58	9315.20	767.88	189.86	679.68	168.05
2	6	**125**	0.203	1.58	0.40	-1.57	-397.24	346.16	87.53	6077.76	1283.95	30783.82	7783.91	2386.88	603.54	155.58	39.34
2	6	**128**	0.2029	0.75	0.19	-1.72	-436.14	328.02	82.98	8673.98	2194.36	24017.08	6075.88	2300.44	581.97	343.76	86.97
2	6	**131**	0.2073	3.58	0.89	-1.63	-402.37	253.04	62.66	1992.61	493.39	26982.33	6681.15	890.27	220.44	144.87	35.87
2	6	**134**	0.2039	17.36	4.37	-0.64	-161.37	217.85	54.84	3397.57	855.31	26650.14	6708.93	1100.31	276.99	136.23	34.30
2	6	**137**	0.2017	23.07	5.87	-1.01	-257.03	166.02	42.25	3223.52	820.34	36098.34	9186.55	955.22	243.09	63.65	16.20
2	6	**140**	0.2063	3.70	0.92	-1.52	-378.94	254.75	63.39	4919.86	1224.12	38826.22	9660.45	1367.18	340.17	160.30	39.89
3	4	**141**	0.2024	4.68	1.19	-0.86	-217.34	148.02	37.54	1491.87	378.35	27966.57	7092.51	833.69	211.43	2548.66	646.36
3	4	**144**	0.2025	8.87	2.25	-0.70	-177.69	206.08	52.24	2436.99	617.73	70667.62	17912.93	1180.75	299.30	4027.79	1020.97
3	4	**147**	0.2063	1.74	0.43	-0.82	-205.02	156.05	38.83	3154.23	784.81	36966.96	9197.84	1903.32	473.57	4253.56	1058.34
3	4	**150**	0.2023	2.62	0.66	-0.87	-221.51	147.62	37.46	1904.11	483.13	33329.46	8456.75	1229.97	312.08	2625.77	666.24
3	4	**153**	0.2028	8.55	2.16	-1.34	-339.92	249.75	63.21	9796.43	2479.54	45390.35	11488.59	1897.93	480.38	6490.31	1642.74
3	4	**156**	0.2021	10.34	2.63	-0.81	-204.46	643.50	163.44	8542.55	2169.66	44945.74	11415.46	1964.71	499.00	4939.21	1254.48
3	4	**159**	0.2025	4.22	1.07	0.35	87.70	213.61	54.15	2306.36	584.62	42706.83	10825.39	1692.09	428.91	5403.25	1369.62
3	4	**162**	0.2007	5.70	1.46	1.12	286.70	230.00	58.82	2829.45	723.64	75366.40	19275.32	1935.44	495.00	2756.25	704.92
3	4	**165**	0.2041	9.70	2.44	16.63	4181.60	2076.32	522.18	4161.12	1046.50	130207.27	32746.39	103.01	25.91	7942.97	1997.61
3	4	**168**	0.2011	9.68	2.47	46.38	11839.34	4515.98	1152.69	6100.16	1557.04	106870.66	27278.32	742.75	189.59	12351.44	3152.66
3	4	**171**	0.2031	7.30	1.85	-1.03	-261.33	210.70	53.25	2523.39	637.74	33037.24	8349.59	1291.31	326.36	4525.91	1143.84
3	4	**174**	0.2012	13.72	3.50	-0.52	-133.68	284.47	72.57	2850.20	727.14	89531.99	22841.34	1369.13	349.29	7186.23	1833.35
3	4	**177**	0.2034	1.71	0.43	-1.23	-310.40	220.45	55.63	3561.52	898.78	28367.41	7158.80	1621.07	409.09	1681.75	424.41
3	4	**180**	0.2065	6.47	1.61	-0.26	-60.63	150.23	39.30	2106.30	523.57	51970.20	12910.33	1271.41	316.04	1100.59	293.46
3	4	**183**	0.2015	37.10	9.45	-1.21	-307.98	207.08	52.75	9245.78	2355.26	42039.13	10709.02	1276.21	325.10	3171.17	807.82
3	4	**186**	0.2018	50.61	12.87	-1.46	-372.13	361.59	91.97	10871.44	2765.27	48719.15	12392.24	1190.62	302.85	2658.15	676.13
3	5	**142**	0.2033	5.54	1.40	-1.78	-450.43	98.01	24.75	665.65	168.06	31295.55	7901.63	1122.13	283.32	74.79	18.88
3	5	**145**	0.2034	9.91	2.50	10.05	2537.23	819.99	206.93	1394.32	351.87	286701.64	72351.99	469.90	118.58	621.72	156.90
3	5	**148**	0.2036	0.99	0.25	15.95	4020.18	501.70	126.48	976.53	246.19	37282.75	9399.43	1074.83	270.98	180.40	45.48
3	5	**151**	0.2032	4.31	1.09	-1.57	-396.09	106.35	26.87	933.46	235.80	37810.64	9551.28	1154.39	291.61	208.58	52.69
3	5	**154**	0.2006	3.05	0.78	31.86	8151.39	339.02	86.75	687.94	176.03	387672.17	99198.47	3113.11	796.59	316.37	80.95
3	5	**157**	0.2088	9.54	2.34	-1.52	-374.40	519.49	127.71	8418.40	2069.52	45605.29	11211.30	2044.00	502.48	1007.86	247.77
3	5	**160**	0.201	2.22	0.57	-1.08	-275.80	175.71	44.87	1091.15	278.65	41956.26	10714.50	1675.53	427.89	420.42	107.36
3	5	**163**	0.2022	2.93	0.74	-1.07	-272.39	199.01	50.52	884.37	224.50	89669.47	22763.27	1532.04	388.92	90.36	22.94
3	5	**166**	0.2034	13.38	3.38	-1.71	-430.78	81.41	20.55	1112.30	280.70	63748.92	16087.67	1352.60	341.34	336.74	84.98
3	5	**169**	0.2083	11.37	2.80	-1.56	-385.41	320.77	79.04	1752.73	431.91	48229.62	11884.91	1554.61	383.09	367.03	90.44
3	5	**172**	0.2039	10.47	2.64	-1.87	-471.26	130.89	32.95	1201.79	302.54	46752.87	11769.62	1472.86	370.78	196.04	49.35
3	5	**175**	0.2016	9.43	2.40	-1.92	-488.86	243.18	61.92	1945.84	495.44	48705.75	12401.12	1851.43	471.40	200.92	51.16
3	5	**178**	0.202	1.84	0.47	-1.63	-412.93	198.19	50.36	1401.90	356.24	47886.52	12168.39	1862.57	473.30	375.30	95.37
3	5	**181**	0.2005	2.00	0.51	-1.12	-285.45	145.13	37.15	801.69	205.24	33444.26	8562.06	1422.22	364.10	107.97	27.64
3	5	**184**	0.203	37.20	9.41	-1.42	-359.06	267.99	67.76	9107.18	2302.82	42752.12	10810.18	1730.53	437.58	938.28	237.25
3	5	**187**	0.2042	16.54	4.16	-1.89	-474.34	269.08	67.64	3390.76	852.34	37896.86	9526.18	1356.56	341.00	177.75	44.68
3	6	**143**	0.2065	9.94	2.47	-1.28	-316.93	205.31	51.04	1055.31	262.32	41712.39	10368.51	1287.54	320.04	158.70	39.45
3	6	**146**	0.2037	8.03	2.02	-1.48	-372.19	243.19	61.28	1607.11	404.97	60889.18	15343.36	1733.31	436.77	136.15	34.31
3	6	**149**	0.2088	0.62	0.15	-1.65	-404.40	226.44	55.67	2069.70	508.80	25824.11	6348.43	1705.57	419.29	62.27	15.31
3	6	**152**	0.2045	3.73	0.93	-1.52	-381.77	144.84	36.36	861.02	216.12	32108.58	8059.33	1298.37	325.89	254.22	63.81
3	6	**155**	0.2095	8.45	2.07	-1.13	-275.88	475.90	116.60	9618.83	2356.73	47459.01	11628.02	2313.04	566.72	577.44	141.48
3	6	**158**	0.2147	11.42	2.73	-1.23	-294.54	444.11	106.18	9390.97	2245.17	44457.46	10628.79	1860.95	444.91	757.40	181.08
3	6	**161**	0.2016	2.57	0.65	0.12	31.06	301.60	76.79	3169.57	807.01	36197.12	9216.26	2175.24	553.85	207.87	52.93
3	6	**164**	0.2041	3.53	0.89	-1.06	-267.34	365.55	91.93	3888.08	977.83	34641.17	8712.06	2203.45	554.16	624.98	157.18
3	6	**167**	0.204	16.18	4.07	-1.91	-480.09	260.76	65.61	5259.15	1323.29	33032.88	8311.66	1164.12	292.91	606.98	152.73
3	6	**170**	0.205	5.56	1.39	-1.93	-484.00	237.69	59.51	2553.85	639.46	40720.80	10196.09	1451.01	363.32	293.37	73.46
3	6	**173**	0.2037	5.59	1.41	-1.84	-463.66	196.92	49.62	1628.98	410.48	36149.08	9109.14	1482.48	373.57	181.84	45.82
3	6	**176**	0.2043	5.58	1.40	-1.81	-454.26	203.58	51.15	1229.42	308.89	32215.73	8094.14	1589.59	399.38	189.99	47.73
3	6	**179**	0.203	3.81	0.96	-1.58	-400.27	314.77	79.59	6282.43	1588.56	39189.32	9909.30	2501.31	632.47	123.02	31.11
3	6	**182**	0.2065	1.95	0.49	-1.24	-308.23	175.07	43.52	1103.31	274.25	26670.28	6629.47	1474.70	366.57	330.38	82.12
3	6	**185**	0.2022	39.61	10.06	-1.96	-497.56	311.81	79.16	10629.94	2698.49	47762.19	12124.79	1758.47	446.40	1214.14	308.22
3	6	**188**	0.2015	47.96	12.22	-1.57	-400.96	321.75	81.96	9342.16	2379.82	41025.35	10450.78	1245.72	317.33	787.17	200.52

Landuse	Position	Sample	Weight	S 34	S-corr	K 39	K-corr	Ca 43	Ca-corr	V 51	V-corr	Cr 52	Cr-corr	Fe 54	Fe-corr	Mn 55	Mn-corr
1=N,2=Ex, 3=Ag	4=surf, 5=sub	#			PPM		PPM		PPM		PPM		PPM		PPM		PPM
4=sink	6=bank, 100=slip																
1	4	**34**	0.2139	625.35	150.07	2869.16	688.52	1881.00	451.39	166.73	40.01	30.26	7.26	81588.44	19578.94	2982.55	715.73
1	4	**38**	0.2004	880.36	225.49	3943.71	1010.13	2363.59	605.40	48.72	12.48	12.36	3.17	52001.52	13319.55	486.12	124.51
1	4	**41**	0.2016	828.14	210.86	2289.86	583.03	2318.05	590.21	133.17	33.91	20.61	5.25	48905.00	12451.85	1307.88	333.00
1	4	**47**	0.2018	1122.51	285.52	3107.45	790.41	2224.53	565.83	117.47	29.88	26.29	6.69	74666.42	18992.21	4017.57	1021.91
1	4	**53**	0.2005	4344.66	1112.28	2136.41	546.94	3340.27	855.14	52.86	13.53	39.19	10.03	39761.65	10179.38	1687.38	431.99
1	4	**56**	0.2079	1146.17	282.99	1587.32	391.91	5347.63	1320.32	198.67	49.05	38.27	9.45	80850.03	19961.67	1951.31	481.77
1	4	**63**	0.207	3692.47	915.62	1044.08	258.90	4912.77	1218.22	95.00	23.56	21.93	5.44	36734.94	9109.20	1327.84	329.26
1	4	**R-63**	**0.2012**	-1094.94	-279.34	510.41	130.22	1005.06	256.41	153.00	39.03	34.15	8.71	81795.16	20867.52	133.05	33.94
1	4	**66**	0.2026	1977.99	501.14	1730.76	438.50	2436.66	617.34	133.73	33.88	156.74	39.71	49724.51	12598.02	903.27	228.85
1	4	**69**	0.2053	2660.85	665.28	2724.62	681.22	6554.37	1638.75	66.24	16.56	12.21	3.05	51825.54	12957.65	1134.65	283.69
1	4	**72**	0.2042	2758.02	693.29	3476.12	873.80	6010.21	1259.42	91.00	22.88	25.04	6.29	67030.79	16849.61	1200.14	301.68
1	4	**75**	0.2023	2412.10	612.03	2347.73	595.70	6660.23	1689.92	141.91	36.01	30.53	7.75	66737.81	16933.52	1073.11	272.28
1	5	**35**	0.2031	242.65	61.32	1901.67	480.61	475.43	120.16	127.85	32.31	23.38	5.91	103035.84	26040.52	2115.07	534.55
1	5	**39**	0.2025	-214.31	-54.32	1706.55	432.58	426.07	108.00	6.61	1.68	3.38	0.86	25937.31	6574.63	26.41	6.69
1	5	**42**	0.2068	-255.41	-63.39	1093.19	271.34	204.22	50.69	141.39	35.09	20.40	5.06	61952.34	15377.24	204.83	50.84
1	5	**48**	0.2031	172.42	43.58	793.26	200.48	155.68	39.35	140.75	35.57	26.03	6.58	86196.28	21784.61	1353.37	342.04
1	5	**54**	0.2021	1800.70	457.35	549.27	139.51	263.47	66.92	75.66	19.22	56.91	14.46	75613.88	19204.65	213.34	54.18
1	5	**57**	0.206	148.78	37.07	609.91	151.97	1172.00	292.03	243.65	60.71	45.18	11.26	122489.93	30521.40	781.10	194.63
1	5	**64**	0.2094	816.80	200.22	241.06	59.09	147.65	36.19	125.66	30.80	30.44	7.46	49742.36	12193.29	205.24	50.31
1	5	**67**	0.2025	941.45	238.64	487.45	123.56	381.67	96.75	114.68	29.07	139.09	35.26	48159.36	12207.51	181.45	45.99
1	5	**70**	0.2031	1167.84	295.15	806.87	203.92	339.74	85.86	72.34	18.28	14.43	3.65	64821.27	16382.45	106.92	27.02
1	5	**73**	0.2046	1383.69	347.14	1222.64	306.74	2932.71	735.76	121.72	30.54	29.20	7.33	74164.93	18606.48	491.28	123.25
1	5	**76**	0.2017	1699.27	432.44	1161.96	295.70	1678.04	427.04	88.16	22.44	10.33	2.63	59693.05	15191.10	354.37	90.18
1	6	**37**	0.2086	989.60	243.51	1269.15	312.30	633.74	155.94	241.05	59.31	31.91	7.85	91635.90	22548.76	837.51	206.09
1	6	**40**	0.2047	264.04	66.21	3538.28	887.25	680.15	170.55	77.20	19.36	22.29	5.59	64727.57	16230.90	1177.57	295.28
1	6	**43**	0.2033	149.81	37.82	1901.04	479.98	3092.75	780.87	252.07	63.64	69.96	17.66	81550.47	20590.19	2000.81	505.17
1	6	**49**	0.2225	-24.11	-5.56	3183.43	734.41	1775.23	409.54	121.73	28.08	38.27	8.83	69217.21	15968.18	2156.53	497.50
1	6	**55**	0.2007	432.04	110.50	1217.66	311.42	1867.25	477.56	102.04	26.10	55.37	14.16	77977.62	19943.15	2949.42	754.33
1	6	**58**	0.204	-43.90	-11.05	499.16	125.60	2057.77	517.77	291.76	73.41	70.02	17.62	102139.78	25700.17	675.29	169.92
1	6	**65**	0.2066	873.80	217.10	675.21	167.76	4762.19	1183.17	175.13	43.51	40.16	9.98	44723.37	11111.57	1402.80	348.53
1	6	**68**	0.2036	1835.81	462.83	1337.25	337.14	960.79	242.23	74.84	18.87	40.36	10.17	76613.86	19315.27	267.83	67.52
1	6	**71**	0.2029	1440.72	364.48	835.96	211.48	2656.68	672.09	127.05	32.14	18.97	4.80	63257.49	16002.99	241.78	61.16
1	6	**R-74**	0.2086	-1757.99	-432.59	1086.00	267.23	4824.42	1187.14	150.56	37.05	16.78	4.13	126586.64	31149.05	1821.00	448.09
1	6	**77**	0.2033	2533.55	639.68	1262.20	318.69	5978.02	1509.35	179.92	45.43	29.28	7.39	113837.37	28742.12	1622.91	409.76
2	4	**50**	0.205	958.90	240.10	1833.40	459.07	1068.12	267.45	59.06	14.79	10.02	2.51	19808.50	4959.85	117.76	29.49
2	4	**59**	0.2037	389.85	98.24	747.00	188.23	1929.62	486.24	172.66	43.51	35.35	8.91	54538.01	13742.94	1010.80	254.71
2	4	**78**	0.2026	3119.21	790.27	1573.36	398.62	3423.20	867.29	136.70	34.63	32.67	8.28	72091.98	18264.96	2227.72	564.41
2	4	**81**	0.2037	1282.95	323.29	2587.22	651.95	1650.46	415.90	134.78	33.96	62.66	15.79	69760.09	17578.72	1064.60	268.27
2	4	**84**	0.2059	2275.28	567.22	3721.24	927.69	3484.62	868.70	112.61	28.07	38.59	9.62	70277.19	17519.81	747.57	186.37
2	4	**87**	0.2237	744.59	170.85	1945.93	446.51	2095.81	480.90	159.48	36.59	49.10	11.27	70726.32	16228.80	386.90	88.55
2	4	**90**	0.2038	1386.59	349.23	695.49	175.17	1805.29	454.69	106.62	26.85	37.71	9.50	56558.05	14244.97	549.73	138.46
2	4	**93**	0.2022	1263.11	320.65	2543.18	645.61	5595.98	1420.58	166.11	42.17	75.47	19.16	71718.77	18206.35	1725.64	438.07
2	4	**96**	0.2026	1395.98	353.68	762.65	193.22	1458.77	369.59	137.01	34.71	14.55	3.69	51813.04	13127.16	472.60	119.74
2	4	**99**	0.2099	1452.30	355.15	1045.73	255.73	3614.48	883.90	121.56	29.73	19.45	4.76	47100.21	11518.12	1241.63	303.63
2	4	**102**	0.2016	1043.92	265.80	686.77	174.86	2604.32	663.09	110.49	28.13	41.50	10.57	44534.04	11338.95	743.73	189.36
2	4	**105**	0.2103	2228.75	543.99	1474.53	359.90	6611.62	1613.76	94.40	23.04	38.10	9.30	58220.30	14210.40	1355.81	330.93
2	4	**108**	0.2088	1791.28	440.36	644.43	158.42	2564.24	630.38	111.97	27.53	83.89	20.62	59086.59	14525.45	1062.58	261.22
2	4	**111**	0.2028	1655.27	418.96	2853.90	722.34	9201.31	2328.91	117.11	29.64	35.35	8.95	43657.20	11049.92	3127.72	791.65
2	4	**114**	0.2061	905.48	225.51	1395.14	347.46	4963.27	1236.12	83.98	20.92	21.38	5.32	61872.59	15409.61	559.30	139.30
2	4	**117**	0.2016	1290.48	328.57	2551.35	649.61	3254.81	828.72	160.70	40.92	66.18	16.85	73943.09	18826.88	1137.22	289.55
2	4	**120**	0.2063	1724.20	429.00	1425.65	354.72	2851.72	709.54	128.90	32.07	35.37	8.80	70598.61	17565.81	513.48	127.76
2	4	**123**	0.2034	1884.01	475.45	1285.80	324.48	6644.36	1676.77	125.49	31.67	39.84	10.05	90836.15	22923.40	3700.87	933.95
2	4	**126**	0.2036	1426.33	359.59	1953.07	492.39	5905.39	1488.82	64.03	16.14	18.44	4.65	79789.35	20115.85	1341.93	338.32
2	4	**129**	0.2026	1296.41	328.45	1422.02	360.28	2287.49	579.55	122.59	31.06	24.00	6.08	68029.11	17235.61	704.27	178.43
2	4	**132**	0.207	1595.22	395.57	1189.85	295.05	2075.62	514.69	122.95	30.49	16.50	4.09	77085.16	19114.88	117.00	29.01
2	4	**135**	0.2048	1199.27	300.58	3740.49	937.50	4505.58	1129.25	99.81	25.02	13.37	3.35	35555.19	8911.37	1214.32	304.35
2	4	**138**	0.2084	708.97	174.62	2123.03	522.91	3162.13	778.85	69.30	17.07	19.13	4.71	51228.00	12617.72	131.79	32.46
2	5	**51**	0.2034	-333.49	-84.16	1031.55	260.32	214.25	54.07	57.82	14.59	27.70	6.99	46321.82	11689.77	27.85	7.03
2	5	**60**	0.2015	-292.23	-74.44	256.39	65.31	149.75	38.15	144.50	36.81	38.28	9.75	46680.52	11891.37	81.40	20.74
2	5	**79**	0.2021	1480.66	376.06	4070.97	1033.96	1790.41	454.74	171.11	43.46	44.64	11.34	101071.75	25670.52	2462.80	625.51
2	5	**82**	0.2091	1555.83	381.93	1483.83	364.25	874.71	214.72	149.91	36.80	69.77	17.13	78519.62	19275.05	452.80	111.15
2	5	**85**	0.2028	1551.94	392.81	1055.36	267.12	292.07	73.93	82.20	20.80	29.63	7.50	48984.52	12398.30	116.20	29.41
2	5	**88**	0.2087	13495.07	3319.13	493.77	121.44	787.16	193.60	44.90	11.04	37.28	9.17	48979.81	12046.64	30.97	7.62
2	5	**91**	0.2096	1034.73	253.40	285.37	69.89	357.16	87.47	182.88	44.79	43.72	10.71	82764.45	20268.60	249.94	61.21
2	5	**94**	0.2007	562.87	143.96	192.58	49.25	485.22	124.10	130.97	33.49	77.55	19.83	53323.71	13637.80	76.33	19.52
2	5	**97**	0.2047	403.57	101.20	257.60	64.59	141.45	35.47	102.61	25.73	29.71	7.45	41919.14	10511.53	24.77	6.21
2	5	**100**	0.2072	563.79	139.67	143.55	35.56	637.60	157.95	87.85	21.76	7.67	1.90	32411.13	8029.26	66.67	16.52
2	5	**103**	0.2031	703.88	177.89	273.23	69.05	131.84	33.32	151.59	38.31	67.10	16.96	66105.13	16706.93	47.90	12.10
2	5	**106**	0.2052	1391.49	348.08	750.62	187.76	1486.74	371.90	128.97	32.26	38.49	9.63	62883.27	15730.01	483.80	121.02
2	5	**109**	0.2204	1538.56	358.32	190.94	44.47	1276.88	297.38	112.89	26.29	90.20	21.01	64181.41	14947.51	301.70	70.26
2	5	**112**	0.2015	236.38	60.22	334.18	85.13	1144.09	291.44	122.68	31.25	20.07	5.11	42485.63	10822.77	170.50	43.43
2	5	**115**	0.2029	683.86	173.00	688.97	174.30	3495.28	884.24	53.94	13.65	32.78	8.29	37833.14	9571.09	67.97	17.19
2	5	**118**	0.2043	24.84	6.24	500.51	125.75	509.13	127.92	89.58	22.51	47.54	11.94	83239.71	20913.82	3133.24	787.22
2	5	**121**	0.1714	887.13	265.67	507.88	152.10	586.08	175.52	158.18	47.37	59.31	17.76	68159.67	20412.11	48.98	14.67
2	5	**124**	0.2159	638.53	151.81	596.68	141.86	5629.04	1338.30	140.27	33.35	39.61	9.42	75727.43	18004.12	456.03	108.42
2	5	**127**	0.2014	1545.51	393.90	845.68	215.53	4042.69	1030.34	71.55	18.24	19.36	4.93	55064.43	14034.05	697.77	177.84
2	5	**130**	0.2027	1053.55	266.79	1034.21	261.89	1194.18	302.40	174.57	44.21	20.68	5.24	69628.92	17632.23	129.28	32.74
2	5	**133**	0.2059	747.66	186.39	1516.69	378.10	1048.33	261.34	168.46	42.00	118.46	29.53	83461.67	20806.64	97.32	24.26
2	5	**136**	0.2044	360.94	90.64	890.03	223.51	213.55	53.63	183.34	46.04	28.31	7.11	45378.69	11395.73	46.65	11.71
2	5	**139**	0.2098	805.90	197.17	1890.04	462.42	1043.44	255.29	43.56	10.66	16.16	3.95	49544.69	12121.68	35.28	8.63
2	6	**52**	0.2022	1622.20	411.81	4154.66	1054.69	231.96	58.89	150.15	38.12	53.19	13.50	74974.02	19032.72	531.81	135.00
2	6	**61**	0.2037	1100.83	277.40	2293.07	577.83	5625.80	1417.64	239.08	60.24	48.89	12.32	89839.83	22638.58	682.53	171.99
2	6	**80**	0.2067	1734.38	430.70	709.40	176.17	1827.05	453.71	257.83	64.03	64.95	16.13	129846.45	32244.89	1754.50	435.70
2	6	**83**	0.2036	1935.99	488.09	2015.96	508.25	2382.98	600.78	161.80	40.79	61.42	15.49	65685.61	16560.13	1487.33	374.97
2	6	**86**	0.2041	986.96	248.22	662.17	166.53	279.50	70.29	87.34	21.96	47.16	11.86	81914.03	20600.92	845.06	212.53
2	6	**89**	0.2063	1590.82	395.82	630.34	156.84	4553.28	1132.91	172.43	42.90	47.77	11.89	62098.52	15450.88	1574.75	391.82

Landuse	Position	Sample	Weight	S 34	S-corr	K 39	K-corr	Ca 43	Ca-corr	V 51	V-corr	Cr 52	Cr-corr	Fe 54	Fe-corr	Mn 55	Mn-corr
1=N,2=Ex, 3=Ag	4=surf, 5=sub	#			PPM		PPM		PPM		PPM		PPM		PPM		PPM
4=sink	6=bank, 100=slip																
2	6	**92**	0.2015	869.15	221.41	660.56	168.27	3432.51	874.40	219.49	55.91	36.08	9.19	65114.47	16587.22	1111.37	283.11
2	6	**95**	0.2033	885.79	223.65	687.63	173.61	2780.36	702.00	270.24	68.23	77.21	19.49	102711.78	25933.08	878.01	221.68
2	6	**98**	0.2006	514.67	131.70	634.39	162.33	2355.47	602.72	200.84	51.39	51.59	13.20	66259.56	16954.65	439.31	112.41
2	6	**101**	0.206	1322.08	329.43	877.65	218.69	2846.24	709.21	162.67	40.53	24.66	6.15	56294.26	14027.11	813.07	202.60
2	6	**104**	0.2009	712.29	181.99	428.94	109.59	877.60	224.23	106.38	27.18	38.47	9.83	42848.35	10947.76	332.59	84.98
2	6	**107**	0.207	1545.99	383.36	817.08	202.61	3855.94	956.16	164.89	40.89	66.78	16.56	67677.52	16782.06	863.97	214.24
2	6	**110**	0.2027	-50.48	-12.78	490.11	124.11	2040.22	516.65	222.62	56.37	157.62	39.91	123495.41	31272.91	168.00	42.54
2	6	**113**	0.2041	1134.86	285.41	1565.17	393.63	5006.04	1258.99	137.84	34.67	34.78	8.75	43635.86	10974.17	1513.56	380.65
2	6	**116**	0.2038	1558.98	392.65	611.49	154.01	2764.91	696.38	178.98	45.08	38.88	9.79	96646.63	24341.86	1101.77	277.50
2	6	**119**	0.2009	-93.28	-23.83	783.85	200.27	3607.58	921.74	247.70	63.29	107.33	27.42	203391.72	51966.63	571.58	146.04
2	6	**122**	0.2076	1721.11	425.55	1969.01	486.85	2939.70	726.85	172.76	42.72	69.43	17.17	134034.55	33140.62	1373.58	339.62
2	6	**125**	0.203	1008.85	255.09	835.22	211.19	3427.92	866.78	122.93	31.08	36.66	9.27	72638.34	18367.12	590.19	149.23
2	6	**128**	0.2029	742.55	187.85	777.73	196.75	12051.88	3048.91	81.37	20.58	20.71	5.24	93059.44	23542.34	456.97	115.60
2	6	**131**	0.2073	1075.47	266.30	1183.53	293.06	2343.35	580.24	197.34	48.86	26.61	6.59	64797.27	16044.59	193.27	47.86
2	6	**134**	0.2039	-183.29	-46.14	1474.82	371.27	2809.45	707.25	186.25	46.89	141.26	35.56	78871.38	19855.16	90.51	22.78
2	6	**137**	0.2017	445.88	113.47	1438.45	366.07	1249.62	318.01	122.68	31.22	45.59	11.60	48680.05	12388.43	98.13	24.97
2	6	**140**	0.2063	281.05	69.93	1803.58	448.75	4156.08	1034.08	130.08	32.37	34.91	8.69	83111.43	20679.16	279.55	69.56
3	4	**141**	0.2024	3776.25	957.68	2058.90	522.15	5602.75	1420.90	54.45	13.81	12.12	3.07	24064.10	6102.82	285.71	72.46
3	4	**144**	0.2025	7495.19	1899.89	1497.09	379.49	8157.20	2067.70	117.89	29.88	29.13	7.38	43834.80	11111.31	774.43	196.30
3	4	**147**	0.2063	4497.84	1119.12	1742.95	433.67	10328.97	2569.98	104.74	26.06	31.69	7.89	52965.76	13178.54	437.70	108.90
3	4	**150**	0.2023	2677.17	679.28	910.78	231.10	6770.03	1717.77	121.55	30.84	40.68	10.32	45265.86	11485.40	767.12	194.64
3	4	**153**	0.2028	4252.75	1076.40	2393.63	605.84	10857.79	2748.18	184.24	46.63	79.90	20.22	73218.43	18532.06	2417.51	611.89
3	4	**156**	0.2021	4010.79	1018.67	2305.75	585.62	14600.33	3708.24	170.14	43.21	67.81	17.22	69739.95	17712.77	1342.49	340.97
3	4	**159**	0.2025	3994.57	1012.55	2411.57	611.29	12184.70	3088.60	111.90	28.36	48.01	12.17	49787.26	12620.15	992.43	251.56
3	4	**162**	0.2007	4018.39	1027.72	3174.20	811.82	10916.51	2791.95	162.88	41.66	61.89	15.83	62681.78	16031.17	1571.94	402.03
3	4	**165**	0.2041	12679.62	3188.85	12195.47	3067.09	19938.58	5014.44	60.40	15.19	25.97	6.53	29532.32	7427.21	2558.12	643.35
3	4	**168**	0.2011	19020.01	4854.78	30148.17	7695.20	28775.81	7344.92	50.40	12.86	25.72	6.57	27424.60	7000.02	1745.62	445.56
3	4	**171**	0.2031	4074.38	1029.73	2188.61	553.13	12068.64	3050.14	91.00	23.00	31.32	7.92	31294.93	7909.25	586.62	148.26
3	4	**174**	0.2012	6700.78	1709.50	4708.75	1201.29	11868.39	3027.85	105.93	27.02	33.30	8.50	40961.09	10449.96	2130.69	543.58
3	4	**177**	0.2034	4447.05	1122.26	1245.92	314.42	5036.87	1271.10	106.93	26.99	22.37	5.65	42595.21	10749.32	771.16	194.61
3	4	**180**	0.2009	3254.77	009.04	592.30	147.24	2311.92	574.60	200.03	51.71	56.69	14.09	57012.41	14171.66	3927.32	976.22
3	4	**183**	0.2015	3162.44	805.60	4775.18	1216.43	5534.68	1409.90	191.88	48.88	49.79	12.68	90133.79	22960.63	2338.20	595.63
3	4	**186**	0.2018	4005.40	1018.82	3642.33	926.46	4670.36	1187.96	175.97	44.76	46.74	11.89	89221.35	22694.41	2583.22	657.07
3	5	**142**	0.2033	607.56	153.40	420.10	106.07	538.26	135.90	107.87	27.23	18.16	4.58	37186.04	9388.88	30.84	7.79
3	5	**145**	0.2034	5772.77	1456.81	353.96	89.32	1841.04	464.60	207.26	52.30	32.73	8.26	84925.38	21431.76	612.29	154.52
3	5	**148**	0.2036	1379.90	347.89	221.46	55.83	984.30	248.15	228.74	57.67	97.49	24.58	87458.83	22049.42	347.42	87.59
3	5	**151**	0.2032	1140.61	288.13	426.91	107.84	630.65	159.31	118.83	30.02	57.96	14.64	41064.25	10373.17	228.69	57.77
3	5	**154**	0.2006	8031.11	2055.02	758.40	194.06	413.80	105.88	38.17	9.77	6.38	1.63	40411.88	10340.69	323.83	82.86
3	5	**157**	0.2088	1867.81	459.17	1372.15	337.32	7552.82	1856.74	184.89	45.45	60.29	14.82	80278.57	19735.15	1367.89	336.27
3	5	**160**	0.201	419.67	107.17	715.61	182.75	2273.99	580.72	87.83	22.43	43.45	11.10	81760.35	20879.40	159.69	40.78
3	5	**163**	0.2022	177.13	44.97	985.31	250.13	8128.79	2063.56	200.16	50.81	47.35	12.02	51793.53	13148.18	196.99	50.01
3	5	**166**	0.2034	1099.61	277.50	505.20	127.49	2445.21	617.07	172.38	43.50	43.82	11.06	100959.84	25478.21	509.87	128.67
3	5	**169**	0.2083	357.94	88.20	2779.78	685.00	526.84	129.83	219.34	54.05	56.04	13.81	86226.16	21248.14	108.89	26.83
3	5	**172**	0.2039	692.67	174.37	666.79	167.86	1402.77	353.13	176.69	44.48	54.08	13.61	80593.19	20288.61	49.22	12.39
3	5	**175**	0.2016	795.73	202.60	1000.83	254.82	1138.49	289.88	168.77	42.97	36.69	9.34	74171.87	18885.13	82.10	20.90
3	5	**178**	0.202	882.46	224.24	253.29	64.36	600.55	152.60	168.44	42.80	75.49	19.18	101375.17	25760.33	134.20	34.10
3	5	**181**	0.2005	948.31	242.78	228.38	58.47	788.42	201.84	291.27	74.57	54.84	14.04	65141.21	16676.80	78.07	19.99
3	5	**184**	0.203	1158.70	292.99	2081.51	526.32	5743.52	1452.29	193.67	48.97	51.12	12.93	97192.49	24575.81	2689.30	680.01
3	5	**187**	0.2042	564.30	141.85	853.12	214.45	1065.68	267.88	139.68	35.11	25.70	6.46	69612.84	17498.66	289.18	72.69
3	6	**143**	0.2065	724.01	179.97	1093.64	271.85	1227.21	305.05	120.80	30.03	22.82	5.67	37667.98	9363.18	55.07	13.69
3	6	**146**	0.2037	615.34	155.06	722.03	181.94	1621.18	408.52	208.67	52.58	48.94	12.33	87963.31	22165.72	130.47	32.88
3	6	**149**	0.2088	344.13	84.60	419.64	103.16	2238.63	550.33	169.98	41.79	45.37	11.15	33822.72	8314.75	207.79	51.08
3	6	**152**	0.2045	1022.53	256.66	317.93	79.80	1405.75	352.85	100.22	25.15	46.89	11.77	58028.23	14565.23	80.35	20.17
3	6	**155**	0.2095	1090.14	267.10	1205.60	295.39	6147.84	1506.29	190.90	46.77	62.15	15.23	88971.34	21799.04	2338.55	572.97
3	6	**158**	0.2147	260.36	62.25	1047.89	250.53	8899.67	2127.71	262.28	62.71	84.80	20.27	103301.83	24697.17	1196.06	285.95
3	6	**161**	0.2016	360.09	91.68	576.83	146.87	2584.26	657.99	182.19	46.39	77.33	19.69	90955.92	23158.57	1860.47	473.70
3	6	**164**	0.2041	818.22	205.78	856.43	215.39	5184.00	1303.75	185.88	46.75	72.80	18.31	78944.68	19854.14	2067.27	519.91
3	6	**167**	0.204	797.43	200.65	1730.37	435.39	5095.76	1282.18	186.44	46.91	49.33	12.41	123965.24	31191.84	2712.03	682.40
3	6	**170**	0.205	694.21	173.82	1792.42	448.81	1687.76	422.60	154.94	38.79	45.73	11.45	122954.65	30786.65	1173.48	293.83
3	6	**173**	0.2037	864.75	217.91	620.83	156.44	582.62	146.81	184.11	46.39	48.60	12.25	60298.31	15194.46	97.39	24.54
3	6	**176**	0.2043	1156.94	290.68	340.53	85.56	1403.04	352.51	102.87	25.85	22.28	5.60	16928.94	4253.37	172.97	43.46
3	6	**179**	0.203	901.32	227.91	836.50	211.52	4544.84	1149.20	162.14	41.00	38.45	9.72	88349.26	22339.74	240.46	60.80
3	6	**182**	0.2065	626.28	155.67	184.76	45.93	1380.16	343.07	196.00	48.72	48.11	11.96	51054.91	12690.79	220.37	54.78
3	6	**185**	0.2022	1452.82	368.81	2870.16	728.61	6045.46	1534.69	287.46	72.97	63.15	16.03	153367.49	38933.50	2450.84	622.16
3	6	**188**	0.2015	1095.71	279.12	2597.19	661.61	4548.72	1158.74	166.53	42.42	46.19	11.77	94875.27	24168.47	2311.79	588.90

Landuse	Position	Sample	Weight	Co 59	Co-corr	Ni 60	Ni-corr	Cu 63	Cu-corr	Zn 66	Zn-corr	As 75	As-corr	Se 82	Se-corr	Sr 88	Sr-corr	Ag 109	Ag-corr
1=N,2=Ex, 3=Ag	4=surf, 5=sub	#			PPM		PPM		PPM		PPM		PPM		PPB		PPM		PPB
4=sink	6=bank, 100=slip																		
1	4	**34**	0.2139	36.48	8.75	14.93	3.58	74.15	17.79	184.06	44.17	17.63	4.23	5.09	1222.42	48.14	11.55	0.56	133.18
1	4	**38**	0.2004	16.74	4.29	2.92	0.75	20.12	5.15	33.41	8.56	21.57	5.53	2.83	724.36	57.61	14.76	0.26	66.85
1	4	**41**	0.2016	28.11	7.16	5.82	1.48	29.22	7.44	57.24	14.57	5.44	1.39	4.70	1196.68	67.22	17.11	0.22	55.25
1	4	**47**	0.2018	37.42	9.52	12.23	3.11	50.06	12.73	129.24	32.87	70.27	17.87	4.56	1159.12	50.56	12.86	1.08	274.71
1	4	**53**	0.2005	19.03	4.87	15.97	4.09	37.69	9.65	50.69	12.98	23.92	6.12	6.07	1552.70	64.10	16.41	0.74	189.19
1	4	**56**	0.2079	42.97	10.61	4.67	1.15	55.42	13.68	41.30	10.20	2.94	0.72	4.65	1148.07	105.65	26.08	0.05	12.84
1	4	**63**	0.207	10.12	2.51	5.67	1.41	44.82	11.11	78.61	19.49	2.06	0.51	4.43	1099.26	64.63	16.03	0.28	68.69
1	4	**R-63**	**0.2012**	7.07	1.80	7.97	2.03	36.41	9.29	48.38	12.34	3.94	1.01	7.89	2012.89	22.34	5.70	0.28	71.43
1	4	**66**	0.2026	16.83	4.26	17.39	4.41	44.86	11.36	34.26	8.68	13.09	3.32	3.36	860.77	37.54	9.51	0.15	37.50
1	4	**69**	0.2053	6.25	1.56	1.97	0.49	22.71	5.68	30.72	7.68	3.26	0.82	3.14	785.08	78.22	19.56	0.08	18.75
1	4	**72**	0.2042	13.80	3.47	2.09	0.52	22.09	5.55	43.21	10.86	15.15	3.81	6.02	1514.01	55.39	13.92	0.20	51.03
1	4	**75**	0.2023	25.84	6.56	4.22	1.07	30.11	7.64	81.81	20.76	1.43	0.36	2.74	695.48	90.30	22.91	0.05	12.18
1	5	**35**	0.2031	32.03	8.10	12.36	3.12	36.75	9.29	128.60	32.50	69.41	17.54	3.22	813.55	20.34	5.14	0.26	66.22
1	5	**39**	0.2025	1.80	0.46	0.76	0.19	12.25	3.10	3.95	1.00	5.55	1.41	0.51	129.78	11.37	2.88	0.04	9.63
1	5	**42**	0.2068	9.07	2.25	3.00	0.74	15.87	3.94	30.81	7.65	3.66	0.91	3.13	777.64	12.18	3.02	0.16	40.71
1	5	**48**	0.2031	26.49	6.70	5.07	1.28	41.56	10.50	51.33	12.97	37.71	9.53	3.13	791.31	6.01	1.52	0.64	160.74
1	5	**54**	0.2021	6.29	1.60	30.29	7.69	23.49	5.97	25.95	6.59	14.33	3.64	10.39	2638.63	6.59	1.67	0.80	202.42
1	5	**57**	0.206	33.13	8.26	4.19	1.04	51.23	12.76	39.37	9.81	3.37	0.84	3.89	968.79	32.71	8.15	-0.02	-3.74
1	5	**64**	0.2094	40.27	9.87	7.68	1.88	25.77	6.32	32.90	8.06	1.48	0.36	4.16	1020.47	1.97	0.48	0.05	11.28
1	5	**67**	0.2025	7.03	1.78	9.74	2.47	29.26	7.42	16.87	4.27	6.47	1.64	3.12	791.12	12.24	3.10	0.08	20.28
1	5	**70**	0.2031	2.67	0.68	1.01	0.26	18.33	4.63	11.08	2.80	2.71	0.69	2.52	637.64	6.90	1.74	0.02	6.07
1	5	**73**	0.2046	9.23	2.31	1.70	0.43	19.94	5.00	37.20	9.33	9.61	2.41	2.55	639.24	48.04	12.05	0.03	8.53
1	5	**76**	0.2017	4.77	1.21	1.01	0.26	19.17	4.88	19.23	4.89	1.35	0.34	2.80	711.80	46.07	11.73	0.00	0.00
1	6	**37**	0.2086	37.78	9.30	11.63	2.86	97.83	24.07	166.78	41.04	86.16	21.20	4.82	1186.05	23.41	5.76	3.20	787.42
1	6	**40**	0.2047	47.63	11.94	7.61	1.91	44.91	11.26	58.98	14.79	27.39	6.87	3.05	765.56	20.51	5.14	0.43	108.83
1	6	**43**	0.2033	72.85	18.39	24.57	6.20	43.83	11.07	118.91	30.02	8.18	2.07	4.69	1185.16	50.88	12.85	0.11	28.78
1	6	**49**	0.2225	52.59	12.13	12.74	2.94	50.84	11.73	101.98	23.53	20.72	4.78	3.07	708.24	34.48	7.95	0.78	178.79
1	6	**55**	0.2007	56.29	14.40	19.50	4.99	46.15	11.80	97.95	25.05	14.72	3.77	5.27	1347.32	35.99	9.21	0.25	64.45
1	6	**58**	0.204	34.86	8.77	9.61	2.42	44.79	11.27	61.07	15.37	2.10	0.53	3.16	795.62	43.47	10.94	0.03	7.05
1	6	**65**	0.2066	27.82	6.91	8.06	2.00	37.41	9.29	55.17	13.71	1.39	0.34	2.50	620.38	62.74	15.59	0.01	2.24
1	6	**68**	0.2036	12.06	3.04	5.86	1.48	59.45	14.99	25.60	6.45	31.07	7.83	1.31	329.26	15.04	3.79	-0.04	-9.33
1	6	**71**	0.2029	4.55	1.15	1.63	0.41	22.29	5.64	19.63	4.97	3.67	0.93	2.06	520.89	35.03	8.86	0.02	4.05
1	6	**R-74**	0.2086	42.20	10.38	4.92	1.21	42.35	10.42	102.21	25.15	11.19	2.75	6.20	1525.63	69.89	17.20	0.21	51.67
1	6	**77**	0.2033	55.60	14.04	7.37	1.86	34.83	8.79	105.98	26.76	3.63	0.92	2.95	745.59	80.28	20.27	0.09	22.22
2	4	**50**	0.205	4.15	1.04	1.92	0.48	7.36	1.84	8.79	2.20	6.15	1.54	2.82	705.35	19.84	4.97	0.46	114.93
2	4	**59**	0.2037	22.80	5.75	5.17	1.30	26.79	6.75	42.26	10.65	7.09	1.79	3.31	833.83	38.69	9.75	0.25	63.50
2	4	**78**	0.2026	30.02	7.61	12.06	3.05	57.25	14.50	136.14	34.49	21.69	5.50	2.72	690.14	30.08	7.62	0.78	196.86
2	4	**81**	0.2037	20.79	5.24	10.65	2.68	38.63	9.73	52.69	13.28	1.95	0.49	2.07	520.36	32.89	8.29	0.02	4.28
2	4	**84**	0.2059	17.29	4.31	7.39	1.84	46.84	11.68	50.68	12.64	16.44	4.10	3.58	891.23	63.86	15.92	0.15	36.15
2	4	**87**	0.2237	10.75	2.47	3.59	0.82	28.07	6.44	26.10	5.99	12.50	2.87	2.38	545.88	31.24	7.17	0.04	8.49
2	4	**90**	0.2038	10.53	2.65	2.37	0.60	16.58	4.17	22.67	5.71	2.96	0.74	3.75	945.50	46.19	11.63	0.06	15.36
2	4	**93**	0.2022	53.07	13.47	23.12	5.87	61.08	15.51	82.90	21.05	5.67	1.44	2.53	641.75	75.56	19.18	0.05	12.19
2	4	**96**	0.2026	18.80	4.76	4.87	1.23	25.85	6.55	30.61	7.75	2.47	0.63	2.59	655.94	21.77	5.51	0.09	23.06
2	4	**99**	0.2099	9.98	2.44	5.80	1.42	25.05	6.12	41.93	10.25	1.40	0.34	2.16	528.71	46.37	11.34	0.00	-0.24
2	4	**102**	0.2016	3.13	0.80	2.72	0.69	20.97	5.34	21.59	5.50	1.44	0.37	1.55	394.40	41.48	10.56	-0.04	-9.68
2	4	**105**	0.2103	10.96	2.68	6.71	1.64	30.71	7.49	47.93	11.70	2.07	0.50	3.18	775.20	89.62	21.88	0.02	5.37
2	4	**108**	0.2088	4.64	1.14	5.42	1.33	40.53	9.96	38.50	9.47	1.70	0.42	4.80	1178.77	61.47	15.11	0.05	12.54
2	4	**111**	0.2028	44.19	11.18	16.69	4.22	58.42	14.79	160.22	40.55	2.08	0.53	4.22	1068.36	120.17	30.42	0.14	34.17
2	4	**114**	0.2061	3.48	0.87	2.38	0.59	30.39	7.57	21.26	5.30	18.39	4.58	2.78	691.12	70.46	17.55	0.08	19.68
2	4	**117**	0.2016	10.65	2.71	11.84	3.02	69.27	17.64	48.33	12.31	2.48	0.63	2.62	665.81	88.45	22.52	0.04	11.20
2	4	**120**	0.2063	4.42	1.10	4.69	1.17	22.05	5.49	25.69	6.39	10.91	2.71	2.20	548.38	38.04	9.47	0.04	10.20
2	4	**123**	0.2034	53.48	13.50	12.93	3.26	46.16	11.65	71.75	18.11	11.52	2.91	4.14	1045.78	90.42	22.82	0.08	20.19
2	4	**126**	0.2036	17.81	4.49	6.73	1.70	30.99	7.81	45.76	11.54	1.59	0.40	2.18	548.34	68.24	17.20	0.01	1.76
2	4	**129**	0.2026	8.77	2.22	2.83	0.72	20.33	5.15	40.09	10.16	3.63	0.92	3.23	818.85	35.17	8.91	0.11	26.86
2	4	**132**	0.207	10.09	2.50	1.10	0.27	20.29	5.03	21.68	5.38	14.11	3.50	1.65	408.16	35.21	8.73	0.16	39.18
2	4	**135**	0.2048	22.69	5.69	3.94	0.99	19.22	4.82	29.54	7.40	47.95	12.02	1.25	313.79	74.04	18.56	0.89	224.07
2	4	**138**	0.2084	6.01	1.48	1.46	0.36	16.23	4.00	16.76	4.13	8.02	1.98	1.84	452.22	40.09	9.88	-0.03	-8.13
2	5	**51**	0.2034	0.65	0.16	0.61	0.15	5.46	1.38	1.56	0.39	2.74	0.69	1.61	406.55	6.72	1.70	0.02	4.04
2	5	**60**	0.2015	3.98	1.01	2.41	0.61	13.64	3.47	14.57	3.71	3.10	0.79	2.24	571.13	4.47	1.14	0.13	34.14
2	5	**79**	0.2021	56.97	14.47	14.64	3.72	72.17	18.33	124.91	31.73	21.18	5.38	3.75	951.42	29.57	7.51	0.54	135.88
2	5	**82**	0.2091	13.84	3.40	9.14	2.24	40.64	9.98	41.61	10.22	1.69	0.42	2.95	724.41	28.05	6.89	0.03	7.12
2	5	**85**	0.2028	5.37	1.36	3.27	0.83	18.78	4.75	18.30	4.63	4.58	1.16	2.61	661.62	11.31	2.86	0.11	28.09
2	5	**88**	0.2087	5.49	1.35	13.53	3.33	37.00	9.10	25.29	6.22	19.09	4.70	1.59	390.57	9.51	2.34	-0.03	-7.13
2	5	**91**	0.2096	8.97	2.20	4.27	1.05	19.87	4.87	33.44	8.19	2.09	0.51	2.31	565.46	11.40	2.79	0.00	-0.73
2	5	**94**	0.2007	8.08	2.07	8.83	2.26	24.15	6.18	21.86	5.59	1.32	0.34	1.68	428.39	7.82	2.00	0.00	-0.26
2	5	**97**	0.2047	11.79	2.96	2.25	0.56	11.54	2.89	12.35	3.10	0.59	0.15	0.76	190.07	3.06	0.77	-0.04	-10.78
2	5	**100**	0.2072	4.66	1.15	2.26	0.56	22.08	5.47	15.65	3.88	0.49	0.12	1.16	288.11	12.70	3.15	-0.05	-11.64
2	5	**103**	0.2031	13.70	3.46	5.09	1.29	33.72	8.52	16.65	4.21	1.13	0.29	1.67	421.05	3.74	0.94	-0.04	-10.11
2	5	**106**	0.2052	15.03	3.76	3.31	0.83	20.48	5.12	27.65	6.92	1.38	0.35	2.97	742.18	44.71	11.18	0.01	2.50
2	5	**109**	0.2204	2.89	0.67	3.39	0.79	34.01	7.92	18.41	4.29	1.65	0.38	3.76	874.52	46.11	10.74	0.06	13.28
2	5	**112**	0.2015	5.18	1.32	2.71	0.69	15.33	3.91	25.34	6.46	1.64	0.42	2.09	532.66	24.73	6.30	0.09	23.44
2	5	**115**	0.2029	1.39	0.35	1.52	0.38	46.47	11.76	9.28	2.35	21.82	5.52	2.94	744.78	56.25	14.23	0.03	7.84
2	5	**118**	0.2043	79.48	19.97	19.60	4.92	80.67	20.27	49.39	12.41	5.75	1.45	4.08	1024.59	15.63	3.93	-0.02	-4.27
2	5	**121**	0.1714	2.25	0.67	10.79	3.23	234.89	70.34	119.43	35.77	1.84	0.55	1.65	495.33	11.87	3.56	3.57	1069.13
2	5	**124**	0.2159	8.10	1.93	6.32	1.50	33.01	7.85	44.05	10.47	2.76	0.66	1.52	360.19	79.43	18.88	0.00	0.00
2	5	**127**	0.2014	13.73	3.50	4.13	1.05	31.07	7.92	28.75	7.33	3.98	1.01	2.11	538.02	48.57	12.38	0.01	2.55
2	5	**130**	0.2027	5.84	1.48	1.81	0.46	25.53	6.47	24.59	6.23	13.66	3.46	2.53	639.41	33.14	8.39	0.01	1.27
2	5	**133**	0.2059	3.69	0.92	6.48	1.62	54.76	13.65	28.47	7.10	323.83	80.73	1.41	351.01	16.90	4.21	0.24	60.83
2	5	**136**	0.2044	1.23	0.31	0.98	0.25	26.68	6.70	9.87	2.48	28.28	7.10	1.24	311.65	10.05	2.52	0.10	24.11
2	5	**139**	0.2098	3.02	0.74	0.91	0.22	19.63	4.80	8.85	2.17	6.06	1.48	1.56	382.41	12.65	3.09	-0.03	-6.12
2	6	**52**	0.2022	41.12	10.44	11.83	3.00	77.34	19.63	90.10	22.87	83.48	21.19	4.97	1261.16	6.25	1.59	1.00	253.60
2	6	**61**	0.2037	37.83	9.53	8.92	2.25	59.92	15.10	79.29	19.98	14.19	3.57	3.31	834.33	64.12	16.16	0.09	22.93
2	6	**80**	0.2067	36.07	8.96	15.44	3.83	57.41	14.26	133.42	33.13	32.81	8.15	3.15	781.50	32.79	8.14	0.25	62.58
2	6	**83**	0.2036	33.77	8.51	9.63	2.43	41.91	10.57	54.34	13.70	2.25	0.57	2.72	684.48	45.27	11.41	0.05	13.36
2	6	**86**	0.2041	21.18	5.33	3.93	0.99	45.53	11.45	25.14	6.32	20.48	5.15	3.82	959.95	6.75	1.70	0.17	42.25
2	6	**89**	0.2063	35.18	8.75	11.60	2.89	47.66	11.86	76.50	19.03	3.84	0.96	2.78	692.44	54.05	13.45	0.06	14.93

Landuse	Position	Sample	Weight	Co 59	Co-corr	Ni 60	Ni-corr	Cu 63	Cu-corr	Zn 66	Zn-corr	As 75	As-corr	Se 82	Se-corr	Sr 88	Sr-corr	Ag 109	Ag-corr
1=N,2=Ex, 3=Ag	4=surf, 5=sub	#			PPM		PPM		PPM		PPM		PPM		PPB		PPM		PPB
4=sink	6=bank, 100=slip																		
2	6	**92**	0.2015	23.62	6.02	6.75	1.72	36.25	9.23	64.31	16.38	2.52	0.64	2.85	725.75	48.51	12.36	0.00	-0.51
2	6	**95**	0.2033	22.49	5.68	6.42	1.62	31.22	7.88	60.48	15.27	2.49	0.63	1.60	402.71	36.42	9.19	-0.04	-9.59
2	6	**98**	0.2006	11.97	3.06	4.05	1.04	31.31	8.01	33.69	8.62	1.79	0.46	1.95	499.99	36.43	9.32	-0.01	-1.79
2	6	**101**	0.206	17.12	4.26	5.96	1.48	42.99	10.71	54.81	13.66	1.43	0.36	3.24	808.07	55.33	13.79	0.00	0.00
2	6	**104**	0.2009	10.10	2.58	2.53	0.65	20.84	5.32	16.84	4.30	0.89	0.23	1.63	417.23	20.26	5.18	-0.03	-6.64
2	6	**107**	0.207	24.70	6.12	9.48	2.35	41.35	10.25	51.72	12.83	2.89	0.72	2.41	597.86	61.46	15.24	0.00	0.99
2	6	**110**	0.2027	6.67	1.69	6.71	1.70	51.12	12.94	30.76	7.79	1.32	0.33	1.42	358.83	37.08	9.39	0.10	25.32
2	6	**113**	0.2041	23.53	5.92	8.51	2.14	37.86	9.52	100.91	25.38	1.86	0.47	3.63	911.92	63.17	15.89	0.08	19.11
2	6	**116**	0.2038	36.61	9.22	7.92	2.00	89.15	22.45	50.40	12.69	15.61	3.93	3.42	862.13	41.70	10.50	0.08	19.90
2	6	**119**	0.2009	18.79	4.80	10.89	2.78	75.21	19.22	40.92	10.45	4.75	1.21	1.51	384.78	58.36	14.91	-0.03	-8.43
2	6	**122**	0.2076	38.15	9.43	23.69	5.86	76.64	18.95	96.10	23.76	54.29	13.42	3.09	764.26	33.22	8.21	0.09	22.99
2	6	**125**	0.203	12.64	3.20	5.24	1.32	23.06	5.83	39.77	10.06	1.99	0.50	1.13	285.98	59.08	14.94	-0.04	-9.36
2	6	**128**	0.2029	12.58	3.18	12.11	3.06	45.94	11.62	71.21	18.02	3.99	1.01	2.29	580.09	85.75	21.69	-0.01	-2.02
2	6	**131**	0.2073	7.95	1.97	3.25	0.80	36.70	9.09	29.80	7.38	6.65	1.65	1.60	395.19	22.11	5.47	0.08	18.82
2	6	**134**	0.2039	6.40	1.61	14.50	3.65	64.21	16.16	50.20	12.64	384.06	96.68	1.02	257.03	21.95	5.53	0.63	157.59
2	6	**137**	0.2017	2.92	0.74	4.06	1.03	26.66	6.78	33.99	8.65	30.90	7.86	1.00	255.25	21.67	5.51	1.24	316.07
2	6	**140**	0.2063	11.37	2.83	6.77	1.68	37.10	9.23	32.36	8.05	18.29	4.55	1.62	403.32	47.26	11.76	-0.06	-13.68
3	4	**141**	0.2024	76.04	19.28	2.55	0.65	50.77	12.88	33.86	8.59	34.47	8.74	1.56	396.39	48.79	12.37	0.06	14.20
3	4	**144**	0.2025	66.57	16.87	7.44	1.89	45.25	11.47	106.91	27.10	25.57	6.48	3.93	997.20	59.51	15.08	0.16	41.32
3	4	**147**	0.2063	18.75	4.66	3.61	0.90	54.77	13.63	51.11	12.72	4.55	1.13	2.46	612.33	76.16	18.95	-0.01	-2.99
3	4	**150**	0.2023	9.96	2.53	3.99	1.01	28.70	7.28	33.22	8.43	5.32	1.35	2.03	514.06	58.40	14.82	0.01	1.27
3	4	**153**	0.2028	55.12	13.95	23.18	5.87	74.50	18.86	171.69	43.46	11.82	2.99	2.65	669.47	91.76	23.22	0.00	0.76
3	4	**156**	0.2021	45.56	11.57	20.65	5.24	79.37	20.16	167.94	42.65	11.75	2.98	2.85	723.34	75.95	19.29	0.07	18.79
3	4	**159**	0.2025	46.58	11.81	8.52	2.16	138.38	35.08	114.91	29.13	14.97	3.79	2.31	585.04	61.61	15.62	0.07	18.76
3	4	**162**	0.2007	29.01	7.42	13.01	3.33	52.60	13.45	123.25	31.52	20.17	5.16	3.15	804.35	93.43	23.90	0.16	39.64
3	4	**165**	0.2041	14.21	3.57	17.16	4.32	79.32	19.95	178.13	44.80	15.64	3.93	9.21	2317.27	91.20	22.94	1.16	291.73
3	4	**168**	0.2011	7.88	2.01	19.28	4.92	99.41	25.37	281.68	71.90	17.15	4.38	8.03	2049.88	139.84	35.69	0.76	194.75
3	4	**171**	0.2031	29.69	7.50	6.94	1.75	53.96	13.64	73.09	18.47	8.15	2.06	2.06	521.64	77.82	19.67	0.09	22.75
3	4	**174**	0.2012	57.28	14.61	11.26	2.87	145.90	37.22	218.89	55.84	10.09	2.57	3.43	874.29	65.44	16.70	0.38	96.69
3	4	**177**	0.2034	37.53	9.47	4.68	1.18	20.63	5.21	67.60	17.06	4.27	1.08	1.86	468.13	55.98	14.13	0.00	-0.76
3	4	**180**	0.2065	63.00	15.75	16.27	4.04	43.19	10.74	120.90	30.05	2.67	0.66	2.32	576.44	31.44	7.02	0.00	6.46
3	4	**183**	0.2015	55.16	14.05	18.83	4.80	95.37	24.29	231.75	59.04	34.25	8.72	3.45	879.11	50.64	12.90	0.19	47.38
3	4	**186**	0.2018	60.21	15.31	17.11	4.35	80.22	20.41	213.44	54.29	27.34	6.95	2.30	584.52	42.74	10.87	0.08	19.84
3	5	**142**	0.2033	2.18	0.55	1.20	0.30	10.83	2.73	8.55	2.16	1.61	0.41	1.17	296.42	8.41	2.12	0.04	9.34
3	5	**145**	0.2034	10.15	2.56	23.10	5.83	25.36	6.40	261.98	66.11	28.32	7.15	6.47	1633.27	33.79	8.53	0.52	129.97
3	5	**148**	0.2036	11.50	2.90	5.77	1.45	33.85	8.53	38.56	9.72	1.79	0.45	1.33	336.32	19.64	4.95	-0.04	-10.08
3	5	**151**	0.2032	2.31	0.58	1.92	0.48	10.63	2.68	10.17	2.57	2.43	0.61	1.56	394.57	9.99	2.52	-0.03	-8.34
3	5	**154**	0.2006	9.00	2.30	2.05	0.52	11.60	2.97	22.88	5.86	17.51	4.48	2.67	682.18	4.03	1.03	0.02	3.84
3	5	**157**	0.2088	23.68	5.82	18.39	4.52	67.00	16.47	90.87	22.34	10.23	2.51	2.90	713.16	78.77	19.36	0.06	14.01
3	5	**160**	0.201	3.26	0.83	8.32	2.12	27.63	7.06	41.01	10.47	2.97	0.76	1.74	445.37	17.81	4.55	-0.01	-3.58
3	5	**163**	0.2022	6.41	1.63	2.51	0.64	21.15	5.37	22.77	5.78	16.16	4.10	1.89	480.04	53.53	13.59	0.01	3.05
3	5	**166**	0.2034	7.70	1.94	3.42	0.86	23.00	5.80	43.49	10.97	26.41	6.66	2.10	529.96	31.71	8.00	0.43	108.26
3	5	**169**	0.2083	10.48	2.58	3.45	0.85	35.39	8.72	36.31	8.95	19.35	4.77	1.05	259.73	11.24	2.77	0.02	5.67
3	5	**172**	0.2039	2.48	0.62	3.09	0.76	28.05	7.06	20.96	5.28	5.64	1.42	1.38	347.91	12.76	3.21	0.00	-1.01
3	5	**175**	0.2016	6.05	1.54	4.27	1.09	30.61	7.79	35.67	9.08	7.28	1.85	1.59	403.56	15.41	3.92	0.12	30.81
3	5	**178**	0.202	14.79	3.76	14.75	3.75	74.81	19.01	26.69	6.78	3.02	0.77	2.12	537.95	14.34	3.64	-0.03	-8.39
3	5	**181**	0.2005	1.38	0.35	1.41	0.36	13.43	3.44	12.74	3.26	4.38	1.12	2.12	541.72	10.40	2.66	-0.02	-5.63
3	5	**184**	0.203	52.01	13.15	16.80	4.25	72.49	18.33	139.82	35.35	27.40	6.93	2.88	727.47	65.77	16.63	0.15	37.93
3	5	**187**	0.2042	6.54	1.64	3.99	1.00	20.69	5.20	47.80	12.02	9.95	2.50	1.04	261.68	11.54	2.90	0.09	22.62
3	6	**143**	0.2065	2.40	0.60	1.94	0.48	14.98	3.72	22.73	5.65	81.92	20.36	1.24	308.23	18.06	4.49	-0.05	-11.93
3	6	**146**	0.2037	9.22	2.32	4.36	1.10	16.03	4.04	37.01	9.33	10.09	2.54	1.64	413.51	24.13	6.08	0.19	48.63
3	6	**149**	0.2088	3.44	0.85	3.50	0.86	26.30	6.47	11.11	2.73	1.09	0.27	1.01	249.03	31.47	7.74	-0.07	-18.19
3	6	**152**	0.2045	4.44	1.11	3.04	0.76	14.35	3.60	17.67	4.43	3.05	0.77	1.45	364.96	14.14	3.55	-0.03	-8.53
3	6	**155**	0.2095	47.65	11.67	16.63	4.07	56.33	13.80	79.98	19.60	5.33	1.31	2.39	584.35	79.62	19.51	-0.03	-7.84
3	6	**158**	0.2147	39.11	9.35	23.33	5.58	90.88	21.73	127.07	30.38	14.87	3.55	3.90	933.12	97.73	23.36	0.08	18.89
3	6	**161**	0.2016	33.10	8.43	8.55	2.18	33.93	8.64	83.04	21.14	5.08	1.29	0.87	221.77	41.55	10.58	-0.01	-2.04
3	6	**164**	0.2041	33.00	8.30	12.43	3.13	40.74	10.25	61.78	15.54	14.67	3.69	2.02	507.01	58.35	14.67	0.00	0.00
3	6	**167**	0.204	43.15	10.86	16.06	4.04	59.43	14.95	113.68	28.60	38.76	9.75	3.43	862.29	60.82	15.30	0.29	73.72
3	6	**170**	0.205	29.96	7.50	5.89	1.47	44.28	11.09	51.35	12.86	14.74	3.69	1.97	492.02	25.83	6.47	0.12	29.05
3	6	**173**	0.2037	7.95	2.00	3.38	0.85	31.00	7.81	26.45	6.66	6.40	1.61	1.24	313.47	8.29	2.09	0.02	5.29
3	6	**176**	0.2043	6.62	1.66	2.75	0.69	24.00	6.03	19.06	4.79	3.77	0.95	3.05	765.05	14.98	3.76	0.13	33.67
3	6	**179**	0.203	21.90	5.54	7.95	2.01	30.69	7.76	30.82	7.79	2.83	0.71	1.30	328.46	55.83	14.12	-0.03	-8.09
3	6	**182**	0.2065	5.16	1.28	1.27	0.32	20.42	5.08	18.98	4.72	3.27	0.81	1.71	424.56	16.24	4.04	-0.10	-24.86
3	6	**185**	0.2022	72.30	18.35	19.00	4.82	87.84	22.30	158.34	40.20	57.92	14.70	3.54	899.42	68.08	17.28	0.16	41.38
3	6	**188**	0.2015	41.99	10.70	17.62	4.49	75.63	19.27	145.31	37.02	23.51	5.99	2.64	671.75	54.86	13.97	0.22	55.02

Landuse	Position	Sample	Weight	Cd 111	Cd-corr	In 115	In-corr	Ba 137	Ba-corr	Tl 205	Tl-corr	Pb 207	Pb-corr	Bi 209	Bi-corr	U 238	U-corr
1=N,2=Ex, 3=Ag	4=surf, 5=sub	#			PPB		PPB		PPM		PPB		PPM		PPB		
4=sink	6=bank, 100=slip																
1	4	34	0.2139	0.48	115.91	0.11	26.40	245.39	58.89	0.85	203.98	45.97	11.03	0.50	119.27	2.04	490.26
1	4	38	0.2004	0.13	32.79	0.05	11.78	116.34	29.80	0.31	80.43	17.14	4.39	2.50	639.32	0.92	235.90
1	4	41	0.2016	0.20	51.69	0.12	30.81	224.55	57.17	0.42	107.45	29.56	7.53	0.84	213.62	1.98	504.90
1	4	47	0.2018	0.35	88.52	0.09	23.66	196.78	50.05	0.39	97.93	38.52	9.80	2.41	611.74	1.11	283.36
1	4	53	0.2005	0.19	49.41	0.06	14.59	87.46	22.39	0.25	64.77	20.67	5.29	0.30	76.29	1.18	302.60
1	4	56	0.2079	0.15	36.05	0.10	25.18	243.58	60.14	0.31	75.30	20.77	5.13	0.39	95.06	2.35	580.46
1	4	63	0.207	0.22	53.81	0.01	2.98	199.43	49.45	0.18	44.39	19.41	4.81	0.12	29.26	1.31	323.85
1	4	R-63	**0.2012**	0.29	73.98	0.11	28.06	186.93	47.69	0.25	63.78	23.45	5.98	0.36	90.82	2.25	574.02
1	4	66	0.2026	0.10	25.08	0.05	11.40	132.06	33.46	0.16	41.30	27.61	7.00	0.66	166.71	1.47	371.93
1	4	69	0.2053	0.05	12.50	0.03	6.25	97.81	24.46	0.08	19.50	13.13	3.28	0.11	26.75	1.28	319.53
1	4	72	0.2042	0.15	36.45	0.03	7.79	109.84	27.61	0.41	103.82	18.07	4.54	1.20	302.65	1.05	264.44
1	4	75	0.2023	0.08	19.54	0.02	5.07	202.56	51.40	0.23	57.60	14.76	3.74	0.02	5.58	1.28	324.02
1	5	35	0.2031	0.24	60.15	0.07	17.44	247.44	62.54	0.37	93.76	43.74	11.05	1.54	388.20	1.23	310.10
1	5	39	0.2025	0.04	10.65	0.02	5.58	26.54	6.73	0.12	30.92	5.92	1.50	2.04	517.86	0.31	79.59
1	5	42	0.2068	0.07	17.87	0.14	34.50	109.86	27.27	0.48	119.89	26.86	6.67	1.00	248.21	2.41	598.44
1	5	48	0.2031	0.15	37.66	0.11	26.79	103.79	26.23	0.39	98.82	34.64	8.76	2.39	605.04	1.25	316.42
1	5	54	0.2021	0.14	36.07	0.12	30.22	45.46	11.55	0.43	107.94	19.80	5.03	0.49	123.69	2.70	684.48
1	5	57	0.206	0.09	23.42	0.11	27.66	142.69	35.55	0.47	115.87	21.00	5.23	0.44	108.89	2.15	535.23
1	5	64	0.2094	0.10	23.78	0.05	11.52	209.39	51.33	0.14	33.83	26.42	6.48	0.08	19.61	2.96	726.07
1	5	67	0.2025	0.04	10.90	0.05	11.66	127.08	32.21	0.27	69.45	29.68	7.52	0.43	109.25	1.71	432.44
1	5	70	0.2031	0.04	9.35	0.05	13.65	40.40	10.21	0.15	37.91	13.98	3.53	0.13	32.60	1.44	364.44
1	5	73	0.2046	0.04	9.28	0.05	12.29	148.97	37.37	0.58	145.01	22.36	5.61	1.08	269.70	1.55	387.61
1	5	76	0.2017	0.02	4.84	0.02	6.11	78.73	20.04	0.19	48.35	14.85	3.78	0.04	9.67	1.28	325.23
1	6	37	0.2086	0.81	198.33	0.16	39.12	228.15	56.14	0.67	165.36	109.26	26.89	6.20	1525.87	1.75	429.39
1	6	40	0.2047	0.16	39.12	0.08	21.06	174.00	43.63	0.44	110.83	32.77	8.22	2.89	725.44	1.35	337.27
1	6	43	0.2033	0.20	49.99	0.12	29.29	344.64	87.02	0.33	83.82	29.12	7.35	0.43	107.56	1.37	344.64
1	6	49	0.2225	0.21	48.91	0.12	28.38	231.03	53.30	0.46	106.58	40.12	9.26	1.94	447.55	1.63	376.50
1	6	55	0.2007	0.22	57.29	0.10	24.81	147.40	37.70	0.28	72.38	28.16	7.20	0.29	73.66	1.44	367.78
1	6	58	0.204	0.09	22.39	0.13	31.96	398.74	100.33	0.34	86.05	28.82	7.25	0.32	80.27	2.06	518.58
1	6	65	0.2066	0.11	28.07	0.04	10.19	325.55	80.88	0.16	39.75	26.22	6.51	0.13	32.55	1.94	481.50
1	6	68	0.2036	0.03	6.81	0.02	4.54	60.80	15.33	0.11	27.23	24.74	6.24	0.73	184.04	0.62	156.81
1	6	71	0.2029	0.04	10.63	0.06	15.43	74.56	18.86	0.16	41.24	14.43	3.65	0.19	48.07	1.67	421.47
1	6	R-74	0.2086	0.25	61.52	0.11	27.07	282.70	69.56	0.65	159.94	49.92	12.28	0.59	144.69	3.11	765.27
1	6	77	0.2033	0.15	37.62	0.04	10.60	390.40	98.57	0.38	96.95	28.31	7.15	0.13	31.56	1.35	340.85
2	4	50	0.205	0.20	49.58	0.03	8.01	100.26	25.10	0.27	67.35	16.80	4.21	0.66	165.01	1.53	382.10
2	4	59	0.2037	0.15	38.30	0.12	29.73	149.84	37.76	0.40	100.04	23.99	6.05	0.26	65.26	2.42	609.31
2	4	78	0.2026	0.51	129.72	0.03	7.35	157.71	39.96	0.14	35.98	42.94	10.88	0.81	203.95	0.96	243.73
2	4	81	0.2037	0.10	25.20	0.04	10.84	99.33	25.03	0.28	70.81	23.56	5.94	0.19	46.62	1.52	382.52
2	4	84	0.2059	0.32	79.53	0.10	25.18	248.75	62.01	0.61	151.07	46.30	11.54	2.68	668.61	2.09	521.28
2	4	87	0.2237	0.15	35.11	0.06	14.46	166.18	38.13	0.32	72.74	47.15	10.82	4.92	1128.25	1.48	338.91
2	4	90	0.2038	0.13	31.99	0.05	13.60	59.07	14.88	0.04	10.33	14.78	3.72	0.24	59.69	2.06	519.60
2	4	93	0.2022	0.38	97.23	0.04	11.17	309.22	78.50	0.30	76.16	26.15	6.64	0.37	92.66	1.25	317.58
2	4	96	0.2026	0.09	23.06	0.04	9.37	71.78	18.18	0.09	23.56	15.94	4.04	0.13	33.95	1.48	374.71
2	4	99	0.2099	0.14	33.99	0.01	3.18	77.74	19.01	0.15	37.66	11.87	2.90	0.03	8.07	1.38	337.47
2	4	102	0.2016	0.16	40.48	0.03	6.87	47.30	12.04	0.16	40.74	18.27	4.65	0.04	9.42	2.02	513.05
2	4	105	0.2103	0.41	100.07	0.04	10.25	150.19	36.66	0.72	175.74	22.91	5.59	0.29	71.27	2.36	575.78
2	4	108	0.2088	0.21	51.63	0.07	15.98	122.61	30.14	0.35	86.29	20.15	4.95	0.29	71.05	3.02	741.68
2	4	111	0.2028	0.45	113.64	-0.01	-2.02	406.75	102.95	0.49	125.03	20.02	5.07	-0.01	-2.53	1.23	312.08
2	4	114	0.2061	0.23	56.78	0.03	6.97	70.62	17.59	0.19	47.32	14.38	3.58	0.44	108.34	1.62	404.46
2	4	117	0.2016	0.05	13.49	0.04	10.18	110.10	28.03	0.09	22.92	16.29	4.15	0.10	25.21	1.42	360.28
2	4	120	0.2063	0.09	22.39	0.06	15.18	110.60	27.52	0.30	74.39	19.04	4.74	1.02	253.29	2.07	515.79
2	4	123	0.2034	0.32	80.25	0.03	6.56	265.34	66.96	1.33	334.38	19.39	4.89	1.00	251.60	2.06	519.86
2	4	126	0.2036	0.06	15.63	0.03	8.57	152.25	38.38	0.39	99.33	19.75	4.98	0.01	2.02	1.55	390.02
2	4	129	0.2026	0.19	47.88	0.08	20.78	103.50	26.22	0.25	62.58	24.77	6.28	0.42	106.66	1.65	417.78
2	4	132	0.207	0.01	2.73	0.00	0.00	55.28	13.71	0.06	14.13	5.47	1.36	0.15	37.44	0.54	134.65
2	4	135	0.2048	0.27	67.42	-0.05	-12.28	159.83	40.06	0.52	129.83	13.24	3.32	0.28	68.92	0.56	141.36
2	4	138	0.2084	0.07	16.01	0.04	9.61	21.49	5.29	0.04	9.11	7.35	1.81	0.02	3.94	0.93	230.05
2	5	51	0.2034	0.07	16.66	0.10	25.49	37.30	9.41	0.26	66.12	15.97	4.03	2.95	744.46	1.54	388.38
2	5	60	0.2015	0.09	22.67	0.12	31.59	74.89	19.08	0.25	62.67	22.00	5.60	0.32	82.03	3.02	769.57
2	5	79	0.2021	0.25	64.51	0.06	14.99	257.29	65.35	0.41	104.13	38.04	9.66	1.18	299.45	1.10	279.13
2	5	82	0.2091	0.11	27.00	0.08	18.41	129.55	31.80	0.36	89.11	22.03	5.41	0.18	44.19	2.15	526.80
2	5	85	0.2028	0.12	31.39	0.09	21.77	109.71	27.77	0.56	140.47	35.06	8.87	3.58	905.11	2.53	639.60
2	5	88	0.2087	0.27	66.90	0.06	13.77	13.58	3.34	0.15	37.38	26.39	6.49	5.96	1466.61	0.52	127.89
2	5	91	0.2096	0.13	31.59	0.05	12.73	328.78	80.52	0.24	59.26	38.10	9.33	0.36	87.18	2.41	589.46
2	5	94	0.2007	0.05	12.02	0.03	8.70	97.19	24.86	0.22	56.52	20.95	5.36	0.10	24.30	1.90	486.70
2	5	97	0.2047	0.08	19.06	0.05	11.28	53.64	13.45	-0.02	-4.01	37.98	9.52	0.09	22.32	2.44	611.35
2	5	100	0.2072	0.04	9.17	0.00	0.00	23.92	5.92	-0.04	-8.92	11.64	2.88	0.03	7.68	0.97	239.80
2	5	103	0.2031	0.06	15.67	0.05	13.39	56.31	14.23	0.15	37.91	25.80	6.52	0.13	33.87	2.55	643.46
2	5	106	0.2052	0.17	42.02	0.08	20.01	217.16	54.32	0.37	92.05	34.64	8.66	0.31	78.30	3.97	993.33
2	5	109	0.2204	0.15	35.63	0.08	17.93	139.79	32.56	0.27	62.18	23.87	5.56	0.34	78.49	3.21	748.29
2	5	112	0.2015	0.04	10.44	0.02	4.33	98.98	25.21	0.15	38.72	20.91	5.33	0.12	29.80	2.03	517.38
2	5	115	0.2029	0.03	8.60	0.00	-0.51	30.47	7.71	0.19	48.07	14.15	3.58	-0.01	-1.52	1.49	377.70
2	5	118	0.2043	0.09	23.37	0.04	8.79	157.84	39.66	0.32	80.15	24.23	6.09	-0.04	-9.55	0.91	228.89
2	5	121	0.1714	0.27	81.46	0.14	41.93	153.05	45.84	0.02	4.49	49.53	14.83	0.52	154.53	2.83	848.11
2	5	124	0.2159	0.09	20.45	0.02	4.99	172.08	40.91	0.39	93.20	16.23	3.86	0.15	35.90	1.48	352.11
2	5	127	0.2014	0.03	7.65	0.01	3.57	77.63	19.79	0.27	69.07	18.03	4.59	0.08	19.37	1.91	485.77
2	5	130	0.2027	0.04	9.37	0.08	20.26	92.90	23.53	0.31	77.24	28.80	7.29	0.43	108.89	1.15	290.96
2	5	133	0.2059	0.01	1.99	0.03	8.23	84.02	20.95	0.20	49.86	18.33	4.57	0.06	15.71	0.97	240.82
2	5	136	0.2044	-0.03	-8.29	-0.05	-11.55	49.83	12.51	0.18	43.95	5.19	1.30	0.03	8.04	0.37	93.92
2	5	139	0.2098	-0.02	-4.40	0.01	1.71	11.01	2.69	0.03	7.83	5.75	1.41	0.02	3.91	0.78	189.86
2	6	52	0.2022	0.28	70.57	0.13	33.00	147.95	37.56	0.57	145.46	66.31	16.83	2.50	633.88	1.88	476.24
2	6	61	0.2037	0.16	39.81	0.06	15.88	331.09	83.43	0.36	90.46	24.08	6.07	0.43	108.35	1.50	377.98
2	6	80	0.2067	0.24	58.61	0.06	13.91	319.41	79.32	0.27	67.55	47.39	11.77	1.04	258.51	1.16	286.82
2	6	83	0.2036	0.25	63.03	0.05	13.36	199.39	50.27	0.28	70.34	19.24	4.85	0.18	44.88	1.92	485.06
2	6	86	0.2041	0.22	55.58	0.12	30.18	58.82	14.79	0.48	121.72	54.64	13.74	5.31	1335.18	1.31	328.95
2	6	89	0.2063	0.21	52.25	0.04	9.21	299.52	74.52	0.24	59.96	26.01	6.47	0.32	78.87	2.02	502.85

Landuse	Position	Sample	Weight	Cd 111	Cd-corr	In 115	In-corr	Ba 137	Ba-corr	Tl 205	Tl-corr	Pb 207	Pb-corr	Bi 209	Bi-corr	U 238	U-corr
1=N,2=Ex, 3=Ag	4=surf, 5=sub	#			PPB		PPB		PPM		PPB		PPM		PPB		
4=sink	6=bank, 100=slip																
2	6	**92**	0.2015	0.14	36.68	0.04	8.92	308.22	78.52	0.29	73.36	25.15	6.41	0.22	56.04	1.58	402.49
2	6	**95**	0.2033	0.06	14.39	0.04	9.85	335.09	84.61	0.29	73.22	25.15	6.35	0.16	39.64	1.36	344.39
2	6	**98**	0.2006	0.11	27.12	0.06	14.07	221.27	56.62	0.19	48.36	32.41	8.29	0.11	28.91	2.57	656.34
2	6	**101**	0.206	0.17	43.11	0.02	4.73	111.23	27.72	0.23	58.31	18.23	4.54	0.00	-1.00	1.50	374.51
2	6	**104**	0.2009	0.06	14.05	0.03	7.15	51.29	13.10	0.13	33.98	24.27	6.20	0.07	17.89	2.01	513.30
2	6	**107**	0.207	0.10	24.55	0.05	12.15	231.99	57.53	0.25	61.99	35.84	8.89	0.38	95.22	2.55	632.82
2	6	**110**	0.2027	0.15	39.00	0.11	27.35	166.13	42.07	0.10	25.83	27.20	6.89	0.29	73.69	3.23	816.92
2	6	**113**	0.2041	0.09	23.64	-0.01	-2.51	206.57	51.95	0.36	90.03	23.26	5.85	0.02	4.78	1.21	304.81
2	6	**116**	0.2038	0.18	44.33	0.04	9.07	162.05	40.82	0.25	62.71	29.77	7.50	0.08	19.14	2.04	513.80
2	6	**119**	0.2009	0.08	20.18	0.06	16.35	348.64	89.08	0.14	34.75	13.60	3.47	0.09	23.76	1.31	334.45
2	6	**122**	0.2076	0.16	40.30	0.10	24.73	212.27	52.48	0.28	68.98	44.80	11.08	2.03	501.43	1.11	273.71
2	6	**125**	0.203	0.03	6.83	0.02	5.31	183.01	46.28	0.21	52.34	13.36	3.38	0.15	37.93	1.30	329.47
2	6	**128**	0.2029	0.04	10.88	0.00	1.01	162.82	41.19	0.05	13.16	18.78	4.75	0.07	17.46	1.90	481.17
2	6	**131**	0.2073	0.10	25.50	0.12	28.97	131.50	32.56	0.16	39.62	31.38	7.77	0.36	89.88	1.55	384.05
2	6	**134**	0.2039	-0.01	-3.02	0.04	9.06	138.30	34.82	0.19	47.08	19.35	4.87	0.11	27.69	1.09	273.64
2	6	**137**	0.2017	-0.02	-5.60	-0.01	-1.53	77.46	19.71	0.41	103.83	27.21	6.92	0.05	13.23	1.19	303.35
2	6	**140**	0.2063	0.00	1.00	0.01	2.99	145.38	36.17	0.19	47.52	20.75	5.16	0.06	14.43	1.27	316.99
3	4	**141**	0.2024	0.89	225.20	-0.03	-8.12	81.15	20.58	0.13	33.22	12.08	3.06	0.15	38.29	2.36	599.53
3	4	**144**	0.2025	1.47	372.36	0.02	5.58	217.51	55.14	0.30	76.04	26.24	6.65	0.24	60.84	2.88	730.79
3	4	**147**	0.2063	1.79	444.88	-0.01	-1.74	57.36	14.27	0.04	9.45	11.65	2.90	0.07	16.92	3.34	832.03
3	4	**150**	0.2023	1.31	331.37	0.00	-1.01	77.30	19.61	0.10	24.87	12.86	3.26	0.14	36.54	2.90	736.33
3	4	**153**	0.2028	2.34	591.51	0.03	6.58	449.58	113.79	0.32	79.73	23.98	6.07	0.37	94.41	5.78	1463.71
3	4	**156**	0.2021	2.14	542.25	0.02	5.59	247.32	62.81	0.19	49.02	20.66	5.25	0.51	129.28	3.20	813.25
3	4	**159**	0.2025	2.64	670.21	0.00	0.51	144.47	36.62	0.28	71.48	17.19	4.36	0.19	49.18	5.14	1302.64
3	4	**162**	0.2007	1.17	298.72	0.03	6.91	336.30	86.01	0.65	166.50	31.75	8.12	0.25	64.96	4.26	1088.49
3	4	**165**	0.2041	4.54	1142.54	0.02	5.78	321.64	80.89	0.70	176.30	35.69	8.98	0.38	94.81	6.49	1631.70
3	4	**168**	0.2011	3.96	1010.01	0.01	2.55	334.69	85.43	0.51	130.43	31.97	8.16	0.35	88.06	5.19	1324.73
3	4	**171**	0.2031	2.76	696.78	-0.03	-6.32	147.31	37.23	0.19	46.76	13.99	3.53	0.34	86.43	4.58	1157.52
3	4	**174**	0.2012	9.91	2528.23	0.03	7.91	308.63	78.74	0.75	191.85	35.89	9.16	0.47	120.42	6.95	1773.59
3	4	**177**	0.2034	1.26	318.23	-0.03	-7.32	119.01	30.03	0.01	2.78	11.16	2.82	0.13	32.55	1.96	494.88
3	4	**180**	0.2065	0.04	209.79	0.01	2.73	159.95	39.76	0.62	154.06	20.07	5.19	0.00	19.39	2.30	572.71
3	4	**183**	0.2015	0.96	243.79	0.02	5.86	308.18	78.51	0.31	78.21	37.43	9.54	0.82	207.61	2.23	568.32
3	4	**186**	0.2018	1.84	467.52	0.02	3.82	310.89	79.08	0.40	102.51	44.33	11.28	0.92	233.76	2.83	720.10
3	5	**142**	0.2033	0.00	0.76	0.00	-0.25	36.32	9.17	0.05	12.62	16.40	4.14	0.16	39.89	1.52	383.02
3	5	**145**	0.2034	0.60	150.91	0.17	41.89	99.26	25.05	0.28	70.91	70.59	17.82	1.19	300.81	7.77	1960.33
3	5	**148**	0.2036	0.09	22.19	0.03	8.07	170.73	43.04	0.17	42.10	29.30	7.39	0.06	14.87	1.92	482.79
3	5	**151**	0.2032	0.03	8.08	0.02	4.04	25.94	6.55	0.06	14.40	16.88	4.26	0.30	76.29	1.47	372.34
3	5	**154**	0.2006	0.32	82.14	0.11	28.66	96.20	24.62	0.01	3.58	44.23	11.32	0.63	162.23	10.23	2617.16
3	5	**157**	0.2088	0.73	179.46	0.03	6.64	350.60	86.19	0.32	78.42	21.65	5.32	0.56	137.91	2.01	495.11
3	5	**160**	0.201	0.23	57.46	0.00	0.26	79.46	20.29	0.17	44.43	23.98	6.12	0.13	33.96	3.47	884.87
3	5	**163**	0.2022	0.11	28.69	0.06	15.49	173.83	44.13	0.50	127.18	36.69	9.32	0.36	91.64	5.02	1275.13
3	5	**166**	0.2034	0.13	32.05	0.07	17.67	102.98	25.99	0.90	227.63	34.19	8.63	1.34	337.15	3.80	959.22
3	5	**169**	0.2083	0.07	16.51	0.09	22.42	219.85	54.18	0.77	190.73	29.51	7.27	1.81	445.04	2.31	568.75
3	5	**172**	0.2039	0.11	28.19	0.06	15.36	62.67	15.78	0.25	63.19	23.93	6.02	0.55	139.21	1.82	456.91
3	5	**175**	0.2016	0.12	30.81	0.04	9.17	238.41	60.70	0.67	169.83	28.73	7.31	0.56	143.35	2.37	603.43
3	5	**178**	0.202	0.06	14.23	-0.01	-1.78	139.92	35.56	0.22	55.65	36.43	9.26	0.01	1.78	1.82	462.48
3	5	**181**	0.2005	0.10	26.11	0.03	7.17	20.64	5.28	-0.03	-7.94	9.69	2.48	0.10	26.37	1.16	297.74
3	5	**184**	0.203	0.44	111.00	0.03	7.59	371.49	93.93	0.34	84.96	43.64	11.03	0.79	200.26	1.38	349.70
3	5	**187**	0.2042	0.02	4.78	0.04	9.80	149.92	37.69	0.48	119.90	35.44	8.91	0.90	227.24	2.12	532.66
3	6	**143**	0.2065	0.05	11.43	0.03	8.20	94.76	23.56	0.20	50.71	10.74	2.67	0.14	34.05	1.26	313.70
3	6	**146**	0.2037	0.14	34.02	0.11	26.46	263.79	66.47	0.42	106.59	39.57	9.97	0.72	180.42	3.75	943.95
3	6	**149**	0.2088	0.03	7.13	0.01	1.23	199.12	48.95	0.02	4.18	21.80	5.36	0.05	12.29	1.50	367.52
3	6	**152**	0.2045	0.11	27.36	0.01	2.76	37.60	9.44	0.07	18.32	16.27	4.08	0.18	45.93	1.42	357.43
3	6	**155**	0.2095	0.12	29.40	0.03	7.35	384.15	94.12	0.24	59.78	27.26	6.68	0.26	63.95	1.44	351.84
3	6	**158**	0.2147	0.23	54.03	0.05	12.91	409.25	97.84	0.29	70.29	33.75	8.07	0.72	172.85	1.93	461.90
3	6	**161**	0.2016	0.05	11.71	0.03	6.37	274.33	69.85	0.27	67.73	39.94	10.17	0.17	43.03	2.30	584.34
3	6	**164**	0.2041	0.25	62.37	0.02	5.03	322.97	81.23	0.49	122.48	32.33	8.13	0.13	33.70	2.43	610.13
3	6	**167**	0.204	0.20	50.83	0.05	12.58	320.22	80.57	0.37	92.85	39.96	10.06	1.94	487.13	1.46	367.61
3	6	**170**	0.205	0.03	7.76	0.02	3.76	144.12	36.08	0.41	102.41	38.49	9.64	0.47	118.68	1.75	437.68
3	6	**173**	0.2037	0.02	5.80	0.04	9.32	96.98	24.44	0.36	90.97	20.53	5.17	0.57	142.37	1.47	371.43
3	6	**176**	0.2043	0.11	26.38	0.00	-0.50	161.48	40.57	0.28	69.85	27.55	6.92	0.29	72.36	1.87	470.09
3	6	**179**	0.203	0.03	7.59	0.02	4.30	139.72	35.33	0.10	24.27	19.03	4.81	0.14	34.39	1.80	455.65
3	6	**182**	0.2065	0.26	63.63	0.00	0.99	37.22	9.25	0.08	20.13	10.67	2.65	0.15	37.53	1.34	333.09
3	6	**185**	0.2022	0.34	86.31	0.05	11.93	464.89	118.02	0.36	92.15	75.26	19.10	1.07	270.87	1.63	414.55
3	6	**188**	0.2015	0.31	79.99	0.02	6.11	297.20	75.71	0.29	72.60	45.85	11.68	0.94	239.20	1.10	279.96

APPENDIX L

ICP-MS RESULTS – SINK

Landuse	Position	Sample	Weight	Li 7	Li-corr	B 10	B-corr	Na 23	Na-corr	Mg 24	Mg-corr	Al 27	Al-corr	Si 28	Si-corr	P 31	P-corr
1=N,2=Ex, 3=Ag	4=surf, 5=sub	#			PPM		PPB		PPM		PPM		PPM		PPM		PPM
4=sink	6=bank, 100=slip																
4	Mouth	189	0.2037	58.68	14.79	17.85	4497.99	131675.57	33180.69	27449.61	6916.98	47094.72	11867.31	269.43	67.89	3873.11	975.98
4	East	190	0.2041	54.28	13.65	11.70	2942.74	70133.12	17638.08	24490.52	6159.23	52011.41	13080.58	175.85	44.23	3635.19	914.23
4	Middle	191	0.207	57.40	14.23	7.76	1924.75	108219.94	26835.41	22250.33	5517.44	48640.70	12061.48	502.81	124.68	1720.66	426.67
4	West	192	0.2014	95.66	24.38	2.84	724.33	50222.57	12800.02	21917.17	5585.94	59641.36	15200.55	236.09	60.17	1992.83	507.90

Landuse	Position	Sample	Weight	S 34	S-corr	K 39	K-corr	Ca 43	Ca-corr	V 51	V-corr	Cr 52	Cr-corr	Fe 54	Fe-corr	Mn 55	Mn-corr
1=N,2=Ex, 3=Ag	4=surf, 5=sub	#			PPM		PPM		PPM		PPM		PPM		PPM		PPM
4=sink	6=bank, 100=slip																
4	Mouth	189	0.2037	85271.1	21487.3	11774.55	2967.05	110413.3	27822.9	189.91	47.85	101.96	25.69	118722.88	29916.77	271.64	68.45
4	East	190	0.2041	43388.9	10912.1	9745.84	2451.02	22178.80	5577.84	227.00	57.09	92.82	23.34	109100.41	27438.14	382.91	96.30
4	Middle	191	0.207	85690.1	21248.7	12236.58	3034.32	49788.30	12346.05	231.95	57.52	75.84	18.80	131133.38	32517.28	379.42	94.08
4	West	192	0.2014	8505.22	2167.69	9903.08	2523.96	3943.35	1005.03	314.89	80.25	86.90	22.15	161019.20	41038.31	1396.02	355.80

Landuse	Position	Sample	Weight	Co 59	Co-corr	Ni 60	Ni-corr	Cu 63	Cu-corr	Zn 66	Zn-corr	As 75	As-corr	Se 82	Se-corr	Sr 88	Sr-corr
1=N,2=Ex, 3=Ag	4=surf, 5=sub	#			PPM		PPM		PPM		PPM		PPM		PPB		PPM
4=sink	6=bank, 100=slip																
4	Mouth	189	0.2037	28.92	7.29	74.44	18.76	64.23	16.19	207.29	52.23	131.63	33.17	9.51	2395.65	1266.0	319.03
4	East	190	0.2041	23.53	5.92	30.52	7.68	60.58	15.24	177.97	44.76	75.29	18.93	6.57	1651.06	335.78	84.45
4	Middle	191	0.207	27.13	6.73	30.39	7.54	60.62	15.03	132.93	32.96	102.94	25.52	7.02	1740.51	562.55	139.50
4	West	192	0.2014	61.86	15.77	30.14	7.68	116.06	29.58	249.11	63.49	62.67	15.97	4.56	1161.42	101.43	25.85

Landuse	Position	Sample	Weight	Ag 109	Ag-corr	Cd 111	Cd-corr	In 115	In-corr	Ba 137	Ba-corr	Tl 205	Tl-corr	Pb 207	Pb-corr	Bi 209	Bi-corr	U 238	U-corr
1=N,2=Ex, 3=Ag	4=surf, 5=sub	#			PPB		PPB		PPB		PPM		PPB		PPM		PPB		
4=sink	6=bank, 100=slip																		
4	Mouth	189	0.2037	0.39	98.53	2.84	715.65	0.16	41.07	53.33	13.44	1.00	252.49	39.85	10.04	0.65	164.55	7.30	1839.77
4	East	190	0.2041	0.33	83.24	0.83	207.73	0.13	31.69	52.37	13.17	0.62	155.68	56.31	14.16	0.95	239.67	7.28	1830.63
4	Middle	191	0.207	0.31	76.62	0.63	156.22	0.09	23.06	47.11	11.68	0.46	113.32	44.88	11.13	0.87	215.73	13.30	3297.02
4	West	192	0.2014	0.37	94.30	0.37	93.03	0.12	30.33	74.98	19.11	0.34	85.63	53.98	13.76	1.34	341.01	4.95	1262.35

APPENDIX M

FULL PROGRAMME KRUSKALL-WALLIS H-TEST RESULTS

M-1 Landscape units

Kruskal-Wallis ANOVA by Ranks; Li-corr (ICP_data in Project_KWall&D
Independent (grouping) variable: Landuse
Kruskal-Wallis test: H (2, N= 150) =10.34055 p =.0057

Depend.: Li-corr	Code	Valid N	Sum of Ranks
1	1	33	2899.000
2	2	69	4361.000
3	3	48	4065.000

Kruskal-Wallis ANOVA by Ranks; Al-corr (ICP_data in Project_K
Independent (grouping) variable: Landuse
Kruskal-Wallis test: H (2, N= 150) =10.95316 p =.0042

Depend.: Al-corr	Code	Valid N	Sum of Ranks
1	1	33	1844.000
2	2	69	5239.000
3	3	48	4242.000

Kruskal-Wallis ANOVA by Ranks; Si-corr (ICP_data in Project_I
Independent (grouping) variable: Landuse
Kruskal-Wallis test: H (2, N= 150) =68.22049 p =.0000

Depend.: Si-corr	Code	Valid N	Sum of Ranks
1	1	33	978.000
2	2	69	5041.000
3	3	48	5306.000

Kruskal-Wallis ANOVA by Ranks; P-corr (ICP_data in Project_K
Independent (grouping) variable: Landuse
Kruskal-Wallis test: H (2, N= 150) =10.38613 p =.0056

Depend.: P-corr	Code	Valid N	Sum of Ranks
1	1	33	2763.000
2	2	69	4361.000
3	3	48	4201.000

Kruskal-Wallis ANOVA by Ranks; Ca-corr (ICP_data in Project_
Independent (grouping) variable: Landuse
Kruskal-Wallis test: H (2, N= 150) =9.331021 p =.0094

Depend.: Ca-corr	Code	Valid N	Sum of Ranks
1	1	33	2147.000
2	2	69	4806.000
3	3	48	4372.000

Kruskal-Wallis ANOVA by Ranks; V-corr (ICP_data in Project_KW
Independent (grouping) variable: Landuse
Kruskal-Wallis test: H (2, N= 150) =7.233503 p =.0269

Depend.: V-corr	Code	Valid N	Sum of Ranks
1	1	33	2125.000
2	2	69	4937.000
3	3	48	4263.000

Kruskal-Wallis ANOVA by Ranks; Cr-corr (ICP_data in Project_KWall&I
Independent (grouping) variable: Landuse
Kruskal-Wallis test: H (2, N= 150) =10.28219 p =.0059

Depend.: Cr-corr	Code	Valid N	Sum of Ranks
1	1	33	1852.000
2	2	69	5271.000
3	3	48	4202.000

Kruskal-Wallis ANOVA by Ranks; Mn-corr (ICP_data in Project_KW
Independent (grouping) variable: Landuse
Kruskal-Wallis test: H (2, N= 150) =6.467282 p =.0394

Depend.: Mn-corr	Code	Valid N	Sum of Ranks
1	1	33	2969.000
2	2	69	4620.000
3	3	48	3736.000

Kruskal-Wallis ANOVA by Ranks; Co-corr (ICP_data in Project_KWa
Independent (grouping) variable: Landuse
Kruskal-Wallis test: H (2, N= 150) =6.658967 p =.0358

Depend.: Co-corr	Code	Valid N	Sum of Ranks
1	1	33	2888.000
2	2	69	4548.000
3	3	48	3889.000

Kruskal-Wallis ANOVA by Ranks; Zn-corr (ICP_data in Project_KW
Independent (grouping) variable: Landuse
Kruskal-Wallis test: H (2, N= 150) =8.328391 p =.0155

Depend.: Zn-corr	Code	Valid N	Sum of Ranks
1	1	33	2697.000
2	2	69	4457.000
3	3	48	4171.000

Kruskal-Wallis ANOVA by Ranks; As-corr (ICP_data in Project_KWall
Independent (grouping) variable: Landuse
Kruskal-Wallis test: H (2, N= 150) =9.118547 p =.0105

Depend.: As-corr	Code	Valid N	Sum of Ranks
1	1	33	2666.000
2	2	69	4433.000
3	3	48	4226.000

Kruskal-Wallis ANOVA by Ranks; Se-corr (ICP_data in Project_KWa
Independent (grouping) variable: Landuse
Kruskal-Wallis test: H (2, N= 150) =23.28324 p =.0000

Depend.: Se-corr	Code	Valid N	Sum of Ranks
1	1	33	3543.000
2	2	69	4757.000
3	3	48	3025.000

Kruskal-Wallis ANOVA by Ranks; Ag-corr (ICP_data in Project_KWa
Independent (grouping) variable: Landuse
Kruskal-Wallis test: H (2, N= 150) =10.21543 p =.0061

Depend.: Ag-corr	Code	Valid N	Sum of Ranks
1	1	33	3188.000
2	2	69	4833.000
3	3	48	3304.000

Kruskal-Wallis ANOVA by Ranks; Cd-corr (ICP_data in Project_KWa
Independent (grouping) variable: Landuse
Kruskal-Wallis test: H (2, N= 150) =11.30231 p =.0035

Depend.: Cd-corr	Code	Valid N	Sum of Ranks
1	1	33	2319.000
2	2	69	4555.500
3	3	48	4450.500

Kruskal-Wallis ANOVA by Ranks; In-corr (ICP_data in Project_KWal
Independent (grouping) variable: Landuse
Kruskal-Wallis test: H (2, N= 150) =25.24109 p =.0000

Depend.: In-corr	Code	Valid N	Sum of Ranks
1	1	33	3364.500
2	2	69	5408.000
3	3	48	2552.500

Kruskal-Wallis ANOVA by Ranks; Bi-corr (ICP_data in Project_KWall
Independent (grouping) variable: Landuse
Kruskal-Wallis test: H (2, N= 150) =10.10894 p =.0064

Depend.: Bi-corr	Code	Valid N	Sum of Ranks
1	1	33	3064.000
2	2	69	4448.000
3	3	48	3813.000

Kruskal-Wallis ANOVA by Ranks; U-corr (ICP_data in Project_KWall
Independent (grouping) variable: Landuse
Kruskal-Wallis test: H (2, N= 150) =21.23868 p =.0000

Depend.: U-corr	Code	Valid N	Sum of Ranks
1	1	33	1984.000
2	2	69	4586.000
3	3	48	4755.000

M-2 Erosion position

Kruskal-Wallis ANOVA by Ranks; Mg-corr (ICP_data in Project_KWall&DFA.stv
Independent (grouping) variable: Position
Kruskal-Wallis test: H (2, N= 150) =31.90947 p =.0000

Depend.: Mg-corr	Code	Valid N	Sum of Ranks
4	4	50	4439.000
5	5	50	2359.000
6	6	50	4527.000

Kruskal-Wallis ANOVA by Ranks; P-corr (ICP_data in Project_KWall&DFA.stw)
Independent (grouping) variable: Position
Kruskal-Wallis test: H (2, N= 150) =64.27365 p =.0000

Depend.: P-corr	Code	Valid N	Sum of Ranks
4	4	50	5711.000
5	5	50	2336.000
6	6	50	3278.000

Kruskal-Wallis ANOVA by Ranks; S-corr (ICP_data in Project_KWall&DFA.stw)
Independent (grouping) variable: Position
Kruskal-Wallis test: H (2, N= 150) =41.24327 p =.0000

Depend.: S-corr	Code	Valid N	Sum of Ranks
4	4	50	5385.000
5	5	50	3009.000
6	6	50	2931.000

Kruskal-Wallis ANOVA by Ranks; K-corr (ICP_data in Project_KWall&DFA.stw)
Independent (grouping) variable: Position
Kruskal-Wallis test: H (2, N= 150) =45.55971 p =.0000

Depend.: K-corr	Code	Valid N	Sum of Ranks
4	4	50	5367.000
5	5	50	2480.000
6	6	50	3478.000

Kruskal-Wallis ANOVA by Ranks; Ca-corr (ICP_data in Project_KWall&DFA.st
Independent (grouping) variable: Position
Kruskal-Wallis test: H (2, N= 150) =56.48426 p =.0000

Depend.: Ca-corr	Code	Valid N	Sum of Ranks
4	4	50	5281.000
5	5	50	2040.000
6	6	50	4004.000

Kruskal-Wallis ANOVA by Ranks; V-corr (ICP_data in Project_KWall&DFA.stw
Independent (grouping) variable: Position
Kruskal-Wallis test: H (2, N= 150) =21.53975 p =.0000

Depend.: V-corr	Code	Valid N	Sum of Ranks
4	4	50	2893.000
5	5	50	3558.000
6	6	50	4874.000

Kruskal-Wallis ANOVA by Ranks; Cr-corr (ICP_data in Project_KWall&DFA.stw)
Independent (grouping) variable: Position
Kruskal-Wallis test: H (2, N= 150) =10.40235 p =.0055

Depend.: Cr-corr	Code	Valid N	Sum of Ranks
4	4	50	3139.000
5	5	50	3660.000
6	6	50	4526.000

Kruskal-Wallis ANOVA by Ranks; Fe-corr (ICP_data in Project_KWall&DFA.stw)
Independent (grouping) variable: Position
Kruskal-Wallis test: H (2, N= 150) =19.30314 p =.0001

Depend.: Fe-corr	Code	Valid N	Sum of Ranks
4	4	50	2862.000
5	5	50	3697.000
6	6	50	4766.000

Kruskal-Wallis ANOVA by Ranks; Mn-corr (ICP_data in Project_KWall&DFA.stw
Independent (grouping) variable: Position
Kruskal-Wallis test: H (2, N= 150) =40.43103 p =.0000

Depend.: Mn-corr	Code	Valid N	Sum of Ranks
4	4	50	4942.000
5	5	50	2250.000
6	6	50	4133.000

Kruskal-Wallis ANOVA by Ranks; Co-corr (ICP_data in Project_KWall&DFA.s
Independent (grouping) variable: Position
Kruskal-Wallis test: H (2, N= 150) =28.37855 p =.0000

Depend.: Co-corr	Code	Valid N	Sum of Ranks
4	4	50	4422.000
5	5	50	2439.000
6	6	50	4464.000

Kruskal-Wallis ANOVA by Ranks; Ni-corr (ICP_data in Project_KWall&DFA
Independent (grouping) variable: Position
Kruskal-Wallis test: H (2, N= 150) =11.21909 p =.0037

Depend.: Ni-corr	Code	Valid N	Sum of Ranks
4	4	50	4031.000
5	5	50	2954.000
6	6	50	4340.000

Kruskal-Wallis ANOVA by Ranks; Cu-corr (ICP_data in Project_KWall&I
Independent (grouping) variable: Position
Kruskal-Wallis test: H (2, N= 150) =17.14117 p =.0002

Depend.: Cu-corr	Code	Valid N	Sum of Ranks
4	4	50	4143.000
5	5	50	2750.000
6	6	50	4432.000

Kruskal-Wallis ANOVA by Ranks; Zn-corr (ICP_data in Project_KWa
Independent (grouping) variable: Position
Kruskal-Wallis test: H (2, N= 150) =25.24332 p =.0000

Depend.: Zn-corr	Code	Valid N	Sum of Ranks
4	4	50	4502.000
5	5	50	2520.000
6	6	50	4303.000

Kruskal-Wallis ANOVA by Ranks; Se-corr (ICP_data in Project_KWall&
Independent (grouping) variable: Position
Kruskal-Wallis test: H (2, N= 150) =11.94331 p =.0026

Depend.: Se-corr	Code	Valid N	Sum of Ranks
4	4	50	4620.000
5	5	50	3185.000
6	6	50	3520.000

Kruskal-Wallis ANOVA by Ranks; Sr-corr (ICP_data in Project_KWall&DFA.st
Independent (grouping) variable: Position
Kruskal-Wallis test: H (2, N= 150) =55.28235 p =.0000

Depend.: Sr-corr	Code	Valid N	Sum of Ranks
4	4	50	5329.000
5	5	50	2105.000
6	6	50	3891.000

Kruskal-Wallis ANOVA by Ranks; Ag-corr (ICP_data in Project_KWall&DFA
Independent (grouping) variable: Position
Kruskal-Wallis test: H (2, N= 150) =7.033881 p =.0297

Depend.: Ag-corr	Code	Valid N	Sum of Ranks
4	4	50	4398.000
5	5	50	3279.000
6	6	50	3648.000

Kruskal-Wallis ANOVA by Ranks; Cd-corr (ICP_data in Project_KWall&
Independent (grouping) variable: Position
Kruskal-Wallis test: H (2, N= 150) =31.73955 p =.0000

Depend.: Cd-corr	Code	Valid N	Sum of Ranks
4	4	50	5142.000
5	5	50	2781.500
6	6	50	3401.500

Kruskal-Wallis ANOVA by Ranks; In-corr (ICP_data in Project_KWall&DF
Independent (grouping) variable: Position
Kruskal-Wallis test: H (2, N= 150) =6.318903 p =.0425

Depend.: In-corr	Code	Valid N	Sum of Ranks
4	4	50	3152.500
5	5	50	4171.000
6	6	50	4001.500

Kruskal-Wallis ANOVA by Ranks; Ba-corr (ICP_data in Project_KWall&D
Independent (grouping) variable: Position
Kruskal-Wallis test: H (2, N= 150) =20.24589 p =.0000

Depend.: Ba-corr	Code	Valid N	Sum of Ranks
4	4	50	3876.000
5	5	50	2751.000
6	6	50	4698.000

Kruskal-Wallis ANOVA by Ranks; Pb-corr (ICP_data in Project_KWall&DF
Independent (grouping) variable: Position
Kruskal-Wallis test: H (2, N= 150) =9.898109 p =.0071

Depend.: Pb-corr	Code	Valid N	Sum of Ranks
4	4	50	3072.000
5	5	50	3816.000
6	6	50	4437.000

APPENDIX N

RADIONUCLIDE RESULTS

N-1 Source area

Landuse code 1=N, 2=Ex 3=Ag	Position code 4=S, 5=SS 6=SB	Number	Cs-137 Bq/kg	Err	Pb-210 Bq/kg	Err	Pb-210-EX Bq/kg	*Err* (est)	Ra-226 Bq/kg	Err	Ra-228 Bq/kg	Err
1	4	WA060034	7.1	1.00	35.9	6.50	14.10	2.55	21.8	3.20	25.2	3.00
1	4	WA060038	8.4	1.30	37.9	7.00	11.70	2.16	26.2	2.40	33.4	3.70
1	4	WA060047	13.1	1.70	45.5	8.00	25.70	4.52	19.8	1.90	24	3.20
1	4	WA060056	17.2	2.30	44.4	8.70	26.20	5.13	18.2	2.10	23.5	3.50
1	4	WA060063	6.7	1.30	35.5	7.60	11.70	2.50	23.8	2.30	32.1	3.90
1	5	WA060035	1.83	0.73	21.3	5.80	-6.50	-1.77	27.8	2.50	38.1	4.00
1	5	WA060039	2.4	0.00	18.4	5.50	-5.00	-1.49	23.4	3.50	36.7	3.80
1	5	WA060048	1.41	0.66	17	5.10	-6.90	-2.07	23.9	2.30	32.7	3.70
1	5	WA060057	1.4	0.00	12	4.10	-6.10	-2.08	18.1	1.90	26	3.10
1	5	WA060064	1.34	0.67	20.1	5.80	-7.00	-2.02	27.1	2.50	42.4	4.40
1	6	WA060037	2	0.00	39.6	8.30	-3.80	-0.80	43.4	3.60	54.6	5.40
1	6	WA060040	2.1	0.00	25.4	6.90	-3.10	-0.84	28.5	2.80	29.6	3.90
1	6	WA060049	1.57	0.70	15.6	5.50	-6.90	-2.43	22.5	2.30	31.3	3.80
1	6	WA060058	1.5	0.00	18.4	4.90	-5.30	-1.41	23.7	2.10	28.4	3.30
1	6	WA060065	1.6	0.00	20.9	5.50	-3.40	-0.89	24.3	2.30	37.8	3.90
2	4	WA060081	5.3	1.10	21.6	5.70	-0.60	-0.16	22.2	2.30	28.1	3.50
2	4	WA060084	15.9	1.80	60.6	9.00	32.60	4.84	28	4.00	28	3.50
2	4	WA060105	18.6	2.10	41.2	7.00	16.90	2.87	24.3	2.10	24.6	2.90
2	4	WA060123	4.2	0.96	29.8	6.40	1.20	0.26	28.6	2.50	28.4	3.40
2	4	WA060132	7.8	1.10	24.8	5.40	6.00	1.31	18.8	2.90	19.1	2.60
2	5	WA060082	3.09	0.86	5.2	4.20	-13.90	-11.23	19.1	2.00	25.4	3.30
2	5	WA060085	2.6	0.00	18.4	5.70	-14.30	-4.43	32.7	4.60	32.9	3.90
2	5	WA060106	1.7	0.00	11.2	4.50	-14.50	-5.83	25.7	2.40	33.9	3.60
2	5	WA060124	1.37	0.65	15.2	4.90	-8.00	-2.58	23.2	2.20	26.9	3.40
2	5	WA060133	1.4	0.00	13.2	4.60	-7.30	-2.54	20.5	1.90	24.7	3.00
2	6	WA060083	6	1.10	26.1	5.90	4.10	0.93	22	2.20	29	3.40
2	6	WA060086	0.83	0.75	18.9	6.40	-2.70	-0.91	21.6	2.40	27.6	4.00
2	6	WA060107	1.57	0.56	21.7	5.30	-2.30	-0.56	24	3.40	29	3.30
2	6	WA060125	2.1	0.00	17.3	4.80	-6.80	-1.89	24.1	3.40	27.1	3.20
2	6	WA060134	1.5	0.00	10.7	4.50	-11.00	-4.63	21.7	2.00	24.9	3.00
3	4	WA060147	9.2	1.40	76	11.00	40.70	5.89	35.3	2.90	23.9	3.10
3	4	WA060156	2.46	0.80	46.2	8.00	18.30	3.17	27.9	2.60	27.3	3.10
3	4	WA060168	12.1	1.70	86	12.00	38.70	5.40	47.3	3.90	31.1	3.80
3	4	WA060174	7.7	1.30	64	9.60	24.60	3.69	39.4	3.20	34.1	3.90
3	4	WA060183	2.62	0.72	37	6.60	14.50	2.59	22.5	2.10	26	3.10
3	4	WA060186	11.3	1.40	52.8	8.40	24.30	3.87	28.5	4.10	21.6	3.00
3	5	WA060148	1.9	0.00	15.3	5.20	-8.00	-2.72	23.3	2.60	29.4	3.60
3	5	WA060157	3.97	0.87	21.6	5.00	-5.80	-1.34	27.4	2.40	30.8	3.40
3	5	WA060169	1.8	0.00	18.4	5.60	-8.20	-2.50	26.6	2.40	35.3	3.90
3	5	WA060175	1.5	0.00	19.4	5.20	-12.00	-3.22	31.4	2.70	32.8	3.60
3	5	WA060184	2.23	0.74	30.2	6.30	7.50	1.56	22.7	2.20	29.5	3.50
3	5	WA060187	2.5	0.00	23.8	6.20	-3.90	-1.02	27.7	4.10	35.7	3.90
3	6	WA060149	1.5	0.00	29.2	5.70	-9.20	-1.80	38.4	3.10	40.5	4.10
3	6	WA060158	1.55	0.62	20.4	4.90	-1.70	-0.41	22.1	2.10	25	3.10
3	6	WA060170	1.5	0.00	18.6	5.00	-4.10	-1.10	22.7	2.10	28.2	3.20
3	6	WA060176	1.6	0.00	29.2	6.10	-1.40	-0.29	30.6	2.70	34.1	3.70
3	6	WA060185	1.86	0.64	30.5	5.90	7.90	1.53	22.6	2.10	29.3	3.30
3	6	WA060188	2.32	0.62	32.1	6.20	10.80	2.09	21.3	3.10	25.9	3.10

N-2 Sink

		Number	Cs-137 Bq/kg	Err	Pb-210 Bq/kg	Err	Pb-210-EX Bq/kg	*Err* (est)	Ra-226 Bq/kg	Err	Ra-228 Bq/kg	Err
Mouth		WA060189	1.8	0.00	114	14.00	106.80	13.12	7.2	1.20	10.6	2.30
East		WA060190	2.34	0.75	135	15.00	123.20	13.69	11.8	1.50	16.8	2.80
South		WA060191	2.99	0.82	66.7	9.80	57.30	8.42	9.4	1.40	17	2.70
West		WA060192	1.17	0.68	43.3	7.80	31.30	5.64	12	1.50	18.5	2.80

APPENDIX O

STUDENT T-TEST RESULTS

Table O-1. Student *t*-test results showing a significant difference between the mean of ^{226}Ra and concentrations of the sink and the surface samples (top) and all subsurface samples (bottom).

$\overline{X}$ of sink*	$\overline{X}$ of surface*	*n* of sink	*n* of surface	Degrees of freedom	**t-test result**	***p* value**
$15.73_{(3.5)}$	$27.04_{(7.86)}$	4	16	18	**2.77**	**0.01**
$\overline{X}$ of sink*	$\overline{X}$ of all subsurface*	*n* of sink	*n* of subsurface	Degrees of freedom	**t-test result**	***p* value**
$15.73_{(3.5)}$	$25.44_{(5.32)}$	4	32	18	**3.53**	**<0.01**

* Subscripts are one standard deviation

Table O-2. Student *t*-test results showing a significant difference between the mean $^{210}Pb_{ex}$ concentrations of the sink and the surface samples (top) and all subsurface samples (bottom).

$\overline{X}$ of sink*	$\overline{X}$ of surface*	*n* of sink	*n* of surface	Degrees of freedom	**t-test result**	***p* value**
$79.65_{(42.7)}$	$21.78_{(13.07)}$	4	16	18	**-4.05**	**<0.01**
$\overline{X}$ of sink*	$\overline{X}$ of all subsurface*	*n* of sink	*n* of surface	Degrees of freedom	**t-test result**	***p* value**
$79.65_{(42.7)}$	$1.25_{(2.91)}$	4	32	18	**-10.25**	**<0.01**

* Subscripts are one standard deviation

Table O-3. Student *t*-test results showing a significant difference between the mean ^{137}Cs concentrations of the sink and the surface samples (top) and all subsurface samples (bottom)..

$\overline{X}$ of sink*	$\overline{X}$ of surface*	*n* of sink	*n* of surface	Degrees of freedom	**t-test result**	***p* value**
$2.08_{(0.78)}$	$9.36_{(4.96)}$	4	16	18	**2.87**	**0.01**
$\overline{X}$ of sink*	$\overline{X}$ of subsurface*	*n* of sink	*n* of subsurface	Degrees of freedom	**t-test result**	***p* value**
$2.08_{(0.78)}$	$1.99_{(0.94)}$	4	32	34	**-0.18**	**0.86**

* Subscripts are one standard deviation

APPENDIX P

PROBE CALIBRATION METHOD

P.1 Standard solution (Formazin)

The following calibration procedure is from (Anderson 1998; Clesceri *et al.* 1998; EPA 1999). A stock Formazin solution was prepared in the laboratory. Care was taken to ensure the quality of the Formazin solution by the use of turbidity-free (deionised) water and preparing the stock turbidity suspension at the time of calibration due to the instability of the solution.

Method for preparing the 4,000 NTU turbidity-unit formazin stock

1.Wearing laboratory powderless disposable gloves, quantitatively transfer 5.0 g of reagent-grade hydrazine sulphate [$(NH_2)_2 \cdot H_2SO_4$] into approximately 400 ml of turbidity-free water in a 1-L volumetric flask.

2.Quantitatively transfer 50.0 g of reagent-grade hexamethylenetetramine [$(CH_2)_6N_4$] into approximately 400 ml of turbidity-free water in a separate, clean flask; stopper and swirl until the $(CH_2)_6N_4$ is completely dissolved. Filter through a 0.2 μm filter into a clean flask.

3.Quantitatively transfer the filtered hexamethylenetetramine into the flask containing hydrazine sulphate (from step 1). Dilute solution to the 1 L mark with turbidity-free water. Stopper and mix for at least 5 minutes, but no more than 10 minutes.

4.Let stand for 24 hours at 25º ± 1ºC to develop the 4,000 turbidity-unit suspension.

5.Transfer the solution to an opaque, light-blocking, polyethylene bottle and store refrigerated. The 4,000 turbidity-unit stock suspension is stable for about a year, if stored at 20 to 25ºC in amber polyethylene bottles.

Method to prepare 500 ml of a 400 NTU turbidity-unit calibrant solution

Dilute the 4,000 turbidity-unit stock solution by a 1:10 ratio as follows:

1. Mix 50 ml of the 4,000 turbidity-unit stock solution in a 500 ml flask.

2. Dilute to the mark with turbidity-free water and mix.

3. Transfer the solution to an opaque, light blocking, polyethylene bottle and store refrigerated. The 400 turbidity-unit stock solution is stable only for about one day.

The above is given as an example to prepare 500 ml of the calibration solution. As the probes were required to be immersed for calibration, a slightly different method was required. Information by the manufacturers required that the probes should be immersed in non-reflective vessels with at least 300 mm of clearance between the probe lens and the tube bottom. This was accomplished by the manufacture of calibration tubes using 100 mm PVC pipe painted internally with automotive bumper-bar matt black paint. A rig was set up to hold the probe in the calibration tube which was mounted on a magnetic stirring stand so as to ensure the Formazin solution remained constant and no settling occurred (Figure P.1).

The calibration tube required approximately 5 L of solution to fill it to ensure the required 300mm separation between the probe lens and the base. To calculate the calibration solution the following formula was used:

$$\frac{\text{NTU required}}{\text{Reference NTU}} \times \text{Final volume}$$

For example, if 5 L of 500 NTU solution is required from the 4,000 NTU stock, then to find the amount to dilute in 5 L will be:

$$\frac{500 NTU}{4{,}000 NTU} \times 5000 ml = 625 ml$$

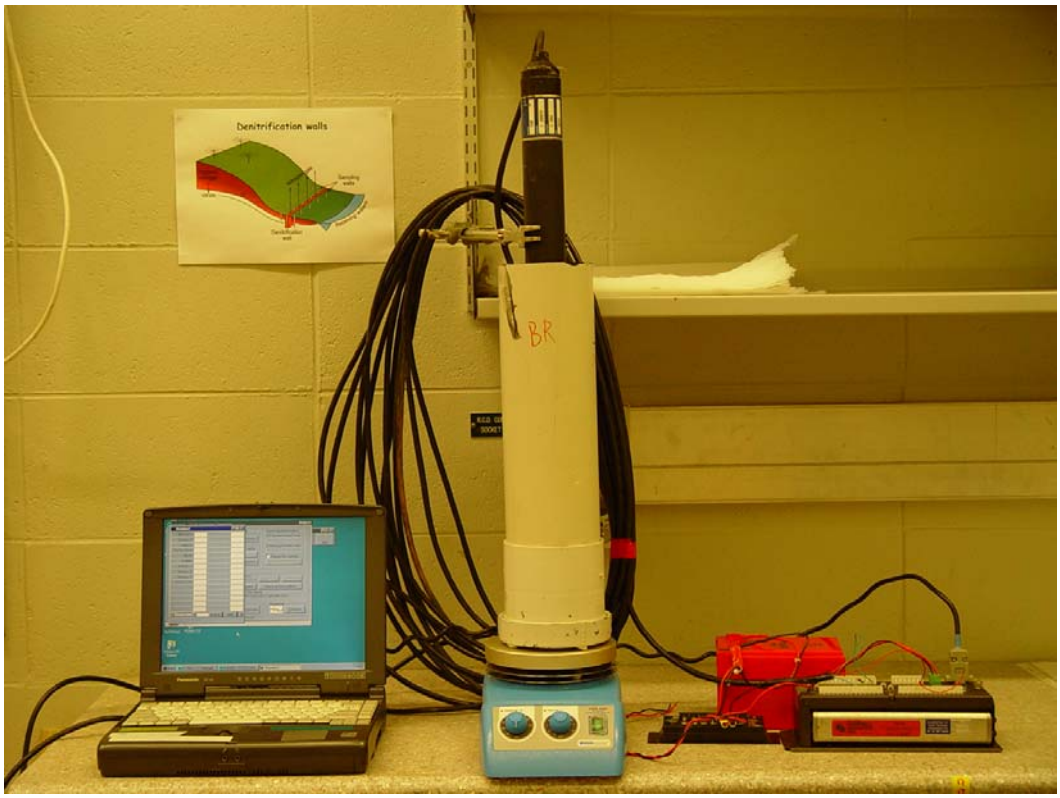

Figure P.1. Probe calibration rig with turbidity probe connected to a CR10 data logger. The probe is mounted into the Formazin container which is on a magnetic stirring base

P.2 Probe to logger signal conversion

As the probes produce information in milliamps (mA) and the Campbells loggers record information in millivolts (mV), a conversion is necessary. This is achieved by the formula:

$$V = I \times R$$

Where V is mV, I is mA, and R is resistance measured in ohms. A loop resistor of 125 ohms converts the mA signal to mV at the logger interface. The Greenspan probes have a reported range of 4mA (~0 NTU) and 20 mA (~2000 NTU). So the calculation becomes:

4mA × 125 ohms = 500 mV

20mA × 125 ohms = 2500 mV

Thus the raw logger readings will be 500mV for 0 NTU and 2500 for 2000 NTU. For convenience, the protocol in the logger can be programmed with a multiplier and an offset, which in this case is set at 1 and 500 respectively. So 0 NTU readings becomes a 500 mV signal recorded and 2000 NTU becomes 2000 mV.

P.3 Calibration of the probes against Formazin standards

The manufactures of other brands of probes recommend a four point measurement to calibrate the probes against a polymer standard (e.g., Arnerich 2003). This study will use eight points of comparison to measure the performance of the probes against the standards, particularly to test the assumption of linearity and scatter. A zero point of comparison of DI water against the probes will also be included.

For each of the eight Formazin standards and the one DI standard, the probe was mounted into the calibration rig as per the photos in Figure P.1. The magnetic stirrer was turned on to ensure an even mix of the standard and this was left for 30 minutes while the probe equalised with the standards temperature and to ensure there was no bubbles around the lens. After this time the magnetic stirrer was turned off and the reading from the probe was recorded. This process was repeated for each probe at each standard level and the results are shown in Table P-1 and graphically in Figure P.2.

Table P-1. Results of probe readings in NTU against Formazin standards.

Standards (NTU)	BR 1	BR 2	BR 3	BR 4
0	-0.09	-3.9	-3.9	-1.43
10	10.6	7	4	20
50	44	49	47	78
100	102	115	120	174
150	136	155	151	212
250	220	251	253	365
500	415	399	383	588
1000	850	703	720	989
1500	1707	1278	1298	1774

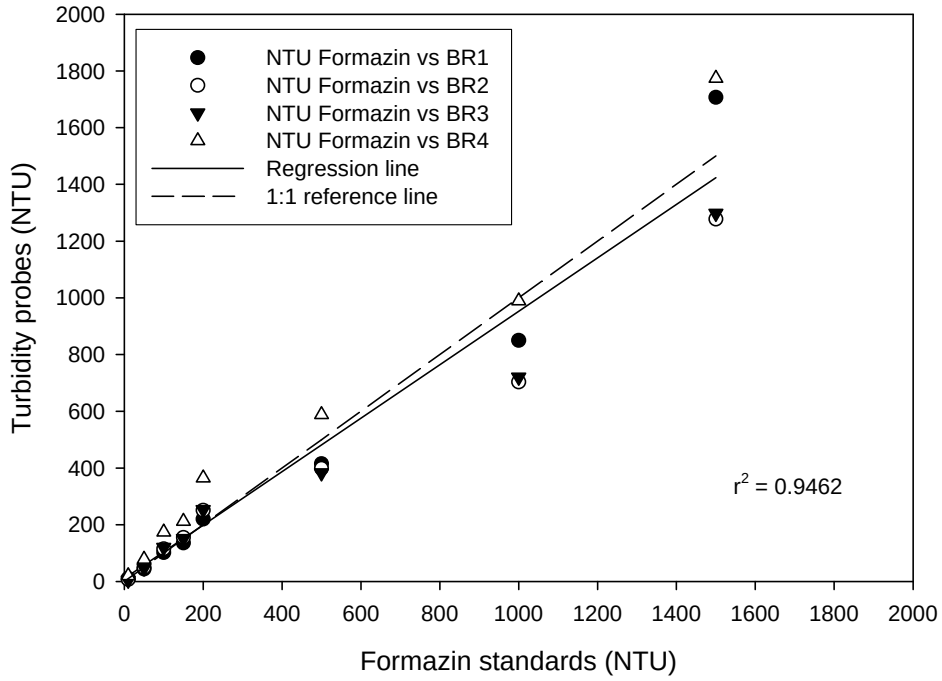

Figure P.2. Results of probe readings in NTU against Formazin standards.

The results show a good fit of the probe readings against the standards with an r^2 of 0.9462 for all 36 results. As seen if Figure P.2, there is some scatter at the higher ranges and a slight underestimation for all values, but for the purposes of this study linearity will be assumed and errors acceptable provided no electronic drift is found during recalibration.

APPENDIX Q

BASE FLOW SEPARATION

It is normal practice when calculating a peak flow/sediment yield storm event to firstly identify that portion of the hydrograph that is over and above base flow (i.e., what flow is caused by the storm?). Thus it is necessary to separate base flow from storm flow. An example of base flow separation is shown in Figure Q.1 where base flow is separated from the peak flow using the constant slope method. Then total sediment derived during the storm event ('duration of quickflow') is calculated by multiplying the discharge by the sediment concentration at each time interval for the event duration. The storm events 'peak discharge' value was recorded along with the total sediment yielded. A range of storm events would then be examined to derive their peak discharge/total sediment yield values that would then be plotted to form a peak discharge/total sediment yield relationship. The flow records were then used to identify all the peak flow values, and using the peak discharge/total sediment yield relationship a catchment erosion rate was calculated. The details of the SSY process as used in this thesis will now be detailed.

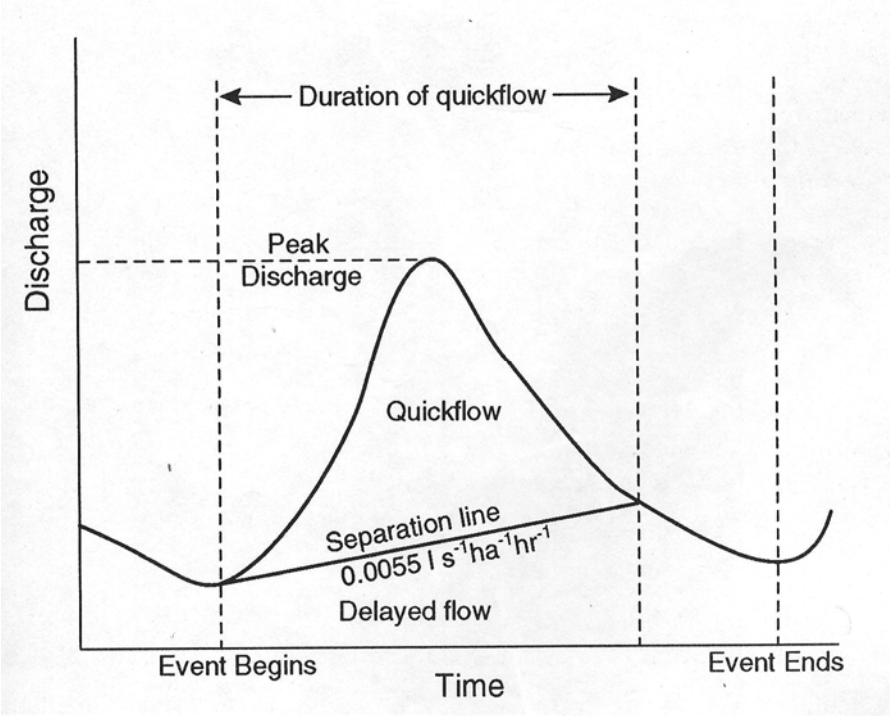

Figure Q.1. Diagram of a storm event elements (Fahey & Rowe 1992). Base flow is separated from quickflow by a constant slope method in this example.

Base flow is defined as the volume of water contributed by ground water. Quick flow is the 'extra' volume contributed by a rainfall event (Gordon *et al.* 2004). The identification of the peak flow component of stream flow is the first step in the SSY method. There are a number of methods to separate peak flow from base flow, the simplest being a graphical approach. There are three different graphical approaches that can be adopted; there is the constant discharge method, constant slope method, and concave method (Figure Q.2). There are also more complicated methods using spreadsheets, algorithms, and computing software (Arnold *et al.* 1995; Bidin & Greer 1997; Brodie & Hostetler 2005; Blume *et al.* 2007). There are arguments for and against each approach and a selection is based on the users preference (Dingman 1994; Davie 2002).

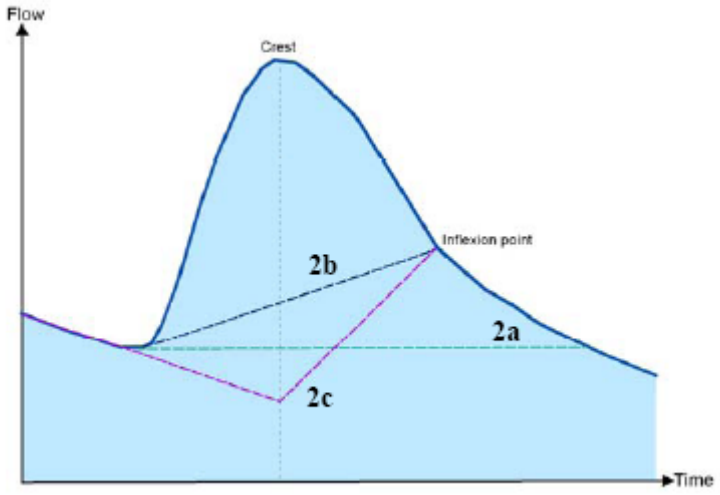

Figure Q.2. Representation of a storm hydrograph with the base flow separation methods of 2a) constant discharge method, 2b) constant slope method, and 2c) concave method (Brodie & Hostetler 2005).

In this study, a modified constant discharge method was used (Figure Q.2, method 2a). While containing some errors, manual identification of base flow separation would only constitute a minor addition to the total error when compared with other assumptions used in my study (Rob Davies-Colley *pers comm*.). Other authors have also reported that the accurate measurement of baseflow is not warranted due to the negligible sediment content of the baseflow (Burney & Edwards 1994).

APPENDIX R

MODIFICATION OF TURBIDITY AND FLOW RECORDS

R-1 Data alteration

Gaps that appear in the data (flow and turbidity) are mainly due to technical problems such as power failure. The other reason for gaps is that parts of the turbidity data has been removed by the author. This occurs primarily for two reasons; one is during periods of weir failure and the other for algae growth over the lens.

An example of weir failure is from the EX-10 subcatchment where a storm event beginning on the 20/12/2006 caused the temporary plywood weir to fail by allowing water around and under the structure (Figure R-1). A site visit on the 25/2/2007 was able to restore the integrity of the weir and return the EX-10 site to the average flows of around 0.4 to 0.5 l sec^{-1}.

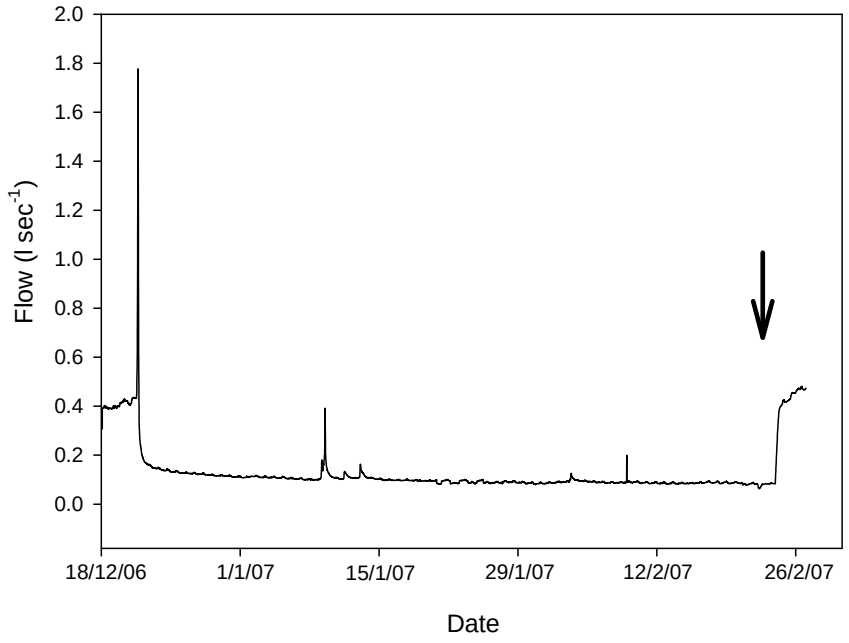

Figure R.1. EX-10 flow data showing the response to a rainfall event that caused the weir to fail. The flow drops until the next site visit where repairs were made and normal flow rates were restored. The date of the site visit is indicated by the arrow.

The second example is also from the EX-10 site where algae has accumulated on the turbidity probe lens causing a rise in NTU readings (Figure P-2). The data shown in Figure R-2 is the NTU readings from the turbidity probe and the stage height values (mm) from the capacitance sensor for July 2006. The NTU values steadily increase over a 15 day period although it doesn't correspond to a rainfall event over the same period. A storm event can be seen around the 20th of July causing a rise in the NTU and flow (or stage height) values, but the NTU continue to climb until a site visit on the 27th of July where the probe was cleaned and NTU values dropped to normal low flow levels.

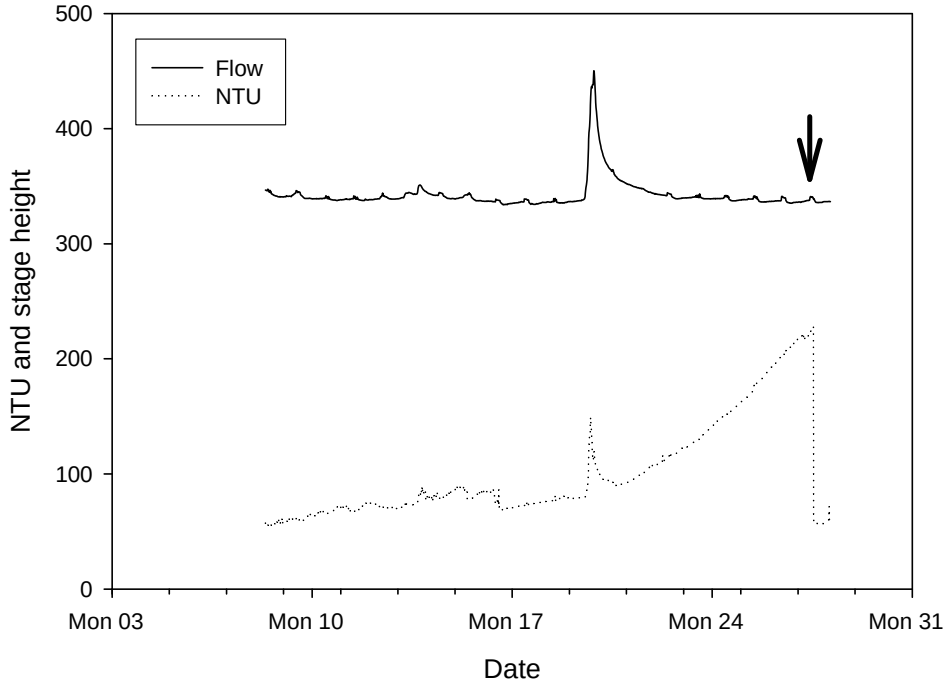

Figure P.2. EX-10 site where algae began to build up on the OBS turbidity probe. This caused a steady increase in NTU readings until a site visit allowed the probe to be cleaned with an immediate response in NTU values. The date of the site visit is indicated by the arrow.

Periods where weirs have failed caused a sudden drop off to low flow values. Periods of algae growth resulted in a 'saw toothed' pattern and that corresponded with site visits that caused a sharp decline in NTU values. The sudden drop off data and saw

tooth data were removed from the data set. Sections of the data missing flow records were patched so as to form the peak flow/sediment yield relationships in the SSY method.

R-2 Method for patching flow records

To begin calculating an averaged erosion figure from storm/sediment relationships, the SSY method requires a continuous flow record to derive a catchment erosion estimate. Due to data drop out caused by a range of problems (power failure, moisture/condensation, insects, and vandalism), it was necessary to patch the flow record.

Of all the four monitoring subcatchments, EX-H was the 'best' site in terms of the reliability of the instrumentation and had the least amount of missing data. The EX-H record was firstly examined for gaps of less than 12 hours and these were filled by linear interpolation. The existing EX-H flow record was compared against all the other variables (flow and rainfall records at all sites) using multivariate analysis in the R statistical software package. The flow record for EX-10 was found to be highly correlated with the flow at EX-H (probably because they were located close to one another), followed by the rainfall record at Castle Rock. So gaps were filled in EX-H by EX-10 and where the EX-10 record was missing, the Castle Rock data was used to fill the gaps.

Multivariate analyse of the flow record from AG-P, EX-H6, and EX-10 was conducted against the flow record for EX-H and the continuous rainfall records obtained from Environment Waikato rainfall records at Castle Rock and Opitonui. The result from the correlation matrix was that the flow record from EX-H was the best predictor of flow in the other three sites, so the EX-H data was used to patch EX-H6, EX-10, and AG-P sites. The Castle Rock rainfall record was used to ensure that the patched spikes are not outliers and are in fact correlated with real events. The resulting p values were in the order of 1×10^{-16} confirming the significance of the patches.

APPENDIX S

FLOW AND RAINFALL RECORDS

The flow results show the data where data drop out has occurred and data that has been removed due to weir failure and algal growth over the turbidity probes (Appendix R). The flow results have been matched with the rainfall records from Castle Rock and Opitonui, as well as the rainfall records from the exotic forest six month post harvest (EX-H6), exotic forest 10 year post harvest (EX-10), and the agricultural pasture (AG-P) suspended sediment monitoring sites (Figure S.1 and Figure S.2).

The EX-H site has the highest flows and has the greatest variability in comparison with the other three sites in spite of being only the second largest catchment. This may indicate that the EX-H site had another source of water other than that from runoff, such as a spring system although this was not observed in the field. The other three sites (EX-H6, EX-10, and AG-P) show a stable flow pattern outside of rainfall events. For both the 2006 and 2007 periods there is a slight decrease in the base flow from a mid year high down to a summer low.

Missing data makes many comparisons between rainfall and flow difficult in the 2006 period. Two events are highlighted in Figure S-1. The first is an August rainfall event that is the largest daily total for the year for the Opitonui site and second largest for Castle Rock and is also captured at the EX-10 site. There is a large response in the EX-H site and EX-10. Another example is the smaller September event which is captured by all five rainfall monitoring stations. All four flow records show a response but in the EX-H site this is harder to detect as the flow moves from a high base flow to a lower base flow.

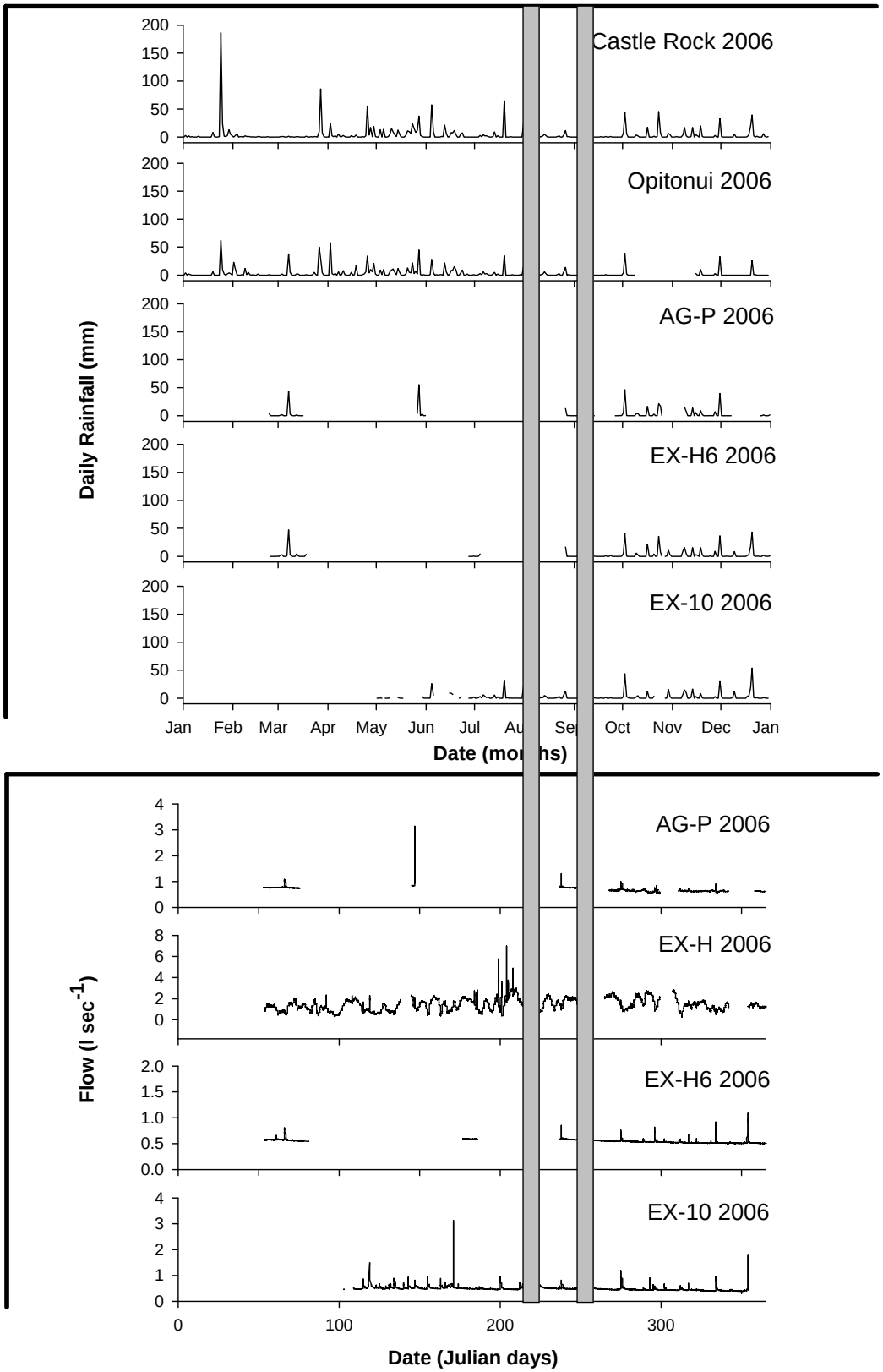

Figure S-1. Rainfall data for the Castle Rock, Opitonui, AG-P, EX-H6, and EX-10, and the corresponding flow records for the four monitoring sites for the year 2006.

In the 2007 results (Figure S-2), the highest rainfall event (April) for that year clearly shows as a flow response in all four stream monitoring sites (and causes a weir failure in EX-10). The second highest rainfall event for the Castle Rock record in August does not come through as a large event on the local rainfall records, nor the Opitonui record. The corresponding flow responses in the monitoring catchments (except AG-P where the record is missing) are more in line with the local/Opitonui records than that of Castle Rock. The rainfall in 2007 became more frequent from July onwards. This shows in the flow response for EX-10 and EX-H6 before the records is lost. This trend is not so evident in the AG-P site where only the larger events influence flow. The EX-H site trend is hard to distinguish from the 'noise' of the data, but an increasing trend in the base flow is evident as a response to the wetter winter month rainfall.

Figure S-2. (next page) Rainfall data for the Castle Rock, Opitonui, AG-P, EX-H6, and EX-10, and the corresponding flow records for the four monitoring sites for the year 2007.

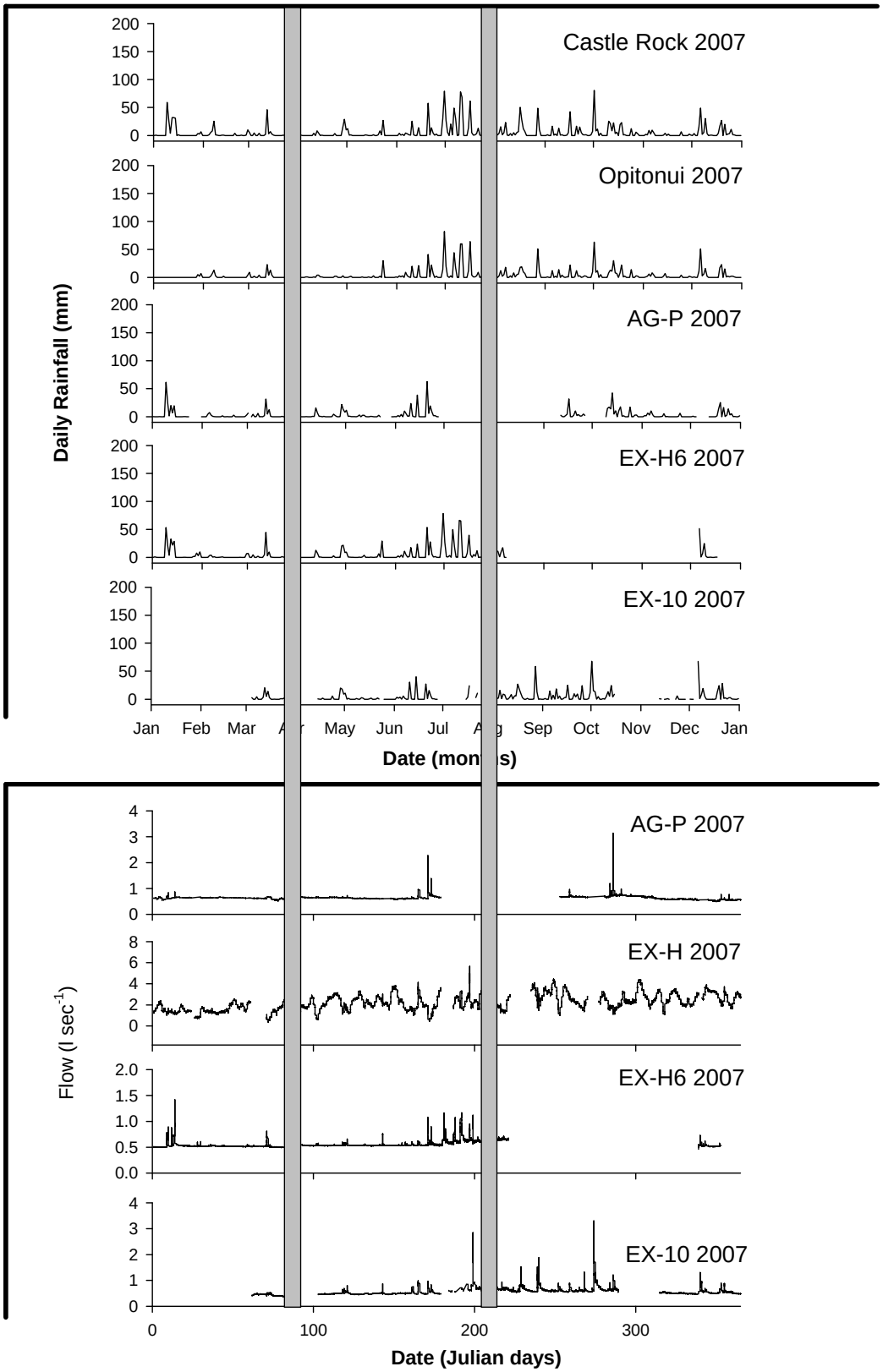
Castle Rock 2007
Opitonui 2007
AG-P 2007
EX-H6 2007
EX-10 2007
Daily Rainfall (mm)
Jan Feb Mar May Jun Jul Sep Oct Nov Dec Jan
Date (mon s)
AG-P 2007
EX-H 2007
EX-H6 2007
EX-10 2007
Flow (l sec-1)
Date (Julian days)

APPENDIX T

PEAK FLOW AND SEDIMENT YIELD STORM EVENTS FOR THE FOUR SUSPENDED SEDIMENT MONITORING SITES

Table T-1. The storm event peak flow and total sediment results for the exotic forest post harvested monitoring site.

Start date & time (dd/mm/yyyy_hh:mm)	End date & time (dd/mm/yyyy_hh:mm)	Sediment yield (kg)	Peak flow (l sec^{-1})
01/04/2006 04:30	03/04/2006 02:30	66	2.34
18/04/2006 18:15	19/04/2006 16:45	83	2.3
24/04/2006 21:00	26/04/2006 06:00	23.5	1.69
29/04/2006 03:30	29/04/2006 22:45	67.4	2.3
26/05/2006 21:15	28/05/2006 21:15	106	2.1
04/06/2006 04:30	05/06/2006 08:00	5.6	0.9
19/07/2006 13:00	20/07/2006 08:45	18.7	3.6
05/08/2006 14:15	06/08/2006 21:45	228	3.8
09/09/2006 11:15	10/09/2006 14:45	56.8	2.57
13/11/2006 01:30	14/11/2006 05:00	31.1	1.79
30/11/2006 11:30	01/12/2006 14:45	25.3	1.09
28/03/2007 16:30	30/03/2007 18:15	547.7	4.94
23/05/2007 14:15	24/05/2007 13:30	58	3.02
16/07/2007 07:00	16/07/2007 20:30	60.5	5.67
29/07/2007 05:30	30/07/2007 13:30	60.3	4.2
23/02/2008 04:30	24/02/2008 00:15	38.9	2.9

Table T-2. The storm event peak flow and total sediment results for the exotic forest six month post harvested monitoring site.

Start date & time (dd/mm/yyyy_hh:mm)	End date & time (dd/mm/yyyy_hh:mm)	Sediment yield (kg)	Peak flow (l sec^{-1})
02/03/2006 20:45	*03/03/2006 04:45*	*2.4*	*2.59*
07/03/2006 12:00	*08/03/2006 14:15*	*50.21*	*0.81*
26/08/2006 20:30	27/08/2006 08:15	2	0.85
02/10/2006 20:30	03/10/2006 10:15	1.7	0.76
30/11/2006 11:00	30/11/2006 21:45	3.1	0.92
09/01/2007 06:30	10/01/2007 14:00	14.2	0.89
13/01/2007 16:30	14/01/2007 22:45	20	1.42
29/03/2007 03:00	31/03/2007 17:00	87.1	1.66
23/05/2007 13:15	24/05/2007 02:45	6.6	0.76
20/06/2007 10:45	21/06/2007 11:30	17.2	1.08
22/06/2007 07:45	22/06/2007 22:45	10	0.9
29/06/2007 14:30	01/07/2007 06:45	33.2	1.16
01/07/2007 10:00	02/07/2007 10:00	14.3	0.86
06/07/2007 11:45	08/07/2007 00:15	26.3	1.07
10/07/2007 06:15	12/07/2007 18:30	47.3	1.17
16/07/2007 06:15	17/07/2007 21:00	18	0.95

Table T-3. The storm event peak flow and total sediment results for the exotic forest 10 year post harvested monitoring site.

Start date & time (dd/mm/yyyy_hh:mm)	End date & time (dd/mm/yyyy_hh:mm)	Sediment yield (kg)	Peak flow (l sec^{-1})
04/06/2006 04:00	04/06/2006 18:00	3.6	0.99
19/07/2006 09:45	20/07/2006 07:30	3.8	0.95
02/10/2006 07:00	03/10/2006 14:00	5	1.2
30/11/2006 09:30	01/12/2006 06:30	18.5	0.95
28/03/2007 08:15	30/03/2007 06:30	13.3	2.1
30/04/2007 18:30	01/05/2007 14:45	1.6	0.8
23/05/2007 13:00	24/05/2007 20:30	2.8	0.87
14/06/2007 03:15	15/06/2007 15:15	3.9	0.98
20/06/2007 10:15	21/06/2007 11:15	2.8	0.97
22/06/2007 07:45	23/06/2007 03:15	1.8	0.82
30/07/2007 03:30	01/08/2007 23:30	16.5	1.9
05/08/2007 15:00	06/08/2007 11:15	4.3	0.94
09/09/2007 06:15	10/09/2007 15:45	4.1	0.89
16/09/2007 09:30	17/09/2007 08:45	4	0.9
01/10/2007 13:45	02/10/2007 16:15	22.3	3.3

Table T-4. The storm event peak flow and total sediment results for the agricultural pasture monitoring site.

Start date & time (dd/mm/yyyy_hh:mm)	End date & time (dd/mm/yyyy_hh:mm)	Sediment yield (kg)	Peak flow (l sec^{-1})
07/03/2006 15:30	08/03/2006 15:00	1.03	1.08
26/05/2006 14:00	27/05/2006 15:30	55.1	3.14
26/08/2006 15:15	27/08/2006 17:00	7.6	1.3
09/09/2006 08:30	10/09/2006 09:45	14.7	1.88
02/10/2006 21:00	03/10/2006 14:15	4	1
23/10/2006 10:45	24/10/2006 06:00	13.8	0.84
30/11/2006 09:00	30/11/2006 20:00	1.6	0.9
09/01/2007 06:30	10/01/2007 13:15	8.3	0.83
29/03/2007 02:15	30/03/2007 21:45	31	2.6
14/06/2007 12:45	15/06/2007 20:30	9.5	0.96
20/06/2007 10:15	21/06/2007 16:00	17.2	2.3
18/12/2007 20:45	19/12/2007 18:15	3.8	0.77
01/03/2008 18:15	02/03/2008 14:15	6.1	0.81

APPENDIX U

PEAK FLOW AND SEDIMENT YIELD STORM EVENTS

U.1 Introduction

The graphs in this appendix are summaries of the storm event data that was used to form the peak flow and sediment yield relationships for the Suspended Sediment Yield (SSY) method. The graphs summarise the flow (from which the peak flow is identified) and the suspended sediment concentration (SSC) in mg L^{-1} for each storm event. The total sediment yield is calculated by multiplying the SSC by the flow for each 15 minute period of the storm event. The detail of the 15 minute logged data is contained in the CD accompanying this thesis.

U.2 Exotic forest recently harvested (EX-H)

U.2.1 Storm event 1-4-2006

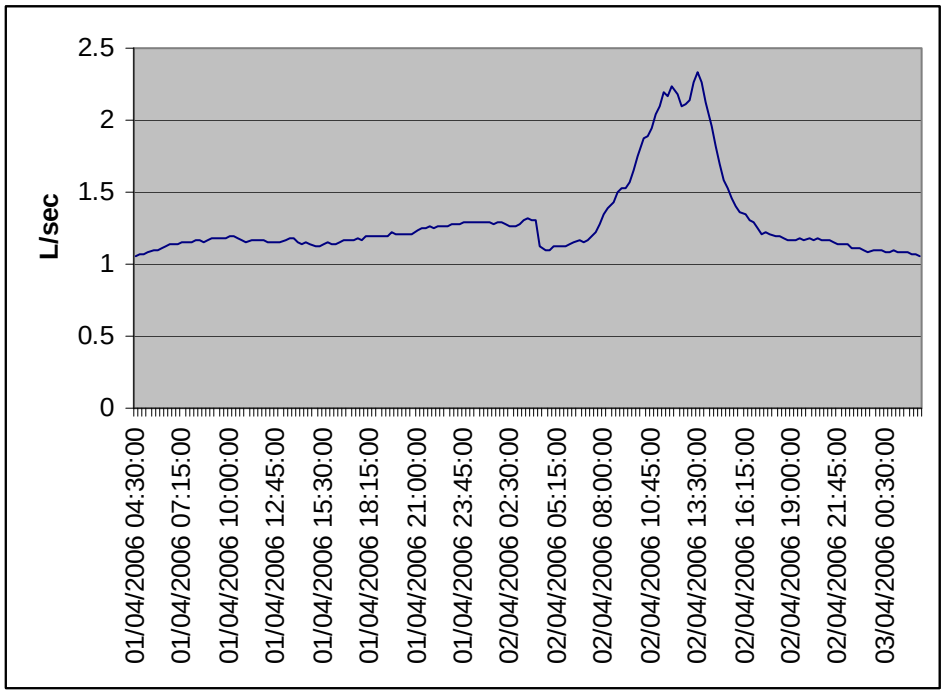

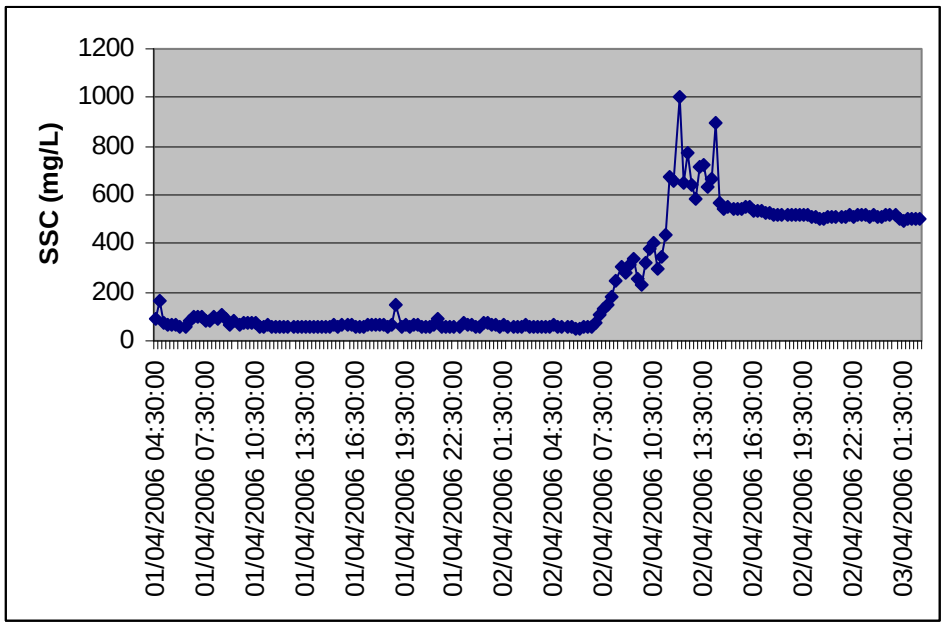

U.2.2 Storm event 18-4-2006

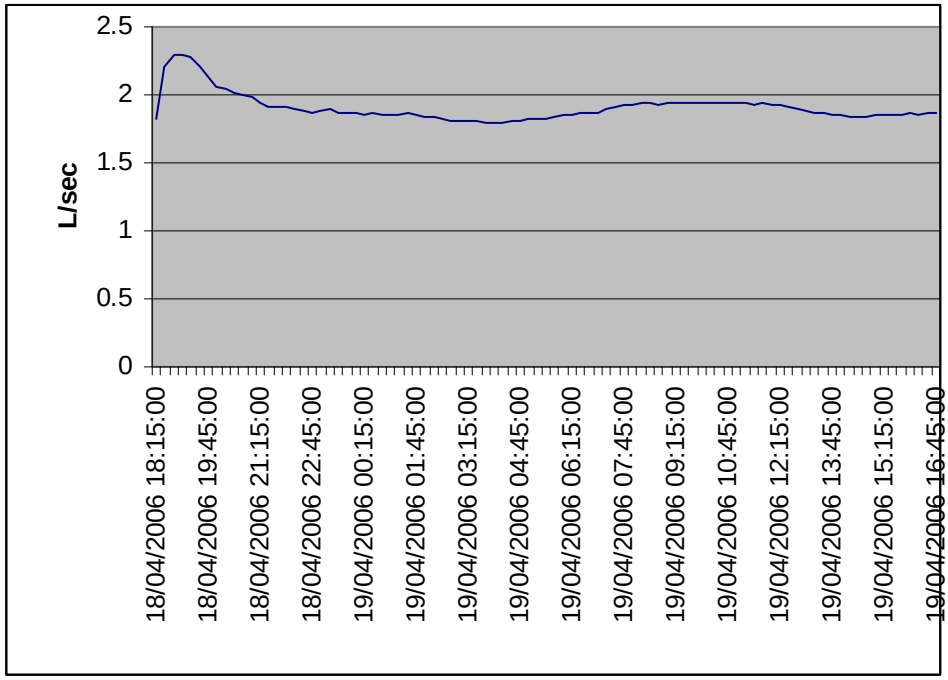

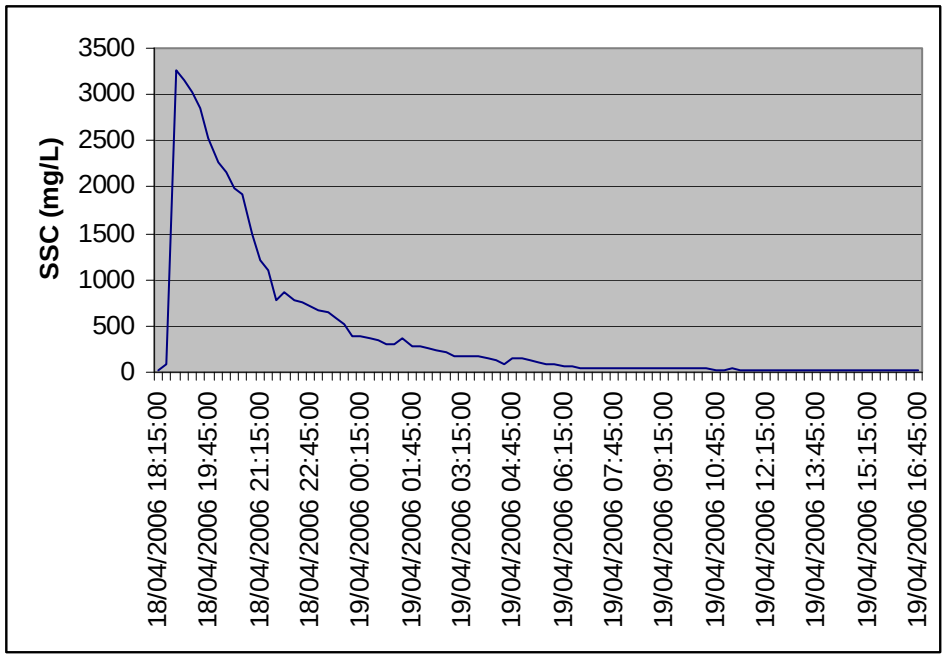

U.2.3 Storm event 24-4-2006

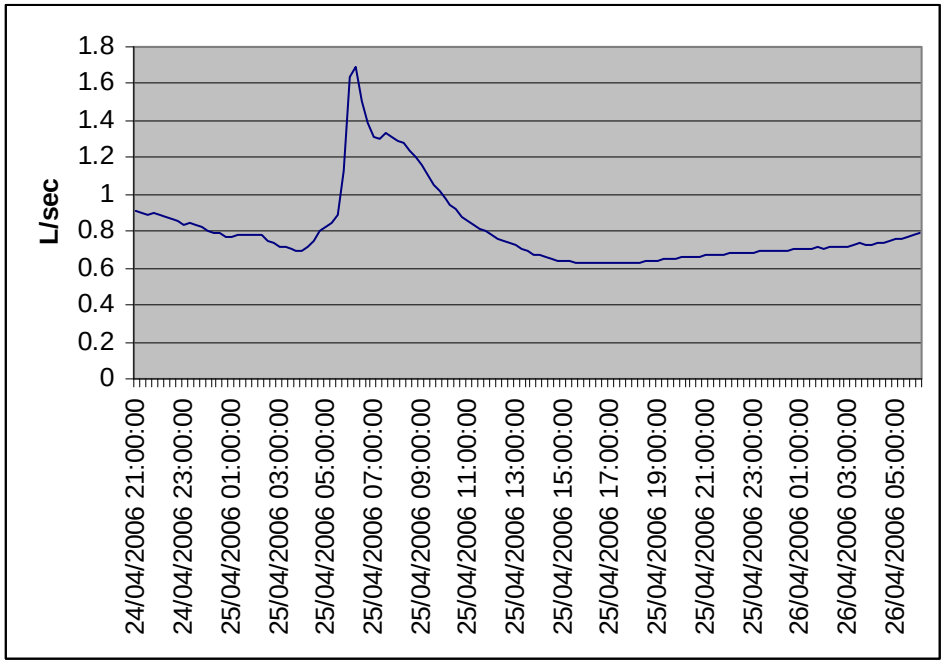

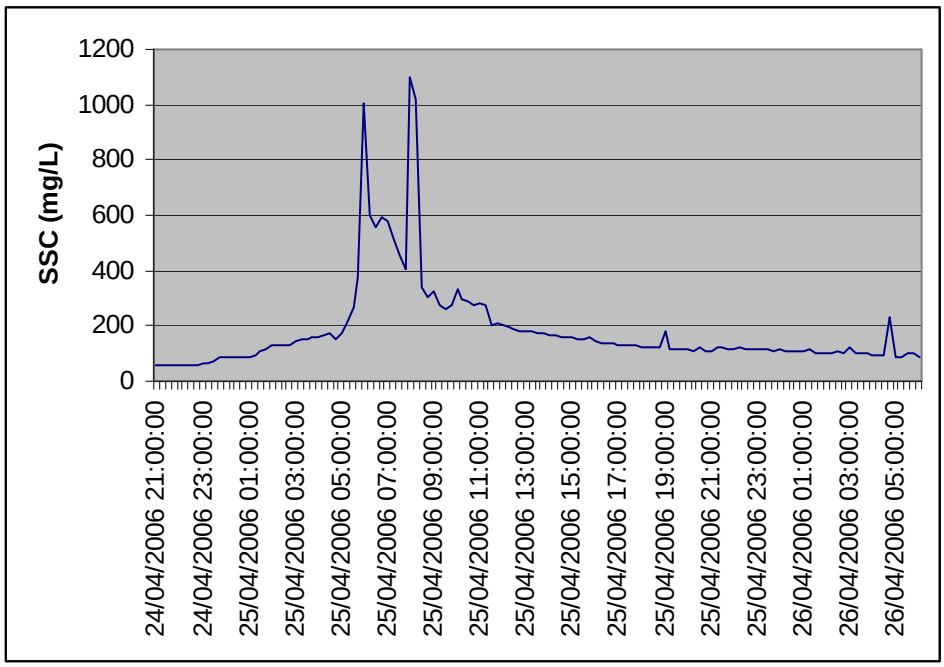

U.2.4 Storm event 29-4-2006

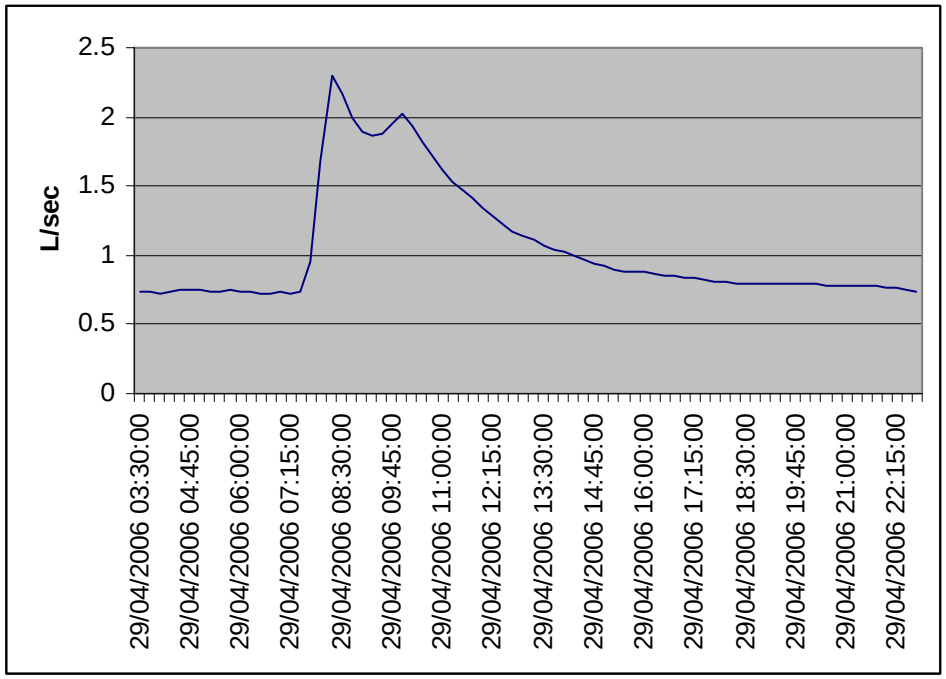

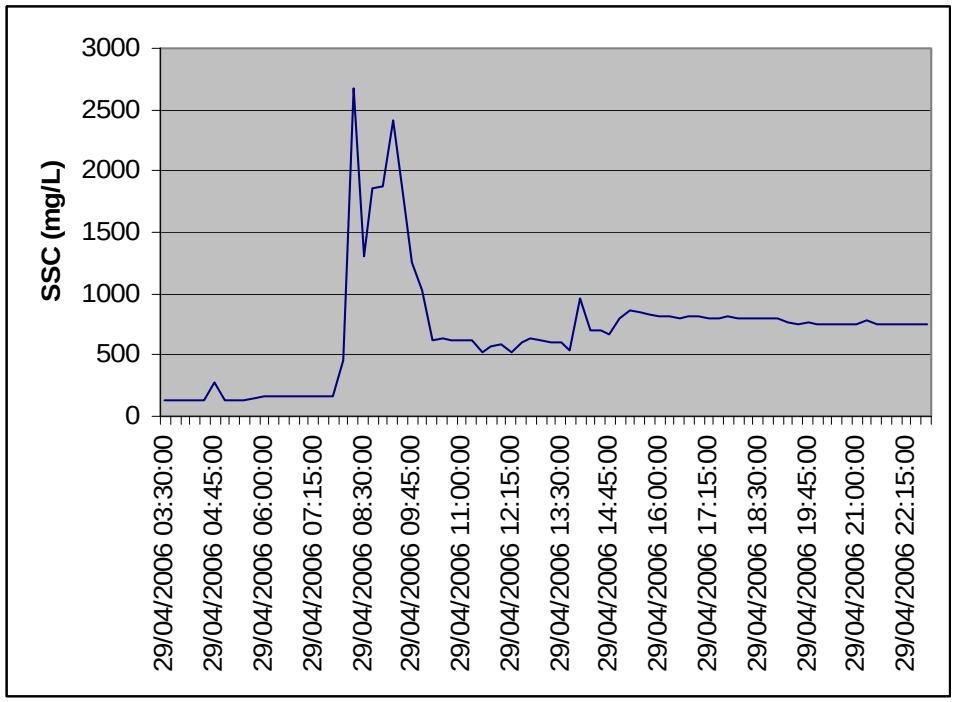

U.2.5 Storm event 26-5-2006

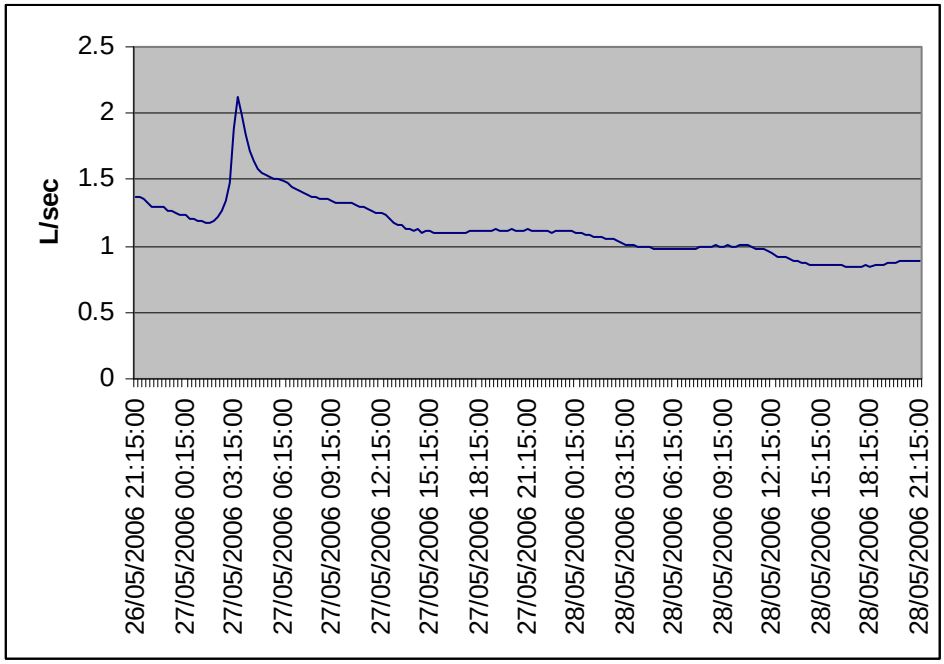

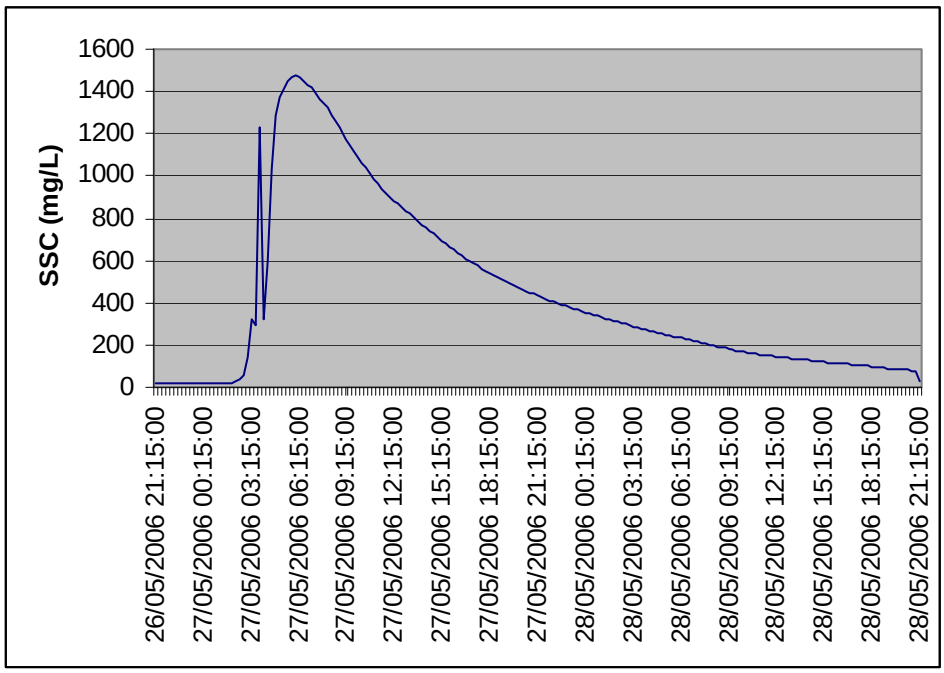

U.2.6 Storm event 4-6-2006

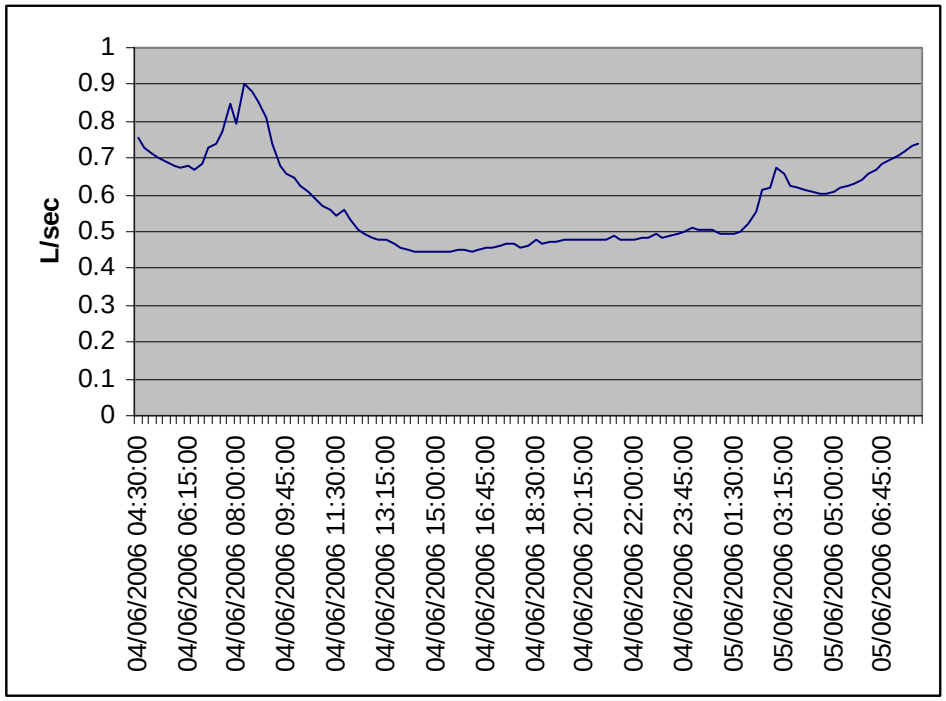

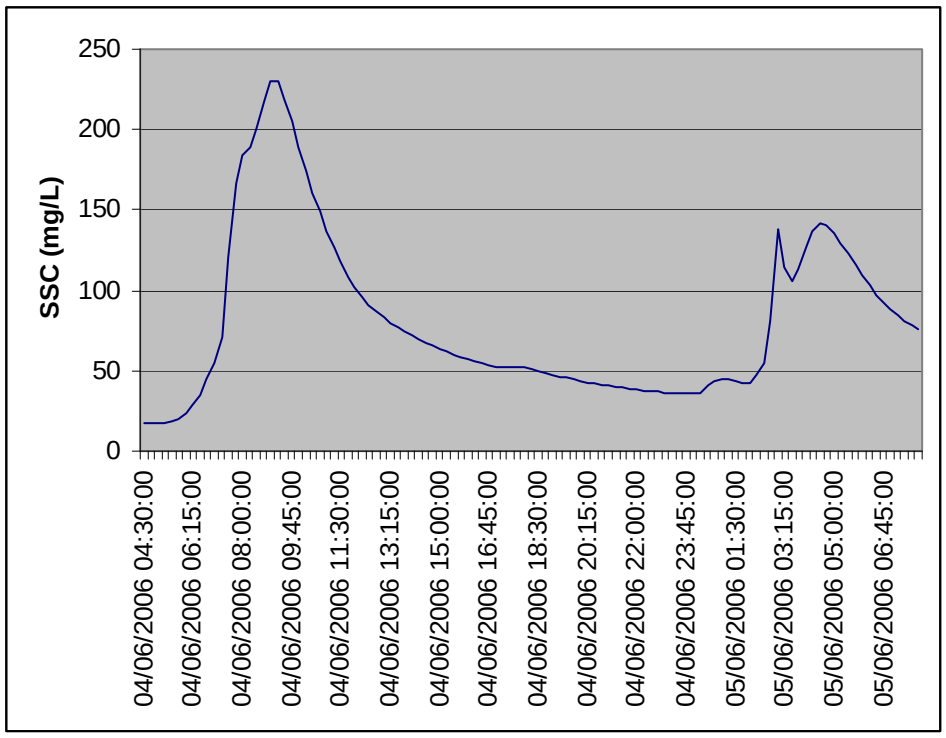

U.2.7 Storm event 19-7-2006

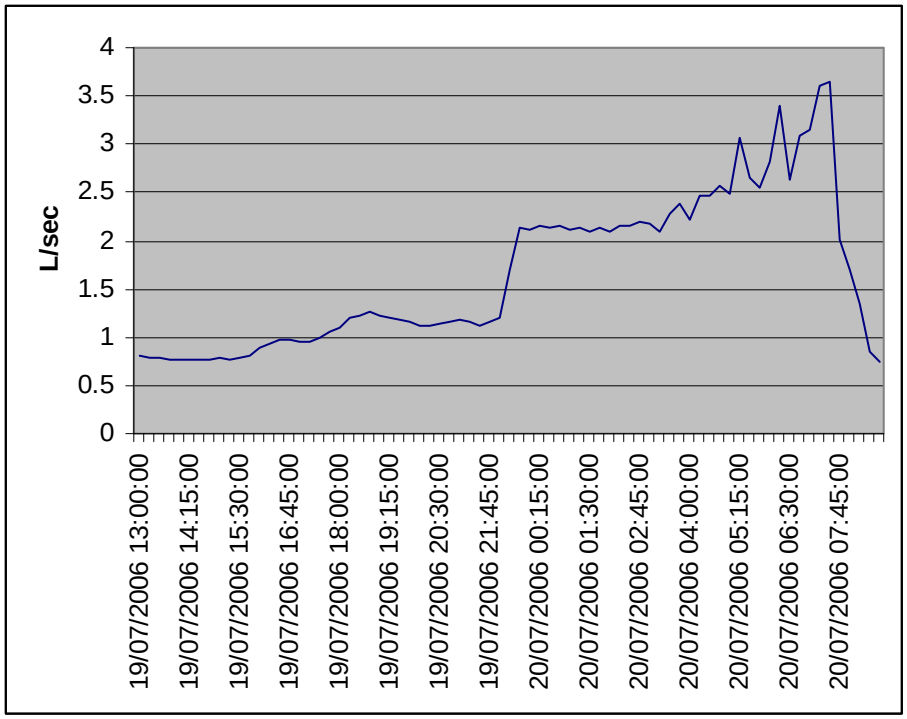

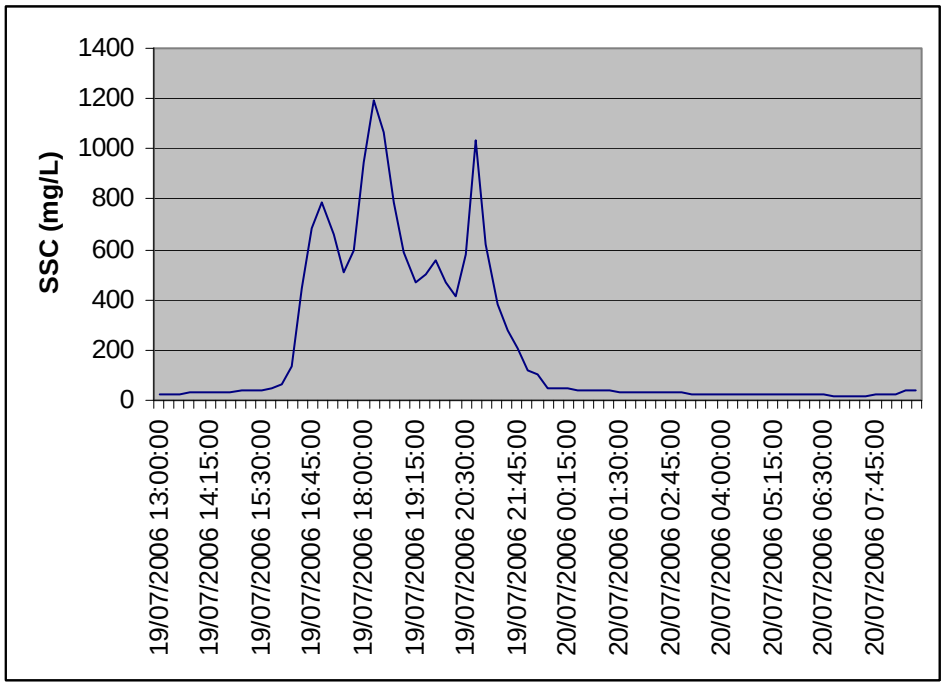

U.2.8 Storm event 5-8-2006

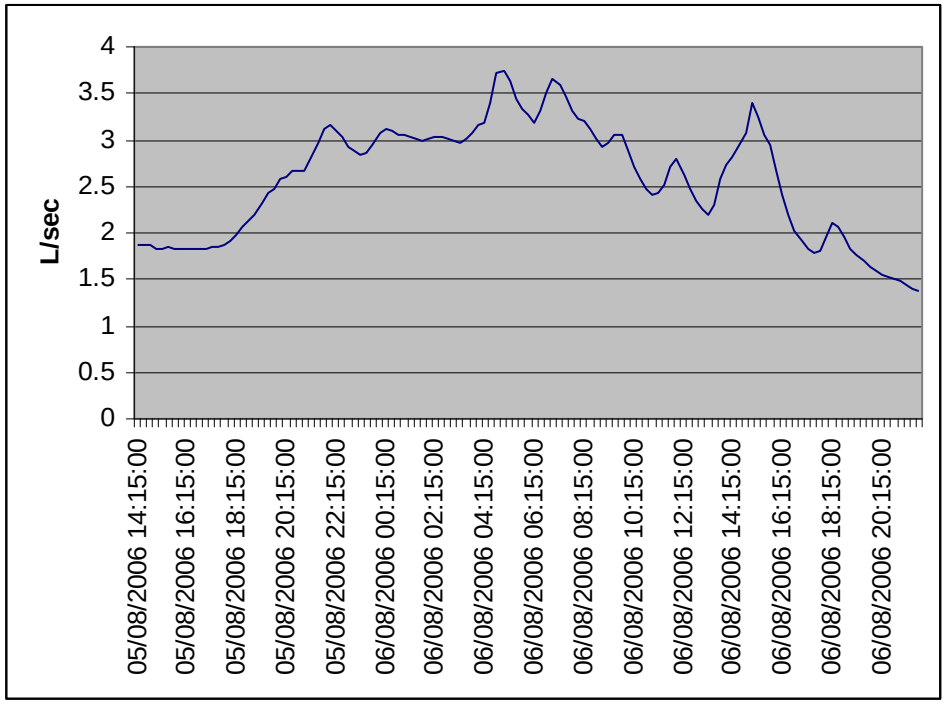

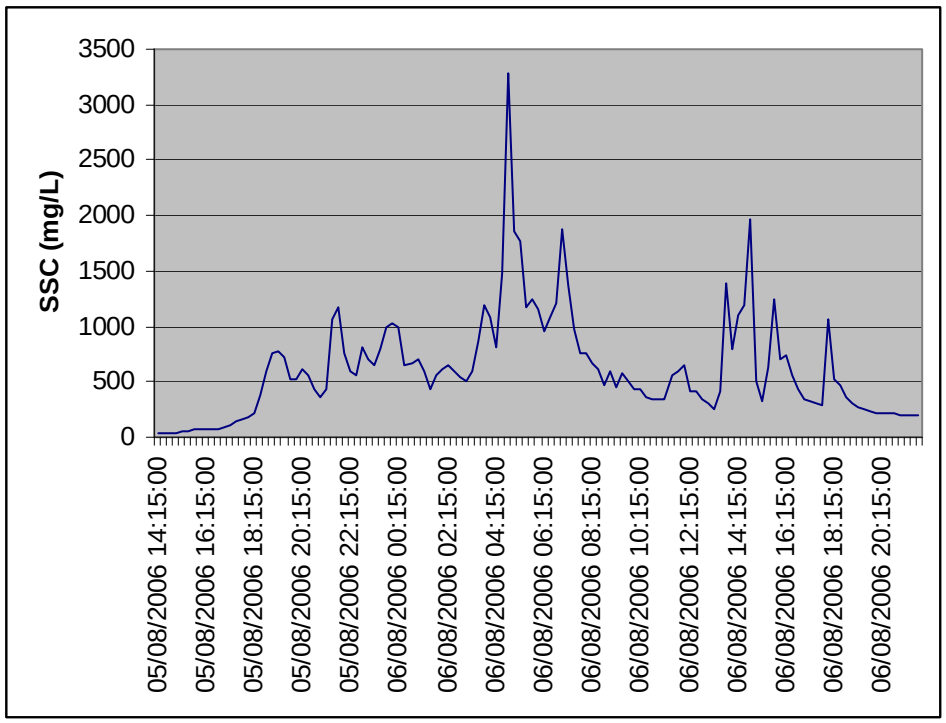

U.2.9 Storm event 9-9-2006

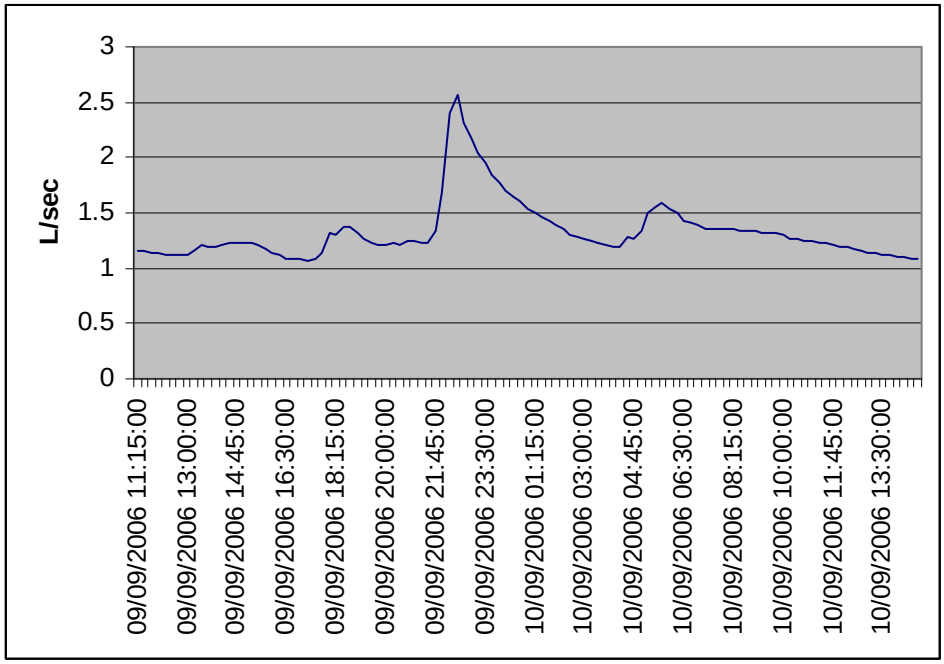

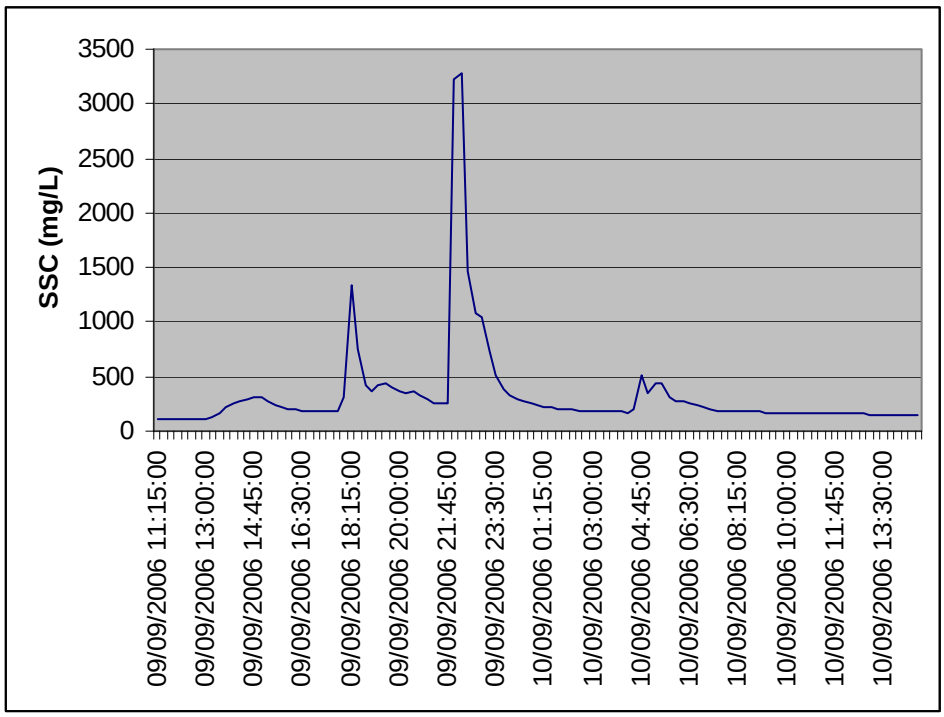

U.2.10 Storm event 13-11-2006

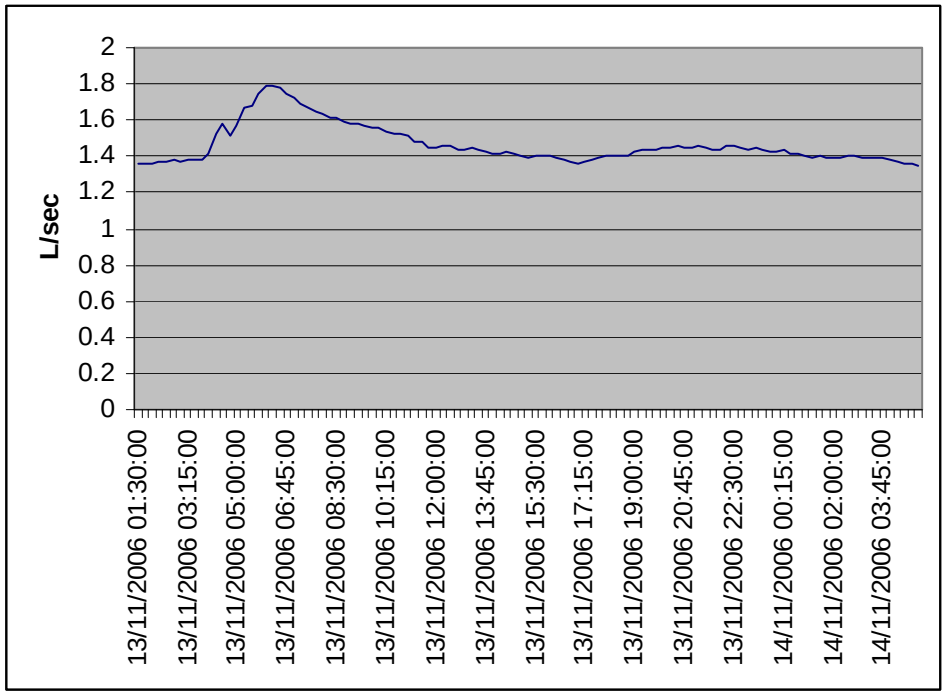

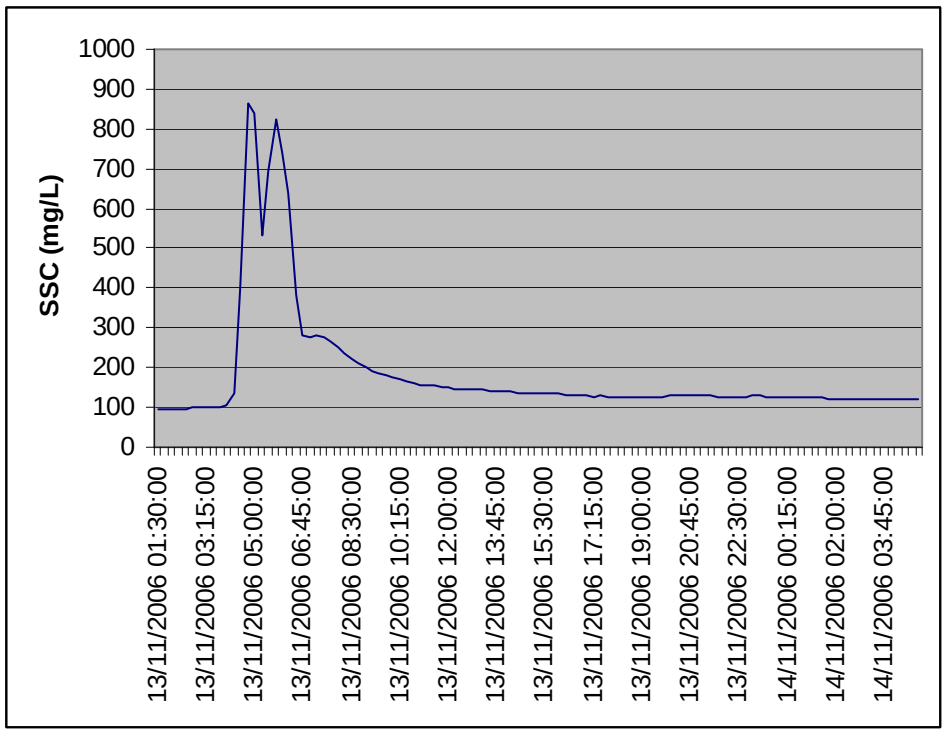

U.2.11 Storm event 30-11-2006

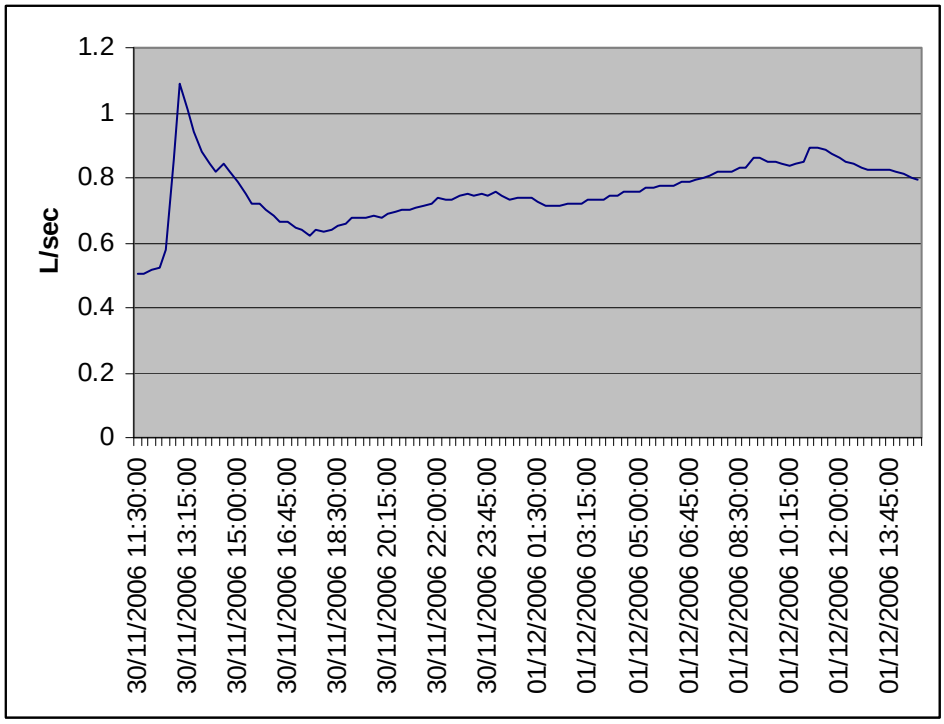

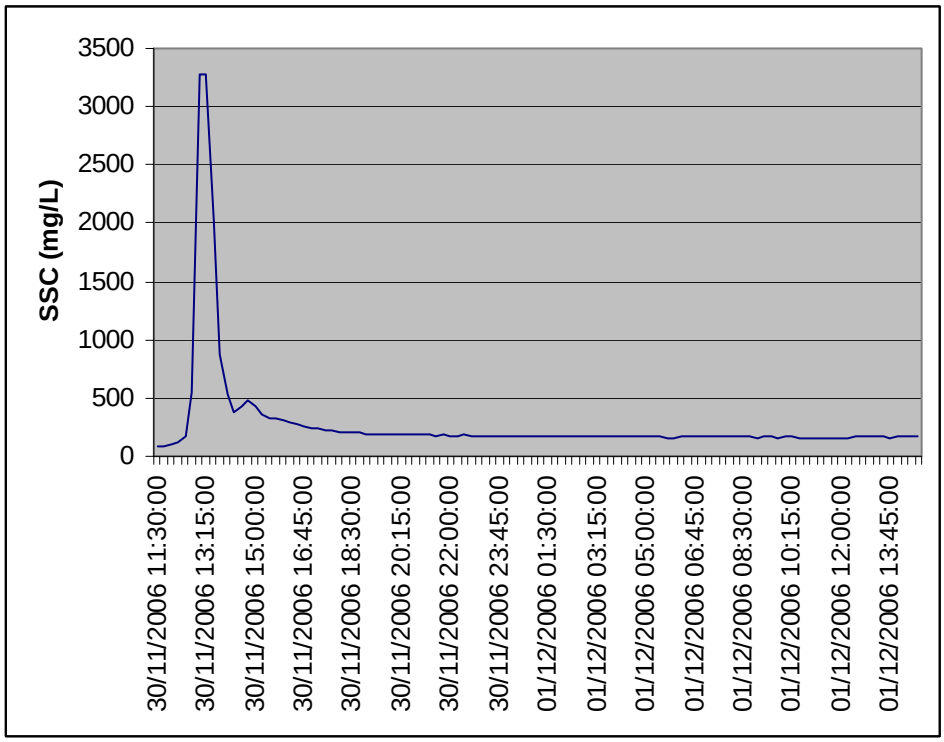

U.2.12 Storm event 28-3-2007

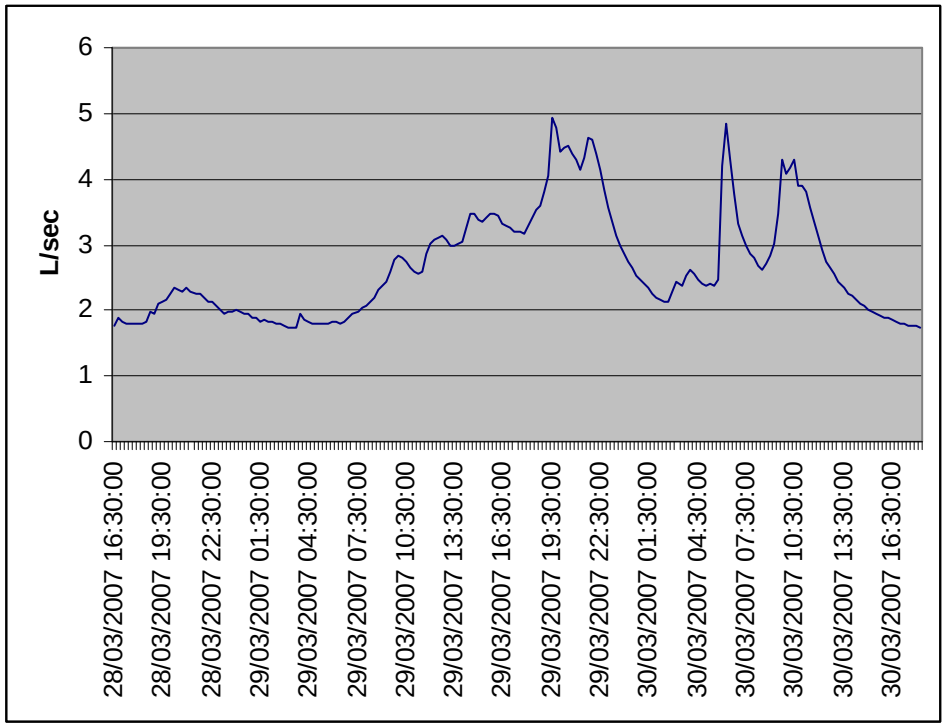

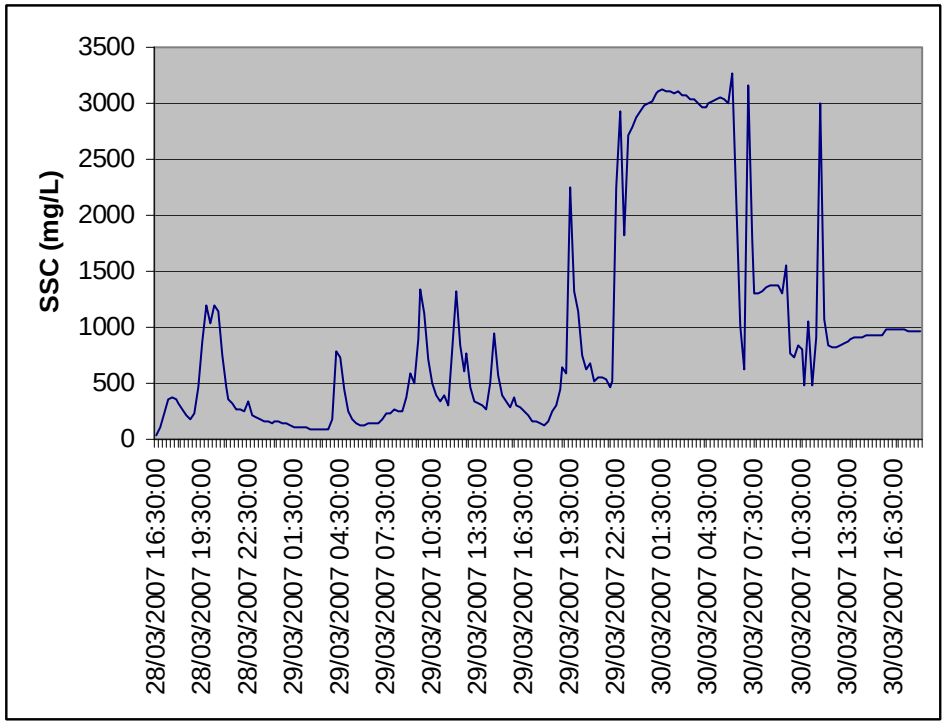

U.2.13 Storm event 23-5-2007

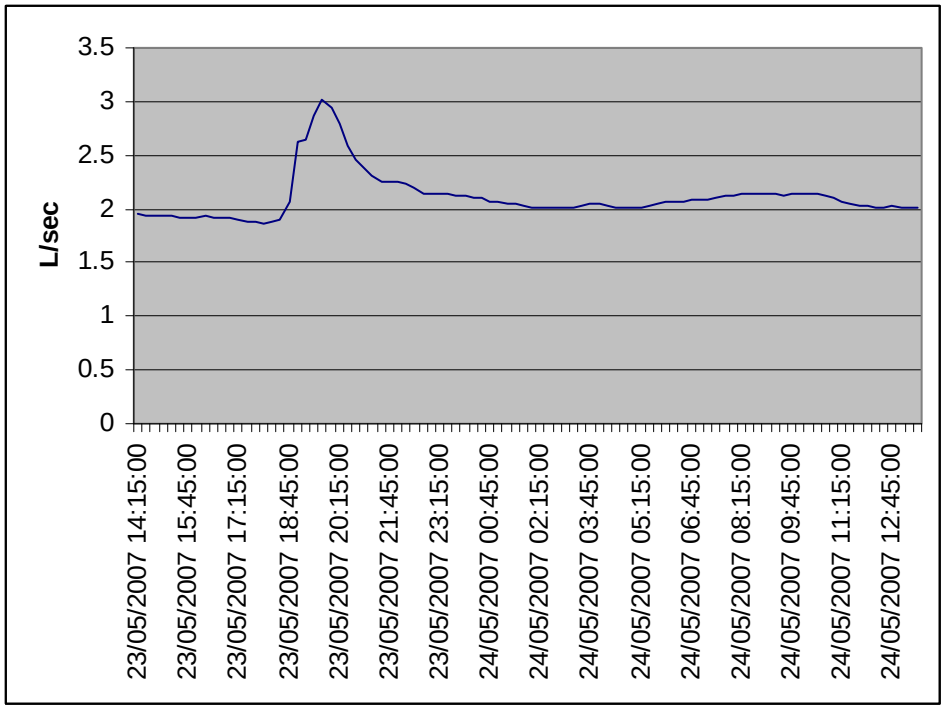

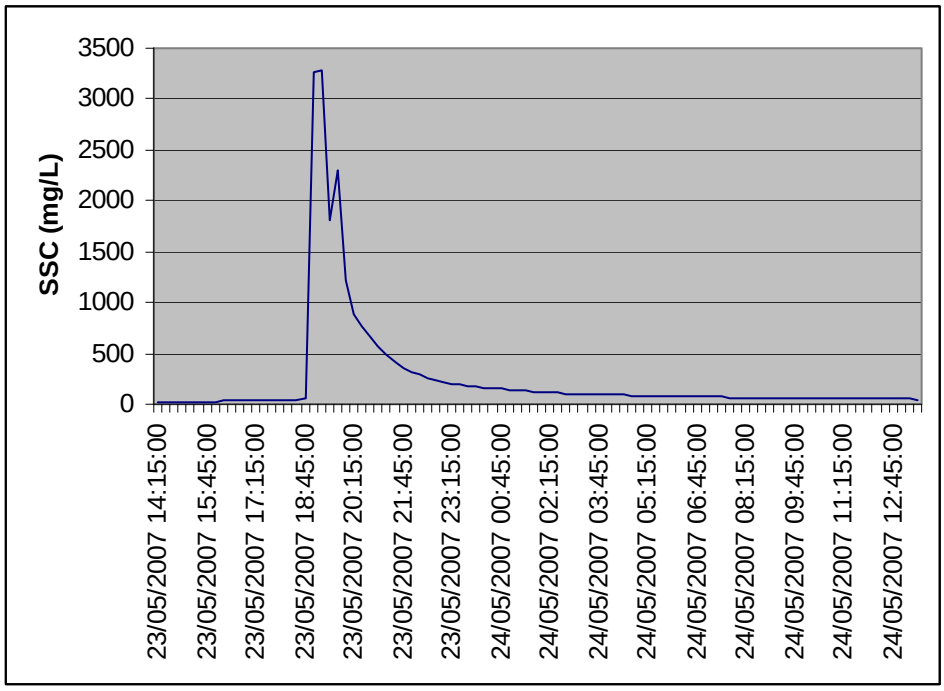

U.2.14 Storm event 16-7-2007

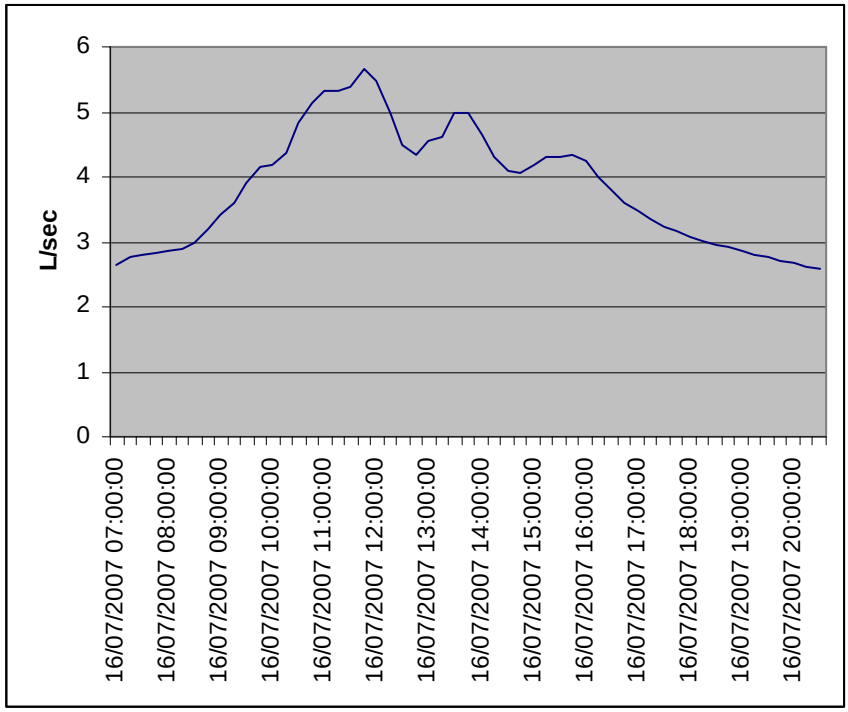

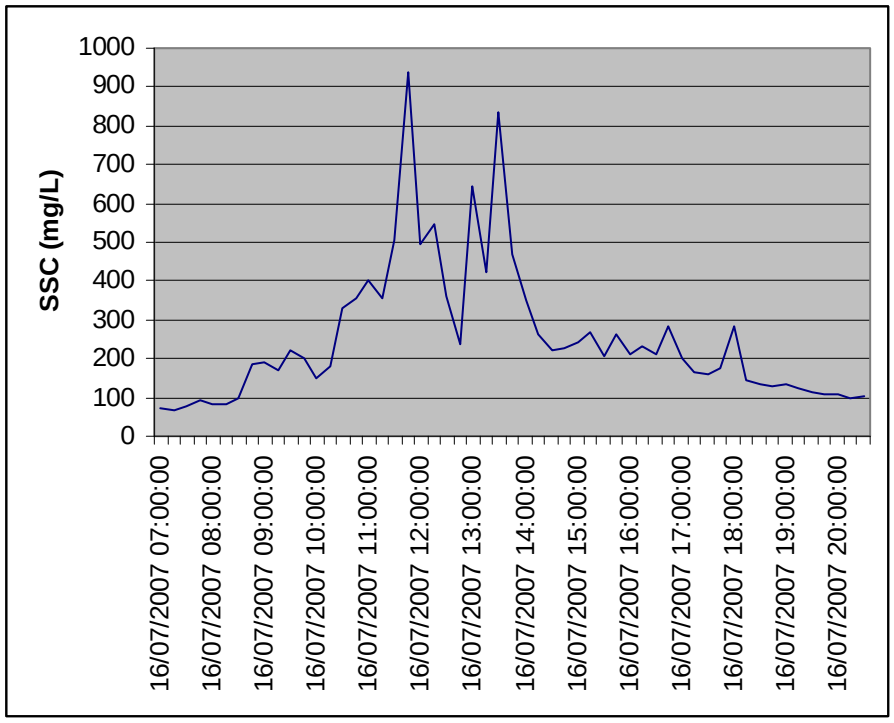

U.2.15 Storm event 29-7-2007

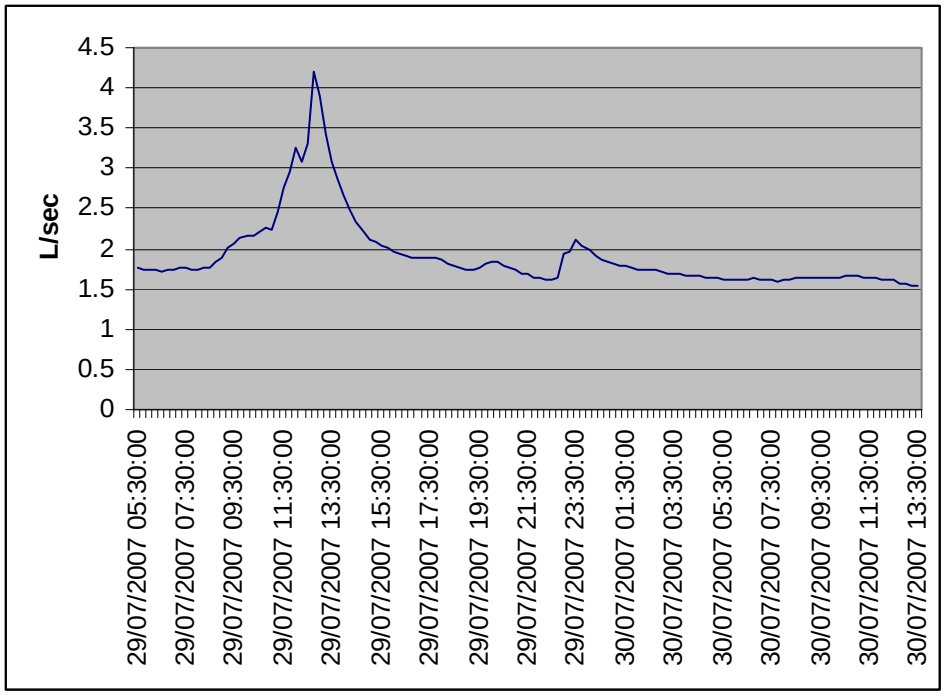

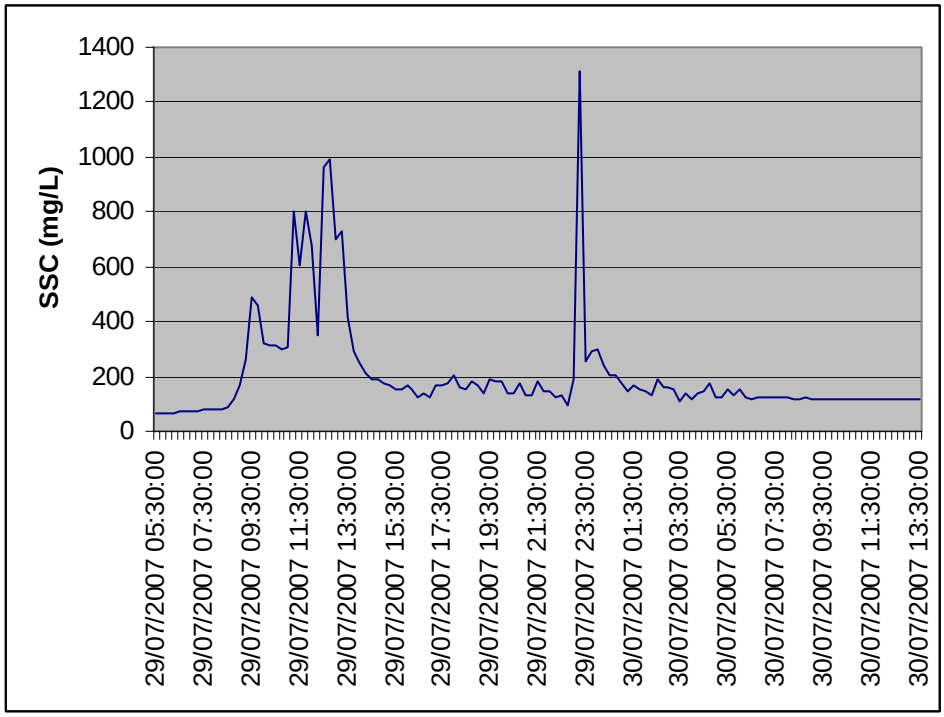

U.2.16 Storm event 23-2-2008

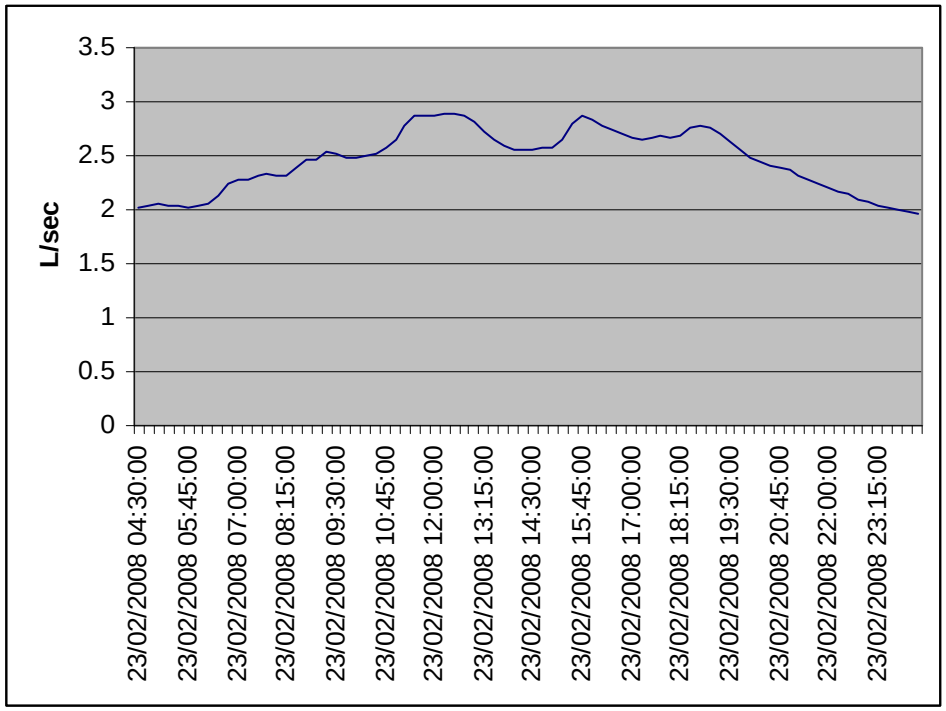

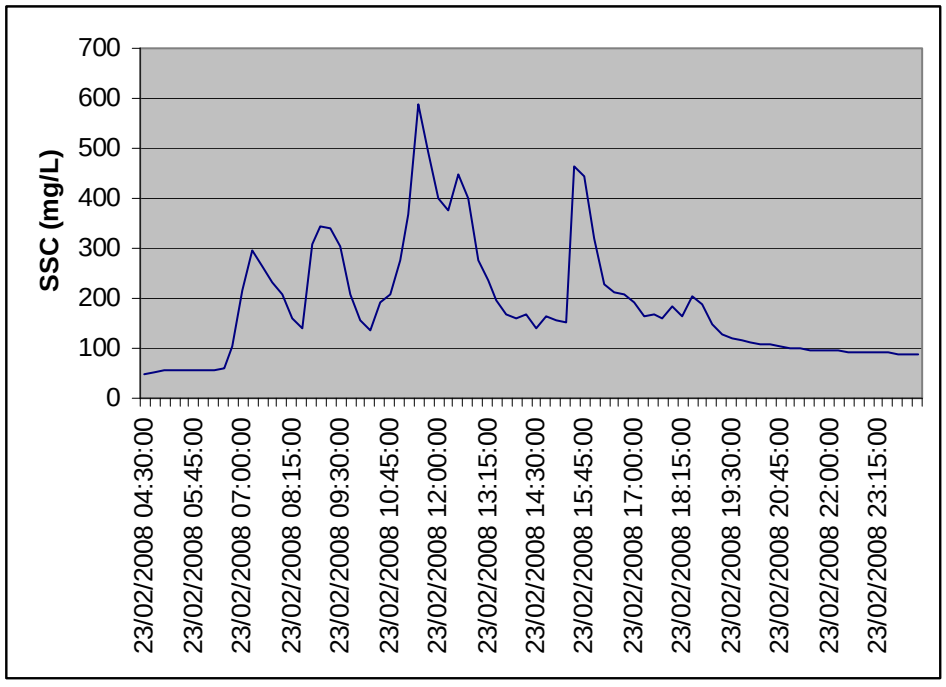

U.3 Exotic forest six month post harvest (EX-H6)

U.3.1 Storm event 2-3-2006

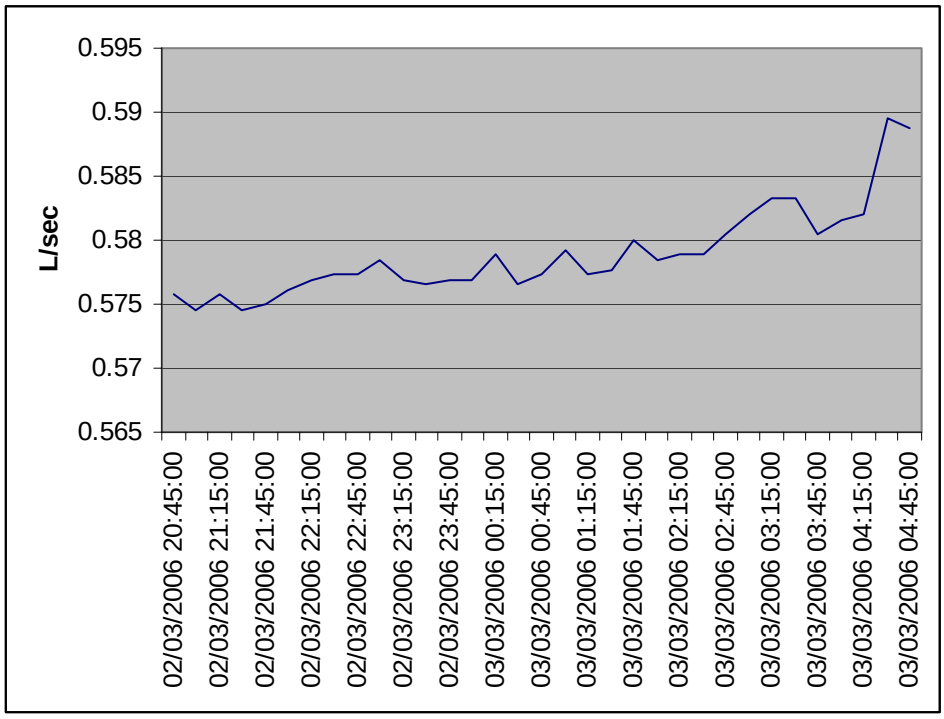

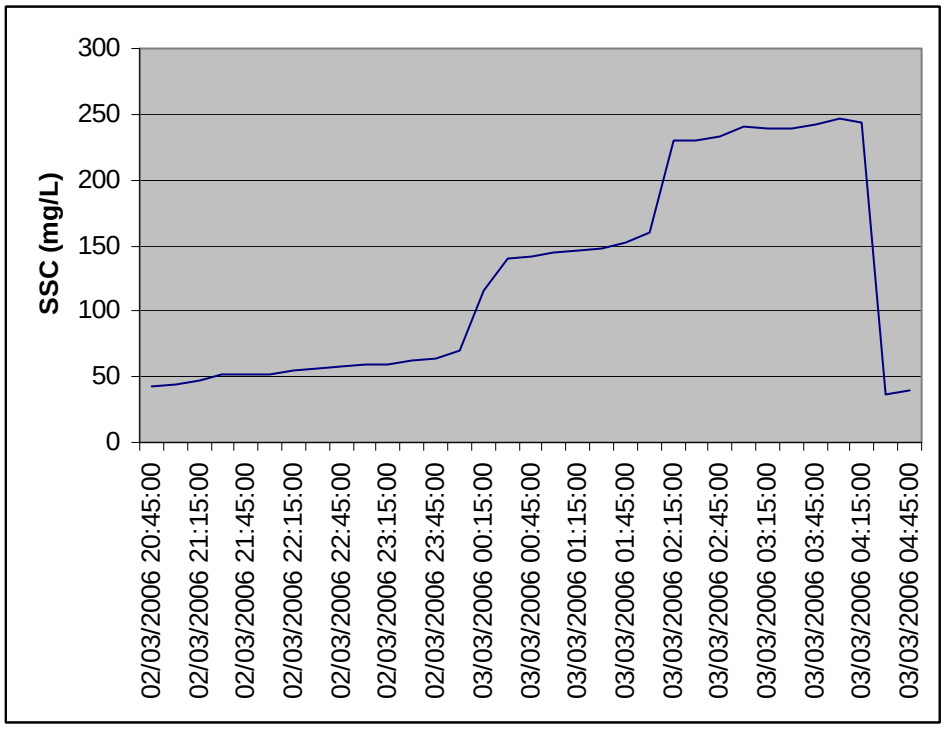

U.3.2 Storm event 7-3-2006

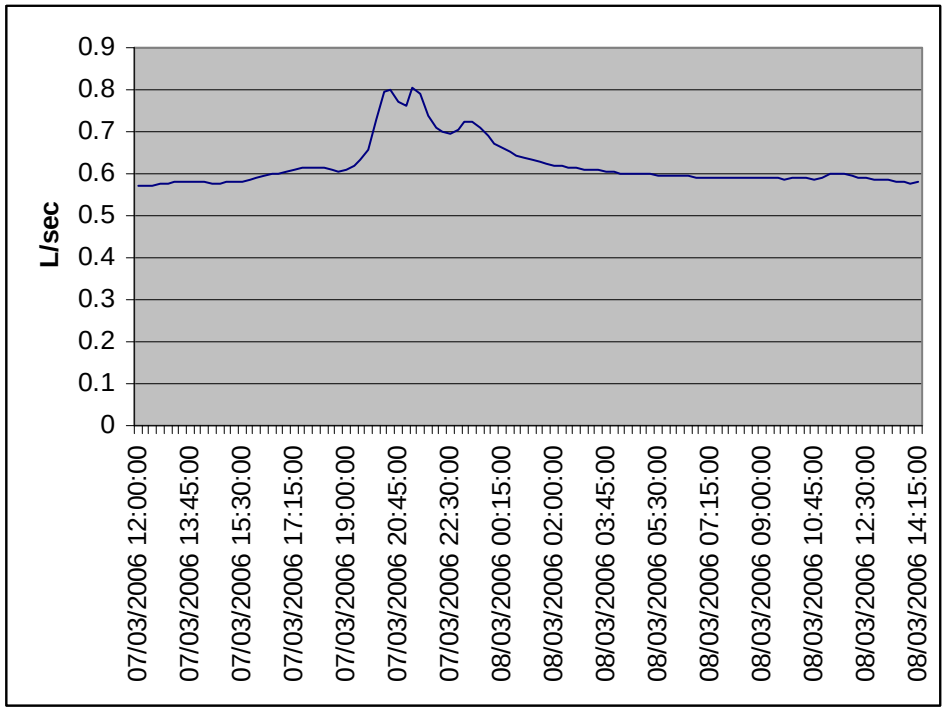

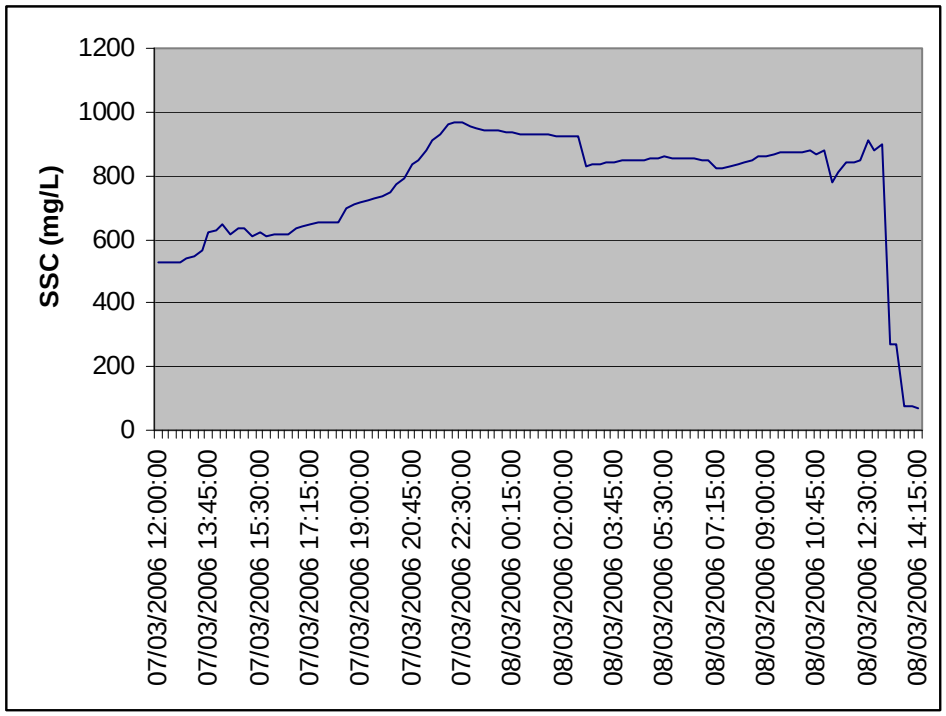

U.3.3 Storm event 26-8-2006

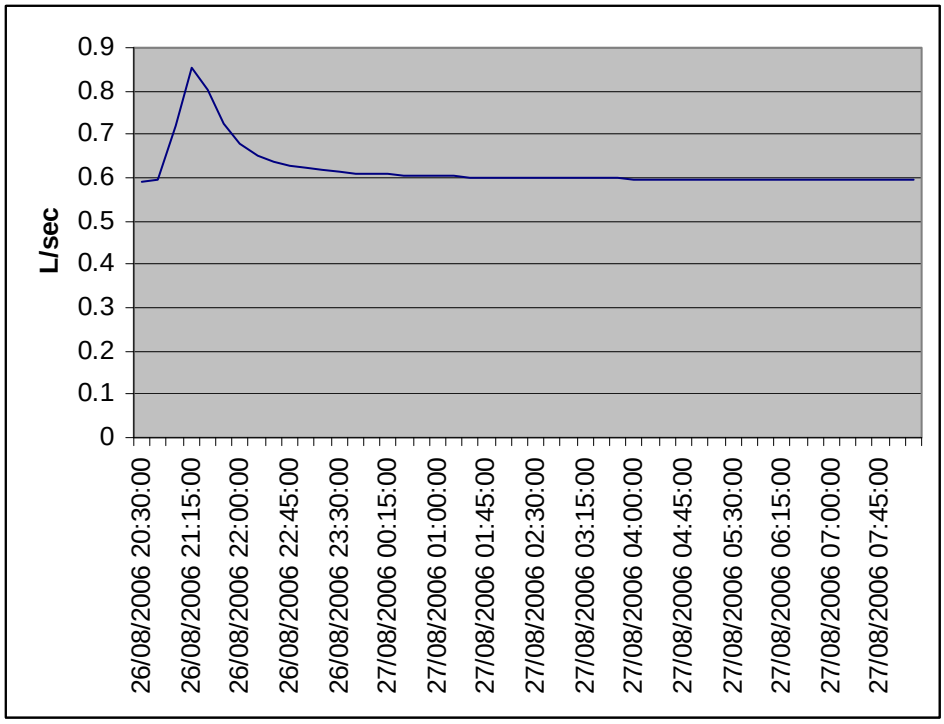

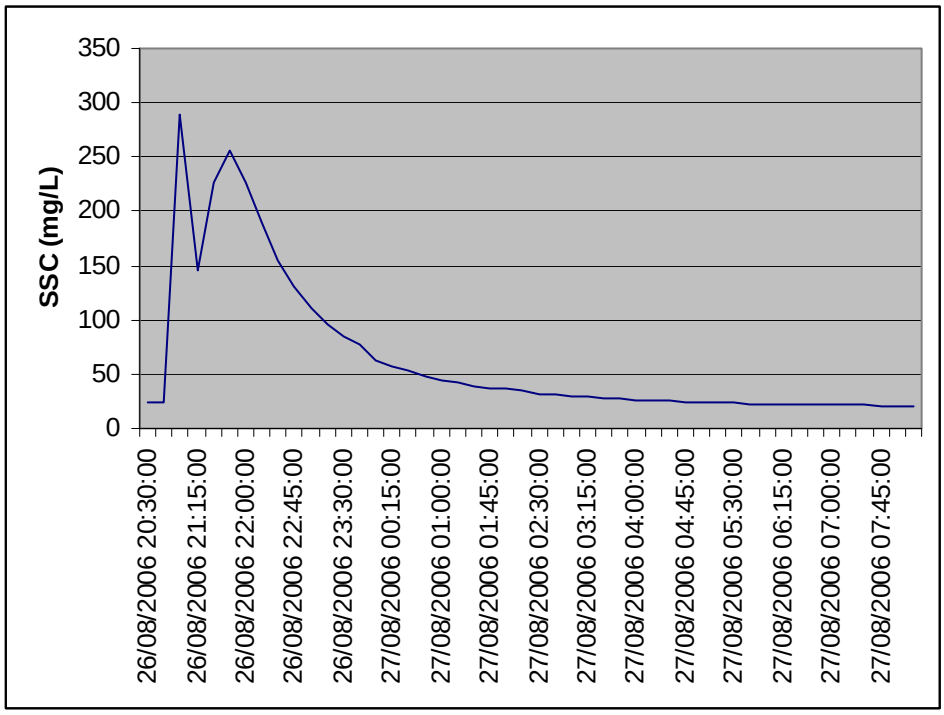

U.3.4 Storm event 2-10-2006

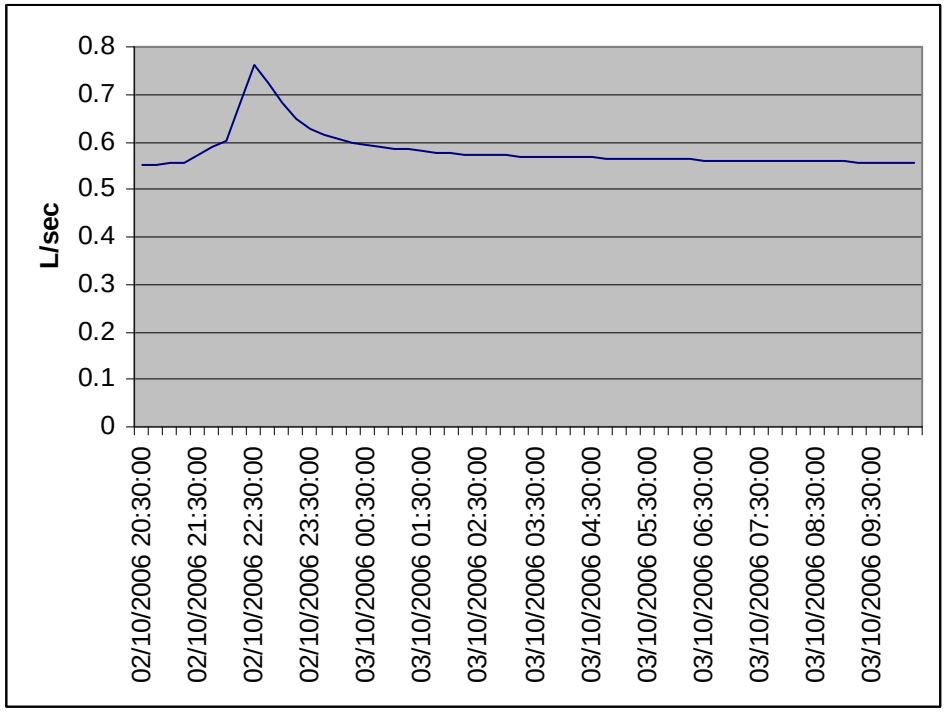

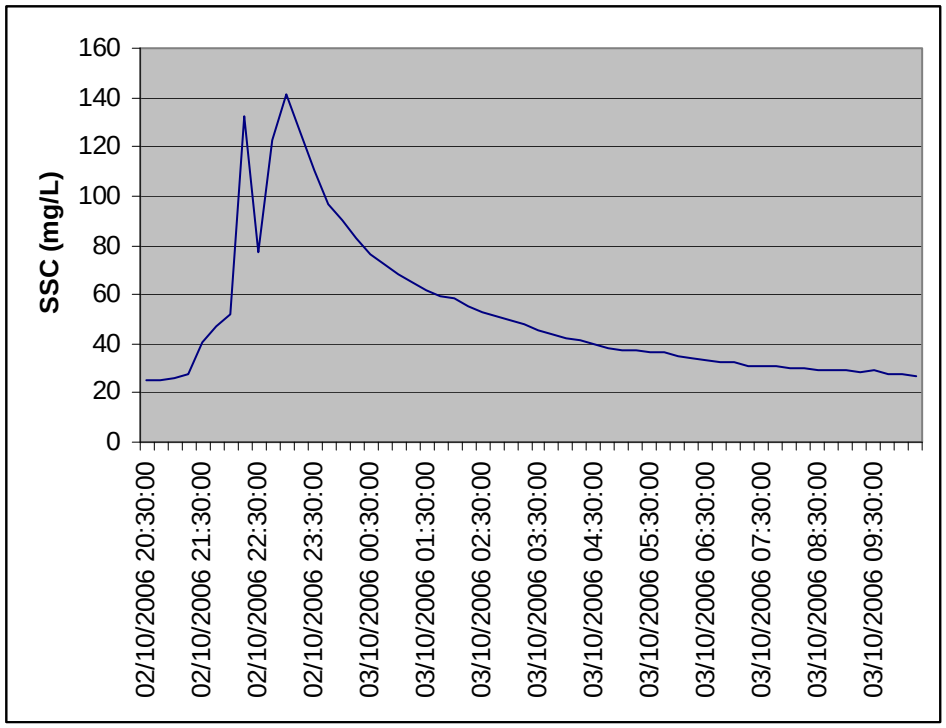

U.3.5 Storm event 30-11-2006

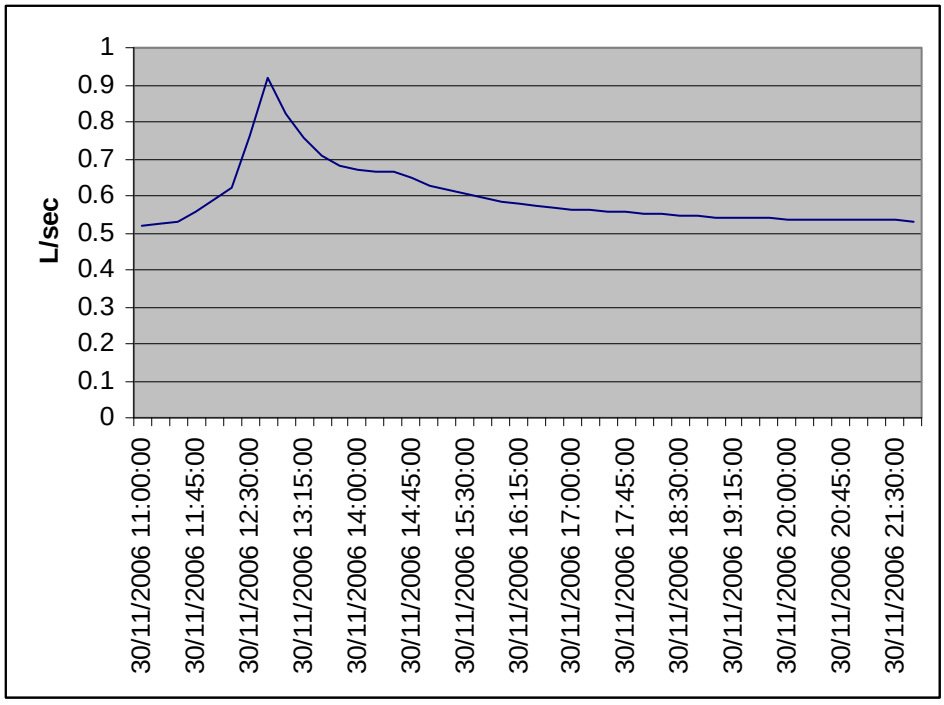

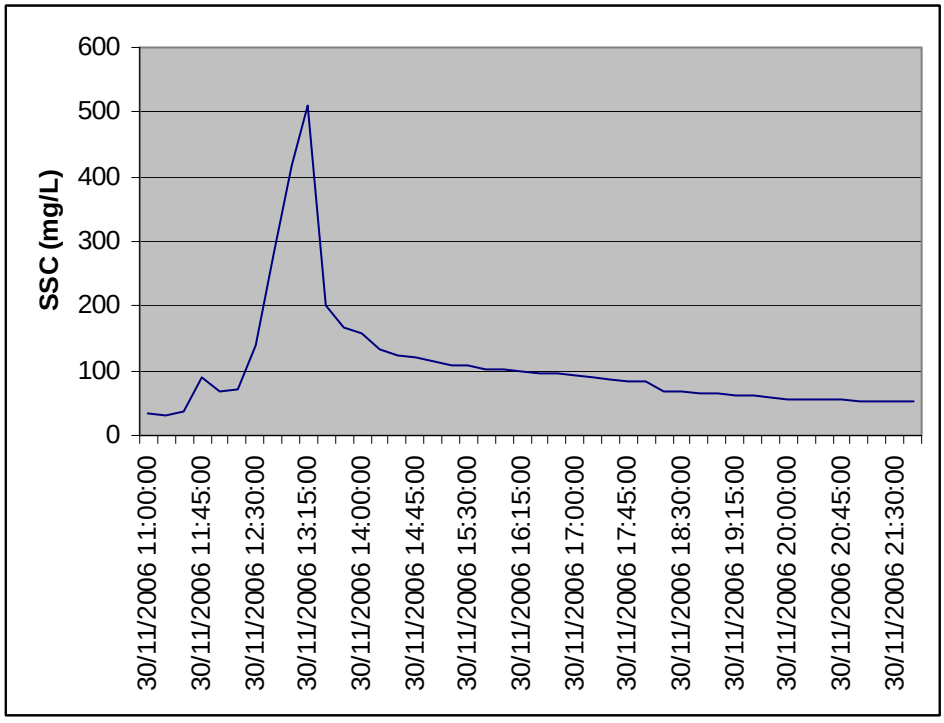

U.3.6 Storm event 9-1-2007

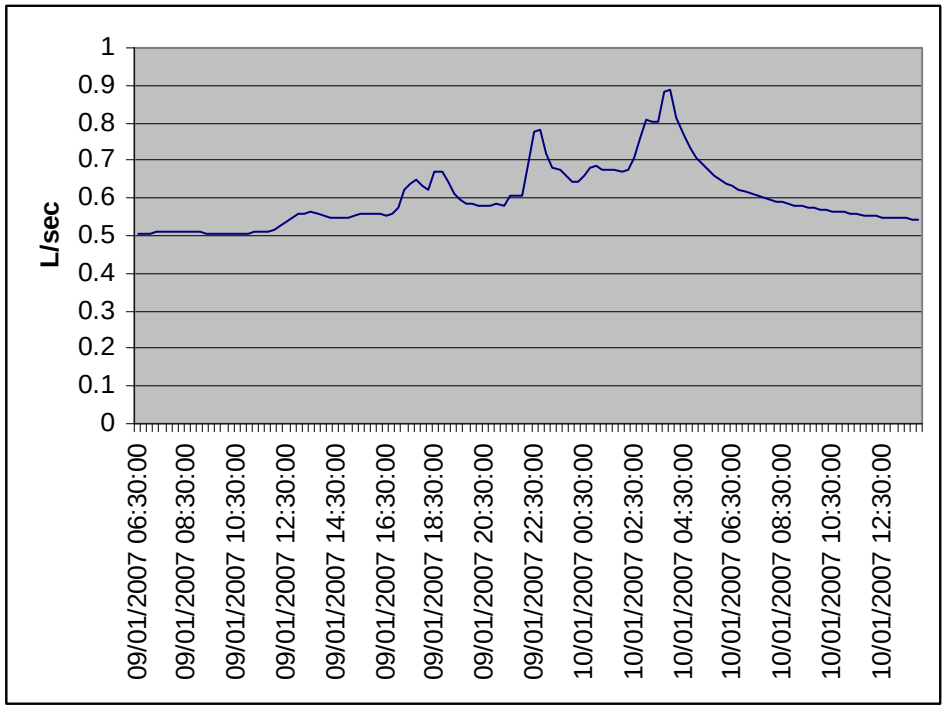

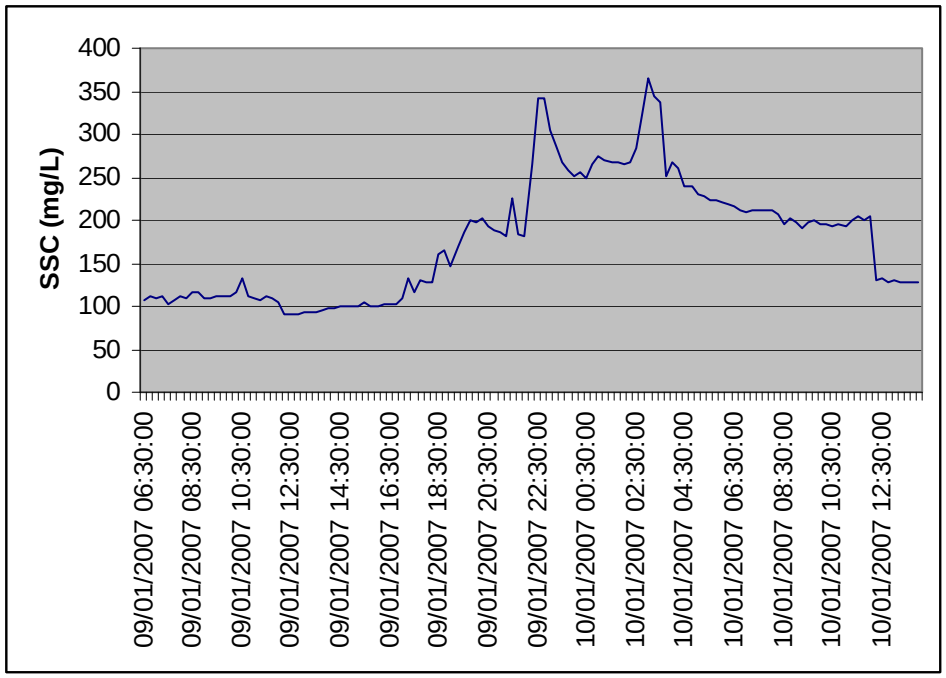

U.3.7 Storm event 13-1-2007

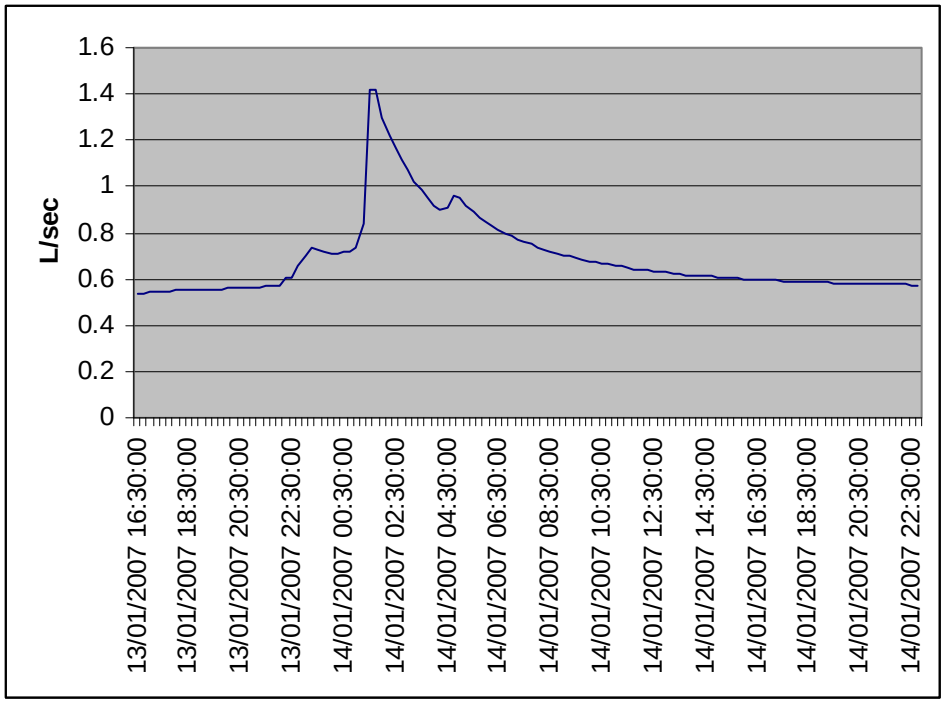

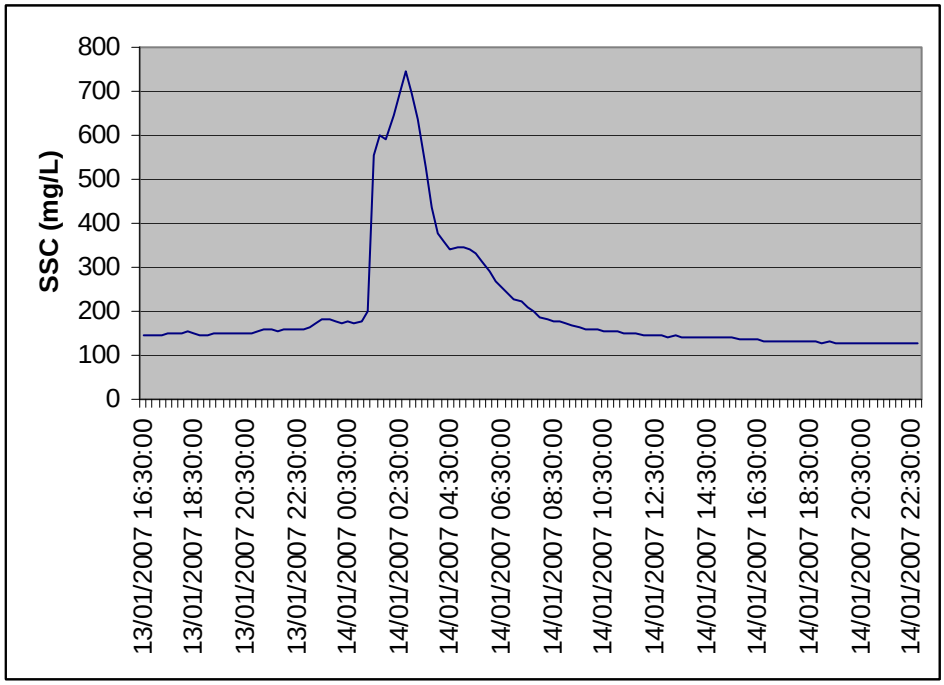

U.3.8 Storm event 29-3-2007

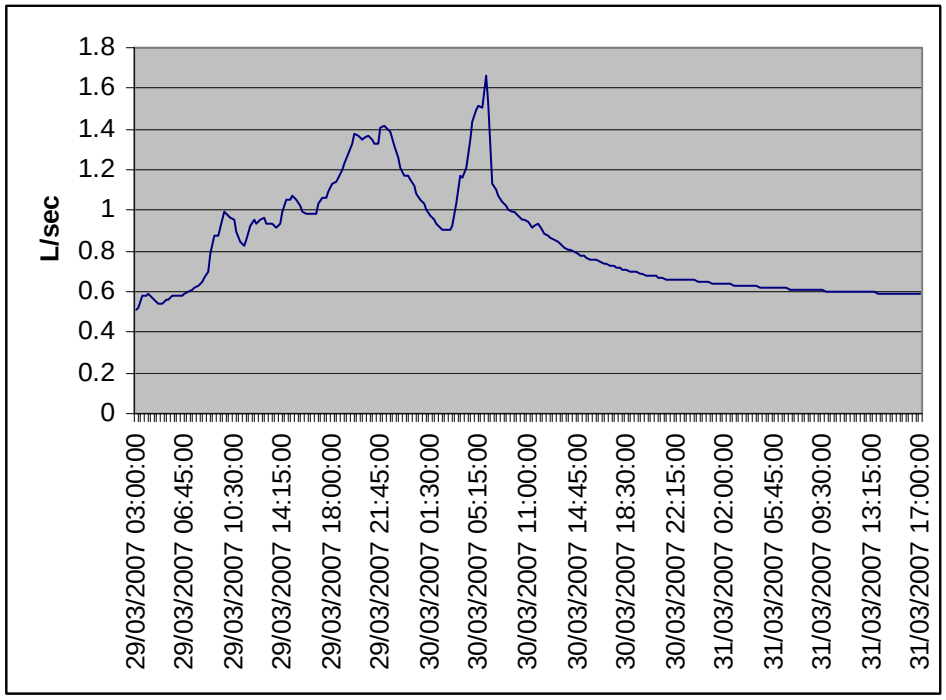

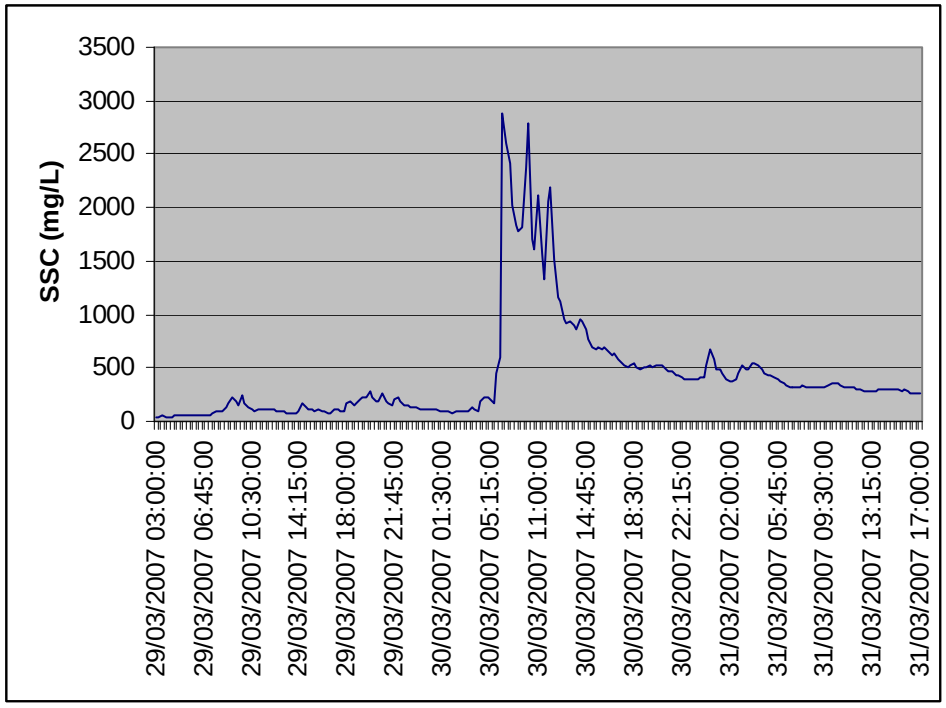

U.3.9 Storm event 23-5-2007

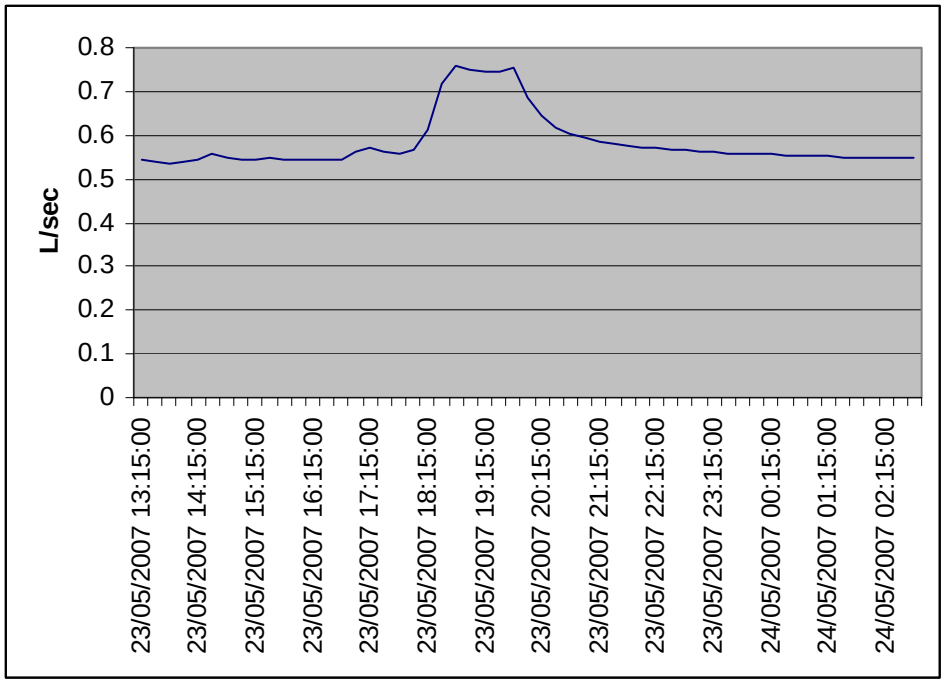

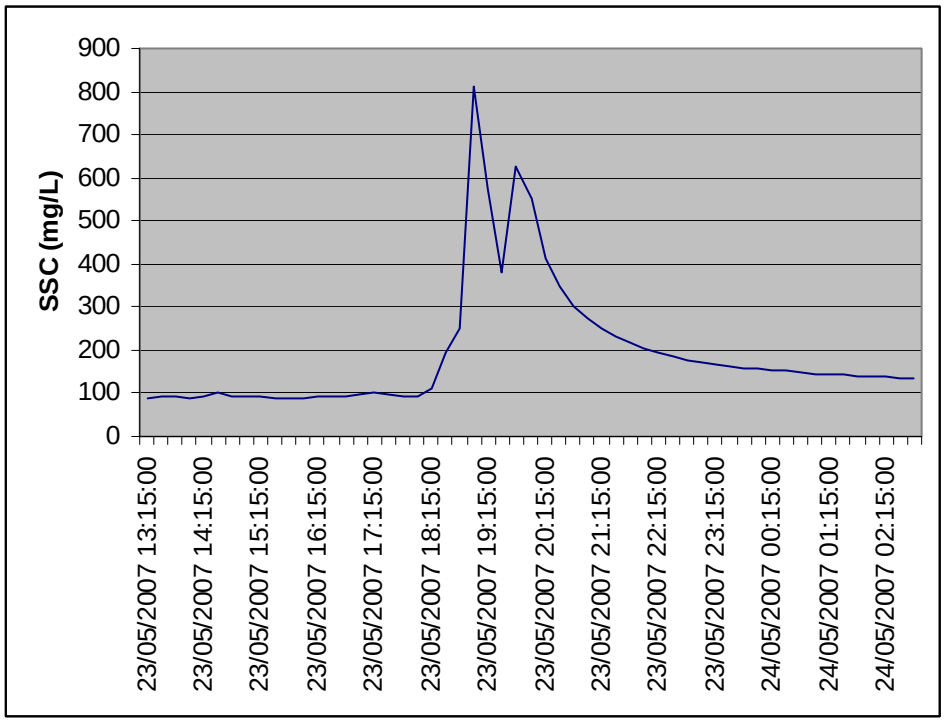

U.3.10 Storm event 20-6-2007

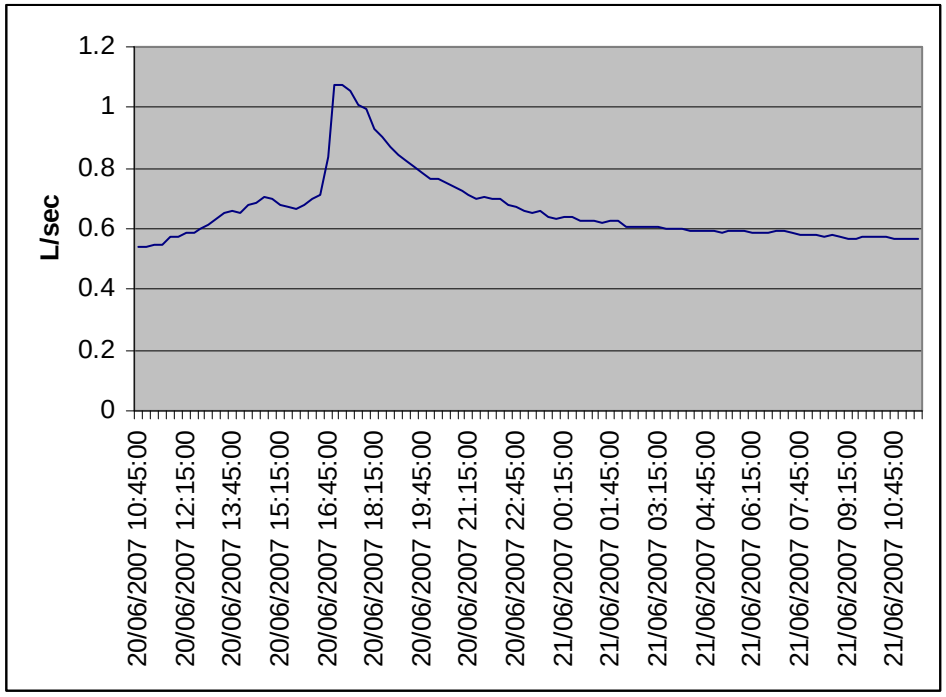

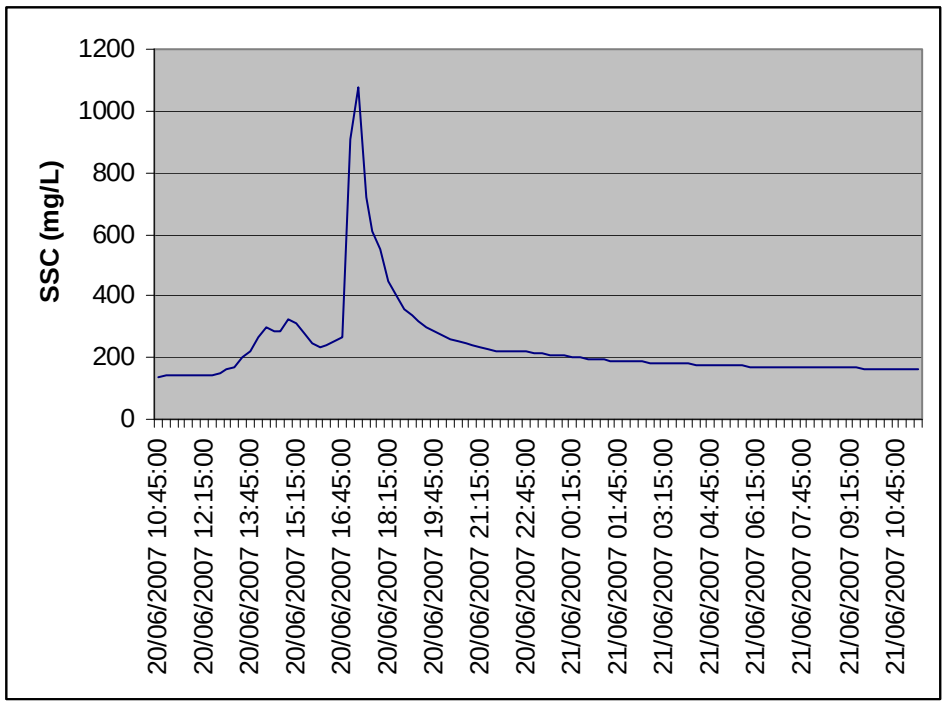

U.3.11 Storm event 22-6-2007

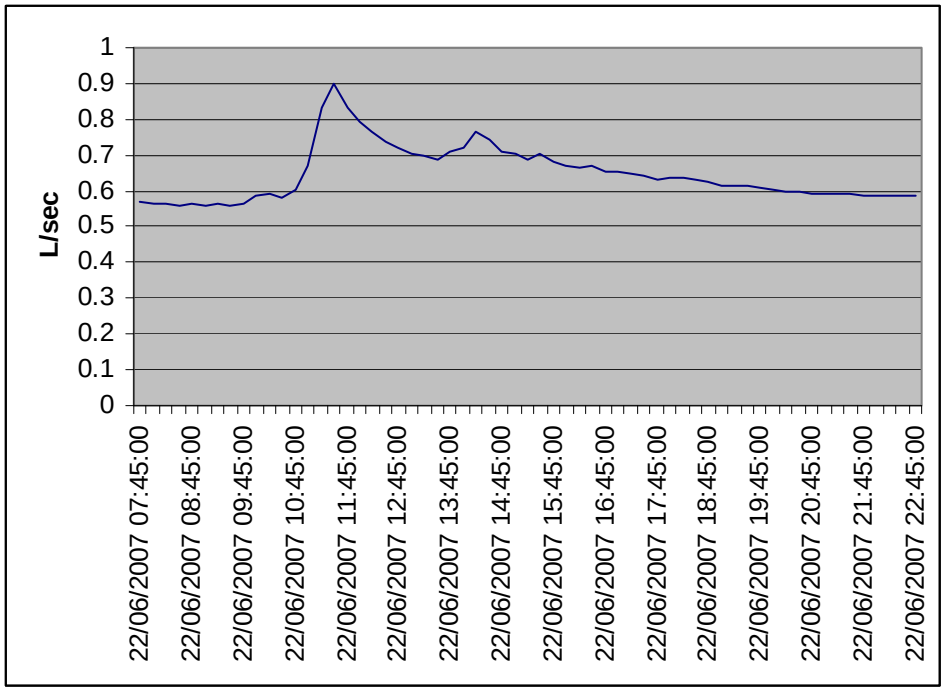

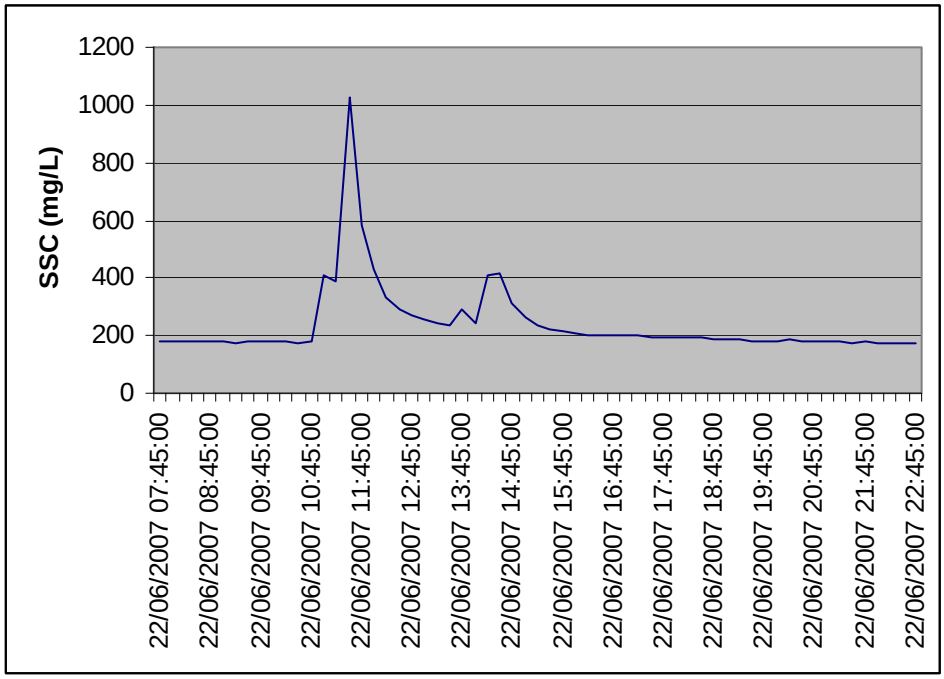

U.3.12 Storm event 29-6-2007

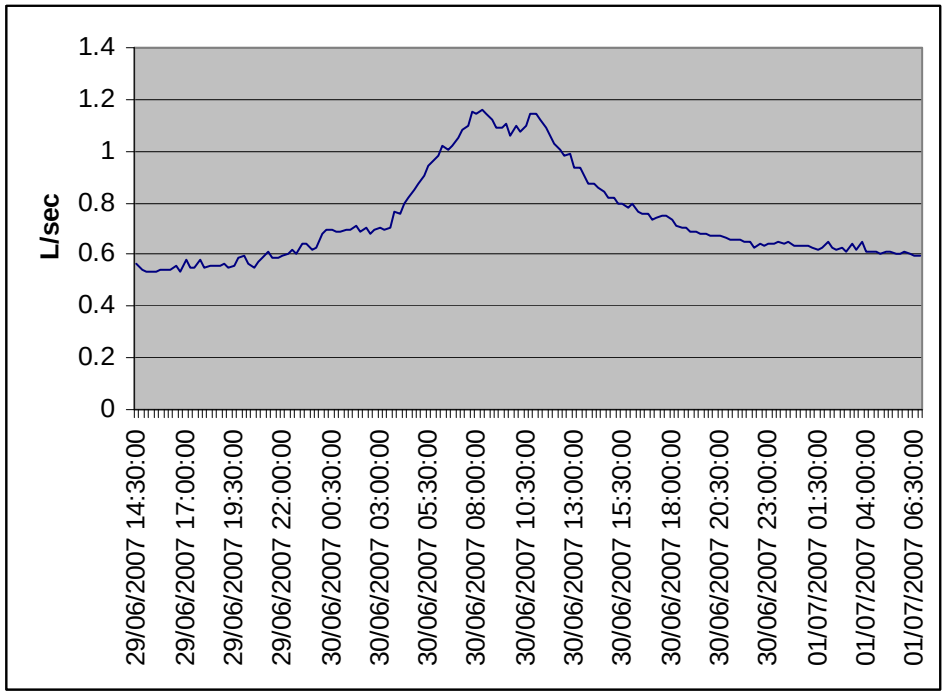

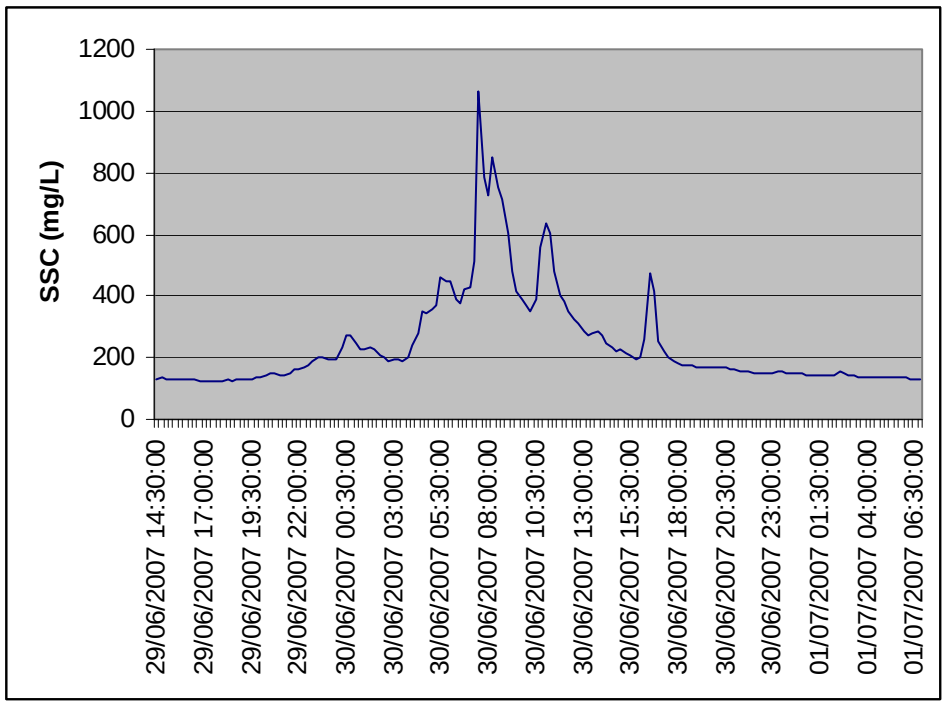

U.3.13 Storm event 1-7-2007

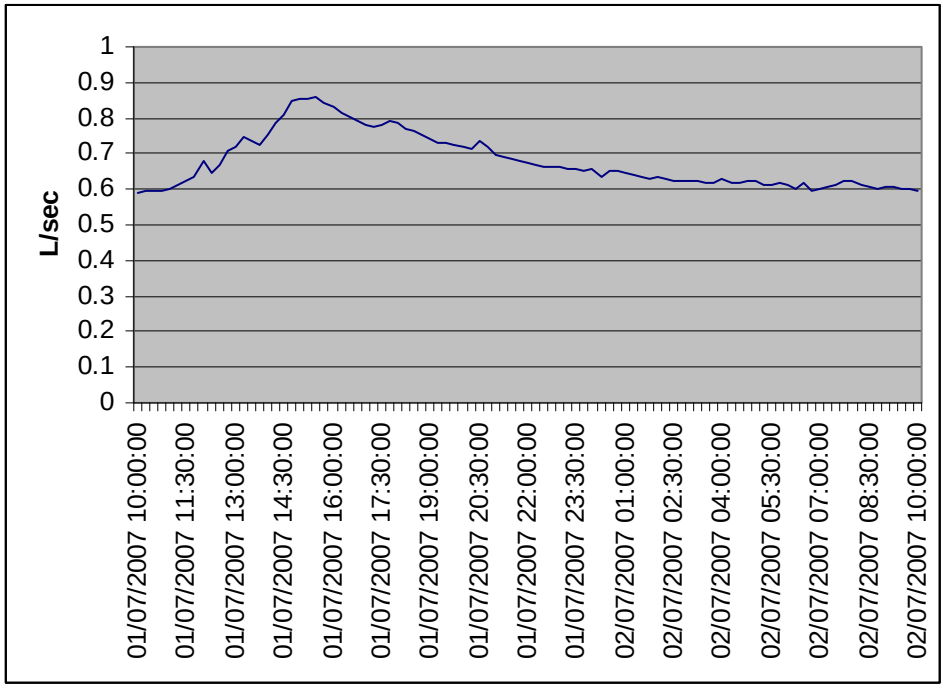

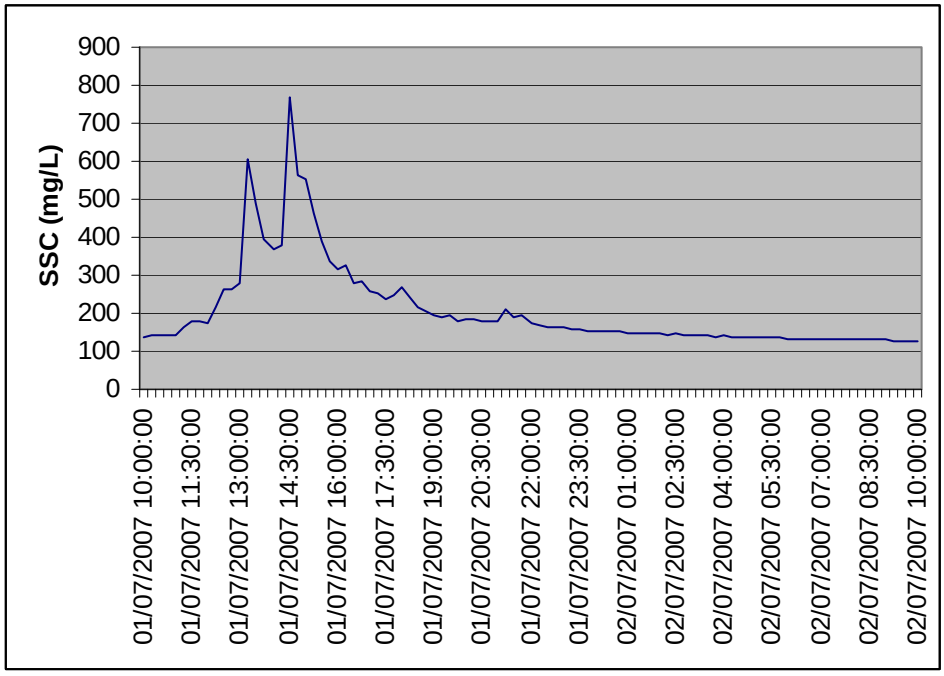

U.3.14 Storm event 6-7-2007

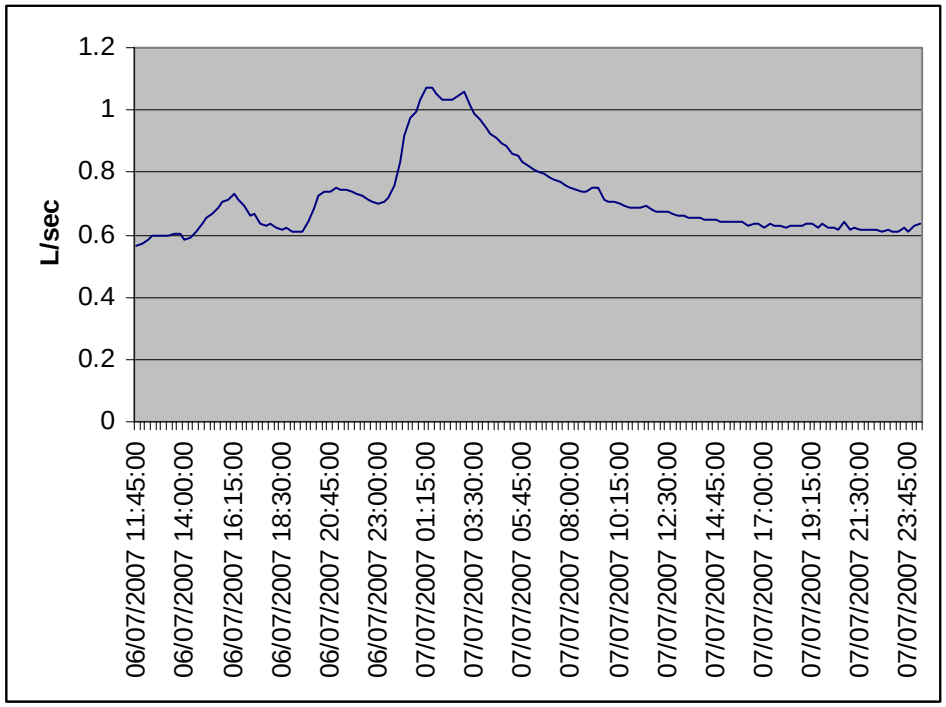

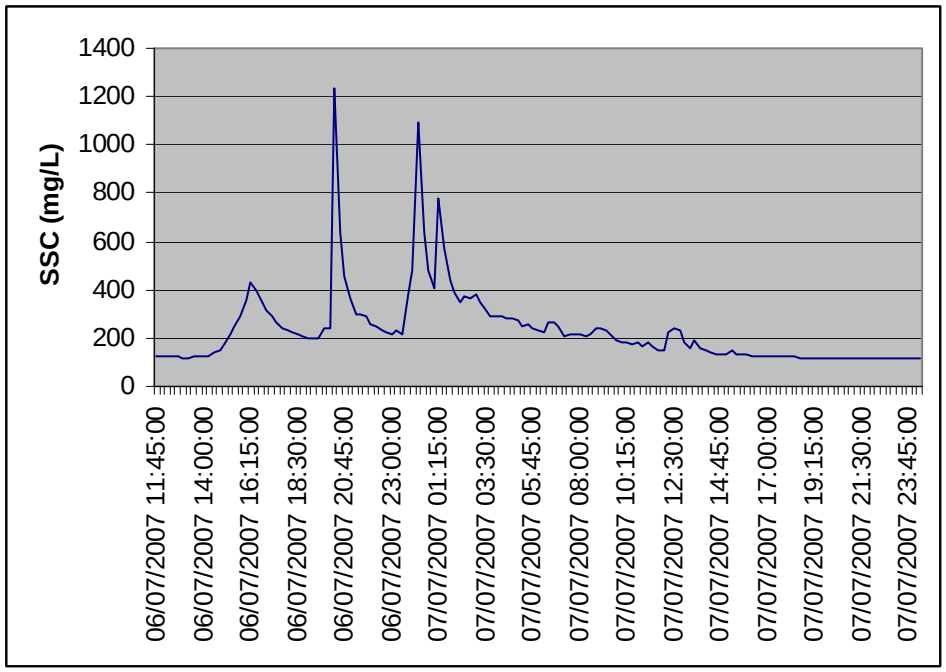

U.3.15 Storm event 10-7-2007

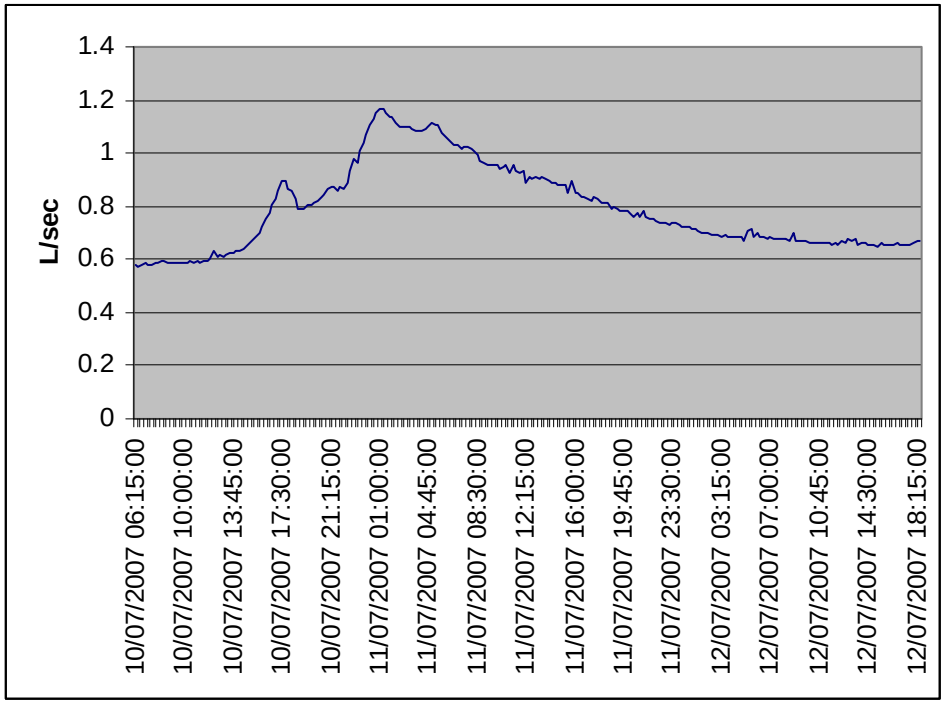

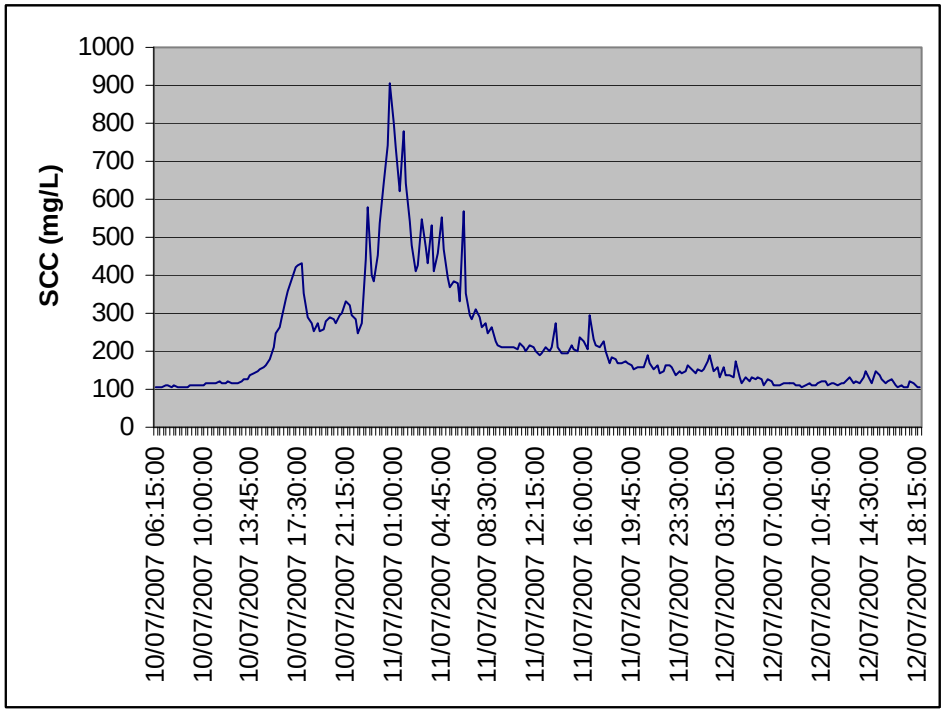

U.3.16 Storm event 16-7-2007

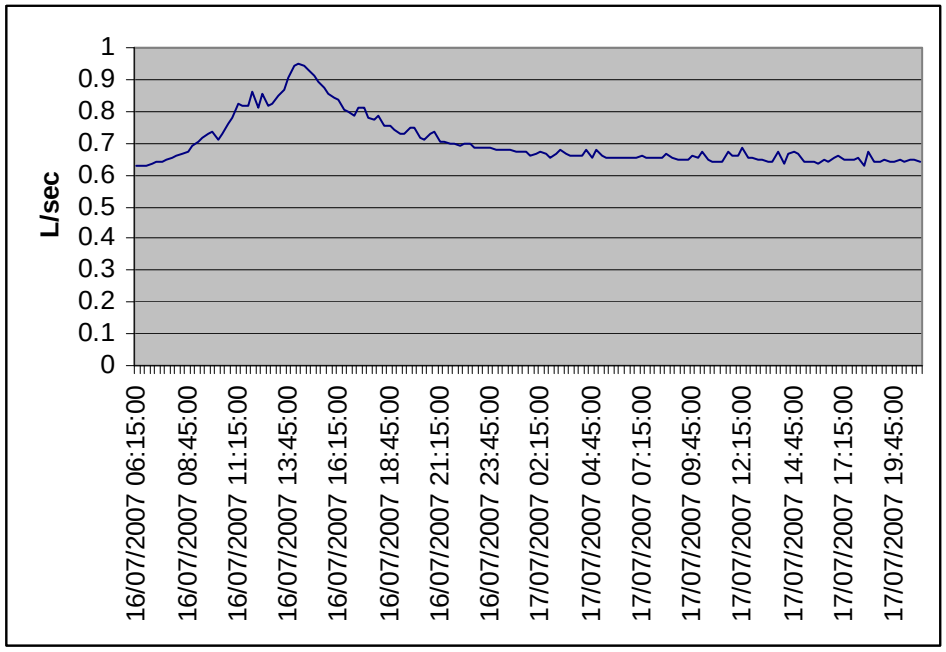

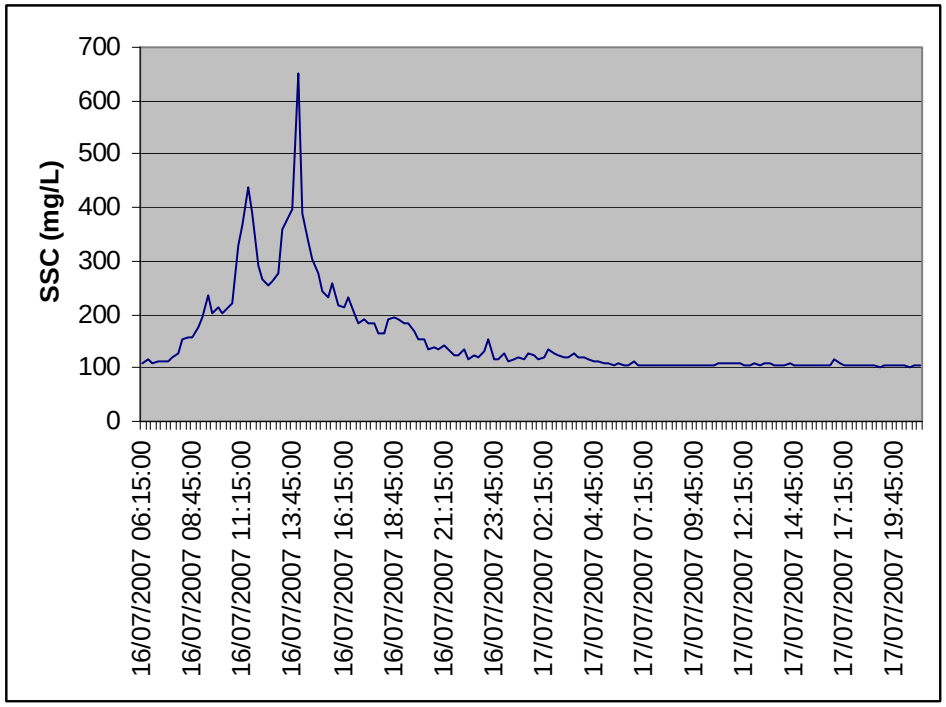

U.4 Exotic forest ten years post harvest (EX-10)

U.4.1 Storm event 4-6-2006

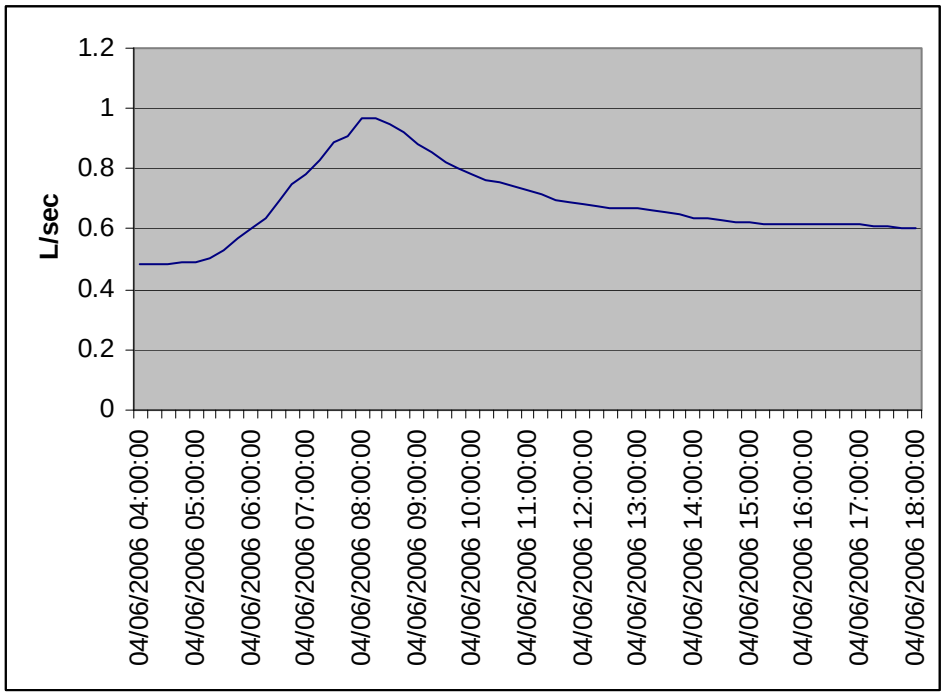

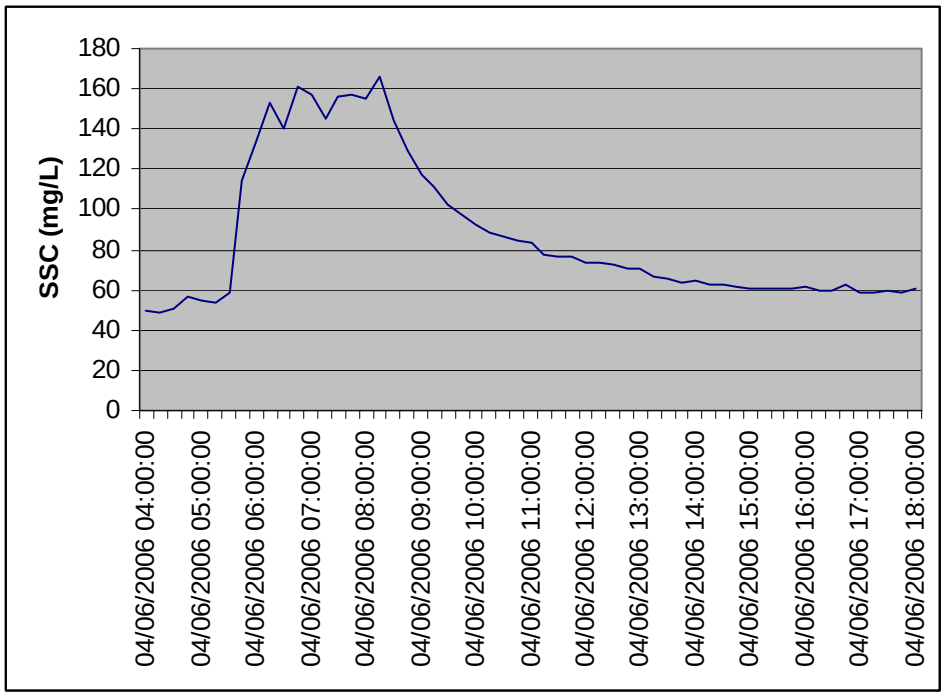

U.4.2 Storm event 19-7-2006

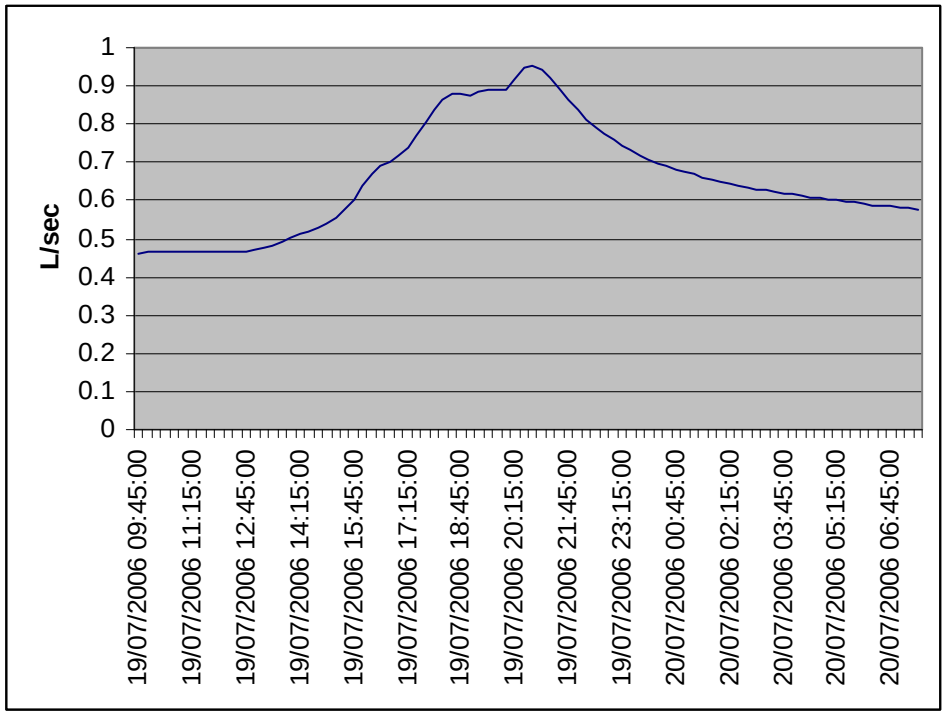

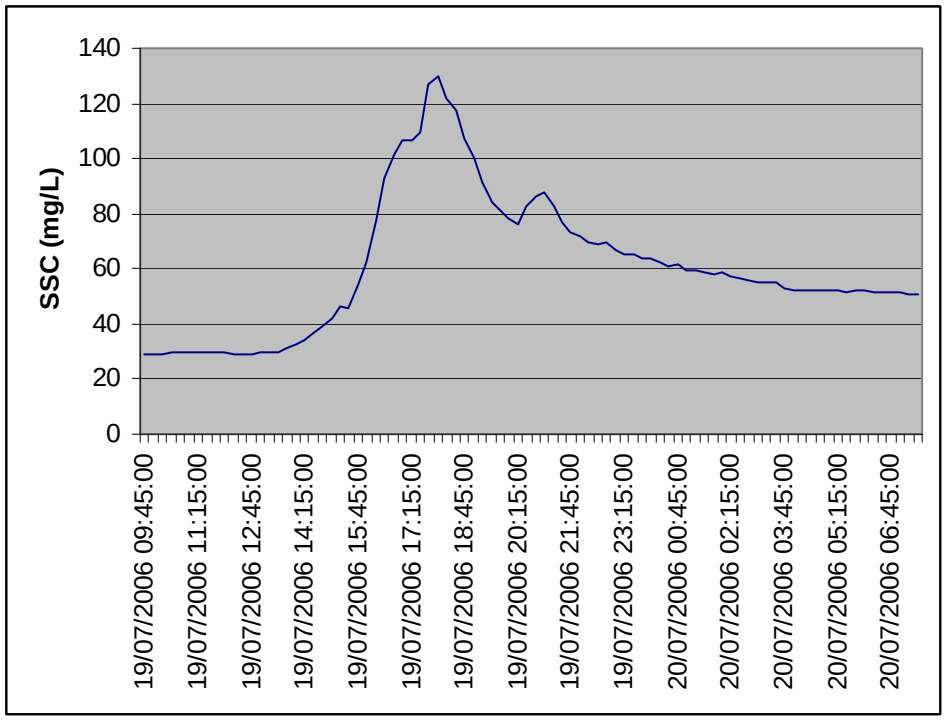

U.4.3 Storm event 2-10-2006

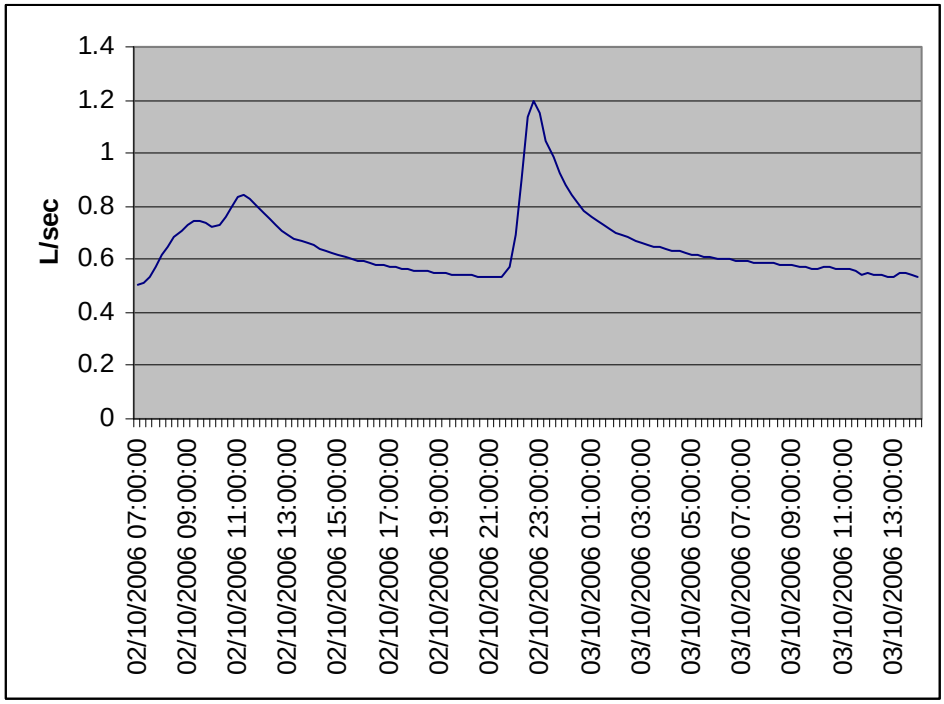

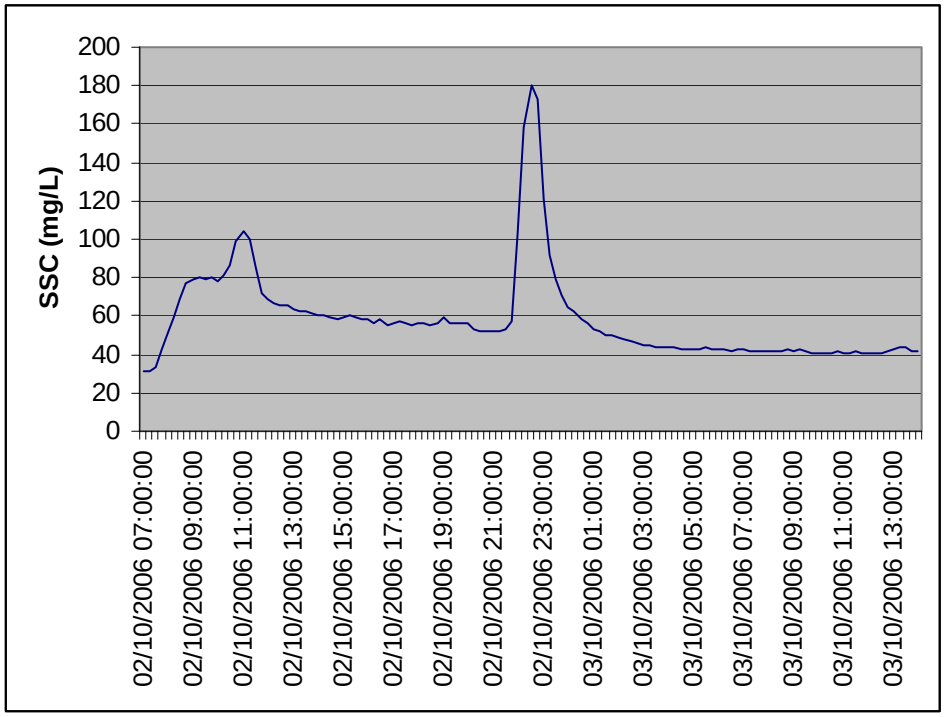

U.4.4 Storm event 30-11-2006

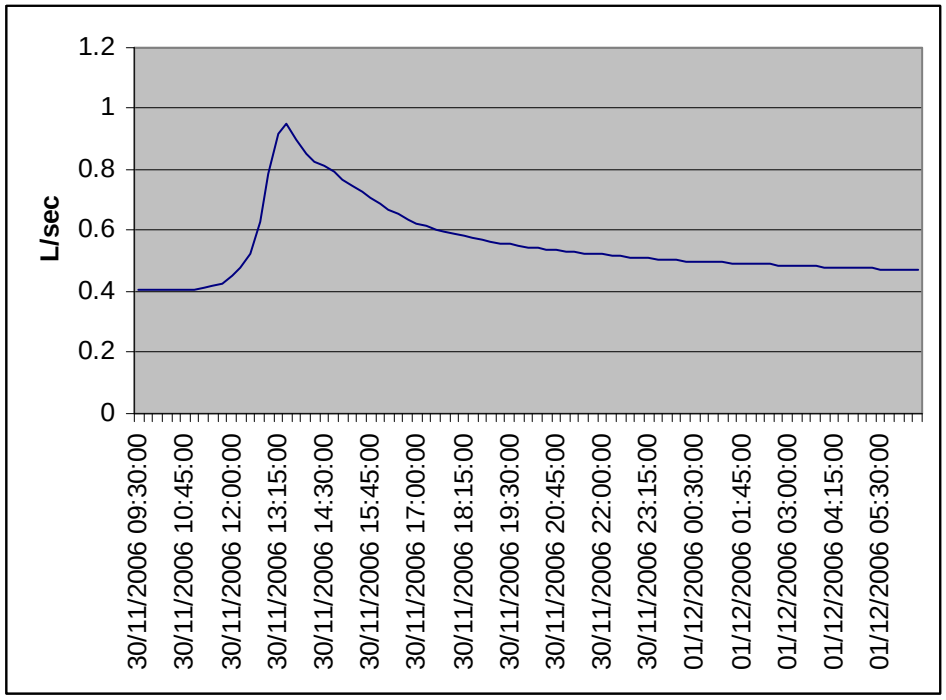

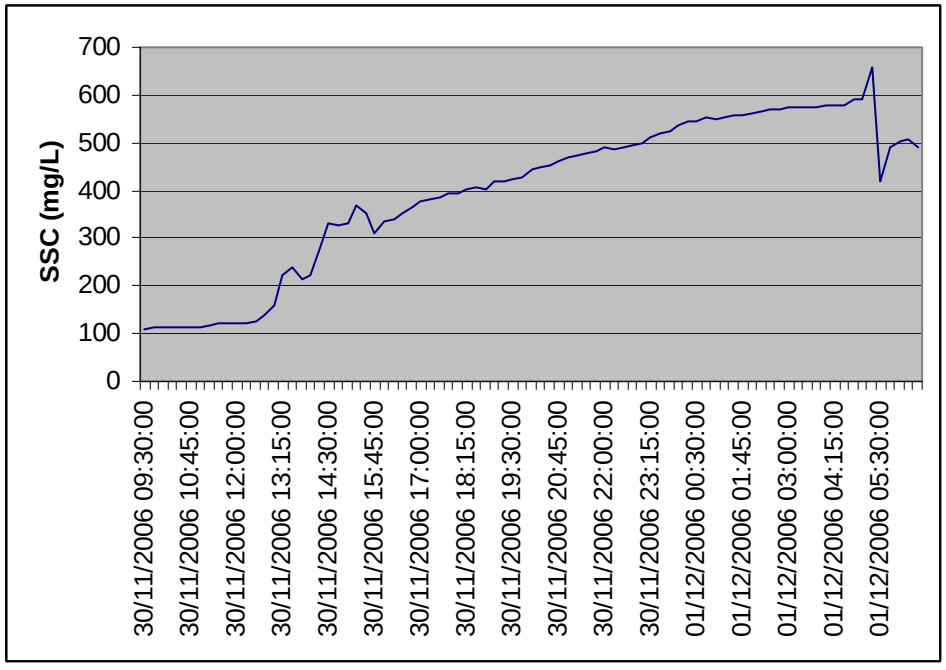

U.4.5 Storm event 28-3-2007

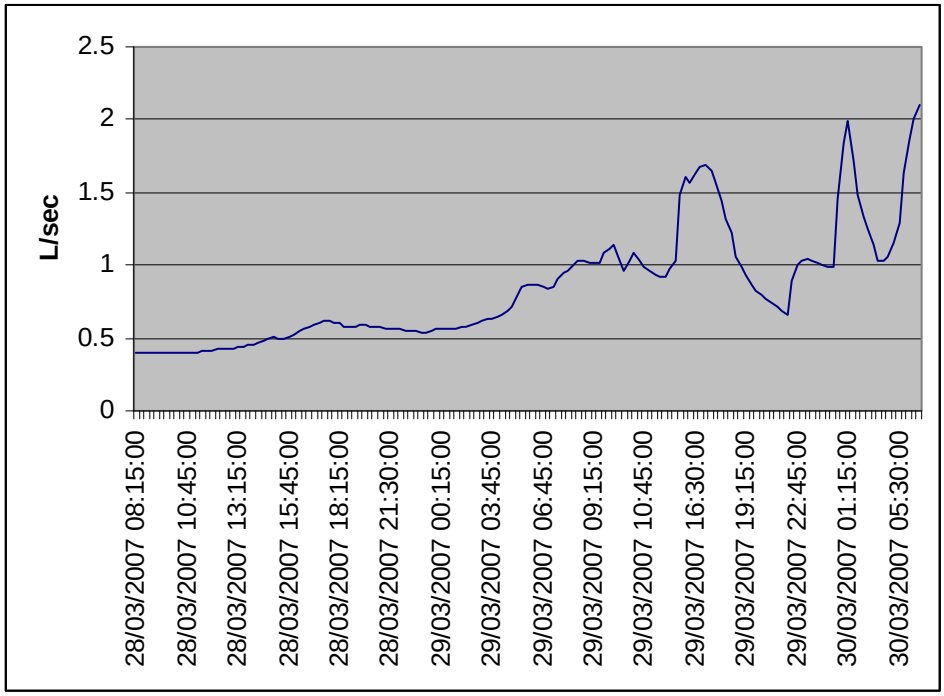

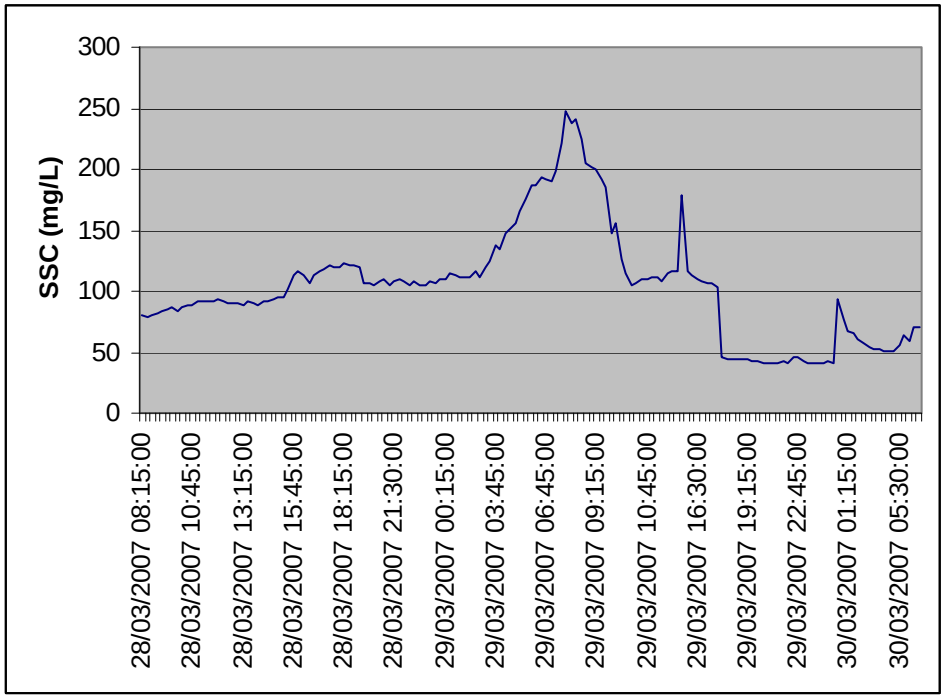

U.4.6 Storm event 30-4-2007

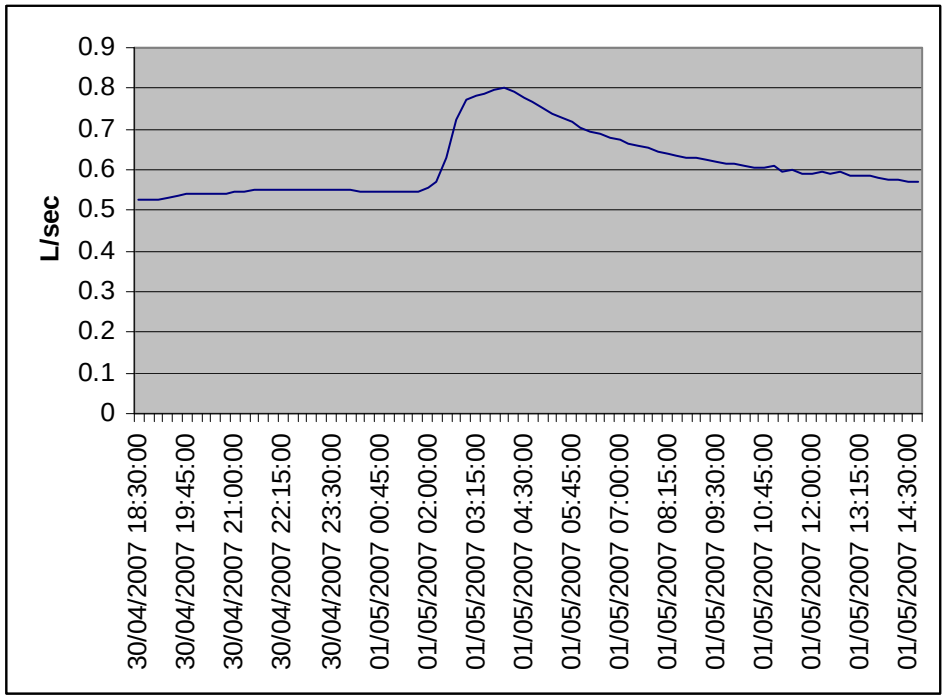

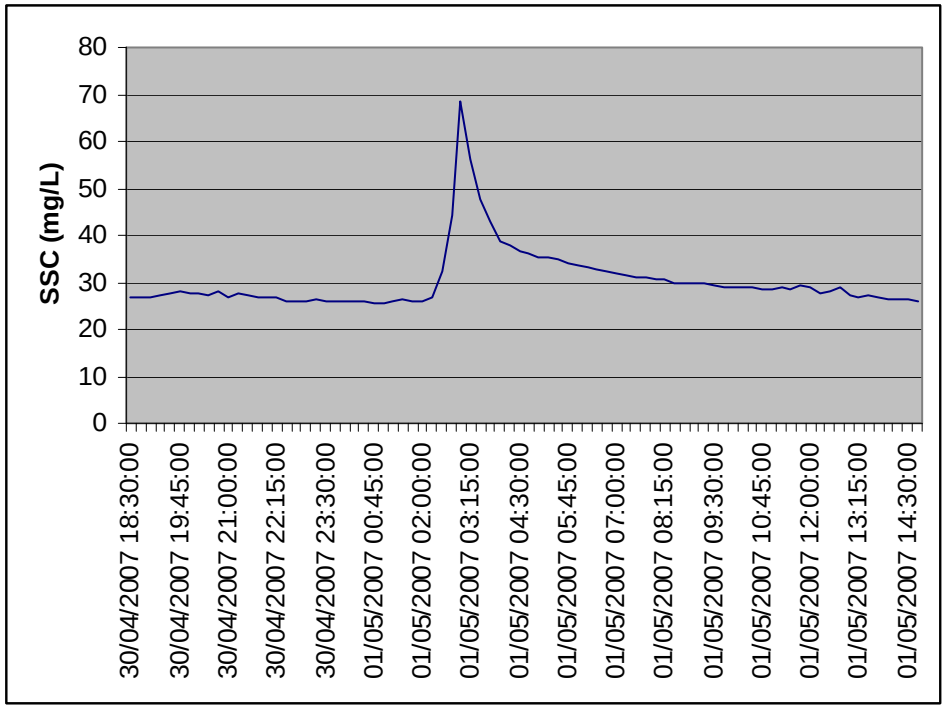

U.4.7 Storm event 23-5-2007

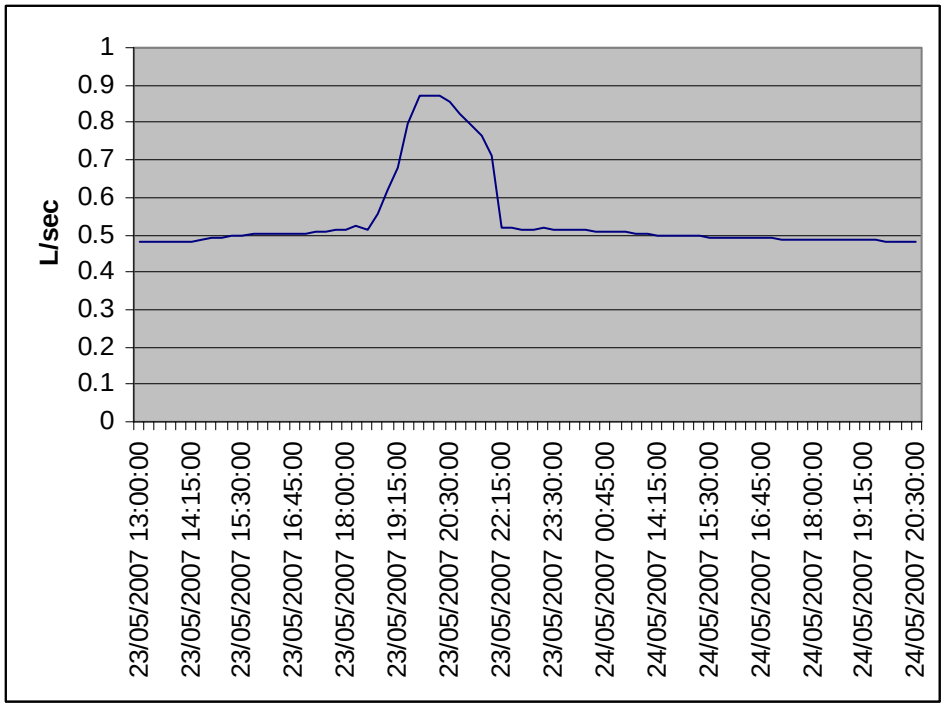

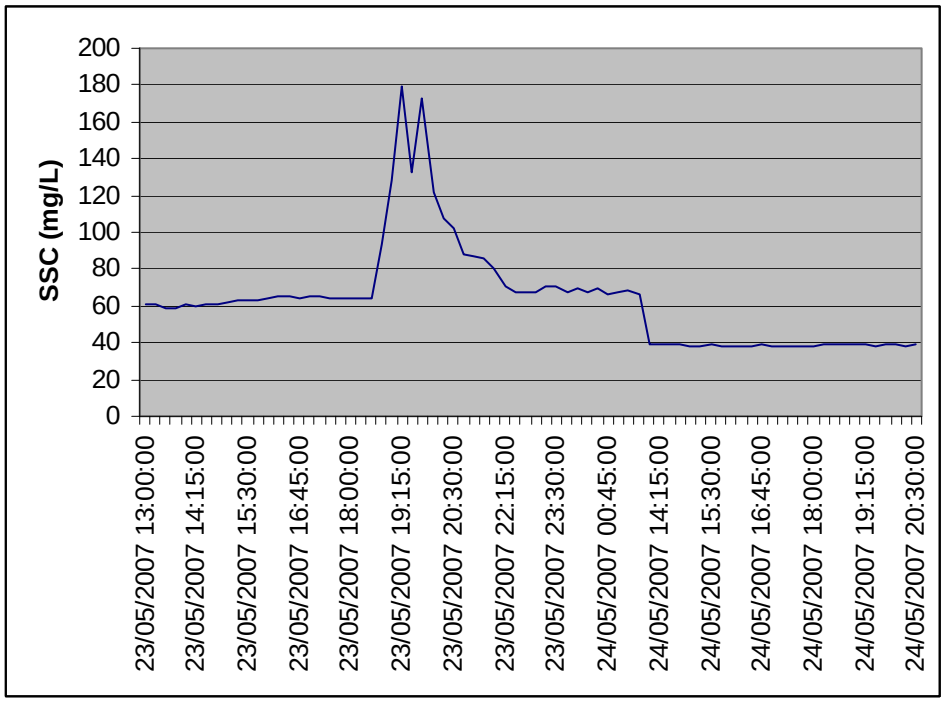

U.4.8 Storm event 14-6-2007

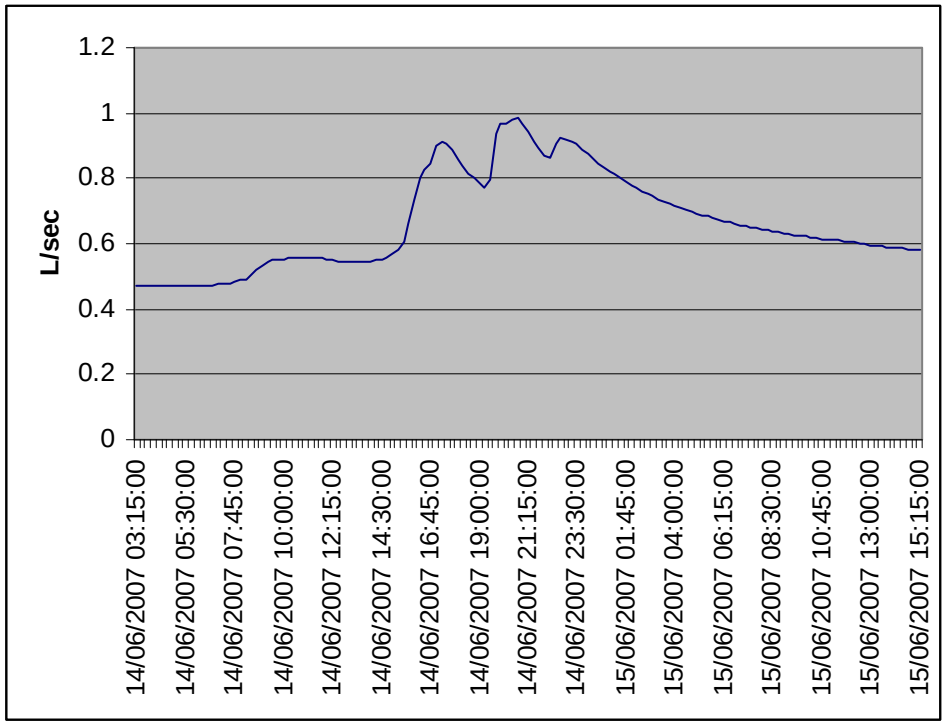

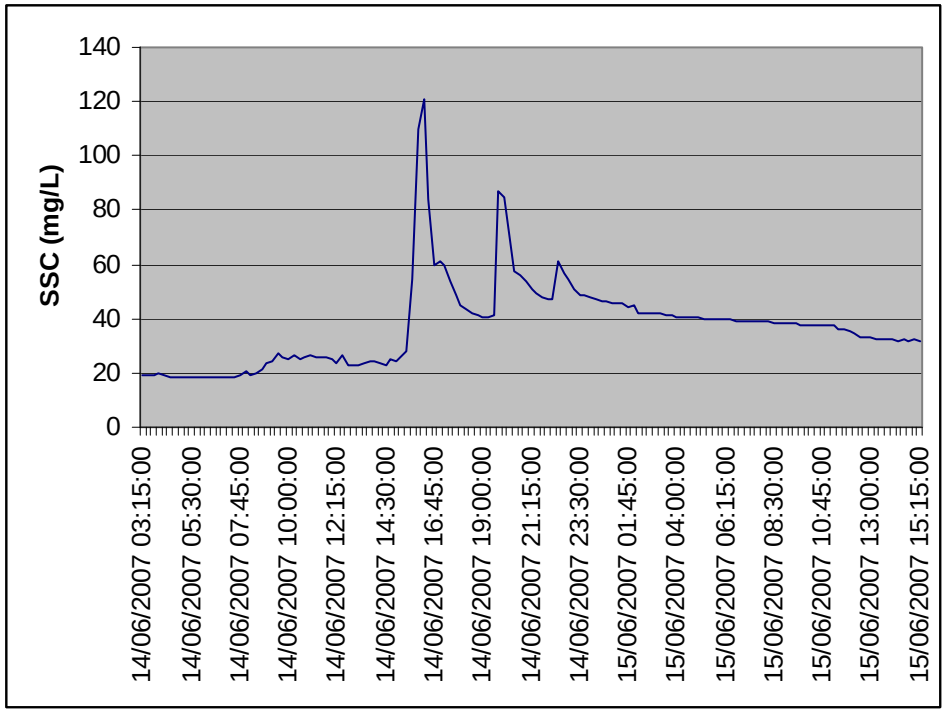

U.4.9 Storm event 20-6-2007

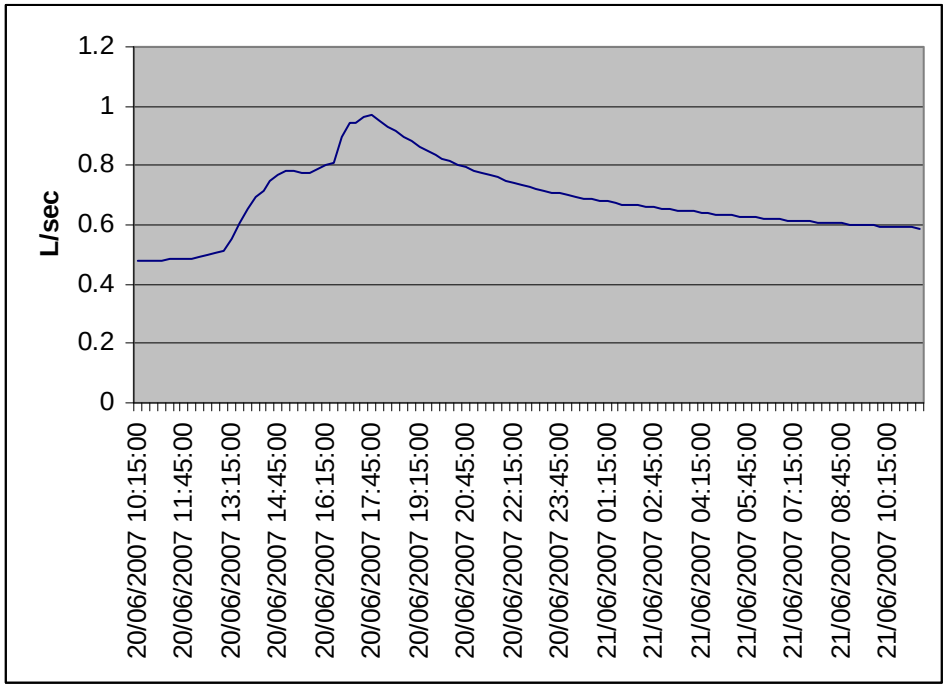

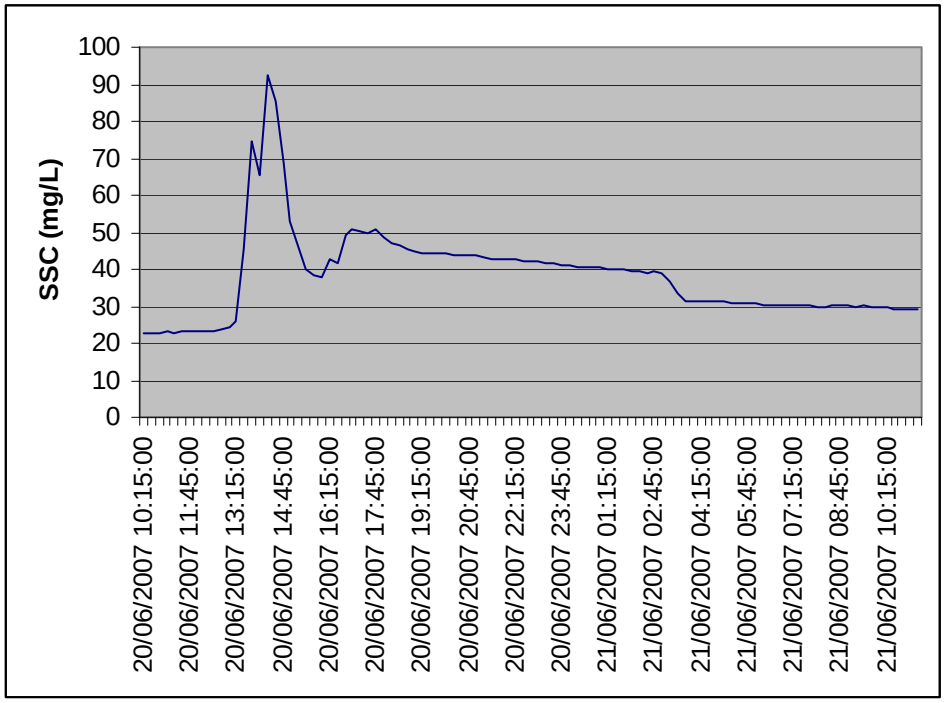

U.4.10 Storm event 22-6-2007

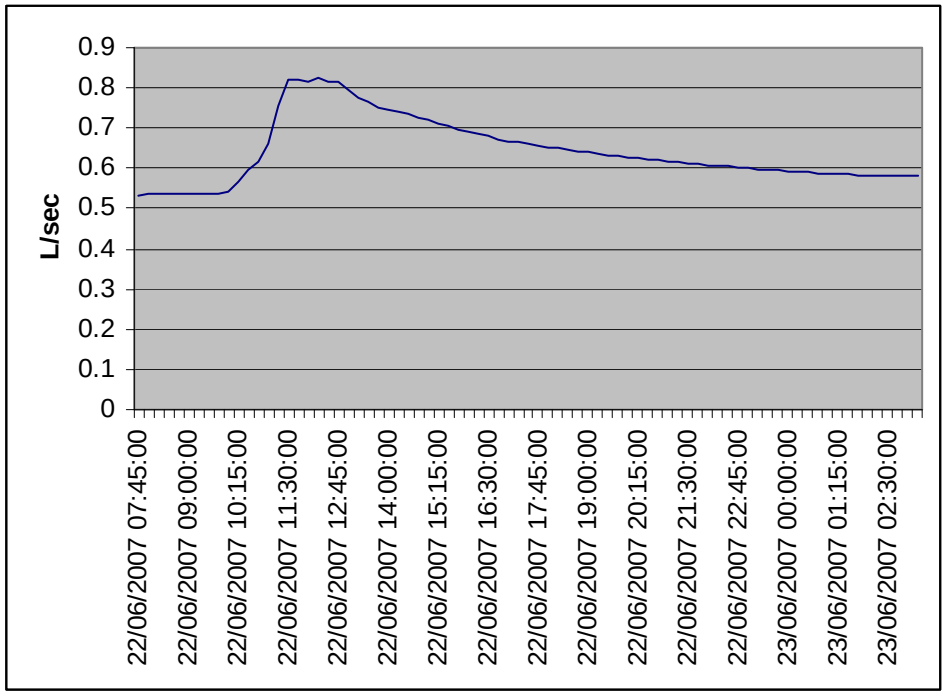

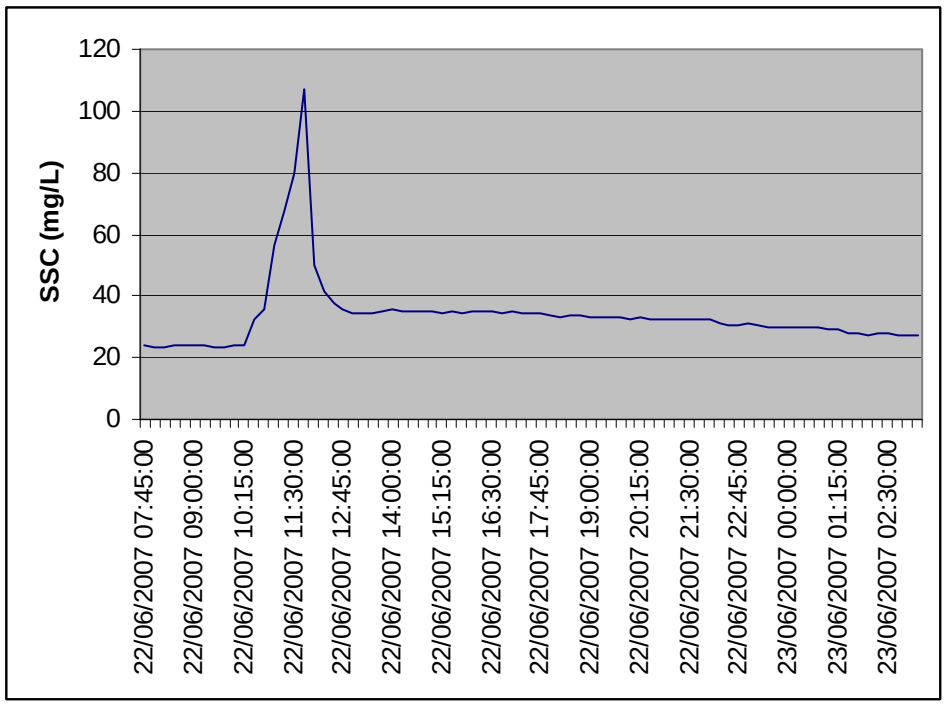

U.4.11 Storm event 30-7-2007

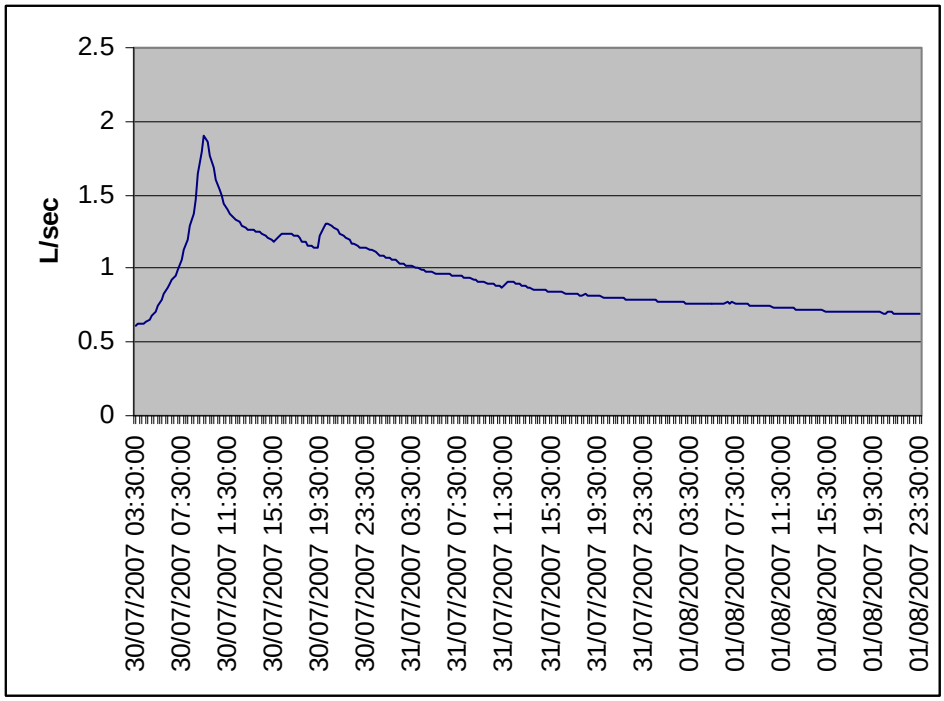

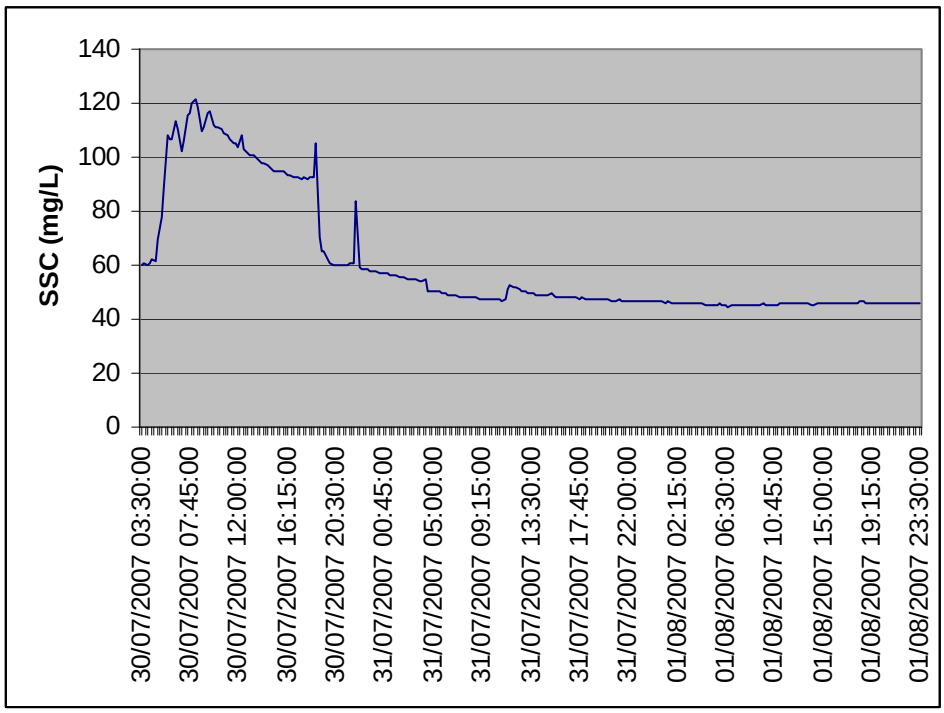

U.4.12 Storm event 5-8-2007

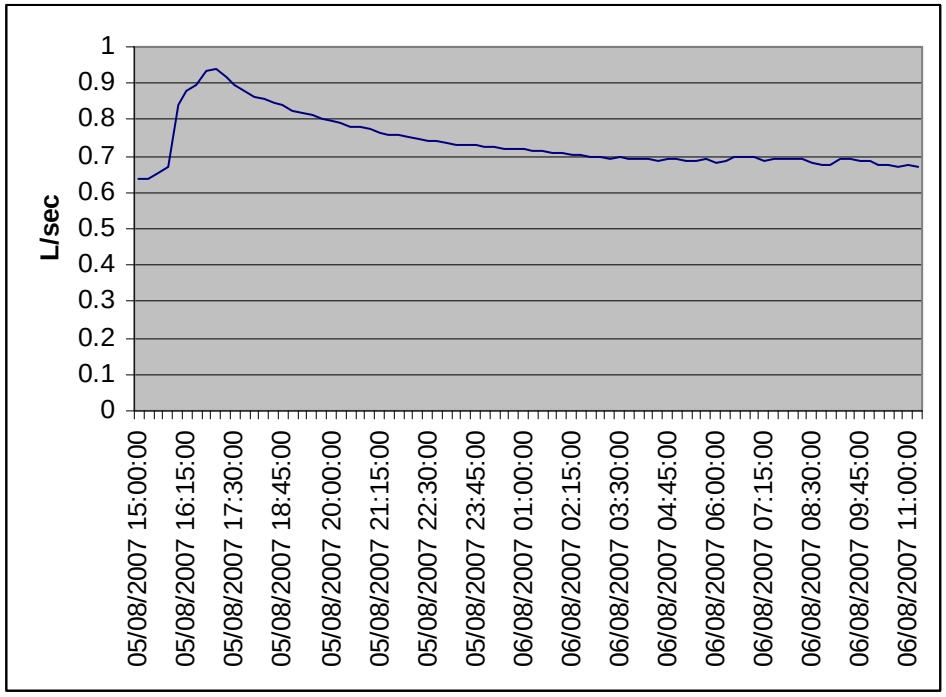

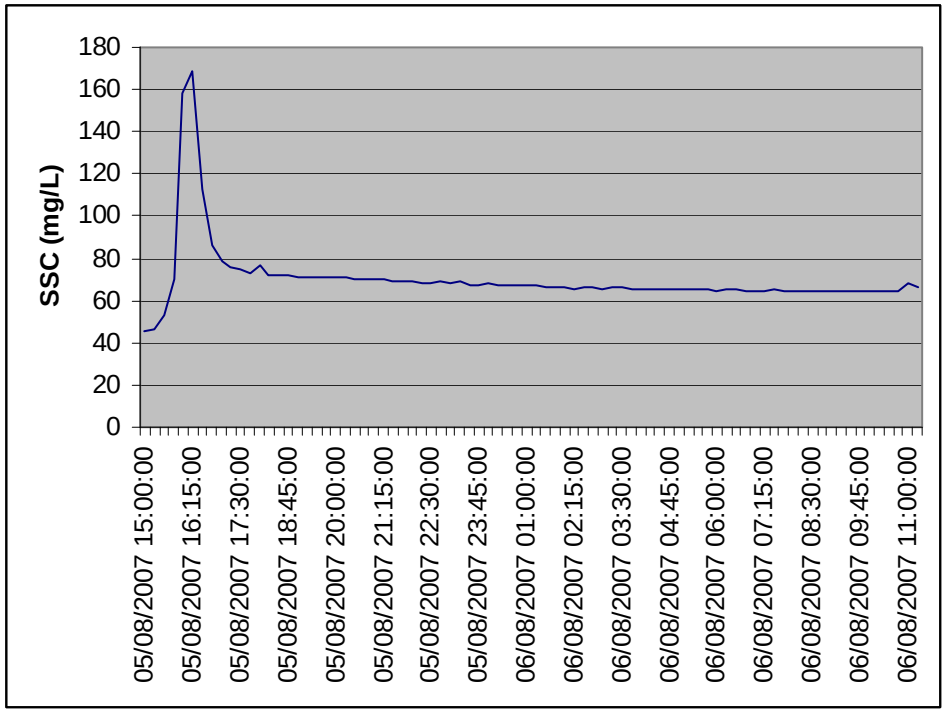

U.4.13 Storm event 9-9-2007

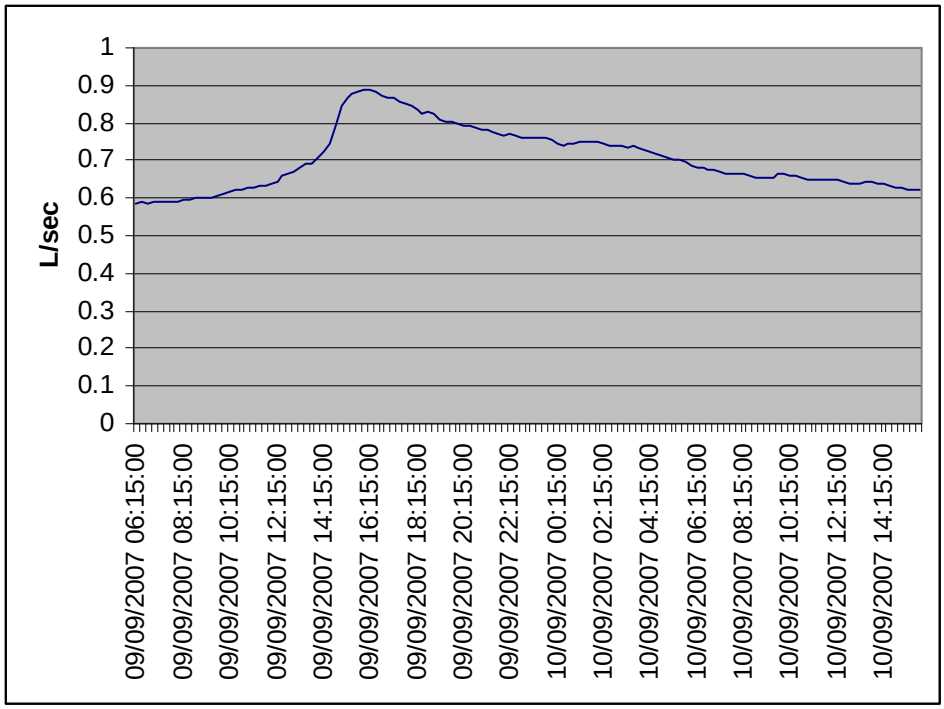

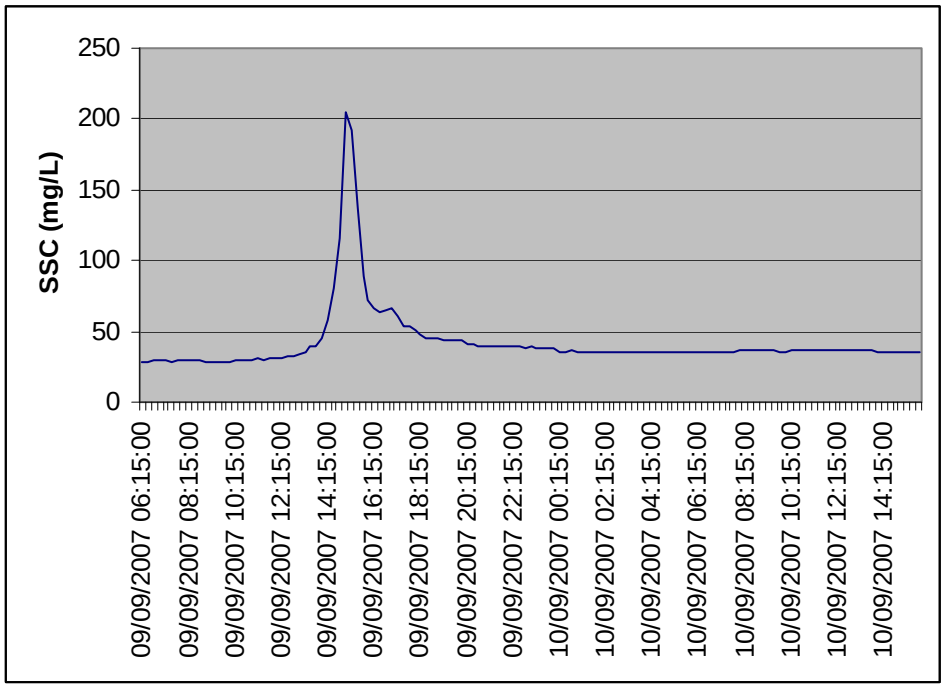

U.4.14 Storm event 16-9-2007

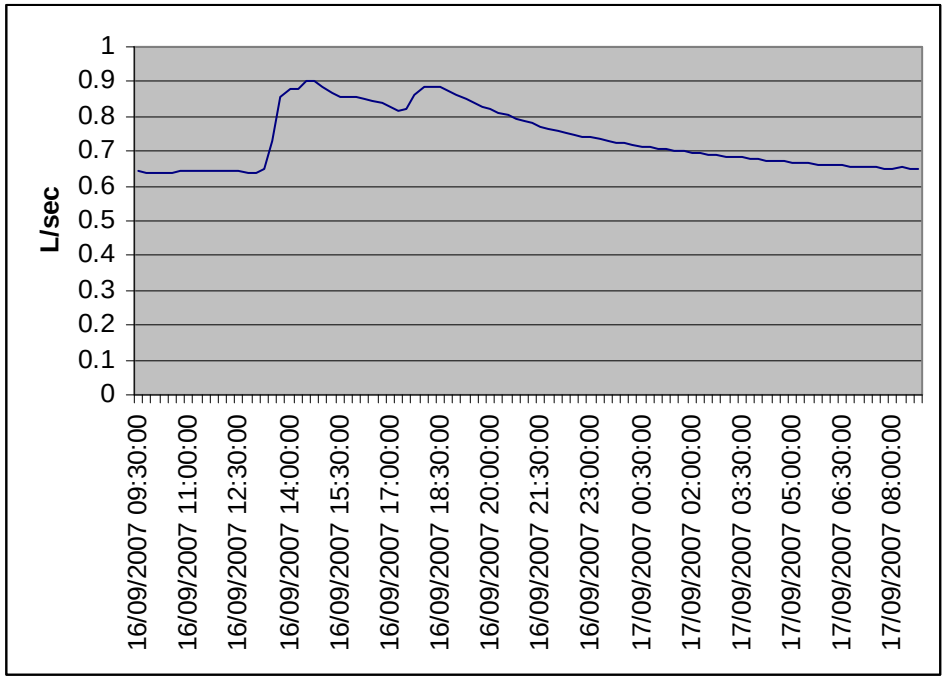

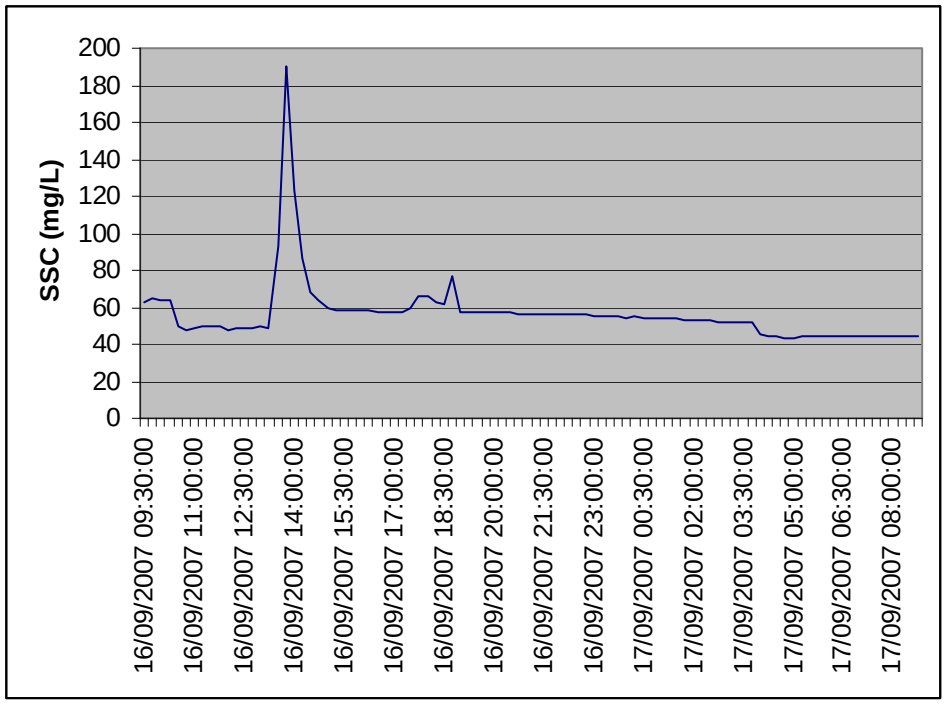

U.4.15 Storm event 1-10-2007

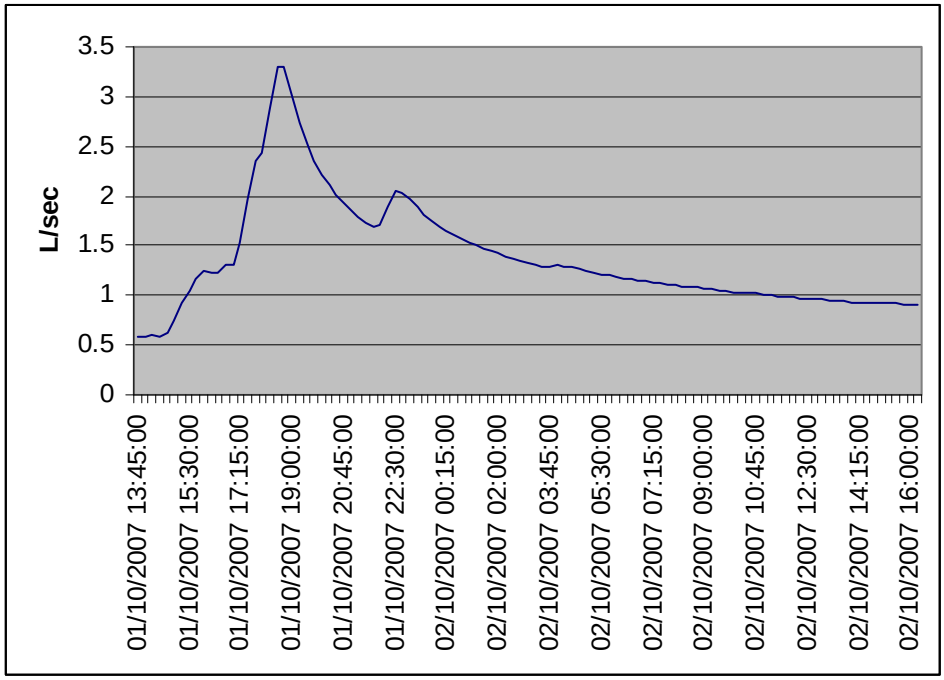

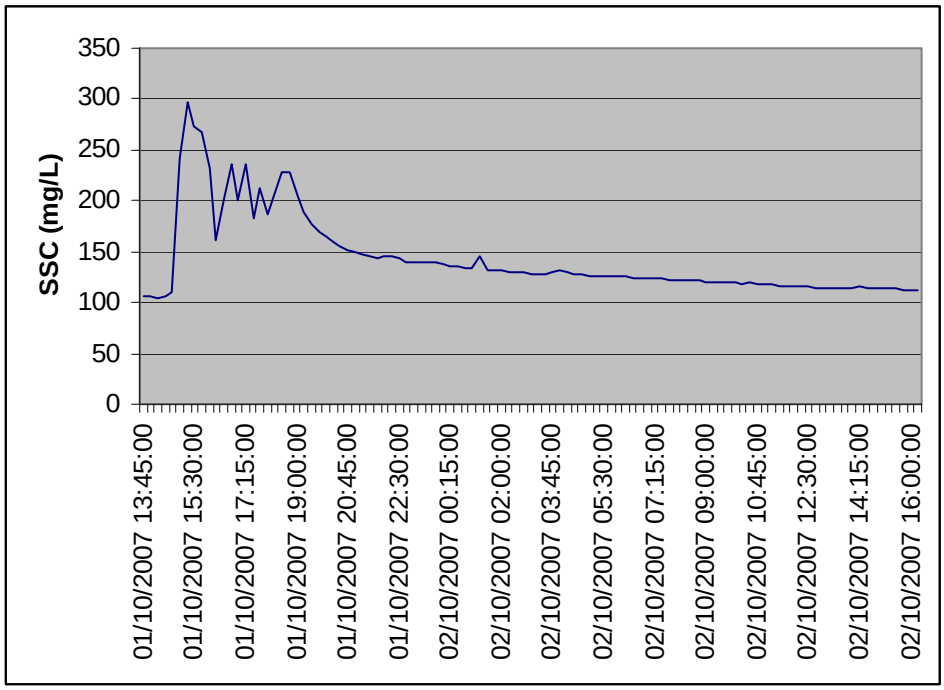

U.5 Agricultural pastures (AG-P)

U.5.1 Storm event 7-3-2006

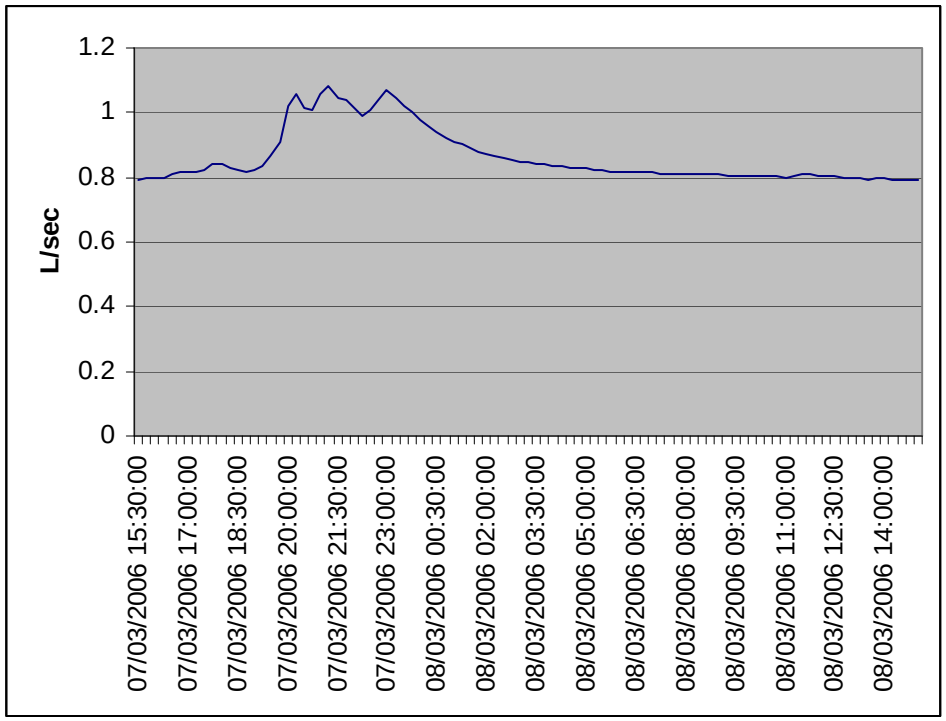

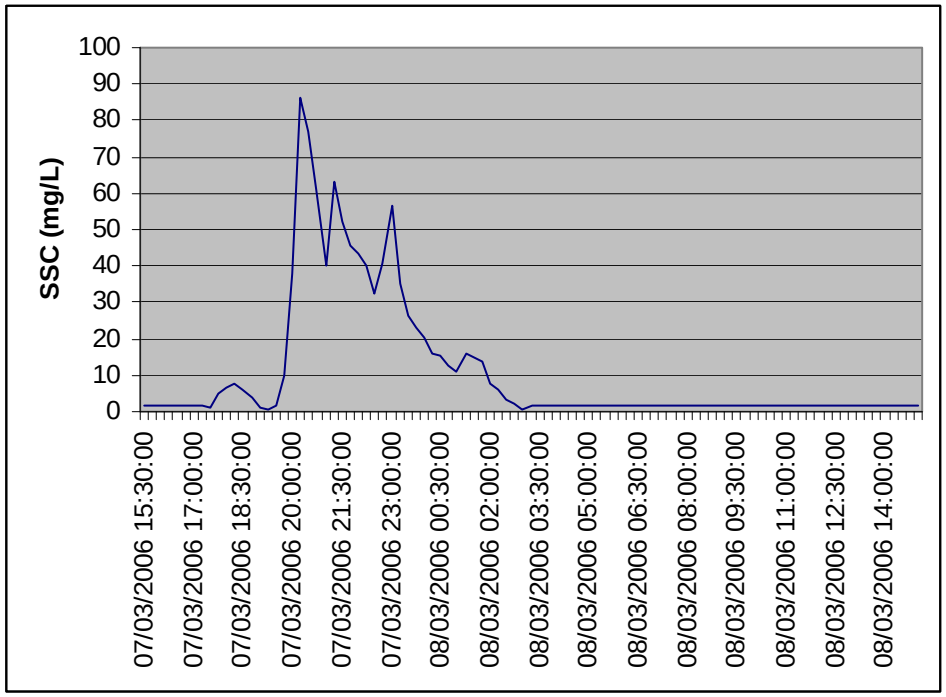

U.5.2 Storm event 26-5-2006

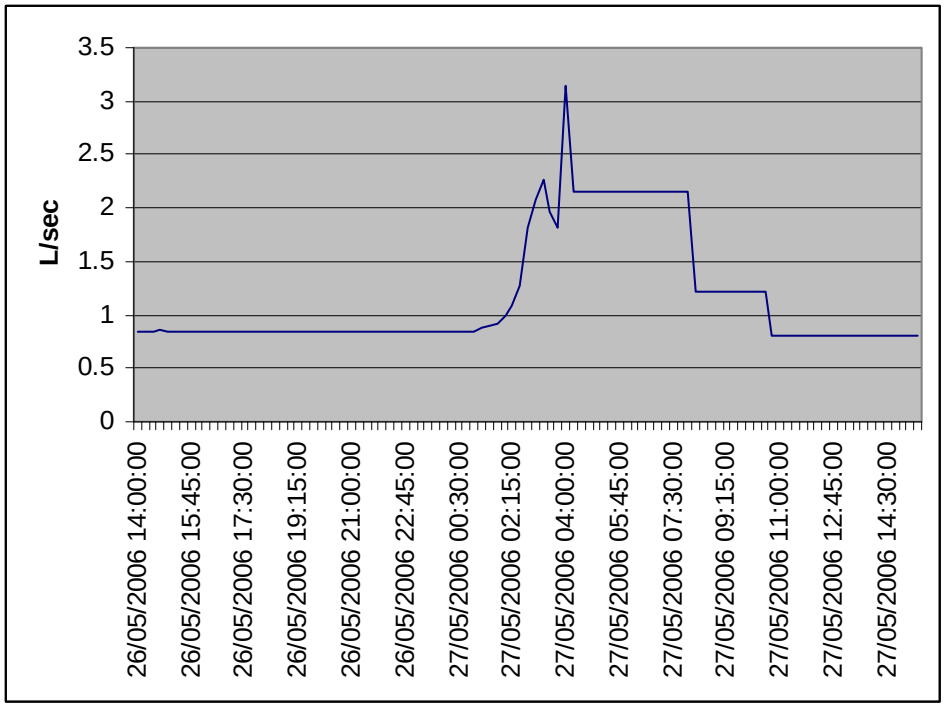

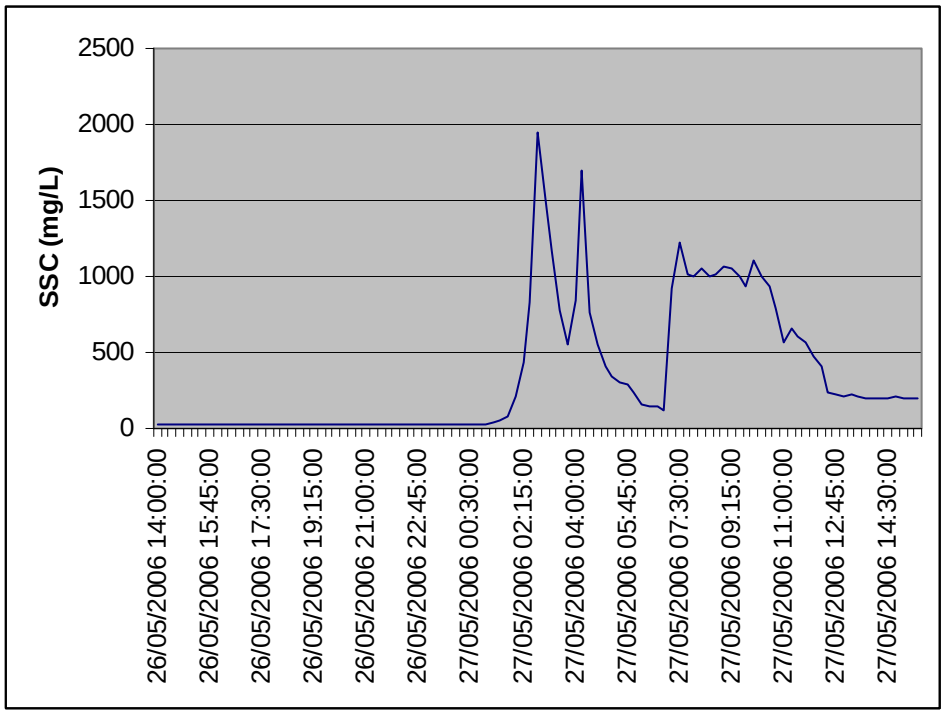

U.5.3 Storm event 26-8-2006

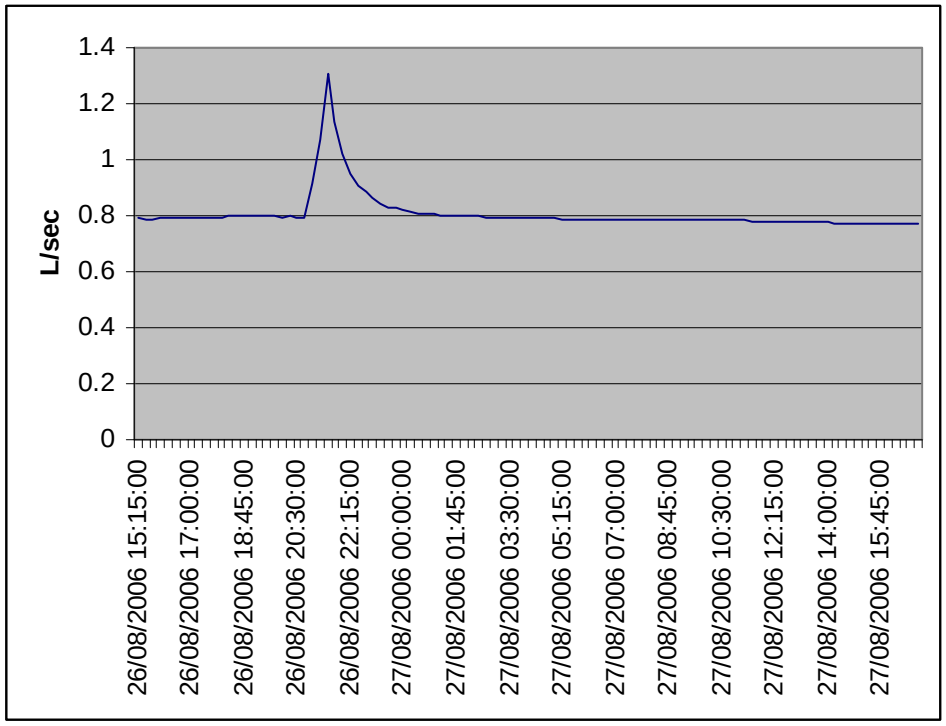

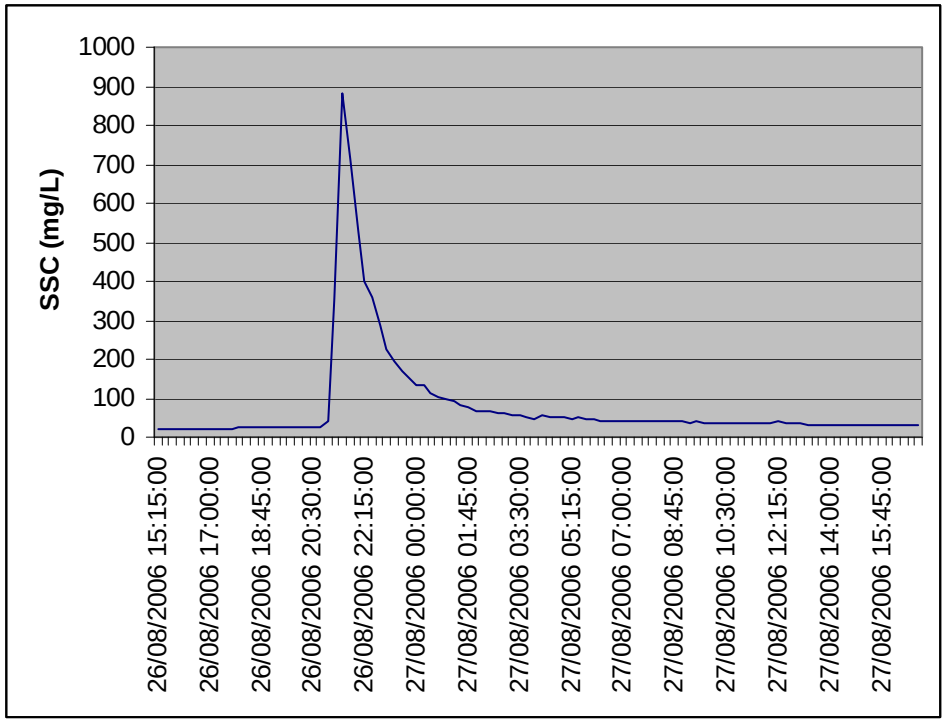

U.5.4 Storm event 9-9-2006

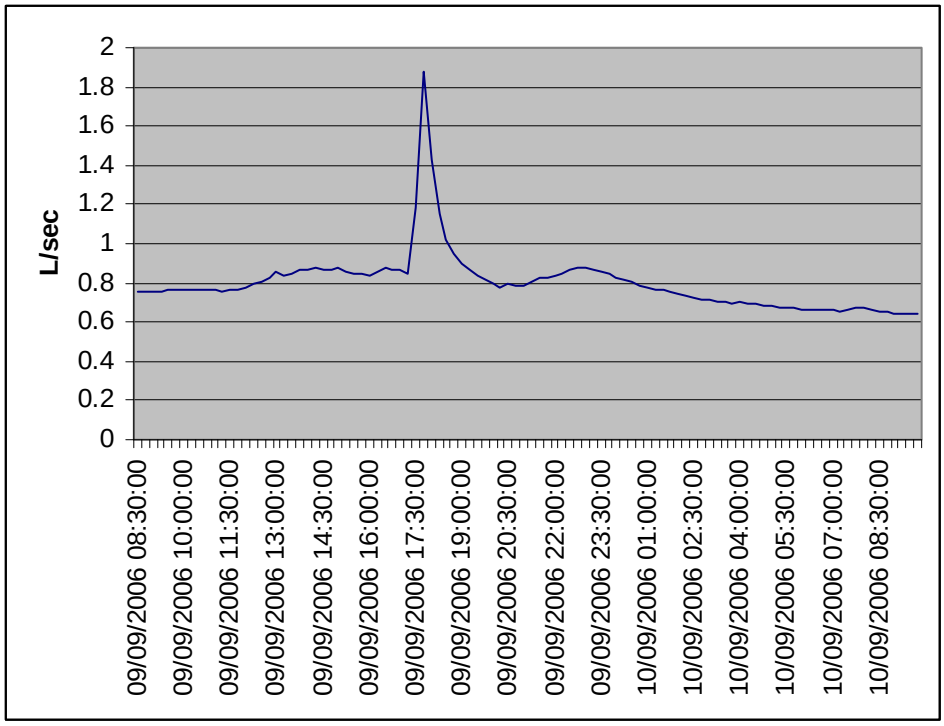

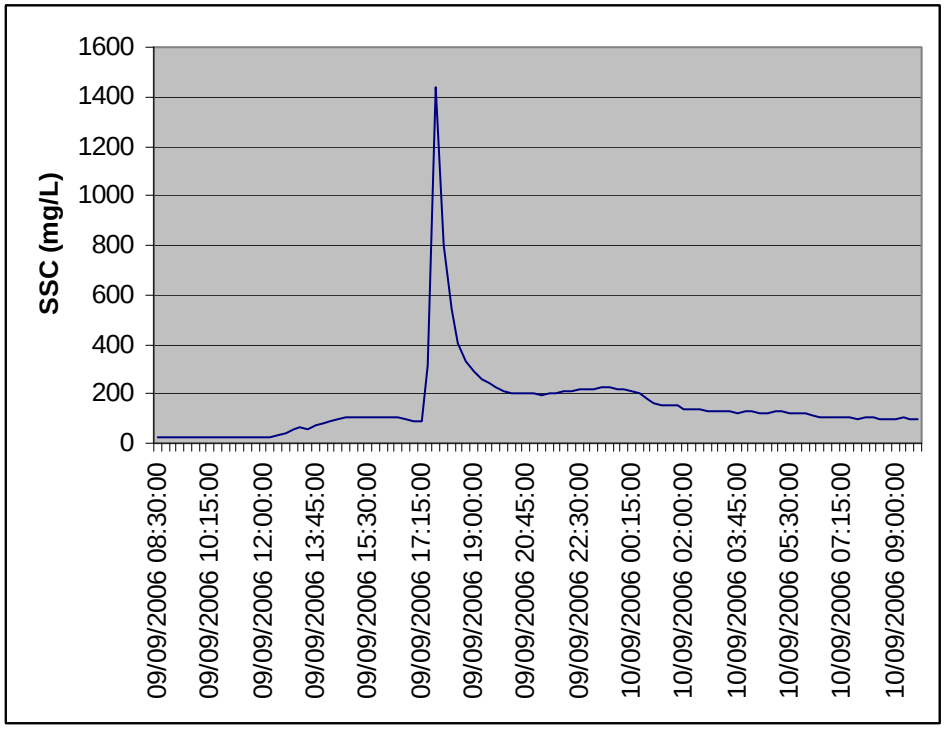

U.5.5 Storm event 2-10-2006

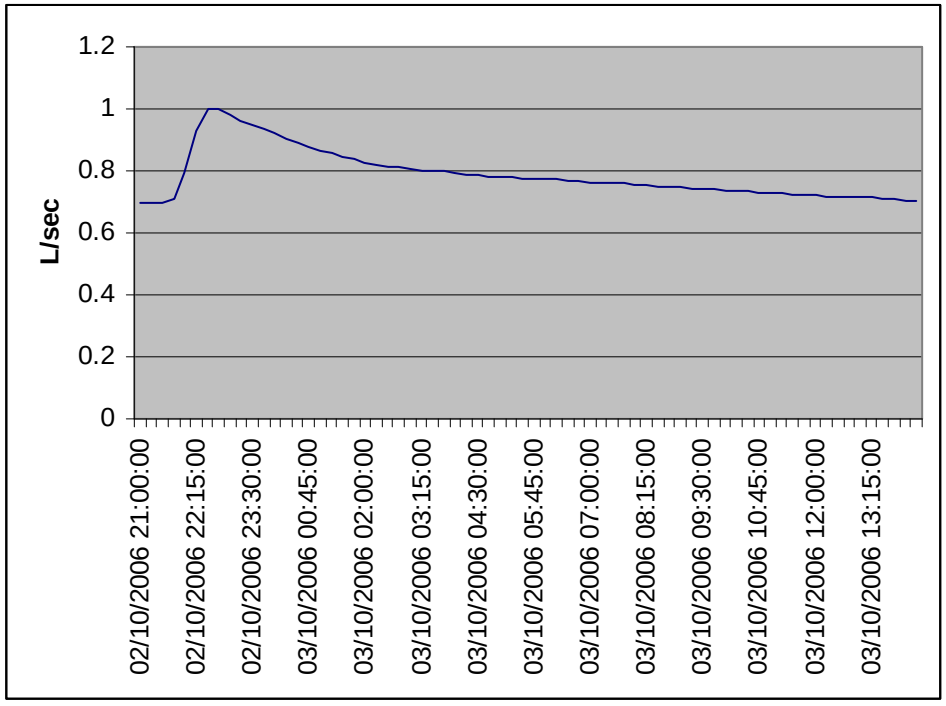

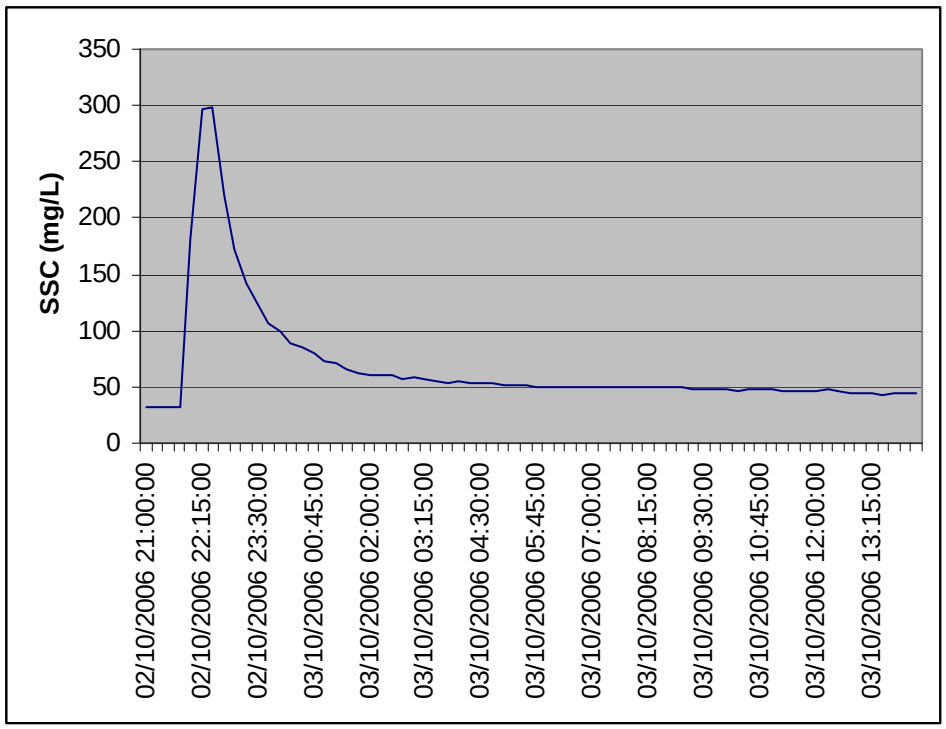

U.5.6 Storm event 23-10-2006

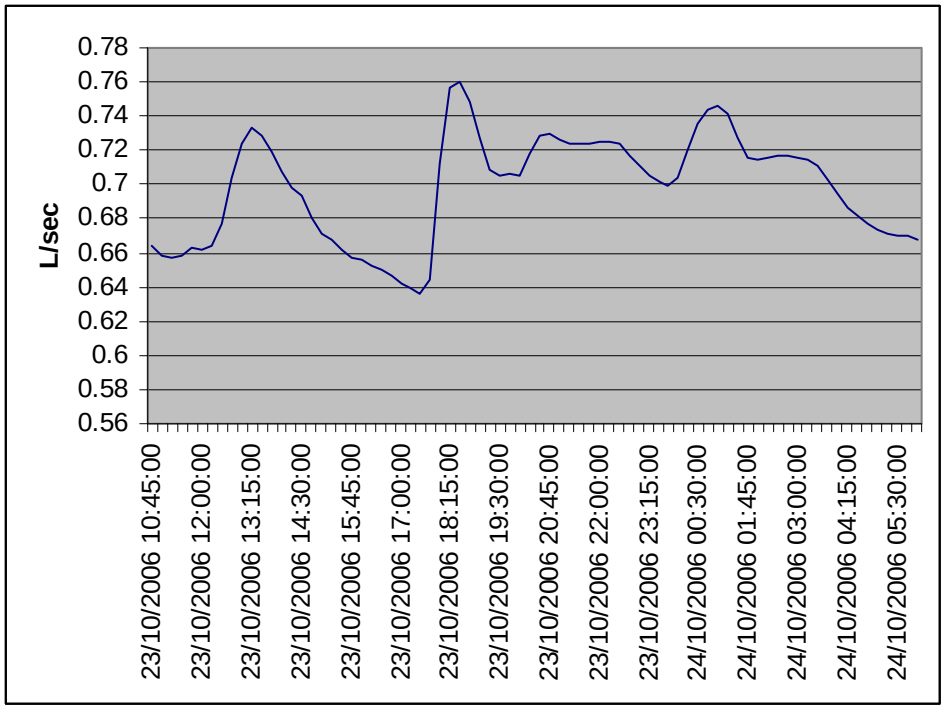

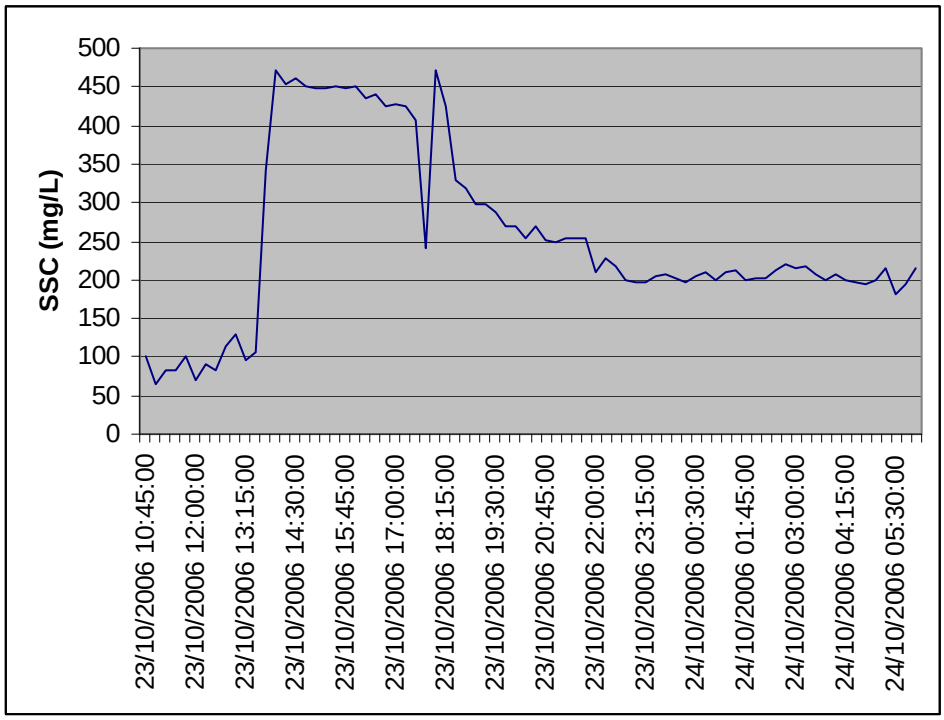

U.5.7 Storm event 30-11-2006

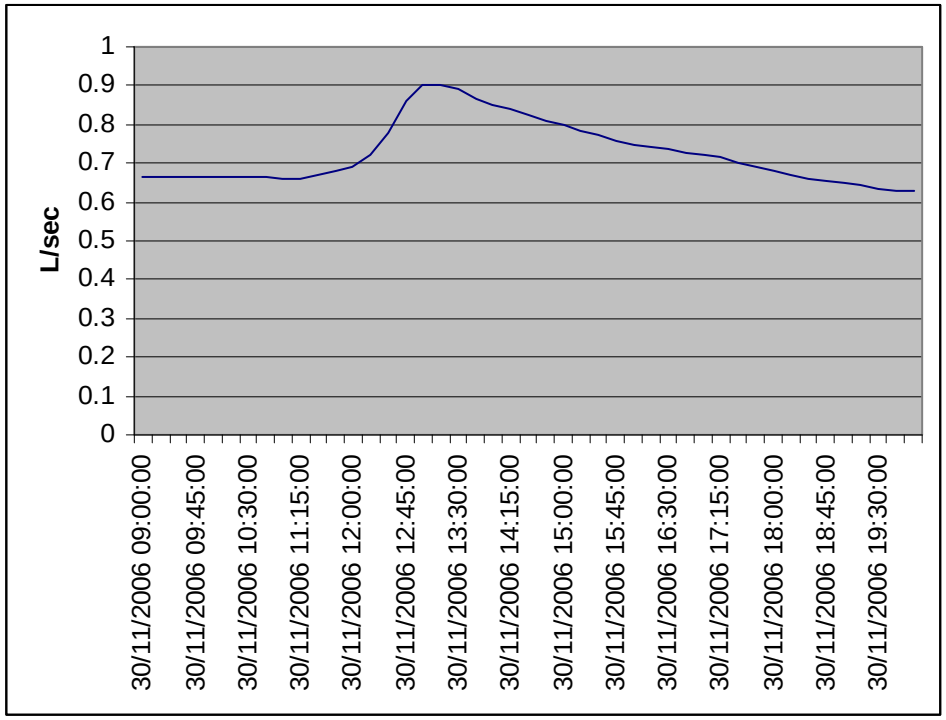

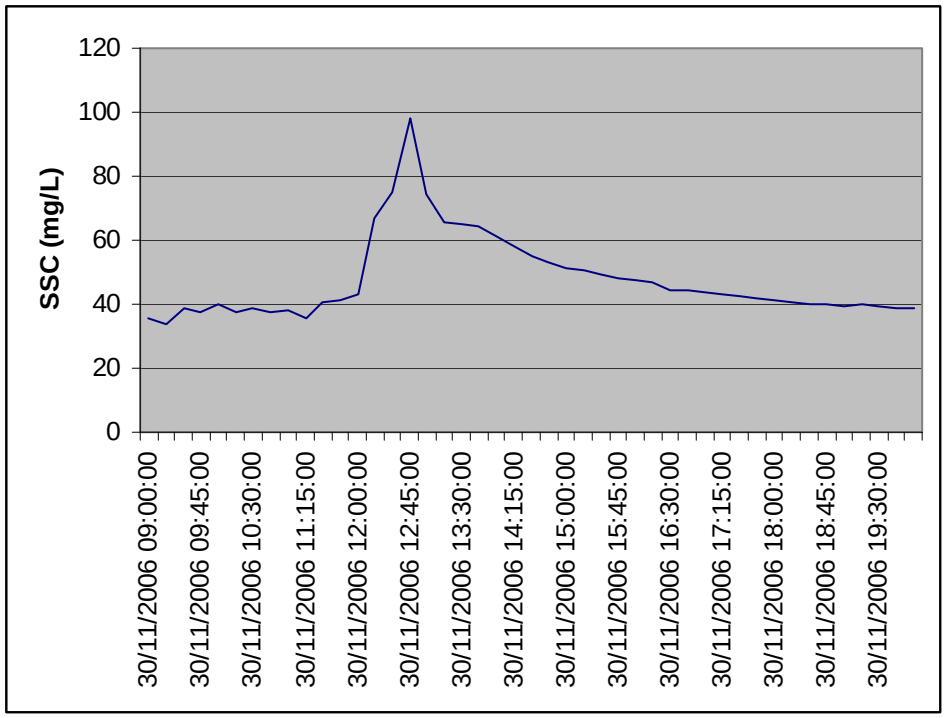

U.5.8 Storm event 9-1-2007

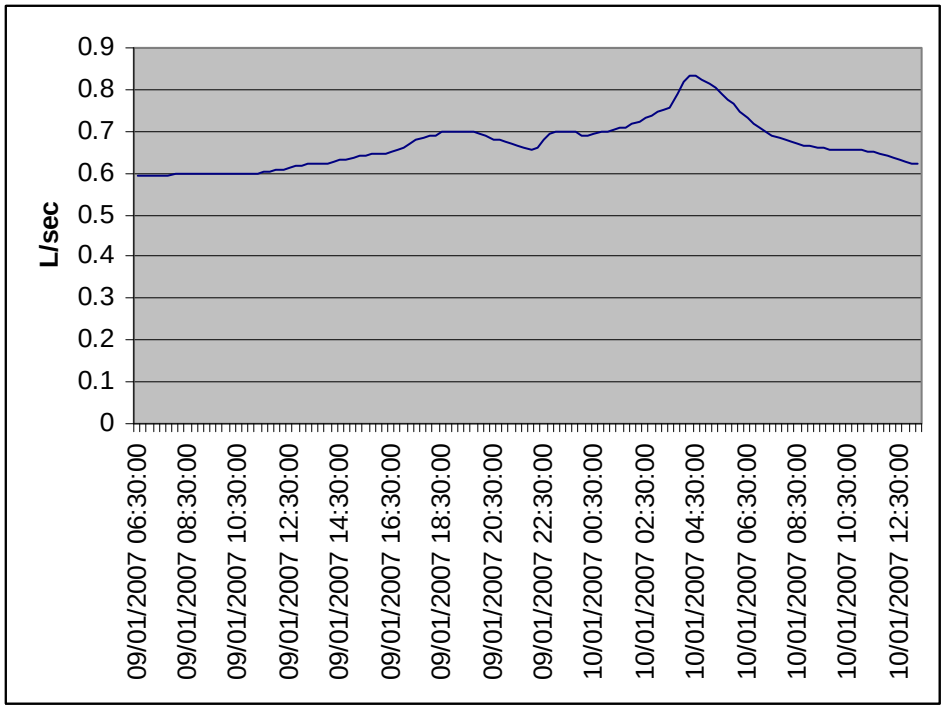

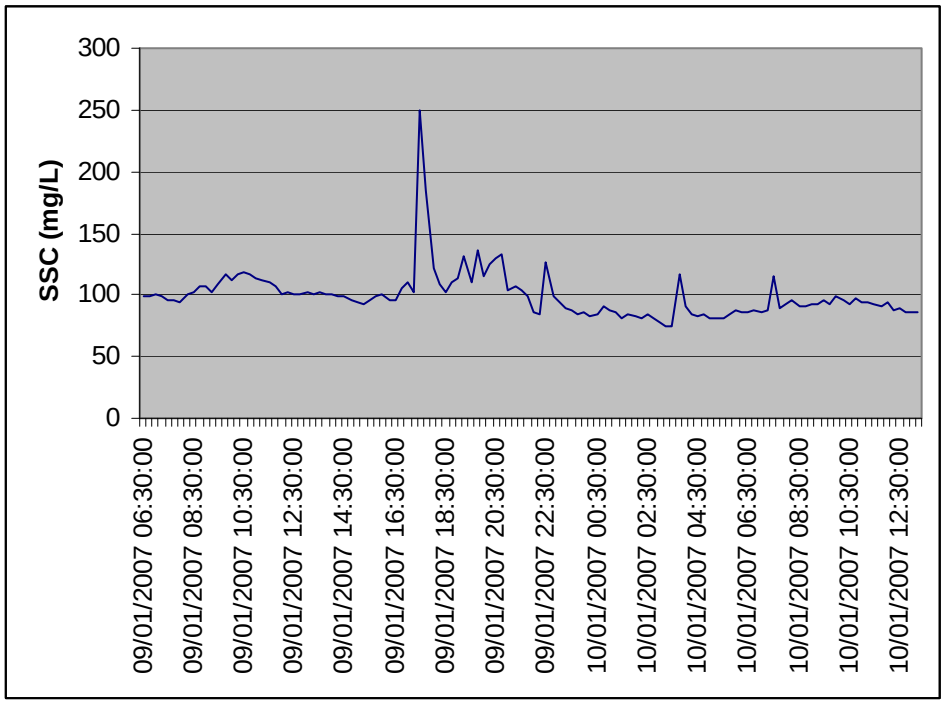

U.5.9 Storm event 29-3-2007

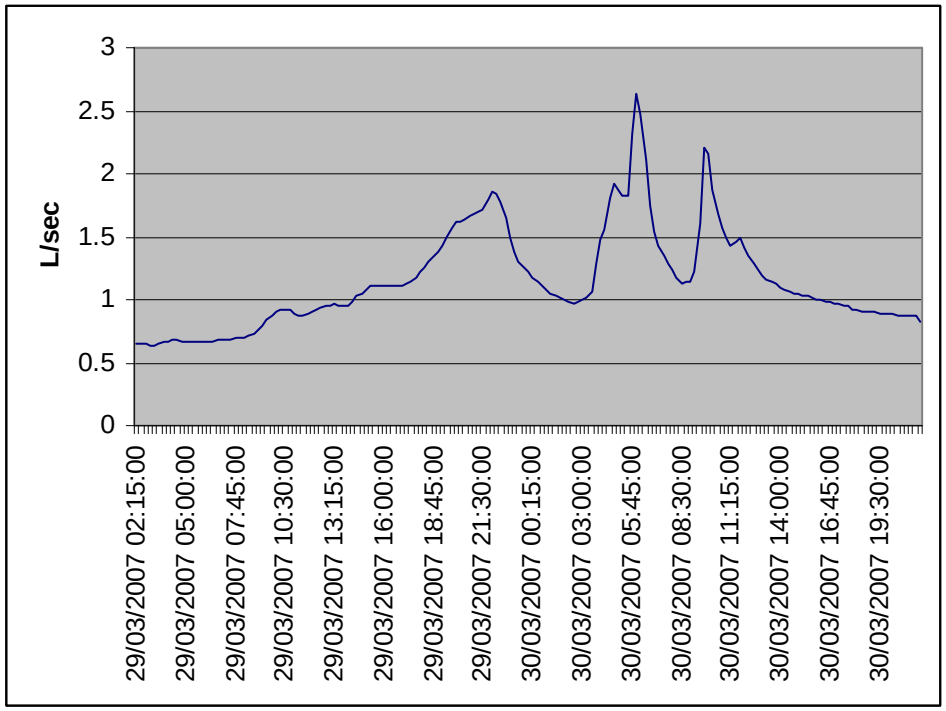

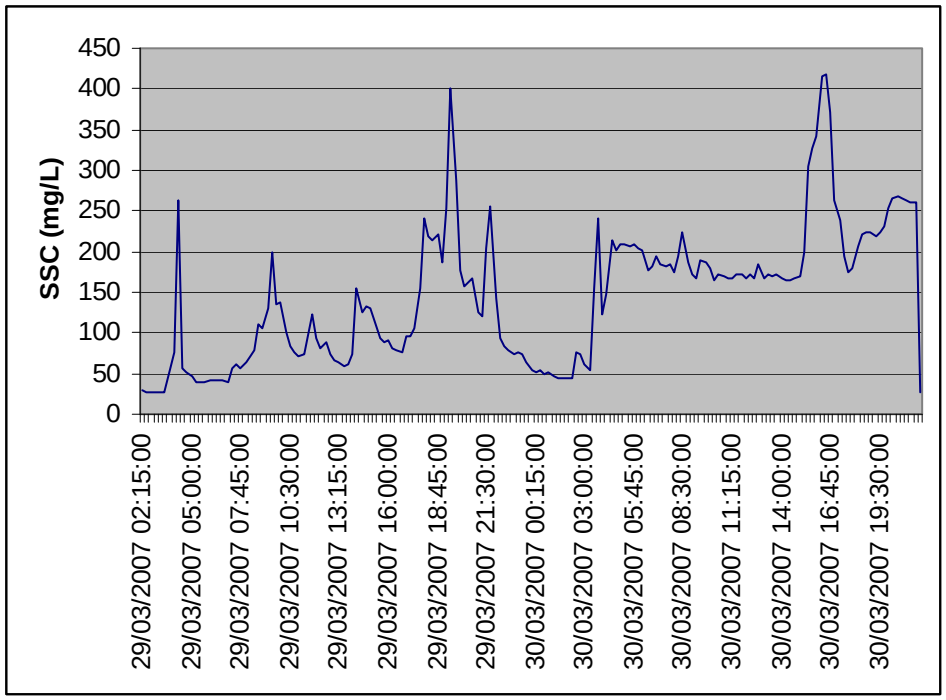

U.5.9 Storm event 14-6-2007

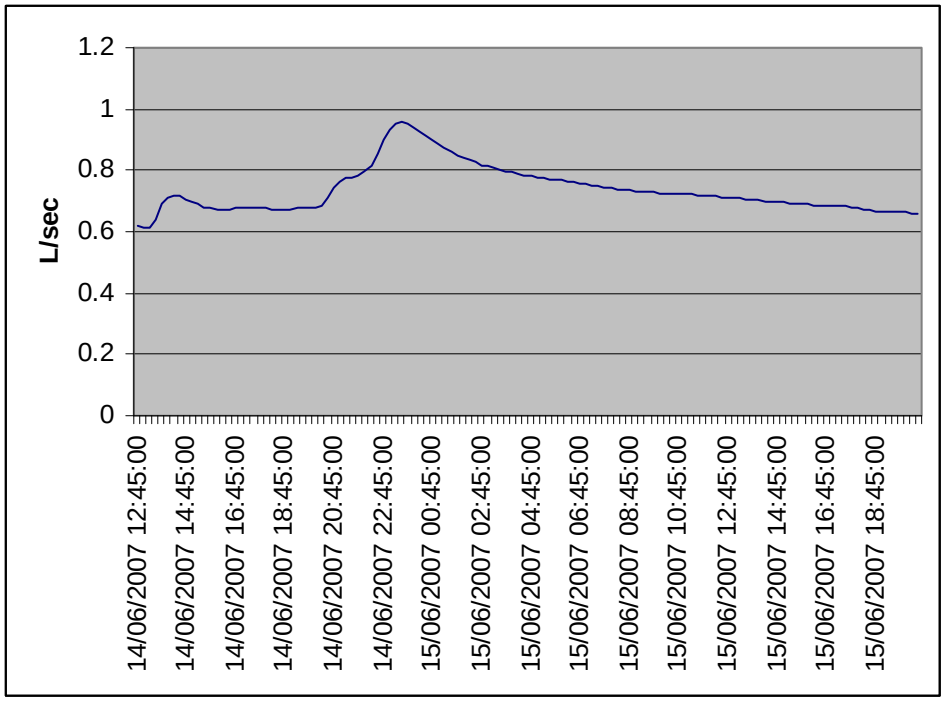

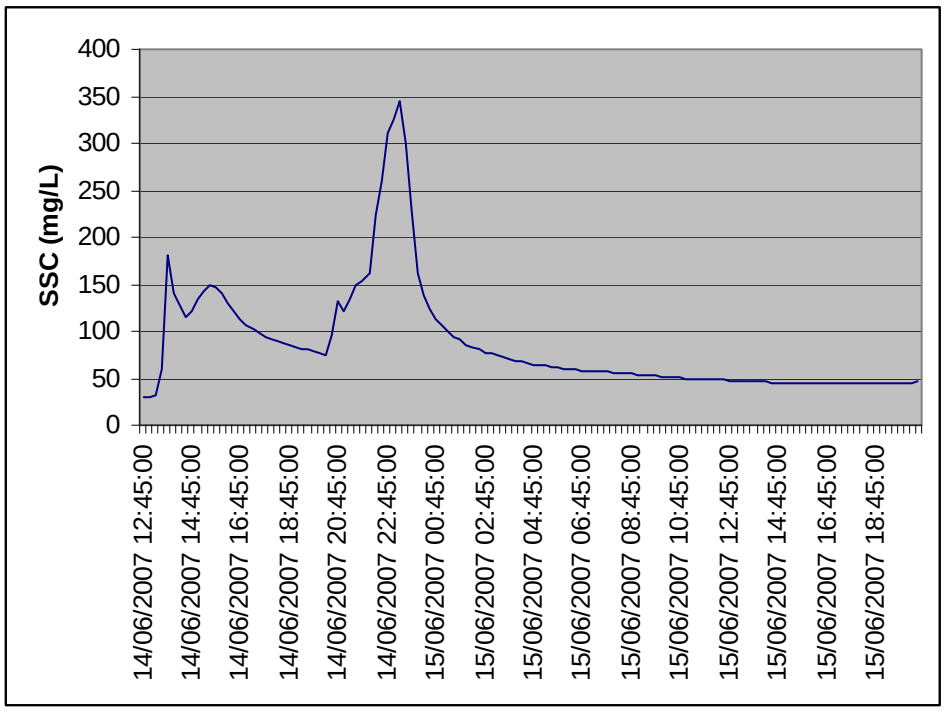

U.5.10 Storm event 20-6-2007

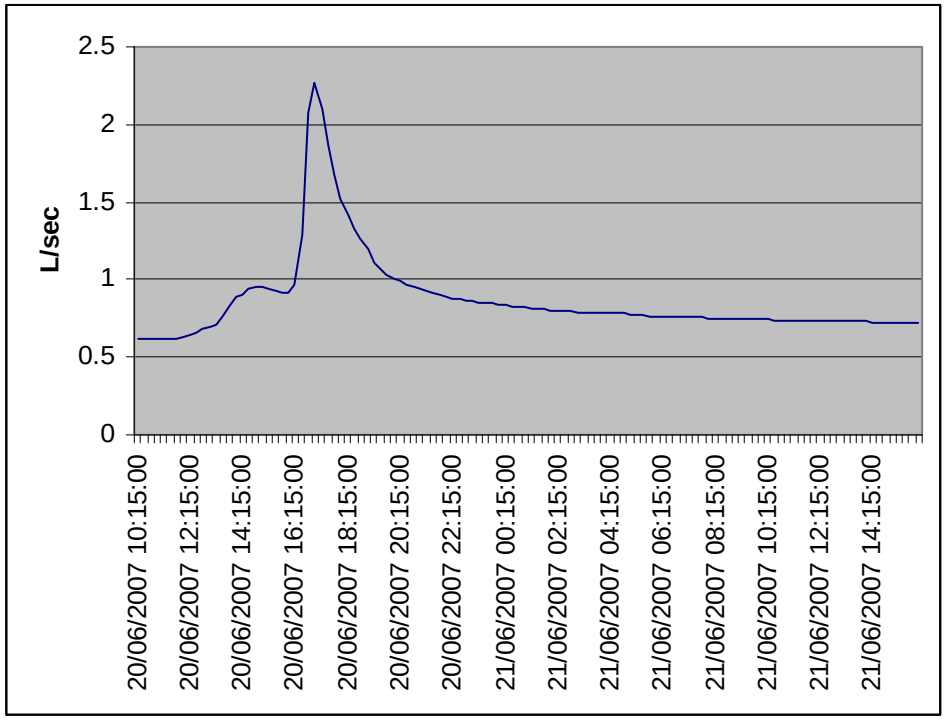

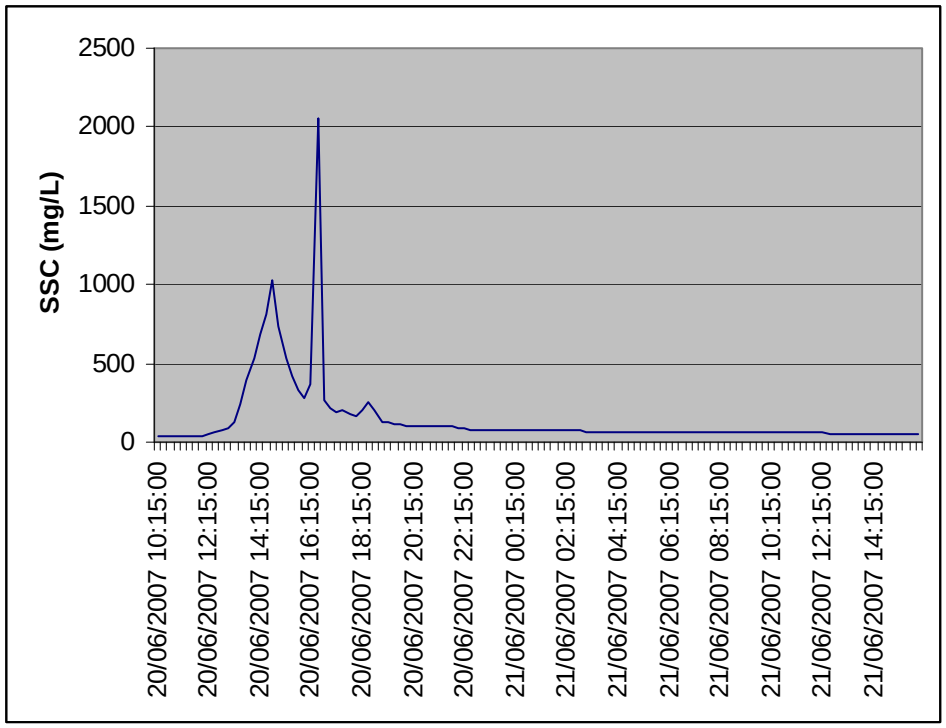

U.5.11 Storm event 18-12-2007

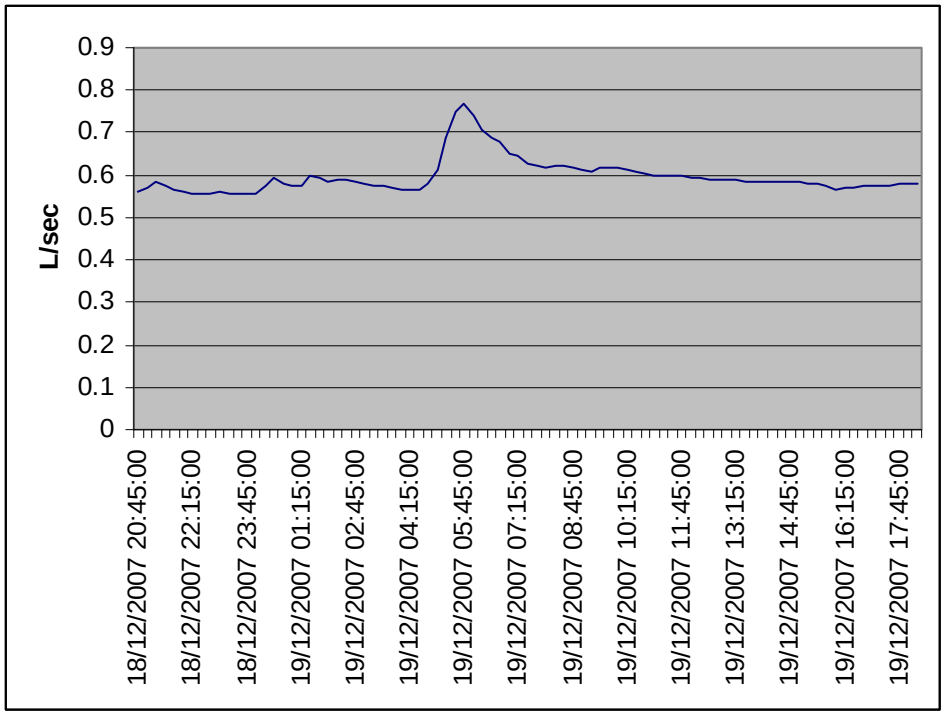

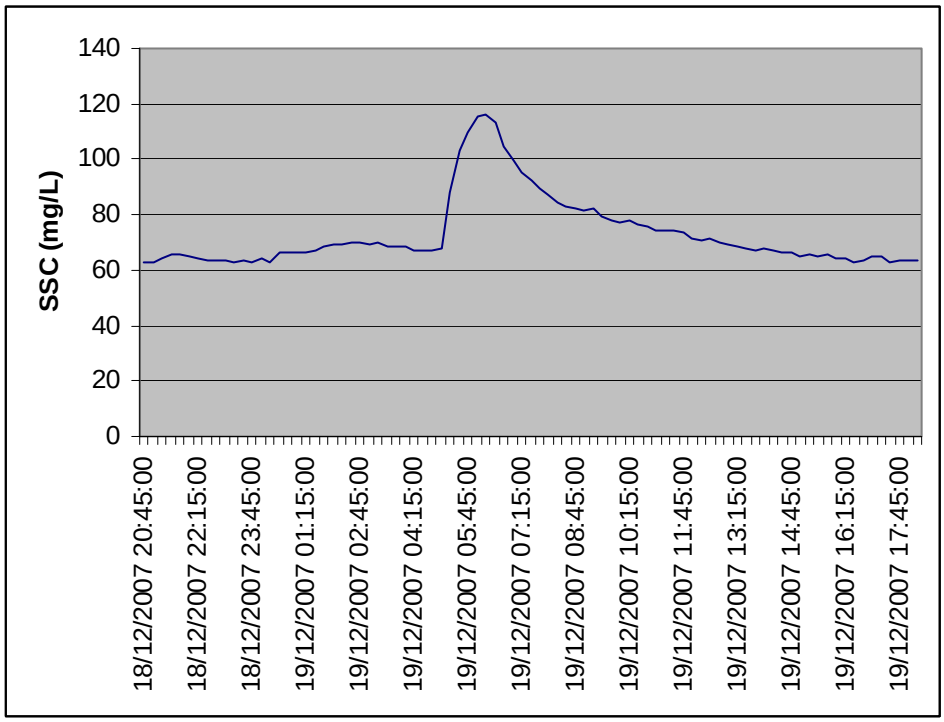

U.5.12 Storm event 1-3-2008

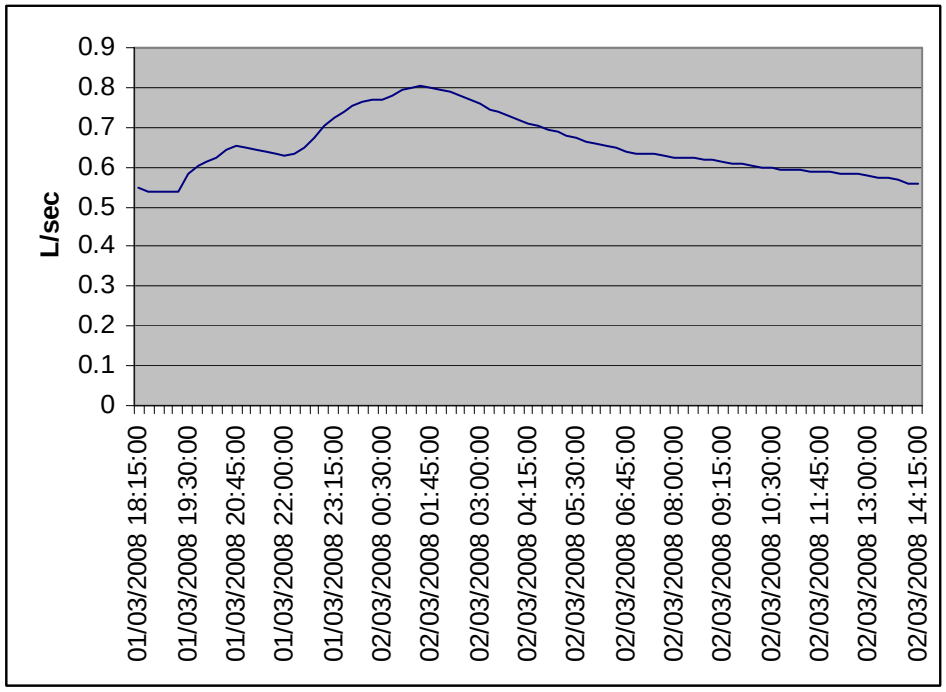

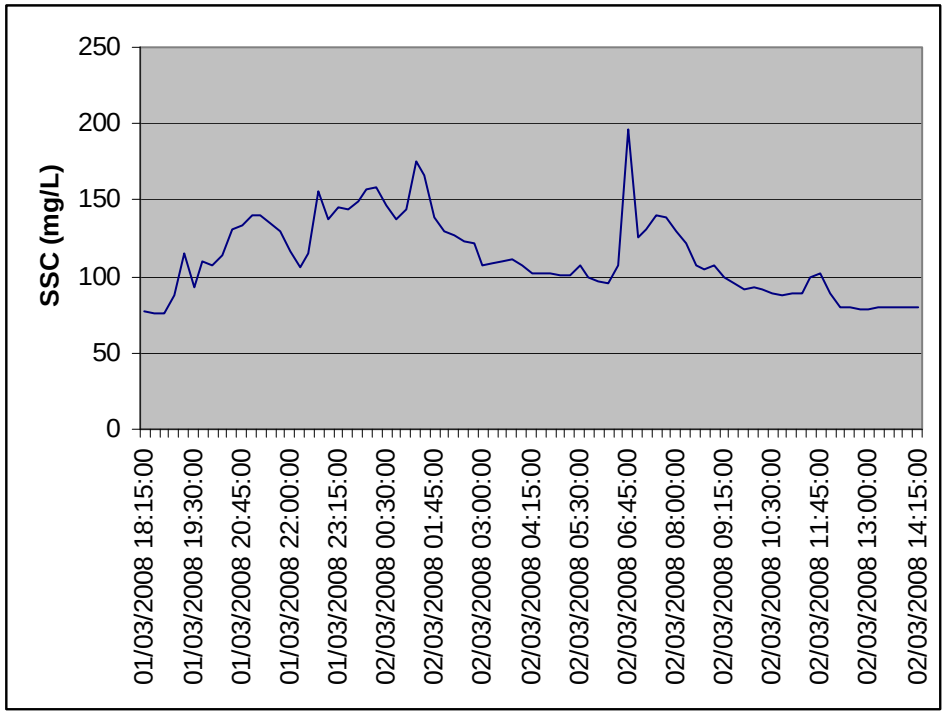

APPENDIX V

STORM SEDIMENT YIELD CALCULATION

The peak flow/sediment yield relationships *xy* pairs were established by linear regression on a log-log plot in Sigmaplot. To accurately calculate the total sediment yielded from all identified peak flows, the peak flows were converted to log base 10. The Sigmaplot regression relationship was then used to calculate sediment yield for each peak flow in an Excel spreadsheet, and the final sediment value in kilograms was calculated (or 'converted back') by taking the anti-logs of the fitted values. All the sediment yields were summed to calculate a total sediment yield.

Start date	End date	Peak discharge l/sec																Peak discharge l/sec			
	Peak discharge l/sec	BR1	b [0]	b [1]	Sed	BR2	b [0]	b [1]	Sed	BR3	b [0]	b [1]	Sed	BR4	b [0]	b [1]	Sed	BR1	b [0]	b [1]	Sed
			1.33797	1.36073	KG		0.69606	1.60704			1.05141	3.99110			0.59830	1.55972			1.00009	1.88408	KG
09/01/2007 @ 06:30:00	10/01/2007 @ 04:15:00	1.68	0.22	1.64	44.00	0.83	-0.08	0.57	3.71	0.89	-0.05	0.85	7.07	0.70	-0.15	0.36	2.28	1.68	0.22	1.42	26.49
12/01/2007 @ 23:30:00	14/01/2007 @ 06:45:00	1.44	0.16	1.55	35.66	0.86	-0.06	0.59	3.93	1.42	0.15	1.66	45.63	1.42	0.15	0.84	6.88	1.44	0.16	1.30	19.80
30/01/2007 @ 02:45:00	30/01/2007 @ 09:00:00	1.18	0.07	1.44	27.40	*				*				*				1.18	0.07	1.14	13.75
28/03/2007 16:30:00	30/03/2007 18:15:00	4.94	0.69	2.28	191.40	2.60	0.41	1.36	23.06	1.66	0.22	1.93	85.09	2.10	0.32	1.10	12.61	4.94	0.69	2.31	202.83
28/04/2007 @ 01:00:00	28/04/2007 @ 12:00:00	1.85	0.27	1.70	50.22	*				*				*				1.85	0.27	1.50	31.81
30/04/2007 @ 06:15:00	01/05/2007 @ 08:15:00	1.81	0.26	1.69	48.82	*				*				0.80	-0.10	0.45	2.81	1.81	0.26	1.49	30.59
21/05/2007 @ 18:30:00	22/05/2007 @ 05:15:00	3.02	0.48	1.99	98.11	1.16	0.06	0.80	6.30	*				0.87	-0.06	0.51	3.20	3.02	0.48	1.91	80.40
14/06/2007 @ 02:00:00	15/06/2007 @ 00:15:00	4.13	0.62	2.18	150.01	0.958	-0.02	0.67	4.64	*				0.98	-0.01	0.59	3.87	4.13	0.62	2.16	144.74
20/06/2007 @ 09:45:00	20/06/2007 @ 20:00:00	1.44	0.16	1.55	35.77	2.27	0.36	1.27	18.60	1.08	0.03	1.18	15.14	0.97	-0.01	0.58	3.78	1.44	0.16	1.30	19.88
21/06/2007 @ 15:45:00	22/06/2007 @ 14:00:00	2.04	0.31	1.76	57.34	1.38	0.14	0.92	8.37	0.90	-0.05	0.86	7.29	0.83	-0.08	0.47	2.95	2.04	0.31	1.58	38.22
23/06/2007 @ 11:15:00	25/06/2007 @ 06:30:00	2.04	0.31	1.76	57.34	*				*				*				2.04	0.31	1.58	38.22
29/06/2007 @ 14:30:00	30/06/2007 @ 13:30:00	2.64	0.42	1.91	81.75	1.00	0.00	0.69	4.95	1.16	0.06	1.31	20.42	0.88	-0.06	0.51	3.24	2.64	0.42	1.80	62.45
06/07/2007 @ 11:30:00	07/07/2007 @ 11:00:00	2.75	0.44	1.94	86.25	1.32	0.12	0.89	7.71	1.07	0.03	1.17	14.86	1.15	0.06	0.69	4.94	2.75	0.44	1.83	67.27
09/07/2007 @ 08:15:00	11/07/2007 @ 20:00:00	3.35	0.53	2.05	112.87	0.95	-0.02	0.66	4.55	1.17	0.07	1.32	20.78	0.83	-0.08	0.48	2.99	3.35	0.53	1.99	97.62
15/07/2007 @ 07:15:00	18/07/2007 @ 12:45:00	5.67	0.75	2.36	230.88	0.74	-0.13	0.49	3.07	1.12	0.05	1.25	17.69	2.85	0.45	1.31	20.27	5.67	0.75	2.42	262.97
28/07/2007 @ 18:15:00	30/07/2007 @ 23:15:00	4.21	0.62	2.19	153.83	1.94	0.29	1.16	14.45	1.14	0.06	1.28	19.06	1.91	0.28	1.04	10.85	4.21	0.62	2.18	149.87
04/08/2007 @ 05:30:00	04/08/2007 @ 12:00:00	*				*				*				0.942	-0.03	0.56	3.61	*		1.00	
15/08/2007 @ 09:30:00	17/08/2007 @ 05:30:00	2.34	0.37	1.84	69.18	1.31	0.12	0.89	7.69	1.18	0.07	1.33	21.47	1.53	0.18	0.88	7.66	2.34	0.37	1.70	49.56
26/08/2007 @ 23:45:00	28/08/2007 @ 23:45:00	3.62	0.56	2.10	125.14	1.06	0.02	0.73	5.41	0.93	-0.03	0.92	8.37	1.88	0.27	1.03	10.62	3.62	0.56	2.05	112.62
07/09/2007 @ 05:15:00	10/09/2007 @ 01:15:00	1.98	0.30	1.74	55.20	0.79	-0.10	0.53	3.42	0.69	-0.16	0.41	2.57	0.89	-0.05	0.52	3.29	1.98	0.30	1.56	36.26
13/09/2007 @ 23:30:00	16/09/2007 @ 19:00:00	3.09	0.49	2.00	100.95	0.957	-0.02	0.67	4.63	0.85	-0.07	0.77	5.85	0.90	-0.04	0.53	3.39	3.09	0.49	1.92	83.64
30/09/2007 @ 15:45:00	30/09/2007 @ 21:15:00	2.34	0.37	1.84	69.24	1.783822	0.25	1.10	12.59	1.60	0.21	1.87	74.28	3.31	0.52	1.41	25.60	2.34	0.37	1.70	49.63
10/10/2007 @ 07:15:00	11/10/2007 @ 02:45:00	1.98	0.30	1.74	55.13	1.19	0.07	0.82	6.55	1.36	0.13	1.58	38.01	0.91	-0.04	0.54	3.43	1.98	0.30	1.56	36.19
11/10/2007 @ 23:00:00	12/10/2007 @ 11:15:00	1.94	0.29	1.73	53.77	3.13	0.50	1.49	31.08	0.88	-0.05	0.83	6.81	1.21	0.08	0.73	5.37	1.94	0.29	1.54	34.96
15/10/2007 @ 13:30:00	16/10/2007 @ 00:15:00	2.22	0.35	1.81	64.57	0.98	-0.01	0.68	4.84	1.03	0.01	1.10	12.46	1.02	0.01	0.61	4.07	2.22	0.35	1.65	45.06
24/10/2007 @ 14:45:00	24/10/2007 @ 23:30:00	2.08	0.32	1.77	59.14	*				0.84	-0.08	0.74	5.54	0.84	-0.08	0.48	2.99	2.08	0.32	1.60	39.89
05/12/2007 @ 17:15:00	07/12/2007 @ 04:15:00	2.77	0.44	1.94	87.28	1.16	0.06	0.80	6.28	*				1.31	0.12	0.78	6.01	2.77	0.44	1.83	68.38
18/12/2007 @ 15:45:00	19/12/2007 @ 10:15:00	2.47	0.39	1.87	74.53	*				*				0.89	-0.05	0.52	3.30	2.47	0.39	1.74	54.95
21/12/2007 @ 01:15:00	21/12/2007 @ 14:30:00	3.72	0.57	2.11	130.21	*				0.86	-0.07	0.78	6.07	0.88	-0.06	0.51	3.24	3.72	0.57	2.08	118.98
				TOTAL	2405.99				185.83				434.46				163.25			**TOTAL**	2017.05
				AREA (KM)	0.050182				0.024818				0.01564				0.099542			**AREA (KM)**	0.050182
				T/KM/YR	**47.95**				**7.49**				**27.78**				**1.64**			**T/KM/YR**	**40.19**

APPENDIX W

STORM HYSTERISIS

The flow data was also used on an event basis to examine the response of suspended sediment concentrations by plotting the data to form storm hysteresis graphs. Storm hysteresis graphs are useful in that they can indicate conditions of the catchment and sediment supply conditions by clockwise, anticlockwise, or linear responses during rainfall events (Baca 2008; Gao 2008) (Figure W.1).

Class	C-Q relationship plots	Interpretation
Single line	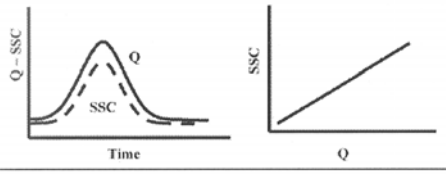	• uninterrupted supply • strong dependence of SSC on Q e.g., sediment derived from entrainment of bed material • possible after a large event if the majority of supply of fine sediment was exhausted during the previous event
Clockwise loop	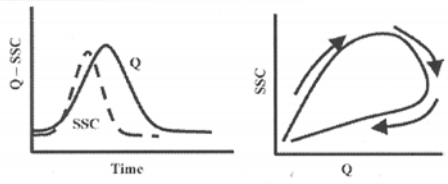	• depletion of available sediment (small supply or long lasting/intense flood) before the Q peak • presence of an armoured layer prior to peak Q
Anti-clockwise loop	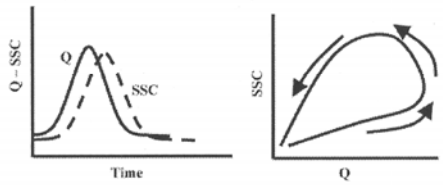	• relative travel times of the flood wave and sediment flux, either kinematic wave theory or channel irregularities that inhibit sediment movement (e.g., lakes) • high soil erosion • temporal variability of rainfall distribution and sediment production • sediment sourced from distal portions of the catchment • bank erosion on the falling limb when bank material is saturated • minor event after a major event providing additional fine sediment from runoff-derived sources

Figure W.1. Storm hysteresis graphs showing the three typical responses; linear, clockwise, and anticlockwise along with the interpretation of sediment supply conditions (after (Williams 1989) and (Hudson 2003) as cited in (McKergow *et al.* 2007).

Storm hysteresis examples for the four monitoring sites are presented in Figure W.2. In Figure W.2-A shows a first storm event for the EX-H site after logging operations and it is the only hysteresis of the group to show an anti-clockwise trend. This would indicate the ample supply of sediment and high soil erosion conditions after tree removal and surface disturbance from logging operations. In contrast, Figure W.2-B shows the EX-H site approximately 13 months after logging and the hysteresis has reversed into a clock-wise trend. As the catchment recovers by ground cover increase, sediment supply is not so available and is depleted near the peak flow or on the falling limb of the hydrograph. Figure W.2-C shows the EX-10 site with a clock-wise trend, also indicating that there is sediment depletion. The AG-P site in Figure W.2-D also shows a clockwise trend, but it is very narrow in comparison with the other catchments and is approaching a liner relationship. This would indicate that sediment supply is more readily available, possible from in-stream sources such as stock crossing points and stock disturbance of the stream line. Figure W.2-E is from the EX-H6 site which also shows a clockwise trend that would indicate that recovery of the catchment after logging is constraining the supply of sediment.

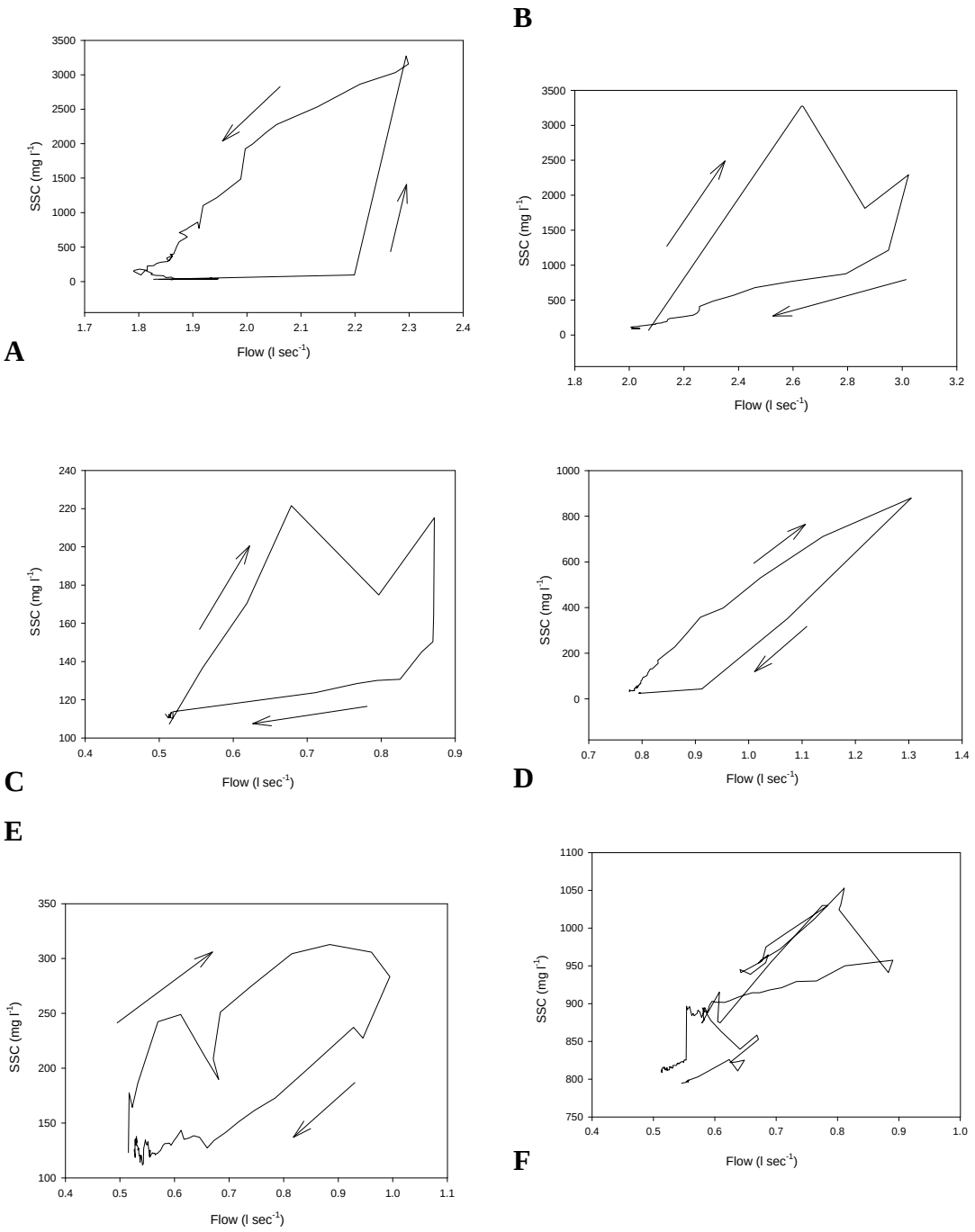

Figure W.2. Storm hysteresis graphs for the four subcatchments. A) EX-H first storm event after harvesting on 21-4-06; B) EX-H 13 month later on 24-5-07; C) EX-10 storm event on 24-5-2007; D) AG-P storm event on 27-8-2006; E) EX-H6 storm event on 20-12-06 and F) EX-H6 storm event for 11-1-2007.

It should be noted that the storm hysteresis examples from the four monitoring sites were selected as they displayed clear relationships between flow and SSC. As often

as not, a storm hysteresis would have a more complex behaviour during an event as shown in Figure W.2-F. This is not unexpected as a Spanish study found four types of hysteretic loops (line, clockwise, anticlockwise, and 8 shaped) for the one catchment (Zabaleta *et al.* 2007).

APPENDIX X

STREAM SEDIMENT STORAGE RESULTS

mg/m2 of channel		Mean sed store	SD	SD % or CV	Stream length	Stream width	Stream area	TOTAL (mg)	SD%
		(mg/m2)			(m)		(m2)		
NATIVE	27000.00								
(Upper)	18128.57								
	32200.00								
	29120.00	26612.14286	6045.243647	22.71611001	20950	2	41900	1115048786	253295708.8
								1.115048786	0.253295709
NATIVE	88500.00								
(Lower)	61800.00	75150	18879.75106	25.1227559	26440	4	105760	7947864000	1996722472
								7.947864	1.996722472
EXOTIC	52900.00								
	52857.14								
	89400.00								
	142800.00								
	230720.00								
	165880.00	122426.1905	70420.66126	57.52091198	104950	4	419800	51394514762	29562593598
								51.39451476	29.5625936
AG	186750.00								
	257500.00								
	329166.67								
	347000.00								
	412000.00								
	1144000.00	446069.44	350586.31	78.59455888	32910	5	164550	73400727083	57688977665
								73.40072708	57.68897766
							Total (t)	**133.8581548**	**64.85380593**

REFERENCES

Ackers, P., White, W. R., Perkins, J. A. & Harrison, A. J. M. 1978, *Weirs and Flumes for Flow Measurement*, John Wiley and Sons,

Adams, C., Graham, I., Seward, D. & Skinner, D. 1994, 'Geochronological and geochemical evolution of late Cenozoic volcanism on the Coromandel Peninsula, New Zealand', *New Zealand Journal of Geology and Geophysics*, vol. 37, pp. 359-379.

Adams, J. 1979, 'Sediment loads of North Island rivers, New Zealand - a reconnaissance', *Journal of Hydrology*, vol. 18, no. 1, pp. 36-48.

Adams, R. & Elliott, S. 2006, 'Physically based modelling of sediment generation and transport under a large rainfall simulator', *Hydrological Processes*, vol. 20, no. 11, pp. 2253-2270.

Adams, R., Parkin, G., Rutherford, J. C., Ibbitt, R. P. & Elliott, A. H. 2005, 'Using a rainfall simulator and a physically based hydrological model to investigate runoff processes in a hillslope', *Hydrological Processes*, vol. 19, pp. 2209-2223.

Agouridis, C. T., Workman, S. R., Warner, R. C. & Jennings, G. D. 2005, 'Livestock grazing management impacts on stream water quality: a review', *Journal of the American Water Resources Association*, vol. 41, no. 3, pp. 591-606.

Akerjord, M. & Christophersen, N. 1996, 'Assessing mixing models with a common framework', *Environmental Science and Technology*, vol. 30, no. 7, pp. 2105-2112.

Aksoy, H. & Kavvas, M. L. 2005, 'A review of hillslope and watershed scale erosion and sediment transport models', *Catena*, vol. 64, no. 2-3, pp. 247-271.

Akyil, S., Aslani, M. A. A., Gurboga, G., Aytas, S. & Eral, M. 2002, 'Activity concentration of radium-226 in agricultural soils', *Journal of Radioanalytical and Nuclear Chemistry*, vol. 254, no. 1, pp. 9-14.

Akyil, S., Gurboga, G., Aslani, M. A. A. & Aytas, S. 2008, 'Vertical distribution of Ra-226 and Po-210 in agricultural soils in Buyuk Menderes Basin, Turkey', *Journal of Hazardous Materials*, vol. 157, no. 2-3, pp. 328-334.

American Public Health Association and American Water Works Association and Water Environment Federation 1992, *Standard Methods for the Examination of Water and Wastewater*, American Public Health Association and American Water Works Association and Water Environment Federation., Maryland, USA.

Amp-Tek 2007, *X-Ray Fluorescence (XRF),* viewed 14-1-2008 http://www.amptek.com/pdf/xrf.pdf

Andersen, M. K., Raulund-Rasmussen, K., Strobel, B. W. & Hansen, H. C. B. 2003, 'The effects of tree species and site on the solubility of Cd, Cu, Ni, Pb, and Zn in soils', *Water, Air and Soil Pollution*, vol. 154, pp. 357-370.

Anderson, C. W. 1998, 'Turbidity', in F. D. Wilke & D. B. Radke (ed.), *National Field Manual for the Collection of Water-Quality Data: Field Measurements*, US Geological Survey. USGS-TWRI Book 9, Chapter A6, pp. TBY1-TBY64

Armstrong, J. D., Kempa, P. S., Kennedy, G. J. A., Ladled, M. & Milnere, N. J. 2003, 'Habitat requirements of Atlantic salmon and brown trout in rivers and streams ', *Fisheries Research* vol. 62, no. 2, pp. 143-170.

Armstrong, J. L. & MacKenzie, D. H. 2002, 'Sediment yields and turbidity records from small upland subcatchments in the Warragamba Dam Catchment, southern New South Wales', *Australian Journal of Soil Research*, vol. 40, pp. 557-579.

Arnerich, T. 2003, *Formazin calibration of the Troll 9000 turbidity sensor*, In-Situ Inc. Technical Note TECH 003 01/03.

Arnold, J. G., Allen, P. M., Muttiah, R. & Bernhardt, G. 1995, 'Automated base flow separation and recession analysis techniques', *Ground Water*, vol. 33, no. 6, pp. 1010-1018.

Asadi, H., Gnadiri, H., Rose, C. W. & Rouhipour, H. 2007, 'Interrill soil erosion processes and their interaction', *Earth Surface Processes and Landforms*, vol. 32, no. 5, pp. 711–724.

Atterberg, A. 1916, 'Die Klassifikation der humusfreien und der humusarmen Mineralboden Schwedens nach den Konsistenzverhaltnissen derselben', *Internationale Mitteilungen für Bodenkunde*, vol. 6, pp. 27-37.

Baca, P. 2008, 'Hysterisis effect in suspended sediment concentration in the Rybarik basin, Slovakia', *Hydrological Sciences*, vol. 53, no. 1, pp. 224-235.

Baeza, A., Delrio, M., Miro, C. & Paniagua, J. 1994, 'Natural Radionuclide Distribution in Soils of Caceres (Spain) - Dosimetry Implications', *Journal of Environmental Radioactivity*, vol. 23, no. 1, pp. 19-37.

Bai, Z. G., Wan, G. J., Wang, C. S., Wan, X. & Huang, R. G. 2000, 'A multitracer study of radionuclides on the surface soil erosion in the Yunnan-Guizhou Plateau, china. I. Distribution and geochemical speciation of Be-7, Cs-137, Ra-226, Ra-228 in the soils', in J. M. Laflen, J. L. Tian & C. H. Huang (ed.), *Soil Erosion and Dryland Farming*, Crc Press-Taylor & Francis Group, Boca Raton, pp. 499-521.

Basher, L. R., Hicks, D. M., Handyside, B. & Ross, C. W. 1997, 'Erosion and sediment transport from the market gardening lands at Pukekohe, Auckland, New Zealand', *Journal of Hydrology*, vol. 36, no. 1, pp. 73-95.

Basher, L. R. & Matthews, K. M. 1993, 'Relationship between 137Cs in some undisturbed New Zealand soils and rainfall', *Australian Journal of Soil Research*, vol. 31, pp. 655-663.

Basher, L. R., Matthews, K. M. & Zhi, L. 1995, 'Surface erosion assessment in the South Canterbury Downlands, New Zealand using 137Cs distribution', *Australian Journal of Soil Research*, vol. 33, pp. 787-803.

Basher, L. R. & Ross, C. W. 2002, 'Soil erosion rates under intensive vegetable production on clay loam, strongly structured soils at Pukekohe, New Zealand', *Australian Journal of Soil Research*, vol. 40, pp. 947-961.

Belyaev, V. R., Wallbrink, P. J., Golosov, V. N., Murray, A. S. & Sidorchuk, A. Y. 2004, 'Reconstructing the development of a gully in the Upper Kalaus basin, Stavropol Region (southern Russia)', *Earth Surface Processes and Landforms*, vol. 29, no. 3, pp. 323-341.

Betts, H., Trustrum, N. A. & De Rose, R. 2003, 'Geomorphic changes in a complex gully system measured from sequential digital elevation models, and implications for management', *Earth Surface Processes and Landforms*, vol. 28, no. 10, pp. 1043-1058.

Bhattarai, R. & Dutta, D. 2007, 'Estimation of soil erosion and sediment yield using GIS at catchment scale', *Water Resource Management*, vol. 21, pp. 1635-1647.

Bidin, K. & Greer, T. 1997, 'A spreadsheet-based technique (LOTUS 1-2-3) for separating tropical forest storm hydrographs using Hewlett and Hibbert's slope ', *Earth Surface Processes and Landforms*, vol. 22, pp. 1231-1237.

Blair, I. 2004, *Suspended Sediment Monitoring Report 2004*, Environment Waikato Document No. 1184249. 1st November, 2004.

Blake, W. H., Walling, D. E. & He, Q. 2002, 'Using cosmogenic beryllium-7 as a tracer in sediment budget investigations', *Geografiska Annaler*, vol. 84, no. 2, pp. 89-102.

Blaschke, P. M., Hicks, D. L. & A., M. 2008, *Quantification of the Flood and Erosion Reduction Benefits, and Costs of Climate Change Mitigation Measures in New Zealand.*, Report prepared by Blaschke and Rutherford Environmental Consultants for MfE. Wellington: Ministry for the Environment. iv + 76 p.

Blaschke, P. M., Trustrum, N. A. & Hicks, D. L. 2000, 'Impacts of mass movement erosion on land productivity: a review', *Progress in Physical Geography*, vol. 24, no. 1, pp. 21-52.

Blume, T., Zehe, E. & Bronstert, A. 2007, 'Rainfall-runoff response, event-based runoff coefficients and hydrograph separation', *Hydrological Sciences,* vol. 52, no. 5, pp. 843-862.

Boix-Fayos, C., Martinez-Mena, M., Arnau-Rosalen, E., Calvo-Cases, A., Castillo, V. & Albaladejo, J. 2006, 'Measuring soil erosion by field plots: Understanding the sources of variation', *Earth-Sciences Reviews*, vol. 78, pp. 267-285.

Boix-Fayos, C., Martinez-Mena, M., Calvo-Cases, A., Arnau-Rosalen, E., Albaladejo, J. & Castillo, V. 2007, 'Causes and underlying processes of measurement variability in field erosion plots in Mediterranean conditions', *Earth Surface Processes and Landforms*, vol. 32, no. 1, pp. 85-101.

Bonniwell, E. C., Matisoff, G. & Whiting, P. J. 1999, 'Determining the times and distances of particle transit in a mountain stream using fallout radionuclides', *Geomorphology*, vol. 27, pp. 75-92.

Bonta, J. V. 1998, 'Modified drop-box weir for monitoring flows from erosion plots and small watersheds', *American Society of Agricultural Engineers*, vol. 41, no. 3, pp. 565-573.

Boothroyd, I. K. G., Quinn, J. M., Langer, E. R., Costley, K. J. & Steward, G. 2004, 'Riparian buffers mitigate effects of pine plantation logging on New Zealand streams 1. Riparian vegetation structure, stream geomorphology, and periphyton', *Forest Ecology and Management*, vol. 194, pp. 199-213.

Brazier, R. 2004, 'Quantifying soil erosion by water in the UK: a review of monitoring and modelling approaches', *Progress in Physical Geography*, vol. 28, no. 3, pp. 340-365.

Bridge, J. S. 2003, *Rivers and Floodplains: Forms, Processes, and Sedimentary Record*, Blackwell Publishing, Oxford.

Brierley, G. & Fryirs, K. 2005, *Geomorphology and River Management*, Blackwell Publishing, Oxford.

Brodie, R. S. & Hostetler, J. J. 2005, *A review of techniques for analysing baseflow from stream hydrographs,* viewed 27-12-2008 www.connectedwater.gov.au/documents/IAH05−Baseflow.pdf

Brooks, S., Crozier, M., Glade, T. & Anderson, M. 2004, 'Towards establishing climatic thresholds for slope instability: use of a physically-based combined soil hydrology-slope stability model', *Pure and Applied Geophysics*, vol. 161, no. 4, pp. 881-905.

Brown, A. J. 2001, 'Soil sampling and sample handling for chemical analysis', in K. I. Peverill, L. A. Sparrow & D. J. Reuter (ed.), *Soil Analysis: An Interpretation Manual*, CSIRO Publishing, pp. 35-54.

Brown, R. B., Kling, G. F. & Cutshall, N. H. 1981, 'Agricultural erosion indicated by ^{137}Cs redistribution: II. Estimates of soil erosion', *Soil Science Society of America Journal*, vol. 45, pp. 1191-1197.

Bruijnzeel, L. A. 2004, 'Hydrological functions of tropical forests: not seeing the soil for the trees?' *Agriculture Ecosystems and Environment*, vol. 104, pp. 185-228.

Bull, L. J. 1997, 'Magnitude and variation in the contribution of bank erosion to the suspended sediment load of the River Severn, UK', *Earth Surface Processes and Landforms*, vol. 22, pp. 1109-1123.

Bungartz, H. & Wanner, S. C. 2004, 'Significance of particle interaction to the modelling of cohesive sediment transport in rivers', *Hydrological Processes*, vol. 18, pp. 1685-1702.

Burney, J. R. & Edwards, L. M. 1994, 'Facilities for continuous monitoring of soil erosion in warm and cool seasons in Prince Edward Island, Canada. I. Watersheds', *Catena*, vol. 21, pp. 329-340.

Burns, B. R. & Smale, M. C. 1990, 'Changes in structure and composition over fifteen years in a secondary kauri (*Agathis australis*) Tanekaha (*Phyllocladus trichomanoides*) forest stand, Coromandel Peninsula, New Zealand', *New Zealand Journal of Botany*, vol. 28, pp. 141-158.

Burt, R., Wilson, M. A., Mays, M. D. & Lee, C. W. 2003, 'Major and trace elements of selected pedons in the USA', *Journal of Environmental Quality*, vol. 32, no. 6, pp. 2109-2121.

Buzzelli, C. P., Wetzel, R. L. & Meyers, M. B. 1998, 'Dynamic simulation of littoral zone habitats in lower Chesapeake Bay. II. Seagrass habitat primary production and water quality relationships ', *Estuaries*, vol. 21, pp. 673-689

Byrami, M., Ogden, J., Horrocks, M., Deng, Y., Shane, P. & Palmer, J. 2002, 'A palynological study of Polynesian and European effects on vegetation in Coromandel, New Zealand, showing the variability between four records from a single swamp', *Journal of The Royal Society of New Zealand*, vol. 32, pp. 507-531.

Caitcheon, G. G. 1998, 'The significance of various sediment magnetic mineral fractions for tracing sediment sources in Killimicat Creek', *Catena*, vol. 32, no. 2, pp. 131-142.

Campbell, D. 2006, *River Flow Measurement and Analysis*, ERTH345-06A Catchment hydrology practical manual, Department of Earth Sciences, University of Waikato.

Cannell, R. Q. & Hawes, J. D. 1994, 'Trends in tillage practices in relation to sustainable crop production with special reference to temperate climates', *Soil and Tillage Research*, vol. 30, pp. 245-282.

Carvalho, F. P. 1997, 'Distribution, cycling and mean residence time of ^{226}Ra, ^{210}Pb and ^{210}Po in the Tagus estuary', *The Science of the Total Environment*, vol. 196, pp. 151-161.

Chandler, J. 1999, 'Effective application of automated digital photogrammetry for geomorphological research', *Earth Surface Processes and Landforms*, vol. 24, no. 1, pp. 51-63.

Chang, M., Roth, F. A. & Hunt, E. V. 1982, 'Sediment production under various forest site conditions', *Recent Developments in the Explanation and Prediction of Erosion and Sediment Yield.* IAHS Publication No. 137, pp. 13-22.

Chappell, B. W. 1992, 'Trace element analysis of rocks by x-ray spectrometry', *Advances in X-ray Analysis*, vol. 34, pp. 263-276.

Chartres, C. 1987, 'Australia's land resources at risk', in A. Chisholm & R. Dumsday (ed.), *Land Degradation: Problems and Policies*, Cambridge University Press, Cambridge, UK, pp. 7-26.

Claessens, L., Heuvelink, G. B. M., Schoorl, J. M. & Veldkamp, A. 2005, 'DEM resolution effects on shallow landslide hazard and soil redistribution modelling', *Earth Surface Processes and Landforms*, vol. 30, no. 4, pp. 461-477.

Claessens, L., Verburg, P. H., Schoorl, J. M. & Veldkamp, A. 2006, 'Contribution of topographically based landslide hazard modelling to the analysis of the spatial distribution and ecology of kauri (*Agathis australis*)', *Landscape Ecology*, vol. 21, pp. 63-76.

Clesceri, L. S., Greenberg, A. E. & Eaton, A. D. 1998, *Standard Methods for the Examination of Water and Wastewater*, American Public Health Association, American Water Works Association, and Water Environment Federation,1998. Section 2130, Turbidity., Washington, D.C.

Clifton, J., McDonald, P., Plater, A. & Oldfield, F. 1999, 'An investigation into the efficiency of particle size separation using Stokes Law', *Earth Surface Processes and Landforms*, vol. 24, no. 8, pp. 725-730.

Clough, P. & Hicks, D. 1993, *Soil Conservation and the Resource Management Act. Summary.* , MAF policy technical paper 93/2, Ministry of Agriculture and Fisheries.

Cogle, A., Lane, L. & Basher, L. 2003, 'Testing the hill slope erosion model for application in India, New Zealand and Australia', *Environmental Modelling and Software*, vol. 18, no. 8-9, pp. 825-830.

Collins, A. J. & Owens, P. N. 2006, 'Introduction to soil erosion and sediment redistribution in river catchments: measurement, modelling and management in the 21st century', in P. N. Owens (ed.), *Soil Erosion and Sediment Redistribution in River Catchments: Measurement, Modelling and Management* CABI Publishing, Wallingford, UK, pp. 3-9.

Collins, A. J. & Walling, D. E. 2007a, 'Fine-grained bed sediment storage within the main systems of the Frome and Piddle catchments, Dorset, UK', *Hydrological Processes*, vol. 21, pp. 1488-1459.

Collins, A. L. & Walling, D. E. 2002, 'Selecting fingerprint properties for discriminating potential suspended sediment sources in river basins', *Journal of Hydrology*, vol. 261, no. 1-4, pp. 218-244.

Collins, A. L. & Walling, D. E. 2004, 'Documenting catchment suspended sediment sources: problems, approaches and prospects', *Progress in Physical Geography*, vol. 28, no. 2, pp. 159-196.

Collins, A. L. & Walling, D. E. 2007b, 'The storage and provenance of fine sediment on the channel bed of two contrasting lowland permeable catchments, UK', *River Research and Applications*, vol. 23, pp. 429-450.

Collins, A. L., Walling, D. E. & Leeks, G. 1997, 'Source type ascription for fluvial suspended sediment based on a quantitative composite fingerprint technique', *Catena*, vol. 29, no. 1, pp. 1-27.

Collins, A. L., Walling, D. E. & Leeks, G. J. L. 1996, 'Composite fingerprinting of the spatial source of fluvial suspended sediment: a case study of the Exe and Severn River basins, UK', *Geomorphologie*, vol. 2, pp. 41-54.

Collins, A. L., Walling, D. E. & Leeks, G. J. L. 1998, 'Use of composite fingerprints to determine the provenance of the contemporary suspended sediment load transported by rivers', *Earth Surface Processes and Landforms*, vol. 23, pp. 31-52.

Collins, A. L., Walling, D. E., Sichingabula, H. & Leeks, G. J. L. 2001, 'Suspended sediment fingerprinting in a small tropical catchment and some management implications', *Applied Geography*, vol. 21, pp. 387-412.

Cooper, A. B. & Bottcher, A. B. 1993, 'Basin-Scale Modelling as Tool for Water-Resource Planning', *Journal of Water Resources Planning and Management-Asce*, vol. 119, no. 3, pp. 306-323.

Cooperative Centre for Catchment Hydrology 2004, *Catchment modelling toolkit,* viewed 31-3-2005, http://www.toolkit.net.au/cgi-bin/WebObjects/toolkit.woa/wa/productDetails?productID=1000013

Coppus, R. & Imeson, A. C. 2002, 'Extreme events controlling erosion and sediment transport in a semi-arid sub-Andean valley', *Earth Surface Processes and Landforms*, vol. 27, no. 13, pp. 1365-1375.

Corbett, J. R. 1969, *The Living Soil: The Processes of Soil Formation*, Martindale Press, Sydney.

Costantini, A. & Loch, R. J. 2002, 'Effects of site preparation on runoff, erosion, and nutrient losses from Pinus plantations established on the coastal lowlands of south-east Queensland, Australia', *Australian Journal of Soil Research*, vol. 40, no. 8, pp. 1287-1303.

Couper, P., Stott, T. & Maddock, I. 2002, 'Insights into river bank erosion processes derived from analysis of negative erosion-pin recordings: observations from three recent UK studies', *Earth Surface Processes and Landforms*, vol. 27, no. 1, pp. 59-79.

Couper, P. R. & Maddock, I. P. 2001, 'Subaerial river bank erosion processes and their interaction with other bank erosion mechanisms on the River Arrow, Warwickshire, UK', *Earth Surface Processes and Landforms*, vol. 26, pp. 631-646.

Crawley, M. J. 2005, *Statistics: An Introduction Using R*, J. Wiley and Sons.

Crichton, N. 2000, 'Information point: Wilks' lambda', *Journal of Clinical Nursing*, vol. 9, no. 3, pp. 381-381.

Croke, J., Hairsine, P. B. & Fogarty, P. 1999, 'Sediment transport, redistribution and storage on logged forest hillslopes in south-eastern Australia', *Hydrological Processes*, vol. 13, pp. 2705-2720.

Croke, J. & Mockler, S. 2001, 'Gully initiation and road-to-stream linkage in a forested catchment, south-eastern Australia', *Earth Surface Processes and Landforms*, vol. 26, pp. 205-217.

Cronin, S. J., Manoharan, V., Hedley, M. J. & Loganathan, P. 2000, 'Fluoride: A review of its fate, bioavailability, and risks of fluorosis in grazed-pasture systems in New Zealand', *New Zealand Journal of Agricultural Research*, vol. 43, pp. 295-321.

Crozier, M. J. 1986, *Landslides: Causes, Consequences and Environment*, Croom Helm, London.

Crozier, M. J., Gage, M., Pettinga, J. R., Selby, M. J. & Wasson, R. J. 1992, 'The stability of hillslopes', in J. M. Soons & M. J. Selby (ed.), *Landforms of New Zealand*, Longman Paul Limited, pp. 63-90.

Crozier, M. J. & Glade, T. W. 2005, 'Landslide hazard and risk: Issues, concepts and approach', in T. W. Glade, M. Anderson & M. J. Crozier (ed.), *Landslide Hazard and Risk*, John Wiley and Sons, Chichester, UK, pp. 1-40.

Dai, F. & Lee, C. 2003, 'A spatiotemporal probabilistic modelling of storm-induced shallow landsliding using aerial photographs and logistic regression', *Earth Surface Processes and Landforms*, vol. 28, no. 5, pp. 527-545.

Dallal, G. E. 2007, *Multiple Comparison Procedures,* viewed 14-2-2006 http://www.jerrydallal.com/LHSP/mc.htm

Davie, T. 2002, *Fundamentals of Hydrology*, Routledge, London.

Davies-Colley, R. J. & Smith, D. G. 2001, 'Turbidity, suspended sediment, and water clarity: a review', *Journal of the American Water Resources Association*, vol. 37, no. 5, pp. 1085-1101.

Davis, C. M. & Fox, J. F. 2009, 'Sediment fingerprinting: review of the method and future improvements for allocating nonpoint source pollution', *Journal of Environmental Engineering*, vol. 135, no. 7, pp. 490-504.

Davis, J. J. 1963, 'Cesium and its relationship to potassium in ecology', in V. Shultz & A. W. Klement (ed.), *Radioecology*, Reinhold, New York, pp. 539-556.

De Boer, D. H. & Crosby, G. 1995, 'Evaluating the potential of SEM/EDS analysis for fingerprinting suspended sediment derived from two contrasting topsoils', *Catena*, vol. 24, pp. 243-258.

De Boer, D. H. & Crosby, G. 1996, 'Specific sediment yield and drainage basin scale', *Erosion and Sediment Yield: Global and Regional Perspectives. July, 1996.* IAHS Publication No. 236 pp. 333-338.

De Rose, R., Gomez, B., Marden, M. & Trustrum, N. A. 1998, 'Gully erosion and Mangatu forest, New Zealand, estimated from digital elevation models', *Earth Surface Processes and Landforms*, vol. 23, no. 11, pp. 1045-1053.

De Rose, R. C., Trustrum, N. A., Thomson, N. A. & Roberts, A. H. C. 1995, 'Effect of landslide erosion on Taranaki hill pasture production and composition.' *New Zealand Journal of Agricultural Research*, vol. 38, no. 4, pp. 457-471.

de Vente, J. & Poesen, J. 2005, 'Predicting soil erosion and sediment yield at the basin scale: scale issues and semi-quantative models', *Earth-Science Reviews*, vol. 71, no. 1-2, pp. 95-125.

de Vente, J., Poesen, J., Arabkhedri, M. & Verstraeten, G. 2007, 'The sediment delivery problem revisited', *Progress in Physical Geography*, vol. 31, no. 2, pp. 155-178.

de Vente, J., Poesen, J., Bazzoffi, P., Van Rompaey, A. & Verstraeten, G. 2006, 'Predicting catchment sediment yield in Mediterranean environments: the importance of sediment sources and connectivity in Italian drainage basins', *Earth Surface Processes and Landforms*, vol. 31, pp. 1017-1034.

De Vita, P. & Reichenbach, P. 1998, 'Rainfall-triggered landslides: a reference list', *Environmental Geology*, vol. 35, no. 2-3, pp. 219-233.

Dedkov, A. P. & Mozzherin, V. I. 1996, 'Erosion and sediment yield on the Earth', *Erosion and Sediment Yield: Global and Regional Perspectives. July, 1996.* IAHS Publication No. 236, pp. 29-33.

Delange, W. P. & Delange, P. J. 1994, 'An Appraisal of Factors Controlling the Latitudinal Distribution of Mangrove (Avicannia-Marina Var Resinifera) in New-Zealand', *Journal of Coastal Research*, vol. 10, no. 3, pp. 539-548.

Di Stefano, C., Ferro, V. & Porto, P. 1999, 'Linking sediment yield and Caesium-137 spatial distribution at basin scale', *Journal of Agricultural Engineering Research*, vol. 74, pp. 41-62.

Dingman, S. L. 1994, *Physical Hydrology*, Prentice Hall, New Jersey.

Doe, K. 1969, 'Lead', in G. Wedepohl (ed.), *Handbook of Geochemistry*, Springer-Verlag, Berlin.

Doering, C., Akber, R. & Heijnis, H. 2006, 'Vertical distributions of Pb-210 excess, Be-7 and Cs-137 in selected grass covered soils in Southeast Queensland, Australia', *Journal of Environmental Radioactivity*, vol. 87, no. 2, pp. 135-147.

Donald, L. A. 1990, *Whangapoua Estuary and Environs Preliminary Physical Assessment Study*, Waikato Regional Council Technical Report 1990/4 February 1990.

Donohue, I., Duck, R. W. & Irvine, K. 2003, 'Land use, sediment loads and dispersal pathways from two catchments at the southern end of Lake Tanganyika, Africa: implications for lake management', *Environmental Geology*, vol. 44, pp. 448-455.

Dosseto, A., Turner, S. P. & Douglas, G. B. 2006, 'Uranium-series isotopes in colloids and suspended sediments: Timescales for sediment production and transport in the Murray-Darling River system', *Earth and Planetary Science Letters*, vol. 246, pp. 418-431.

Douglas, G., Ford, P., Jones, G. & Palmer, M. 2003, 'Identification of sources of sediment to Lake Samsonvale (North Pine Dam), southeast Queensland, Australia', *Erosion Prediction in Ungauged Basins: Integrating Methods and Techniques*, Proceedings of the symposium HS01 held at Sapporo, Japan. 8-9 July, 2003.

Douglas, G., Palmer, M., Caitcheon, G. & Orr, P. 2007, 'Identification of sediment sources to Lake Wivenhoe, south-east Queensland, Australia', *Marine and Freshwater Research*, vol. 58, no. 9, pp. 793-810.

Dowdall, M., Gerland, S. & Lind, B. 2003, 'Gamma-emitting natural and anthropogenic radionuclides in the terrestrial environment of Kongsfjord, Svalbard', *Science of the Total Environment*, vol. 305, no. 1-3, pp. 229-240.

Downes, B., Barmuta, L., Fairweather, P., Faith, D., Keough, M., Lake, P., Mapstone, B. & Quinn, G. 2002, *Monitoring Ecological Impacts. Concepts and Practice in Flowing Water*, Cambridge University Press.

Drenge, H. E. 1995, 'Erosion and soil productivity in Australia and New Zealand', *Land Degradation and Rehabilitation*, vol. 6, pp. 71-78.

Drewry, J. J. 2006, 'Natural recovery of soil physical properties from treading damage of pastoral soils in New Zealand and Australia: a review', *Agriculture Ecosystems and Environment*, vol. 114, pp. 159-169.

Droppo, I. G. & Stone, M. 1994, 'In-Channel Surficial Fine-Grained Sediment Laminae .1. Physical Characteristics and Formational Processes', *Hydrological Processes*, vol. 8, no. 2, pp. 101-111.

Dunne, T. 1979, 'Sediment yield and land use in tropical catchments', *Journal of Hydrology*, vol. 42, pp. 281-300.

Dyer, F. J. 1998, *Sources of sediment and associated phosphorus for Tarago reservoir*, PhD Thesis, The University of Melbourne.

Dyer, F. J. & Olley, J. M. 1999, 'The effects of grain abrasion and disaggregation on ^{137}Cs concentrations in different size fractions of soils developed on three different rock types', *Catena*, vol. 36, pp. 143-151.

Dymond, J. R., Ausseil, A., Shepherd, J. D. & Buettner, L. 2006, 'Validation of a region-wide model of landslide susceptibility in the Manawatu-Wanganui region of New Zealand', *Geomorphology*, vol. 74, no. 1-4, pp. 70-79.

Dymond, J. R. & Betts, H. D. In prep., 'An erosion model for evaluating regional land-use scenarios in New Zealand', *Environmental Modelling and Software*.

Dymond, J. R., Shepherd, J. D. & Page, M. 2008, *Regional Council Erosion Model Rollout: Workshop Notes 18 March 2008*, Landcare Research.

Eads, R. E. & Lewis, J. 2002, 'Continuous turbidity monitoring in streams of north-western California', *Turbidity and Other Sediment Surrogates Workshop, April-May 2002*, Reno, Nevada.

Efron, B. 1982, *The Jackknife, the Bootstrap and Other Resampling Plans,* Society of industrial and applied mathematics, Philadelphia.

Egli, M., Mirabella, A. & Fitze, P. 2001, 'Clay mineral transformations in soils affected by fluorine and depletion of organic matter within a time span of 24 years', *Geoderma*, vol. 103, pp. 307-334.

El-Reefy, H. I., Sharshar, T., Zaghloul, R. & Badran, H. M. 2006, 'Distribution of gamma-ray emitting radionuclides in environment of Burullus Lake: I. Soils and vegetation', *Journal of Environmental Radioactivity*, vol. 87, pp. 148-169.

Eldridge, D. J. 1993, 'Soils and range management', in P. E. V. Charman & B. W. Murphy (ed.), *Soils - Their Properties and Management*, Sydney University Press.

Elliott, A. H., Tian, Y. Q., Rutherford, J. C. & Carlson, W. T. 2002, 'Effect of cattle treading on interill erosion from hill pasture: modelling concepts and analysis of rainfall simulator data', *Australian Journal of Soil Research*, vol. 40, no. 6, pp. 963-976.

Elliott, G. L., Campbell, B. L. & Loughran, R. J. 1990, 'Correlation of erosion measurements and soil Caesium-137 content', *Applied Radiation and Isotopes*, vol. 41, no. 8, pp. 713-717.

Ellis, J. I., Nicholls, P., Craggs, R., Hofstra, D. & Hewitt, J. E. 2004, 'Effects of terrigenous sedimentation on mangrove physiology and associated macrobenthic communities', *Marine Ecology - Progress Series*, vol. 270, pp. 71-82.

Ellison, W. D. 1944, 'Studies of raindrop erosion', *Agricultural Engineering*, vol. 25, pp. 131-182.

Environment Southland 2007, *Regional Coastal Plan for Southland*, Report no. 2007/03 April 2007 Environment Southland.

Environment Waikato 2005a, *Report on Resource Consent Applications (110661-110664) Lodged by Ernslaw One Ltd to Undertake Forest Harvesting and Related Activities at Whangapoua Forest, Te Rerenga. Report to Hearings Committee. Document number 969355*.

Environment Waikato 2005b, *Waikato Regional Coastal Plan*, Environment Waikato Policy Series 2005/06. Prepared by the Policy and Strategy Group. Report number 1021525, 1021525, Environment Waikato, Hamilton.

Environment Waikato 2006, *Proposed Waikato Regional Plan*, Environment Waikato. November, 2006.

Environment Waikato ND, *What to plant in the Coromandel ecological region. Environment Waikato local area planting guide series 2.,* viewed 17-7-2009 http://www.ew.govt.nz/PageFiles/2900/Coromandel%20planting%20guide%20-%20part%201.pdf

Environmental Protection Agency 2007, *Discriminant Function Analysis. Biological Indicators of Watershed Health (Statistical Primer Multivariate Methods)* viewed 6-2-2008, http://epa.gov/bioindicators/statprimer/dfa.html#simple

EPA 1999, *Guidance Manual for Compliance with the Interim Enhanced Surface Water Treatment Rule: Turbidity Provisions*, United States Environmental Protection Agency (Office of Water) EPA Report 815-R-99-010 April 1999.

EPA 2004, *Understanding Variation in Partition Coefficient, Kd, Values. Volume III: Review of Geochemistry and Available Kd Valuesfor Americium, Arsenic, Curium, Iodine, Neptunium, Radium, and Technetium*, Office of Air and Radiation. U.S. Environmental Protection Agency. July 2004 (EPA402-R-04-002C).

Eshetu, Z., Geisler, R. & Hogberg, P. 2004, 'Historical land use patterns affects the chemistry of forest soils in the Ethiopian highlands', *Geoderma*, vol. 118, pp. 149-165.

Evans, D. J., Gibson, C. E. & Rossell, R. S. 2006, 'Sediment loads and sources in heavily modified Irish catchments: a move towards informed management strategies', *Geomorphology*, vol. 79, pp. 93-113.

Eyles, G. & Fahey, B. D. 2006, *The Pakuratahi Landuse Study*, HBRC plan no. 3868, Hawkes Bay Regional Council.

Eyles, G. O. 1983, 'The distribution and severity of present soil erosion in New Zealand', *New Zealand Geographer*, vol. 39, no. 1, pp. 12-28.

Fahey, B. D., Duncan, M. J. & Quinn, J. M. 2004, 'Impacts of forestry', in J. S. Harding, M. P. Mosley, C. P. Pearson & B. K. Sorrell (ed.), *Freshwaters of New Zealand*, New Zealand Hydrological Society Inc. and New Zealand Limnological Society Inc., Christchurch, New Zealand.

Fahey, B. D. & Marden, M. 2000, 'Sediment yields from a forested and a pasture catchment, coastal Hawke's Bay, North Island, New Zealand', *Journal of Hydrology*, vol. 39, no. 1, pp. 49-63.

Fahey, B. D. & Marden, M. 2006, *Forestry Effects on Sediment Yield and Erosion*, The Pakuratahi Land Use Study, Hawke's Bay Regional Council.

Fahey, B. D. & Rowe, L. K. 1992, 'Land-use impacts', in M. P. Mosley (ed.), *Waters of New Zealand*, New Zealand Hydrological Society, Wellington, pp. 265-284.

Fangmeier, D. D., Elliot, W. J., Workman, S. R., Huffman, R. L. & Schwab, G. O. 2005, *Soil and Water Conservation*, Thompson Delmar.

Fenwick, J. K. 1994, *Hydrologists Field Manual*, NIWA Science and Technology Series No. 5. August 1994.

Findlay, S., Quinn, J., Hickey, C., Burrell, G. & Downes, M. 2001, 'Effects of land use and riparian flowpath on deliver of dissolved organic carbon to streams', *Limnology and Oceanography*, vol. 46, no. 2, pp. 345-355.

Flanagan, D. C., Huang, C., Norton, L. D. & Parker, S. C. 1995, 'Laser scanner for erosion plot measurements', *American Society of Agricultural Engineers*, vol. 38, no. 3, pp. 703-710.

Franks, S. W. & Rowan, J. 2000, 'Multi-parameter fingerprinting of sediment sources: Uncertainty estimation and tracer selection', *Computational Methods in Water Resources*, Proceedings of the XIII international conference on computational methods in water resources. Alberta, Canada, 25-29th June, 2000, pp. 1067-1074.

Fransen, P., Phillips, C. & Fahey, B. 2001, 'Forest road erosion in New Zealand: overview', *Earth Surface Processes and Landforms*, vol. 26, no. 2, pp. 165-174.

Fredericks, D. J., Norris, V. & Perrens, S. J. 1988, 'Estimating erosion using Caesium-137: I. Measuring Caesium-137 activity in a soil', *Sediment Budgets*, IAHS Publication no. 174, Porto Alegre, pp. 225-231.

Fu, B., Newham, L. T. H. & Field, J. B. 2008, 'Influence of particle size on geochemical suspended sediment tracing in Australia', *Sediment dynamics in changing environments*, IAHS Publication 325, Christchurch, New Zealand.

Fukuyama, T., Onda, Y., Takenaka, C. & Walling, D. E. 2008, 'Investigating erosion rates within a Japanese cypress plantation using Cs-137 and Pb-210_{ex} measurements', *Journal of Geophysical Research*, vol. 113, pp. F02007.

Fuller, I. C. & Hutchinson, E. L. 2007, 'Sediment flux in a small gravel-bed stream: Response to channel remediation works', *New Zealand Geographer*, vol. 63, no. 3, pp. 169-180.

Gabet, E. J. & Dunne, T. 2002, 'Landslides on coastal sage-scrub and grassland hillslopes in a severe El Nino winter: the effects of vegetation conversion on sediment delivery', *Geological Society of America Bulletin*, vol. 114, no. 8, pp. 983-990.

Gao, P. 2008, 'Understanding watershed suspended sediment transport', *Progress in Physical Geography*, vol. 32, no. 2, pp. 243-263.

Garde, R. J. & Ranga Raju, K. G. 1977, *Mechanics of Sediment Transport and Alluvial Stream Problems*, John Wiley and Sons.

Garson, D. 2007, *Discriminant Function Analysis. Quantitative research in public administration (PA.765). North Carolina State University,* viewed 6-2-2008 http://www2.chass.ncsu.edu/garson/pa765/discrim.htm

Gibbs, M. 2006, *Whangapoua Harbour Sediment Sources*, NIWA Client Report: HAM2006-056 prepared for Environment Waikato, May 2006.

Gibbs, M. M. 2008, 'Identifying source soils in contemporary estuarine sediments: a new compound-specific isotope method', *Estuaries and Coasts*, vol. 31, pp. 344-359.

Gilley, J. E. 2005, 'Erosion/wind induced', in D. Hillel (ed.), *Encyclopaedia of Soils in the Environment*, Elsevier Academic Press, Oxford, UK, pp. 463-469.

Gillison, D. S., Wallbrink, P. J., Murray, A. S. & Cochrane, J. A. 1996, 'Estimates of wind erosion risk and rates using GIS modelling and Caesium-137 on the Nullarbor Plain karst, Australia', *Zeitschrift fur Geomorphol*, vol. 105, pp. 73-90.

Gippel, C. J. 1989, 'The use of turbidimeters in suspended sediment research', *Hydrobiologia*, vol. 176-177, no. 1, pp. 465-480.

Gippel, C. J. 1993, 'Potential of turbidity monitors for measuring the transport of suspended solids in streams', *Hydrological Processes*, vol. 9, pp. 83-97.

Gippel, C. J. 1994, 'Monitoring turbidity of stream water', *Australian Journal of Soil and Water Conservation*, vol. 7, pp. 37-44.

Gippel, C. J. 1995, 'Potential of turbidity monitoring for measuring the transport of suspended solids in streams', *Hydrological Processes*, vol. 9, no. 1, pp. 83-97.

Glade, T. 2003, 'Landslide occurrence as a response to land use change: a review of evidence from New Zealand', *Catena*, vol. 51, no. 3-4, pp. 297-314.

Glade, T. W. 1998, 'Establishing the frequency and magnitude of landslide-triggering rainstorms events in New Zealand', *Environmental Geology*, vol. 35, no. 2-3, pp. 160-174.

Glendinning, J. S. 2000, *Australian Soil Fertility Manual*, CSIRO Publishing, Collingwood, Victoria.

Gomez, B., Coleman, S. E., Sy, V. W. K., Peacock, D. H. & Kent, M. 2007, 'Channel change, bankfull and effective discharges on a vertically accreting, meandering, gravel-bed river', *Earth Surface Processes and Landforms*, vol. 32, no. 5, pp. 770-785.

Gomi, T., Moore, R. D. & Hassan, M. A. 2005, 'Suspended sediment dynamics in small forest streams of the Pacific Northwest', *Journal Of The American Water Resources Association*, vol. 41, no. 4, pp. 877-898.

Gordon, N. D., McMahon, T. A., Finlayson, B. L., Gippel, C. J. & Nathan, R. J. 2004, *Stream Hydrology: An Introduction for Ecologists*, John Wiley and Sons, Ltd.

Govers, G., Gimenez, R. & Van Oost, K. 2007, 'Rill erosion: Exploring the relationship between experiments, modelling and field observations', *Earth-Science Reviews*, vol. 84, no. 3-4, pp. 87-102.

Govers, G., Quine, T. A., Desmet, P. J. J. & Walling, D. E. 1996, 'The relative contribution of soil tillage and overland flow erosion to soil redistribution on agricultural land', *Earth Surface Processes and Landforms*, vol. 21, pp. 929-946.

Grayson, R. B., Finlayson, B. L., Gippel, C. J. & Hart, B. T. 1996, 'The potential of field turbidity measurements for the computation of total phosphorus and suspended solids loads', *Journal of Environmental Management*, vol. 47, no. 3, pp. 257-267.

Green, T. R., Beavis, S. G., Dietrich, C. R. & Jakeman, A. J. 1999, 'Relating stream-bank erosion to in-stream transport of suspended sediment', *Hydrological Processes*, vol. 13, pp. 777-787.

Gregory, J. 2006, *Particles in Water: Properties and Processes*, IWA Publishing and CRC Press.

Hale, R. L. 2000, *Investigating statistics. Penn State University, Department of Educational Psychology,* viewed 4-8-2008 http://espse.educ.psu.edu/edpsych/faculty/rhale/statistics/Investigating.htm

Halliday, J., Thrush, S. F. & Hewitt, J. 2006, *Ecological Monitoring for Potential Effects of Forestry Activity on the Intertidal Habitats of Whangapoua Harbour*, NIWA Client Report: HAM2006-113,

Hamilton, C. L. 2003, *The variation in sediment properties at the interface between fresh and estuarine water in the Whangapoua estuary, Coromandel Peninsula*, Master of Science in Earth Sciences Thesis, University of Waikato.

Hancock, G. R., Loughran, R. J., Evans, K. G. & Balog, R. M. 2008, 'Estimation of soil erosion using field and modelling approaches in an undisturbed Arnhem land catchment, Northern Territory, Australia', *Geographical Research*, vol. 46, no. 3, pp. 333-349.

Happ, S. C., Rittenhouse, G. & Dobson, G. C. 1940, *Some Principles of Accelerated Stream and Valley Sedimentation*, US Department of Agriculture Technical Bulletin 695.

Hardle, W. & Simar, L. 2007, *Applied Multivariate Statistical Analysis*, Springer, Berlin.

Harris, R. R., Sullivan, K., Cafferata, P. H., Munn, J. R. & Faucher, K. M. 2007, 'Applications of turbidity monitoring to forest management in California', *Environmental Management*, vol. 40, pp. 531-543.

Harrison, W. 1988, *Palynological Study of Whangapoua and Whitianga Estuaries - The Historical Record*, Hauraki Catchment Board technical report No. 232. June 1988.

Harvey, A. M. 2002, 'Effective timescales of coupling within fluvial systems', *Geomorphology*, vol. 44, no. 3-4, pp. 175-201.

Hatch, D., Goulding, K. & Murphy, D. 2002, 'Nitrogen', in P. M. Haygarth & S. C. Jarvis (ed.), *Agriculture, Hydrology and Water Quality*, CABI Publishing, Wallingford, UK., pp. 7-28.

Haygarth, P. M. & Jarvis, S. C. 1999, 'Transfer of phosphorus from agricultural soils', *Advances in Agronomy*, vol. 66, pp. 195-249.

He, Q. & Walling, D. E. 1996, 'Interpreting particle size effects in the adsorption of Cs-137 and unsupported Pb-210 by mineral soils and sediments ', *Journal of Environmental Radioactivity*, vol. 30, no. 2, pp. 117-137.

He, Q., Walling, D. E. & Wallbrink, P. J. 2002, 'Alternative methods of radionuclides for us in soil erosion and sedimentation investigations', in F. Zapata (ed.), *Handbook for the Assessment of Soil Erosion and Sedimentation Using Environmental Radionuclides*, Kluwer Academic Publishers, pp. 185-216.

Healy, T., Cole, R. & de Lange, W. 1996, 'Geomorphology and New Zealand shallow estuaries and shorelines', in K. Nordstrom & C. Roman (ed.), *Estuarine Shores: Evolution, Environments, and Human Alterations*, John Wiley and Sons.

Healy, T. & Kirk, R. 1991, 'Coasts', in J. Soons & M. Selby (ed.), *Landforms of New Zealand*, Longman Paul, Auckland.

Herpin, U., Cerri, C. C., Carvalho, M. C. S., Markert, B., Enzweiler, J., Friese, K. & Breulmann, G. 2002, 'Biogeochemical dynamics following land use change from forest to pasture in a humid tropical area (Rondonia, Brazil): a multi-element approach by means of XRF-spectroscopy', *The Science of the Total Environment*, vol. 286, pp. 97-109.

Hewawasam, T., von Blanckenburg, F., Schaller, M. & Kubik, P. W. 2003, 'Increase in human over natural erosion rates in tropical highlands constrained by cosmogenic nuclides', *Geology*, vol. 31, no. 7, pp. 597-600.

Hewitt, A. 1998, *New Zealand Soil Classification*, Manaaki Whenua Press, Lincoln.

Hibbert, A. R. 1967, 'Forest treatment effects on water yield', *Proceedings of the International Symposium of Forest Hydrology.* Penn State University, pp. 527-543.

Hicks, D. 1995, *Control of Soil Erosion on Farmland. A Summary of Erosion's Impact on New Zealand Agriculture, and Farm Management Practices Which Counteract It. Report number 95/4*, 95/4, Ministry of Agriculture and Forestry.

Hicks, D. & Griffiths, G. A. 1992, 'Sediment load', in M. P. Mosley (ed.), *Waters of New Zealand*, New Zealand Hydrological Society, Christchurch, pp. 229-248.

Hicks, D. M. 1990, 'Suspended sediment yields from pasture and exotic forest basins', *Proceedings of the New Zealand Hydrological Society*, Taupo.

Hicks, D. M. 1994a, 'Land-use effects on magnitude-frequency characteristics of storm sediment yields: some New Zealand examples', *Variability in Stream Erosion and Sediment Transport*, IAHS Publication no. 224, Canberra, pp. 395-402.

Hicks, D. M. 1994b, *Storm Sediment Yields from Basins with Various Landuses in the Auckland Area*, Prepared for the Auckland Regional Council, July 1994. ARC802/1.

Hicks, D. M. & Basher, L. R. 2008, 'The signature of an extreme erosion event on suspended sediment loads: Motueka River catchment, South Island, New Zealand', *Sediment Dynamics in Changing Environments*, Christchurch, New Zealand, pp. 184-191.

Hicks, D. M., Gomez, B. & Trustrum, N. A. 2000, 'Erosion thresholds and suspended sediment yields, Waipaoa River Basin, New Zealand', *Water Resources Research*, vol. 36, no. 4, pp. 1129-1142.

Hicks, M., Shankar, U. & McKerchar, A. 2003, *Sediment yield estimates : a GIS tool. Water and atmosphere. V. 11, n4. National Institute of Water and Atmospheric Research,* viewed 10-10-2008 http://www.niwa.cri.nz/pubs/wa/ma/11-4/estimates

Hicks, M., Shankar, U., McKerchar, A., Hume, T., Basher, L., Lynn, I., Jessen, M., Page, M. & Webb, T. ND, *'River suspended sediment yields to the New Zealand coast and estuaries'*.

Hill, R. 2002, *Whangapoua Catchment - Geology and Soil Characteristics*, Environment Waikato Regional Council Document No. 765707 July, 2002, Hamilton, New Zealand.

Hooke, J. M. 2007, 'Monitoring morphological and vegetation changes and flow events in dryland river channels', *Environmental Monitoring and Assessment*, vol. 127, no. 1-3, pp. 445-457.

Horrocks, M., Nichol, S. L., D'Costa, D. M., Augustinus, P., Jacobi, T. & Shane, P. A. 2007, 'A late Quaternary record of natural change and human impact from Rangihoua Bay, Bay of Islands, Northern New Zealand', *Journal of Coastal Research*, vol. 23, no. 3, pp. 592-604.

Horrocks, M., Nichol, S. L., Gregory, M. R., Creese, R. & Augustinus, P. C. 2001, 'A Holocene pollen and sediment record of Whangape Harbour, far northern New Zealand', *Journal of The Royal Society of New Zealand*, vol. 31, no. 2, pp. 411-424.

House, W. A., Jickells, T. D., Edwards, A. C., Praska, K. E. & Denison, F. H. 1998, 'Reactions of phosphorus with sediments in fresh and marine waters', *Soil Use and Management*, vol. 14, pp. 139-146.

Howard, A. D., Dietrich, W. E. & Seidl, M. A. 1994, 'Modelling fluvial erosion on regional to continental scales', *Journal of Geophysical Research*, vol. 99, no. B7, pp. 13971-13986.

Hudson, P. F. 2003, 'Event sequence and sediment exhaustion in the lower Panuco Basin, Mexico. ' *Catena*, vol. 52, pp. 57-76.

Hughes, A. O., Olley, J. M., Croke, J. C. & McKergow, L. A. 2009, 'Sediment source changes over the last 250 years in a dry-tropical catchment, central Queensland, Australia', *Geomorphology*, vol. 104, no. 3-4, pp. 262-275.

Hume, T. 2003, 'Estuaries and tidal inlets', in J. Goff, S. Nichol & H. Rouse (ed.), *The New Zealand coast Te Tai o Aotearoa*, Dunmore Press, pp. 191-214.

Hume, T. & Herdendorf, C. 1998, 'A geomorphic classification of estuaries and its application to coastal resource management - a New Zealand example', *Ocean and Shoreline Management*, vol. 11, pp. 249-274.

Hume, T. M. & Dahm, J. 1992, *An Investigation of the Effects of Polynesian and European Land Use on Sedimentation in Coromandel Estuaries.* , DSIR Consultancy Report No. 6104 for the Department of Conservation (Waikato Conservancy), Hamilton.

Hutchings, P., Haynes, D., Goudkamp, K. & McCook, L. 2005, 'Catchment to Reef: Water quality issues in the Great Barrier Reef Region - An overview of papers', *Marine Pollution Bulletin*, vol. 51, pp. 3-8.

Imaizumu, F., Sidle, R. C. & Kamei, R. 2007, 'Effects of forest harvesting on the occurrence of landslides and debris flows in steep terrain of central Japan', *Earth Surface Processes and Landforms*, vol. 33, pp. 827-840.

Istanbulluogulu, E., Tarboton, D. G. & Pack, R. T. 2004, 'Modelling of the interactions between forest vegetation, disturbances, and sediment yields', *Journal of Geophysical Research*, vol. 109, pp. F01009.

Iverson, R. M. 1997, 'The physics of debris flows', *Reviews of Geophysics*, vol. 35, no. 3, pp. 245-296.

Jansson, M. B. 2002, 'Determining sediment source areas in a tropical river basin, Costa Rica', *Catena*, vol. 47, no. 1, pp. 63-84.

Jayasuriya, R. T. 2003, 'Measurement of the scarcity of soil in agriculture', *Resources Policy*, vol. 29, no. 3-4, pp. 119-129.

Jenkins, B. 2006, *Assessment of the 'Hobo rainomatic' gauges installed in the Whangapoua estuary catchment.* Internal Memo, Environment Waikato. 8th September, 2006.

Johnson, A. C., Edwards, R. T. & Erhardt, R. 2007, 'Ground-water response to forest harvest: Implications for hillslope stability', *Journal of the American Water Resources Association*, vol. 43, no. 1, pp. 134-147.

Jones, H. 2008, *Coastal Sedimentation: What We Know and Information Gaps*, Environment Waikato Technical Report 2008/12.

Kasai, M. 2006, 'Channel processes following land use changes in a degrading steep headwater stream in North Island, New Zealand', *Geomorphology*, vol. 81, no. pp. 421-439.

Kasai, M., Brierley, G. J., Page, M. J., Marutani, T. & Trustrum, N. A. 2005, 'Impacts of land use change on patterns of sediment flux in Weraamaia catchment, New Zealand', *Catena*, vol. 64, pp. 27-60.

Kasai, M., Marutani, T., Reid, L. & Trustrum, N. A. 2001, 'Estimation of temporally averaged sediment delivery ration using aggradational terraces in headwater catchment of the Waipaoa River, North Island, New Zealand', *Earth Surface Processes and Landforms*, vol. 26, no. 1, pp. 1-16.

Kato, Y., Kitazato, H., Shimanaga, M., Nakatsuka, T., Shirayama, Y. & Masuzawa, T. 2003, '^{210}Pb and ^{137}Cs in sediments from Sagami Bay, Japan: sedimentation rates and inventories', *Progress in Oceanography*, vol. 57, pp. 77-95.

Kelley, D. W., Brachfeld, S. A., Nater, E. A. & Wright, H. E. 2006, 'Sources of sediment in Lake Pepin on the Upper Mississippi River in response to Holocene climatic changes', *Journal of Paleolimnology*, vol. 35, no. pp. 193-206.

Kelley, D. W. & Nater, E. A. 2000a, 'Historical sediment flux from three watersheds in Lake Pepin, Ninnesota, USA', *Journal of Environmental Quality*, vol. 29, no. 2, pp. 561-568.

Kelley, D. W. & Nater, E. A. 2000b, 'Source apportionment of lake bed sediments to watersheds in an Upper Mississippi basin using a chemical mass balance method', *Catena*, vol. 41, pp. 277-292.

Kettner, A. J., Gomez, B. & Syvitski, J. P. M. 2007, 'Modelling suspended sediment discharge from the Waipaoa River system, New Zealand: The last 3000 years', *Water Resources Research*, vol. 43, pp. W07411.

Khanchoul, K. & Jansson, M. B. 2008, 'Sediment rating curves developed on stage and seasonal means in discharge classes for the Mellah wadi, Algeria', *Geografiska Annaler Series a-Physical Geography*, vol. 90A, no. 3, pp. 227-236.

Kim, N., Taylor, M., Chapman, R., Harris, J. & Robinson, P. 2008, 'Inadvertent sources of trace elements in Waikato's rural soils', *NZ Trace Elements Group Conference 2008.* University of Waikato, Hamilton, 13-15 Feb 2008.

Kinnell, P. I. A. 2004, 'Sediment delivery ratios: a misaligned approach to determining sediment delivery from hillslopes', *Hydrological Processes*, vol. 18, no. 16, pp. 3191-3194.

Kinnell, P. I. A. 2005, 'Raindrop-impact-induced erosion processes and prediction: a review', *Hydrological Processes*, vol. 19, pp. 2815-2844.

Kinsey-Henderson, A. E., Post, D. A. & Prosser, I. P. 2005, 'Modelling sources of sediment at sub-catchment scale: An example from the Burdekin catchment, North Queensland, Australia', *Mathematics and Computers in Simulation*, vol. 69, no. 1-2, pp. 90-102.

Kochanoski, R. G. & De Jong, E. 1984, 'Predicting the temporal relationship between soil ^{137}Cs and erosion rate', *Journal of Environmental Quality*, vol. 13, no. pp. 301-304.

Kohavi, R. 1995, 'A study of cross-validation and bootstrap for accuracy estimation and model selection', *Proceedings of the Fourteenth International Joint Conference on Artificial Intelligence,* San Mateo, CA, USA, pp. 1137-1143.

Koide, M., Soutar, A. & Goldberg, D. 1972, 'Marine geochronology with ^{210}Pb', *Earth and Planetary Science Letters*, vol. 14, pp. 442-446.

Krause, A. K., Franks, S. W., Kalma, J. D., Loughran, R. J. & Rowan, J. S. 2003, 'Multi-parameter fingerprinting of sediment deposition in a small gullied catchment in SE Australia', *Catena*, vol. 53, no. 4, pp. 327-348.

Krausse, M., Eastwood, C. & Alexander, R. R. 2001, *Muddies Waters: Estimating the National Economic Cost of Soil Erosion and Sedimentation in New Zealand.*, Landcare Research., Palmerston North, N.Z.

Kronvang, B., Grant, R. & Laubel, A. L. 1997, 'Sediment and phosphorus export from a lowland catchment: quantification of sources', *Water, Air and Soil Pollution*, vol. 99, pp. 465-476.

Laffan, M., Jordan, G. & Duhig, N. 2001, 'Impacts on soils from cable-logging steep slopes in north-eastern Tasmania, Australia', *Forest Ecology and Management*, vol. 144, pp. 91-99.

Lal, R. 1998, 'Soil erosion impact on agronomic productivity and environment quality', *Critical Reviews in Plant Science*, vol. 17, no. 4, pp. 319-464.

Lal, R. 2001, 'Soil degradation by erosion', *Land Degradation and Development*, vol. 12, no. 6, pp. 519-539.

Lambert, C. P. & Walling, D. E. 1988, 'Measurement of channel storage of suspended sediment in a gravel-bed river ', *Catena*, vol. 15, pp. 65-80.

Landcare Research 2007, *2007 Annual Report*, Landcare Research New Zealand Limited.

Lane, P. N. J. & Sheridan, G. J. 2002, 'Impact of an unsealed forest road stream crossing: water quality and sediment sources', *Hydrological Processes*, vol. 16, pp. 2599-2612.

Lanyon, S. M. 1987, 'Jackknifing and bootstrapping: Important "new" statistical techniques for ornithologists', *The Auk*, vol. 104, no. 1, pp. 144-146.

Laubel, A. L., Svendsen, L. M., Kronvang, B. & Larsen, S. E. 1999, 'Bank erosion in a Danish lowland stream system', *Hydrobiologia*, vol. 410, pp. 279-285.

Lawler, D. M. 1993, 'The measurement of river bank erosion and lateral channel change: a review', *Earth Surface Processes and Landforms*, vol. 18, pp. 777-821.

Lawler, D. M. 2005, 'The importance of high-resolution monitoring in erosion and deposition studies: examples from estuarine and fluvial systems', *Geomorphology*, vol. 64, pp. 1-23.

Lawler, D. M., Couperthwaite, J., Bull, L. J. & Harris, N. M. 1997, 'Bank erosion events and processes in the Upper Severn basin', *Hydrology and Earth Systems Sciences*, vol. 1, no. 3, pp. 523-534.

Lawler, D. M., Grove, J. R., Couperthwaite, J. S. & Leeks, G. J. L. 1999, 'Downstream change in river bank erosion rates in the Swale-Ouse system, northern England', *Hydrological Processes*, vol. 13, pp. 977-992.

Lawler, D. M., Petts, G. E., Foster, I. D. L. & Harper, S. 2006, 'Turbidity dynamics during spring storm events in an urban headwater river system: The Upper Tame, West Midlands, UK', *Science of the Total Environment*, vol. 360, pp. 109-126.

Le Cloarec, M., Bonte, P., Lefevre, I., Mouchel, J. & Colbert, S. 2007, 'Distribution of ^{7}Be, ^{210}Pb and ^{137}Cs in watersheds of different scales in the Seine River basin: Inventories and residence times ', *Science of the Total Environment*, vol. 375, pp. 125-139.

Leroy, M. 1995, 'Alpha rays emitting impurities in ultra pure aluminium evolution through the successive refining steps', *Journal De Physique Iv*, vol. 5, no. C7, pp. 99-110.

Leslie, L., Leplastrier, M., Buckley, B. & Qi, L. 2005, 'Climatology of meteorological "bombs" in the New Zealand region', *Meteorology and Atmospheric Physics*, vol. 89, pp. 207-214.

Lewis, J. 2002a, 'Estimation of suspended sediment flux in streams using continuous turbidity and flow data coupled with laboratory concentrations', *Turbidity and Other Surrogates Workshop, April 30 - May 2, 2002*, Reno, Nevada, pp.

Lewis, J. 2002b, 'Turbidity-controlled sampling for suspended sediment load estimation', *Erosion and Sediment Transport Measurement in Rivers: Technological and Methodological Advances*, IAHS Publication no. 283, Oslo, pp. 13-20.

Lind, P. R., Robson, B. J. & Mitchell, B. D. 2007, 'Multiple lines of evidence for the beneficial effects of environmental flows in tow lowland rivers in Victoria, Australia', *River Research and Applications*, vol. 23, pp. 933-946.

Loganathan, P., Hedley, M. J., Grace, N. D., Lee, J., Cronin, S. J., Bolan, N. S. & Zanders, J. M. 2003, 'Fertiliser contaminants in New Zealand grazed pasture with special reference to cadmium and flourine: a review', *Australian Journal of Soil Research*, vol. 41, pp. 501-532.

Lohrer, A. M., Thrush, S. F., Lundquist, C. J., Vopel, K., Hewitt, J. E. & Nicholls, P. E. 2006, 'Deposition of terrigenous sediment on subtidal marine macrobenthos: response of two contrasting community types', *Marine Ecology - Progress Series*, vol. 307, pp. 115-125.

Lomenick, T. F. & Tamura, T. 1965, 'Naturally occurring fixation of Cs-137 on sediment of lacustrine origin', *Soil Science Society of America Proceedings*, vol. 29, pp. 383-387.

Longmore, M. E. 1982, 'The caesium-137 dating technique and associated applications in Australia - a review', in W. Ambrose & P. Duerden (ed.), *Archaeometry: An Australian Perspective*, Australian National University Press, Canberra, pp. 310-321.

Loughran, R. J. & Campbell, B. L. 1995, 'The identification of catchment sediment sources', in I. D. L. Foster, A. M. Gurnell & B. W. Webb (ed.), *Sediment and Water Quality in River Catchments*, John Wiley and Sons Ltd.

Loughran, R. J., Campbell, B. L., Shelly, D. J. & Elliott, G. L. 1992, 'Developing a sediment budget for a small drainage basin in Australia', *Hydrological Processes*, vol. 6, pp. 145-158.

Lovell, C. J. & Rose, C. W. 1988, 'Measurement of soil aggregate settling velocities. I. A modified bottom withdrawl tube method', *Australian Journal of Soil Research*, vol. 25, pp. 55-71.

Lovelock, C. E., Feller, I. C., Ellis, J., Schwarz, A., Hancock, N., Nichols, P. & Sorrell, B. 2007, 'Mangrove growth in New Zealand estuaries: the role of nutrient enrichment at sites with contrasting rates of sedimentation', *Oecologia* vol. 153, pp. 633-641.

Lowe, D., Newnham, R., McFadgen, B. & Higham, T. 2000, 'Tephras and New Zealand archaeology', *Journal of Archaeological Science*, vol. 27, pp. 859-870.

Luckman, P., Gibson, R. & De Rose, R. 1998, 'Landslide erosion risk to New Zealand pastoral steeplands productivity', *Land Degradation and Development*, vol. 10, pp. 49-65.

Maclaren, J. P. 1996, *Environmental Effects of Planted Forests in New Zealand*, FRI Bulletin No 198. New Zealand Forest Research Institute.

Madej, M. A. 2001, 'Erosion and sediment delivery following removal of forest roads', *Earth Surface Processes and Landforms*, vol. 26, pp. 175-190.

Malengreau, B., Skinner, D., Bromley, C. & Black, P. 2000, 'Geophysical characterisation of large silicic volcanic structures in the Coromandel Peninsula, New Zealand', *New Zealand Journal of Geology and Geophysics*, vol. 43, pp. 171-186.

Malet, J. P., Maquaire, O. & Calais, E. 2002, 'The use of Global Positioning System techniques for the continuous monitoring of landslides: application to the Super-Sauze earthflow (Alpes-de-Haute-Provence, France)', *Geomorphology*, vol. 43, no. 1-2, pp. 33-54.

Manoharan, V., Loganathan, P., Tillman, R. W. & Parfitt, R. L. 2007, 'Interactive effects of soil acidity and fluoride on soil solution aluminium chemistry and barley (*Hordeum vulgare* L.) root growth', *Environmental Pollution*, vol. 145, pp. 778-786.

Marden, M., Arnold, G., Gomez, B. & Rowan, D. 2005, 'Pre- and post-reforestation gully development in Mangatu Forest, east coast, North Island, New Zealand', *River Research and Applications*, vol. 21, pp. 757-771.

Marden, M. & Rowan, D. 1995, *Assessment of Storm Damage to Whangapoua Forest and its Immediate Environs Following the Storms of March 1995*, Landcare Research Contract Report LC9495/172 July 1995.

Marden, M., Rowan, D. & Phillips, C. 2006, 'Sediment sources and delivery following plantation harvesting in a weathered volcanic terrain, Coromandel Peninsula, North Island, New Zealand', *Australian Journal of Soil Research*, vol. 44, pp. 219-232.

Marks, G. & Nelson, C. 1979, 'Sedimentology and evolution of Omaro Spit, Coromandel Peninsula', *New Zealand Journal of Marine and Freshwater Research*, vol. 13, pp. 347-372.

Martin, A. J., Crusius, J., Jay McNee, J. & Yanful, E. K. 2003, 'The mobility of radium-226 and trace metals in pre-oxidized subaqueous uranium mill tailings', *Applied Geochemistry*, vol. 18, no. 7, pp. 1095-1110.

Martin, C. E. & McCulloch, M. T. 1999, 'Nd-Sr isotopic and trace element geochemistry of river sediments and soils in a fertilized catchment, New South Wales, Australia', *Geochimica et Cosmochimica Acta*, vol. 63, no. 2, pp. 287-305.

Matisoff, G., Bonniwell, E. C. & Whiting, P. J. 2002, 'Soil erosion and sediment sources in an Ohio watershed using beryllium-7, cesium-137, and lead-210 ', *Journal of Environmental Quality*, vol. 31, no. 1, pp. 54-61.

Matisoff, G., Wilson, C. G. & Whiting, P. J. 2005, 'The $^{7}Be/^{210}Pb_{ex}$ ratio as an indicator of suspended sediment age or fraction new sediment in suspension', *Earth Surface Processes and Landforms*, vol. 30, pp. 1191-1201.

McCave, I. N. & Syvitski, J. P. M. 1991, 'Principles and methods of geological particle size analysis', in J. P. M. Syvitski (ed.), *Principles, Methods, and Applications of Particle Size Analysis* Cambridge Press, pp. 3-21.

McKee, L. J., Ganju, N. K. & Schoellhamer, D. H. 2006, 'Estimates of suspended sediment entering San Francisco Bay from the Sacramento and San Joaquin Delta, San Francisco Bay, California', *Journal of Hydrology*, vol. 323, no. 1-4, pp. 335-352.

McKenzie, N., Jacquier, D., Isbell, R. & Brown, K. 2004, *Australian Soils and Landscapes*, CSIRO Publishing.

McKergow, L. A., Elliott, A. H. & Costley, K. J. 2007, *Waitetuna Flood Experiment: 24-28 January, 2006*, NIWA Client Report: HAM2007-114.

McKergow, L. A., Prosser, I. P., Hughes, A. O. & Brodie, J. 2005, 'Sources of sediment to the Great Barrier Reef World Heritage Area', *Marine Pollution Bulletin*, vol. 51, no. 1-4, pp. 200-211.

McLaren, R. & Cameron, K. 1990, *Soil Science: An Introduction to the Properties and Management of New Zealand Soils*, Oxford University Press, Auckland.

McLaughlin, M. J., Tiller, K. G., Naidu, R. & Stevens, D. P. 1996, 'Review: the behaviour and environmental impact of contaminants in fertilisers', *Australian Journal of Soil Research*, vol. 34, pp. 1-54.

Mead, S. & Moores, A. 2004, *Estuary Sedimentation: A Review of Estuarine Sedimentation in the Waikato Region*, Environment Waikato Technical Report Series 2005/13.

Merritt, W. S., Letcher, R. A. & Jakeman, A. J. 2003, 'A review of erosion and sediment transport models.' *Environmental Modelling and Software*, vol. 18, no. 8-9, pp. 761-799.

Miller, D. C., Muir, C. L. & Hauser, O. A. 2002, 'Detrimental effects of sedimentation on marine benthos: what can be learned from natural processes and rates?' *Ecological Engineering*, vol. 19, pp. 211-232.

Miller, J. E. 2005, *The Chicago Guide to Writing About Multivariate Analysis*, The University of Chicago Press, Chicago.

Miller, J. R., Lord, M., Yurkovich, S., Mackin, G. & Kolenbrander, L. 2005, 'Historical trends in sedimentation rates and sediment provenance, Fairfield Lake, western North Carolina', *Journal Of The American Water Resources Association*, vol. 41, no. 5, pp. 1053-1075.

Miller, S. R., Slingerland, R. L. & Kirby, E. 2007, 'Characteristics of steady state fluvial topography above fault-bend folds', *Journal of Geophysical Research-Earth Surface*, vol. 112, no. F4, pp FO4004.

Milliman, J. D. & Syvitski, J. P. M. 1992, 'Geomorphic/tectonic control of sediment discharge to the ocean: the importance of small mountainous rivers', *The Journal of Geology*, vol. 100, no. 5, pp. 525-544.

Minella, J. P. G., Walling, D. E. & Merten, G. H. 2008, 'Combining sediment source tracing techniques with traditional monitoring to assess the impact of improved land management on catchment sediment yields', *Journal of Hydrology*, vol. 348, pp. 546-563.

Ministry of Culture and Heritage 2007, 'Kauri Gum', in A. H. McLintock (ed.), *An Encyclopaedia of New Zealand.* First published in 1966.

Mitchell, S. B., Lawler, D. M., West, J. R. & Couperthwaite, J. 2003, 'Use of continuous turbidity sensor in the prediction of fine sediment transport in the turbidity maximum of the Trent Estuary, UK', *Estuarine, Coastal, and Shelf Sciences*, vol. 58, pp. 645-652.

Mizagaki, S., Onda, Y., Fukuyama, T., Koga, S., Asai, H. & Hiramatsu, S. 2008, 'Estimation of suspended sediment sources using 137Cs and 210Pbex in unmanaged Japanese cypress plantation watersheds in southern Japan', *Hydrological Processes*, vol. 22, pp. 4519-4531.

Molina, M., Aburto, F., Calderon, R., Cazanga, M. & Escudey, M. 2009, 'Trace Element Composition of Selected Fertilizers Used in Chile: Phosphorus Fertilizers as a Source of Long-Term Soil Contamination', *Soil & Sediment Contamination*, vol. 18, no. 4, pp. 497-511.

Molloy, L. 1993, *Soils in the New Zealand Landscape: The Living Mantle*, New Zealand Society of Soil Science.

Montagne, D., Cornu, S., Bourennane, H., Baize, D., Ratie, C. & King, D. 2007, 'Effect of agricultural practices on trace-element distribution in soil', *Communications in Soil Science and Plant Analysis*, vol. 38, pp. 473-491.

Montgomery, D. R., Schmidt, K. M., Greenberg, H. M. & Dietrich, W. E. 2000, 'Forest clearing and regional landsliding', *Geology*, vol. 28, pp. 311-314.

Montgomery, J. A., Busacca, A. J., Frazier, B. E. & McCool, D. K. 1997, 'Evaluating soil movement using Cesium-137 and the Revised Universal Soil Loss Equation', *Soil Science Society of America Journal*, vol. 61, pp. 571-579.

Moon, V. G., De Lange, A. & De Lange, W. 2003, 'Mudslides developed on Waitemata Group rocks, Tawharanui Peninsula, North Auckland', *New Zealand Geographer*, vol. 59, no. 2, pp. 44-53.

Moore, R. D. & Wondzell, S. M. 2005, 'Physical hydrology and the effects of forest harvesting in the Pacific Northwest: a review', *Journal of the American Water Resources Association*, vol. 41, no. 4, pp. 763-784.

Moore, W. S., DeMaster, D. J., Smoak, J. M., McKee, B. A. & Swarzenski, P. W. 1996, 'Radionuclide tracers of sediment-water interactions on the Amazon shelf', *Continental Shelf Research*, vol. 16, no. 5/6, pp. 645-665.

Moore, W. S. & Shaw, T. J. 2008, 'Fluxes and behaviour of radium isotopes, barium, and uranium in seven Southeastern US rivers and estuaries', *Marine Chemistry*, vol. 108, pp. 236-254.

Morgan, R. P. C. 2005, *Soil Erosion and Conservation*, Blackwell Publishing, Oxford.

Mosley, P. & Jowett, I. 1999, 'River morphology and management in New Zealand', *Progress in Physical Geography*, vol. 23, no. 4, pp. 541-565.

Motha, J., Wallbrink, P. J., Hairsine, P. & Grayson, R. 2002, 'Tracer properties of eroded sediment and source material', *Hydrological Processes*, vol. 16, pp. 1983-2000.

Motha, J., Wallbrink, P. J., Hairsine, P. & Grayson, R. 2004, 'Unsealed roads as suspended sediment sources in an agricultural catchment in south-eastern Australia', *Journal of Hydrology*, vol. 286, pp. 1-18.

Motha, J. A., Wallbrink, P. J., Hairsine, P. B. & Grayson, R. B. 2003, 'Determining the sources of suspended sediment in a forested catchment in south-eastern Australia', *Water Resources Research*, vol. 39, no. 3, pp. 1056.

Muller, G., Ottenstein, R. & Yahya, A. 2001, 'Standardized particle size for monitoring, inventory, and assessment of metals and other trace elements in sediments: < 20 μm or < 2 μm', *Journal of Analytical Chemistry*, vol. 371, pp. 637-642.

Murphy, B. W. 1993, 'The nature of soil', in P. E. V. Charman & B. W. Murphy (ed.), *Soils: Their Properties and Management*, Oxford University Press, Melbourne, pp. 3-11.

Nagle, G. N., Fahey, T. J., Ritchie, J. C. & Woodbury, P. B. 2007, 'Variations in sediment sources and yields in the Finger Lakes and Catskills regions of New York', *Hydrological Processes*, vol. 21, pp. 828-838.

Nagle, G. N. & Ritchie, J. C. 1999, 'The use of tracers to study sediment sources in three streams in Northeastern Oregon', *Physical Geography*, vol. 20, no. 4, pp. 348-366.

Nath, B., Norra, S., Chatterjee, D. & Stuben, D. 2007, 'Fingerprinting of land-use related chemical patterns in street sediments from Kolkata, India', *Environmental Forensics*, vol. 8, pp. 313-328.

Navas, A., Machin, J. & Soto, J. 2005, 'Mobility of natural radionuclides and selected major and trace elements along a soil toposequence in the Central Spanish Pyrenees', *Soil Science* vol. 170, no. 9, pp. 743-757.

Nearing, M. A. 2006, 'Can soil erosion be predicted?' in P. N. Owens (ed.), *Soil Erosion and Sediment Redistribution in River Catchments: Measurement, Modelling and Management*, CABI Publishing, Oxfordshire, pp. 145-152.

Nearing, M. A., Govers, G. & Norton, L. D. 1999, 'Variability on soil erosion data from replicated plots', *Soil Science Society of America Journal*, vol. 63, no. 6, pp. 1829-1835.

Newsome, P., Wilde, R. & Willoughby, E. 2000, *Volume 1: Label Formats*, Land resource information system spatial data layers, Landcare Research New Zealand, Palmerston North.

Nichol, S. L., Augustinus, P. C., Gregory, M. R., Creese, R. & Horrocks, M. 2000, 'Geomorphic and sedimentary evidence of human impact on the New Zealand coastal landscape', *Physical Geography*, vol. 21, no. 2, pp. 109-132.

NIWA 2007, *National climate centre,* viewed 10-9-2007 http://cliflo.niwa.co.nz

Norrish, K. & Hutton, J. T. 1977, 'Plant analysis by X-ray spectroscopy. I. Low atomic number elements, sodium to calcium', *X-ray Spectrometry*, vol. 6, no. 1, pp. 6-11.

Novotny, V. 1999, 'Diffuse pollution from agriculture - a worldwide outlook', *Water Science Technology*, vol. 39, no. 3, pp. 1-13.

Nriagu, J. O. 1978, 'Properties and the biogeochemical cycle of lead', in J. O. Nriagu (ed.), *Biogeochemistry of Lead in the Environment*, Elsevier Press, pp. 1-14.

O'Loughlin, C. L., Rowe, L. K. & Pearse, A. J. 1980, 'Sediment yield and water quality responses to clearfelling of evergreen mixed forests in Western New Zealand', *The Influence of Man on the Hydrological Regime, with Special Reference to Representative and Experimental Basins.* IAHS Publication No. 130, pp. 285-292.

Oden, S. 1915, 'A neue Methode zur mechanischen Bodenanalyse.' *Internationale Mitteilungen f˙ur Bodenkunde*, vol. 5, pp. 257-311.

Ogden, J. 1985, 'An introduction to plant demography with special reference to New Zealand trees', *New Zealand Journal of Botany*, vol. 23, pp. 751-772.

Ogden, J., Braggins, J., Stretton, K. & Anderson, S. 1997, 'Plant species richness under *Pinus radiata* stands on the central North Island volcanic plateau, New Zealand', *New Zealand Journal of Ecology*, vol. 21, no. 1, pp. 17-29.

Ogden, J., Deng, Y., Horrocks, M., Nichol, S. & Anderson, S. 2006, 'Sequential impacts of Polynesian and European settlement on vegetation and environment processes recorded in sediments at Whangapoua Estuary, Great Barrier Island, New Zealand', *Regional Environmental Change*, vol. 6, no. 1-2, pp. 25-40.

Olley, J. M., Murray, A. S., MacKenzie, D. H. & Edwards, K. 1993, 'Identifying sediment sources in a gullied catchment using natural and anthropogenic radioactivity', *Water Resources Research*, vol. 29, no. 4, pp. 1037-1043.

Olley, J. M. & Wasson, R. J. 2003, 'Changes in the flux of sediment in the Upper Murrumbidgee catchment, Southeastern Australia, since European settlement ', *Hydrological Processes*, vol. 17, no. 16, pp. 3307-3320.

Orbell, G. 1974, *Soils of the Waikato Coromandel King Country Region*, Department of Scientific and Industrial Research. Soil Bureau Publication 603, Wellington.

Osan, J., Kurunczi, S., Torok, S. & Van Grieken, R. 2002, 'X-ray analysis of riverbank sediment of the Tisza (Hungary): identification of particles from a mine pollution event', *Spectrochimica Acta Part B*, vol. 57, pp. 413-422.

Owens, P. N., Batalla, R. J., Collins, A. J., Gomez, B., Hicks, D. M., Horowitz, A. J., Kondolf, G. M., Marden, M., Page, M. J., Peacock, D. H., Petticrew, E. L., Salomons, W. & Trustrum, N. A. 2005, 'Fine-grained sediment in river systems: environmental significance and management issues', *River Research and Applications*, vol. 21, pp. 693-717.

Owens, P. N., Walling, D. E., He, Q. P., Shanahan, J. & Foster, I. D. L. 1997, 'The use of caesium-137 measurements to establish a sediment budget for the Start catchment, Devon, UK', *Hydrological Sciences Journal* vol. 42, no. 3, pp. 405-423.

Owens, P. N., Walling, D. E. & Leeks, G. J. L. 1999a, 'Deposition and storage of fine-grained sediment within the main channel system of the River Tweed, Scotland', *Earth Surface Processes and Landforms*, vol. 24, pp. 1061-1076.

Owens, P. N., Walling, D. E. & Leeks, G. J. L. 1999b, 'Use of floodplain sediment cores to investigate recent historical changes in overbank sedimentation rates and sediment sources in the catchment of the River Ouse, Yorkshire, UK', *Catena*, vol. 36, no. 1-2, pp. 21-47.

Page, M., Trustrum, N. A., Brackley, H. & Baisden, T. 2004, 'Erosion-related soil carbon fluxes in a pastoral steepland catchment, New Zealand', *Agriculture Ecosystems and Environment*, vol. 103, pp. 561-579.

Page, M. J. & Trustrum, N. A. 1997, 'A late Holocene lake sediment record of the erosion response to land use change in a steepland catchment, New Zealand', *Zeitschrift Fur Geomorphologie*, vol. 41, no. 3, pp. 369-392.

Page, M. J., Trustrum, N. A. & DeRose, R. C. 1994a, 'A high resolution record of storm-induced erosion from lake sediments, New Zealand', *Journal of Paleolimnology*, vol. 11, pp. 333-348.

Page, M. J., Trustrum, N. A. & Dymond, J. R. 1994b, 'Sediment Budget to Assess the Geomorphic Effect of a Cyclonic Storm, New-Zealand', *Geomorphology*, vol. 9, no. 3, pp. 169-188.

Painter, R. B., Blyth, K., Mosedale, J. C. & Kelly, M. 1974, 'The effect of afforestation on erosion processes and sediment yield.' *Effects of Man on the Interface of the Hydrological Cycle with the Physical Environment.* IAHS Publication No. 113, pp. 150-157.

Parkner, T., Page, M. J., Marutani, T. & Trustrum, N. A. 2006, 'Development and controlling factors of gullies and gully complexes, East Coast, New Zealand ', *Earth Surface Processes and Landforms*, vol. 31, no. 2, pp. 187-199.

Parkyn, S. & Wilcock, B. 2004, 'Impacts of agricultural land use', in J. S. Harding, M. P. Mosley, C. P. Pearson & B. K. Sorrell (ed.), *Freshwaters of New Zealand*, New Zealand Hydrological Society Inc. and New Zealand Limnological Society Inc., Christchurch, New Zealand.

Parkyn, S. M., Davies-Colley, R. J., Cooper, A. B. & Stroud, M. J. 2005, 'Predictions of stream nutrient and sediment yield changes following restoration of forested riparian buffers', *Ecological Engineering*, vol. 24, no. 5, pp. 551-558.

Parsons, A. J., Wainwright, J., Brazier, R. E. & Powell, D. M. 2006, 'Is sediment delivery a fallacy?' *Earth Surface Processes and Landforms*, vol. 31, pp. 1325-1328.

Parsons, A. J., Wainwright, J., Powell, D. M., Kaduk, J. & Brazier, R. E. 2004, 'A conceptual model for determining soil erosion by water', *Earth Surface Processes and Landforms*, vol. 29, pp. 1293-1302.

Peart, M. R., Ng, K. Y. & Zhang, D. D. 2005, 'Landslides and sediment delivery to a drainage system: some observations from Hong Kong', *Journal of Asian Earth Sciences*, vol. 25, pp. 821-836.

Peeters, I., Van Oost, K., Govers, G., Verstraeten, G., Rommens, T. & Poesen, J. 2008, 'The compatibility of erosion data at different temporal scales', *Earth and Planetary Science Letters*, vol. 265, pp. 138-152.

Peng, J. 2003, 'Unusually high Lead-210 inventory in the sediment column of a tidal embayment', *American Geophysical Union, Fall Meeting, 2003.* Abstract # OS32B-0247.

Pereira, H. C. 1973, *Land Use and Water Resources in Temperate and Tropical Climates*, Cambridge University Press, London.

Phillips, C., Marden, M. & Rowan, D. 2005, 'Sediment yield following plantation forest harvesting, Coromandel Peninsula, North Island, New Zealand', *Journal of Hydrology*, vol. 44, no. 1, pp. 29-44.

Phillips, J. D. & Gomez, B. 2007, 'Controls on sediment export from the Waipaoa River basin, New Zealand', *Basin Research*, vol. 19, no. 2, pp. 241-252.

Phillips, J. D., Marden, M. & Gomez, B. 2007, 'Residence time of alluvium in an aggrading fluvial system ', *Earth Surface Processes and Landforms*, vol. 32, no. 2, pp. 307-316.

Phillips, J. D. & Marion, D. A. 2001, 'Residence times of alluvium in an east Texas stream as indicated by sediment color', *Catena*, vol. 45, pp. 49-71.

Phillips, J. D. & Slattery, M. C. 2007, 'Downstream trends in discharge, slope, and stream power in a lower coastal plain river', *Journal of Hydrology*, vol. 334, pp. 290-303.

Phillips, J. M., Russell, M. A. & Walling, D. E. 2000, 'Time-integrated sampling of fluvial suspended sediment: a simple methodology for small catchments', *Hydrological Processes*, vol. 14, pp. 2589-2602.

Pickup, G. & Marks, A. 2001, 'Regional-scale sedimentation process models from airborne gamma ray remote sensing and digital elevation data', *Earth Surface Processes and Landforms*, vol. 26, no. 3, pp. 273-293.

Pimentel, D., Harvey, C., Resosudarmo, P., Sinclair, K., Kurz, D., McNair, M., Crist, S., Shpritz, L., Fitton, I., Saffouri, R. & Blair, R. 1995, 'Environmental and economic costs of soil erosion and conservation benefits', *Science*, vol. 267, no. 5210, pp. 1117-1123.

Poesen, J., Nachtergaele, J., Verstraeten, G. & Valentin, C. 2003, 'Gully erosion and environmental change: importance and research needs', *Catena*, vol. 50, pp. 91-133.

Poesen, J. W., Vandaele, K. & Van Wesemael, B. 1996, 'Contribution of gully erosion to sediment production on cultivated lands and rangelands', *Erosion and Sediment Yield: Global and Regional Perspectives.* July, 1996. IAHS Publication No. 236, pp. 251-266.

Polyakov, V., Nearing, M. & Shipitalo, M. 2004, 'Tracking sediment redistribution in a small scale watershed: implications for agro-landscape evolution', *Earth Surface Processes and Landforms*, vol. 29, pp. 1275-1291.

Porto, P., Walling, D. E., Tamburino, V. & Callegari, G. 2003, 'Relating caesium-137 and soil loss from cultivated land', *Catena*, vol. 53, pp. 303-326.

Pouyat, R. V., Yesilonis, I. D., Russell-Anelli, J. & Neerchal, N. K. 2007, 'Soil chemical and physical properties that differentiate urban land-use and cover types', *Soil Science Society of America Journal*, vol. 71, no. 3, pp. 1010-1019.

Prosser, I., Rustomji, P., Young, B., Moran, C. & Hughes, A. 2001a, *Constructing River Basin Sediment Budgets for the National Land and Water Resources Audit*, Technical Report 15/01, CSIRO Land and Water, Canberra.

Prosser, I. P., Hughes, A. O. & Rutherford, I. D. 2000, 'Bank erosion of an incised upland channel by subaerial processes: Tasmania, Australia', *Earth Surface Processes and Landforms*, vol. 25, pp. 1085-1101.

Prosser, I. P., Rutherford, I. D., Olley, J. M., Young, W. J., Wallbrink, P. J. & Moran, C. J. 2001b, 'Large-scale patterns of erosion and sediment transport in river networks, with examples from Australia', *Marine and Freshwater Research*, vol. 52, pp. 81-99.

Purkait, R. 2005, 'Triangle identified at the proximal end of femur: a new sex determinant', *Forensic Science International*, vol. 147, no. 2-3, pp. 135-139.

Pye, K. 1994, 'Properties of sediment particles', in K. Pye (ed.), *Sediment Transport and Depositional Processes*, Blackwell Scientific Publications, Oxford, pp. 1-24.

Quinn, J. & Stroud, M. 2002, 'Water quality and sediment and nutrient export from New Zealand hill-land catchments of contrasting land use', *New Zealand Journal of Marine and Freshwater Research*, vol. 36, pp. 409-429.

Quinn, J. M., Boothroyd, I. K. G. & Smith, B. J. 2004, 'Riparian buffers mitigate effects of pine plantation logging on New Zealand streams 2. Invertebrate communities', *Forest Ecology and Management*, vol. 191, pp. 129-146.

Reid, L. & Page, M. 2002, 'Magnitude and frequency of landsliding in a large New Zealand catchment', *Geomorphology*, vol. 49, pp. 71-88.

Reimann, C., Arnoldussen, A., Englmaier, P., Filzmoser, P., Erik Finne, T., Garrett, R. G., Koller, F. & Nordgulen, O. 2007, 'Element concentrations and variations along a 120km transect in southern Norway - Anthropogenic vs. geogenic vs. biogenic elemental sources and cycles', *Applied Geochemistry*, vol. 22, pp. 851-871.

Richter, D. D., Markewitz, D., Wells, C. G., Allen, H. L., April, R., Heine, P. R. & Urrego, B. 1994, 'Soil chemical change during three decades in an old-field Loblolly Pine (*Pinus Taeda* L.) ecosystem', *Ecology*, vol. 75, no. 2, pp. 1463-1473.

Ritchie, J. C. & McHenry, J. R. 1990, 'Application of radioactive fallout Cesium-137 for measuring soil erosion and sediment accumulation rates and patterns: a review', *Journal of Environmental Quality*, vol. 19, no. 2, pp. 215-233.

Ritchie, J. C. & Ritchie, C. A. 2001, *Bibliography of publications of ^{137}Cs studies related to soil erosion and sediment deposition,* viewed 9-12-2007 http://hydrolab.arsusda.gov/cesium137bib.htm

Ritsema, C. J., van Lynden, G. W. J., Jetten, V. G. & de Jong, S. M. 2005, 'Degradation', in D. Hillel (ed.), *Encyclopaedia of Soils in the Environment*, Elsevier Academic Press, Oxford, UK, pp. 370-377.

Rivaie, A. A., Loganathan, P., Graham, J. D., Tillman, R. W. & Payn, T. W. 2008, 'Effect of phosphate rock and triple superphosphate on soil phosphorus fractions and their plant-availability and downward movement in two volcanic ash soils under *Pinus radiata* plantations in New Zealand', *Nutrient Cycling in Agroecosystems*, vol. 82, pp. 75-88.

Rodda, H., Stroud, M., Shankar, U. & Thorrold, B. 2001, 'A GIS based approach to modelling the effects of land-use change on soil erosion in New Zealand', *Soil Use and Management*, vol. 17, pp. 30-40.

Roddy, B. P. 1997, *The use of fallout radionuclides to estimate soil redistribution in a logged coupe in the south east of NSW*, Honours Thesis, Australian National University.

Roddy, B. P., McWhirter, J. L., Moon, V. G., Balks, M. R. & Dyer, F. J. 2008, 'Sediment fingerprinting in New Zealand: a pilot study into the feasibility of the application of the technique.' *Sediment Dynamics in Changing Environments Symposium*, International Hydrological Sciences Association Publication 325, Christchurch, NZ. December 2008.

Roering, J. J. 2008, 'How well can hillslope evolution models "explain" topography? Simulating soil transport and production with high-resolution topographic data', *Geological Society of America Bulletin*, vol. 120, no. 9/10, pp. 1248-1262.

Rommens, T., Verstraeten, G., Bogman, P., Peeters, I., Poesen, J., Govers, G., Van Rompaey, A. & Lang, A. 2006, 'Holocene alluvial sediment storage in a small river catchment in the loess area of central Belgium', *Geomorphology*, vol. 77, no. 1-2, pp. 187-201.

Rommens, T., Verstraeten, G., Poesen, J., Govers, G., Van Rompaey, A., Peeters, I. & Lang, A. 2005, 'Soil erosion and sediment deposition in the Belgian loess belt during the Holocene: establishing a sediment budget for a small agricultural catchment', *Holocene*, vol. 15, no. 7, pp. 1032-1043.

Rosewell, C., Crouch, R., Morse, R., Leys, J., Hicks, R. & Stanley, R. 1993, 'Forms of erosion', in P. Charman & B. W. Murphy (ed.), *Soils: Their Properties and Management*, Sydney University Press.

Russell, M. A., Walling, D. E. & Hodgkinson, R. A. 2001, 'Suspended sediment sources in two lowland agricultural catchments in the UK', *Journal of Hydrology*, vol. 252, pp. 1-24.

Ryan, P. 1991, 'Environmental effects of sediment on New Zealand's streams: a review', *New Zealand Journal of Marine and Freshwater Research*, vol. 25, pp. 207-221.

Schaub, D. & Prasuhn, V. 1993, 'The role of test plot measurements in a long-term soil erosion research project in Switzerland', in S. Wicherek (ed.), *Farm Land Erosion: In Temperate Plains Environments and Hills*, Elsevier, Amsterdam, pp. 111-123.

Schierlitz, C., Dymond, J. & Shepherd, J. 2006, *Erosion/Sedimentation in the Manawatu Catchment Associated with Scenarios of Whole Farm Plans*, Landcare Research Contract Report: 0607/028. September 2006.

Schoellhamer, D. H. & Wright, S. A. 2002, 'Continuous measurement of suspended-sediment discharge in rivers by use of optical backscatterance sensors', *Erosion and Sediment Transport Measurement in Rivers: Technological and Methodological Advances*, IAHS Publication no. 283, Oslo, pp. 28-36.

Schuster, R. L. & Highland, L. M. 2007, 'Overview of the effects of mass wasting on the natural environment', *Environmental and Engineering Geoscience*, vol. 13, no. 1, pp. 25-44.

Schwarz, A. 2004, 'Contribution of photosynthetic gains during tidal emersion to production of *Zostera capricorni* in a North Island, New Zealand estuary', *New Zealand Journal of Marine and Freshwater Research*, vol. 38, pp. 809-818.

Selby, M. J. 1972, 'The relationship between land use and erosion in the central North Island, New Zealand', *Journal of Hydrology*, vol. 11, no. 2, pp. 73-87.

Selby, M. J. 1994, 'Hillslope sediment transport and deposition', in K. Pye (ed.), *Sediment Transport and Depositional Processes*, Blackwell Scientific Publications, Oxford.

Shao, J. & Tu, D. 1995, *The Jackknife and Bootstrap*, Springer-Verlag, New York.

Sheffield, A., Healy, T. & McGlone, M. 1995, 'Infilling rates of a steepland catchment estuary, Whangamata, New Zealand', *Journal of Coastal Research*, vol. 11, no. 4, pp. 1294-1308.

Sheridan, G. J. & Noske, P. J. 2007, 'Catchment-scale contribution of forest roads to stream exports of sediment, phosphorus and nitrogen', *Hydrological Processes*, vol. 21, pp. 3107-3122.

Sheridan, G. J., Noske, P. J., Whipp, R. K. & Wijesinghe, N. 2006, 'The effect of truck traffic and road water content on sediment delivery from unpaved forest roads', *Hydrological Processes*, vol. 20, pp. 1683-1699.

Sidle, R. C., Ziegler, A. D., Negishi, J. N., Nik, A. R., Siew, R. & Turkelboom, F. 2006, 'Erosion processes in steep terrain - truths, myths, and uncertainties related to forest management in Southeast Asia', *Forest Ecology and Management*, vol. 224, pp. 199-225.

Simkiss, K., Baxter, M. S., Bell, J. N. B., Davidson, W., Duncan, K., Fry, F., Horrill, A. D., Kelly, M., Mather, J. D., Parsons, J. W., Peterson, P., Kennedy, V. & Vanderborght, O. 1993, 'Radiocesium in natural systems - a UK coordinated study', *Journal of Environmental Radioactivity,* vol. 18, no. 2, pp. 133-149.

Singleton, P. L. & Addison, B. 1999, 'Effects of cattle treading on physical properties of three soils used for dairy farming in the Waikato, North Island, New Zealand', *Australian Journal of Soil Research*, vol. 37, pp. 891-902.

Sirvent, J., Desir, G., Gutierrez, M., Sancho, C. & Benito, G. 1997, 'Erosion rates in badland areas recorded by collectors, erosion pins and profilometer techniques (Ebro Basin, NE-Spain)', *Geomorphology*, vol. 18, pp. 61-75.

Skinner, D. 1986, 'Neogene volcanism of the Hauraki Volcanic Region', in I. Smith (ed.), *Late Cenozoic volcanism in New Zealand*, Royal Society of New Zealand Bulletin 23: 21-47, pp. 21-47.

Skinner, D. 1993, *Geology of the Coromandel Harbour Area*, Institute of Geological and Nuclear Sciences.

Slattery, M. C. & Burt, T. P. 1997, 'Particle size characteristics of suspended sediment in hillslope runoff and stream flow', *Earth Surface Processes and Landforms*, vol. 22, pp. 705-719.

Small, I. F., Rowan, J. S. & Franks, S. W. 2002, 'Quantitative sediment fingerprinting using a Bayesian uncertainty estimation framework ', *The Structure, Function and Management Implications of Fluvial Sedimentary Systems.* IAHS Publication no. 276, Alice Springs, pp. 443-450.

Smith, B. & Amonette, A. 2006, *The Environmental Transport of Radium and Plutonium: A Review*, Institute for Energy and Environmental Research, June 23, 2006.

Smith, H. G. & Dragovich, D. 2008, 'Improving precision in sediment source and erosion process distinction in an upland catchment, south-eastern Australia', *Catena*, vol. 72, no. 1, pp. 191-203.

Smith, J. D. 1982, 'Lead-210 dating of sediments', in W. Ambrose & P. Duerden (ed.), *Archaeometry: An Australian perspective*, Australian National University Press, Canberra, pp. 303-309.

Stanley, D. J. 1996, 'Nile delta: extreme case of sediment entrapment on a delta plain and consequent coastal land loss', *Marine Geology*, vol. 129, pp. 189-195.

StatSoft Inc 2007, *Electronic Statistics Textbook,* viewed 23-5-2006 http://www.statsoft.com/textbook/stathome.html

Stewart, G. J., Caldwell, J. M. & Cloutier, A. R. 2003, *Water Resources Data - Maine (USA) 2002*, Water Data Report ME-02-1, US Geological Survey, Augusta, Maine.

Stott, T. & Mount, N. 2004, 'Plantation forestry impacts on sediment yields and downstream channel dynamics in the UK: a review', *Progress in Physical Geography*, vol. 28, no. 2, pp. 197-240.

Stubblefield, A. P., Reuter, J. E., Dahlgren, R. A. & Goldman, C. R. 2006, 'Use of turbidometry to characterize suspended sediment and phosphorus fluxes in the Lake Tahoe basin, California, USA', *Hydrological Processes*, vol. 21, no. 3, pp. 281-291.

Sun, H., Cornish, P. & Daniell, T. 2001, 'Turbidity-based erosion estimation in a catchment in South Australia', *Journal of Hydrology*, vol. 253, pp. 227-238.

Sutherland, R. A. 1991, '^{137}Cs and sediment budgeting within a partially closed drainage basin', *Zeitschrift fur Geomorphol*, vol. 35, pp. 47-63.

Sutherland, R. A. 1994, 'Spatial variability of ^{137}Cs and the influence of sampling on estimates of sediment redistribution', *Catena*, vol. 21, pp. 57-71.

Sutherland, R. A. 1996, 'Caesium-137 soil sampling and inventory variability in reference locations: a literature survey', *Hydrological Processes*, vol. 10, pp. 43-53.

Swales, A., Bentley, S. J., Lovelock, C. & Bell, R. G. 2007, 'Sediment processes and mangrove-habitat expansion on a rapidly prograding muddy coast, New Zealand', *Coastal Sediment '07, American Society of Civil Engineers*, New Orleans, Louisiana,, pp. 1441-1454.

Swank, W. T., Vose, J. M. & Elliott, K. J. 2001, 'Long-term hydrologic and water quality responses following commercial clearcutting of mixed hardwoods on a southern Appalachian catchment', *Forest Ecology and Management*, vol. 143, pp. 163-178.

Syvitski, J. P. M. & Millman, J. D. 2007, 'Geology, geography, and humans battle for dominance over the delivery of fluvial sediment to the coastal ocean', *The Journal of Geology*, vol. 115, pp. 1-19.

Tabachnick, B. G. & Fidell, L. S. 1996, *Using Multivariate Statistics*, Harper Collins, New York.

Tanberg, A., Da Veiga, M., Dechens, S. C. F. & Stocking, M. A. 1998, 'Modelling the impact of erosion and soil productivity: a comparative evaluation of approaches on data from southern Brazil', *Experimental Agriculture*, vol. 34, pp. 55-71.

Taylor, M. D. & Kim, N. D. 2009, 'Dealumination as a mechanism for increased acid recoverable aluminium in Waikato mineral soils', *Australian Journal of Soil Research*, vol. 47, no. 8, pp. 828-838.

Thoma, D. P., Gupta, S. C., Bauer, M. E. & Kirchoff, C. E. 2005, 'Airborne laser scanning of riverbank erosion assessment', *Remote Sensing of Environment*, vol. 95, pp. 493-501.

Thompson, S. 2008, *More than two treatment levels for ANOVA. Stat 650 - Quantitative Analysis in Resource Management and Field Biology, Simon Fraser University, Canada,* viewed 6-9-2008 http://www.stat.sfu.ca/~thompson/stat403-650/three_or_more-ANOVA.html

Thrush, S. F., Hewitt, J. E., Cummings, V., Ellis, J. I., Hatton, C. & Lohrer, A. 2004, 'Muddy waters: elevating sediment input to coastal and estuarine habitats', *Frontiers in Ecology and the Environment*, vol. 2, no. 6, pp. 299-306.

Timm, N. H. 2002, *Applied Multivariate Analysis*, Springer-Verlag, New York.

Tims, S. G., Hancock, G. J., Wacker, L. & Fifield, L. K. 2004, 'Measurements of Pu and Ra isotopes in soils and sediments by AMS', *Nuclear Instruments and Methods in Physics Research B*, vol. 223-224, pp. 796-801.

Trefil, J. & Hazen, R. M. 2004, *The Sciences: An Integrated Approach*, Wiley Higher Education.

Trimble, S. W. 1999, 'Decreased rates of alluvial sediment storage in the Coon Creek Basin, Wisconsin, 1975-93', *Science*, vol. 285, pp. 1244-1246.

Turekian, K. K. 1997, *Radium on Soil Mineral Surfaces: Its Mobility Under Environmental Conditions and its Role in Radon Emanation.*, DOE FINAL REPORT 1997, DOE/ER/60576-TI.

Turekian, K. K., Nozaki, Y. & Benninger, L. K. 1977, 'Geochemistry of atmospheric radon and radon products: annual review', *Earth and Planetary Science*, vol. 5, pp. 227-255.

Turner, J. & Lambert, M. J. 1986, 'Nutrition and Nutritional Relationships of Pinus Radiata ', *Annual Review of Ecology and Systematics*, vol. 17, pp. 325-350.

University of Missouri Research Reactor Center 2007, *Inductively Coupled Plasma Mass Spectrometry (ICP-MS),* viewed 10-1-2007 http://web.missouri.edu/~umcreactorweb/pages/ac_icpms1.shtml

Valentin, C., Poesen, J. & Li, Y. 2005, 'Gully erosion: Impacts, factors and control', *Catena*, vol. 63, no. 2-3, pp. 132-153.

van Dijk, P. M., Auzet, A. V. & Lemmel, M. 2005, 'Rapid assessment of field erosion and sediment transport pathways in cultivated catchments after heavy rainfall events', *Earth Surface Processes and Landforms*, vol. 30, no. 2, pp. 169-182.

VandenBygaart, A. J. & Protz, R. 1995, 'Gamma radioactivity on a chronosequence, Pinery Provincial Park, Ontario', *Canadian Journal of Soil Science*, vol. 75, no. 1, pp. 73-84.

Vanoni, V. 1975, *Sedimentation Engineering*, American Society of Civil Engineers, New York.

Varnes, D. J. 1975, 'Slope movements in the Western United States', in E. Yatsu, A. J. Ward & F. Adams (ed.), *Mass Wasting 4th Guelph Symposium on Geomorphology*, pp. 1-17.

Ventura, E., Nearing, M. A. & Darrell Norton, L. 2001, 'Developing a magnetic tracer to study soil erosion', *Catena*, vol. 43, pp. 277-291.

Vrana, D. 2007, 'A Pox Upon the Kauri', *Smithsonian*, vol. 38, pp. 4-5.

Walden, J., Slattery, M. & Burt, T. 1997, 'Use of mineral magnetic measurements to fingerprint suspended sediment sources: approaches and techniques for data analysis', *Journal of Hydrology*, vol. 202, pp. 353-372.

Wallbrink, P., Roddy, B. & Olley, J. 2002a, 'A tracer budget quantifying soil redistribution on hillslopes after forest harvesting', *Catena*, vol. 47, pp. 179-201.

Wallbrink, P. J. 2004, 'Quantifying the erosion processes and landuses which dominate fine sediment supply to Moreton Bay, Southeast Queensland, Australia', *Journal of Environmental Radioactivity*, vol. 76, pp. 67-80.

Wallbrink, P. J. & Croke, J. 2002, 'A combined rainfall simulator and tracer approach to assess the role of Best Management Practices in minimising sediment redistribution and loss in forests after harvesting', *Forest Ecology and Management*, vol. 170, no. 1-3, pp. 217-232.

Wallbrink, P. J., Martin, C. E. & Wilson, C. J. 2003a, 'Quantifying the contributions of sediment, sediment-P and fertiliser-P from forested, cultivated and pasture areas at the landuse and catchment scale using fallout radionuclides and geochemistry', *Soil and Tillage Research*, vol. 69, pp. 53-68.

Wallbrink, P. J. & Murray, A. S. 1993, 'The use of fallout radionuclides as indicators of erosion processes', *Hydrological Processes*, vol. 7, pp. 297-304.

Wallbrink, P. J. & Murray, A. S. 1996, 'Determining soil loss using the inventory ratio of excess Lead-210 to Cesium-137', *Soil Science Society of America Journal*, vol. 60, no. 4, pp. 1201-1208.

Wallbrink, P. J., Murray, A. S. & Olley, J. M. 1999, 'Relating suspended sediment to its original soil depth using fallout radionuclides', *Soil Science Society of America Journal*, vol. 63, no. 2, pp. 369-378.

Wallbrink, P. J., Murray, A. S., Olley, J. M. & Olive, L. J. 1998, 'Determining sources and transit times of suspended sediment in the Murrumbidgee River, New South Wales, Australia, using fallout ^{137}Cs and ^{210}Pb', *Water Resources Research*, vol. 34, no. 4, pp. 879-887.

Wallbrink, P. J., Olley, J. M. & Hancock, G. 2002b, 'Estimating residence times of fine grained sediment in river channels using fallout ^{210}Pb', *The Structure, Function and Management Implications of Fluvial Sedimentary Systems.* IAHS Publication no. *276*, Alice Springs, pp. 425-432.

Wallbrink, P. J., Olley, J. M. & Hancock, G. 2003b, *Tracer Assessment of Catchment Sediment Contributions to Western Port, Victoria*, Technical Report 8/03, January 2003, CSIRO Land and Water, Canberra.

Wallbrink, P. J., Olley, J. M. & Murray, A. S. 1994a, 'Measuring soil movement using ^{137}Cs: implications of reference site variability', *Variability in Stream Erosion and Sediment Transport.* IAHS Publication no. 224, Canberra, pp. 95-102.

Wallbrink, P. J., Olley, J. M. & Murray, A. S. 1994b, 'Measuring soil movement using ^{137}Cs: implications of reference site variability', *Variability in Stream Erosion and Sediment Transport*, IAHS Publication no. 224, Canberra, December 1994, pp. 95-102.

Wallbrink, P. J., Olley, J. M., Murray, A. S. & Olive, L. J. 1996, 'The contribution of subsoil to sediment yield in the Murrumbidgee River basin, New South Wales, Australia', *Erosion and Sediment Yield: Global and Regional Perspectives. July, 1996.* IAHS Publication No. 236, pp. 347-355.

Walling, D. 1999, 'Linking land use, erosion and sediment yields in river basins', *Hydrobiologia*, vol. 410, pp. 223-240.

Walling, D., Owens, P. & Leeks, G. 1999, 'Fingerprinting suspended sediment sources in the catchment of the River Ouse, Yorkshire, UK', *Hydrological Processes*, vol. 13, pp. 955-975.

Walling, D. E. 1983, 'The sediment delivery problem', *Journal of Hydrology*, vol. 65, pp. 209-237.

Walling, D. E. 2002, 'Using environmental radionuclides as tracers in sediment budget investigations', *Erosion and Sediment Transport Measurement in Rivers: Technological and Methodological Advances*, Olso, Norway, 19-21 June, 2002, pp. 57-78.

Walling, D. E. 2003, 'Using environmental radionuclides as tracers in sediment budget investigations', *Erosion and Sediment Transport Measurement in Rivers: Technological and Methodological Advances*, Olso, Norway, 19-21 June, 2002. IAHS Publication No. 283, pp. 57-78.

Walling, D. E. 2005, 'Tracing suspended sediment sources in catchments and river systems', *Science of the Total Environment*, vol. 344, pp. 159-184.

Walling, D. E. 2006, 'Tracing versus monitoring', in P. Owens (ed.), *Soil Erosion and Sediment Redistribution in River Catchments: Measurement, Modelling and Management*, CABI publishing, Wallingford, Oxfordshire.

Walling, D. E. & Amos, C. M. 1999, 'Source, storage and mobilisation of fine sediment in a chalk stream system', *Hydrological Processes*, vol. 13, pp. 323-340.

Walling, D. E., Collins, A. L., Jones, P. A., Leeks, G. J. L. & Old, G. 2006, 'Establishing fine-grained sediment budgets for the Pang and Lambourn LOCAR catchments, UK', *Journal of Hydrology*, vol. 330, pp. 126-141.

Walling, D. E., Collins, A. L., Sichingabula, H. & Leeks, G. 2001, 'Integrated assessment of catchment suspended sediment budgets: a Zambian example', *Land Degradation and Development*, vol. 12, pp. 387-415.

Walling, D. E., Collins, A. L., Sichingabula, H. M. & Leeks, G. J. L. 2003, 'Use of reconnaissance measurements to establish catchment sediment budgets: a Zambian example', *Erosion Prediction in Ungauged Basins: Integrating Methods and Techniques*, Proceedings of the symposium HS01 held at Sapporo, Japan. 8-9 July, 2003.

Walling, D. E., Collins, A. L. & Stroud, R. W. 2008, 'Tracing suspended sediment and particulate phosphorus sources in catchments', *Journal of Hydrology*, vol. 350, pp. 274-289.

Walling, D. E. & He, Q. 1997, 'Use of fallout ^{137}Cs in investigations of overbank sediment deposition on river floodplains', *Catena*, vol. 29, pp. 263-282.

Walling, D. E., He, Q. & Appleby, P. G. 2002a, 'Conversion models for use in soil-erosion, soil redistribution and sedimentation investigations', in F. Zapata (ed.), *Handbook for the Assessment of Soil Erosion and Sedimentation Using Environmental Radionuclides*, Kluwer Academic Publishers, pp. 111-164.

Walling, D. E. & Kane, P. 1982, 'Temporal variation of suspended sediment properties', *Recent Developments in the Explanation and Prediction of Erosion and Sediment Yield.* , Exeter, UK. IAHS Publication No 137, pp. 409-419.

Walling, D. E. & Moorehead, P. W. 1989, 'The particle size characteristics of fluvial suspended sediment: an overview', *Hydrobiologia*, vol. 176/177, pp. 125-149.

Walling, D. E., Owens, P. N., Waterfall, B. D., Leeks, G. J. L. & Wass, P. D. 2000, 'The particle size characteristics of fluvial suspended sediment in the Humber and Tweed catchments, UK', *The Science of the Total Environment*, vol. 251/252, pp. 205-222.

Walling, D. E. & Quine, T. A. 1993, 'Using Chernobyl-Derived Fallout Radionuclides to Investigate the Role of Downstream Conveyance Losses in the Suspended Sediment Budget of the River Severn, United-Kingdom', *Physical Geography*, vol. 14, no. 3, pp. 239-253.

Walling, D. E., Russell, M. A., Hodgkinson, R. & Zhang, Y. 2002b, 'Establishing sediment budgets for two small lowland agricultural catchments in the UK', *Catena*, vol. 47, pp. 323-353.

Walling, D. E. & Woodward, J. 1995, 'Tracing sources of suspended sediment in river basins: A case study of the River Culm, Devon, UK ', *Marine and Freshwater Research*, vol. 46, pp. 327-36.

Walling, D. E. & Woodward, J. C. 1992, 'Use of radiometric fingerprints to derive information on suspended sediment sources', *Erosion and Sediment Transport Monitoring Programmes in River Basins*, IAHS Publication no. 210, Oslo, August 1992, pp. 153-164.

Wan, G. J., Chen, J. A., Wu, F. C., Xu, S. Q., Bai, Z. G., Wan, E. Y., Wang, C. S., Huang, R. G., Yeager, K. M. & Santschi, P. H. 2005, 'Coupling between 210Pbex and organic matter in sediments of a nutrient-enriched lake: An example from Lake Chenghai, China', *Chemical Geology*, vol. 224, no. 4, pp. 223-236.

Wasson, R. J. 2002, 'Sediment budgets, dynamics, and variability: new approaches and techniques', *The Structure, Function and Management Implications of Fluvial Sedimentary Systems.* IAHS Publication no. 276, Alice Springs, pp. 471-478.

Wasson, R. J., Caitcheon, G., Murray, A. S., McCulloch, M. & Quade, J. 2002, 'Sourcing sediment using multiple tracers in the catchment of Lake Argyle, Northwestern Australia', *Environmental Management*, vol. 29, no. 5, pp. 634-646.

Wasson, R. J., Clark, R. L. & Nanninga, P. M. 1987, '^{210}Pb as a chronometer and tracer, Burrinjuck reservoir, Australia', *Earth Surface Processes and Landforms*, vol. 12, pp. 399-414.

Watson, A., Phillips, C. & Marden, M. 1999, 'Root strength, growth, and rates of decay: root reinforcement changes of two tree species and their contribution to slope stability', *Plant and Soil*, vol. 217, pp. 39-47.

Watson, A. J. & Basher, L. R. 2005, *Stream Bank Erosion: A Review of Processes of Bank Failure, Measurement and Assessment Techniques, and Modelling Approaches*, Landcare ICM Report No. 2005-2006/01.

Weitzman, J. 2008, *Nutrient and Trace Element Contents of Stream Bank Sediments from Big Spring Run and Implications for the Chesapeake Bay*, Honours Thesis, Franklin and Marshall College, Earth and Environment Department.

White, P. A., Sharp, B. M. H. & Reeves, R. R. 2006, *New Zealand Water Bodies of National Importance for Domestic Use and Industrial Use* viewed 21-4-2006 http://www.med.govt.nz/templates/MultipageDocumentPage____12540.aspx

White, W. R. 1978, 'Flow measuring structures', in R. W. Herschy (ed.), *Hydrometry: Principles and Practices.* John Wiley and Sons, Chichester, pp. 83-109.

Whiting, P. J., Matisoff, G., Fornes, W. & Soster, F. M. 2005, 'Suspended sediment sources and transport distances in the Yellowstone River basin', *Geological Society of America Bulletin*, vol. 117, no. 3/4, pp. 515-529.

Wilbanks, T. J. & Kates, R. W. 1999, 'Global change in local places: How scale matters', *Climatic Change*, vol. 43, no. 3, pp. 601-628.

Wilcock, R. J., Nagles, J. W., H.J.E., R., O'Connor, M. B., Thorrold, B. S. & Barnett, J. W. 1999, 'Water quality of a lowland stream in a New Zealand dairy farming catchment', *New Zealand Journal of Marine and Freshwater Research*, vol. 33, pp. 683-696.

Wild, M. & Hicks, M. 2005, *Opitonui Stream Suspended Sediment Analysis.* , Environment Waikato Technical Report 2005/45. October 2005.

Will, G. M. 1968, 'The uptake, cycling and removal of mineral nutrients by crops of pinus radiata', *Proceedings of the New Zealand Ecological Society*, vol. 15, pp. 20-24.

Williams, G. P. 1989, 'Sediment concentration versus water discharge during single hydrologic events in rivers.' *Journal of Hydrology*, vol. 111, pp. 89-106.

Wilmshurst, J. 1997, 'The impact of human settlement on vegetation and soil stability in Hawke's Bay, New Zealand', *New Zealand Journal of Botany*, vol. 35, pp. 97-111.

Wilmshurst, J. & McGlone, M. 2005, 'Corroded pollen and spores as indicators of changing lake sediment sources and catchment disturbance', *Journal of Paleolimnology*, vol. 34, pp. 503-517.

Wilson, C. G., Matisoff, G. & Whiting, P. J. 2003, 'Short-term erosion rates from a Be-7 inventory balance', *Earth Surface Processes and Landforms*, vol. 28, no. 9, pp. 967-977.

Wilson, C. G., Matisoff, G., Whiting, P. J. & Klarer, D. M. 2005, 'Transport of fine sediment through a wetland using radionuclide tracers: Old Woman Creek, OH', *Journal of Great Lakes Research*, vol. 31, no. 1, pp. 56-67.

Wilson, J. P. & Gallant, J. C. 1996, 'EROS: A grid-based program for estimating spatially-distributed erosion indices', *Computers & Geosciences*, vol. 22, no. 7, pp. 707-712.

Winter, S., Conrad, V. & Ross, J. 2002, *Direct Reaction Cell ICP-MS vs. XRF: Which is the Superior Technique for the Analysis of Water-Soluble and Total Elements in Fine Particulate Matter?,* viewed 25-3-2009 http://www.netl.doe.gov/publications/proceedings/02/PM25/1.4.1Winter_p.pdf

Wise, S. M. 1980, 'Caesium-137 and Lead-210: a review of the techniques and some applications in geomorphology', in R. A. Cullingford, D. A. Davidson & J. Lewin (ed.), *Timescales in Geomorphology*, John Wiley and Sons, pp. 109-127.

Wolman, M. G. & Schick, A. P. 1967, 'Effects of Construction on Fluvial Sediment, Urban and Suburban Areas of Maryland', *Water Resources Research*, vol. 3, no. 2, pp. 451-464.

Wood, G. & Fahey, B. D. 2006, 'Forestry effects on stream flow and water yield', in G. Eyles & B. D. Fahey (ed.), *The Pakuratahi Land Use Study*, pp. 31-50.

Wren, D., Barkdoll, B., Kuhnle, R. & Derrow, R. 2000, 'Field techniques for suspended sediment measurement', *Journal of Hydraulic Engineering*, vol. 126, no. 2, pp. 97-104.

Yeager, K. M. & Santschi, P. H. 2003, 'Invariance of isotope ratios of lithogenic radionuclides: more evidence for their use as sediment source tracers', *Journal of Environmental Radioactivity*, vol. 69, no. 3, pp. 159-176.

Yeager, K. M., Santschi, P. H., Phillips, J. D. & Herbert, B. E. 2005, 'Suspended sediment sources and tributary effects in the lower reaches of a coastal plain stream as indicated by radionuclides, Loco Bayou, Texas', *Environmental Geology*, vol. 47, pp. 382-395.

Yeates, G. W., Hawke, M. F. & Rijkse, W. C. 2000, 'Changes in soil fauna and soil conditions under *P. radiata* agroforestry regimes during a 25-year tree rotation', *Biology and Fertility of Soils*, vol. 31, pp. 391-406.

Yu, L. 2002, 'The Huanghe (Yellow) River: a review of its development, characteristics, and future management issues ', *Continental Shelf Research*, vol. 22, no. 3, pp. 389-403.

Zabaleta, A., Martinez, M., Uriarte, J. A. & Antiguedad, I. 2007, 'Factors controlling suspended sediment yield during runoff events in small headwater catchments of the Basque Country ', *Catena*, vol. 71, no. 1, pp. 179-190

Zaimes, G. N., Schultz, R. C. & Isenhart, T. M. 2004, 'Stream bank erosion adjacent to riparian forest buffers, row-crop fields, and continuously-grazed pastures along Bear Creek in central Iowa', *Journal of Soil and Water Conservation*, vol. 59, no. 1, pp. 19-27.

Zapata, F., Garcia-Agudo, E., Ritchie, J. & Appleby, P. G. 2002, 'Introduction', in F. Zapata (ed.), *Handbook for the Assessment of Soil Erosion and Sedimentation Using Environmental Radionuclides*, Kluwer Academic Publishers, Secaucus, NJ, USA, pp. 1-14.

Zehetner, F., Vemuri, N. L., Huh, C., Kao, S., Hsu, S., Huang, J. & Chen, Z. 2008, 'Soil and phosphorus redistribution along a steep tea plantation in the Feitsui reservoir catchment on northern Taiwan', *Soil Science and Plant Nutrition*, vol. 54, pp. 618-626.

Zhang, C., Fay, D., McGrath, D., Grennan, E. & Carton, O. T. 2008, 'Statistical analyses of geochemical variables in soils of Ireland', *Geoderma*, vol. 146, pp. 378-390.

Zhang, X. B., He, X. B., Wen, A. B., Walling, D. E., Feng, M. Y. & Zou, X. 2004, 'Sediment source identification by using Cs-137 and Pb-210 radionuclides in a small catchment of the Hilly Sichuan Basin, China', *Chinese Science Bulletin*, vol. 49, no. 18, pp. 1953-1957.

Zhang, X. B., Higgitt, D. L. & Walling, D. E. 1990, 'A preliminary assessment of the potential for using Caesium-137 to estimate soil erosion in the Loess Plateau of China ', *Hydrological Sciences Journal*, vol. 35, pp. 267-276.

Zheng, F. 2006, 'Effects of vegetation changes on soil erosion on the Loess Plateau', *Pedosphere*, vol. 16, no. 4, pp. 420-427.

Zhenli, L. H., Xiaoe, E. Y. & Stoffella, P. J. 2005, 'Trace elements in agroecosystems and impacts on the environment', *Journal of Trace Elements in Medicine and Biology*, vol. 19, pp. 125-140.